frontiers | Research Topics

Precision medicine in pediatrics

Edited by
Jian Gao, Xiaoling Wang, Yang Zhou and Samuel Seward

Published in
Frontiers in Pharmacology
Frontiers in Pediatrics

ISSN 1664-8714
ISBN 978-2-8325-2663-7
DOI 10.3389/978-2-8325-2663-7

About Frontiers

Frontiers is more than just an open access publisher of scholarly articles: it is a pioneering approach to the world of academia, radically improving the way scholarly research is managed. The grand vision of Frontiers is a world where all people have an equal opportunity to seek, share and generate knowledge. Frontiers provides immediate and permanent online open access to all its publications, but this alone is not enough to realize our grand goals.

Frontiers journal series

The Frontiers journal series is a multi-tier and interdisciplinary set of open-access, online journals, promising a paradigm shift from the current review, selection and dissemination processes in academic publishing. All Frontiers journals are driven by researchers for researchers; therefore, they constitute a service to the scholarly community. At the same time, the *Frontiers journal series* operates on a revolutionary invention, the tiered publishing system, initially addressing specific communities of scholars, and gradually climbing up to broader public understanding, thus serving the interests of the lay society, too.

Dedication to quality

Each Frontiers article is a landmark of the highest quality, thanks to genuinely collaborative interactions between authors and review editors, who include some of the world's best academicians. Research must be certified by peers before entering a stream of knowledge that may eventually reach the public - and shape society; therefore, Frontiers only applies the most rigorous and unbiased reviews. Frontiers revolutionizes research publishing by freely delivering the most outstanding research, evaluated with no bias from both the academic and social point of view. By applying the most advanced information technologies, Frontiers is catapulting scholarly publishing into a new generation.

What are Frontiers Research Topics?

Frontiers Research Topics are very popular trademarks of the *Frontiers journals series*: they are collections of at least ten articles, all centered on a particular subject. With their unique mix of varied contributions from Original Research to Review Articles, Frontiers Research Topics unify the most influential researchers, the latest key findings and historical advances in a hot research area.

Find out more on how to host your own Frontiers Research Topic or contribute to one as an author by contacting the Frontiers editorial office: frontiersin.org/about/contact

Precision medicine in pediatrics

Topic editors

Jian Gao — Shanghai Children's Medical Center, China
Xiaoling Wang — Capital Medical University, China
Yang Zhou — Brown University, United States
Samuel Seward — Department of Medicine, Icahn School of Medicine at Mount Sinai, United States

Citation

Gao, J., Wang, X., Zhou, Y., Seward, S., eds. (2023). *Precision medicine in pediatrics*. Lausanne: Frontiers Media SA. doi: 10.3389/978-2-8325-2663-7

Table of contents

06 Effects of Fuyou Formula on GnRH Secretion and Related Gene Expression in Treating Precocious Puberty
Yi Zhang, Ning Sun, Meng Zhang, Qian Ding, Qian Wang, Yuguang Liang, Huan He, Yuxin Yang and Chunyan Guo

16 Related Markers for the Precision Diagnosis of Complex Appendicitis in Children
Jialin Zhou, Wenjing Xu, Jitao Wang and Zhe Fan

23 Evaluation of the Clinical Effectiveness of Oseltamivir for Influenza Treatment in Children
Jianru Qin, Jilei Lin, Xiangfei Zhang, Shuhua Yuan, Chiyu Zhang and Yong Yin

32 Metabolomic Differential Compounds Reflecting the Clinical Efficacy of Polyethylene Glycol Recombinant Human Growth Hormone in the Treatment of Childhood Growth Hormone Deficiency
Ji Li, Weiwei Pan, Jianqin Qian, Yan Ni, Junfen Fu and Shaoqing Ni

43 Stevens-Johnson Syndrome Following Vancomycin and Linezolid: A Real-World Analysis of Post-Marketing Surveillance Data
Ming Ni, Xue-Dong Yin, Wen-Juan Hu, Na Zeng, Bin Zhao and Zhi-Ling Li

49 Antifungal Drugs and Drug-Induced Liver Injury: A Real-World Study Leveraging the FDA Adverse Event Reporting System Database
Zhi-Xuan Zhou, Xue-Dong Yin, Yu Zhang, Qi-Hui Shao, Xin-Yu Mao, Wen-Juan Hu, Yun-Lin Shen, Bin Zhao and Zhi-Ling Li

57 Stevens-Johnson Syndrome Following Non-steroidal Anti-inflammatory Drugs: A Real-World Analysis of Post-marketing Surveillance Data
Qi-hui Shao, Xue-dong Yin, Na Zeng, Zhi-xuan Zhou, Xin-yu Mao, Yan Zhu, Bin Zhao and Zhi-ling Li

64 Spina Bifida Occulta Is a Risk Factor for Spinal Cord Injury Without Fracture or Dislocation for Children Performing a Backbend During Dance
Guoqing Liu, Wei Jiang, Xiang Tang, Shali Tan, Mingqiang Zhang, Liang Tao, Nong Xiao and Yuxia Chen

71 The Correlation Between Busulfan Exposure and Clinical Outcomes in Chinese Pediatric Patients: A Population Pharmacokinetic Study
Xiaohuan Du, Chenrong Huang, Ling Xue, Zheng Jiao, Min Zhu, Jie Li, Jun Lu, Peifang Xiao, Xuemei Zhou, Chenmei Mao, Zengyan Zhu, Ji Dong, Xiaoxue Liu, Zhiyao Chen, Shichao Zhang, Yiduo Ding, Shaoyan Hu and Liyan Miao

83 A Multi-Centre Prospective Study of the Efficacy and Safety of Alglucosidase Alfa in Chinese Patients With Infantile-Onset Pompe Disease
Diqi Zhu, Jiacong Zhu, Wenjuan Qiu, Benzhen Wang, Lin Liu, Xiaodan Yu, Zhenheng Ou, Guangsong Shan, Jian Wang, Bin Li, Xiaokang Chen, Cong Liu, Zipu Li and Lijun Fu

91 Signal Detection of Pediatric Drug–Induced Coagulopathy Using Routine Electronic Health Records
Xiaolu Nie, Yuncui Yu, Lulu Jia, Houyu Zhao, Zhenping Chen, Liqiang Zhang, Xiaoling Cheng, Yaqi Lyu, Wang Cao, Xiaoling Wang and Xiaoxia Peng

101 Population Pharmacokinetics of Cyclosporine in Chinese Pediatric Patients With Acquired Aplastic Anemia
Xuan Gao, Zhu-Li Bian, Xiao-Hong Qiao, Xiao-Wen Qian, Jun Li, Guo-Mei Shen, Hui Miao, Yi Yu, Jian-Hua Meng, Xiao-Hua Zhu, Jun-Ye Jiang, Jun Le, Ling Yu, Hong-Sheng Wang and Xiao-Wen Zhai

110 Short-term efficacy and safety of a lower dose of polyethylene glycol recombinant human growth hormone in children with growth hormone deficiency: A randomized, dose-comparison study
Zhouhong Jiang, Xuefeng Chen, Guanping Dong, Yin Lou, Jianping Zhang, Xinran Cheng, Jiayan Pan, Wei Liao, Jinzhun Wu, Xiaodong Huang, Xianjiang Jin, Deyun Liu, Ting Zeng, Shunye Zhu, Qin Dong, Xiaoming Luo, Dan Lan, Lizhi Cao, Xingxing Zhang, Jing Liu, Mingjuan Dai, Manyan Zhang, Li Liu, Junhua Dong, Dongmei Zhao, Shaoqing Ni and Junfen Fu

119 A randomized, double-blinded, placebo-controlled, single dose analgesic study of preoperative intravenous ibuprofen for tonsillectomy in children
Xiaohuan Cui, Jianmin Zhang, Zhengzheng Gao, Lan Sun and Fuzhou Zhang

126 Prophylactic administration of tranexamic acid combined with thromboelastography-guided hemostatic algorithm reduces allogeneic transfusion requirements during pediatric resective epilepsy surgery: A randomized controlled trial
Ting Zhang, Hua Feng, Wei Xiao, Jingsheng Li, Qinghai Liu, Xuexin Feng, Dezhou Qi, Xiaotong Fan, Yongzhi Shan, Tao Yu, Guoguang Zhao and Tianlong Wang

138 Effect of ranibizumab on retinopathy of prematurity: A meta-analysis
Zhibin Wang, Zhaobo Zhang, Yue Wang and Yu Di

147 Comparison of LC-MS/MS and EMIT methods for the precise determination of blood sirolimus in children with vascular anomalies
Yue-Tao Zhao, Hao-Ran Dai, Yue Li, Yuan-Yuan Zhang, Hong-Li Guo, Xuan-Sheng Ding, Ya-Hui Hu and Feng Chen

162 Plasma lacosamide monitoring in children with epilepsy: Focus on reference therapeutic range and influencing factors
Yue Li, Hong-Li Guo, Yuan-Yuan Zhang, Na Dong, Ya-Hui Hu, Jing chen, Xiao-Peng Lu and Feng Chen

173 Optimal dose of cefotaxime in neonates with early-onset sepsis: A developmental pharmacokinetic model-based evaluation
Zhen-Hai Shang, Yue-E Wu, Dong-Mei Lv, Wei Zhang, Wen-Qiang Liu, John van den Anker, Yan Xu and Wei Zhao

183 The medication for pneumocystis pneumonia with glucose-6-phosphate dehydrogenase deficiency patients
Ziyu Zhang, Qinhui Li, Xiaoyan Shen, Lankai Liao, Xia Wang, Min Song, Xi Zheng, Yulian Zhu and Yong Yang

196 Detection of pediatric drug-induced kidney injury signals using a hospital electronic medical record database
Yuncui Yu, Xiaolu Nie, Yiming Zhao, Wang Cao, Yuefeng Xie, Xiaoxia Peng and Xiaoling Wang

206 Drug-induced kidney injury in Chinese critically ill pediatric patients
Biwen Hu, Ling Ye, Tong Li, Zeying Feng, Longjian Huang, Chengjun Guo, Li He, Wei Tan, Guoping Yang, Zhiling Li and Chengxian Guo

214 Optimizing thiopurine therapy in children with acute lymphoblastic leukemia: A promising “MINT” sequencing strategy and therapeutic “DNA-TG” monitoring
Hong-Li Guo, Yue-Tao Zhao, Wei-Jun Wang, Na Dong, Ya-Hui Hu, Yuan-Yuan Zhang, Feng Chen, Li Zhou and Tao Li

232 Improving the efficacy for meropenem therapy requires a high probability of target attainment in critically ill infants and children
Zeming Wang, Jing Bi, Dianping You, Yu Tang, Gang Liu, Jinqian Yu, Zhipeng Jin, Tingting Jiang, Xue Tian, Hui Qi, Lei Dong, Lili Dong, Qunqun Zhang, Wei Zhao and Adong Shen

239 Associations between *CES1* variants and dosing and adverse effects in children taking methylphenidate
Jacob T. Brown, Nancy Beery, Allise Taran, Tyler Stevens, Christine Henzler, Jonathan Badalamenti, Ron Regal and Catherine A. McCarty

frontiers in Pharmacology

ORIGINAL RESEARCH
published: 11 March 2022
doi: 10.3389/fphar.2022.852550

Effects of Fuyou Formula on GnRH Secretion and Related Gene Expression in Treating Precocious Puberty

*Yi Zhang[1], Ning Sun[1], Meng Zhang[1,2], Qian Ding[1,2], Qian Wang[1], Yuguang Liang[1], Huan He[1], Yuxin Yang[1] and Chunyan Guo[1,2]**

[1]Clinical Research Center, Beijing Children's Hospital, Capital Medical University, National Center for Children's Health, Beijing, China, [2]Department of Pharmacy, Beijing Children's Hospital, Capital Medical University, National Center for Children's Health, Beijing, China

The Fuyou (Fy) formula is an in-hospital preparation consisting of traditional Chinese medicine (TCM) that has been used for treating precocious puberty (PP) for more than 20 years. In this study, we aimed to clarify the effect of the Fy formula and its major components on PP. To confirm the effect of the Fy formula on the release of hypothalamic gonadotropin-releasing hormone (GnRH), GT1-7 cells were treated with estrogen to build the model group and subsequently treated with the Fy formula and its major components to explore their effects on the secretion of GnRH. The level of GnRH in GT1-7 cells was determined using enzyme-linked immunosorbent assay. The results illustrated that, compared to the model group, the Fy formula inhibited the release of GnRH. In addition, the expression levels of proteins related to GnRH secretion, including GnRH, gonadotropin-releasing hormone receptor (GnRHR), Kiss-1 metastasis-suppressor (Kiss1), G-protein coupled receptor 54 (GPR54), estrogen receptor α (ERα), insulin-like growth factor-1 (IGF-1), and insulin-like growth factor-1 receptor (IGF-1R), were detected by real-time polymerase chain reaction (RT-qPCR). The results demonstrated that the Fy formula significantly reduced the level of GnRH secretion in the GT1-7 cell lines compared with the model group. Moreover, it significantly downregulated the expression of GnRH, GnRHR, Kiss1, GPR54, ERα, IGF-1, and IGF-1R. In summary, our results indicate that the Fy formula and its major components may inhibit the effects of estrogen, which alleviates PP through transcriptional regulation of target genes.

Keywords: precocious puberty, fuyou formula, GnRH, gene expression, KISS1, ER

OPEN ACCESS

Edited by:
Jian Gao,
Shanghai Children's Medical Center, China

Reviewed by:
Hui Zhao,
Capital Medical University, China
Mao Chenmei,
Children's Hospital of Soochow University, China

***Correspondence:**
Chunyan Guo
guochunyan205@163.com

Specialty section:
This article was submitted to Obstetric and Pediatric Pharmacology, a section of the journal Frontiers in Pharmacology

Received: *11 January 2022*
Accepted: *03 February 2022*
Published: *11 March 2022*

Citation:
Zhang Y, Sun N, Zhang M, Ding Q, Wang Q, Liang Y, He H, Yang Y and Guo C (2022) Effects of Fuyou Formula on GnRH Secretion and Related Gene Expression in Treating Precocious Puberty. Front. Pharmacol. 13:852550. doi: 10.3389/fphar.2022.852550

INTRODUCTION

Precocious puberty (PP) is an endocrine disorder that is defined as puberty starting before the age of 9 in boys and eight in girls. Observational data from Europe show that breast development begins before the age of 8 years in 5% of girls. In China, the incidence of PP is approximately 1/50,000–10,000 population, and the male-to-female ratio is approximately 1:5–10 (Dong et al., 2019). The causes of pathological PP are normally categorized into central precocious puberty (CPP) and peripheral precocious puberty (PPP). Idiopathic CPP is the most common form of CPP, originating from the early activation of the hypothalamic-pituitary-gonadal (HPG) axis with

pulsatile secretion of hypothalamic gonadotropin-releasing hormone (GnRH). Approximately 74% of girls with CPP have the idiopathic form (Bradley et al., 2020). CPP may also occur secondary to tumors involving the hypothalamus and congenital defects in neuronal migration, resulting in a heterotopic mass of GnRH-secreting neurons acting as an ectopic GnRH pulse generator. In the remaining situations, disruption of a normal inhibitory restraint on the onset of puberty is caused by an extensive variety of insults to the central nervous system (CNS) (Eugster and Pescovitz, 2001). These include hypothalamic tumors, cerebral malformations involving the hypothalamus, and congenital brain disorders, infections, or acquired injuries. PPP is often related to increased sex steroid levels independent of GnRH. It can be caused by virilizing tumors, including adrenal tumors, gonadal tumors, or human chorionic gonadotropin (hCG)-secreting germ cell tumors. Neoclassic tissues can then lead to an increase in androgen or estrogen production (Latronico et al., 2016). Familial male precocious puberty (FMPP) is caused by an activating mutation in the luteinizing hormone (LH) receptor gene. The activating mutation leads to the continuous activation of adenylate cyclase, resulting in gonadal autonomic hyperfunction. Congenital adrenal hyperplasia may lead to the excessive production of adrenal androgens. McCune-Albright syndrome and recurrent autonomous ovarian cysts caused by somatic activating mutations in the *GNAS* gene lead to an increase in the signal transduction of the GnRH signaling pathway. Children with PPP can easily develop CPP due to their early bone age and long-term hyperestrogenemia (Carel and Léger, 2008).

Puberty onset is thought to integrate diverse genetic and environmental signals (Leka-Emiri et al., 2017). The hypothalamic secretion of GnRH has been established as a pivotal pathway for initiating puberty onset. The synthesis and secretion of GnRH neurons in the hypothalamus are essential for the regulation of hormonal cascade effects, including pituitary gonadotropin release, ovarian maturation, and estrogen production. All of these hormonal events are necessary for normal sexual maturation and reproductive function. The release of GnRH activates the synthesis and secretion of LH and follicle-stimulating hormone (FSH) from the anterior pituitary, thus leading to the stimulation of gonadal function (Carel et al., 2004). Briefly, LH initiates the growth and ovulation of the corpus luteum in girls and release of androgen in boys. FSH mediates the formation and maturation of ovarian follicles in girls and spermatogenesis in boys, inducing secondary sexual characteristics (Kanasaki et al., 2017). Reproductive control of the HPG axis also facilitates negative gonadal feedback. GnRH is not the only hormone involved in puberty onset but is the most important factor identified to date. Therefore, the regulation of GnRH secretion and expression is critical for the pathogenesis of PP.

The pharmacological therapy for PP includes GnRH analogs (GnRHas), GnRH antagonists, and traditional Chinese medicine (TCM) Fy formula. GnRHas are the gold-standard management for CPP, as they provide continuous stimulation of pituitary gonadotrophs, resulting in the downregulation of the HPG axis and thus leading to decreased secretion of LH and FSH (Eugster and Pescovitz, 2001). Numerous studies have demonstrated that the use of GnRHas results in the stabilization of pubertal symptoms. Local side effects include pain at the injection site, sterile abscesses, and implant site reactions (Aguirre and Eugster, 2018). Other side effects include headache, hot flashes, decreased bone density, and vaginal bleeding (Fuqua, 2013). Several GnRHas have been synthesized and are currently under investigation in clinical trials. They exhibit high-affinity binding to the human GnRH receptor (GnRHR), leading to a rapid decrease in gonadal sex steroids to castrate levels; however, the detailed mechanism for this is still under investigation (M. Chen and Eugster, 2015).

TCM treating PP includes Zhibai Dihuang wan, Dabuyin wan and Fy formula. Zhibai Dihuang wan and Dabuyin wan were applied to yin deficiency, fire hyperactivity syndrome, phlegm dampness stagnation syndrome, liver depression and fire transformation syndrome. However, the recommendation level for the use of these two medicines are low, and there is no indication in the drug instruction. At present, there is no Chinese patent medicine with definite curative effect for treating PP are commercially available. The Fy formula is an in-hospital preparation used at Beijing Children's Hospital, and it is composed of TCM and was developed by pediatric gynecologists according to the pathogenesis, etiology, and physical characteristics of children with PP. It was approved by the National Medical Products Administration (NMPA) as a compound preparation for TCM in hospitals in 2001. In the study of Fy formula treatment of 60 female with PP, it has been showed that the total effective rate is 83.3%. The changes of 60 cases before and after treatment were breast nucleus index, blood E_2 level, number of positive cases of vaginal cell smear, bone age, uterine and follicular volume. The treatment can improve the symptoms of liver depression, yin deficiency and fire hyperactivity, reduce the level of estrogen and delay the speed of bone age maturation (Liu et al., 2009). It has also been reported that the Fy formula is able to regulate early pubertal symptoms, reducing the size of the mammary nucleus and effectively controlling estrogen levels and bone age. It has also been shown that the Fy formula exerts an inhibitory effect on female ovarian cysts complicated by PP, leading to a reduction in E_2 levels and postponing the rate of bone maturation with no evident adverse effects (Pan et al., 2019).

It has been showed that the Fy formula induces downregulation of the mRNA expression of kiss1, GPR54, and GnRH in female rats (Bai et al., 2020). A previous integrated pharmacological study on the mechanism of Fy formula in treating PP demonstrated that it can effectively reduce the levels of FSH, LH, and E_2 in Sprague-Dawley rats (Guo et al., 2021b). Also, the TCM-chemical component-target-pathway study based on integrated pharmacology illustrated that ERα, ERβ, IGF, and IGF1 are associated with PP, so these can be potential therapeutic targets for PP (Guo et al., 2021a). Therefore, in this study, we aimed to explore the effects of the Fy formula on the secretion of GnRH and expression of related genes in the treatment of PP.

MATERIALS AND METHODS

Materials and Reagents

Dulbecco's modified Eagle medium (DMEM) was purchased from Corning (NY, United States). Fetal bovine serum (FBS) was obtained from Gibco (Grand Island, NY). Dimethyl sulfoxide (DMSO) was purchased from Sigma-Aldrich (St. Louis, MO, United States). Penicillin-streptomycin and 0.25% trypsin-EDTA were purchased from MacGene (Beijing, China). *Mycoplasma* Prevention Reagent (MycAway™) was obtained from Yeasen Biotech (Hong Kong, China). Phosphate-buffered saline (PBS) was purchased from Solarbio (Beijing, China).

The TCM standards estradiol (E_2, serial number: 100,182-21,906, purity: 96.3%), quercetin (serial number: 100081-201610, purity: 99.90%), and luteolin (serial number: 111520-202006, purity: 94.40%) were purchased from the National Institutes for Food and Drug Control (Beijing, China). Apigenin (serial number: B20981-20 mg, purity: 98.00%) was purchased from Shanghai Yuanye Biotechnology Co., Ltd. (Shanghai, China). The reagents were dissolved in DMSO (Sigma-Aldrich) and stored at 4°C.

Fy Formula Preparation

The Fy formula is an in-hospital preparation obtained by mixing the following 12 herbs: *Prunella vulgarism* L (Xiakucao), *Carapax Trionycis* (Cubiejia), *Gentiana scabra* Bunge (Longdan), *Chrysanthemum morifolium* (Ramat.) Hemsl (Juhua), *Lycium chinense* Mill (Digupi), *Alisma plantago-aquatica* L (Zexie), *Scrophularia ningpoensis* Hemsl (Xuanshen), *Paeonia suffruticosa Andrews* (Mudanpi), *Rehmannia glutinosa* (Gaertn.) DC (Shengdihunag), *Hordeum vulgare* L (Maiya), *Concha oetreae* (Muli), and *Thallus laminariae* (Kunbu) at the ratio of 1.5:1:0.6:0.6:1:1:1.5:0.6:1.2:2:3:1. All herbs were purchased from the Beijing Bencao Fangyuan Pharmaceutical Group Co. Ltd., and the Fy formula was prepared by the Preparation Center of Beijing Children's Hospital (approval number: Z20053679; lot number: 20201202).

Cell Cultures

The GT1-7 cell line (mouse GnRH neuronal cell line) was kindly provided by Prof. P. Mellon (University of California, San Diego, CA, United States). GT1-7 cells were grown in a monolayer culture in DMEM (Corning) supplemented with 10% FBS (Gibco), 1% penicillin-streptomycin (Macgene), and 0.5% *Mycoplasma* Prevention Reagent (Yeasen Biotech). The cultures were incubated at 37°C in an atmosphere of 5% CO_2 in a 25 mm flask (Corning) for 2 days after seeding, with a medium change at 24 h. The cells were then washed twice with PBS and digested with 0.25% trypsin-EDTA (MacGene). When more than half of the cells were observed to become round under a microscope, serum-containing medium was added to terminate the digestion. After obtaining a single-cell suspension, the cells were cultured in an incubator and inoculated three times for subsequent experiments. The cells were treated with different treatments in serum-free medium (SFM) for 24 h depending on the experiment.

TABLE 1 | Primer sequences used in quantitative real-time polymerase chain reaction.

Gene	Forward primer (5′—3′)	Reverse primer (3′—5′)
β-actin	ACTCTTCCAGCCTTCCTTC	ATCTCCTTCTGCATCCTGTC
GnRH	GGGAAGACATCAGTGTCCCAG	CTCGAGCTTCCGTTGGTAGG
GnRHR	TGCAGGACCACAGAACTACAG	GTCCAGCAGACGACAAAGGA
Kiss1	GATGTCTGCAGCCTGAGTCCC	AGGCATTAACGAGTTCCTGGG
GPR54	CTGTCAGCCTCAGCATCTGG	AGCAGCGGCAGCAGATATAG
ERα	AAGACGCTCTTGAACCAGCA	CGAGTTACAGACTGGCTCCC
IGF-1	AAGGCAGTTTACCCAGGCTC	GGCCGAGGTGAACACAAAAC
IGF-1R	TACCAGCATTAACTCCGCTG	GCTCGCCTCTCTCGAGTTC

GnRH, *gonadotropin-releasing hormone;* GnRHR, *gonadotropin-releasing hormone receptor;* Kiss1, *Kiss-1 metastasis-suppressor;* GPR54, *G-protein coupled receptor 54;* ERα, *estrogen receptor α;* IGF-1, *insulin-like growth factor-1;* IGF-1R, *insulin-like growth factor-1 receptor.*

CCK-8 Assay

Cell counting kit-8 (CCK-8) was purchased from Solarbio (Beijing, China). To assay the toxicity of the Fy formula, quercetin, luteolin, apigenin, and GT1-7 cells were seeded in 96-well plates at a density of 2.0×10^5 cells/well. After 24 h of incubation, the cells were pretreated with 100 pmol/L E_2 in SFM overnight. The cells were then incubated with 75, 150, 225, 300, 450, and 525 μg/ml of Fy formula or 5, 10, 15, 20, 30, and 40 μmol/ml of quercetin, luteolin, and apigenin separately in SFM for 24 h. Subsequently, the cells were treated with 10 μL of CCK-8 solution (Gibco) for 1 h at 37°C and 5% CO_2. The optical density (OD) was determined by measuring the absorbance at 450 nm using a microplate reader (BioTek Synergy, United States).

ELISA

To determine the concentration of GnRH, GT1-7 cells were seeded in 24-well plates. The cells were treated with E_2, Fy, quercetin, luteolin, and apigenin, as previously described. After treatment, the supernatants were collected. Relative GnRH concentrations in the supernatant were determined using the mouse GnRH ELISA kit from mlbio (Shanghai, China) with serial dilutions of 80, 40, 20, 10, 5, and 0 mIU/mL as a standard curve.

RNA Extraction and Quantitative Real-Time Polymerase Chain Reaction

The cells were seeded in 6-well plates and treated with E_2, Fy, and TCM, as described previously. At the end of the treatment, total RNA was extracted from GT1-7 cells using an RNA Easy Fast Tissue/Cell Kit (TIANGEN BIOTECH Co., Ltd, Beijing, China) according to the manufacturer's protocol. The RNA samples were quantified using a microplate reader (BioTek Synergy, United States) at 260/280 nm. First-strand cDNA was prepared using 2 μg RNA reverse-transcribed with a FastKing RT Kit (TIANGEN BIOTECH Co., Ltd, Beijing, China). The synthesized first-strand cDNA was stored at −80°C until use. mRNA expression was analyzed using a 7500 Fast Real-Time PCR system (Applied Biosystems, United States) with the following thermocycling conditions: 50°C for 2 min, 95°C for 10 min, and 40 cycles of 95°C for 15 s

TABLE 2 | Composition of the Fy formula.

Chinese name	Scientific name	Family	Lot no	Place of origin	Parts of plant used
Xia Ku Cao	*Prunella vulgaris* L	*Lamiaeae*	20201010	Jiangsu, China	Driod orial parts
Cu Bie Jia	*Carapax Trionycis*	*Trionyxsinensis Wiegmann*	20201018	Hubei, China	Carapace
Long Dan	*Gentiana scabra* Bunge	*Gentianaceae*	20200927	Yunnan, China	Dried roots and rhizomes
Ju Hua	*Chrysanthemum morifolium* (Ramat.) Hemsl	*Compositae*	20201027	Anhui, China	Capitulum
Di Gu Pi	*Lycium chinense* Mill	*Solanaceae*	20201105	Hebei, China	Dried root bark
Ze Xie	*Alisma plantago-aquatica* L	*Alismataceae*	20201126	Fujian, China	Dried tuber
Xuan Shen	*Scroophularia ningpoensis* Hemsl	*Scrophulariaceae*	20201019	Zhejiang, China	Dried root tuber
Mu Dan Pi	*Paeonia suffruticosa Andrews*	*Paeoniaceae*	20201123	Anhui, China	Dried root bark
Sheng Di Huang	*Rehmannia glutinosa* (Gaertn.) DC	*Plantaginaceae*	20201104	Henan, China	Dried root tuber
Mai Ya	*Hordeum vulgare* L	*Triticum*	20201030	Hebei, China	Dried ripe fruit
Mu Li	*Concha oetreae*	*Ostrea*	20200917	Guangdong, China	Shell
Kun Bu	*Thalluslaminariae*	*Laminaria*	20200922	Fujian, China	Dried lobes

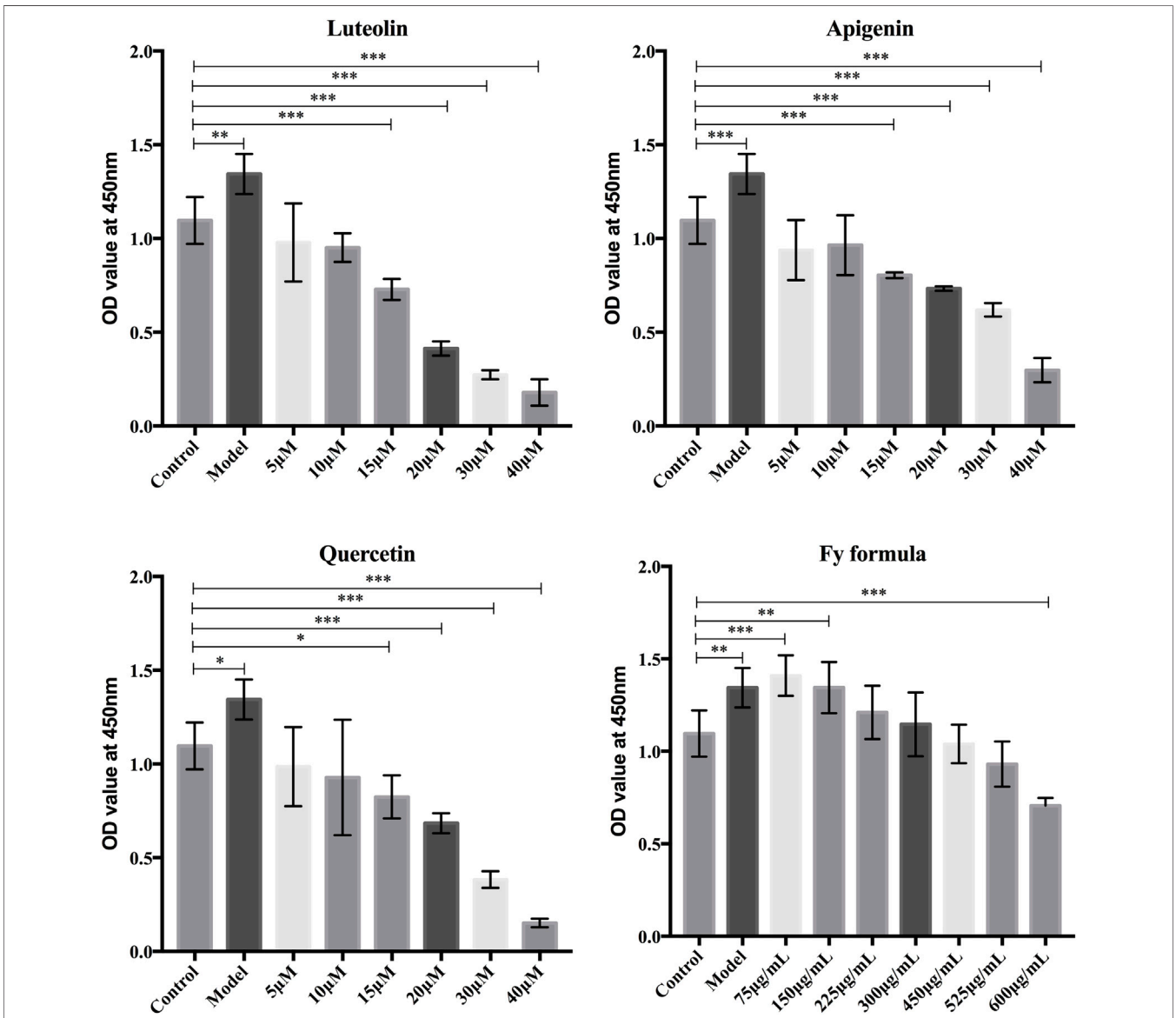

FIGURE 1 | Effects of luteolin, apigenin, quercetin, and the Fy formula, at different concentrations, on GT1-7 cells. The CCK-8 assay was conducted to determine cell proliferation in the GT1-7 cells after treatment with luteolin, apigenin, quercetin, and the Fy formula at different concentrations.

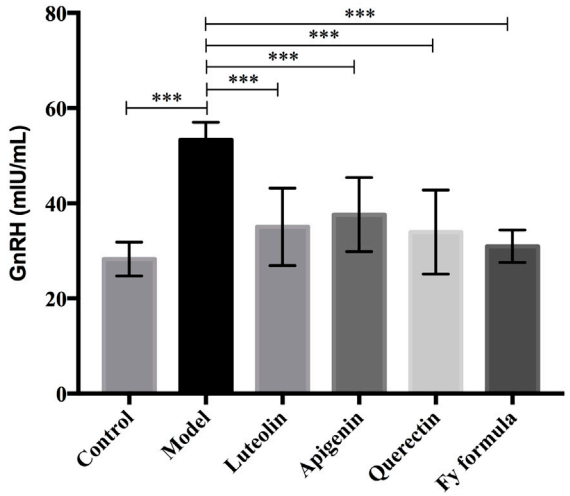

FIGURE 2 | Effects of luteolin, apigenin, quercetin, and the Fy formula on GnRH secretion. Cells pretreated with E_2 stimulate the secretion of GnRH, and the level of GnRH secretion decreases when coincubated with luteolin, apigenin, quercetin, and the Fy formula. ***$p < 0.0001$ compared to the model group.

and 60°C for 60 s. Single-stranded oligonucleotide primer sets were designed (Tianyi Huiyuan, Beijing, China) to target *β-actin, Erα, Kiss1, GPR45, GnRH, GnRHR, IGF1, and IGF1R*. The primer sequences used for qRT-PCR are listed in **Table 1**. Data were analyzed using the $2^{\Delta\Delta Ct}$ method, and mRNA expression was normalized to that of *β-actin*.

Statistical Analysis

All experiments were performed in triplicate independently and data were expressed as mean ± SD. Significant differences were analyzed by one-way analysis of variance (ANOVA), and the data were plotted using Prism7 software (GraphPad software, Inc., San Diego, United States). Statistical significance was determined using $p < 0.05$.

RESULTS

Composition Analysis of the Fy Formula

The TCM components of the Fy formula are listed in **Table 2**. *Prunella vulgaris* L. and *Carapax trionycis* exert effects on the liver that can nourish yin, moderate heat, and relieve congestion. *Gentiana scabra* Bunge, *Chrysanthemum morifolium* (Ramat.) Hemsl, *Lycium chinense* Mill, *Alisma plantago-aquatica* L., *Scroophularia ningpoensis* Hemsl, *Paeonia suffruticosa Andrews*, and *Rehmannia glutinosa* (Gaertn.) DCs can nourish yin, eliminate dampness, and cool blood. *Hordeum vulgare* L, *Concha oetreae* and *Thallus laminariae* act on the liver to relieve congestion and are used as adjuvants. As previously reported, five compounds were recognized with the HPLC-MS/MS method from Fy formula including Luteolin, Quercetin, Apigenin, Kaempferol and Emodin. Also, the concentration of these five target components in Fy Formula were determined using preliminary LC-MS/MS method, the concentration of Luteolin, Quercetin and Apigenin are much higher than Kaempferol and Emodin in Fy formula. Therefore, the compounds with higher concentration were selected in the experiment. (Guo et al., 2021a). We aimed to determine the effects of the Fy formula and its major components, including luteolin, quercetin, and apigenin, on GnRH secretion and related gene expression in PP treatment.

Effects of Luteolin, Apigenin, Quercetin, and the Fy Formula on the Proliferation of GT1-7 Cells

The nontoxic concentrations of Fy and its major chemical components in GT1-7 cells were evaluated based on cell viability. The CCK-8 assay was performed to examine the proliferation of GT1-7 cells following treatment with different concentrations of luteolin, apigenin, quercetin, and Fy. As demonstrated in **Figure 1**, the GT1-7 cells treated with high concentrations of the Fy formula and its major components showed reduced cell proliferation activity compared to the control group cells. The cell proliferation activity of the GT1-7 cells was not significantly different at concentrations of 5 and 10 μM for luteolin, apigenin, and quercetin and concentrations of 450 μg/ml and 525 μg/ml for the Fy formula compared to the control group. To ensure that the Fy formula was administered at a concentration sufficient to exert the desired effect, the final concentrations of 10 μM and 525 μg/ml were selected for use in subsequent experiments.

The Fy Formula, Luteolin, Apigenin, and Quercetin Inhibit GnRH Secretion in GT1-7 Cells

After pretreatment of the GT1-7 cells with E_2, ELISA was performed to determine the level of GnRH in the GT1-7 cells. The GnRH concentration in the culture medium is shown in **Figure 2**. Comparing the model and control groups, the E_2 treatment resulted in an increase in GnRH secretion. Moreover, treatment with the Fy formula, luteolin, apigenin, and quercetin led to a significant reduction in the concentration of GnRH in the culture medium and thus inhibited the increased level of GnRH secretion caused by E_2 in GT1-7 cells.

The Fy Formula, Luteolin, Apigenin, and Quercetin Inhibit *GnRH, GnRHR, Kiss1, GPR54, ERα, IGF-1,* and *IGF-1R* Expression in GT1-7 Cells

To further analyze whether the potential molecular mechanism of the Fy formula on GnRH secretion in GT1-7 cells is via the GnRH receptor, E_2 receptor, Kiss1/GPR54 signaling pathway, or IGF-1, the mRNA expression levels of these genes were quantified by RT-qPCR (**Figure 3**). GT1-7 cells treated with E_2 showed significantly upregulated gene expression of *GnRH, GnRHR*, *Kiss1*, *GPR54*, *ERα*, *IGF-1,* and *IGF-1R*. In contrast, GT1-7 cells treated with the Fy formula, luteolin, apigenin, and quercetin showed downregulated

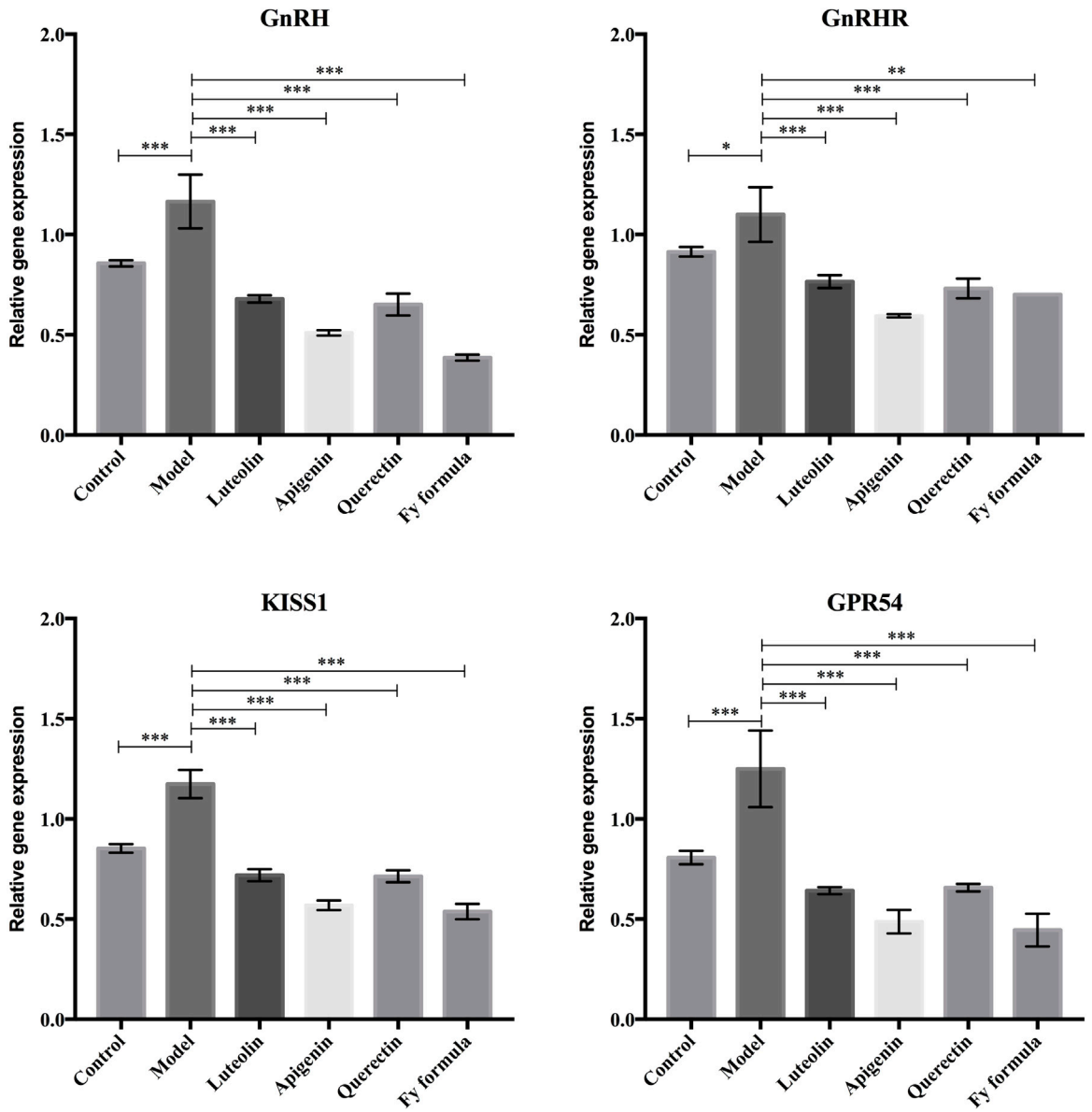

FIGURE 3 | Effects of luteolin, apigenin, quercetin, and the Fy formula on the expression of *GnRH, GnRHRc, Kiss1, GPR54, ERα IGF-1*, and *IGF-1R*, which are involved in GnRH secretion. $^{*}p < 0.05$, $^{**}p < 0.001$, and $^{***}p < 0.0001$ compared to the model group.

expression of all genes involved in GnRH secretion. These results indicate that the effect of the Fy formula is mediated by inhibiting the expression of *GnRH* itself, as well as *GnRHR, Kiss1, GPR54, ERα, IGF-1,* and *IGF-1R*, which are related to GnRH secretion.

DISCUSSION

In our previous study, five major chemical components of the Fy formula were identified using HPLC-MS/MS: luteolin, quercetin, apigenin, kaempferol, and emodin (Guo et al., 2021b). Three compounds with higher concentration were selected in the experiment including Luteolin, Quercetin and Apigenin. The association of ERα, ERβ, IGF, and IGF1 with PP are identified by "TCM-chemical component-target-pathway" study based on integrated pharmacology, which indicated that these proteins can be the potential targets for treating PP (Guo et al., 2021b). Moreover, it has been reported that the treatment with Fy formula can result in a significantly reduction in the level of E2, LH and FSH in Sprague-Dawley rats (Guo et al., 2021b). Furthermore, it has been illustrated that the Fy formula is able to downregulate the expression of Kiss1, GPR54, and GnRH in female rats (Bai et al., 2020).

As an in-hospital preparation at Beijing Children's Hospital, the Fy formula has been used for the treatment of PP for more than 20 years. Clinical data illustrated that the Fy formula

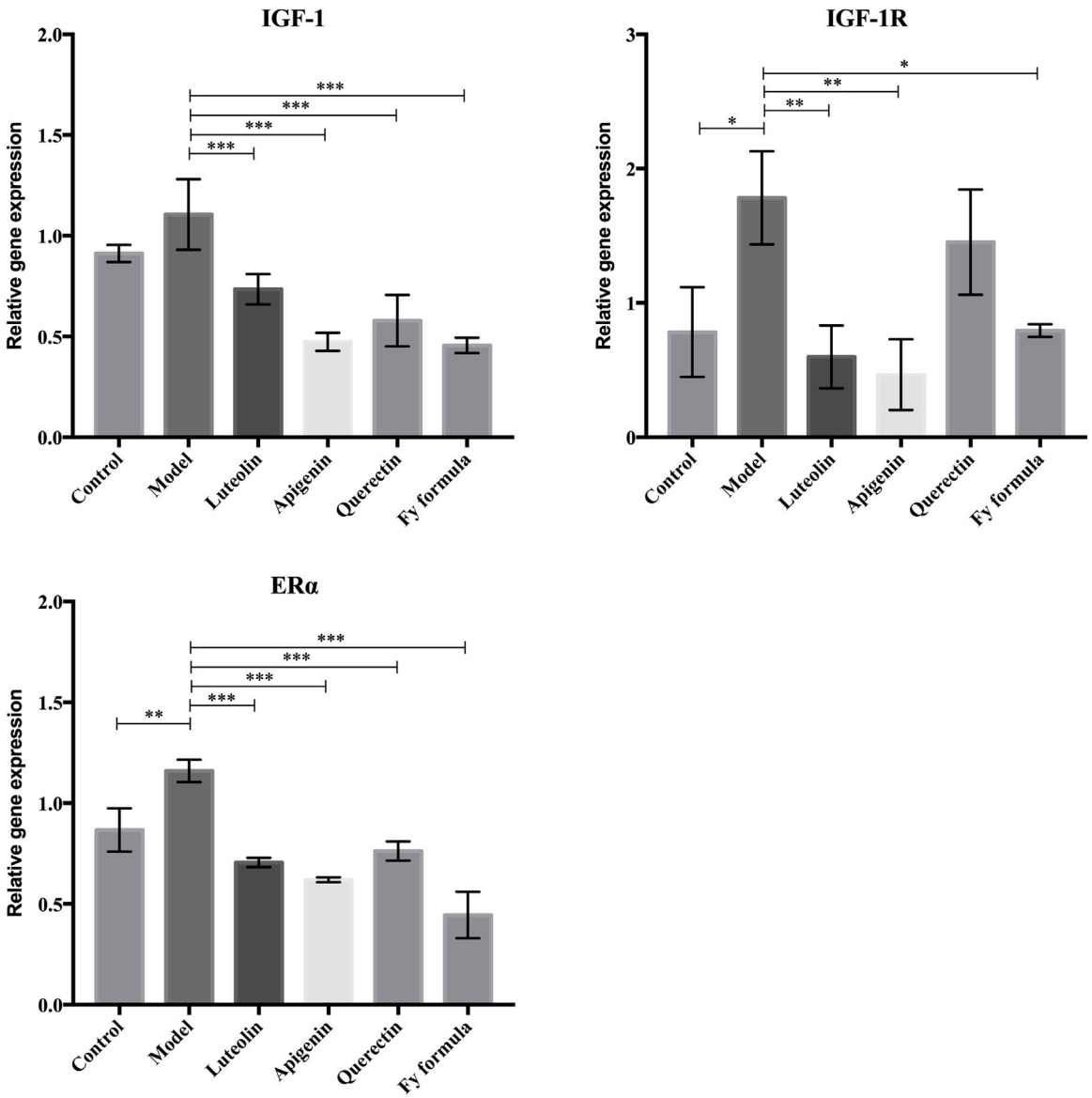

FIGURE 3 | (Continued).

significantly reduced the level of estrogen in the blood serum of patients. It can also delay bone maturation and decrease the mammary gland size in women with PP. Furthermore, TCM research has revealed that the herbs used in the preparation of the Fy formula have intervention effects on ovarian cysts in girls complicated with PP. Taken together, these findings indicate the clinical benefits of the Fy formula, which is an advantageous therapeutic approach owing to its low cost. However, the mechanism of action of the Fy formula in treating PP has not been fully clarified.

GT1-7 cells are a valuable GnRH-expressing cell model with a number of characteristics common to normal GnRH neurons. In addition, GT1-7 cells express a number of genes relevant to reproduction, circadian rhythm, and energy homeostasis, including *GnRH*, *Kiss1*, and *GPR54*. Estrogen has been proven to be the main regulator of GnRH neuronal function in the female brain, which possesses a bimodal effect on the hypothalamic–pituitary axis. In GT1-7 cells, estrogen exerts a stimulatory effect at low concentrations (Qian et al., 2020) and an inhibitory effect at high concentration on the secretion of GnRH and gonadotropin (Roy et al., 1999). It has been suggested that the binding sites for E_2 in the plasma membrane of GT1-7 cells share structural homology with classical estrogen receptors (ERs) at their carboxy-terminal domain (Morales et al., 2007). To investigate the effects of the Fy formula on GnRH secretion and related gene expression in PP treatment, we incubated GT1-7 cells with E_2 (100 pmol/L) for 24 h, followed by the Fy formula, luteolin, apigenin, or quercetin for another 24 h. Our

results showed that E_2 treatment increased the release of GnRH from the GT1-7 cells and established a PP model in GT1-7 cells. However, the level of GnRH in the GT1-7 cells was decreased by treatment with the Fy formula, luteolin, apigenin, and quercetin compared to that in the model group. This suggests that the Fy formula can significantly reduce GnRH secretion.

To determine the role of potential targets associated with GnRH secretion in the effects of the Fy formula on PP, gene expression was analyzed. Our results showed that *GnRHR, Kiss1, GPR54, ERα*, *IGF-1,* and *IGF-1R* mRNA levels were higher in the model group than in the control group. We also found that, compared to the model group, the Fy formula significantly downregulated the expression of GnRH secretion-related genes, including *GnRHR, Kiss1, GPR54, ERα*, *IGF-1,* and *IGF-1R*, in GT1-7 cells. Taken together, these results indicate that the Fy formula and its major components, including luteolin, apigenin, and quercetin, are able to inhibit GnRH secretion in GT1-7 cells by inhibiting the expression of related genes, weakening the binding between signaling molecules and their receptors, and ultimately reducing the pulsed secretion of GnRH, thus reducing the activation of downstream pituitary and gonadal development and alleviating the symptoms of PP.

GnRH is a decapeptide that serves as a vital element in the regulation of the reproductive cycle and sexual maturation. GnRH drives the release of pituitary gonadotropic hormones, including LH, FSH, and gonadotropin, by interacting with pituitary gonadotropes through binding to its high-affinity receptor GnRHR on the cell surface (Tzoupis et al., 2020). GnRHR belongs to the G protein-coupled receptor family (GPCRs) that is characterized by seven transmembrane domains. It has been demonstrated that GnRHR gene expression is dependent on GnRH pulse in rat pituitary cultures, with increased mRNA expression levels being observed under high pulse frequency. In response to varying GnRH pulses, GnRHR appears to differentially activate multiple distinct signaling pathways implicated in the synthesis of both LH and FSH (Stamatiades and Kaiser, 2018). In our study, it was shown that the Fy formula and its major components could significantly suppress the expression of both GnRH and GnRHR, indicating that the Fy formula may delay pituitary gonadotropic hormone release and alleviate PP.

Recent research has demonstrated that signaling by kisspeptin through its receptor, G protein-coupled receptor GPR54 (also called Kiss1R), is the most potent stimulator of GnRH-induced gonadotropin release (Chan et al., 2009 and; Blaustein, 2010). Kisspeptin is encoded by the *KISS1* gene, which contacts GnRH neurons within the hypothalamus and induces GnRH release by binding to its receptor, GPR54 (Mayer and Boehm, 2011). Subsequently, GnRH reaches the pituitary gland through portal circulation and initiates the secretion of pituitary gonadotropins (Trevisan et al., 2018). Kisspeptin treatment in immature rodents and primates was able to induce activation of the gonadotropic axis and precocious pubertal development (Kanasaki et al., 2017). Serum kisspeptin-54 levels were higher in girls with CPP than in prepubescent controls, implying that kisspeptin secretion may stimulate the onset of puberty (C.-Y. Chen et al., 2013). It has also been reported that in GPR54-overexpressing GT1-7 cells, intracellular signaling, such as extracellular signal-regulated kinase (ERK) activation and protein kinase A (PKA) signaling pathways, were activated, resulting in increased GnRH receptor expression in response to kisspeptin (Kanasaki et al., 2017 and; Kang et al., 2009). Therefore, the development of kisspeptin antagonists may be a new approach for treating PP. In our results, we found that the Fy formula can target kisspeptin and its receptor GPR54 by suppressing their mRNA expression, thus inhibiting their activity.

IGF-1 is an important somatotropic hormone that mediates the regulation of the reproductive axis. In addition, it has emerged as a prime candidate for having a significant role in the onset of puberty. IGF-1 may promote the secretion of prepubertal GnRH, and the level of IGF-1 increases in the circulation as puberty approaches, which can advance the timing of puberty (Dees et al., 2021). Multiple findings suggested that IGF-1 may prime pituitary gonadotrophs and stimulate the synthesis of GnRHR and FSH during puberty onset in prepubertal salmon. Also, IGF-1 enhances pituitary gonadotropic hormone release, which accelerates puberty onset in rats (Luckenbach et al., 2010). More recent findings have depicted a later action of IGF-1 in regulating the synthesis and release of kisspeptin. It has been reported that IGF-1 activates kiss-1 in female rats, expressing kisspeptins that are involved in the secretion of pituitary gonadotropins at puberty, as previously described (Hiney et al., 2009). Furthermore, girls with CPP have remarkably higher levels of IGF-1 and insulin than healthy girls (Sørensen et al., 2012 and; Kanety et al., 1996). Our research on GT1-7 cell lines further corroborated that the Fy formula appears to downregulate the expression of IGF-1 and its receptor, inhibiting their activity in pubertal development and hence relieving PP.

With respect to the E_2, several studies have reported that it alters pulsatile GnRH secretion through the binding and activation of ERs (Thomas and Dong, 2006). The ER is a member of the nuclear receptor superfamily that participates in the transcriptional regulation of multiple genes. The classic ER signaling pathway is initiated by the binding of estrogen to its receptor. Two isoforms of ER have been described: ERα and ERβ. This leads to receptor dimerization and subsequent combination with the estrogen response element located on the promoter of target genes, which finally activates gene transcription (Radovick et al., 2012). ERα may contribute to the feedback regulation of kisspeptin expression during pubertal development (Clarkson, 2013), which is associated with the restraint of GnRH release prior to puberty onset, followed by enhanced initiation of GnRH secretion and thus prompt reproductive maturation throughout puberty (Mayer et al., 2010). In contrast, ERβ may directly participate in estrogen regulation by regulating neuronal activity, gene expression, and pulsatile secretion of GnRH (Wolfe and Wu, 2012 and; Fixemer et al., 2003). Our research suggests that the Fy formula can inhibit this effect, demonstrating that the gene expression levels of both ERα and kiss-1 are repressed by the TCM components of the Fy formula.

However, this study remains few limitations that need to be considered. First of all, the effects of Fy formula against PP have been identified *in vitro*, the effects of Fy formula in treating PP *in vivo* still need to be verified in the future by comparing the level of GnRH secretion and gene expression before and after the

treatment of Fy formula. Secondly, the mechanism of protein interactions in treating PP still need to be further clarified.

CONCLUSION

In conclusion, we have shown evidence of inhibitory effect of Fy formula in GnRH secretion in GT1-7 cell lines and have shown that Fy formula down regulates GnRH gene expression *in vitro*. The Fy formula also suppresses the expression level in all genes that involved in the GnRH secretion including GnRHR, Kiss1, GPR54, ERα, IGF-1, and IGF-1R, and hence delay the pituitary gonadotropic hormone release and alleviating the symptoms of PP.

DATA AVAILABILITY STATEMENT

The original contributions presented in the study are included in the article/Supplementary Material, further inquiries can be directed to the corresponding author.

AUTHOR CONTRIBUTIONS

CG designed and performed the experiments. YZ performed the experiments and wrote the manuscript. MZ designed the primers used. NS provided technical support. QD analyzed the data. YY and HH helped construct the illustrations. QW and YL revised the manuscript.

FUNDING

This study was supported by the Beijing Traditional Chinese Medicine Science and Technology Development Fund Project (grant no. QN-2020-26).

ACKNOWLEDGMENTS

We thank Prof. P. Mellon and Prof. T. Feng for supplying the GT1-7 cell lines.

REFERENCES

Aguirre, R. S., and Eugster, E. A. (2018). Central Precocious Puberty: From Genetics to Treatment. *Best Pract. Res. Clin. Endocrinol. Metab.* 32 (4), 343–354. doi:10.1016/j.beem.2018.05.008

Bai, G. L., Hu, K. L., Huan, Y., Wang, X., Lei, L., Zhang, M., et al. (2020). The Traditional Chinese Medicine Fuyou Formula Alleviates Precocious Puberty by Inhibiting GPR54/GnRH in the Hypothalamus. *Front. Pharmacol.* 11, 596525. doi:10.3389/fphar.2020.596525

Blaustein, J. D. (2010). The Year in Neuroendocrinology. *Mol. Endocrinol.* 24 (1), 252–260. doi:10.1210/me.2009-0350

Bradley, S. H., Lawrence, N., Steele, C., and Mohamed, Z. (2020). Precocious Puberty. *BMJ* 368, l6597. doi:10.1136/bmj.l6597

Carel, J. C., Lahlou, N., Roger, M., and Chaussain, J. L. (2004). Precocious Puberty and Statural Growth. *Hum. Reprod. Update* 10 (2), 135–147. doi:10.1093/humupd/dmh012

Carel, J. C., and Léger, J. (2008). Clinical Practice. Precocious Puberty. *N. Engl. J. Med.* 358 (22), 2366–2377. doi:10.1056/NEJMcp0800459

Chan, Y. M., Broder-Fingert, S., Wong, K. M., and Seminara, S. B. (2009). Kisspeptin/Gpr54-independent Gonadotrophin-Releasing Hormone Activity in Kiss1 and Gpr54 Mutant Mice. *J. Neuroendocrinol* 21 (12), 1015–1023. doi:10.1111/j.1365-2826.2009.01926.x

Chen, C. Y., Chou, Y. Y., Wu, Y. M., Lin, C. C., Lin, S. J., and Lee, C. C. (2013). Phthalates May Promote Female Puberty by Increasing Kisspeptin Activity. *Hum. Reprod.* 28 (10), 2765–2773. doi:10.1093/humrep/det325

Chen, M., and Eugster, E. A. (2015). Central Precocious Puberty: Update on Diagnosis and Treatment. *Paediatr. Drugs* 17 (4), 273–281. doi:10.1007/s40272-015-0130-8

Clarkson, J. (2013). Effects of Estradiol on Kisspeptin Neurons during Puberty. *Front. Neuroendocrinol* 34 (2), 120–131. doi:10.1016/j.yfrne.2013.02.002

Dees, W. L., Hiney, J. K., and Srivastava, V. K. (2021). IGF-1 Influences Gonadotropin-Releasing Hormone Regulation of Puberty. *Neuroendocrinology* 111 (12), 1151–1163. doi:10.1159/000514217

Dong, G., Zhang, J., Yang, Z., Feng, X., Li, J., Li, D., et al. (2019). The Association of Gut Microbiota with Idiopathic Central Precocious Puberty in Girls. *Front. Endocrinol. (Lausanne)* 10, 941. doi:10.3389/fendo.2019.00941

Eugster, E. A., and Pescovitz, O. H. (2001). Advances in the Treatment of Precocious Puberty. *Expert Opin. Investig. Drugs* 10 (9), 1623–1630. doi:10.1517/13543784.10.9.1623

Fixemer, T., Remberger, K., and Bonkhoff, H. (2003). Differential Expression of the Estrogen Receptor Beta (ERbeta) in Human Prostate Tissue, Premalignant Changes, and in Primary, Metastatic, and Recurrent Prostatic Adenocarcinoma. *Prostate* 54 (2), 79–87. doi:10.1002/pros.10171

Fuqua, J. S. (2013). Treatment and Outcomes of Precocious Puberty: an Update. *J. Clin. Endocrinol. Metab.* 98 (6), 2198–2207. doi:10.1210/jc.2013-1024

Guo, C., Sun, N., Hu, K., Bai, G., Zhang, M., Wang, Q., et al. (2021b). Integrated Pharmacological Analysis on the Mechanism of Fuyou Formula in Treating Precocious Puberty. *Front. Pharmacol.* 12, 649732. doi:10.3389/fphar.2021.649732

Guo, C., Liu, J., Zhang, M., Wang, Q., Ding, Q., and Zhao, L. (2021a). Study on the "traditional Chinese Medicine - Chemical Component - Target - Pathway" of Fuyou Mixture in the Treatment of Precocious Puberty Based on Integrated Pharmacology. *Chin. J. Clin. Pharmacol.* 37 (5), 572–575.

Hiney, J. K., Srivastava, V. K., Pine, M. D., and Les Dees, W. (2009). Insulin-like Growth Factor-I Activates KiSS-1 Gene Expression in the Brain of the Prepubertal Female Rat. *Endocrinology* 150 (1), 376–384. doi:10.1210/en.2008-0954

Kanasaki, H., Oride, A., Mijiddorj, T., Sukhbaatar, U., and Kyo, S. (2017). How Is GnRH Regulated in GnRH-Producing Neurons? Studies Using GT1-7 Cells as a GnRH-Producing Cell Model. *Gen. Comp. Endocrinol.* 247, 138–142. doi:10.1016/j.ygcen.2017.01.025

Kanety, H., Karasik, A., Pariente, C., and Kauschansky, A. (1996). Insulin-like Growth Factor-I and IGF Binding Protein-3 Remain High after GnRH Analogue Therapy in Girls with central Precocious Puberty. *Clin. Endocrinol. (Oxf)* 45 (1), 7–12. doi:10.1111/j.1365-2265.1996.tb02053.x

Kang, K., Lee, S. B., Jung, S. H., Cha, K. H., Park, W. D., Sohn, Y. C., et al. (2009). Tectoridin, a Poor Ligand of Estrogen Receptor Alpha, Exerts its Estrogenic Effects via an ERK-dependent Pathway. *Mol. Cell* 27 (3), 351–357. doi:10.1007/s10059-009-0045-8

Latronico, A. C., Brito, V. N., and Carel, J. C. (2016). Causes, Diagnosis, and Treatment of central Precocious Puberty. *Lancet Diabetes Endocrinol.* 4 (3), 265–274. doi:10.1016/s2213-8587(15)00380-0

Leka-Emiri, S., Chrousos, G. P., and Kanaka-Gantenbein, C. (2017). The Mystery of Puberty Initiation: Genetics and Epigenetics of Idiopathic central Precocious Puberty (ICPP). *J. Endocrinol. Invest.* 40 (8), 789–802. doi:10.1007/s40618-017-0627-9

Liu, H., Liu, J., and Liu, G. (2009). Clinical Study on 60 Cases of True Precocious Puberty in Girls Treated with Fuyou Mixture. *Beijing Traditional Chin. Med.* 28 (8), 596525. doi:10.3389/fphar.2020.596525

Luckenbach, J. A., Dickey, J. T., and Swanson, P. (2010). Regulation of Pituitary GnRH Receptor and Gonadotropin Subunits by IGF1 and GnRH in Prepubertal Male Coho salmon. *Gen. Comp. Endocrinol.* 167 (3), 387–396. doi:10.1016/j.ygcen.2009.09.010

Mayer, C., Acosta-Martinez, M., Dubois, S. L., Wolfe, A., Radovick, S., Boehm, U., et al. (2010). Timing and Completion of Puberty in Female Mice Depend on Estrogen Receptor Alpha-Signaling in Kisspeptin Neurons. *Proc. Natl. Acad. Sci. U S A.* 107 (52), 22693–22698. doi:10.1073/pnas.1012406108

Mayer, C., and Boehm, U. (2011). Female Reproductive Maturation in the Absence of kisspeptin/GPR54 Signaling. *Nat. Neurosci.* 14 (6), 704–710. doi:10.1038/nn.2818

Morales, A., Gonzalez, M., Marin, R., Diaz, M., and Alonso, R. (2007). Estrogen Inhibition of Norepinephrine Responsiveness Is Initiated at the Plasma Membrane of GnRH-Producing GT1-7 Cells. *J. Endocrinol.* 194 (1), 193–200. doi:10.1677/joe-06-0001

Pan, Y., Liu, J., and Liu, H. (2019). Clinical Observation on Treatment of Ovarian Cyst Complicated with Precocious Puberty in Girls with Chinese Herbal Medicine Fuyou Mixture. *Beijing J. Trad. Chin. Med.* 38 (07), 700–703. doi:10.16025/j.1674-1307.2019.07.021

Qian, F., Shi, N., and Zhou, H. (2020). Estrogen Can Promote the Expression of Genes Related to Precocious Puberty in GT1-7 Mouse Hypothalamic GnRH Neuronal Cell Line via Activating G Protein-Coupled Estrogen Receptor. *Gen. Physiol. Biophys.* 39 (1), 27–36. doi:10.4149/gpb_2019049

Radovick, S., Levine, J. E., and Wolfe, A. (2012). Estrogenic Regulation of the GnRH Neuron. *Front. Endocrinol. (Lausanne)* 3, 52. doi:10.3389/fendo.2012.00052

Roy, D., Angelini, N. L., and Belsham, D. D. (1999). Estrogen Directly Respresses Gonadotropin-Releasing Hormone (GnRH) Gene Expression in Estrogen Receptor-Alpha (ERalpha)- and ERbeta-Expressing GT1-7 GnRH Neurons. *Endocrinology* 140 (11), 5045–5053. doi:10.1210/endo.140.11.7117

Sørensen, K., Aksglaede, L., Petersen, J. H., Andersson, A. M., and Juul, A. (2012). Serum IGF1 and Insulin Levels in Girls with normal and Precocious Puberty. *Eur. J. Endocrinol.* 166 (5), 903–910. doi:10.1530/eje-12-0106

Stamatiades, G. A., and Kaiser, U. B. (2018). Gonadotropin Regulation by Pulsatile GnRH: Signaling and Gene Expression. *Mol. Cel Endocrinol* 463, 131–141. doi:10.1016/j.mce.2017.10.015

Thomas, P., and Dong, J. (2006). Binding and Activation of the Seven-Transmembrane Estrogen Receptor GPR30 by Environmental Estrogens: a Potential Novel Mechanism of Endocrine Disruption. *J. Steroid Biochem. Mol. Biol.* 102 (1-5), 175–179. doi:10.1016/j.jsbmb.2006.09.017

Trevisan, C. M., Montagna, E., de Oliveira, R., Christofolini, D. M., Barbosa, C. P., Crandall, K. A., et al. (2018). Kisspeptin/GPR54 System: What Do We Know about its Role in Human Reproduction? *Cell Physiol Biochem* 49 (4), 1259–1276. doi:10.1159/000493406

Tzoupis, H., Nteli, A., Androutsou, M. E., and Tselios, T. (2020). Gonadotropin-Releasing Hormone and GnRH Receptor: Structure, Function and Drug Development. *Curr. Med. Chem.* 27 (36), 6136–6158. doi:10.2174/0929867326666190712165444

Wolfe, A., and Wu, S. (2012). Estrogen Receptor-β in the Gonadotropin-Releasing Hormone Neuron. *Semin. Reprod. Med.* 30 (1), 23–31. doi:10.1055/s-0031-1299594

Conflict of Interest: The authors declare that the research was conducted in the absence of any commercial or financial relationships that could be construed as a potential conflict of interest.

Publisher's Note: All claims expressed in this article are solely those of the authors and do not necessarily represent those of their affiliated organizations, or those of the publisher, the editors and the reviewers. Any product that may be evaluated in this article, or claim that may be made by its manufacturer, is not guaranteed or endorsed by the publisher.

frontiers in Pharmacology

MINI REVIEW
published: 31 March 2022
doi: 10.3389/fphar.2022.865303

Related Markers for the Precision Diagnosis of Complex Appendicitis in Children

Jialin Zhou[1,2†], *Wenjing Xu*[3†], *Jitao Wang*[4*] *and Zhe Fan*[1,2*]

[1]Department of General Surgery, The Third People's Hospital of Dalian, Dalian Medical University, Dalian, China, [2]Department of Central Laboratory, The Third People's Hospital of Dalian, Dalian Medical University, Dalian, China, [3]Department of General Surgery, Zhongda Hospital, School of Medicine, Southeast University, Nanjing, China, [4]Department of Hepatobiliary Surgery, Xingtai People's Hospital, Xingtai, China

Acute appendicitis is the most common surgical emergency in children. Despite the high incidence rate of appendicitis, it is sometimes misdiagnosed or missed. Complex appendicitis (CA) in children is characterized by a critical condition, several complications, and high mortality. Precision distinguishing between simple appendicitis and CA correctly is key to choosing appropriate treatment. A safe, cheap, rapid, extensive and accurate diagnostic marker of appendicitis will be of great significance for emergency general surgeons to treat suspected CA. Many studies have investigated possible diagnostic markers for the diagnosis of CA in children. In this study, studies related to CA in children in recent years are summarized, and the related markers and scoring system for the diagnosis of CA in children are summarized.

Keywords: complex appendicitis, children, biomarkers, rating related, review

OPEN ACCESS

Edited by:
Jian Gao,
Shanghai Children's Medical Center, China

Reviewed by:
Yang Li,
Zhejiang University School of Medicine, China
Fan Li,
Nanjing Medical University, China

***Correspondence:**
Jitao Wang
wangjt302@163.com
Zhe Fan
fanzhe1982@hotmail.com

[†]*These authors have contributed equally to this work*

Specialty section:
This article was submitted to Obstetric and Pediatric Pharmacology, a section of the journal Frontiers in Pharmacology

Received: *29 January 2022*
Accepted: *03 March 2022*
Published: *31 March 2022*

Citation:
Zhou J, Xu W, Wang J and Fan Z (2022) Related Markers for the Precision Diagnosis of Complex Appendicitis in Children. Front. Pharmacol. 13:865303. doi: 10.3389/fphar.2022.865303

BACKGROUND

Acute appendicitis can be divided into simple appendicitis (SA) and complex appendicitis (CA) according to the severity of the disease. Diagnosis of CA is based on appendix perforation, appendix gangrene, appendix abscess, intra-abdominal abscess, and fecal peritonitis (Pham et al., 2016; Hajibandeh et al., 2020), CA is more common in children, with a prevalence of up to 30% (Yu et al., 2019). However, due to nonspecific symptoms and difficulties in accurate physical examination, distinguishing between SA and CA in children remains a challenge. The application of biomarkers in the diagnosis of CA has the advantages of easy collection, no limitations based on operator skill, and no radiation exposure compared with other diagnostic modalities. Our study summarizes biomarkers and the scoring system related to the diagnosis of CA in children to diagnose this disease more quickly and increasing the time for follow-up treatment. (**Figure 1**).

SINGLE INDEX

Soluble CD40 Ligand

sCD40L has both pro-thrombotic and pro-inflammatory effects (de Lizarrondo et al., 2012; Seibold and Ehrenschwender, 2015; Liu et al., 2018). When the body experiences an inflammatory response, sCD40L stored in unstimulated platelets aggregates, followed by stimulation of nuclear factor-κB signaling, causing upregulation of pro-inflammatory and pro-thrombotic factors.

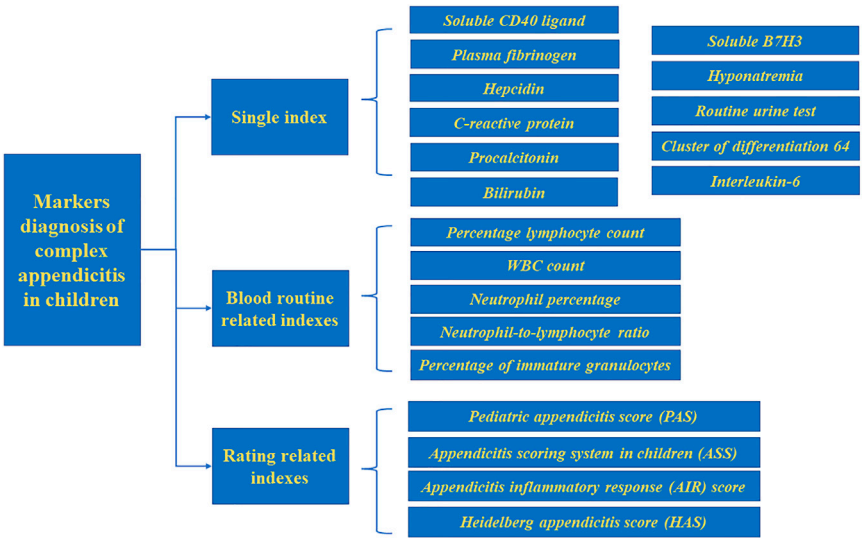

FIGURE 1 | Markers for pediatric complex appendicitis.

Studies have shown that sCD40L has excellent sensitivity and specificity in predicting CA in children. sCD40L levels below 178.00 pg/ml in the first 3 days of appendicitis can exclude the diagnosis of ruptured appendicitis (RA). Conversely, sCD40L above 301.00 pg/ml confirms the diagnosis of appendicitis and may have a high probability of RA (Huang et al., 2021). In these cases, further testing may not be necessary to confirm the diagnosis in patients with suspected appendicitis.

Plasma Fibrinogen

Under physiological conditions, the plasma concentration of fibrinogen ranges from 2 to 4 g/L (Tennent et al., 2007). However, under pathological conditions, such as infection, post-injury inflammation or diseases associated with vascular rupture, plasma fibrinogen concentrations can increase several-fold (Luyendyk et al., 2019). Therefore, fibrinogen is considered to be a marker of acute inflammation (Adams et al., 2004). An increase in fibrinogen in the blood can indicate that inflammation has been increased in the organism; it can also indicate the development of vascular inflammatory disease (Kayapinar et al., 2019; Luyendyk et al., 2019).

Studies have shown that fibrinogen has relatively high specificity and acceptable sensitivity as a laboratory marker for predicting perforated appendicitis (PA) (Feng et al., 2014). Fibrinogen can also be an important indicator to exclude CA (Li et al., 2011). Children with plasma fibrinogen levels > 520 mg/dl are more likely to have CA (Prada-Arias et al., 2017).

Hepcidin

Hepcidin is synthesized in hepatocytes and is a major hormonal regulator of iron metabolism, an antimicrobial peptide, and an acute phase reactant. For healthy children, the interquartile range for hepcidin was shown to be 21.90 ng/ml (Kumar et al., 2019). In inflammatory and infectious conditions, hepcidin synthesis is regulated by interleukin (IL)-6 and lipopolysaccharide (Rodriguez et al., 2014; Arezes et al., 2015). Hepcidin has direct antimicrobial activity and helps host defense by depriving microorganisms of this essential iron mineral (Ganz, 2003; Michels et al., 2015).

Kaiser et al. found that the serum hepcidin level of SA and CA in children was significantly increased. In addition, the accuracy of the combination of leukocytes and C-reactive protein (CRP) for the diagnosis of acute appendicitis can be improved by increasing serum hepcidin levels (Kaiser et al., 2018).

CRP

CRP is an acute temporal protein important for detecting occult inflammation and active disease (Clyne and Olshaker, 1999). Many researchers believe CRP has good diagnostic value for CA. Perforation should be considered in children with high CRP levels and free fluid or abscess formation by ultrasonography (Boettcher et al., 2017). Yang et al. found that increased WBC levels, CRP levels, and absolute value of neutrophils were associated with an increased likelihood of perforation (Yang et al., 2019). Beltran et al. (Beltrán et al., 2007) indicated that the CRP level and its sensitivity increased gradually from symptom to diagnosis, and the specificity at 12, 24, and 48 h from symptom to diagnosis was still very high (90%). However, the diagnostic accuracy of CRP reached its highest value within 12 h, after which it decreased significantly.

Different researchers have reached different conclusions regarding the threshold value of CRP for diagnosis of CA. Several studies have shown that children with CRP values in the range of 10–50 mg/L suggest uncomplicated appendicitis, while CRP > 50 mg/L strongly suggests CA (Kafetzis et al., 2005; Xharra et al., 2012). It has also been suggested that CRP values > 50 mg/L are more likely to indicate CA (Wu et al., 2012). A retrospective study by Zani et al. found that CRP and WBC levels increased in proportion to the severity of appendicitis.

Children with CRP below 40 mg/L had an 80% chance of not having CA (Zani et al., 2017).

Procalcitonin

PCT is a good marker of severe bacterial infection. PCT levels increased with the severity of infection (Meisner, 2014). PCT is less accurate than CRP and WBC in the diagnosis of acute appendicitis, but more accurate in the diagnosis of CA (Yu et al., 2013; Cui et al., 2019). Patients with PCT levels > 0.18 ng/ml and/or CRP > 3 mg/dl are at higher risk of peritonitis and should be closely monitored; more stringent treatment should be administered early (Gavela et al., 2012).

Bilirubin

Hyperbilirubinemia is defined as bilirubin levels greater than 20.5 μmol/l (Emmanuel et al., 2011). One prospective study showed that an increase in total serum bilirubin can be used as an indicator of appendicitis perforation in children (Pogorelić et al., 2021a). Bilirubin levels are highly specific for the diagnosis of complicated appendicitis; a 2.0-fold increase in the likelihood of complicated appendicitis was observed in patients with elevated bilirubin levels (Noh et al., 2012). In addition, total bilirubin > 21.38 mol/L was a predictor of appendicitis perforation (Yamazaki et al., 2021). As serum bilirubin level is an economical, simple, and available laboratory index, it should be recommended for preliminary evaluation of acute appendicitis in pediatric patients.

Soluble B7H3

B7H3, an immune checkpoint molecule belonging to the B7-CD28 family, is associated with the regulation of T cells (Janakiram et al., 2017). Release of sB7H3 may regulate B7H3R/B7H3 interactions *in vivo* (Zhang et al., 2008). This marker has been increasingly used to detect a number of inflammatory conditions (Chen et al., 2009; Chen et al., 2013a; Xu et al., 2019). Du et al. found that sB7H3 is important in predicting acute appendicitis and its severity in children, and sB7H3 > 36.146 ng/ml is statistically significant for the diagnosis of CA. The combination of CRP and sB7H3 increases the accuracy of PA diagnosis (Du et al., 2020).

Hyponatremia

Hyponatremia refers to a serum sodium concentration ≤ 135 mmol/L. Research suggests hyponatremia may be a useful tool for predicting PA (Pogorelić et al., 2021b). It is unclear why hyponatremia usually accompanies CA patients, but it may be mediated by antidiuretic hormone (Käser et al., 2013; Pham et al., 2016; Pogorelić et al., 2019; Yang et al., 2019; Giannis et al., 2020; Lindestam et al., 2020).

Routine Urine Test

A routine urine test is helpful to distinguish SA from PA. Chen et al. (Chen et al., 2013b) found that urinary ketone bodies, nitrate, urinary specific gravity, pH, WBC count and red blood cell (RBC) count all appeared to be important predictors of PA. Compared with children with SA, children with PA are more likely to be positive for ketone bodies and nitrates, higher urinary proportion, lower urinary pH, more urinary WBCs, and more urinary RBCs. In addition, urine RBC count (≥ 2.0/hpf) and WBC count (≥ 4.0/hpf) can be important predictors of appendiceal perforation or appendiceal abscess in children.

Cluster of Differentiation 64

Quantitative expression of neutrophil CD64 serves as a sensitive and specific laboratory indicator of the presence of sepsis or systemic acute inflammatory response, thus suggestive of a variety of inflammatory conditions (Xini et al., 2019; Hashem et al., 2020; Patnaik et al., 2020). Levels of CD64 were found to predict the occurrence of advanced appendicitis or PA; CRP levels and CD64 expression on leukocytes could better predict the diagnosis of CA (Ozguner et al., 2014).

Interleukin (IL)-6

IL-6 is an important natural immune cytokine closely related to the degree of inflammation. Researchers often use IL-6 as an indicator of the degree of systemic inflammation (Raeburn et al., 2002). IL-6 plays an important role in differentiating simple and advanced cases of appendicitis (Türkyilmaz et al., 2006).

BLOOD ROUTINE RELATED INDEXES

Percentage Lymphocyte Count

Virmani et al. demonstrated that the percentage lymphocyte count is a better indicator than the neutrophil to lymphocyte ration (NLR) and total leukocyte count (TLC) in distinguishing SA from CA. The threshold value for lymphocyte count is 14.8%. Values less than this are considered CA whereas values greater are considered SA (Virmani et al., 2018; Celik et al., 2019).

WBC Count

WBC count is not sensitive and specific enough to distinguish PA from non-perforated appendicitis (Grönroos, 2001). However, the use of CRP alone or WBC count in combination with CRP helps to differentiate between PA and non-perforated appendicitis (Grönroos, 2001). CRP levels > 50 mg/l and leukocyte counts > 104/mm^3 were effective adjuncts to predict appendiceal perforation (Kafetzis et al., 2005; Buyukbese Sarsu and Sarac, 2016; Yang et al., 2019; Zvizdic et al., 2021).

However, some studies have reached an opposite conclusion, suggesting the increase in leukocyte count is a risk factor for CA (Beltrán et al., 2007; Siddique et al., 2011; Şahbaz et al., 2014), and its sensitivity increases with the duration of symptoms (Beltrán et al., 2007; Ngim et al., 2014). Okamoto et al. (Okamoto et al., 2006) found that an increase in WBC count 48 h after the onset of pain is a prognosis marker of CA. In addition, Beltra et al. (Beltrán et al., 2007) demonstrated that WBC count can also distinguish between SA and PA. The diagnostic accuracy was high (80%) at 12 and 48 h, and beyond 49 h, decreasing to 70% at 24 h.

Neutrophil Percentage

Neutrophil percentage can be used to diagnose CA, with elevated neutrophil percentage (> 74%) and CRP (> 8 mg/dl) levels

TABLE 1 | Related markers in the diagnosis of complex appendicitis in children and corresponding values.

marker	Value
sCD40L	> 301.00 pg/ml
Plasma Fibrinogen	> 520 mg/dl
CRP	> 50 mg/L/ > 30 mg/L
PCT	> 0.18 ng/m
Bilirubin	> 21.38 mol/L
sB7H3	> 36.146 ng/ml
Serum natrium	≤135 mmol/L
Urine RBC counts	≥2.0/hpf
Urine WBC counts	≥4.0/hpf
Percentage lymphocyte count	< 14.8%
WBC	> 13,500/mm^3
Percentage neutrophil counts	> 74%
NLR	> 8.8
IG%	> 35%

CRP, C-reactive protein; PCT, procalcitonin; RBC, red blood cell; WBC, white blood cell; NLR, neutrophil-to-lymphocyte ratio; IG, immature granulocyte.

predicting a more than five-fold increased risk of PA (Yang et al., 2019). A neutrophil count greater than 75% is considered CA (Virmani et al., 2018).

Neutrophil-to-Lymphocyte Ratio

Neutrophil-to-lymphocyte ratio (NLR) is a simple and easily calculated marker of the body's inflammatory status (Käser et al., 2010). Because it provides information about two different inflammatory and immune pathways, we believe NLR is valuable in predicting appendicitis and its severity. Hajibandeh et al. demonstrated that children with NLR > 8.8 are at higher risk of CA (Hajibandeh et al., 2020).

Percentage of Immature Granulocytes

In recent years, it has been found that the Ig percentage can be used as a marker of infection and that this percentage can be measured automatically in a new generation of hemograms. It has the advantage that it can be measured easily and quickly without incurring additional costs (van der Geest et al., 2014; Pavare et al., 2018; Zeng et al., 2020). Studies have demonstrated that an elevated Ig percentage can predict CA, with a sensitivity of 85.4% and a specificity of 61.5% when the Ig percentage is 35%. Because it is quick and easy to measure, does not require additional blood collection, and does not incur additional costs, IG percentage may be the test of choice for diagnosing patients with CA (Güngör et al., 2021). (**Table 1**)

RATING RELATED INDEXES

Pediatric Appendicitis Score

PAS includes the following indicators: 1) cough/shock/jumping abdominal pressure in the right lower abdomen, 2), anorexia, 3), fever, 4), nausea/vomiting, 5), pain in the right iliac fossa, 6), leukocytosis, 7), polymorphonuclear neutrophilia, and 8) painful migration. All of these variables were scored as 1 except for signs (1 and 5), which were scored as 2, for a total score of 10. The score is now widely used to diagnose acute appendicitis in children. A score ≥ 6 is consistent with a diagnosis of appendicitis (Samuel, 2002). PAS may be related to the pathological progression of appendicitis and the severity of the disease. PAS ≥ 8 can be used for the diagnosis of CA (Fujii et al., 2020). Fujii et al. demonstrated that symptom duration > 1 day, CRP > 4 mg/dl and PAS ≥ 8 predicted CA, which was more convincing than a single indicator of any of these three.

Appendicitis Scoring System in Children

Lee et al. developed a scoring system capable of differentiating CA in children under 10 years of age, which consisted of five risk factors: diarrhea, anorexia, temperature, CRP level, and presence of periappendiceal free fluid on radiological examination. Among them, fever (Bonadio et al., 2018; Obinwa et al., 2015; Peng et al., 2006; van den Bogaard et al., 2016; Atema et al., 2015; Augustin et al., 2011) and CRP level (van den Bogaard et al., 2016; Lee et al.,

TABLE 2 | Different scoring systems for diagnosing complex appendicitis in children, including the different weighing factors for each score.

	PAS	ASS	AIR	HAS	Mod HAS
Nausea/Vomiting	1		1		
Pain in RIF	2		1	1	1
Abdominal Defense (Low/Mild/Severe)			1/2/3		
Temperature >38.5°C	1	3	1		
Neutrophilia (70–84%/>85%)	1		1/2		
Leukocytes (10.0–14.9 × 109/l/>15.0 × 109/l/>11 × 109/l)	1		1/2		1
CRP (10–49 g/l/>50 g/l/>20 mg/l)		5	1/2		1
US demonstrating APP				1	1
Rebound tenderness				1	1
Anorexia	1	2			
Diarrhea		2			
Periappendiceal free fluid on image		3			
Continuous pain				1	
Cough/Percussion/Hopping tenderness	2				
Migration of pain	1				
Positive score	8/10	4/15	9/12	3/4	3/5

RIF, right Iliac Fossa; CRP, C-reactive protein; US demonstrating appendicitis comprises the appendix diameter > 6 mm and/or signs of inflammation such as wall edema, hyperemia, and surrounding inflammation; US, ultrasound; APP, appendicitis.

2021; Barreto et al., 2010; Bröker et al., 2012) were found to be predictors of CA in previous studies. The advantages of this score over other scores is that it includes CRP levels and excludes indistinguishable symptoms, such as pain metastasis and nausea.

To reduce the risk of delaying treatment due to misclassification of CA as uncomplicated appendicitis using this scoring system, this score uses a score of 4 as the threshold value to distinguish CA from SA. Appendectomy should be considered if the patient meets both an ASS score of four and CRP ≥ 50 mg/L or has two or more risk factors (Lee et al., 2021).

Appendicitis Inflammatory Response Score

The AIR score includes vomiting, right iliac fossa pain, muscle tension, temperature, neutrophil grading, WBC, and CRP. Because it is primarily based on objective inflammatory markers, this score has the advantage of high repeatability in different environments, independent of the inspector's experience. Pogoreli et al. found that the AIR score was able to distinguish PA from non-perforated appendicitis; ≥ 9 (AIR score) is a good index of appendix perforation, with a sensitivity of 89.5% and a specificity of 71.9% (Pogorelić et al., 2021c).

Heidelberg Appendicitis Score

HAS includes four factors (persistent pain, right lower abdominal tenderness, rebound tenderness, and appendicitis by ultrasound). Current studies have shown that perforation in children with appendicitis can be identified by using HAS as it can reliably detect PA in children and exclude perforation if the score is negative (Boettcher et al., 2017).

Stiel et al. proposed a modified Heidelberg score including ultrasound showing appendicitis, CRP > 20 mg/L, rebound tenderness, leukocytes > 11 × 10^9/L and right lower abdominal tenderness. Modified Heidelberg appendicitis provides good predictability for both general appendicitis and PA (Stiel et al., 2020). (**Table 2**)

CONCLUSION

Research on relevant markers for the diagnosis of CA in children is gradually increasing. Biomarkers and scoring systems for children allow for earlier diagnosis, which not only reduces the number of unnecessary surgeries, but also reduces complications and helps to significantly reduce the cost of treating patients with acute abdominal disease. All markers list in the manuscript are helpful for diagnosis of CA, however, no index can diagnose CA at an accuracy of 100%; based on the overall consideration, we recommend PAS. Although, the review focuses the markers for the precision diagnosis of complex appendicitis in children. related markers for CA are as same as medical history, physical examination and imaging examinations. Appropriate selection of diagnostic markers and scoring systems for predicting CA in children is important for determining the best treatment strategy. There are several non-routine indexes for diagnosis of CA; therefore, more researches about the non-routine indexes need to be performed to verify their significance and they can be routine test for diagnosis of CA. The research on some biomarkers is still in its infancy, and further investigation is needed to refine the reference value for diagnosing CA, diagnostic accuracy, and clinical applications of CA.

AUTHOR CONTRIBUTIONS

JZ and WX reviewed the relevant literature and wrote the manuscript. ZF designed structure. JW and ZF revised the manuscript. All authors read and approved the final manuscript.

FUNDING

This study was supported by the National Natural Science Foundation of China (Grants No. 81701965 to ZF).

REFERENCES

Adams, R. A., Passino, M., Sachs, B. D., Nuriel, T., and Akassoglou, K. (2004). Fibrin Mechanisms and Functions in Nervous System Pathology. *Mol. Interv.* 4 (3), 163–176. doi:10.1124/mi.4.3.6

Arezes, J., Jung, G., Gabayan, V., Valore, E., Ruchala, P., Gulig, P. A., et al. (2015). Hepcidin-induced Hypoferremia Is a Critical Host Defense Mechanism against the Siderophilic Bacterium Vibrio Vulnificus. *Cell Host Microbe* 17 (1), 47–57. doi:10.1016/j.chom.2014.12.001

Atema, J. J., van Rossem, C. C., Leeuwenburgh, M. M., Stoker, J., and Boermeester, M. A. (2015). Scoring System to Distinguish Uncomplicated from Complicated Acute Appendicitis. *Br. J. Surg.* 102 (8), 979–990. doi:10.1002/bjs.9835

Augustin, T., Cagir, B., and Vandermeer, T. J. (2011). Characteristics of Perforated Appendicitis: Effect of Delay Is Confounded by Age and Gender. *J. Gastrointest. Surg.* 15 (7), 1223–1231. doi:10.1007/s11605-011-1486-x

Barreto, S. G., Travers, E., Thomas, T., Mackillop, C., Tiong, L., Lorimer, M., et al. (2010). Acute Perforated Appendicitis: an Analysis of Risk Factors to Guide Surgical Decision Making. *Indian J. Med. Sci.* 64 (2), 58–65. doi:10.4103/0019-5359.94401

Beltrán, M. A., Almonacid, J., Vicencio, A., Gutiérrez, J., Cruces, K. S., and Cumsille, M. A. (2007). Predictive Value of white Blood Cell Count and C-Reactive Protein in Children with Appendicitis. *J. Pediatr. Surg.* 42 (7), 1208–1214. doi:10.1016/j.jpedsurg.2007.02.010

Boettcher, M., Günther, P., and Breil, T. (2017). The Heidelberg Appendicitis Score Predicts Perforated Appendicitis in Children. *Clin. Pediatr. (Phila)* 56 (12), 1115–1119. doi:10.1177/0009922816678976

Bonadio, W., Shahid, S., Vardi, L., Buckingham, C., Kornblatt, A., Free, C., et al. (2018). A Pre-operative Clinical Scoring System to Distinguish Perforation Risk with Pediatric Appendicitis. *J. Pediatr. Surg.* 53 (3), 441–445. doi:10.1016/j.jpedsurg.2017.05.017

Bröker, M. E., van Lieshout, E. M., van der Elst, M., Stassen, L. P., and Schepers, T. (2012). Discriminating between Simple and Perforated Appendicitis. *J. Surg. Res.* 176 (1), 79–83. doi:10.1016/j.jss.2011.09.049

Buyukbese Sarsu, S., and Sarac, F. (2016). Diagnostic Value of White Blood Cell and C-Reactive Protein in Pediatric Appendicitis. *Biomed. Res. Int.* 2016, 6508619. doi:10.1155/2016/6508619

Celik, B., Nalcacioglu, H., Ozcatal, M., and Altuner Torun, Y. (2019). Role of Neutrophil-To-Lymphocyte Ratio and Platelet-To-Lymphocyte Ratio in Identifying Complicated Appendicitis in the Pediatric Emergency Department. *Ulus Travma Acil Cerrahi Derg* 25 (3), 222–228. doi:10.5505/tjtes.2018.06709

Chen, C. Y., Zhao, L. L., Lin, Y. R., Wu, K. H., and Wu, H. P. (2013). Different Urinalysis Appearances in Children with Simple and Perforated Appendicitis. *Am. J. Emerg. Med.* 31 (11), 1560–1563. doi:10.1016/j.ajem.2013.06.027

Chen, X., Zhang, G., Li, Y., Feng, X., Wan, F., Zhang, L., et al. (2009). Circulating B7-H3(cd276) Elevations in Cerebrospinal Fluid and Plasma of Children with Bacterial Meningitis. *J. Mol. Neurosci.* 37 (1), 86–94. doi:10.1007/s12031-008-9133-z

Chen, Z. R., Zhang, G. B., Wang, Y. Q., Yan, Y. D., Zhou, W. F., Zhu, C. H., et al. (2013). Soluble B7-H3 Elevations in Hospitalized Children with Mycoplasma Pneumoniae Pneumonia. *Diagn. Microbiol. Infect. Dis.* 77 (4), 362–366. doi:10.1016/j.diagmicrobio.2013.09.006

Clyne, B., and Olshaker, J. S. (1999). The C-Reactive Protein. *J. Emerg. Med.* 17 (6), 1019–1025. doi:10.1016/s0736-4679(99)00135-3

Cui, W., Liu, H., Ni, H., Qin, X., and Zhu, L. (2019). Diagnostic Accuracy of Procalcitonin for Overall and Complicated Acute Appendicitis in Children: a Meta-Analysis. *Ital. J. Pediatr.* 45 (1), 78. doi:10.1186/s13052-019-0673-3

de Lizarrondo, S. M., Roncal, C., Calvayrac, O., Rodríguez, C., Varo, N., Purroy, A., et al. (2012). Synergistic Effect of Thrombin and CD40 Ligand on Endothelial Matrix Metalloproteinase-10 Expression and Microparticle Generation *In Vitro* and *In Vivo*. *Atvb* 32 (6), 1477–1487. doi:10.1161/atvbaha.112.248773

Du, X., Chen, Y., Zhu, J., Bai, Z., Hua, J., Li, Y., et al. (2020). sB7H3 in Children with Acute Appendicitis: Its Diagnostic Value and Association with Histological Findings. *J. Immunol. Res.* 2020, 2670527. doi:10.1155/2020/2670527

Emmanuel, A., Murchan, P., Wilson, I., and Balfe, P. (2011). The Value of Hyperbilirubinaemia in the Diagnosis of Acute Appendicitis. *Ann. R. Coll. Surg. Engl.* 93 (3), 213–217. doi:10.1308/147870811x566402

Feng, S., Wu, P., and Chen, X. (2014). Hyperfibrinogenemia in Appendicitis: a New Predictor of Perforation in Children. *Pediatr. Surg. Int.* 30 (11), 1143–1147. doi:10.1007/s00383-014-3585-8

Fujii, T., Tanaka, A., Katami, H., and Shimono, R. (2020). Usefulness of the Pediatric Appendicitis Score for Assessing the Severity of Acute Appendicitis in Children. *Pediatr. Int.* 62 (1), 70–73. doi:10.1111/ped.14032

Ganz, T. (2003). Hepcidin, a Key Regulator of Iron Metabolism and Mediator of Anemia of Inflammation. *Blood* 102 (3), 783–788. doi:10.1182/blood-2003-03-0672

Gavela, T., Cabeza, B., Serrano, A., and Casado-Flores, J. (2012). C-reactive Protein and Procalcitonin Are Predictors of the Severity of Acute Appendicitis in Children. *Pediatr. Emerg. Care* 28 (5), 416–419. doi:10.1097/PEC.0b013e318252d875

Giannis, D., Matenoglou, E., and Moris, D. (2020). Hyponatremia as a Marker of Complicated Appendicitis: A Systematic Review. *Surgeon* 18 (5), 295–304. doi:10.1016/j.surge.2020.01.002

Grönroos, J. M. (2001). Do normal Leucocyte Count and C-Reactive Protein Value Exclude Acute Appendicitis in Children? *Acta Paediatr.* 90 (6), 649–651. doi:10.1080/08035250117900

Güngör, A., Göktuğ, A., Güneylioğlu, M. M., Yaradılmış, R. M., Bodur, i., Öztürk, B., et al. (2021). Utility of Biomarkers in Predicting Complicated Appendicitis: Can Immature Granulocyte Percentage and C-Reactive Protein Be Used? *Postgrad. Med.* 133 (7), 817–821. doi:10.1080/00325481.2021.1948306

Hajibandeh, S., Hajibandeh, S., Hobbs, N., and Mansour, M. (2020). Neutrophil-to-lymphocyte Ratio Predicts Acute Appendicitis and Distinguishes between Complicated and Uncomplicated Appendicitis: A Systematic Review and Meta-Analysis. *Am. J. Surg.* 219 (1), 154–163. doi:10.1016/j.amjsurg.2019.04.018

Hashem, H. E., Abdel Halim, R. M., El Masry, S. A., Mokhtar, A. M., and Abdelaal, N. M. (2020). The Utility of Neutrophil CD64 and Presepsin as Diagnostic, Prognostic, and Monitoring Biomarkers in Neonatal Sepsis. *Int. J. Microbiol.* 2020, 8814892. doi:10.1155/2020/8814892

Huang, W. Y., Chen, C. Y., Chang, Y. J., Lee, E. P., and Wu, H. P. (2021). Serum Soluble CD40 Ligand in Predicting Simple Appendicitis and Complicated Appendicitis at Different Time Points in Children. *Front. Pediatr.* 9, 676370. doi:10.3389/fped.2021.676370

Janakiram, M., Shah, U. A., Liu, W., Zhao, A., Schoenberg, M. P., and Zang, X. (2017). The Third Group of the B7-CD28 Immune Checkpoint Family: HHLA2, TMIGD2, B7x, and B7-H3. *Immunol. Rev.* 276 (1), 26–39. doi:10.1111/imr.12521

Kafetzis, D. A., Velissariou, I. M., Nikolaides, P., Sklavos, M., Maktabi, M., Spyridis, G., et al. (2005). Procalcitonin as a Predictor of Severe Appendicitis in Children. *Eur. J. Clin. Microbiol. Infect. Dis.* 24 (7), 484–487. doi:10.1007/s10096-005-1360-4

Kaiser, M., Schroeckenfuchs, M., Castellani, C., Warncke, G., Till, H., and Singer, G. (2018). The Diagnostic Value of Hepcidin to Predict the Presence and Severity of Appendicitis in Children. *J. Surg. Res.* 222, 102–107. doi:10.1016/j.jss.2017.10.021

Käser, S. A., Fankhauser, G., Willi, N., and Maurer, C. A. (2010). C-reactive Protein Is superior to Bilirubin for Anticipation of Perforation in Acute Appendicitis. *Scand. J. Gastroenterol.* 45 (7-8), 885–892. doi:10.3109/00365521003728572

Käser, S. A., Furler, R., Evequoz, D. C., and Maurer, C. A. (2013). Hyponatremia Is a Specific Marker of Perforation in Sigmoid Diverticulitis or Appendicitis in Patients Older Than 50 Years. *Gastroenterol. Res. Pract.* 2013, 462891. doi:10.1155/2013/462891

Kayapinar, O., Ozde, C., and Kaya, A. (2019). Relationship between the Reciprocal Change in Inflammation-Related Biomarkers (Fibrinogen-To-Albumin and hsCRP-To-Albumin Ratios) and the Presence and Severity of Coronary Slow Flow. *Clin. Appl. Thromb. Hemost.* 25, 1076029619835383. doi:10.1177/1076029619835383

Kumar, S., Bhatia, P., Jain, R., and Bharti, B. (2019). Plasma Hepcidin Levels in Healthy Children: Review of Current Literature Highlights Limited Studies. *J. Pediatr. Hematol. Oncol.* 41 (3), 238–242. doi:10.1097/mph.0000000000001216

Lee, Y., Cho, H., Gwak, G., Bae, B., and Yang, K. (2021). Scoring System for Differentiation of Complicated Appendicitis in Pediatric Patients: Appendicitis Scoring System in Children. *Glob. Pediatr. Health* 8, 2333794X211022268. doi:10.1177/2333794x211022268

Li, J., Liu, Y., Yin, W., Zhang, C., Huang, J., Liao, C., et al. (2011). Alterations of the Preoperative Coagulation Profile in Patients with Acute Appendicitis. *Clin. Chem. Lab. Med.* 49 (8), 1333–1339. doi:10.1515/cclm.2011.214

Lindestam, U., Almström, M., Jacks, J., Malmquist, P., Lönnqvist, P. A., Jensen, B. L., et al. (2020). Low Plasma Sodium Concentration Predicts Perforated Acute Appendicitis in Children: A Prospective Diagnostic Accuracy Study. *Eur. J. Pediatr. Surg.* 30 (4), 350–356. doi:10.1055/s-0039-1687870

Liu, Z. L., Hu, J., Xiao, X. F., Peng, Y., Zhao, S. P., Xiao, X. Z., et al. (2018). The CD40 Rs1883832 Polymorphism Affects Sepsis Susceptibility and sCD40L Levels. *Biomed. Res. Int.* 2018, 7497314. doi:10.1155/2018/7497314

Luyendyk, J. P., Schoenecker, J. G., and Flick, M. J. (2019). The Multifaceted Role of Fibrinogen in Tissue Injury and Inflammation. *Blood* 133 (6), 511–520. doi:10.1182/blood-2018-07-818211

Meisner, M. (2014). Update on Procalcitonin Measurements. *Ann. Lab. Med.* 34 (4), 263–273. doi:10.3343/alm.2014.34.4.263

Michels, K., Nemeth, E., Ganz, T., and Mehrad, B. (2015). Hepcidin and Host Defense against Infectious Diseases. *Plos Pathog.* 11 (8), e1004998. doi:10.1371/journal.ppat.1004998

Ngim, C. F., Quek, K. F., Dhanoa, A., Khoo, J. J., Vellusamy, M., and Ng, C. S. (2014). Pediatric Appendicitis in a Developing Country: what Are the Clinical Predictors and Outcome of Perforation? *J. Trop. Pediatr.* 60 (6), 409–414. doi:10.1093/tropej/fmu037

Noh, H., Chang, S. J., and Han, A. (2012). The Diagnostic Values of Preoperative Laboratory Markers in Children with Complicated Appendicitis. *J. Korean Surg. Soc.* 83 (4), 237–241. doi:10.4174/jkss.2012.83.4.237

Obinwa, O., Peirce, C., Cassidy, M., Fahey, T., and Flynn, J. (2015). A Model Predicting Perforation and Complications in Paediatric Appendicectomy. *Int. J. Colorectal Dis.* 30 (4), 559–565. doi:10.1007/s00384-015-2120-2

Okamoto, T., Sano, K., and Ogasahara, K. (2006). Receiver-operating Characteristic Analysis of Leukocyte Counts and Serum C-Reactive Protein Levels in Children with Advanced Appendicitis. *Surg. Today* 36 (6), 515–518. doi:10.1007/s00595-006-3189-6

Ozguner, İ., Kızılgun, M., Karaman, A., Cavusoğlu, Y. H., Erdoğan, D., Karaman, İ., et al. (2014). Are Neutrophil CD64 Expression and Interleukin-6 Early Useful Markers for Diagnosis of Acute Appendicitis? *Eur. J. Pediatr. Surg.* 24 (2), 179–183. doi:10.1055/s-0033-1347295

Patnaik, R., Azim, A., and Agarwal, V. (2020). Neutrophil CD64 a Diagnostic and Prognostic Marker of Sepsis in Adult Critically Ill Patients: A Brief Review. *Indian J. Crit. Care Med.* 24 (12), 1242–1250. doi:10.5005/jp-journals-10071-23558

Pavare, J., Grope, I., and Gardovska, D. (2018). Assessment of Immature Granulocytes Percentage to Predict Severe Bacterial Infection in Latvian Children: An Analysis of Secondary Data. *Medicina (Kaunas)* 54 (4), 56. doi:10.3390/medicina54040056

Peng, Y. S., Lee, H. C., Yeung, C. Y., Sheu, J. C., Wang, N. L., and Tsai, Y. H. (2006). Clinical Criteria for Diagnosing Perforated Appendix in Pediatric Patients. *Pediatr. Emerg. Care* 22 (7), 475–479. doi:10.1097/01.pec.0000226871.49427.ec

Pham, X. D., Sullins, V. F., Kim, D. Y., Range, B., Kaji, A. H., de Virgilio, C. M., et al. (2016). Factors Predictive of Complicated Appendicitis in Children. *J. Surg. Res.* 206 (1), 62–66. doi:10.1016/j.jss.2016.07.023

Pogorelić, Z., Lukšić, B., Ninčević, S., Lukšić, B., and Polašek, O. (2021). Hyponatremia as a Predictor of Perforated Acute Appendicitis in Pediatric Population: A Prospective Study. *J. Pediatr. Surg.* 56 (10), 1816–1821. doi:10.1016/j.jpedsurg.2020.09.066

Pogorelić, Z., Silov, N., Jukić, M., Elezović Baloević, S., Poklepović Peričić, T., and Jerončić, A. (2019). Ertapenem Monotherapy versus Gentamicin Plus Metronidazole for Perforated Appendicitis in Pediatric Patients. *Surg. Infect. (Larchmt)* 20 (8), 625–630. doi:10.1089/sur.2019.025

Pogorelić, Z., Lukšić, A. M., Mihanović, J., Đikić, D., and Balta, V. (2021). Hyperbilirubinemia as an Indicator of Perforated Acute Appendicitis in Pediatric Population: A Prospective Study. *Surg. Infections* 22, 1064–1071. doi:10.1089/sur.2021.107

Pogorelić, Z., Mihanović, J., Ninčević, S., Lukšić, B., Elezović Baloević, S., and Polašek, O. (2021). Validity of Appendicitis Inflammatory Response Score in Distinguishing Perforated from Non-perforated Appendicitis in Children. *Children* 8 (4), 309. doi:10.3390/children8040309

Prada-Arias, M., Vázquez, J. L., Salgado-Barreira, Á., Gómez-Veiras, J., Montero-Sánchez, M., and Fernández-Lorenzo, J. R. (2017). Diagnostic Accuracy of Fibrinogen to Differentiate Appendicitis from Nonspecific Abdominal Pain in Children. *Am. J. Emerg. Med.* 35 (1), 66–70. doi:10.1016/j.ajem.2016.10.003

Raeburn, C. D., Sheppard, F., Barsness, K. A., Arya, J., and Harken, A. H. (2002). Cytokines for Surgeons. *Am. J. Surg.* 183 (3), 268–273. doi:10.1016/s0002-9610(02)00781-x

Rodriguez, R., Jung, C. L., Gabayan, V., Deng, J. C., Ganz, T., Nemeth, E., et al. (2014). Hepcidin Induction by Pathogens and Pathogen-Derived Molecules Is Strongly Dependent on Interleukin-6. *Infect. Immun.* 82 (2), 745–752. doi:10.1128/iai.00983-13

Şahbaz, N. A., Bat, O., Kaya, B., Ulukent, S. C., İlkgül, Ö., Özgün, M. Y., et al. (2014). The Clinical Value of Leucocyte Count and Neutrophil Percentage in Diagnosing Uncomplicated (Simple) Appendicitis and Predicting Complicated Appendicitis. *Ulus Travma Acil Cerrahi Derg* 20 (6), 423–426. doi:10.5505/tjtes.2014.75044

Samuel, M. (2002). Pediatric Appendicitis Score. *J. Pediatr. Surg.* 37 (6), 877–881. doi:10.1053/jpsu.2002.32893

Seibold, K., and Ehrenschwender, M. (2015). p62 Regulates CD40-Mediated NFκB Activation in Macrophages through Interaction with TRAF6. *Biochem. Biophys. Res. Commun.* 464 (1), 330–335. doi:10.1016/j.bbrc.2015.06.153

Siddique, K., Baruah, P., Bhandari, S., Mirza, S., and Harinath, G. (2011). Diagnostic Accuracy of white Cell Count and C-Reactive Protein for Assessing the Severity of Paediatric Appendicitis. *JRSM Short Rep.* 2 (7), 59. doi:10.1258/shorts.2011.011025

Stiel, C., Elrod, J., Klinke, M., Herrmann, J., Junge, C. M., Ghadban, T., et al. (2020). The Modified Heidelberg and the AI Appendicitis Score Are Superior to Current Scores in Predicting Appendicitis in Children: A Two-Center Cohort Study. *Front. Pediatr.* 8, 592892. doi:10.3389/fped.2020.592892

Tennent, G. A., Brennan, S. O., Stangou, A. J., O'Grady, J., Hawkins, P. N., and Pepys, M. B. (2007). Human Plasma Fibrinogen Is Synthesized in the Liver. *Blood* 109 (5), 1971–1974. doi:10.1182/blood-2006-08-040956

Türkyilmaz, Z., Sönmez, K., Karabulut, R., Elbeğ, Ş., Moralioğlu, S., Demirtola, A., et al. (2006). Sequential Cytokine Levels in the Diagnosis of Appendicitis. *Scand. J. Clin. Lab. Invest.* 66 (8), 723–732. doi:10.1080/00365510600975251

van den Bogaard, V. A., Euser, S. M., van der Ploeg, T., de Korte, N., Sanders, D. G., de Winter, D., et al. (2016). Diagnosing Perforated Appendicitis in Pediatric Patients: a New Model. *J. Pediatr. Surg.* 51 (3), 444–448. doi:10.1016/j.jpedsurg.2015.10.054

van der Geest, P. J., Mohseni, M., Brouwer, R., van der Hoven, B., Steyerberg, E. W., and Groeneveld, A. B. (2014). Immature Granulocytes Predict Microbial Infection and its Adverse Sequelae in the Intensive Care Unit. *J. Crit. Care* 29 (4), 523–527. doi:10.1016/j.jcrc.2014.03.033

Virmani, S., Prabhu, P. S., Sundeep, P. T., and Kumar, V. (2018). Role of Laboratory Markers in Predicting Severity of Acute Appendicitis. *Afr. J. Paediatr. Surg.* 15 (1), 1–4. doi:10.4103/ajps.AJPS_47_16

Wu, H. P., Yang, W. C., Wu, K. H., Chen, C. Y., and Fu, Y. C. (2012). Diagnosing Appendicitis at Different Time Points in Children with Right Lower Quadrant Pain: Comparison between Pediatric Appendicitis Score and the Alvarado Score. *World J. Surg.* 36 (1), 216–221. doi:10.1007/s00268-011-1310-5

Xharra, S., Gashi-Luci, L., Xharra, K., Veselaj, F., Bicaj, B., Sada, F., et al. (2012). Correlation of Serum C-Reactive Protein, white Blood Count and Neutrophil Percentage with Histopathology Findings in Acute Appendicitis. *World J. Emerg. Surg.* 7 (1), 27. doi:10.1186/1749-7922-7-27

Xini, A., Pistiki, A., Lada, M., Giamarellos-Bourboulis, E. J., and Dimopoulos, G. (2019). Association of the Early Absolute CD64-Expressing Neutrophil Count and Sepsis Outcome. *Eur. J. Clin. Microbiol. Infect. Dis.* 38 (6), 1123–1128. doi:10.1007/s10096-019-03507-0

Xu, Y., Yu, L., Hao, C., Wang, Y., Zhu, C., Ji, W., et al. (2019). Plasma Soluble B7-H3 Levels for Severity Evaluation in Pediatric Patients with Mycoplasma Pneumoniae Pneumonia. *Int. Immunopharmacol* 73, 163–171. doi:10.1016/j.intimp.2019.05.014

Yamazaki, S., Shimodaira, Y., Kobayashi, A., Takata, M., Hayashibara, K., Sakon, M., et al. (2021). Predictive Factors of Perforated Appendicitis: Impact of the C-Reactive Protein Level. *Surg. Open Sci.* 6, 1–4. doi:10.1016/j.sopen.2021.06.003

Yang, J., Liu, C., He, Y., and Cai, Z. (2019). Laboratory Markers in the Prediction of Acute Perforated Appendicitis in Children. *Emerg. Med. Int.* 2019, 4608053. doi:10.1155/2019/4608053

Yu, C. W., Juan, L. I., Wu, M. H., Shen, C. J., Wu, J. Y., and Lee, C. C. (2013). Systematic Review and Meta-Analysis of the Diagnostic Accuracy of Procalcitonin, C-Reactive Protein and white Blood Cell Count for Suspected Acute Appendicitis. *Br. J. Surg.* 100 (3), 322–329. doi:10.1002/bjs.9008

Yu, Y. R., Rosenfeld, E. H., Dadjoo, S., Orth, R. C., Lopez, M. E., Shah, S. R., et al. (2019). Accuracy of Surgeon Prediction of Appendicitis Severity in Pediatric Patients. *J. Pediatr. Surg.* 54 (11), 2274–2278. doi:10.1016/j.jpedsurg.2019.04.007

Zani, A., Teague, W. J., Clarke, S. A., Haddad, M. J., Khurana, S., Tsang, T., et al. (2017). Can Common Serum Biomarkers Predict Complicated Appendicitis in Children? *Pediatr. Surg. Int.* 33 (7), 799–805. doi:10.1007/s00383-017-4088-1

Zeng, L., Wang, S., Lin, M., Chen, Y., Deng, Q., Zhong, H., et al. (2020). Evaluation of Time to Positivity for Blood Culture Combined with Immature Granulocytes, Neutrophil-To-Lymphocyte Ratio, and CRP in Identifying Bloodstream Coagulase-Negative Staphylococci Infection in Pediatric Patients. *J. Clin. Lab. Anal.* 34 (11), e23473. doi:10.1002/jcla.23473

Zhang, G., Hou, J., Shi, J., Yu, G., Lu, B., and Zhang, X. (2008). Soluble CD276 (B7-H3) Is Released from Monocytes, Dendritic Cells and Activated T Cells and Is Detectable in normal Human Serum. *Immunology* 123 (4), 538–546. doi:10.1111/j.1365-2567.2007.02723.x

Zvizdic, Z., Golos, A. D., Milisic, E., Jonuzi, A., Zvizdic, D., Glamoclija, U., et al. (2021). The Predictors of Perforated Appendicitis in the Pediatric Emergency Department: A Retrospective Observational Cohort Study. *Am. J. Emerg. Med.* 49, 249–252. doi:10.1016/j.ajem.2021.06.028

Conflict of Interest: The authors declare that the research was conducted in the absence of any commercial or financial relationships that could be construed as a potential conflict of interest.

Publisher's Note: All claims expressed in this article are solely those of the authors and do not necessarily represent those of their affiliated organizations, or those of the publisher, the editors and the reviewers. Any product that may be evaluated in this article, or claim that may be made by its manufacturer, is not guaranteed or endorsed by the publisher.

frontiers | Frontiers in Pharmacology

ORIGINAL RESEARCH
published: 06 April 2022
doi: 10.3389/fphar.2022.849545

Evaluation of the Clinical Effectiveness of Oseltamivir for Influenza Treatment in Children

Jianru Qin[1†], Jilei Lin[2†], Xiangfei Zhang[1], Shuhua Yuan[2], Chiyu Zhang[3] and Yong Yin[2]*

[1]NMPA Key Laboratory for Research and Evaluation of Innovative Drug, College of Life Sciences, Henan Normal University, Xinxiang, China, [2]Department of Respiratory, Shanghai Children's Medical Center Affiliated to Shanghai Jiao Tong University School of Medicine, Shanghai, China, [3]Shanghai Public Health Clinical Center, Fudan University, Shanghai, China

Objective: To estimate the clinical effectiveness of oseltamivir in children with different subtypes of influenza virus infection.

Methods: A total of 998 children with acute respiratory infection were enrolled from January to March 2018, and were divided into influenza A, influenza B, influenza A + B, and non-influenza infection (IV-negative) groups. Influenza-like symptoms and duration of fever were evaluated and compared between oseltamivir-treated and non-treated groups.

Results: There were no significant differences in the reduction in total febrile period and duration of fever from the onset of therapy between the oseltamivir treated and non-treated children infected with influenza A (p = 0.6885 for total febrile period and 0.7904 for the duration of fever from the onset of treatment), influenza B (p = 0.1462 and 0.1966), influenza A + B (p = 0.5568 and 0.9320), and IV-negative (p = 0.7631 and 0.4655). The duration of fever in children received oseltamivir therapy within 48 h was not significantly shorter than that beyond 48 h (p > 0.05). Additionally, percentages and severities of influenza-like symptoms, including headache, myalgia, fatigue, bellyache, vomiting, diarrhea, sore throat, cough, and coryza were not decreased and alleviated after treatment of oseltamivir.

Conclusion: Oseltamivir treatment does not significantly shorten the duration of fever, nor does it significantly relieve influenza-like symptoms in children with infection of influenza.

Keywords: clinical effectiveness, Oseltamivir, treatment, influenza, children

OPEN ACCESS

Edited by:
Yang Zhou,
Brown University, United States

Reviewed by:
Xiaoxia Lu,
Wuhan Medical Center for Women and Children, China
Sheng Wang,
institutes of biomedical sciences, China

***Correspondence:**
Yong Yin
yinyong9999@163.com

†These authors have contributed equally to this work

Specialty section:
This article was submitted to Obstetric and Pediatric Pharmacology, a section of the journal Frontiers in Pharmacology

Received: *06 January 2022*
Accepted: *17 March 2022*
Published: *06 April 2022*

Citation:
Qin J, Lin J, Zhang X, Yuan S, Zhang C and Yin Y (2022) Evaluation of the Clinical Effectiveness of Oseltamivir for Influenza Treatment in Children. Front. Pharmacol. 13:849545. doi: 10.3389/fphar.2022.849545

INTRODUCTION

Seasonal influenza epidemics, caused by the influenza A (H1N1 and H3N2) and influenza B viruses pose a great threat to the health of children each year (Lytras et al., 2019; Mott et al., 2021). The annual incidence rate of seasonal influenza can be up to 30% in the entire pediatric population (Esposito and Principi, 2016). Moreover, seasonal influenza infection is usually characterized by severe clinical manifestations and complications, such as rhinosinusitis, pneumonia, myocarditis, encephalitis, gastroenteritis, acute otitis media, and acute respiratory distress syndrome, resulting in considerably high hospitalization and mortality rates in children (Neuzil et al., 2000; Ferdinands et al., 2011; Antonova et al., 2012; Asseri et al., 2021; RothDiPrinzioFisher, 2021).

Currently, there are only two classes of specific antiviral drugs that have been approved for the treatment of influenza virus infections: M2-ion channel inhibitors and neuraminidase inhibitors

(NAIs) (YipSelim et al., 2018). M2-ion channel inhibitors are only effective against influenza A virus, and are rarely recommended for clinical use because most influenza strains have developed resistance to them (Toledo-Rueda et al., 2018; Vorobjev, 2021). Hence, NAIs, which include oseltamivir, zanamivir, lanimamivir, and peramivir, are the only available anti-influenza virus drugs (Zwillenberg et al., 2021). Oseltamivir is the most widely prescribed NAI and has been extensively used in the prophylaxis and treatment of both influenza A and influenza B virus infections (Davies, 2010). Additionally, oseltamivir is the most commonly used drug in children (Esposito and Principi, 2016).

Despite the fact that influenza poses a great burden on children and oseltamivir is widely used for the treatment of influenza in this population, there are few studies on the clinical efficacy of oseltamivir in children compared to adults, or on the effectiveness of oseltamivir in infection caused by the different subtypes of the influenza virus. In this study, we analyzed a large number of children who were diagnosed with influenza A, influenza B, co-infection with influenza A and influenza B (designated as influenza A + B), and non-infection with influenza A or B (designated as IV-negative) using an influenza antigen detection test kit, and who were treated with oseltamivir or not. The intensity of symptoms and duration of fever were compared to assess the efficacy of oseltamivir treatment.

METHODS

Study Design and Participants

The observational real-world study was conducted in Shanghai Children's Medical Center, a 1000-bed tertiary teaching hospital in Shanghai, China. Patients were enrolled from January 2018 to March 2018.

The criteria for enrollment in this study were formulated in accordance with the guidelines for the diagnosis and treatment of influenza issued by the Ministry of Health of China in 2011, and by the respiratory group of the Chinese Academy of Pediatrics in 2015. The inclusion criteria were children aged 0 months to 16 years with influenza-like illness (such as fever, acute upper respiratory symptoms or other systemic symptoms) or a positive rapid influenza test result who visited the outpatient department or emergency department of the hospital. No exclusion criteria were used for enrollment. Detailed patient information, including the courses of treatment, and influenza-like symptoms, such as fever, cough, coryza (sneezing, runny nose, nasal congestion), sore throat, headache, myalgia, fatigue, bellyache, vomiting, and diarrhea was recorded. Moreover, the body temperature of the children should have been measured at least two times per day (8: 00 and 20:00, body temperature <37.0°C was considered afebrile). The severity of cough and coryza was divided into four degrees: absent, mild, moderate, and severe. The white blood cell (WBC) count, blood platelet count (BPC), C-reactive protein (CRP), hemoglobin (Hb), and percentage of neutrophils (N%) were measured by routine peripheral blood examination before administration of any treatment.

Influenza Antigen Detection Test

Influenza antigens were detected in nasal and laryngeal specimens. A colloidal gold immunochromatographic assay (Wondfo Co., Ltd.) was performed for the rapid detection of influenza virus A and B antigens. This method uses highly unique monoclonal antibodies against the influenza A and B viruses. When the antigen concentration of the sample to be tested is higher than the minimum, it forms a complex with the labeled antibody, moves, and is captured by the monoclonal antibody of influenza virus nucleoprotein under the action of chromatography to form a red reaction line. The test is completed within 15–20 min. The accuracy of the colloidal gold immunochromatographic assay with virus isolation, which is considered the gold standard for influenza detection, was 90.24–92.09% for influenza A, 98.36%–99.59% for influenza B, and 87.39–90.70% for influenza A + B.

Oseltamivir is the only approved anti-influenza drug for the treatment of children. After a comprehensive analysis of the children's symptoms, age, preference, and presence of chronic diseases, children weighing <37.5 kg were treated with oral oseltamivir at a dose of 2 mg/kg, and children weighing ≥37.5 kg were treated with oral oseltamivir at a dose of 75 mg twice a day for five consecutive days. After the initial treatment, a follow-up clinical examination was conducted on days 3 and 10 to monitor the disease progression.

Statistical Analysis

Statistical analyses were performed using SPSS and GraphPad Prism version 6. Chi-square test, unpaired Student's t-test, and one-way ANOVA followed by Tukey's multiple comparison test were used for statistical comparisons and statistical analysis. Statistical differences between the two groups are indicated by *($p < 0.05$), **($p < 0.01$), ***($p < 0.001$), ****($p < 0.0001$).

RESULTS

Characteristics of the Patients

A total of 998 children with the mean age of 4.82 ± 2.73 years were enrolled in the present study. Of these, 325 were infected with influenza A virus (266 were treated with oseltamivir and 59 were not), 232 were infected with influenza B virus (172 were treated with oseltamivir and 60 were not), 51 were co-infected with influenza A and influenza B viruses (45 were treated with oseltamivir and six were not), and 390 were IV-negative (23 were treated with oseltamivir, 365 were not and two were off the record for the information of oseltamivir treatment was not available) according to the results of influenza antigen detection tests. The demographic characteristics of the children are summarized in **table 1**. The sex, average time until treatment, N% and BPC did not differ significantly among the four groups, with p values of 0.142, 0.6714, 0.2410, and 0.1135, respectively (**Table 1**). However, significant differences were observed in the age, peak body temperature (**Supplementary Figure S1**), peak body temperature over the past 24 h, WBC count, and Hb among the four groups, with p values of 0.0002, 0.0000, 0.0000, 0.0023, and 0.0163, respectively (**Table 1**).

TABLE 1 | Characteristics of children patients enrolled in this study.

		Influenza A	Influenza B	Influenza A + B	IV-Negative	*p* Value
Total No. of patients		325	232	51	390	-
Gender	No. of male	184	120	35	208	0.142
	No. of female	140	112	16	178	
Age (years, Mean ± SD)		4.50 ± 2.57	5.45 ± 2.66	4.16 ± 3.14	4.80 ± 2.77	0.0002
Time until treatment (hours, Mean ± SD)		62.28 ± 42.05	61.79 ± 36.15	61.71 ± 40.95	65.92 ± 50.25	0.6714
Temperature	Peak body temperature (°C, Mean ± SD)	39.63 ± 0.70	39.38 ± 0.60	39.63 ± 0.66	39.34 ± 0.68	0.0000
	Peak body temperature over the past 24 h	39.37 ± 0.88	39.16 ± 0.68	39.37 ± 0.86	39.08 ± 0.79	0.0000
Routine peripheral blood examination	WBC (*10^9/L)	6.98 ± 3.75	6.62 ± 3.24	7.12 ± 2.74	7.90 ± 5.20	0.0023
	N%	58.89 ± 18.66	56.52 ± 15.42	55.67 ± 17.56	56.49 ± 17.28	0.2410
	HB (g/L)	122.95 ± 10.74	125.66 ± 10.28	121.69 ± 11.41	125.05 ± 10.56	0.0163
	BPC (*10^9/L)	195.15 ± 76.67	194.07 ± 57.93	212.60 ± 79.92	205.70 ± 76.24	0.1135

Note: The genders of one child in influenza A and four children in IV-negative were off record. -: not applicable.

TABLE 2 | Comparison for the duration of fever of oseltamivir treated and non-treated children infected with different subtypes of influenza.

		Influenza A	Influenza B	Influenza A + B	IV-Negative	*p* Value
Total febrile period	Oseltamivir treated	110.29 ± 48.84 (220)	108.06 ± 38.67 (143)	101.84 ± 37.60 (37)	118.80 ± 51.74 (20)	0.5453
	Oseltamivir non-treated	113.28 ± 41.30 (50)	117.74 ± 47.61 (53)	91.20 ± 38.40 (5)	114.97 ± 55.21 (308)	0.7499
	p value	0.6885	0.1462	0.5568	0.7631	-
Duration of fever from onset of treatment	Oseltamivir treated	47.89 ± 26.34 (220)	47.33 ± 23.91 (143)	44.11 ± 22.67 (37)	44.40 ± 24.33 (20)	0.8069
	Oseltamivir non-treated	48.96 ± 22.49 (50)	52.53 ± 27.60 (53)	43.20 ± 17.96 (5)	49.48 ± 30.45 (308)	0.8502
	p value	0.7904	0.1966	0.9320	0.4655	-

Note: Data are Mean h ± SD (No. of patients)-: not applicable.

Duration of Fever

Inconsistent with the results of previous studies that oseltamivir is effective in shortening the duration of fever after the onset of treatment in influenza (Kawai et al., 2006; Groeneveld et al., 2020), our results showed that though the total febrile periods in children infected with influenza A or influenza B treated with oseltamivir were shorter than those not treated with oseltamivir, the differences were not statistically significant (p = 0.6885 for influenza A and 0.1462 for influenza B). Total febrile periods in patients of infected with A + B or IV-negative treated with oseltamivir were higher than those in patients not treated with oseltamivir (p = 0.5568 for influenza A + B, and 0.7631 for IV-negative) (**Table 2**). Furthermore, the total febrile period in influenza A treated with oseltamivir was not shorter than that in influenza B treated with oseltamivir (p = 0.6457), nor was it shorter in influenza A compared to influenza A + B (p = 0.3168), and in influenza B compared to influenza A + B (p = 0.3817).

The duration of fever from the commencement of oseltamivir therapy was also compared to assess the effectiveness of oseltamivir. There was no statistically significant difference between the oseltamivir treatment and non-treatment groups, with p values of 0.7904 (influenza A), 0.1966 (influenza B), 0.9320 (influenza A + B), and 0.4655 (IV-negative) (**Table 2**). The differences in the fever duration from the start of oseltamivir treatment between influenza A and influenza B (p = 0.8376), influenza A and influenza A + B (p = 0.4114), influenza B and influenza A + B (p = 0.4617) were not statistically significant.

Overall, oseltamivir did not shorten the duration of fever, regardless of the onset of illness or the onset of treatment.

Time From the Onset of Symptoms to the Start of Oseltamivir Treatment

Previous studies have shown that oral oseltamivir treatment should be started within 48 h of symptoms onset (Groeneveld et al., 2020). Hence, we analyzed the effect of the time from the onset of therapy on the effectiveness of oseltamivir. As shown in **Table 3**, regardless of whether treatment was initiated within or beyond 48 h, oseltamivir did not shorten the fever duration (p = 0.1186–0.9003 for the total febrile period and p = 0.0964–0.7716 for fever duration from the onset of treatment). Except the duration of fever from the onset of treatment when treatment was started beyond 48 h in children infected with influenza A (the average duration in oseltamivir treated children was 7.5 h longer than that in non-treated children), oseltamivir treatment reduced the fever period by 2–10 h in children, but there were no statistical differences (**Table 3**).

Although the percentages of children infected with influenza A and influenza B afebrile within 24 and 48 h from onset of oseltamivir treatment were higher than those of oseltamivir non-treatment, no significant difference was observed. The percentage of body temperature of children treated with

TABLE 3 | Effect of time to start of oseltamivir administration on duration of fever.

			Influenza A	Influenza B	Influenza A + B	IV-Negative	*p* Value
Total febrile period	≤48 h	Oseltamivir treated	86.18 ± 24.94 (127)	85.16 ± 28.27 (80)	85.44 ± 19.30 (25)	81.60 ± 30.74 (10)	0.9547
		Oseltamivir non-treated	93.68 ± 18.65 (31)	91.71 ± 24.89 (28)	78.00 ± 31.17 (4)	86.62 ± 34.42 (178)	0.5529
		p value	0.1186	0.2796	0.5153	0.6525	-
	>48 h	Oseltamivir treated	143.23 ± 54.01 (93)	137.14 ± 29.45 (63)	136.00 ± 43.08 (12)	156.00 ± 40.52 (10)	0.5911
		Oseltamivir non-treated	145.26 ± 47.67 (19)	146.88 ± 50.03 (25)	-(1)	153.78 ± 54.70 (130)	0.7134
		p value	0.8794	0.3706	-	0.9003	-
Duration of fever from onset of treatment	≤48 h	Oseltamivir treated	50.65 ± 22.18 (127)	50.70 ± 24.88 (80)	46.08 ± 19.10 (25)	45.60 ± 25.06 (10)	0.7356
		Oseltamivir non-treated	56.52 ± 15.60 (31)	52.29 ± 24.89 (28)	42.00 ± 19.90 (4)	52.04 ± 32.43 (178)	0.7772
		p value	0.1664	0.7716	0.6961	0.5379	-
	>48 h	Oseltamivir treated	44.13 ± 30.71 (93)	43.05 ± 21.87 (63)	40.00 ± 28.28 (12)	43.20 ± 23.52 (10)	0.9668
		Oseltamivir non-treated	36.63 ± 26.25 (19)	52.80 ± 30.36 (25)	-(1)	45.97 ± 27.13 (130)	0.1560
		p value	0.3233	0.0964	-	0.7542	-

Data are Mean h ± SD (No. of patients).-: not applicable.

TABLE 4 | Percentage of patients afebrile within 24 and 48 h from onset of treatment.

		Influenza A	Influenza B	Influenza A + B	IV-Negative
24	Oseltamivir treated	27.27% (60)	30.77% (44)	32.43% (12)	30.00% (6)
	Oseltamivir non-treated	22.00% (11)	26.42% (14)	20.00% (1)	29.22% (90)
48	Oseltamivir treated	71.36% (60 + 97)	69.23% (44 + 55)	72.97% (12 + 15)	70.00% (6 + 8)
	Oseltamivir non-treated	64.00% (11 + 21)	56.60% (14 + 16)	60.00% (1 + 2)	62.66% (90 + 103)

oseltamivir become normal within 24 h were up to 27.27–32.43% compared to 22.00–29.22% in oseltamivir non-treated groups (**Table 4**). Within 48 h, the percentages of children afebrile with oseltamivir treatment were 69.23–72.97%, which were higher than 56.6–64.00% of the oseltamivir non-treated groups (**Table 4**).

Symptoms of Influenza-Like Illness

Coryza and cough were the most common influenza-like symptoms, followed by the less common symptoms of fatigue, sore throat, headache, vomiting, bellyache, and myalgia, with diarrhea being the most common (**Supplementary Figure S2A**). The percentage of each symptom showed a decreasing trend over time (0 d, 3 d, and 10 days after treatment), and there were almost no symptoms at 10 days after treatment except for cough and coryza (**Supplementary Figures S2A–C**), indicating that influenza was in the process of resolution. Comparison of the percentage of symptoms in patients treated and not treated with oseltamivir revealed that there were no significant differences between the two groups, with the exception of diarrhea 3 days after treatment in the IV-negative group (oseltamivir treated vs. oseltamivir non-treated was 4/18 vs. 16/290, $p = 0.0216$), which indicates that oseltamivir treatment may not relieve influenza-like symptoms; conversely, it may have exacerbated some symptoms in IV-negative children (**Figure 1**).

Moreover, the severity of cough and coryza was divided into four degrees. The rate of moderate and severe coryza tended to show a decrease compared to absent and mild coryza, which tended to increase with time. There was a significant difference in the cough severity after 3 days of influenza B treatment between the oseltamivir treated group and the oseltamivir non-treated group (number of cases of absent, mild, moderate, and severe cough in the oseltamivir treated group were 39, 91, 6, and 5, respectively, whereas the number of cases of absent, mild, moderate, and severe cough in the non-treated oseltamivir were 11, 31, 14, and 2, respectively, $p = 0.0000$) (**Figure 2**). In addition, no differences were found in the severity of cough and coryza between the oseltamivir treated and non-treated groups (**Figure 2**).

Adverse Effects

Although oseltamivir is generally well tolerated, adverse effects are reported to be relatively common in patients, especially in infants and young children (Rath et al., 2015). The proportion of adverse events in children treated with oseltamivir (51/506) was significantly higher ($p = 0.0000$) than in those not treated with oseltamivir (14/490), which was consistent with previous studies (Jefferson et al., 2014). The proportions of adverse effects induced by oseltamivir were 4/23 (17.39%) in the IV-negative group, 21/266 (7.89%) in influenza A infection, 19/172 (11.05%) in influenza B infection, and 7/45 (15.56%) in influenza A + B infection, whereas in the non-treated children, adverse effects were observed in proportions of 3/365 (0.82%), 5/59 (8.47%), 6/60 (10.00%), and 0/6, respectively. There was a significant

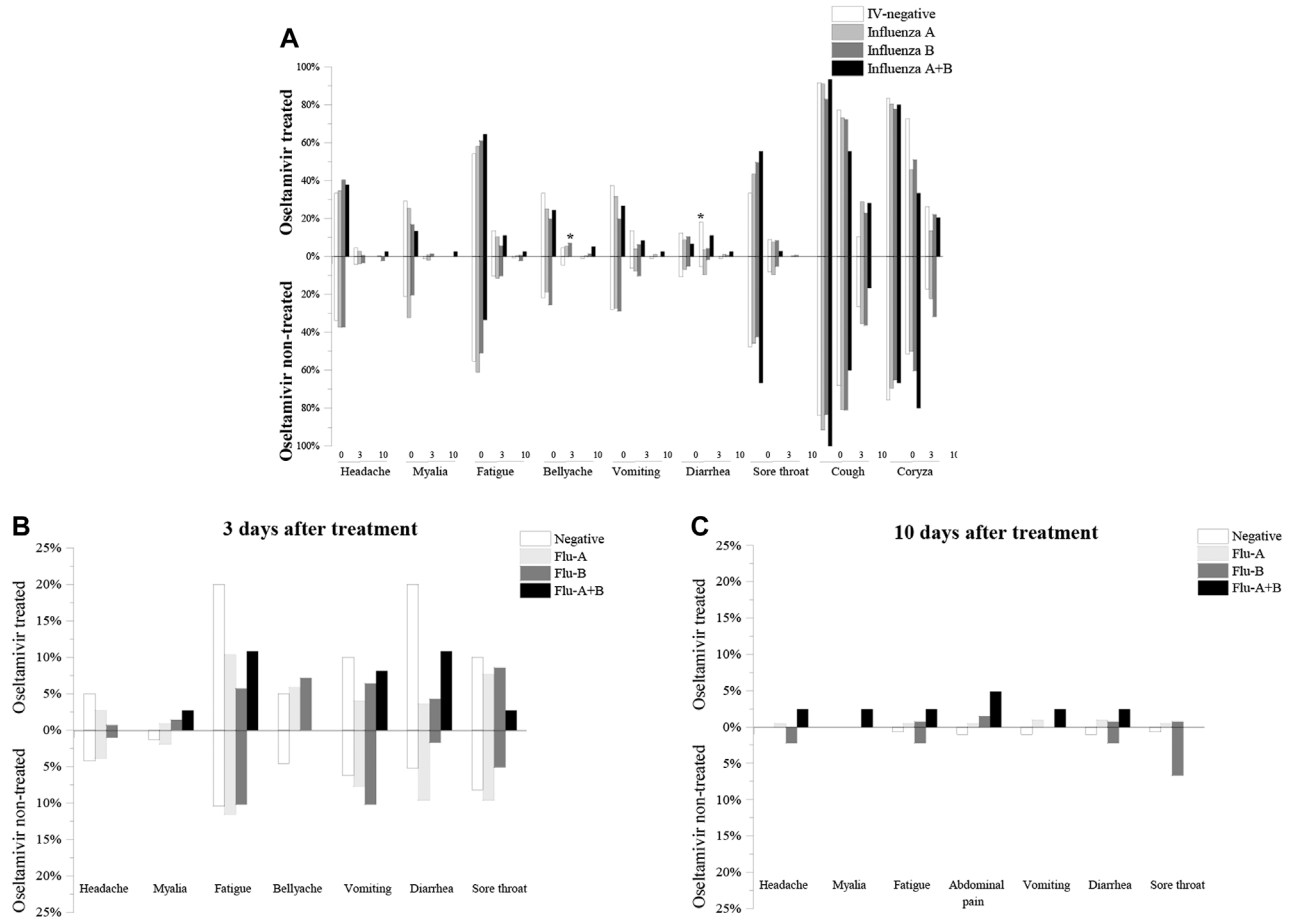

FIGURE 1 | Comparision of influenza-like symptoms of oseltamivir treated and non-treated groups. **(A)**: Percentage of influenza-like symptoms of oseltamivir treated and non-treated groups before treatment. **(B)**: Percentage of influenza-like symptoms of oseltamivir treated and untreated groups after 3 days of treatment. **(C)**: Percentage of influenza-like symptoms of oseltamivir treated and untreated groups after 10 days of treatment.

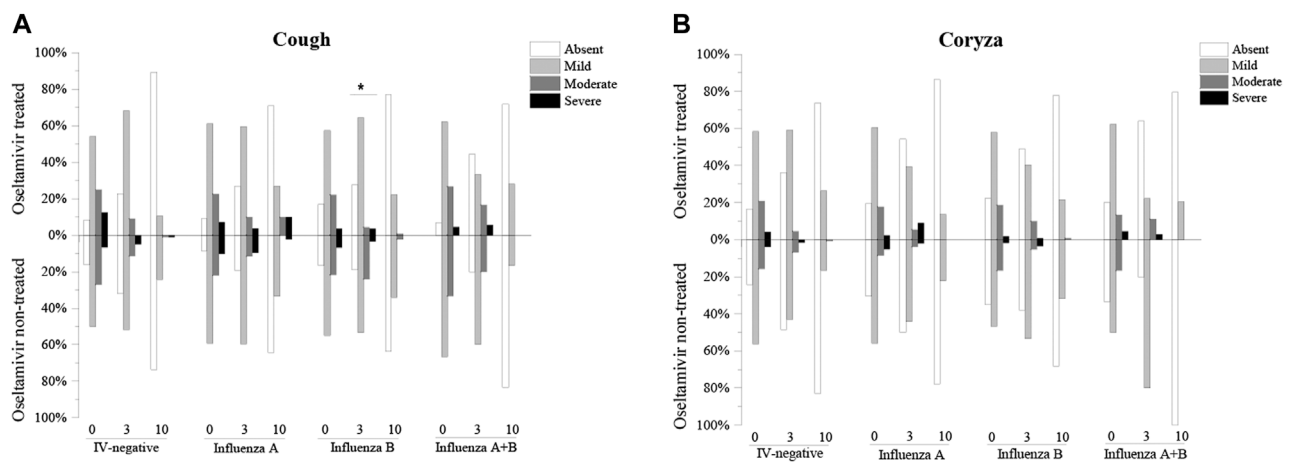

FIGURE 2 | Comparision of the severities of cough and coryza of oseltamivir treated and non-treated groups. **(A)**: Comparision of the severities of cough of oseltamivir treated and non-treated groups. **(B)**: Comparision of the severities of coryza of oseltamivir treated and non-treated groups.

TABLE 5 | Adverse effects after treatment.

	Influenza A	Influenza B	Influenza A + B	IV-Negative
Oseltamivir treated				
Total	7.89% (21)	11.05% (19)	15.56% (7)	17.39% (4)
Nausea	4.14% (11)	6.97% (12)	13.33% (6)	8.70% (2)
Bellyache	2.63% (7)	3.49% (6)	0	8.70% (2)
Others	1.13% (3)	0.58% (1)	2.22% (1)	0
Oseltamivir non-treated				
Total	8.47% (5)	10.00% (6)	0	0.82% (3)
Nausea	5.08% (3)	3.33% (2)	0	0.27% (1)
Bellyache	3.39% (2)	3.33% (2)	0	0.27% (1)
Others	0	3.33% (2)	0	0.27% (1)

Other side effects including dizziness, nosebleed, stomachache and poor appetite. Data are percentage (No. of patients).

difference ($p = 0.000$) in adverse events between the oseltamivir treated (4/23) and non-treated (3/365) children in the IV-negative group, but no significant differences were found in children with influenza A (oseltamivir treated vs. oseltamivir non-treated was 21/266 vs. 5/59, $p = 0.9071$), influenza B (19/172 vs. 6/60, $p = 0.8219$), and A + B (7/45 vs. 0/6, $p = 0.6828$). Nausea ($n = 31$) and bellyache ($n = 15$) were the most common adverse effects reported in children treated with oseltamivir, and all the adverse events were mild to moderate. Other adverse effects induced by oseltamivir, including dizziness, nosebleed, stomachache, and poor appetite, were less common. No neuropsychiatric symptoms were observed, and treatment was not prematurely withdrawn for adverse events in any patient (**Table 5**).

DISCUSSION

Although oseltamivir demonstrated excellent safety and tolerability *in vivo* (Davies, 2010), in recent years, many experts have raised doubts and controversies regarding the efficacy of oseltamivir treatment in patients with influenza, especially children. The most important reason is that there are significantly fewer studies in children than in adults, let alone studies to compare the effectiveness of oseltamivir in the treatment of different subtypes of influenza. In addition, there were some design defects in observational studies on the effect of oseltamivir, such as the number of children being too small for the analysis or the criteria of effectiveness being different for comparison. Furthermore, influenza in children can lead to multiple complications, and whether the children develop a chronic illness remains unknown. In the present study, we enrolled a large number of children who were diagnosed with an influenza-like illness, and they were divided into four groups: influenza A, influenza B, influenza A + B, and IV-negative based on the results of the influenza antigen detection test kit for the identification of the subtypes of influenza. The clinical effectiveness of oseltamivir in the treatment of different subtypes of influenza was evaluated and compared. As an observational study on the efficacy of oseltamivir, this research not only provides a large amount of data on influenza in children, but also has important implications for the management of influenza B, whose epidemiology and impact on public health are less understood and often underestimated.

The limited clinical effectiveness of oseltamivir in the treatment of influenza has been reported previously. Muthuri et al. pointed out that although NAIs treatment was associated with reduced mortality in adult patients infected with influenza A H1N1pdm09, the mortality risk was not reduced in pediatric patients (Muthuri et al., 2014). Santtu et al. demonstrated that oseltamivir could not decrease the incidence of acute otitis media even after starting therapy within 24 h. In addition, oseltamivir was been demonstrated no efficacy against influenza B infection in children (Heinonen et al., 2010). Wang et al. summarized that treatment of children with oseltamivir resulted in a reduction in the duration of the illness and alleviation of symptoms, although it did not achieve statistical significance (Wang et al., 2012). There has been much debate surrounding the efficacy of oseltamivir, including the lack of significant therapeutic effect on the incidence of pneumonia, sinusitis, bronchitis, and otitis media (Heinonen et al., 2010; Toovey et al., 2012; Wang et al., 2012; Jefferson et al., 2014; Muthuri et al., 2014). In accordance with the previous studies, although there were no significant differences between the oseltamivir treated and non-treated groups in the present study, oseltamivir therapy showed a trend towards reducing the duration of fever in children infected with influenza A and influenza B (no. of children not treated with oseltamivir was five, which is too small for statistical analysis). In terms of the symptom relieving effects, oseltamivir treatment and non-treatment groups were comparable. Whether the safety of oseltamivir treatment is greater than its effectiveness has also been questioned. Nguyen reported the case of a 14-year-old girl who was treated with oseltamivir, and developed systemic lupus erythematosus, systemic vasculitis, chronic pancreatitis, and eventually died of the complications (Nguyen et al., 2010). In addition, psychiatric side effects after oseltamivir treatment are more common in children than in adults (JhonKimKangKimLeeKim, 2021). Influenza viruses mutate easily, and there is little treatment for oseltamivir-resistant influenza (HanpaiboolLeelawiwatTakahashiRungrotmongkol, 2021; Macesic et al., 2021).

Considering the fact that oseltamivir has no significant effect on the treatment of influenza in the clinic and the high rate of side effects in children, it is important to identify suitable antiviral alternatives. Favipiravir (T-705), an inhibitor of viral RNA polymerase, has been proven to be effective in the treatment

of influenza viruses, including NAI-resistant variants, and is also a potential drug for treating Ebola virus disease virus (EVD) and severe acute respiratory syndrome coronavirus type 2 (SARS-cov-2) (FangHuangLiChengTanLiu, 2020; DziedziejkoPawlik, 2021). Baloxavir marboxil (baloxavir), a novel influenza cap-dependent inhibitor of endonuclease-selective polymerase acidic protein, has shown clinical efficacy in rapidly reducing the viral load, shortening the duration of fever, and relieving symptoms (Chong et al., 2021; Portsmouth et al., 2021). In addition, compared to the ineffectiveness of NAIs, the efficacy of single and combined use of favipiravir was excellent *in vivo* (Imai et al., 2017; Wang et al., 2020). However, these antiviral drugs are still approved for restricted use or clinical trials in some countries. In addition to anti-influenza drugs, the usefulness of influenza vaccines cannot be overemphasized. Influenza vaccination in susceptible children has been shown to be an effective measure for preventing influenza virus infection, but a "Universal" vaccine with a broad spectrum of protection needs to be developed due to rapid viral mutations (Rolfes et al., 2019; Niang et al., 2021).

This study has some limitations, which must be noted. First, it was performed in a general practice setting instead of in the context of a rigorous clinical protocol. Second, the number of children infected with the different subtypes of the influenza virus varied greatly, as did the number of oseltamivir treated and non-treated children, especially the number of non-treated children infected with influenza A + B, which was too small for statistical analysis. Third, the administration of oseltamivir within 48 h referred to less than 48 h from the onset of fever, instead of the onset of symptoms. It is difficult for infants and young children (aged <2 years) to express the onset of symptoms. Hence, fever, as an important indicator of influenza, can be detected by the measurement of temperature and is much more accurate and convenient to record. Nonetheless, therapy within 48 h from the onset of fever does not mean it was within 48 h from the onset of symptoms, unless fever was the first symptom. In addition, although a lot of efforts had been made to collect children raw data, there are still some gaps. For example, we collected 325 children infected with influenza A, but in terms of statistics of duration of fever, only 270 children were counted, partly because several children were afebrile (n = 1), and partly because of the lack of original data (n = 54). And we displayed the number to statistics in brackets in each table to solve this problem. It is worth mentioning that the data presented here showed that oseltamivir has no significant effect on relieving influenza-like symptoms, instead of in treating influenza. In this study, we did not perform assay on influenza virus isolation or virus resistance. Hence, the role of oseltamivir in reducing viral particle release is hard to clarify in this study. Data of children from 2018 influenza epidemic season was analyzed in this study, more data and other influenza epidemic seasons should be collected for further studies to verify the conclusion.

In conclusion, the evidence presented in this research shows that the duration of fever in children with influenza virus infection was not reduced by the administration of oseltamivir. Moreover, influenza-like symptoms were not relieved, and the severity of cough and coryza was not improved by administering oseltamivir.

DATA AVAILABILITY STATEMENT

The original contributions presented in the study are included in the article/**Supplementary Material**, further inquiries can be directed to the corresponding author.

ETHICS STATEMENT

The studies involving human participants were reviewed and approved by Shanghai Children's Medical Center (Grant No. SCMCIRB-W2021063). Written informed consent to participate in this study was provided by the participants' legal guardian/next of kin.

AUTHOR CONTRIBUTIONS

JQ, JL, SY and YY designed the study; JQ, JL, XZ, and CZ analyzed the data; JQ, JL, XZ and CZ wrote the paper; JQ and XZ performed statistical analysis. CZ and YY offered suggestions; all authors read and approved the final manuscript.

FUNDING

This work was supported by the National Natural Science Foundation of China (Grant No. 32000125) and the doctoral scientific research foundation of Henan Normal University (Grant No. 5101049170188).

ACKNOWLEDGMENTS

We thank Honglian Liu for preprocessing of the data.

SUPPLEMENTARY MATERIAL

The Supplementary Material for this article can be found online at: https://www.frontiersin.org/articles/10.3389/fphar.2022.849545/full#supplementary-material

Supplementary Figure S1 | Peak body temperatures of children with infection of influenza A, influenza B, influenza A+B, and IV negative.

Supplementary Figure S2 | Percentage of influenza-like symptoms before and after oseltamivir treatment. **(A)**: Percentage of influenza like symptoms before oseltamivir treatment. **(B)**: Percentage of influenza like symptoms after 3 days of oseltamivir treatment. **(C)**: Percentage of influenza like symptoms after 10 days of oseltamivir treatment.

Supplementary Figure S3 | The severity of cough and coryza before and after oseltamivir treatment. **(A)**: Cough severity before and after 3 and 10 days of oseltamivir treatment. **(B)**: Coryza severity before and after 3 and 10 days of oseltamivir treatment.

REFERENCES

Antonova, E. N., Rycroft, C. E., Ambrose, C. S., Heikkinen, T., and Principi, N. (2012). Burden of Paediatric Influenza in Western Europe: a Systematic Review. *Bmc Public Health* 12, 968. doi:10.1186/1471-2458-12-968

Asseri, A. A., Shati, A. A., Al-Qahtani, S. M., Alzaydani, I. A., Al-Jarie, A. A., Alaliani, M. J., et al. (2021). Distinctive Clinical and Laboratory Features of COVID-19 and H1N1 Influenza Infections Among Hospitalized Pediatric Patients. *World J. Pediatr.* 17 (3), 272–279. doi:10.1007/s12519-021-00432-1

Chong, Y., Kawai, N., Tani, N., Bando, T., Takasaki, Y., Shindo, S., et al. (2021). Virological and Clinical Outcomes in Outpatients Treated with Baloxavir or Oseltamivir: A Japanese Multicenter Study in the 2019-2020 Influenza Season. *Antivir. Res* 192, 105092. doi:10.1016/j.antiviral.2021.105092

Davies, B. E. (2010). Pharmacokinetics of Oseltamivir: an Oral Antiviral for the Treatment and Prophylaxis of Influenza in Diverse Populations. *J. Antimicrob. Chemother.* 65 Suppl 2, II5–II10. doi:10.1093/jac/dkq015

Esposito, S., and Principi, N. (2016). Oseltamivir for Influenza Infection in Children: Risks and Benefits. *Expert Rev. Respir. Med.* 10 (1), 79–87. doi:10.1586/17476348.2016.1126182

Fang, Q. Q., Huang, W. J., Li, X. Y., Cheng, Y. H., Tan, M. J., Liu, J., et al. (2020). Effectiveness of Favipiravir (T-705) against Wild-type and Oseltamivir-Resistant Influenza B Virus in Mice. *Virology* 545, 1–9. doi:10.1016/j.virol.2020.02.005

Ferdinands, J. M., Denison, A. M., Dowling, N. F., Jost, H. A., Gwinn, M. L., Liu, L., et al. (2011). A Pilot Study of Host Genetic Variants Associated with Influenza-Associated Deaths Among Children and Young Adults. *Emerg. Infect. Dis.* 17 (12), 2294–2302. doi:10.3201/eid1712.111002

Groeneveld, G. H., Marbus, S. D., Ismail, N., de Vries, J. J. C., Schneeberger, P., Oosterheert, J. J., et al. (2020). Effectiveness of Oseltamivir in Reduction of Complications and 30-day Mortality in Severe Seasonal Influenza Infection. *Int. J. Antimicrob. Agents* 56 (5), 106155. doi:10.1016/j.ijantimicag.2020.106155

Hanpaibool, C., Leelawiwat, M., Takahashi, K., and Rungrotmongkol, T. (2020). Source of Oseltamivir Resistance Due to Single E119D and Double E119D/H274Y Mutations in pdm09H1N1 Influenza Neuraminidase. *J. Comput. Aided Mol. Des.* 34 (1), 27–37. doi:10.1007/s10822-019-00251-7

Heinonen, S., Silvennoinen, H., Lehtinen, P., Vainionpää, R., Vahlberg, T., Ziegler, T., et al. (2010). Early Oseltamivir Treatment of Influenza in Children 1-3 Years of Age: A Randomized Controlled Trial. *Clin. Infect. Dis.* 51 (8), 887–894. doi:10.1086/656408

Imai, M., Watanabe, T., Kiso, M., Nakajima, N., Yamayoshi, S., Iwatsuki-Horimoto, K., et al. (2017). A Highly Pathogenic Avian H7N9 Influenza Virus Isolated from A Human Is Lethal in Some Ferrets Infected via Respiratory Droplets. *Cell Host Microbe* 22 (5), 615–e8. doi:10.1016/j.chom.2017.09.008

Jefferson, T., Jones, M., Doshi, P., Spencer, E. A., Onakpoya, I., and Heneghan, C. J. (2014). Oseltamivir for Influenza in Adults and Children: Systematic Review of Clinical Study Reports and Summary of Regulatory Comments. *BMJ* 348, g2545. doi:10.1136/bmj.g2545

Jhon, M., Kim, J.-W., Kang, H.-J., Kim, S.-Y., Lee, J.-Y., Kim, S.-W., et al. (2021). Delayed Onset of Manic Symptoms in a Patient with Influenza A (H1N1) after Administration of Oseltamivir (Tamiflu): A Case Report. *Clin. Psychopharmacol. Neurosci.* 19 (1), 166–169. doi:10.9758/cpn.2021.19.1.166

Kawai, N., Ikematsu, H., Iwaki, N., Maeda, T., Satoh, I., Hirotsu, N., et al. (2006). A Comparison of the Effectiveness of Oseltamivir for the Treatment of Influenza A and Influenza B: A Japanese Multicenter Study of the 2003-2004 and 2004-2005 Influenza Seasons. *Clin. Infect. Dis.* 43 (4), 439–444. doi:10.1086/505868

Łagocka, R., Dziedziejko, V., Kłos, P., and Pawlik, A. (2021). Favipiravir in Therapy of Viral Infections. *Jcm* 10 (2), 273. doi:10.3390/jcm10020273

Lytras, T., Pantavou, K., Mouratidou, E., and Tsiodras, S. (2019). Mortality Attributable to Seasonal Influenza in Greece, 2013 to 2017: Variation by Type/subtype and Age, and a Possible Harvesting Effect. *Euro Surveill.* 24 (14), 11–20. doi:10.2807/1560-7917.ES.2019.24.14.1800118

Macesic, N., Laplante, J. M., Aaron, J. G., DiMango, E. A., Miko, B. A., Pereira, M. R., et al. (2021). Baloxavir Treatment of Oseltamivir-Resistant Influenza A/H1pdm09 in Two Immunocompromised Patients. *Transpl. Infect. Dis.* 23 (3), e13542. doi:10.1111/tid.13542

Mott, J. A., Fry, A. M., Kondor, R., Wentworth, D. E., and Olsen, S. J. (2021). Re-emergence of Influenza Virus Circulation during 2020 in Parts of Tropical Asia: Implications for Other Countries. *Influenza Other Respir. Viruses* 15 (3), 415–418. doi:10.1111/irv.12844

Muthuri, S. G., Venkatesan, S., Myles, P. R., Leonardi-Bee, J., Al Khuwaitir, T. S., Al Mamun, A., et al. (2014). Effectiveness of Neuraminidase Inhibitors in Reducing Mortality in Patients Admitted to Hospital with Influenza A H1N1pdm09 Virus Infection: a Meta-Analysis of Individual Participant Data. *Lancet Respir. Med.* 2 (5), 395–404. doi:10.1016/S2213-2600(14)70041-4

Neuzil, K. M., Mellen, B. G., Wright, P. F., Mitchel, E. F., Jr., and Griffin, M. R. (2000). The Effect of Influenza on Hospitalizations, Outpatient Visits, and Courses of Antibiotics in Children. *N. Engl. J. Med.* 342 (4), 225–231. doi:10.1056/NEJM200001273420401

Nguyen, H. T., Fry, A. M., Loveless, P. A., Klimov, A. I., and Gubareva, L. V. (2010). Recovery of a Multidrug-Resistant Strain of Pandemic Influenza A 2009 (H1N1) Virus Carrying a Dual H275Y/I223R Mutation from a Child after Prolonged Treatment with Oseltamivir. *Clin. Infect. Dis.* 51 (8), 983–984. doi:10.1086/656439

Niang, M. N., Sugimoto, J. D., Diallo, A., Diarra, B., Ortiz, J. R., Lewis, K. D. C., et al. (2021). Estimates of Inactivated Influenza Vaccine Effectiveness Among Children in Senegal: Results from 2 Consecutive Cluster-Randomized Controlled Trials in 2010 and 2011. *Clin. Infect. Dis.* 72 (12), E959–E969. doi:10.1093/cid/ciaa1689

Portsmouth, S., Hayden, F. G., Kawaguchi, K., Ishibashi, T., Kinoshita, M., Shishido, T., et al. (2021). Baloxavir Treatment in Adolescents with Acute Influenza: Subgroup Analysis from the CAPSTONE-1 Trial. *J. Pediatr. Infect Dis Soc* 10 (4), 477–484. doi:10.1093/jpids/piaa145

Rath, B. A., Blumentals, W. A., Miller, M. K., Starzyk, K., Tetiurka, B., and Wollenhaupt, M. (2015). A Prospective Observational Study of Oseltamivir Safety and Tolerability in Infants and Young Children ≤24 months. *Pharmacoepidemiol. Drug Saf.* 24 (3), 286–296. doi:10.1002/pds.3707

Rolfes, M. A., Flannery, B., Chung, J. R., O'Halloran, A., Garg, S., Belongia, E. A., et al. (2019). Effects of Influenza Vaccination in the United States during the 2017-2018 Influenza Season. *Clin. Infect. Dis.* 69 (11), 1845–1853. doi:10.1093/cid/ciz075

Roth, T., DiPrinzio, D., and Fisher, J. D., Rapid and Severe Neurologic Deterioration Due to Influenza Associated Encephalopathy in a Healthy Child. *Am. J. Emerg. Med.*, 2021. 45: 687. e1-687. DOI: doi:10.1016/j.ajem.2020.12.081

Toledo-Rueda, W., Rosas-Murrieta, N. H., Muñoz-Medina, J. E., González-Bonilla, C. R., Reyes-Leyva, J., and Santos-López, G. (2018). Antiviral Resistance Markers in Influenza Virus Sequences in Mexico, 2000-2017. *Infect. Drug Resist.* 11, 1751–1756. doi:10.2147/IDR.S153154

Toovey, S., Prinssen, E. P., Rayner, C. R., Thakrar, B. T., Dutkowski, R., Koerner, A., et al. (2012). Post-marketing Assessment of Neuropsychiatric Adverse Events in Influenza Patients Treated with Oseltamivir: An Updated Review. *Adv. Ther.* 29 (10), 826–848. doi:10.1007/s12325-012-0050-8

Vorobjev, Y. N. (2021). An Effective Molecular Blocker of Ion Channel of M2 Protein as Anti-influenza a Drug. *J. Biomol. Struct. Dyn.* 39 (7), 2352–2363. doi:10.1080/07391102.2020.1747550

Wang, K., Shun-Shin, M., Gill, P., Perera, R., and Harnden, A. (2012). Neuraminidase Inhibitors for Preventing and Treating Influenza in Children (Published Trials Only). *Cochrane Database Syst. Rev.* (4), CD002744. doi:10.1002/14651858.CD002744.pub4

Wang, Y., Fan, G., Salam, A., Horby, P., Hayden, F. G., Chen, C., et al. (2020). Comparative Effectiveness of Combined Favipiravir and Oseltamivir Therapy versus Oseltamivir Monotherapy in Critically Ill Patients with Influenza Virus Infection. *J. Infect. Dis.* 221 (10), 1688–1698. doi:10.1093/infdis/jiz656

Yip, T. F., Selim, A. S. M., Lian, I., and Lee, S. M. (2018). Advancements in Host-Based Interventions for Influenza Treatment. *Front. Immunol.* 9, 1547. doi:10.3389/fimmu.2018.01547

Zwillenberg, M., Tang, E., and Quaas, J. (2021). Neuraminidase Inhibitors for Treatment of Influenza. *Acad. Emerg. Med.* 28 (10), 1195–1197. doi:10.1111/acem.14241

Conflict of Interest: The authors declare that the research was conducted in the absence of any commercial or financial relationships that could be construed as a potential conflict of interest.

Publisher's Note: All claims expressed in this article are solely those of the authors and do not necessarily represent those of their affiliated organizations, or those of the publisher, the editors and the reviewers. Any product that may be evaluated in this article, or claim that may be made by its manufacturer, is not guaranteed or endorsed by the publisher.

frontiers | Frontiers in Pharmacology

ORIGINAL RESEARCH
published: 27 April 2022
doi: 10.3389/fphar.2022.864058

Metabolomic Differential Compounds Reflecting the Clinical Efficacy of Polyethylene Glycol Recombinant Human Growth Hormone in the Treatment of Childhood Growth Hormone Deficiency

Ji Li[1†], *Weiwei Pan*[2†], *Jianqin Qian*[1], *Yan Ni*[3], *Junfen Fu*[3,4*] *and Shaoqing Ni*[1,5*]

[1]National Clinical Trial Institute, The Children's Hospital, Zhejiang University School of Medicine, National Clinical Research Center for Child Health, Hangzhou, China, [2]Department of Pharmacy, Children's Hospital, Zhejiang University School of Medicine, Hangzhou, China, [3]The Children's Hospital, Zhejiang University School of Medicine, National Clinical Research Center for Child Health, Hangzhou, China, [4]Department of Endocrinology, Children's Hospital, Zhejiang University School of Medicine, Hangzhou, China, [5]Research Center for Clinical Pharmacy, Zhejiang University, Hangzhou, China

Understanding metabolite profiles may aid in providing a reference for individualized treatment using PEG-rhGH. Therefore, this study aimed to evaluate the clinical efficacy of PEG-rhGH in treating GHD patients by using a metabolomic approach. Fifty-seven pediatric participants treated with PEG-rhGH were enrolled (28 GHD patients with high clinical efficacy and 29 GHD patients with lower clinical efficacy). Serum samples from all patients were first collected at baseline for biochemical detection; then metabolite levels were measured using gas chromatography time-of-flight mass spectrometry. The candidates included heptadecanoic acid, stearic acid, 2-hydroxybutyric acid, myristic acid, palmitoleic acid, D-galactose, dodecanoic acid, and oleic acid. The related metabolic pathways involved fatty acid metabolism and energy metabolism. This study suggested that growth gains of PEG-rhGH treatment might be differentiated by altered serum levels of fatty acid. Collectively, the metabolomic study provides unique insights into the use of PEG-rhGH as a therapeutic strategy for individualized treatment.

Keywords: growth hormone deficiency, PEG-rhGH, metabolomics, clinical efficacy, biomarkers

OPEN ACCESS

Edited by:
Jian Gao,
Shanghai Children's Medical Center, China

Reviewed by:
Huiwen Zhang,
Xinhua Hospital, China
Liwei Xie,
Guangdong Institute of Microbiology, China

***Correspondence:**
Junfen Fu
fjf68@zju.edu.cn
Shaoqing Ni
chnsq@zju.edu.cn

[†]*These authors have contributed equally to this work and share first authorship*

Specialty section:
This article was submitted to Obstetric and Pediatric Pharmacology, a section of the journal Frontiers in Pharmacology

Received: *28 January 2022*
Accepted: *04 April 2022*
Published: *27 April 2022*

Citation:
Li J, Pan W, Qian J, Ni Y, Fu J and Ni S (2022) Metabolomic Differential Compounds Reflecting the Clinical Efficacy of Polyethylene Glycol Recombinant Human Growth Hormone in the Treatment of Childhood Growth Hormone Deficiency. Front. Pharmacol. 13:864058. doi: 10.3389/fphar.2022.864058

INTRODUCTION

The prevalence of growth hormone deficiency (GHD) in children is on the rise worldwide. The focus on children's health is more urgent owing to their estimated greater vulnerability (Jee et al., 2017; Murray et al., 2018; Halas and Grimberg, 2020). GHD is a developmental disorder caused by either partial or complete deficiency in the synthesis and secretion of growth hormone in the anterior pituitary lobe or by receptor defects and structural abnormalities. Growth failure, the primary apparent feature of GHD, may influence the life quality and psychosocial development of affected children (Chaplin et al., 2015; Chinoy and Murray, 2016; Leonibus et al., 2016). As recorded in recent pharmaceutical studies, recombinant human growth hormone (rhGH) showed a significant therapeutic effect against growth hormone deficiency (Rogol et al., 2013). To achieve this effect, rhGH is required to be administered as a daily injection (López-Siguero et al., 2011; Wit et al., 2013).

Frequent injections cause distress to the children and therefore reduce compliance. PEG-rhGH preparation is a covalent conjugate of rhGH and branched polyethylene glycol (PEG), which can potentially increase the molecular weight of rhGH, reduce drug toxicity and prolong the half-life of elimination *in vivo* (Cutfield et al., 2011; Rogol et al., 2013; Lundberg et al., 2018; Wang et al., 2021). The treatment of polyethylene glycol-modified long-acting rhGH (PEG-rhGH) requires only weekly injections, which can reduce the frequency of injections and can enhance children's compliance with rhGH treatment.

However, to the best of our knowledge, relatively little is known about the metabolic changes that are associated with differences in clinical efficacy of PEG-rhGH replacement therapy (Rasmussen et al., 2010; Schepper et al., 2011; Hou et al., 2015). Therefore, it is of interest to find predictive biological metabolites for monitoring individual responses to PEG-rhGH therapy. Metabolomics has stood out for providing rapid, sensitive, and less invasive analyses that identify and quantify endogenous metabolites present in different biological matrices (McBride et al., 2019). Studies on the disease diagnosis and treatment of rhGH by metabolomics have been reported in recent years (Rahman et al., 2013; Höybye et al., 2014; Xu et al., 2019). Research in 10 adults with GHD demonstrated that the level of serum metabolite was altered in GHD patients and that some specific fatty acid compounds and amino acids had the potential ability to be biomarkers for GHD. (Höybye et al., 2014). Metabolomics may be a powerful method for studying the clinical efficacy of PEG-rhGH intervention in improving GHD. This kind of improvement will be particularly useful for the pediatric population.

The primary objectives of the present study were to investigate the associations between clinical efficacy and metabolites in GHD children treated with PEG-rhGH and to find biomarkers and related metabolic pathways by metabolomic techniques, which are expected to provide a reference for the individualized treatment of PEG-rhGH.

MATERIAL AND METHODS

Patients and Samples

The present study was conducted on the basis of the multi-center drug clinical study project "Phase IV clinical trial of polyethylene glycol-recombinant human growth hormone injection in treating children growth hormone deficiency" led by the Children's Hospital, Zhejiang University School of Medicine, which was registered at www.clinicaltrials.gov (NCT02314676). Sixty subjects with different clinical efficacies of PEG-rhGH treatment were randomly screened from the established PEG-rhGH phase IV clinical trial database, and three of these subjects were excluded due to incomplete data. The study was approved by the Ethics Committee of the Children's Hospital, Zhejiang University School of Medicine and was conducted in accordance with the Declaration of Helsinki. All patients provided written informed consent (2018-IRB-033). The actual height of the patients after treatment was compared with the mean height of the population and its standard deviation (SD) of height for a chronological age, which was considered the primary outcome measure (△Ht SDS). The mean and SD value for height were calculated using reference values with The National Growth Survey of Children under 7 years in the Nine Cities of China in 2005. Patients were divided into two groups using the median △Ht SDS as a cutoff: △Ht SDS >0.44 (high clinical efficacy (HE) group, n = 28), and △Ht SDS ≤0.44 (low clinical efficacy (LE) group, n = 29). Patient inclusion criteria were as follows: diagnosed as GHD based on medical history, clinical symptoms, and signs; GH activation test and imaging criteria before treatment (height below the third percentile of the normal growth curve for children of the same age and sex at age of 2–18, rate of height increase ≤5.0 cm year^{-1}, two-drug GH stimulation tests with different mechanisms of action confirmed that the plasma GH peak was less than 10.0 ng ml^{-1}, for girls ≤9 years old and boys ≤10 years old, the bone age is more than 1 year behind the actual age, that is, the actual age minus bone age ≥1 year); pre-pubertal stage (Tanner I stage), age ≥3 years old, gender is not limited; did not receive growth hormone therapy within 6 months; and the subject is willing and able to complete the scheduled interview, treatment plan, laboratory examination and other procedures, and to sign a written informed consent. Exclusion criteria were as follows: abnormal liver and kidney function (ALT > two times the upper limit of normal (ULN), Cr > ULN); hepatitis B virus detection of HBc, HBsAg, and HBeAg were all positive; subjects with allergy constitution or allergy to the drug; subjects with severe CVD, lung diseases, hematological diseases, malignant cancer, systemic infections or a compromised immune system; subjects with underlying cancer (family history of cancer); subjects with diabetes; abnormal growth and development, such as Turner's Syndrome, constitute delay of puberty; Laron Syndrome; growth hormone receptor deficiency; girls with short stature with chromosomal abnormalities; subjects participated in drug clinical trials within 3 months; subjects with positive anti-hGH antibodies; and other conditions that the investigator considers unsuitable for inclusion in this clinical trial.

Sample Preparation

The metabolomic samples were analyzed with residual serum samples of IGF-1 and IGF-BP3 from 57 cases for freeze-thaw frequency less than 3 times. Samples were thawed at 4°C and were mixed adequately before analysis with chemical derivatization. A 50 μl aliquot of serum sample was spiked with 10 μl internal standard solutions (chlorophenyl alanine) and was vortexed for 10 s. The mixed solution was deproteinized using 200 μl of the extraction solvent (methanol: chloroform = 3:1 [v/v]). After 30 s of vertex, the samples were centrifuged at 13,500 rpm for 20 min at 4°C. A 200 μl supernatant was transferred to an autosampler vial, all samples in autosampler vials were evaporated by CentriVap vacuum concentrator for 5 min, and then they were further lyophilized with a cryogenic freeze-dryer (Labconco, Kansas City, Mo, United States). After the samples were vacuum-dried at room temperature under nitrogen, 50 μl of methoxyamine (20 mg ml^{-1} in pyridine) was added to each

vial and kept at 30°C for 120 min, followed by 50 μl of MSTFA at 37.5°C for 60 min. This silylated derivation was performed using a Gerstel multipurpose sample MPS2 with dual heads (Gerstel GmbH and Co., Mulheim, Germany), and the derived samples were automatically injected into GC/TOFMS for metabolomics analysis.

GC-TOFMS Analysis

Serum metabolite profile was acquired by time-of-flight mass spectrometry system (Pegasus HT, Leco Corp., St. Joseph, MO, United States) coupled with gas chromatography (Agilent 7890B, Santa Clara, CA, United States). The chromatographic separation of the serum sample was performed on an Rxi-5MS capillary column (30 m × 250 μm I.D., 0.25 μm). The column flow rate was set at 1.0 ml min^{-1}, and helium was used as the carrier gas. The temperature programs were set up as follows: 80°C hold on for 2 min, then raised to 300°C at a rate of 12°C·min^{-1} for 4.5 min, and finally to 320°C at a rate of 40°Cmin^{-1} for 1 min. The temperatures for front injection, transfer line, and ion source were 270, 270, and 220°C, respectively. Electron impact ionization of 70 eV in the scan range (50–550 Da) was applied, and the acquisition rate was 20 spectra s^{-1}. The instrument was optimized and maintained every 24 h to monitor its stability.

GC-TOFMS Data Processing and Statistical Analysis

Raw data from GC/TOFMS analysis were processed using ChromaTOF software (v4.51.6.0, Leco., CA, United States) to achieve the following elements of preprocessing: baseline correction and smoothing, deconvolution, extraction, and alignment of original chromatographic peak signals, retention index correction, and metabolite identification using standard materials. The self-developed platform iMAP (v1.0, Metabo-Profile, Shanghai, China) was used for statistical analyses, including data preprocessing (normalization and standardization), statistical analysis (multidimensional statistical analysis and one-dimensional statistical analysis), metabolic network analysis, and reporting. Following preprocessing, the data were presented as mean ± standard deviation (SD). The *p*-value of 0.05 was considered to indicate statistical significance. The SIMCA 14.1 software (MKS Data Analytics Solutions, Umea, Sweden) was applied for principal component analysis (PCA) and orthogonal partial least squares discriminant analysis (OPLS-DA). Permutation tests were performed with 200 iterations to validate the model. The features were filtered initially by variable importance in the projection (VIP) value (VIP > 1) and fold change value (FC > 1) in the comparison of HE and LE patient groups. The Mann-Whitney *U* test was applied to assess the significant difference of these features between the groups. Differential serum metabolites were selected by considering VIP (>1.0), FC (>1.0) and *p*-value (<0.05). The receiver-operating characteristic (ROC) analysis was used to evaluate the specificity and sensitivity of potential biomarkers according to the area under the curve (AUC).

TABLE 1 | Baseline clinical characteristics.

Item	LE group	HE group	[a]FC	[b]*p*
[d]BHEIGHT (cm)	119.27 (13.79)	108.19 (10.12)	0.877	1.10×10^{-3}
HEIGHT (cm)	121.8 (13.19)	110.98 (10.56)	0.885	1.70×10^{-3}
WEIGHT (kg)	25.8 (7.38)	20.18 (5.96)	0.738	2.90×10^{-3}
BONE AGE	6.81 (2.53)	4.79 (2.15)	0.571	3.30×10^{-3}
AGE (year)	11.93 (2.79)	10 (2.29)	0.833	6.70×10^{-3}
BMI	16.99 (2.38)	16.06 (2.24)	0.920	0.067
[c]SEX_STD	1.19 (0.40)	1.3 (0.47)	1.000	0.486
Liver function				
PHOS (mmol/L)	1.57 (0.19)	1.56 (0.16)	1.039	0.947
ALP (IU/L)	219.93 (71.59)	226.76 (58.69)	1.138	0.344
TBIL (μmol/L)	8.41 (5.34)	7.92 (2.95)	1.054	0.966
ALT (IU/L)	15.14 (6.02)	17.02 (7.76)	1.100	0.321
AST (IU/L)	29 (8.42)	31.17 (7.30)	1.089	0.174
ALB (g/L)	44.06 (2.96)	43.56 (2.63)	1.023	0.566
TP (g/L)	70.14 (3.95)	66.95 (4.82)	0.973	1.50×10^{-2}
Renal function				
SG	1.02 (0.01)	1.02 (0.00)	1.001	0.611
BUN (mmol/L)	4.58 (0.97)	4.86 (1.25)	0.980	0.457
PH	6.4 (0.86)	6.25 (0.74)	0.923	0.442
CR (μmol/L)	47.93 (7.81)	41.24 (12.94)	0.856	1.80×10^{-2}
UWBC	1.05 (1.09)	1.38 (1.85)	1.000	0.890
URBC	2.1 (2.31)	2.24 (3.46)	0.763	0.489
Blood lipid				
TG (mmol/L)	0.91 (0.62)	0.84 (0.34)	1.013	0.954
TC (mmol/L)	4.09 (0.68)	4.29 (0.99)	1.040	0.915
HDL (mmol/L)	1.52 (0.28)	1.45 (0.30)	0.980	0.561
LDL (mmol/L)	2.25 (0.54)	2.48 (0.77)	1.039	0.448
Blood glucose and hormone				
HBA1C (%)	5.26 (0.34)	5.31 (0.40)	1.000	0.574
GLU (mmol/L)	5.04 (1.06)	4.81 (0.40)	0.966	0.476
CORT (nmol/L)	97.68 (139.49)	130.75 (223.92)	1.196	0.634
ACTH (pmol/L)	31.63 (26.69)	25.25 (18.18)	1.043	0.595
INS (mIU/L)	14 (22.22)	9.27 (8.01)	0.805	0.574
Thyroid				
TSH (mIU/L)	2.91 (1.20)	2.81 (1.63)	0.936	0.560
T3 (nmol/L)	1.82 (0.49)	2.03 (0.50)	1.319	0.057
T4 (nmol/L)	70.07 (51.35)	82.65 (51.77)	1.135	0.242
Blood routine				
RBC (× 10^{12}/L)	4.7 (0.40)	4.62 (0.41)	0.951	0.212
WBC (× 10^{9}/L)	7.27 (2.16)	6.89 (2.28)	0.949	0.421
HCT	27.06 (20.39)	32.8 (13.12)	1.012	0.844
HB (g/L)	128.54 (11.64)	124.44 (9.16)	0.962	0.076
PLT (× 10^{9}/L)	283.08 (69.01)	293.3 (63.42)	1.007	0.588
Others				
IGF-1 (ng/ml)	174.63 (87.20)	111.4 (69.84)	0.595	4.80×10^{-3}
IGFBP-3 (ng/ml)	3.54 (0.95)	2.96 (1.09)	0.880	0.076
CAL (mmol/L)	2.35 (0.19)	2.38 (0.13)	1.004	0.848

[a]FC, FC (fold change)-value. FC value is the multiple difference of the metabolite concentration between samples. A value less than 1 means that the metabolite content in HE group is lower than that in LE group, and a value greater than 1 means that the metabolite content in HE group is higher than that in LE group.

[b]p, p-value, which is obtained from Mann-Whitney U test, p < 0.05 means the difference is statistically significant.

[c]SEX_STD, 1 represents male and 2 represents female for gender comparison.

[d]BHEIGHT, height 1 year prior to the treatment.

Commercial databases, Kyoto Encyclopedia of Genes and Genomes (KEGG, http://www.genome.jp/kegg/) and Human Metabolome Database (http://www.hmdb.ca/) were utilized to search for the relative metabolites and metabolic pathways. A heatmap was used to show the association between clinical indicators and differential metabolites.

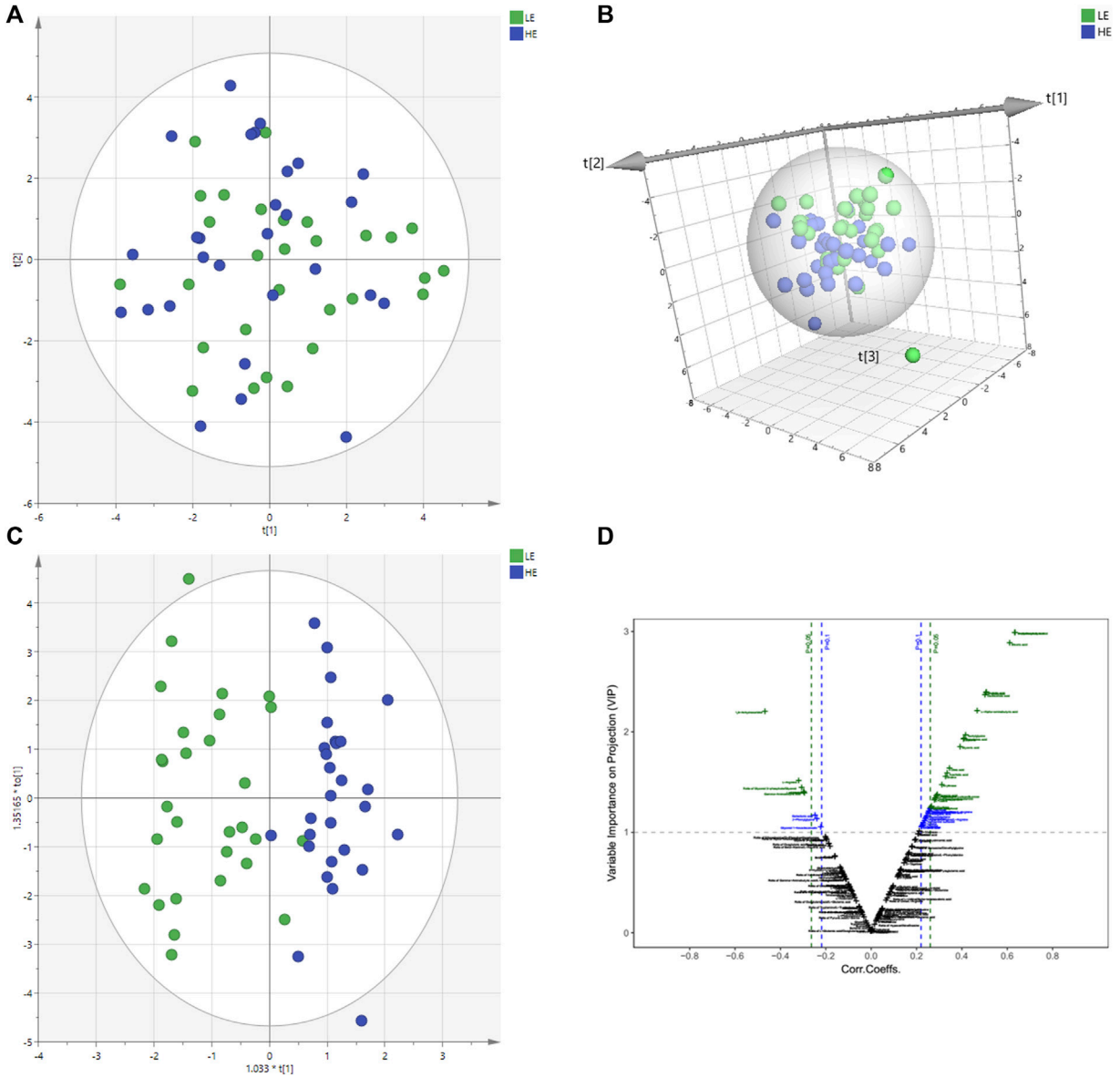

FIGURE 1 | Metabolomics multivariate statistical analysis (MVA). PCA and PCA 3D score plots for pairwise comparisons between HE and LE from serum samples **(A,B)**. OPLS-DA score plots of HE group and LE group. LE (in green) represents low efficacy group and HE (in blue) represents high efficacy group. The clustering of HE group and LE group was obvious **(C)**. V-plot of differential metabolites **(D)**. On the left is the downregulated metabolites in the HE group compared with the LE group, and the correlation coefficient on the X-axis is negative. On the right is the up-regulated metabolites between the HE and the LE group, and the correlation coefficient on the X-axis is positive. HE, high clinical efficacy group; LE, low clinical efficacy group.

RESULTS

Demographics and Serum Biochemical Analysis

The clinical characteristics of GHD patients at baseline were summarized in **Table 1**. Of the 60 GHD children that underwent baseline testing, 3 withdrew owing to incomplete data; therefore, data were reported from the 57 participants who completed the intervention. As anticipated, the improvement in bheight, height, weight, bone age, and age was lower in the HE group than in the LE group. Compared with the LE group, the level of total protein (TP, **Table 1**) in GHD patients of high clinical efficacy was significantly decreased. In addition, it was found that the differences in creatinine (CR, **Table 1**) and IGF-1 in the HE group were statistically significant compared to the LE group. The concentrations of other biochemical indexes did not differ significantly among treatments.

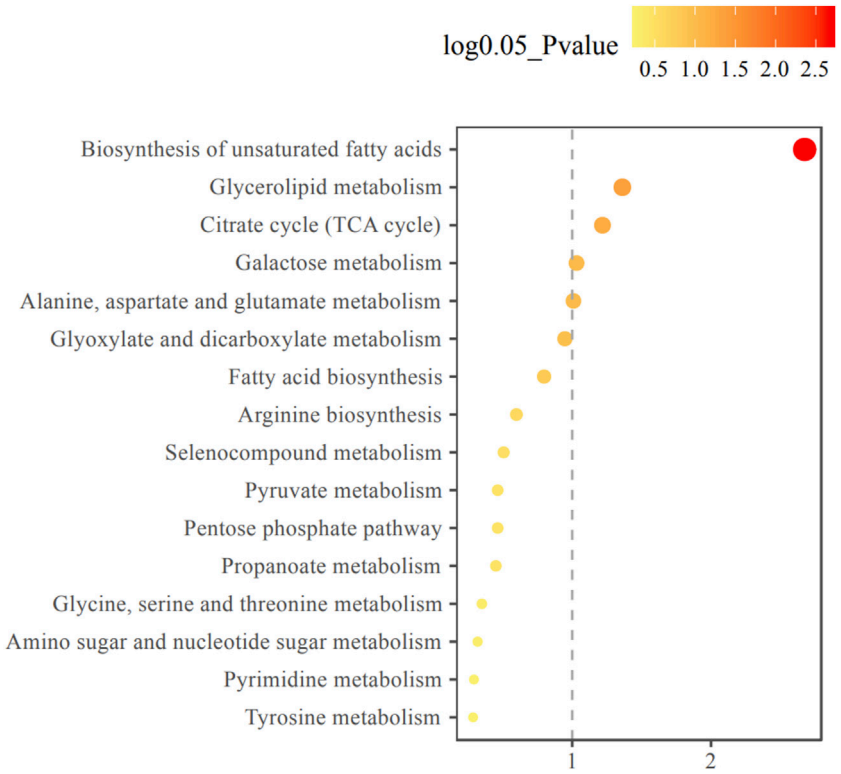

FIGURE 2 | Metabolic pathway enrichment analysis diagram. Among the metabolic pathways associated with efficacy, there were statistically significant differences in glycerol lipid metabolism, TCA cycle, galactose metabolism, alanine, aspartate and glutamate metabolism pathways. The horizontal axis represents the enrichment factor and the vertical axis represents the pathway name. The color ranges from yellow to red, indicating that the adjusted *p*-value grows from small to large, and the enrichment degree becomes more and more significant. The size of the dot represents the number of metabolites enriched in this pathway.

Metabolomic Profiling

The changes of metabolite in serum under different conditions could not be explored simply by visual inspection; thus, multivariate statistical analysis was applied to explore the differences in serum metabolites between groups. PCA, an unsupervised method, was used to obtain general clustering, trends, or outliers among the observations acquired in metabolic changes. The outline of the differences in serum metabolome was provided by an OPLS-DA model, which was used to identify the discriminant metabolic profiles and to determine significantly different metabolites. First, PCA was conducted on serum samples. Slight differences in the serum metabolome were observed between HE and LE groups (**Figures 1A,B**). OPLS-DA and V-plot were then performed and compared to identify and characterize metabolites. The key parameters, R2 and Q2, were used for the evaluation of discrimination and predictive abilities of the models respectively. The results of 200-item permutation test (R^2 = (0.0; 0.746), Q^2 = (0.0; −0.582)) demonstrated the validity and stability of the fitted OPLS-DA model. As shown in **Figures 1C,D**, significant differences in serum samples were observed between HE and LE groups. Biomarkers that differed between the two groups were identified to be involved in four main pathways based on metabolic pathway analysis, including 1) biosynthesis of unsaturated fatty acids; 2) glycerolipid metabolism; 3) citrate cycle; and 4) galactose metabolism (**Figure 2**).

Significantly Disturbed Metabolites Between HE Group and LE Group

To identify distinct biomarkers that may be associated with clinical efficacy among thousands of variables, a comparison was conducted between the HE and LE groups of patients. The metabolite profiles of all serum samples at baseline were analyzed to determine the relative levels of the metabolites based on GC-TOFMS analyses. A total of 119 putative metabolites were annotated, and 23 of the 119 annotated metabolites were identified (**Table 2**). The endogenous metabolite contributing most to the classification between the HE group and LE group was screened out using multiple criteria, including VIP value, FC value, *p*-value, and AUC value. The variables with VIP > 1 (**Figure 1D**), FC > 1 (**Table 3**), AUC > 0.700 (**Figure 3**), and $p < 0.05$ (**Figure 4**) indicated eight differential metabolites, including heptadecanoic acid, stearic acid, 2-hydroxybutyric acid, myristic acid, palmitoleic acid, D-galactose, dodecanoic acid, and oleic acid. Upregulation of metabolites was observed in the HE group compared to the LE group. Compared to the LE group, the levels of several metabolites

TABLE 2 | The identified metabolites with $p < 0.05$ in HE group compared to LE group at baseline.

Metabolites	[a]FC	[b]*p*.value
Heptadecanoic acid	1.687	8.40E-05
Stearic acid	1.684	2.50E-04
2-Hydroxybutyric acid	1.54	8.80E-04
Myristic acid	2.836	1.10E-03
Palmitoleic acid	3.987	2.30E-03
D-Galactose	1.11	4.00E-03
Dodecanoic acid	2.115	4.00E-03
Malic acid	1.204	6.40E-03
Oleic acid	1.692	8.20E-03
Ratio of Glycerol 3-phosphate/Glycerol	0.566	1.30E-02
Uridine	1.593	1.50E-02
Acetylglycine	1.22	2.20E-02
Isocitric acid	1.815	2.50E-02
Glycerol	1.333	2.60E-02
L-Alanine	0.92	2.80E-02
Glyceric acid	1.61	2.80E-02
Decanoyl carnitine	1.298	3.10E-02
Benzoic acid	0.87	3.30E-02
Fumaric acid	1.354	3.30E-02
MG182	1.587	3.40E-02
Docosahexaenoic acid	1.299	3.90E-02
Arachidic acid	1.493	4.10E-02
Erythrose	4.918	4.40E-02

[a]*FC, FC (fold change)-value. FC, value is the multiple difference of the metabolite concentration between samples. A value less than 1 means that the metabolite content in HE, group is lower than that in LE, group, and a value greater than 1 means that the metabolite content in HE, group is higher than that in LE, group.*
[b]*p, p-value, which is obtained from Mann-Whitney U test, $p < 0.05$ means the difference is statistically significant.*

showed an upward trend in the HE group, including heptadecanoic acid, stearic acid, 2-hydroxybutyric acid, myristic acid, palmitoleic acid, D-galactose, dodecanoic acid, and oleic acid (**Table 3**). We correlated the serum biochemical index changes observed in the baseline clinical characteristics of GHD patients with metabolites in HE and LE groups. A heatmap was generated to show the associations between clinical index and metabolites in the two groups (**Figure 5**). CR, age, bheight, height, weight, and sktagey showed strong negative correlations with heptadecanoic acid, stearic acid, myristic acid, palmitoleic acid, and dodecanoic acid. Negative correlations also were observed between the CR and age with pyroglutamic acid. A similar trend was observed between the age, bheight, height, weight, sktagey, and D-galactose.

DISCUSSION

The analysis of metabolomics provides a powerful tool for determining biomarkers that predict the effects of PEG-rhGH therapy through large-scale molecular analyses. The present study confirmed and extended previous studies by showing the favorable effects of PEG-rhGH therapy on GHD patients (Rogol et al., 2013; Luo et al., 2017). To explore the potential mechanism, changes of metabolites of GHD patients in HE and LE groups were monitored using a GC/TOFMS-based metabolomics method. Based on the results of metabolomics analysis, 8 differential metabolites were found to be closely related to growth gains following PEG-rhGH intervention on GHD children. These metabolites were heptadecanoic acid, stearic acid, 2-hydroxybutyric acid, myristic acid, palmitoleic acid, D-galactose, dodecanoic acid, and oleic acid. The related metabolic pathways involved fatty acid metabolism and energy metabolism.

Fatty Acid Metabolism A variety of fatty acids exist in the cells and tissues of humans, which play essential roles in endogenous substance metabolism, cell structure, and function (Judge and Dodd 2020). Neural cell membrane phospholipids, ceramides, and sphingolipids contain some longer-chain, saturated fatty acids, such as palmitic and stearic acids (Simons and Gerl, 2010). The saturated fatty acid content of these structures is related to their membrane location and their function. Moreover, myristic and palmitic acids can covalently modify several proteins involved in cell signaling and can influence fatty acid biosynthesis and metabolism by affecting the regulation of transcription factors, including SREBPs and LXR/RXR (Johnson et al., 1994; Mitchell et al., 2006; Calder, 2015). Previous studies have shown that fatty acids were reduced in GHD patients and became normalized upon rhGH treatment, which might raise the level of total and LDL cholesterol Cuneo et al., 1993; Russell-Jones

TABLE 3 | Statistically significant metabolites in serum samples of HE group versus LE group comparison.

Metabolites	LE group	HE group	[a]FC	[b]VIP	[c]*p*.value	Formula	[d]HMDB ID	HE/LE
Heptadecanoic acid	3,589.11 (1761.33)	6,194.47 (2,885.30)	1.69	2.98	8.40 × 10−5	C17H34O2	HMDB02259	↑
Stearic acid	182,390.78 (65,213.65)	280,726.2 (109,564.96)	1.68	2.87	2.50 × 10−4	C18H36O2	HMDB00827	↑
2-Hydroxybutyric acid	158,827.15 (67,109.12)	242,265.37 (106,426.26)	1.54	2.98	8.80 × 10−4	C4H8O3	HMDB00008	↑
Myristic acid	22,604.22 (19,671.17)	47,192.23 (33,841.80)	2.84	2.39	1.10 × 10−3	C14H28O2	HMDB00806	↑
Palmitoleic acid	20,111.44 (23,314.53)	50,034.73 (48,186.11)	3.99	1.92	2.30 × 10−3	C16H30O2	HMDB03229	↑
D-Galactose	246,084.44 (57,503.14)	285,655.97 (33,157.03)	1.11	2.38	4.00 × 10−3	C6H12O6	HMDB00143	↑
Dodecanoic acid	6,990.11 (5,881.99)	13,504.60 (8,949.79)	2.12	2.36	4.00 × 10−3	C12H24O2	HMDB00638	↑
Oleic acid	172,689.04 (99,261.28)	246,016.00 (142,341.37)	1.69	1.63	8.20 × 10−3	C18H34O2	HMDB00207	↑

[a]*FC, FC (fold change)-value. FC, value is the multiple difference of the metabolite concentration between samples. A value less than 1 means that the metabolite content in HE, group is lower than that in LE, group, and a value greater than 1 means that the metabolite content in HE, group is higher than that in LE, group.*
[b]*VIP, variable importance in projection, the VIP>1 is considered to contribute to group classification.*
[c]*p, p-value, which is obtained from Mann-Whitney U test, $p < 0.05$ means the difference is statistically significant.*
[d]*HMDB ID, Human Metabolome Database ID.*

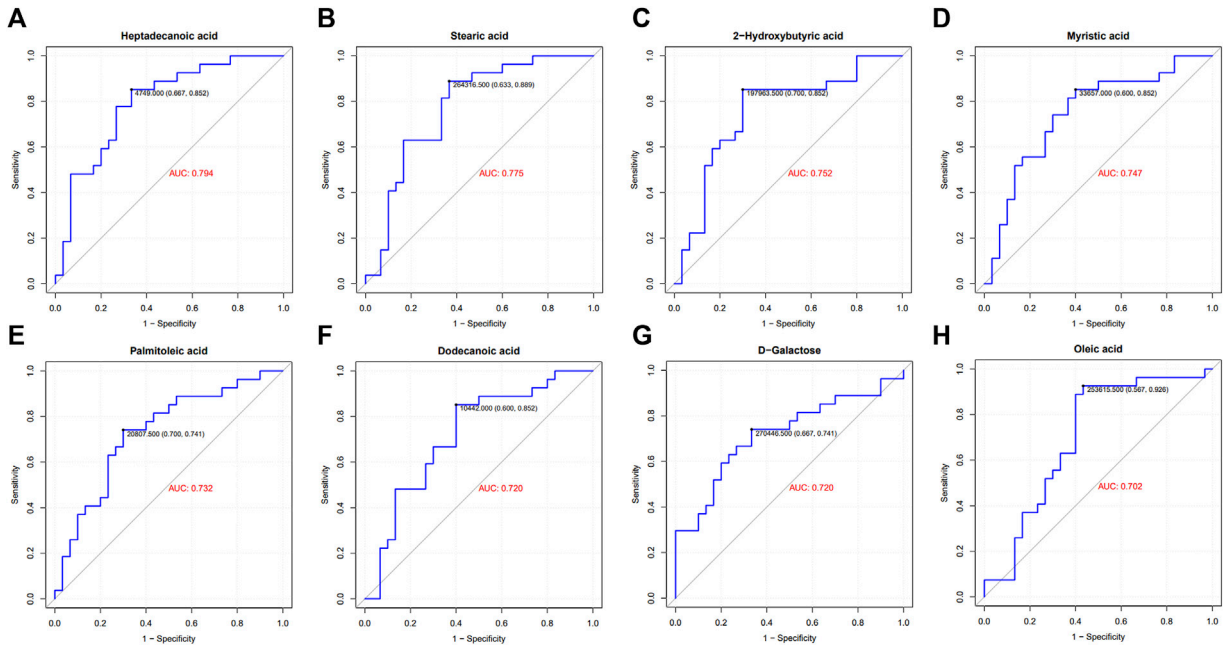

FIGURE 3 | ROC curve and area under the curve (AUC) of differential metabolites. GHD patients were grouped by clinic efficacy to calculate the value of serum metabolites for the diagnosis of GHD. The ROC curve and AUC of heptadecanoic acid **(A)**, stearic acid **(B)**, 2-hydroxybutyric acid **(C)**, myristic acid **(D)**, palmitoleic acid **(E)**, dodecanoic acid **(F)**, D-galactose **(G)** and oleic acid **(H)**.

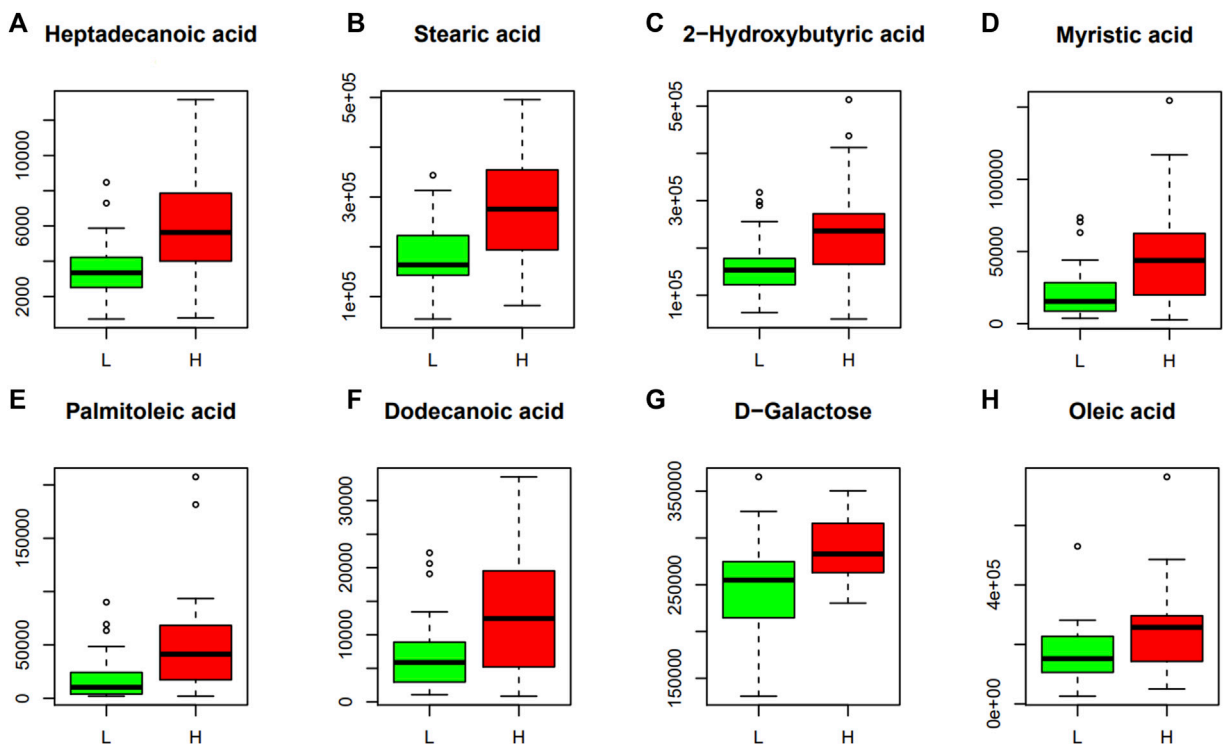

FIGURE 4 | Discriminant metabolites obtained with Mann-Whitney *U* test. The resulted metabolites obtained are shown and expressed on the y axes of the graphs as the relative level of peak signals. The serum levels of heptadecanoic acid **(A)**, stearic acid **(B)**, 2-hydroxybutyric acid **(C)**, myristic acid **(D)**, palmitoleic acid **(E)**, dodecanoic acid **(F)**, D-galactose **(G)** and oleic acid **(H)**. L, LE group; H, HE group. The data are expressed as the mean ± standard deviation (n = 28 HE group; n = 29 LE group).

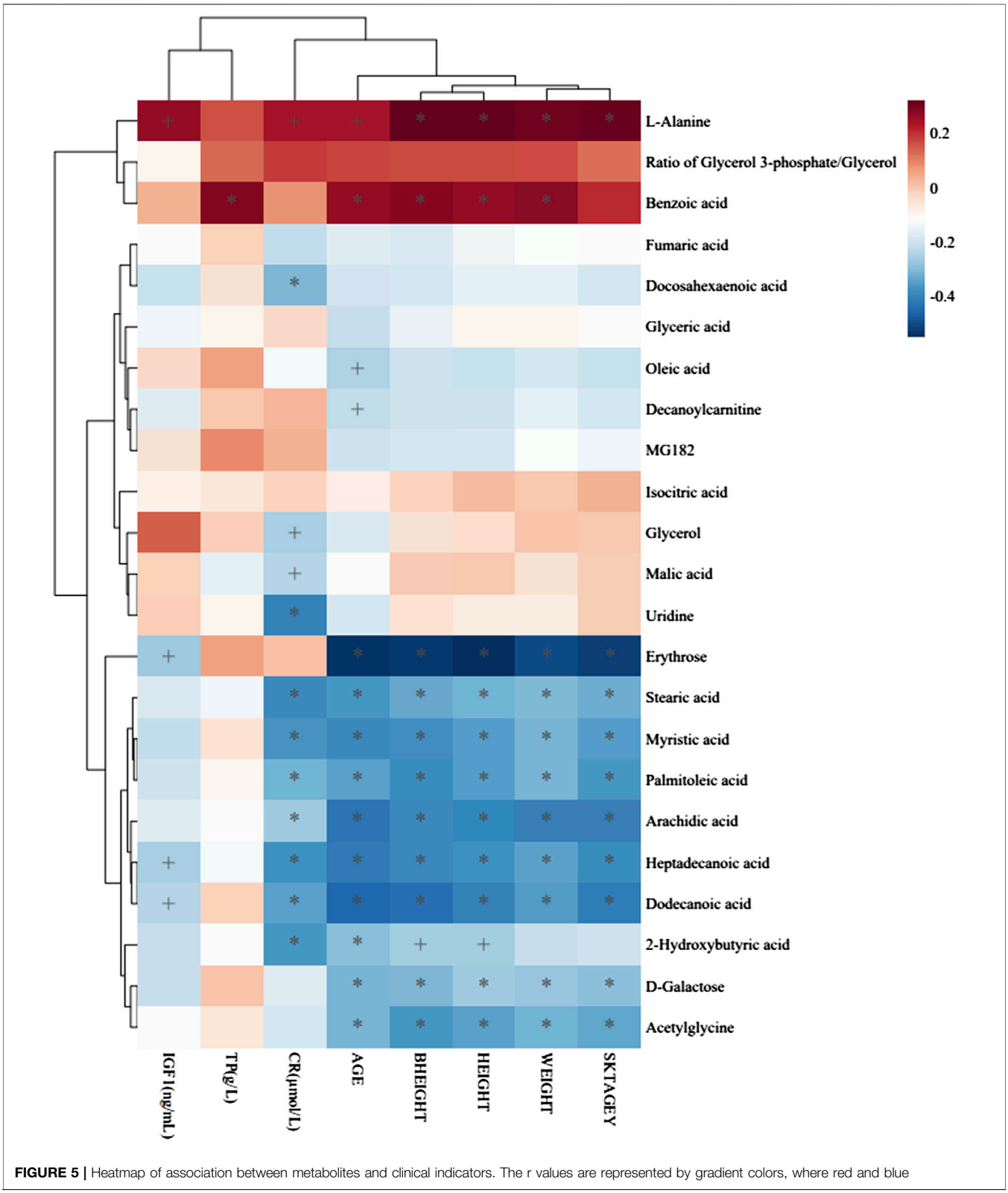

FIGURE 5 | Heatmap of association between metabolites and clinical indicators. The r values are represented by gradient colors, where red and blue

et al., 1994; Beshyah et al., 1995; Mensink et al., 2003; Molitch et al., 2011). In the present study we showed that stearic acid, myristic acid, palmitoleic acid, and dodecanoic acid were significantly increased in the GHD patients of high clinical efficacy. These results were consistent with previous studies, indicating that fatty acid metabolism may be related to the

improvement of growth and development in children with GHD. Moreover, oleic acid is a monounsaturated acid of the ω-9 series in serum, which is present endogenously in the organism and also can be obtained from the diet. Oleic acid is the most prevalent dietary fatty acid in many individuals, and it acts as a neurotrophic factor in neuronal growth (Rodríguez-Rodríguez et al., 2004; Polo-Hernández et al., 2010). There is a direct association between the exogenous administration of oleic acid and brain development in humans (Polo-Hernández et al., 2010). Interestingly, it was found that oleic acid has beneficial effects by preventing lipotoxicity, increasing mitochondrial fatty acid oxidation (Coll et al., 2008), and preventing the desensitization of human growth hormone secretagogue receptors (Delhanty et al., 2010). The present study's results revealed a significant increase in oleic acid in the high efficacy group. More importantly, oleic acid is a biological metabolite implicated in brain growth and development, which is consistent with our GC/TOFMS-based metabolomics study. However, there is evidence that a higher intake of saturated fatty acid can increase body fat and inflammatory biomarkers for inducing incident type 2 diabetes and obesity-related diseases (Cuneo et al., 1993). Several observational studies have investigated the relationship between saturated fatty acids and inflammation in humans and have found that lauric, myristic, and palmitic acids can induce insulin resistance and can promote inflammation (Innes and Calder, 2018); however, oleic acid has the ability to reduce the inflammatory effects of long-chain, saturated fatty acids in human aortic endothelial cells (Harvey et al., 2010; Schenkel and Bakovic, 2014). The published literature is not entirely consistent with these findings, most likely because each type of fatty acid has unique effects on human metabolism. Further investigation is needed to identify the exact mechanisms involved in the function and role of fatty acid metabolism. Our results implied that regulation of fatty acid metabolism may be one of the possible mechanisms by which PEG-rhGH exerts different therapeutic effects in improving GHD. Traditionally, most interest in the health impact of fatty acids has been related to metabolic diseases and inflammatory diseases. It is now clear that they are also related to the difference in the clinical efficacy of PEG-rhGH replacement therapy.

Energy Metabolism Fatty acid oxidation becomes important in times of limited glucose availability. In this context good energy substrate is provided by fatty acids, which can be used to generate energy in most aerobic tissues except for the brain. Furthermore, fatty acids (palmitoleic acid and oleic acid) have distinct ways of regulating energy homeostasis (Innes and Calder, 2018). D-Galactose is completely metabolized upon first pass (from the gut) through the liver, where it is converted into glucose, lactate, glycogen, and lipids (Brouns, 2017; Gonzalez et al., 2017). Glucose is broken down to pyruvic acid, and then pyruvic acid is decarboxylated to acetyl-CoA, which is the source for the tricarboxylic acid cycle (TCA) (Akram, 2014). This cycle is an important energy-producing pathway used in eukaryotes and provides many intermediates required for gluconeogenesis and lipogenesis. In the present study the HE group showed an upward trend of the level of serum D-galactose compared to the LE group, suggesting another possible mechanism for the difference in the clinical efficacy of PEG-rhGH treatment associated with altered energy metabolism.

Our data highlighted that the clinical efficacy of PEG-rhGH treatment was associated with individual factors in GHD patients, including age, sex, and height, which suggests that individualized treatment of PEG-rhGH is needed. Bone age has been accepted as an important criterion for assessing growth and development. Patients with younger bone age before puberty can grow 8–14 cm per year using rhGH treatment (Yuen et al., 2019). As the skeletal age increases (LE group 6.81 ± 2.53 vs. HE group 4.79 ± 2.15), the growth rate of subjects will gradually decrease after PEG-rhGH treatment. Similarly, the sex-related difference is an important contributor to the efficacy of PEG-rhGH. Following general opinion, the first menarche of Asian women is estimated to be 12–16 years, and the annual growth rate is about 6–9 cm (Yang et al., 2017). At the end of the second menarche, the bone age is basically closed, possibly reflecting alterations in ovarian hormone levels *in vivo* combined with earlier developmental risks in girls. The first signs of the voice mutation can be fixed at the age of 10–11 years as the male progressed through puberty (Boskey and Coleman, 2010). Indeed, higher levels of the hormone are known to interfere with the physiological pathways of growth hormone, affecting not only growth rate but also PEG-rhGH efficacy. We note also that older participants in the LE group exhibited lower than their younger counterparts in the HE group in terms of clinical efficacy after PEG-rhGH administration. The stearic acid, myristic acid, palmitoleic acid, heptadecanoic acid, dodecanoic acid, 2-hydroxybutyric acid, and D-galactose were negatively associated with subjects' age and had higher concentrations in the samples of the HE group. A similar trend also was observed with stearic acid, myristic acid, palmitoleic acid, heptadecanoic acid, dodecanoic acid, and D-galactose and the height and weight of GHD patients. We demonstrated that the age, height, and weight of GHD patients might have an association with a fatty acid level in serum, and we observed a possible correlation between the fatty acid level and the difference of clinical efficacy of PEG-rhGH replacement, wherein stearic acid, myristic acid, palmitoleic acid, heptadecanoic acid, dodecanoic acid, 2-hydroxybutyric acid, and D-galactose were suggested as biomarkers for predicting the PEG-rhGH efficacy.

This is a well-designed clinical study with strict inclusion and exclusion criteria although the number of qualified participants was small in this study. Thus, further large-scale and multi-center-based studies are needed for further validation. Moreover, non-targeted metabolomics studies contributed to biomarker discovery initially, so further targeted and quantitative analysis of differential metabolites are required in the future.

CONCLUSION

In conclusion, our results revealed for the first time the identity of important metabolites and pathways that contribute to predicting the efficacy of PEG-rhGH therapy. Several predictive marker candidates for the effects of PEG-rhGH treatment were identified, including heptadecanoic acid, stearic acid, 2-hydroxybutyric acid,

myristic acid, palmitoleic acid, D-galactose, dodecanoic acid, and oleic acid. The results revealed a strong association between the serum metabolic profiles and the clinical efficacy of PEG-rhGH therapy, and this association was most pronounced in fatty acids. The mechanisms are likely to be involved in fatty acid metabolism and energy metabolism. The current study suggested fatty acid as the potential predictive marker for PEG-rhGH treatment effects. These discoveries enabled a better understanding of the mechanism of PEG-rhGH and may lead to the development of metabolic biomarkers and novel therapeutic strategies for individualized treatment of PEG-rhGH.

DATA AVAILABILITY STATEMENT

The original contributions presented in the study are included in the article/**Supplementary Material**, further inquiries can be directed to the corresponding authors.

ETHICS STATEMENT

The studies involving human participants were reviewed and approved by the Ethics Committee of Children's Hospital, Zhejiang University School of Medicine. Written informed consent to participate in this study was provided by the participants' legal guardian/next of kin.

AUTHOR CONTRIBUTIONS

SN and JF conceived and designed the study. WP and YN carried out the experiments. JL drafted this manuscript. JL, WP, YN and JQ analyzed the data. SN provided final approval of the version to be published. All other authors contributed to data collection and data analysis, critically revised the article, and approved the final version of the paper.

FUNDING

This research was supported by the National Natural Science Foundation of China (Grant No.81573516).

ACKNOWLEDGMENTS

We thank Dr. Robert M. Dorazio for English language editing of the manuscript.

SUPPLEMENTARY MATERIAL

The Supplementary Material for this article can be found online at: https://www.frontiersin.org/articles/10.3389/fphar.2022.864058/full#supplementary-material

REFERENCES

Akram, M. (2014). Citric Acid Cycle and Role of its Intermediates in Metabolism. *Cell Biochem. Biophys.* 68 (3), 475–478. doi:10.1007/s12013-013-9750-1

Beshyah, S. A., Henderson, A., Niththyananthan, R., Skinner, E., Anyaoku, V., and Richmond, W. (1995). The Effects of Short and Long Term Growth Hormone Replacement Therapy in Hypopituitary Adults on Lipid Metabolism and Carbohydrate Tolerance. *J. Clin. Endocrinol. Metab.* 80 (2), 356–363. doi:10.1210/jcem.80.2.7852490

Binnerts, A., Swart, G. R., Wilson, J. H. P., Hoogerbrugge, N., Pols, H. A. P., Birkenhager, J. C., et al. (1993). The Effect of Growth Hormone Administration in Growth Hormone Deficient Adults on Bone, Protein, Carbohydrate and Lipid Homeostasis, as Well as on Body Composition. *Clin. Endocrinol. (Oxf).* 37 (1), 79–87. doi:10.1111/j.1365-2265.1992.tb02287.x

Boskey, A. L., and Coleman, R. (2010). Aging and Bone. *J. Dent. Res.* 89 (12), 1333–1348. doi:10.1177/0022034510377791

Brouns, F. (2017). Saccharide Characteristics and Their Potential Health Effects in Perspective. *Front. Nutr.* 7, 75. doi:10.3389/fnut.2020.00075

Calder, P. C. (2015). Functional Roles of Fatty Acids and Their Effects on Human Health. JPEN J. Parenter. Enteral. *Nutr* 39 (1 Suppl. l), 18S–32S. doi:10.1177/0148607115595980

Chaplin, J. E., Kristrom, B., Jonsson, B., Tuvemo, T., and Albertsson-Wikland, K. (2015). Growth Hormone Treatment Improves Cognitive Function in Short Children with Growth Hormone Deficiency. *Horm. Res. Paediatr.* 83, 390–399. doi:10.1159/000375529

Chinoy, A. P., and Murray, G. (2016). Diagnosis of Growth Hormone Deficiency in the Paediatric and Transitional Age. *Best Pract. Res. Clin. Endocrinol. Metab.* 30 (6), 737–747. doi:10.1016/j.beem.2016.11.002

Coll, T., Eyre, E., Rodriguez-Calvo, R., Palomer, X., Sanchez, R. M., Merlos, M., et al. (2008). Oleate Reverses Palmitate-Induced Insulin Resistance and Inflammation in Skeletal Muscle Cells. *J. Biol. Chem.* 283 (17), 11107–11116. doi:10.1074/jbc.M708700200

Cuneo, R. C., Salomon, F., Watts, G. F., Hesp, R., and Sönksen, P. H. (1993). Growth Hormone Treatment Improves Serum Lipids and Lipoproteins in Adults with Growth Hormone Deficiency. *Metabolism* 42 (12), 1519–1523. doi:10.1016/0026-0495(93)90145-e

Cutfield, W. S., Derraik, J. G., Gunn, A. J., Reid, K., Delany, T., Robinson, E., et al. (2011). Non-Compliance with Growth Hormone Treatment in Children Is Common and Impairs Linear Growth. *PLoS One* 6 (1), e16223. doi:10.1371/journal.pone.0016223

Delhanty, J. D., Kerkwijk, A., Huisman, M., Zande, B., Verhoef-Post, M., Gauna, C., et al. (2010). Unsaturated Fatty Acids Prevent Desensitization of the Human Growth Hormone Secretagogue Receptor by Blocking its Internalization. *Am. J. Physiol. Endocrinol. Metab.* 299 (3), E497–E505. doi:10.1152/ajpendo.00414.2009

Gonzalez, J. T., Fuchs, C. J., Betts, J. A., and van Loon, L. J. C. (2017). Glucose Plus Fructose Ingestion for Post-Exercise Recovery-Greater Than the Sum of its Parts? *Nutrients* 9 (4), 344. doi:10.3390/nu9040344

Halas, J. G., and Grimberg, A. (2020). Dilemmas of Growth Hormone Treatment for GH Deficiency and Idiopathic Short Stature: Defining, Distinguishing, and Deciding. *Minerva Pediatr.* 72 (3), 206–225. doi:10.23736/S0026-4946.20.05821-1

Harvey, K. A., Walker, C. L., Xu, Z. D., Whitley, P., Pavlina, T. M., Hise, M., et al. (2010). Oleic Acid Inhibits Stearic Acid-Induced Inhibition of Cell Growth and Pro-inflammatory Responses in Human Aortic Endothelial Cells. *J. Lipid Res.* 51 (12), 3470–3480. doi:10.1194/jlr.M010371

Hou, L., Chen, Z. H., Liu, D., Cheng, Y. G., and Luo., X. P. (2015). Comparative Pharmacokinetics and Pharmacodynamics of A PEGylated Recombinant Human Growth Hormone and Daily Recombinant Human Growth Hormone in Growth Hormone-Deficient Children. *Drug Des. Devel Ther.* 10, 13–21. doi:10.2147/DDDT.S93183

Höybye, C., Wahlström, E., Tollet-Egnell, P., and Norstedt, G. (2014). Metabolomics: A Tool for the Diagnosis of GH Deficiency and for Monitoring GH Replacement? *Endocr. Connect.* 3 (4), 200–206. doi:10.1530/EC-14-0098

Innes, J. K., and Calder, P. C. (2018). Omega-6 Fatty Acids and Inflammation. *Prostaglandins Leukot. Essent. Fatty Acids* 132, 41–48. doi:10.1016/j.plefa.2018.03.004

Jee, Y. H., Andrade, A. C., Baron, J., and Nilsson, O. (2017). Genetics of Short Stature. *Endocrinol. Metab. Clin. North. Am.* 46 (2), 259–281. doi:10.1016/j.ecl.2017.01.001

Johnson, D. R., Bhatnagar, R. S., Knoll, L. J., and Gordon, J. I. (1994). Genetic and Biochemical Studies of Protein N-Myristoylation. *Annu. Rev. Biochem.* 63, 869–914. doi:10.1146/annurev.bi.63.070194.004253

Judge, A., and Dodd, M. S. (2020). Metabolism. *Essays Biochem.* 64, 607–647. doi:10.1042/EBC20190041

Leonibus, C. D., Marco, S. D., Stevens, A., Clayton, P., Chiarelli, F., and Mohn, A. (2016). Growth Hormone Deficiency in Prepubertal Children: Predictive Markers of Cardiovascular Disease. *Horm. Res. Paediatr.* 85 (6), 363–371. doi:10.1159/000444143

López-Siguero, J., Pérez, V. B., Balser, S., and Khan-Boluki, J. (2011). Long-term Safety and Efficacy of the Recombinant Human Growth Hormone Omnitrope(R) in the Treatment of Spanish Growth Hormone Deficient Children: Results of A Phase III Study. *Adv. Ther.* 28 (10), 879–893. doi:10.1007/s12325-011-0063-8

Lundberg, E., Andersson, B., Kriström, B., Rosberg, S., and Albertsson-Wikland, K. (2018). Broad Variability in Pharmacokinetics of GH Following RhGH Injections in Children. *Growth Horm. IGF Res.* 40, 61–68. doi:10.1016/j.ghir.2018.01.004

Luo, X., Hou, L., Liang, L., Dong, G., Shen, S., Zhao, Z., et al. (2017). Long-acting PEGylated Recombinant Human Growth Hormone (Jintrolong) for Children with Growth Hormone Deficiency: Phase II and Phase III Multicenter, Randomized Studies. *Eur. J. Endocrinol.* 177 (2), 195–205. doi:10.1530/EJE-16-0905

McBride, E. M., Lawrence, R. J., McGee, K., Mach, P. M., Demond, P. S., Busch, M. W., et al. (2019). Rapid Liquid Chromatography Tandem Mass Spectrometry Method for Targeted Quantitation of Human Performance Metabolites in Saliva. *J. Chromatogr. A.* 1601, 205–213. doi:10.1016/j.chroma.2019.04.071

Mensink, R. P., Zock, P. L., Kester, A. D., and Katan, M. B. (2003). Effects of Dietary Fatty Acids and Carbohydrates on the Ratio of Serum Total to HDL Cholesterol and on Serum Lipids and Apolipoproteins: A Meta-Analysis of 60 Controlled Trials. *Am. J. Clin. Nutr.* 77 (5), 1146–1155. doi:10.1093/ajcn/77.5.1146

Mitchell, D. A., Vasudevan, A., Linder, M. E., and Deschenes, R. J. (2006). Protein Palmitoylation by A Family of DHHC Protein S-Acyltransferases. *J. Lipid Res.* 47 (6), 1118–1127. doi:10.1194/jlr.R600007-JLR200

Molitch, M. E., Clemmons, D. R., Malozowski, S., Merriam, G. R., and Vance, M. L. (2011). Evaluation and Treatment of Adult Growth Hormone Deficiency: An Endocrine Society Clinical Practice Guideline. *J. Clin. Endocrinol. Metab.* 96 (6), 1587–1609. doi:10.1210/jc.2011-0179

Murray, P. G., Clayton, P. E., and Chernausek, S. D. (2018). A Genetic Approach to Evaluation of Short Stature of Undetermined Cause. *Lancet Diabetes Endocrinol.* 6 (7), 564–574. doi:10.1016/S2213-8587(18)30034-2

Polo-Hernández, E., De Castro, F., García-García, A. G., Tabernero, A., and Medina, J. M. (2010). Oleic Acid Synthesized in the Periventricular Zone Promotes Axonogenesis in the Striatum during Brain Development. *J. Neurochem.* 114 (6), 1756–1766. doi:10.1111/j.1471-4159.2010.06891.x

Rahman, S. A., Schirra, H. J., Lichanska, A. M., Huynh, T., and Leong, G. M. (2013). Urine Metabonomic Profiling of A Female Adolescent with PIT-1 Mutation before and during Growth Hormone Therapy: Insights into the Metabolic Effects of Growth Hormone. *Growth Horm. IGF Res.* 23 (1-2), 29–36. doi:10.1016/j.ghir.2012.12.001

Rasmussen, M. H., Jensen, L., Anderson, T. W., Klitgaard, T., and Madsen, J. (2010). Multiple Doses of Pegylated Long-Acting Growth Hormone Are Well Tolerated in Healthy Male Volunteers and Possess A Potential Once-Weekly Treatment Profile. *Clin. Endocrinol. (Oxf)* 73 (6), 769–776. doi:10.1111/j.1365-2265.2010.03863.x

Rodríguez-Rodríguez, R. A., Tabernero, A., Velasco, A., Lavado, E. M., and Medina, J. M. (2004). The Neurotrophic Effect of Oleic Acid Includes Dendritic Differentiation and the Expression of the Neuronal Basic Helixloop-Helix Transcription Factor NeuroD2. *J. Neurochem.* 88 (5), 1041–1051. doi:10.1046/j.1471-4159.2003.02262.x

Rogol, A. D., Cohen, P., Weng, W., Kappelgaard, A. M., and Germak, J. A. (2013). Prepubertal Children with Growth Hormone Deficiency Treated for Four Years with Growth Hormone Experience Dose-dependent Increase in Height, but Not in the Rate of Puberty Initiation. *Horm. Res. Paediatr.* 80 (1), 28–37. doi:10.1159/000353429

Russell-Jones, D. L., Watts, G. F., Weissberger, A., Naournova, R., Myers, J., Thompson, G. R., et al. (1994). The Effect of Growth Hormone Replacement on Serum Lipids, Lipoproteins, Apolipoproteins and Cholesterol Precursors in Adult Growth Hormone Deficient Patients. *Clin. Endocrinol. (Oxf)* 41 (3), 345–350. doi:10.1111/j.1365-2265.1994.tb02555.x

Schenkel, L. C., and Bakovic, M. (2014). Palmitic Acid and Oleic Acid Differentially Regulate Choline Transporter-like 1 Levels and Glycerolipid Metabolism in Skeletal Muscle Cells. *Lipids* 49 (8), 731–744. doi:10.1007/s11745-014-3925-4

Schepper, J., Rasmussen, M. H., Gucev, Z., Eliakim, A., and Battelino, T. (2011). Long-Acting Pegylated Human GH in Children with GH Deficiency: A Single-Dose, Dose-Escalation Trial Investigating Safety, Tolerability, Pharmacokinetics and Pharmacodynamics. *Eur. J. Endocrinol.* 165 (3), 401–409. doi:10.1530/EJE-11-0536

Simons, K., and Gerl, M. J. (2010). Revitalizing Membrane Rafts: New Tools and Insights. *Nat. Rev. Mol. Cel Biol* 11 (10), 688–699. doi:10.1038/nrm2977

Wang, C. C., Huang, H. Q., Zhao, C., Zhao, J., Xiong, R. J., Jin, R. M., et al. (2021). The Impact of Pegylated Recombinant Human Growth Hormone Replacement Therapy on Glucose and Lipid Metabolism in Children with Growth Hormone Deficiency. *Ann. Palliat. Med.* 10 (2), 1809–1814. doi:10.21037/apm-20-871

Wit, J. M., Ranke, M. B., Albertsson-Wikland, K., Carrascosa, A., Rosenfeld, R. G., Van Buuren, S., et al. (2013). Personalized Approach to Growth Hormone Treatment: Clinical Use of Growth Prediction Models. *Horm. Res. Paediatr.* 79 (5), 257–270. doi:10.1159/000351025

Xu, R., Zhu, H. W., Zhang, C. Y., Shen, G. P., and Feng, J. H. (2019). Metabolomic Analysis Reveals Metabolic Characteristics of Children with Short Stature Caused by Growth Hormone Deficiency. *Clin. Sci. (Lond)* 133 (6), 777–788. doi:10.1042/CS20181005

Yang, L., Li, L. M., Millwood, I. Y., Peters, S. A. E., Chen, Y. P., Guo, Y., et al. (2017). Age at Menarche and Risk of Major Cardiovascular Diseases: Evidence of Birth Cohort Effects from A Prospective Study of 300,000 Chinese Women. *Int. J. Cardiol.* 227, 497–502. doi:10.1016/j.ijcard.2016.10.115

Yuen, K. C. J., Biller, B. M. K., Radovick, S., Carmichael, J. D., Jasim, S., Pantalone, K. M., et al. (2019). American Association of Clinical Endocrinologists and American College of Endocrinology Guidelines for Management of Growth Hormone Deficiency in Adults and Patients Transitioning from Pediatric to Adult Care. *Endocr. Pract.* 25 (11), 1191–1232. doi:10.4158/GL-2019-0405

Conflict of Interest: The authors declare that the research was conducted in the absence of any commercial or financial relationships that could be construed as a potential conflict of interest.

Publisher's Note: All claims expressed in this article are solely those of the authors and do not necessarily represent those of their affiliated organizations, or those of the publisher, the editors and the reviewers. Any product that may be evaluated in this article, or claim that may be made by its manufacturer, is not guaranteed or endorsed by the publisher.

frontiers | Frontiers in Pharmacology

ORIGINAL RESEARCH
published: 28 April 2022
doi: 10.3389/fphar.2022.872854

Stevens-Johnson Syndrome Following Vancomycin and Linezolid: A Real-World Analysis of Post-Marketing Surveillance Data

Ming Ni[1,2†], *Xue-Dong Yin*[1,3†], *Wen-Juan Hu*[1†], *Na Zeng*[1], *Bin Zhao*[4*] and *Zhi-Ling Li*[1*]

[1]Department of Pharmacy, Shanghai Children's Hospital, Shanghai Jiao Tong University, Shanghai, China, [2]Department of Clinical Pharmacy, Shaoxing Maternity and Child Health Care Hospital, Shaoxing, China, [3]Shanghai Jiao Tong University School of Medicine, Shanghai, China, [4]Department of Pharmacy, Peking Union Medical College Hospital, Peking Union Medical College, Chinese Academy of Medical Sciences, Beijing, China

Background: Stevens-Johnson syndrome (SJS) has been reported as a serious adverse effect in patients treated with vancomycin or linezolid, and there is currently a lack of real-world studies comparing specific differences in adverse effects of SJS.

Methods: According to the FDA's Adverse Event Reporting System (FAERS), from January 2004 to July 2021, the data of suspected SJS after the use of vancomycin and linezolid were analyzed by imbalance and Bayesian analysis. The onset time, fatality rate and hospitalization rate of vancomycin-associated SJS and linezolid-associated SJS were also investigated.

Results: 276 cases of vancomycin-related SJS reports and 63 cases of linezolid-related SJS reports were identified. These two drugs are more common in middle-aged patients (45–64 years) than other age groups, and less common in underage children (<18). Among them, linezolid-related SJS is more common in middle-aged and elderly patients (45–74 years old) than other groups. Except for unspecified data, in vancomycin-associated SJS cases, there are more men than women (49.28% vs 43.84%), while in linezolid-associated SJS cases, the proportion of men and women is almost equal (44.44%). From the point of view of the areas where adverse reactions were reported, about 1/2 of the reports on Vancomycin-related SJS came from North America, and 1/3 of the reports came from Europe. The median onset time of Linezolid-related SJS was 5 days (interquartile range [IQR] 2–7.75), which was significantly earlier than that of Vancomycin-related SJS (12 days, IQR 4–20) (Mann-Whitney test, $p < 0.0001$). There were no significant differences in mortality and hospitalization rates after vancomycin and linezolid caused SJS.

Conclusion: The analysis of faers data provides a comprehensive overview of the adverse reactions of SJS caused by the use of vancomycin and linezolid, and can warn clinical workers to timely intervene and continuously monitor the patients at risk of SJS when using such drugs.

Keywords: vancomycin, linezolid, epidemiology, SJS, adverse event reporting system

OPEN ACCESS

Edited by:
Jian Gao,
Shanghai Children's Medical Center, China

Reviewed by:
Zhao Libo,
Capital Medical University, China
Haibin Dai,
Zhejiang University, China

***Correspondence:**
Bin Zhao
zhaobin@pumch.cn
Zhi-Ling Li
lizhiling22@163.com

†*These authors have contributed equally to this work*

Specialty section:
This article was submitted to Obstetric and Pediatric Pharmacology, a section of the journal Frontiers in Pharmacology

Received: *10 February 2022*
Accepted: *06 April 2022*
Published: *28 April 2022*

Citation:
Ni M, Yin X-D, Hu W-J, Zeng N, Zhao B and Li Z-L (2022) Stevens-Johnson Syndrome Following Vancomycin and Linezolid: A Real-World Analysis of Post-Marketing Surveillance Data. Front. Pharmacol. 13:872854. doi: 10.3389/fphar.2022.872854

INTRODUCTION

With the emergence of highly resistant β-lactam gram-positive bacteria, the use of vancomycin and linezolid has greatly increased (National Nosocomial Infections Surveillance System, 2004; Fridkin et al., 1999; Jones et al., 1999). Vancomycin was the first glycopeptide antibiotic to be introduced and is widely used in the treatment of MRSA and other Gram-positive bacteria. Linezolid is a new generation of fully synthetic oxazolidinone antibacterial drugs, which can be clinically used for the anti-infection treatment of pneumonia and vancomycin-resistant bacteria. The adverse reactions of vancomycin during use mainly include nephrotoxicity, ototoxicity and hematological toxicity. Therefore, vancomycin often needs to monitor the blood concentration during use, and adjust the dose to benefit while reducing the risk of adverse reactions. Common adverse reactions of linezolid are more prominent, such as thrombocytopenia, optic neuropathy, peripheral neuropathy, and lactic acidosis (Kishor et al., 2015).

With the increasing use of drugs, there are also concerns about serious adverse drug reactions. Drug eruptions are skin eruptions that are induced by drugs. Many drug eruptions belong to immunologically mediated reac-tions which are dose-independent and also termed type B adverse reactions. SJS is a potentially life-threatening immune-mediated adverse reaction characterized by extensive erythema, epidermal necrosis, and sloughing of the skin and mucosa. SJS is a rare but high burden disease. It is necessary to strengthen prevention, early diagnosis and long-term management (Chang et al., 2020).

The literature on vancomycin and linezolid-induced SJS is rare (Alexander and Greenberger, 1996; Jones et al., 2004; Minhas et al., 2016). Therefore, we can only obtain the association between vancomycin, linezolid and SJS through the reports in the faers database, which helps us to further study the differences between vancomycin related SJS and linezolid related SJS in time of onset, mortality and hospitalization.

METHODS

Data Source

A retrospective pharmacovigilance study was conducted with data retrieved from January 2004 to July 2021 through the FAERS database. From the FAERS database, we selected reports of SJS caused by vancomycin or linezolid, and retrieved a total of 339 reports. Among them, there were 276 cases of vancomycin-related SJS reports and 63 cases of linezolid-related SJS reports, and duplicate data reports were deleted after referring to FDA recommendations.

Adverse Event and Drug Identification

We investigated adverse events by using the MedDRA (Version 24.0) Preferred Terms as follows: epidermal necrosis (10059284), epidermal necrolysis (10014986), SJS (10042033), toxic epidermal necrolysis (10044223), Stevens Johnson reaction (10042029). Therefore, MICROMEDEX ® (index nominum) was used like a dictionary. In addition, the trade names and common names of vancomycin and linezolid in the drug archives will also be listed.

Data Mining

Based on the basic principles of Bayesian analysis and non proportional analysis, we applied reporting odds ratio (ROR), proportional reporting ratio (PRR), Bayesian confidence propagation neural network (BCPNN) and multiple gamma Poisson constrictor (MGPS) algorithms to explore the relationship between vancomycin or linezolid and SJS adverse reactions. The equations and standards of the four algorithms (DuMouchel, 1999; Evans et al., 2001; Szarfman et al., 2002; Van Puijenbroek et al., 2002; Hauben, 2003; Hauben et al., 2005; Norén et al., 2006; Ooba and Kubota, 2010; Szumilas, 2010) have been compiled into a table. See **Table 1** for details. The extraction of these algorithms is mainly used to judge the tightness of the relationship between drugs and adverse events. As long as any one of the four algorithms meets the standard, it will be considered as a positive signal of SJS adverse events.

We separately counted the time to onset of SJS adverse reactions induced by vancomycin and linezolid, and recorded

TABLE 1 | Summary of major algorithms used for signal detection.

Algorithms	Equation[a]	Criteria
ROR	$ROR = (a/b)/(c/d)$	95% CI > 1, N ≥ 2
	$95\%CI = e^{\ln(ROR)\pm1.96(1/a+1/b+1/c+1/d)\hat{0}.5}$	
PRR	$PRR = (a/(a+c))/(b/(b+d))$	PRR≥2, $\chi^2 \geq 4$, N ≥ 3
	$\chi^2 = \sum((O-E)^2/E)$; $(O = a, E = (a+b)(a+c)/(a+b+c+d))$	
BCPNN	$IC = \log_2 a(a+b+c+d)/((a+c)(a+b))$	IC025 > 0
	$IC025 = e^{\ln(IC)-1.96(1/a+1/b+1/c+1/d)\hat{0}.5}$	
MGPS	$EBGM = a(a+b+c+d)/((a+c)(a+b))$	EB05 ≥ 2, N > 0
	$EB05 = e^{\ln(EBGM)-1.64(1/a+1/b+1/c+1/d)\hat{0}.5}$	

[a]*a: number of reports containing both the suspect drug and the suspect adverse drug reaction. b: number of reports containing the suspect adverse drug reaction with other medications (except the drug of interest). c: number of reports containing the suspect drug with other adverse drug reactions (except the event of interest). d: number of reports containing other medications and other adverse drug reactions. Abbreviations: ROR, reporting odds ratio; CI, confidence interval; N, the number of co-occurrences; PRR, proportional reporting ratio; χ^2, chi-squared; BCPNN, Bayesian confidence propagation neural network; IC, information component; IC025, the lower limit of the 95% two-sided CI, of the IC; MGPS, multi-item gamma Poisson shrinker; EBGM, empirical Bayesian geometric mean; EB05, the lower 90% one-sided CI of EBGM.*

TABLE 2 | Signal detection for vancomycin-associated SJS and linezolid-associated SJS.

Drugs	N	ROR (95% two-sided CI)	PRR (χ2)	IC (IC025)	EBGM (EBGM05)
Vancomycin	276	9.72 (8.62,10.96)*	9.56 (2097.18)*	3.24 (2.88)*	9.47 (8.57)*
Linezolid	63	3.46 (2.7,4.43)*	3.44 (109.19)*	1.78 (1.39)*	3.44 (2.79)*

ROR, reporting odds ratio; CI, confidence interval; PRR, proportional reporting ratio; χ^2, chi-squared; IC, information component; EBGM, empirical Bayesian geometric mean.

TABLE 3 | Clinical characteristics of patients with vancomycin-associated SJS and Linezolid-associated SJS collected from the FAERS database (January 2004 to July 2021).

Characteristics	Reports (N, %)	
	Vancomycin	Linezolid
Patient age (year)		
<18	17 (6.16)	1 (1.59)
18–44	41 (14.86)	2 (3.17)
45–64	87 (31.52)	23 (36.51)
65–74	55 (19.93)	17 (26.98)
>74	41 (14.86)	4 (6.35)
Unknown	35 (12.68)	16 (25.40)
Patient gender		
Female	121 (43.84)	29 (46.03)
Male	136 (49.28)	28 (44.44)
Unknown	19 (0.36)	6 (1.59)
Area		
Africa	0 (0.00)	0 (0.00)
Asia	26 (9.42)	8 (12.70)
Europe	90 (32.61)	26 (41.27)
Oceania	0 (0.00)	0 (0.00)
North America	130 (47.10)	26 (41.27)
South America	6 (2.17)	1 (1.59)
Unknown	24 (8.70)	2 (3.17)
Reporters		
Consumer	7 (2.54)	3 (4.76)
Lawyer	11 (3.99)	0 (0.00)
Pharmacist	77 (27.90)	19 (30.16)
Physician	68 (24.64)	10 (15.87)
Other health-professional	66 (23.91)	21 (33.33)
Unknown	47 (17.03)	10 (15.87)
Outcome event		
Death	93 (33.70)	25 (39.68)
Disability	18 (6.52)	3 (4.76)
Hospitalization-Initial or Prolonged	144 (52.17)	28 (44.44)
Life-Threatening	59 (21.38)	17 (26.98)
Other Serious (Important Medical Event)	122 (44.20)	35 (55.56)
Required Intervention to Prevent Permanent Impairment/Damage	17 (6.16)	1 (1.59)

FAERS, FDA, adverse event reporting system.

as the time interval between the start of drug administration and the occurrence of adverse events. Mortality data were reported as the ratio of reported deaths to vancomycin- or linezolid-related SJS reports. Also, all of the above reports are valid reports.

Statistical Analysis

An applied descriptive analysis was made based on the clinical characteristics of patients with SJS induced by vancomycin and linezolid in the FAERS database. The time to onset of SJS induced by vancomycin and linezolid was compared using the Mann-Whitney test. Pearson's chi-square test or Fisher's exact test was utilized to compare the mortality and hospitalization rates between Vancomycin and Linezolid. The statistical significance was set at $p < 0.001$ with 95% confidence intervals. All statistical analyses were performed by the software GraphPad Prism 8 (GraphPad Software, CA, United States).

RESULTS

Disproportionality Analysis and Bayesian Analysis

We searched the FARS database of 339 cases for all reports of vancomycin or linezolid-induced SJS from January 2004 to July 2021. Of these, 276 were SJS caused by vancomycin and 63 were SJS caused by linezolid. As shown in **Table 2**, according to the

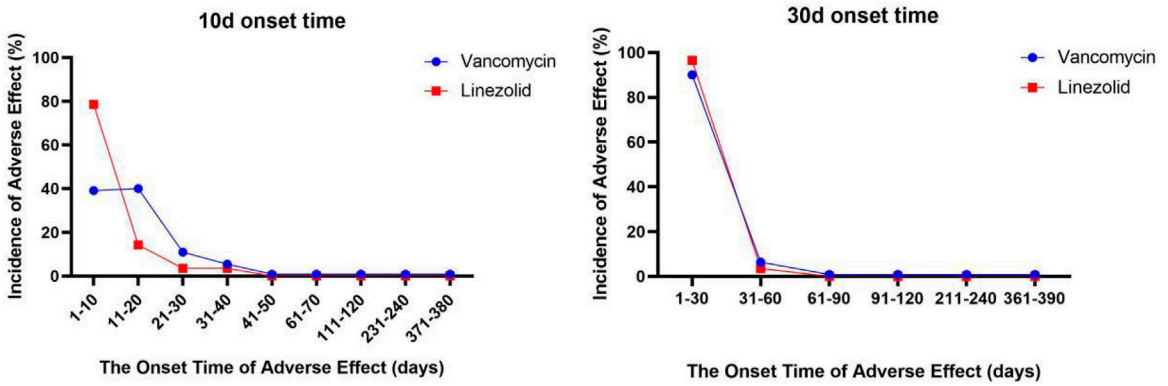

FIGURE 1 | The onset time of vancomycin- and linezolid-associated SJS.

four algorithm criteria, vancomycin- and linezolid-induced SJS signals were detected, in which ROR, PRR, information component (IC), and empirical Bayesian geometric mean (EBGM) were all statistically significant.

Descriptive Analysis

A summary of the clinical features reporting vancomycin- and linezolid-related SJS is presented in **Table 3**. With the exception of unspecified age, we found that SJS adverse reactions due to vancomycin and linezolid were more common in middle-aged patients (45–64 years) than in other age groups, minors (<18 years) are less common. Among them, the reported rate of linezolid-related SJS was more common in middle-aged and elderly patients (45–74) compared with other groups. In terms of patient gender, in vancomycin-related SJS cases, males were more likely to report than females (49.28% vs 43.84%), while in linezolid-related SJS cases, the proportion of males and females was almost Equal (29–28). In terms of regions reporting adverse reactions, approximately one-half of vancomycin-related SJ reports were from North America, and one-third were from Europe. Most reports on linezolid come from North America and Europe. Most reports are submitted by pharmacists, other health professionals and physicians, and reporting adverse drug events is the responsibility and obligation of every medical professional. Among them, pharmacists reported the most cases of vancomycin (27.9%) and doctors reported the most cases of linezolid (33.33%).

Time to Onset of Vancomycin- and Linezolid-Associated SJS

We describe the time to onset of vancomycin and linezolid in **Figure 1**. The median time to onset of linezolid-related SJS was 5 days (interquartile range [IQR] 2–7.75), significantly earlier than vancomycin-related SJS (12 days, IQR 4–20) (Mann-Whitney test, $p < 0.0001$). In general, vancomycin and linezolid-induced SJS had a higher onset time overall, while vancomycin and linezolid were special-use antibacterial drugs and should not be used for a long time. During use, more attention should be paid to monitoring adverse reactions at the initial stage of medication, especially linezolid.

Fatality and Hospitalization Due to Vancomycin- and Linezolid-Associated SJS

To assess the mortality and hospitalization rates of SJS caused by vancomycin and linezolid to analyze the prognosis of SJS associated with vancomycin and linezolid. According to the report analysis, the hospitalization rate of vancomycin-related SJS was 52.17%, and the hospitalization rate of linezolid-related SJS was 44.44%. Unfortunately, vancomycin and linezolid did not differ significantly in mortality (33.7% VS 39.68%) and hospitalization after SJS.

The left figure only shows the change in the incidence of SJS every 10 days after administration for 380 days. The graph on the right shows the change in the incidence of SJS every 30 days after administration for 390 days.

DISCUSSION

As of now, this study is the first and largest report based on the FAES pharmacovigilance database from January 2004 to July 2021 to describe vancomycin- and linezolid-induced SJS in different vulnerable populations, onset time and adverse outcomes in real-world practice. The sample size of previous related studies is small, and most of them are single cases (Alexander and Greenberger, 1996; Waldman et al., 2004; Craycraft et al., 2005; Nasr et al., 2014), among which the literature reports of vancomycin causing SJS are more than that of linezolid. This article discusses the characteristics of SJS caused by vancomycin and linezolid from multiple perspectives, including mortality, hospitalization rate, and time to adverse reactions.

In the results of this study, we found that vancomycin-induced SJS is more common in middle-aged and elderly people. The population of case reports we collected in the PubMed database is also mostly middle-aged and elderly (Laurencin et al., 1992; Waldman et al., 2004; Craycraft et al.,

2005; Craycraft et al., 2005). There are great differences in the pharmacokinetic behavior of vancomycin in different groups. After entering the human body, vancomycin is mainly metabolized through the kidney. Many factors may affect the pharmacokinetic behavior of vancomycin in the body, such as age, obesity, combined diseases, receiving other treatments and so on. There is evidence that infection is a serious cause of death in the elderly population over the age of 65 (Centers for Disease Control and Prevention, 2013). The risk of colonization and infection with methicillin-resistant *Staphylococcus aureus* (MRSA) in elderly patients is five times higher than in younger patients, resulting in a substantial increase in the frequency of vancomycin use (Barber et al., 2016). Changes in the physiological conditions of elderly patients are also potential factors that induce adverse drug reactions.

When SJS occurs, it is usually accompanied by eye diseases, and ophthalmologists need to intervene as soon as possible and follow up in a timely manner. The mechanism by which vancomycin and linezolid cause SJS is still unclear, mainly the immune pathogenesis, thus hindering the prevention and treatment of the disease. T cells may be the key mediators that induce SJS. Drugs, considered as foreign antigens, likely interact with particular HLA/peptide/T-cell receptor (TCR) complexes on keratinocytes to trigger the adaptive immune response and adverse reactions (Chang et al., 2020). The risk of SJS varies significantly by race or ethnicity with respect to the drugs used. It is not difficult to see from our research that North America and Europe have the highest incidence of SJS. We speculate that this may be related to the higher use of vancomycin and linezolid in North America and Europe. The more frequently antibiotics are used, the higher the resistance rate.

The global clinical and financial burden of SJS/ten is quite large, and the mortality rate of the elderly is even as high as 50% (White et al., 2018). In this study, hospitalization and mortality were also high after drug-induced SJS. The adverse outcomes of vancomycin-related SJS led to a hospitalization rate of 52.17%, and linezolid-related SJS led to a hospitalization rate of 44.44%, which was similar to mortality (44.44% vs 39.68%). Due to the low number of reported SJS associated with linezolid, we did not expect a significant difference between vancomycin and linezolid. The data can only show that once SJS is induced, both will lead to an increase in hospitalization rate and mortality, and the prognosis of patients is not ideal. However, we believe that early prediction and diagnosis will be more helpful for subsequent treatment.

Based on the FAERS database, the time to onsets of SJS for vancomycin and linezolid mainly occurred within 1 month after administration (vancomycin: median 12 days, IQR 4–20; linezolid: median 5 days, IQR 2–7.75), but there was a significant difference in average time to onset of SJS among vancomycin and linezolid (Mann-Whitney test, $p < 0.0001$). It can be seen that the time of SJS in patients using linezolid will be earlier than that of vancomycin. This requires our physicians and pharmacists to pay early attention to the occurrence of serious adverse skin reactions, especially SJS, when using linezolid. For vancomycin, the attention of physicians and pharmacists is required after 1 week of use.

The data in this study are all from professionals, including Pharmacist, Physician and Other health-professionals. This study fully demonstrates the advantages of real-world research and data mining technology, but there are also some limitations. Firstly, in the process of data mining, there will be incomplete information, such as input errors, report lack of important information and so on. These situations may lead to deviation in report analysis, which is an inevitable limitation of faers database. Secondly, we need to remove some duplicate or overlapping reports. When we try to delete some duplicate data based on event_dt, age, sex and reporter_country, a small part of the report may be lost. Due to the limited time, we can't check all the report information one by one, so we can only eliminate the reports lacking information. Of course, our method needs further consideration. Third, confounding factors are difficult to control. The patient may already have a potential immune disease, which may aggravate the incidence of skin adverse reactions such as SJS. Fourth, disproportionate measurements lack incidence denominators, suffer from severe reporting bias, and are not subject to confounding adjustment (Michel et al., 2017; Raschi et al., 2018). Therefore, pharmacovigilance (analysis of spontaneous reporting system) cannot provide safety comparison or evaluate the association between drugs, especially the incidence of adverse events. The assumptions generated by disproportionate analysis also need to be further verified by more reliable and accurate methods. Although the above shortcomings do exist, the faers database can still help us identify the signals of vancomycin or linezolid and SJS. Our research may provide some help to the clinic for vancomycin and linezolid in the incidence of SJS.

CONCLUSION

In his study, the signal of SJS after Vancomycin and Linezolid in real-world practice were determined according to the analysis of FAERS database. Compared with vancomycin, linezolid is less prone to skin rash and less prone to SJS. This may be related to the frequency of drug use, or it may be related to the fact that the drug itself is not easy to induce immune-related adverse reactions. However, the sample size of this study is limited, and more scientific researchers are required to work together to advance science and transform it into prediction, prevention, early diagnosis and treatment. Our study lays the foundation for a pharmacovigilance investigation, and further clinical pharmacy and pharmacoepidemiology may be required to test the hypotheses generated by this study for a more precise reporting analysis.

DATA AVAILABILITY STATEMENT

The original contributions presented in the study are included in the article/**Supplementary Material**, further inquiries can be directed to the corresponding authors.

AUTHOR CONTRIBUTIONS

All authors listed have made a substantial, direct, and intellectual contribution to the work and approved it for publication. MN,

X-DY, and W-JH analyzed and interpreted data, plotted figures, and wrote the manuscript draft. NZ and BZ participated in the interpretation of data. Z-LL designed and directed the research and assisted in preparing this manuscript and providing constructive suggestions.

FUNDING

Project Sponsored by Science and Technology Commission of Shanghai Municipality (No. 21DZ2300700), Shanghai "Rising Stars of Medical Talent" Youth Development Program "Outstanding Youth Medical Talent" (No. SHWSRS (2021)_099), Shanghai Talent Development Funding (No. 2020110).

SUPPLEMENTARY MATERIAL

The Supplementary Material for this article can be found online at: https://www.frontiersin.org/articles/10.3389/fphar.2022.872854/full#supplementary-material

REFERENCES

Alexander, II, and Greenberger, P. A. (1996). Vancomycin-Induced Stevens-Johnson Syndrome. *Allergy Asthma Proc.* 17 (2), 75–78. doi:10.2500/108854196778645029

Barber, K. E., Bell, A. M., Stover, K. R., and Wagner, J. L. (2016). Intravenous Vancomycin Dosing in the Elderly: A Focus on Clinical Issues and Practical Application. *Drugs Aging.* 33 (12), 845–854. doi:10.1007/s40266-016-0420-z

Centers for Disease Control and Prevention (2013). *The State of Aging and Health in America 2013*. Atlanta: Centers for Disease Control and Prevention, U.S. Department of Health and Human Services.

Chang, W. C., Abe, R., Anderson, P., Anderson, W., Ardern-Jones, M. R., Beachkofsky, T. M., et al. (2020). SJS/TEN 2019: From Science to Translation. *J. Dermatol. Sci.* 98 (1), 2–12. doi:10.1016/j.jdermsci.2020.02.003

Craycraft, M. E., Arunakul, V. L., and Humeniuk, J. M. (2005). Probable Vancomycin-Associated Toxic Epidermal Necrolysis. *Pharmacotherapy.* 25 (2), 308–312. doi:10.1592/phco.25.2.308.56953

DuMouchel, W. (1999). Bayesian Data Mining in Large Frequency Tables, with an Application to the FDA Spontaneous Reporting System. *The Am. Statistician.* 53 (3), 177–190. doi:10.1080/00031305.1999.10474456

Evans, S. J., Waller, P. C., and Davis, S. (2001). Use of Proportional Reporting Ratios (PRRs) for Signal Generation from Spontaneous Adverse Drug Reaction Reports. *Pharmacoepidemiol. Drug Saf.* 10 (6), 483–486. doi:10.1002/pds.677

Fridkin, S. K., Steward, C. D., Edwards, J. R., Pryor, E. R., McGowan, J. E., Jr, Archibald, L. K., et al. (1999). Surveillance of Antimicrobial Use and Antimicrobial Resistance in United States Hospitals: Project ICARE Phase 2. Project Intensive Care Antimicrobial Resistance Epidemiology (ICARE) Hospitals. *Clin. Infect. Dis.* 29 (2), 245–252. doi:10.1086/520193

Hauben, M. (2003). A Brief Primer on Automated Signal Detection. *Ann. Pharmacother.* 37 (7-8), 1117–1123. doi:10.1345/aph.1C515

Hauben, M., Madigan, D., Gerrits, C. M., Walsh, L., and Van Puijenbroek, E. P. (2005). The Role of Data Mining in Pharmacovigilance. *Expert Opin. Drug Saf.* 4 (5), 929–948. doi:10.1517/14740338.4.5.929

Jones, D. H., Todd, M., and Craig, T. J. (2004). Early Diagnosis Is Key in Vancomycin-Induced Linear IgA Bullous Dermatosis and Stevens-Johnson Syndrome. *J. Am. Osteopath Assoc.* 104 (4), 157–163. doi:10.1016/S0091-6749(03)80563-8

Jones, R. N., Low, D. E., and Pfaller, M. A. (1999). Epidemiologic Trends in Nosocomial and Community-Acquired Infections Due to Antibiotic-Resistant Gram-Positive Bacteria: the Role of Streptogramins and Other Newer Compounds. *Diagn. Microbiol. Infect. Dis.* 33 (2), 101–112. doi:10.1016/s0732-8893(98)00108-4

Kishor, K., Dhasmana, N., Kamble, S. S., and Sahu, R. K. (2015). Linezolid Induced Adverse Drug Reactions - an Update. *Curr. Drug Metab.* 16 (7), 553–559. doi:10.2174/1389200216666151001121004

Laurencin, C. T., Horan, R. F., Senatus, P. B., Wheeler, C. B., and Lipson, S. J. (1992). Stevens-Johnson-type Reaction with Vancomycin Treatment. *Ann. Pharmacother.* 26 (12), 1520–1521. doi:10.1177/106002809202601206

Michel, C., Scosyrev, E., Petrin, M., and Schmouder, R. (2017). Can Disproportionality Analysis of Post-marketing Case Reports Be Used for Comparison of Drug Safety Profiles? *Clin. Drug Investig.* 37 (5), 415–422. doi:10.1007/s40261-017-0503-6

Minhas, J. S., Wickner, P. G., Long, A. A., Banerji, A., and Blumenthal, K. G. (2016). Immune-mediated Reactions to Vancomycin: A Systematic Case Review and Analysis. *Ann. Allergy Asthma Immunol.* 116 (6), 544–553. doi:10.1016/j.anai.2016.03.030

Nasr, J., Ammoury, A., Chouairy, C., Mégarbané, H., and El Habr, C. (2014). Drug-induced Linear IgA Bullous Dermatosis Simulating Toxic Epidermal Necrolysis. *J. Med. Liban* 62 (3), 176–179. doi:10.12816/0006220

National Nosocomial Infections Surveillance System (2004). National Nosocomial Infections Surveillance (NNIS) System Report, Data Summary from January 1992 through June 2004, Issued October 2004. *Am. J. Infect. Control.* 32 (8), 470–485. doi:10.1016/S0196655304005425

Norén, G. N., Bate, A., Orre, R., and Edwards, I. R. (2006). Extending the Methods Used to Screen the WHO Drug Safety Database towards Analysis of Complex Associations and Improved Accuracy for Rare Events. *Stat. Med.* 25 (21), 3740–3757. doi:10.1002/sim.2473

Ooba, N., and Kubota, K. (2010). Selected Control Events and Reporting Odds Ratio in Signal Detection Methodology. *Pharmacoepidemiol. Drug Saf.* 19 (11), 1159–1165. doi:10.1002/pds.2014

Raschi, E., Poluzzi, E., Salvo, F., Pariente, A., De Ponti, F., Marchesini, G., et al. (2018). Pharmacovigilance of Sodium-Glucose Co-transporter-2 Inhibitors: What a Clinician Should Know on Disproportionality Analysis of Spontaneous Reporting Systems. *Nutr. Metab. Cardiovasc. Dis.* 28 (6), 533–542. doi:10.1016/j.numecd.2018.02.014

Szarfman, A., Machado, S. G., and O'Neill, R. T. (2002). Use of Screening Algorithms and Computer Systems to Efficiently Signal higher-Than-expected Combinations of Drugs and Events in the US FDA's Spontaneous Reports Database. *Drug Saf.* 25 (6), 381–392. doi:10.2165/00002018-200225060-00001

Szumilas, M. (2010). Explaining Odds Ratios. *J. Can. Acad. Child. Adolesc. Psychiatry* 19 (3), 227–229.

Van Puijenbroek, E. P., Bate, A., Leufkens, H. G., Lindquist, M., Orre, R., and Egberts, A. C. (2002). A Comparison of Measures of Disproportionality for Signal Detection in Spontaneous Reporting Systems for Adverse Drug Reactions. *Pharmacoepidemiol. Drug Saf.* 11 (1), 3–10. doi:10.1002/pds.668

Waldman, M. A., Black, D. R., and Callen, J. P. (2004). Vancomycin-induced Linear IgA Bullous Disease Presenting as Toxic Epidermal Necrolysis. *Clin. Exp. Dermatol.* 29 (6), 633–636. doi:10.1111/j.1365-2230.2004.01649.x

White, K. D., Abe, R., Ardern-Jones, M., Beachkofsky, T., Bouchard, C., Carleton, B., et al. (2018). SJS/TEN 2017: Building Multidisciplinary Networks to Drive Science and Translation. *J. Allergy Clin. Immunol. Pract.* 6 (1), 38–69. doi:10.1016/j.jaip.2017.11.023

Conflict of Interest: The authors declare that the research was conducted in the absence of any commercial or financial relationships that could be construed as a potential conflict of interest.

Publisher's Note: All claims expressed in this article are solely those of the authors and do not necessarily represent those of their affiliated organizations, or those of the publisher, the editors and the reviewers. Any product that may be evaluated in this article, or claim that may be made by its manufacturer, is not guaranteed or endorsed by the publisher.

frontiers | Frontiers in Pharmacology

ORIGINAL RESEARCH
published: 28 April 2022
doi: 10.3389/fphar.2022.891336

Antifungal Drugs and Drug-Induced Liver Injury: A Real-World Study Leveraging the FDA Adverse Event Reporting System Database

Zhi-Xuan Zhou[1,2†], Xue-Dong Yin[1,2†], Yu Zhang[1,3†], Qi-Hui Shao[1,2], Xin-Yu Mao[1,2], Wen-Juan Hu[1], Yun-Lin Shen[4], Bin Zhao[5]* and Zhi-Ling Li[1]**

[1]Department of Pharmacy, Shanghai Children's Hospital, Shanghai Jiao Tong University, Shanghai, China, [2]Shanghai Jiao Tong University School of Medicine, Shanghai, China, [3]Department of Pharmacy, Nanyang Central Hospital, Affiliated Hospital of Zhengzhou University, Nanyang, China, [4]Department of Neonatology, Shanghai Children's Hospital, Shanghai Jiao Tong University, Shanghai, China, [5]Pharmacy Department, Peking Union Medical College Hospital, Peking Union Medical College, Chinese Academy of Medical Sciences, Beijing, China

OPEN ACCESS

Edited by:
Jian Gao,
Shanghai Children's Medical Center, China

Reviewed by:
Lujuan Gao,
Fudan University, China
Yi Sun,
Jingzhou Hospital Affiliated to Yangtze University, China

***Correspondence:**
Yun-Lin Shen
shenyl@shchildren.com.cn
Bin Zhao
zhaobin@pumch.cn
Zhi-Ling Li
lizhiling22@163.com

†These authors have contributed equally to this work

Specialty section:
This article was submitted to Obstetric and Pediatric Pharmacology, a section of the journal Frontiers in Pharmacology

Received: 07 March 2022
Accepted: 28 March 2022
Published: 28 April 2022

Citation:
Zhou Z-X, Yin X-D, Zhang Y, Shao Q-H, Mao X-Y, Hu W-J, Shen Y-L, Zhao B and Li Z-L (2022) Antifungal Drugs and Drug-Induced Liver Injury: A Real-World Study Leveraging the FDA Adverse Event Reporting System Database. Front. Pharmacol. 13:891336. doi: 10.3389/fphar.2022.891336

Aims: We aimed to estimate the risk of drug-induced liver injury (DILI) from various antifungal treatments with azoles and echinocandins causing in real-world practice.

Methods: We performed disproportionality and Bayesian analyses based on data from the first quarter in 2004 to the third quarter in 2021 in the Food and Drug Administration Adverse Event Reporting System to characterize the signal differences of antifungal drugs-related DILI. We also compared the onset time and mortality differences of different antifungal agents.

Results: A total of 2943 antifungal drugs-related DILI were identified. Affected patients tended to be aged >45 years (51.38%), with more males than females (49.03% vs. 38.09%). Antifungal drug-induced liver injury is most commonly reported with voriconazole (32.45%), fluconazole (19.37%), and itraconazole (14.51%). Almost all antifungal drugs were shown to be associated with DILI under disproportionality and Bayesian analyses. The intraclass analysis of correlation between different antifungal agents and DILI showed the following ranking: caspofungin (ROR = 6.12; 95%CI: 5.36–6.98) > anidulafungin (5.15; 3.69–7.18) > itraconazole (5.06; 4.58–5.60) > voriconazole (4.58; 4.29–4.90) > micafungin (4.53; 3.89–5.27) > posaconazole (3.99; 3.47–4.59) > fluconazole (3.19; 2.93–3.47) > ketoconazole (2.28; 1.96–2.64). The onset time of DILI was significantly different among different antifungal drugs ($p < 0.0001$), and anidulafungin result in the highest mortality rate (50.00%), while ketoconazole has the lowest mortality rate (9.60%).

Conclusion: Based on the Food and Drug Administration Adverse Event Reporting System database, antifungal drugs are significantly associated with DILI, and itraconazole and voriconazole had the greatest risk of liver injury. Due to indication bias, more clinical studies are needed to confirm the safety of echinocandins.

Keywords: DILI, antifungal drugs, pharmacovigilance, adverse event reporting system, epidemiology

INTRODUCTION

Drug-induced liver injury (DILI) is a common and serious adverse drug reaction, defined as liver damage caused by a drug or herbal product resulting in abnormal liver tests or liver dysfunction, after reasonable exclusion of competing etiologies (Raschi E et al., 2014). Antifungal drugs can be classified as polyenes, antimetabolite—flucytosine (5-FC), azoles, echinocandins, the latter two being more common, which are the first-line option for the prevention and treatment of fungal infections caused by immunosuppression (Nett and Andes, 2016). In recent years, due to the epidemic of acquired immunodeficiency syndrome (AIDS) and the advancement of immunosuppressive techniques, the number of patients with severely weakened immune systems has increased, and the incidence of fungal infections has continued to rise (Tverdek et al., 2016). With the wide application of antifungal drugs, the safety of antifungal drugs has been concerned.

There are many adverse reactions to antifungal drugs, such as hepatotoxicity and hormone-related effects (gynecomastia, alopecia, decreased libido, oligospermia, azoospermia and so on), among which hepatotoxicity is the most common. An article summarized that all azoles have abnormal liver function and hepatotoxicity, and the frequency of adverse reactions varies by drug and patient population (Benitez and Carver, 2019). A real-world study found that about 2.9% of all reported drug-induced liver injuries are associated with antifungal drugs (Raschi et al., 2014). Another retrospective study reported the prevalence of micafungin-associated DILI was 10.6% (Mullins et al., 2020). It can be seen that almost all antifungal drugs have certain hepatotoxicity.

However, the current studies are based on a case or retrospective study of a drug, and there are few real-world studies. The existing real-world study was in 2014, and the data need to be further updated. In this context, this study aims to characterize the liver injury induced by various antifungal drugs in a large population by using FAERS. We further examined and compared the onset-time and outcomes of liver injury with different antifungal drugs.

METHODS

Data Source

We conducted a retrospective pharmacovigilance study using the FAERS database from the first quarter of 2004 to the third quarter of 2021. FDA adverse event reporting system (FAERS) is a

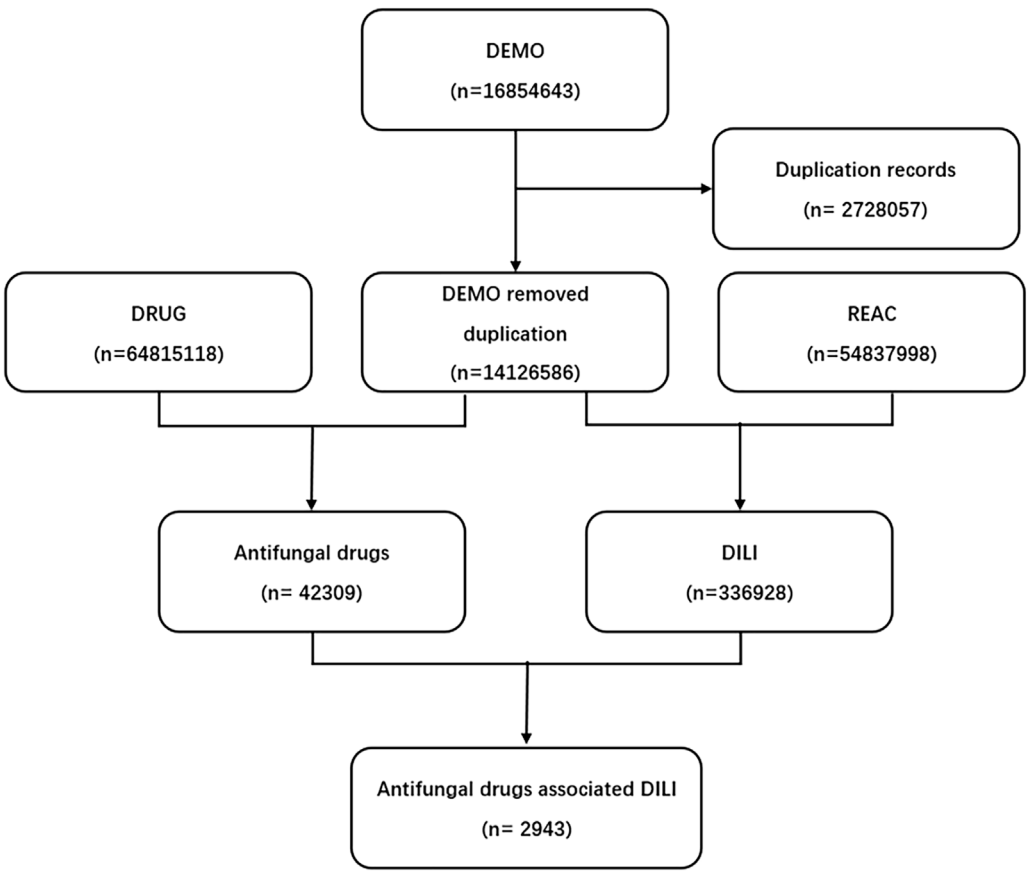

FIGURE 1 | Process of the selection of cases of antifungal drugs-associated liver injury from the Food and Drug Administration's Adverse Event Reporting System database. DEMO, demographic information; DRUG, drug information; REAC, adverse events.

TABLE 1 | MedDRA preferred terms used to retrieve liver events in FAERS.

PT
Liver injury
Liver damage
Liver necrosis
Hepatic damage
Hepatotoxicity
Hepatopathy
Hepatic disease
Hepatitis
Nonalcoholic fatty liver disease
Liver fatty infiltration
Steatohepatitis
Hepatic steatosis
Jaundice
Icterus
Cholestasis
Bile duct damage
Biliary cholangitis
Hepatobiliary disease
Hepatic encephalopathy
Hepatic failure
Hepatic vascular injury
Hepatic cirrhosis
Portal hypertension
DILI
Hepatic necrosis
Hepatocellular injury
Hepatomegaly
Hepatic enzyme abnormal
Hepatic enzyme increased
Transaminases increased
Transaminases abnormal
Blood bilirubin abnormal
Blood bilirubin increased
Aspartate aminotransferase abnormal
Aspartate aminotransferase increased
Hepatic injury
Hepatic function abnormal
Hepatocellular damage
Cirrhosis
Hyperbilirubinaemia
Liver transplant
Alanine aminotransferase abnormal
Alanine aminotransferase increased
Ammonia increased
Bilirubin conjugated increased
Bilirubin urine
Blood bilirubin unconjugated
Increased
Coma hepatic
Hyperammonaemia
Liver function test abnormal
Mixed hepatocellular-cholestatic injury
Urine bilirubin increased

PT, preferred terms.

database designed to support FDA's post-marketing monitoring plan for drugs and therapeutic biological products, which includes all Adverse drug reaction (ADR) signals and medication error information collected by FDA. A FAERS data contains demographic information, drug information, adverse events, patient outcomes, indications, duration of use, time to adverse reactions, and more. Finally, a total of 16854643 reports were obtained from the FAERS database (**Figure 1**).

Adverse Event and Drug Identification

DILI cases were obtained by searching using the Medical Dictionary for Regulatory Activities (MedDRA) (version 23.0), and the preferred terms are shown in **Table 1**. Study drugs were antifungal triazoles (ketoconazole, miconazole, clotrimazole, fluconazole, voriconazole, itraconazole, isavuconazole, posaconazole) and echinocandins (caspofungin, micafungin, anidulafungin) on the market.

Data Mining

Based on the principles of Bayesian analysis and disproportionality analysis, we used the reporting odds ratio (ROR), the proportional reporting ratio (PRR), the Bayesian confidence propagation neural network and the multi-item gamma Poisson shrinker algorithms to explore the associations between antifungal drugs and DILI (Evans et al., 2001; Szarfman et al., 2002; van Puijenbroek et al., 2002; Hauben et al., 2005; Norén et al., 2006; Ooba and Kubota, 2010; Szumilas, 2010). A two-by-two contingency table (**Table 2**) of reported event counts for specific drug and other drugs was constructed to calculate ROR, PRR, information component (IC), and empirical Bayesian geometric mean (EBGM). The former two belong to disproportionality analysis, while the latter two belong to Bayesian analysis. The calculation formula and criteria follow: **Table 2**.

Statistical Analysis

Descriptive analyses were used to summarize the characteristics of adverse event reports on antifungal drug-related liver injuries collected from the FAERS database. We analyzed the age, sex, reporters, country, area and reporting time distribution of different antifungal agents, and compared the onset time and mortality differences of different antifungal agents.

RESULTS

Descriptive Analysis

FAERS database from the first quarter in 2004 to the third quarter in 2021 contained 42309 antifungal drugs-related adverse events and 336928 DILI-related reports, among these 2943 were reported for DILI after using antifungal (**Figure 1**). The clinical characteristics of patients with antifungal drug-induced liver injuries were described in **Table 3** and **Figure 2**. Most of the patients were older than 45 years (51.38%), and men accounted for a larger proportion than women in all reports (49.03% vs. 38.09%). Most cases were reported from Europe (40.88%), Asia (25.35%) and North America (23.41%), and were reported by the physician (40.47%). More and more cases were reported from 2016 (5.27%) to 2020 (9.14%), reflecting the significantly increased usage of antifungal drugs in recent years. Voriconazole ranked first in the number of cases (955), followed by fluconazole and itraconazole.

TABLE 2 | Two-by-two contingency table for disproportional analysis.

	DILI	All other adverse drug reactions	Total
Antifungal drugs	a	c	a + c
All other drugs	b	d	b + d
Total	a + b	c + d	a+b + c + d

ROR = (a/b)/(c/d), 95% CI = $e^{\ln(ROR)\pm1.96\sqrt{1/a+1/b+1/c+1/d}}$ (criteria: 95% CI > 1, n ≥ 2);
PRR = (a / [a + c]) / (b / [b + d]), $\chi^2 = \Sigma([O-E]^2/E)$,
(O = a, E = [a + b] [a + c]/[a + b + c + d]) (criteria : PRR ≥ 2, $\chi^2 \geq 4$, n ≥ 3);
IC = $\log 2a^*(a+b+c+d)/([a+c][a+b])$,
IC025 = $e^{\ln(IC)-1.96\sqrt{1/a+1/b+1/c+1/d}}$ (criteria : IC025 > 0);
EBGM = $a^*(a+b+c+d)/([a+c][a+b])$, EBGM05 = $e^{\ln(EBGM)-1.64\sqrt{1/a+1/b+1/c+1/d}}$ (criteria: EBGM05 ≥ 2, n > 0).

CI, indicates confidence interval; n, indicates the number of co-occurrences; $\chi 2$, indicates chi-squared; IC, indicates information component; IC025, indicates the lower limit of the 95% two-sided CI of the IC; EBGM05, the lower limit of the 90% one-sided CI of the EBGM.

Disproportionality Analysis and Bayesian Analysis

Data showed a strong association between antifungals and DILI, with no positive signals detected only for miconazole and clotrimazole. In addition, there were two other drugs with one or two negative signals according to the criteria of the four algorithms: which are ketoconazole in EBGM: 2.21(1.95), and isavuconazole in ROR: 1.22(0.92–1.63), PRR: 1.22(1.88) and EBGM: 1.22(0.96). The intraclass analysis of correlation between different antifungal agents and DILI showed the following ranking: caspofungin (ROR = 6.12; 95%CI: 5.36–6.98) > anidulafungin (5.15; 3.69–7.18) > itraconazole (5.06; 4.58–5.60) > voriconazole (4.58; 4.29–4.90) > micafungin (4.53; 3.89–5.27) > posaconazole (3.99; 3.47–4.59) > fluconazole (3.19; 2.93–3.47) > ketoconazole (2.28; 1.96–2.64) (**Table 4**).

Onset Times of DILI

The median onset times of DILI for each antifungal drugs are summarized in **Table 5**. The onset time of DILI was significantly different among different antifungal drugs ($p < 0.0001$). Significant differences were noted for ketoconazole vs. posaconazole ($p = 0.0460$), ketoconazole vs. caspofungin ($p = 0.0006$), ketoconazole vs. micafungin ($p = 0.0018$), voriconazole vs. caspofungin ($p = 0.0248$), itraconazole vs. caspofungin ($p < 0.0001$), itraconazole vs. micafungin ($p = 0.0005$).

Outcomes due to DILI

To analyze the prognosis of antifungal drugs-induced liver injuries, we calculated the proportion of outcomes (death, disability, hospitalization, life-threatening, other serious and required intervention) due to DILI after various antifungal drugs treatments, and the results are shown in **Table 6**. Patients with antifungal-related liver damage tended to have poor outcomes, with approximately 42.21% of patients hospitalized and 22.86% dying. In addition, a significant difference in the mortality rate of DILI was found between different antifungal drugs ($p < 0.0001$). Anidulafungin results in the highest mortality rate (50.00%), while ketoconazole has the lowest mortality rate (9.60%). The mortality rate for each drug is shown in **Figure 3**.

TABLE 3 | Clinical characteristics of patients with antifungal drugs-associated DILI sourced from the FDA Adverse Event Reporting System database (2004q1 to 2021q3).

Characteristics	Reports, n (%)
Patient age (year)	
<18	218(7.41%)
18–44	511 (17.36%)
45–64	755(25.65%)
65–74	432 (14.68%)
75–84	264 (8.97%)
≥85	61 (2.07%)
Unknow	702(23.85%)
Reporter	
Consumer	306 (10.40%)
Lawyer	1 (0.03%)
Other health-professional	808(27.45%)
Pharmacist	345 (11.72%)
Physician	1191(40.47%)
Unknow	292 (9.92%)
Patient gender	
Female	1121 (38.09%)
Male	1443(49.03%)
Unknow	379(12.88%)
Year	
2004	136 (4.62%)
2005	132 (4.49%)
2006	134 (4.55%)
2007	120 (4.08%)
2008	117(3.98%)
2009	137 (4.66%)
2010	152 (5.16%)
2011	129 (4.38%)
2012	154 (5.23%)
2013	156(5.30%)
2014	124 (4.21%)
2015	174 (5.91%)
2016	155 (5.27%)
2017	183 (6.22%)
2018	231(7.85%)
2019	262 (8.90%)
2020	269 (9.14%)
2021	171 (5.81%)
Unknow	6 (0.20%)
Area	
Africa	26 (0.88%)
Asian	746(25.35%)
Europe	1203(40.88%)
North America	689 (23.41%)
Oceania	39 (1.33%)
South America	34 (1.16%)
Unknow	206 (7.00%)
Antifungal drugs	
Ketoconazole	188 (6.29%)
Miconazole	48 (1.63%)
Clotrimazole	10 (0.34%)
Fluconazole	570 (19.37%)
Voriconazole	955 (32.45%)
Itraconazole	427 (14.51%)
Isavuconazole	48 (1.63%)
Posaconazole	216 (7.34%)
Caspofungin	256 (8.70%)
Micafungin	186 (6.32%)
Anidulafungin	39 (1.33%)

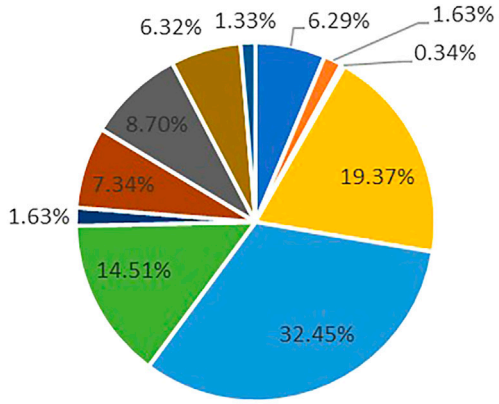

FIGURE 2 | Proportion of antifungal drugs-related liver injury.

TABLE 4 | Association of antifungal drugs with DILI.

Drugs	N	ROR (95% Two-sided CI)	PRR (χ2)	IC (IC025)	EBGM (EBGM05)
Ketoconazole	188	2.28 (1.96, 2.64)*	2.21 (127.22)*	1.14 (0.99)*	2.21(1.95)
Miconazole	48	0.30 (0.23, 0.40)	0.31 (77.37)	−1.71()	0.31 (0.24)
Clotrimazole	10	0.16 (0.08, 0.29)	0.16 (44.96)	−2.64 ()	0.16 (0.10)
Fluconazole	570	3.19 (2.93, 3.47)*	3.03 (793.68)*	1.60 (1.47)*	3.03 (2.82)*
Voriconazole	955	4.58 (4.29, 4.90)*	4.22 (2400.98)*	2.08 (1.94)*	4.22 (3.99)*
Itraconazole	427	5.06 (4.58, 5.60)*	4.62 (1237.69)*	2.21 (1.99)*	4.61 (4.24)*
Isavuconazole	48	1.22 (0.92, 1.63)	1.22 (1.88)	0.28 (0.21)*	1.22 (0.96)
Posaconazole	216	3.99 (3.47, 4.59)*	3.72 (440.63)*	1.90 (1.65)*	3.72 (3.31)*
Caspofungin	256	6.12 (5.36, 6.98)*	5.45 (952.64)*	2.45 (2.14)*	5.45 (4.88)*
Micafungin	186	4.53 (3.89, 5.27)*	4.18 (460.10)*	2.06 (1.77)*	4.17 (3.68)*
Anidulafungin	39	5.15 (3.69, 7.18)*	4.69 (115.82)*	2.23 (1.60)*	4.69 (3.55)*

ROR, reporting odds ratio; CI, confidence interval; PRR, proportional reporting ratio; χ^2, chi-squared; IC, information component; EBGM, empirical Bayesian geometric mean; "" suggests that antifungal agents are associated with DILI.*

TABLE 5 | Onset times of DILI associated with antifungals.

Antifungal drugs	M(IQR)(d)
Ketoconazole	21 (7–40)
Miconazole	22 (2.5–45.75)
Fluconazole	8 (3–17.25)
Voriconazole	8 (2–20)
Itraconazole	11 (4–32.5)
Isavuconazole	7 (0–56.5)
Posaconazole	6 (2–19)
Caspofungin	5 (2–11)
Micafungin	5 (1.5–12.5)
Anidulafungin	4 (1–12)

M, median; IQR, interquartile range; d, days.

DISCUSSION

Drug-induced liver injury is classified as intrinsic, idiosyncratic and indirect, and the idiosyncratic type can be divided into hepatocellular injury, cholestatic liver injury and mixed liver injury (Garcia-Cortes et al., 2020). Patients with alanine aminotransferase (ALT) > 5 times the upper limit of normal or alkaline phosphatase (ALP) > 2 times the upper limit of normal were considered suspected DILI. If ALT/ALP ≥5, it is defined as Hepatocellular injury; if ALT/ALP ≤2, it is defined as Cholestatic liver injury; if 2 < ALT/ALP <5, it is defined as Mixed liver injury (Danan and Theschke, 2015).

Triazole drugs prevent the synthesis of ergosterol by inhibiting C14 (a sterol demethylase), thereby reducing sterol precursors and ergosterol, and destroying the integrity of the fungal cell membrane, thus achieving the antifungal effect (Nett and Andes, 2016). The exact mechanism of hepatotoxicity induced by triazole drugs remains unclear. They competitively inhibit liver oxidative metabolism by rapidly and reversibly binding CYP450 metabolic enzymes, and are both substrates and inhibitors of various CYP450 metabolic enzymes, with potential for drug interactions (Zonios and Bennett, 2008). Drug interactions increase the risk of increased toxicity leading to liver damage. Itraconazole is metabolized primarily by the CYP450 isoenzyme CYP3A4; voriconazole is metabolized by the CYP450 isoenzymes CYP2C9, CYP2C19, and CYP3A4 (Haria et al., 1996; Alffenaar et al., 2009). In addition, itraconazole, but not voriconazole, is an inhibitor of gastric P-glycoprotein, a transmembrane efflux pump that limits blood drug concentrations by expelling the drug into

TABLE 6 | Outcomes events of DILI.

	Ketoconazole	Miconazole	Clotrimazole	Fluconazole	Voriconazole	Itraconazole	Isavuconazole	Posaconazole	Caspofungin	Micafungin	Anidulafungin
Congenital Anomaly	0(0.00)	1(2.22)	0(0.00)	0(0.00)	0(0.00)	2(0.48)	0(0.00)	0(0.00)	0(0.00)	0(0.00)	0(0.00)
Death	17(9.60)	6(13.33)	0(0.00)	100(18.28)	196(22.17)	75(17.99)	9(20.93)	38(20.32)	87(36.40)	85(47.49)	19(50.00)
Disability	3(1.69)	1(2.22)	0(0.00)	10(1.83)	24(2.71)	9(2.16)	0(0.00)	7(3.74)	8(3.35)	9(5.03)	1(2.63)
Hospitalization - Initial or Prolonged	67(37.85)	24(53.33)	6(66.67)	292(53.38)	322(36.43)	157(37.65)	17(39.53)	88(47.06)	123(51.46)	57(31.84)	14(36.84)
Life-Threatening	11(6.21)	3(6.67)	0(0.00)	51(9.32)	86(9.73)	22(5.28)	0(0.00)	23(12.30)	41(17.15)	31(17.32)	6(15.79)
Other Serious	117(66.10)	28(62.22)	7(77.78)	327(59.78)	638(72.17)	265(63.55)	39(90.70)	132(70.59)	126(52.72)	101(56.42)	21(55.26)
Required Intervention to Prevent Permanent Impairment/Damage	3(1.69)	0(0.00)	0(0.00)	4(0.73)	6(0.68)	2(0.48)	0(0.00)	2(1.07)	1(0.42)	0(0.00)	0(0.00)

the intestinal lumen (Wang et al., 2002). Itraconazole inhibits drug efflux by inhibiting P-glycoprotein, resulting in increased plasma concentrations and increased systemic exposure of the drug, so itraconazole has a higher risk of liver damage. Fluconazole is metabolized mainly through the kidney (Shiba et al., 1990), but not extensively through the liver, so its hepatotoxicity is relatively low. The echinocandins damage fungal cell walls by inhibiting the synthesis of B-1,3 glucan, a fungal cell wall polysaccharide essential to many fungi. The echinocandins are eliminated mainly by non-enzymatic degradation to an inactive product. Although they are not significantly metabolized by CYP450 enzymes, caspofungin and micafungin are metabolized in the liver and thus have less hepatotoxicity (Nett and Andes, 2016).

This study found that almost all antifungal drugs can cause liver damage, and the association of echinocandins is significantly higher than that of triazoles. In previous studies, hepatotoxicity of echinocandins was considered to be significantly lower than that of triazoles (Tverdek et al., 2016; Kyriakidis et al., 2017). An *in vitro* study found that caspofungin exhibited mild hepatotoxicity, whereas fluconazole and voriconazole exhibited higher hepatotoxicity (Doß et al., 2017). Due to the low hepatotoxicity of echinocandins, some echinocandins have been used safely in patients with pre-existing liver damage, namely caspofungin in patients with chronic liver disease and post-liver transplantation (Mycamine., 2010). A retrospective study found that patients with abnormal liver enzymes at baseline had an increased overall incidence of liver injury compared with patients without elevated liver enzymes at baseline (Takeda et al., 2007). Since echinocandins are widely used in patients with liver damage themselves, if the liver damage worsens after medication, the case may be reported to FAERS as DILI. Therefore, patients with echinocandins-related liver damage will be higher than the actual liver damage caused by drugs. The basic number of patients is large, so there is a strong correlation between echinocandins and liver damage, which is also a shortcoming of this study. Due to indication bias in real-world studies, the ROR of echinocandins was higher than that of triazoles.

Of note, we also found that the correlation between different triazoles and DILI showed the following ranking: itraconazole > voriconazole > fluconazole > ketoconazole. Previous studies considered ketoconazole to be the most hepatotoxic triazole, and ketoconazole was withdrawn from the market precisely due to its hepatotoxic effect and better-evaluated alternatives, so the ROR of this study was reduced accordingly. Numerous studies have shown that voriconazole and itraconazole are more hepatotoxic than other triazoles (Kullberg et al., 2005; Wang et al., 2010), possibly due to their ability to inhibit CYP450, resulting in significant drug-drug interactions, which in turn alter circulating plasma levels of concomitant drugs and increase liver toxicity.

Another finding is that the mortality rate of echinocandins was significantly higher than that of triazole. Among echinocandins, anidulafungin has the highest mortality rate. Anidulafungin is the only echinocandin that is not metabolized through the liver, and dose adjustment is not

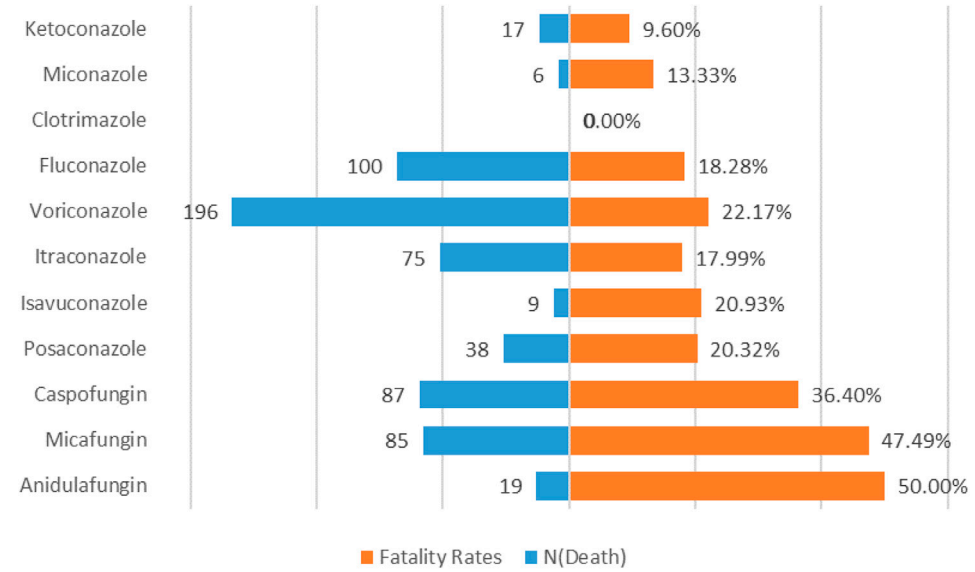

FIGURE 3 | Mortality rate for DILI associated with antifungal drugs.

required even in patients with severe hepatic insufficiency (Patil and Majumdar, 2017), therefore, clinicians may prefer to use anidulafungin in patients with a history of hepatotoxicity. A small retrospective study found that anidulafungin was used more than micafungin in patients with liver failure, confirming real-world channel bias (van der Geest et al., 2016). Another retrospective study also found that baseline liver function impairment and other more serious comorbidities were more likely to be in patients using anidulafungin (van der Geest et al., 2016; Vekeman et al., 2018). Therefore, the highest mortality rate of anidulafungin may be affected by the patients' condition. However, due to the significant risk of liver injury of azole drugs, clinicians will strictly grasp the indications and monitor the level of liver function when using them and stop taking them in time to relieve the condition when liver enzymes are significantly increased. In most cases using triazoles, liver enzymes returned to normal and symptoms disappeared within a few weeks after drug withdrawal (Song and Deresinski, 2005), so triazole mortality is relatively low.

We acknowledge that our research has certain limitations. First, the FAERS database is a fully open website, so the absolute authenticity of data cannot be guaranteed, and there may be duplicate samples and imperfect data. Due to underdeveloped information in some regions, a lot of data have not been recorded in the database, for example, the sample of Africa is only 0.88%. Secondly, this study selected all patients with liver damage after medication, which could not exclude further aggravation of liver damage in patients with abnormal liver function, so there was a certain bias. Finally, this paper did not use Roussel Uclaf Causality Assessment Method (RUCAM) to define DILI, but screened all patients with liver enzyme abnormalities or liver damage, so the data were not accurate to some extent. Therefore, the FAERS database cannot be directly used to calculate the incidence of DILI, but it can be used as a pharmacovigilance tool to remind pharmacists to use antifungals with caution.

The current study showed that antifungal drugs are significantly associated with DILI, and itraconazole and voriconazole had the greatest risk of liver injury. Clinicians are advised to monitor and consider patients' liver function when taking antifungal drugs. At the same time, due to indication bias, more clinical studies are needed to confirm the safety of echinocandins.

DATA AVAILABILITY STATEMENT

The original contributions presented in the study are included in the article/Supplementary Material, further inquiries can be directed to the corresponding authors.

AUTHOR CONTRIBUTIONS

Z-XZ analyzed and interpreted data, plotted figures, and wrote the manuscript draft. X-DY, YZ, Q-HS and X-YM participated in the interpretation of data. BZ, Y-LS and Z-LL designed and directed the research. W-JH, Y-LS and Z-LL assisted in preparing this manuscript and providing constructive suggestions.

FUNDING

Project Sponsored by Science and Technology Commission of Shanghai Municipality (No. 21DZ2300700), Shanghai

"Rising Stars of Medical Talent" Youth Development Program "Outstanding Youth Medical Talent" (No.SHWSRS (2021)_099), Shanghai Talent Development Funding(No. 2020110), "Innovative Training Program for College Students," School of Medicine, Shanghai Jiaotong University (No. 1521Y424).

ACKNOWLEDGMENTS

I would like to express my gratitude to all those who helped me during the writing of this paper. My deepest gratitude goes to Huajun Sun, director of the Department of Pharmacy, Shanghai Children's Hospital, for his support and help in this article.

REFERENCES

Alffenaar, J. W., de Vos, T., Uges, D. R., and Daenen, S. M. (2009). High Voriconazole Trough Levels in Relation to Hepatic Function: How to Adjust the Dosage? *Br. J. Clin. Pharmacol.* 67 (2), 262–263. doi:10.1111/j.1365-2125.2008.03315.x

Benitez, L. L., and Carver, P. L. (2019). Adverse Effects Associated with Long-Term Administration of Azole Antifungal Agents. *Drugs* 79 (8), 833–853. doi:10.1007/s40265-019-01127-8

Danan, G., and Teschke, R. (2015). RUCAM in Drug and Herb Induced Liver Injury: The Update. *Int. J. Mol. Sci.* 17 (1), 14. doi:10.3390/ijms17010014

Doß, S., Potschka, H., Doß, F., Mitzner, S., and Sauer, M. (2017). Hepatotoxicity of Antimycotics Used for Invasive Fungal Infections: *In Vitro* Results. *Biomed. Res. Int.* 2017, 9658018. doi:10.1155/2017/9658018

Evans, S. J., Waller, P. C., and Davis, S. (2001). Use of Proportional Reporting Ratios (PRRs) for Signal Generation from Spontaneous Adverse Drug Reaction Reports. *Pharmacoepidemiol. Drug Saf.* 10 (6), 483–486. doi:10.1002/pds.677

Garcia-Cortes, M., Robles-Diaz, M., Stephens, C., Ortega-Alonso, A., Lucena, M. I., and Andrade, R. J. (2020). Drug Induced Liver Injury: an Update. *Arch. Toxicol.* 94 (10), 3381–3407. doi:10.1007/s00204-020-02885-1

Haria, M., Bryson, H. M., and Goa, K. L. (1996). Itraconazole. A Reappraisal of its Pharmacological Properties and Therapeutic Use in the Management of Superficial Fungal Infections. *Drugs* 51 (4), 585–620. doi:10.2165/00003495-199651040-00006

Hauben, M., Madigan, D., Gerrits, C. M., Walsh, L., and Van Puijenbroek, E. P. (2005). The Role of Data Mining in Pharmacovigilance. *Expert Opin. Drug Saf.* 4 (5), 929–948. doi:10.1517/14740338.4.5.929

Kullberg, B. J., Sobel, J. D., Ruhnke, M., Pappas, P. G., Viscoli, C., Rex, J. H., et al. (2005). Voriconazole versus a Regimen of Amphotericin B Followed by Fluconazole for Candidaemia in Non-neutropenic Patients: a Randomised Non-inferiority Trial. *Lancet* 366 (9495), 1435–1442. doi:10.1016/S0140-6736(05)67490-9

Kyriakidis, I., Tragiannidis, A., Munchen, S., and Groll, A. H. (2017). Clinical Hepatotoxicity Associated with Antifungal Agents. *Expert Opin. Drug Saf.* 16 (2), 149–165. doi:10.1080/14740338.2017.1270264

Mullins, C., Beaulac, K., and Sylvia, L. (2020). Drug-Induced Liver Injury (DILI) with Micafungin: The Importance of Causality Assessment. *Ann. Pharmacother.* 54 (6), 526–532. doi:10.1177/1060028019892587

Mycamine[Package_Insert] (2010). Deerfield (IL): Astellas Pharma Inc.

Nett, J. E., and Andes, D. R. (2016). Antifungal Agents: Spectrum of Activity, Pharmacology, and Clinical Indications. *Infect. Dis. Clin. North. Am.* 30 (1), 51–83. doi:10.1016/j.idc.2015.10.012

Norén, G. N., Bate, A., Orre, R., and Edwards, I. R. (2006). Extending the Methods Used to Screen the WHO Drug Safety Database towards Analysis of Complex Associations and Improved Accuracy for Rare Events. *Stat. Med.* 25 (21), 3740–3757. doi:10.1002/sim.2473

Ooba, N., and Kubota, K. (2010). Selected Control Events and Reporting Odds Ratio in Signal Detection Methodology. *Pharmacoepidemiol. Drug Saf.* 19 (11), 1159–1165. doi:10.1002/pds.2014

Patil, A., and Majumdar, S. (2017). Echinocandins in Antifungal Pharmacotherapy. *J. Pharm. Pharmacol.* 69 (12), 1635–1660. doi:10.1111/jphp.12780

Raschi, E., Poluzzi, E., Koci, A., Caraceni, P., and Ponti, F. D. (2014). Assessing Liver Injury Associated with Antimycotics: Concise Literature Review and Clues from Data Mining of the FAERS Database. *World J. Hepatol.* 6 (8), 601–612. doi:10.4254/wjh.v6.i8.601

Shiba, K., Saito, A., and Miyahara, T. (1990). Safety and Pharmacokinetics of Single Oral and Intravenous Doses of Fluconazole in Healthy Subjects. *Clin. Ther.* 12 (3), 206–215.

Song, J. C., and Deresinski, S. (2005). Hepatotoxicity of Antifungal Agents. *Curr. Opin. Investig. Drugs* 6 (2), 170–177.

Szarfman, A., Machado, S. G., and O'Neill, R. T. (2002). Use of Screening Algorithms and Computer Systems to Efficiently Signal higher-Than-expected Combinations of Drugs and Events in the US FDA's Spontaneous Reports Database. *Drug Saf.* 25 (6), 381–392. doi:10.2165/00002018-200225060-00001

Szumilas, M. (2010). Explaining Odds Ratios. *J. Can. Acad. Child. Adolesc. Psychiatry* 19 (3), 227–229.

Takeda, K., Morioka, D., Matsuo, K., Endo, I., Sekido, H., Moroboshi, T., et al. (2007). A Case of Successful Resection after Long-Term Medical Treatment of Invasive Pulmonary Aspergillosis Following Living Donor Liver Transplantation. *Transpl. Proc* 39 (10), 3505–3508. doi:10.1016/j.transproceed.2007.05.085

Tverdek, F. P., Kofteridis, D., and Kontoyiannis, D. P. (2016). Antifungal Agents and Liver Toxicity: a Complex Interaction. *Expert Rev. Anti Infect. Ther.* 14 (8), 765–776. doi:10.1080/14787210.2016.1199272

van der Geest, P. J., Hunfeld, N. G., Ladage, S. E., and Groeneveld, A. B. (2016). Micafungin versus Anidulafungin in Critically Ill Patients with Invasive Candidiasis: a Retrospective Study. *BMC Infect. Dis.* 16, 490. doi:10.1186/s12879-016-1825-3

van Puijenbroek, E. P., Bate, A., Leufkens, H. G., Lindquist, M., Orre, R., and Egberts, A. C. (2002). A Comparison of Measures of Disproportionality for Signal Detection in Spontaneous Reporting Systems for Adverse Drug Reactions. *Pharmacoepidemiol. Drug Saf.* 11 (1), 3–10. doi:10.1002/pds.668

Vekeman, F., Weiss, L., Aram, J., Ionescu-Ittu, R., Moosavi, S., Xiao, Y., et al. (2018). Retrospective Cohort Study Comparing the Risk of Severe Hepatotoxicity in Hospitalized Patients Treated with Echinocandins for Invasive Candidiasis in the Presence of Confounding by Indication. *BMC Infect. Dis.* 18 (1), 438. doi:10.1186/s12879-018-3333-0

Wang, E. J., Lew, K., Casciano, C. N., Clement, R. P., and Johnson, W. W. (2002). Interaction of Common Azole Antifungals with P Glycoprotein. *Antimicrob. Agents Chemother.* 46 (1), 160–165. doi:10.1128/aac.46.1.160-165.2002

Wang, J. L., Chang, C. H., Young-Xu, Y., and Chan, K. A. (2010). Systematic Review and Meta-Analysis of the Tolerability and Hepatotoxicity of Antifungals in Empirical and Definitive Therapy for Invasive Fungal Infection. *Antimicrob. Agents Chemother.* 54 (6), 2409–2419. doi:10.1128/AAC.01657-09

Zonios, D. I., and Bennett, J. E. (2008). Update on Azole Antifungals. *Semin. Respir. Crit. Care Med.* 29 (2), 198–210. doi:10.1055/s-2008-1063858

Conflict of Interest: The authors declare that the research was conducted in the absence of any commercial or financial relationships that could be construed as a potential conflict of interest.

Publisher's Note: All claims expressed in this article are solely those of the authors and do not necessarily represent those of their affiliated organizations, or those of the publisher, the editors and the reviewers. Any product that may be evaluated in this article, or claim that may be made by its manufacturer, is not guaranteed or endorsed by the publisher.

frontiers | Frontiers in Pediatrics

ORIGINAL RESEARCH
published: 06 May 2022
doi: 10.3389/fped.2022.896867

Stevens-Johnson Syndrome Following Non-steroidal Anti-inflammatory Drugs: A Real-World Analysis of Post-marketing Surveillance Data

Qi-hui Shao[1,2†], Xue-dong Yin[1,2†], Na Zeng[1†], Zhi-xuan Zhou[1,2], Xin-yu Mao[1,2], Yan Zhu[1], Bin Zhao[3] and Zhi-ling Li[1*]*

[1] Department of Pharmacy, Shanghai Children's Hospital, School of Medicine, Shanghai Jiao Tong University, Shanghai, China, [2] Shanghai Jiao Tong University School of Medicine, Shanghai, China, [3] Department of Pharmacy, Peking Union Medical College Hospital, Peking Union Medical College, Chinese Academy of Medical Sciences, Beijing, China

OPEN ACCESS

Edited by:
Jian Gao,
Shanghai Children's Medical Center, China

Reviewed by:
Chao Ai,
Tsinghua University, China
Zhaohui Jin,
Sichuan University, China

***Correspondence:**
Bin Zhao
zhaobin@pumch.cn
Zhi-ling Li
lizhiling22@163.com

[†] These authors have contributed equally to this work

Specialty section:
This article was submitted to Obstetric and Pediatric Pharmacology, a section of the journal Frontiers in Pediatrics

Received: 15 March 2022
Accepted: 18 April 2022
Published: 06 May 2022

Citation:
Shao Q-h, Yin X-d, Zeng N, Zhou Z-x, Mao X-y, Zhu Y, Zhao B and Li Z-l (2022) Stevens-Johnson Syndrome Following Non-steroidal Anti-inflammatory Drugs: A Real-World Analysis of Post-marketing Surveillance Data. Front. Pediatr. 10:896867. doi: 10.3389/fped.2022.896867

Background: The Stevens-Johnson syndrome (SJS) is a severe skin reaction to non-steroidal anti-inflammatory drugs (NSAIDs), and can even be life-threatening. However, there are still few real-world studies to compare the specific differences in the adverse effects of skin and mucosal invasion.

Methods: Disproportionality analysis and Bayesian analysis were devoted to data-mining of the suspected SJS after using NSAIDs based on the FDA's Adverse Event Reporting System (FAERS) from January 2004 to March 2021. The times to onset, fatality, and hospitalization rates of antipyretic analgesic-associated SJS were also investigated.

Results: A total of 1,868 reports of SJS adverse events were identified with NSAIDs. Among 5 NSAIDs monotherapies we studied (acetaminophen, ibuprofen, aspirin, diclofenac and celecoxib), ibuprofen had the highest association with SJS based on the highest reporting odds ratio (ROR = 7.06, 95% two-sided CI = 6.59–7.56), proportional reporting ratio (PRR = 6.98, $\chi^2 = 4201.14$) and empirical Bayes geometric mean (EBGM = 6.78, 95% one-sided CI = 6.40). However, ibuprofen-associated SJS had the lowest fatality rate (6.87%, $p < 0.0001$) and the highest hospitalization rate (79.27%, $p < 0.0001$). Celecoxib-associated SJS had the latest time to onset (317.56 days, $p < 0.0001$). Diclofenac-associated SJS cases appeared to be associated with the highest risk of death (25.00%, $p < 0.0001$).

Conclusions: The analysis of FAERS data provides a more accurate profile of the incidence and prognosis of SJS after NSAIDs treatment, enabling continued surveillance and timely intervention in patients at risk of SJS following these NSAIDs.

Keywords: non-steroidal anti-inflammatory drugs, real-world study, FAERS, spontaneous reporting system, pharmacovigilance, Stevens-Johnson syndrome

INTRODUCTION

Due to its efficacy in reducing pain and inflammation, non-steroidal anti-inflammatory drugs (NSAIDs) are one of the most popularly used medicines. NSAIDs are traditionally divided into seven groups according to their different chemical structures, the most popular of which are the main derivatives of salicylic acid, acetic acid, enolic acid, anthranilic acid, or propionic acid (1). Meanwhile, NSAIDs can also be classified into non-selective and selective cyclooxygenase (COX) inhibitors according to their mechanism (2). The COX enzyme comes in two forms, COX-1 and COX-2. Non-selective NSAIDs (NS-NSAIDs), represented by aspirin, ibuprofen, acetaminophen, and diclofenac, inhibit COX-1 and COX-2 simultaneously, while selective NSAIDs (S-NSAIDs) specifically inhibit COX-2, represented by celecoxib. However, studies (3, 4) have now found that COX-3 is more sensitive than COX-1 or COX-2 to inhibition by acetaminophen, diclofenac, ibuprofen, and aspirin.

Stevens-Johnson syndrome (SJS) and toxic epidermal necrolysis (TEN) are serious adverse skin drug reactions, mainly involving the skin and mucous membranes. The single difference between them lies in the degree of skin detachment (5). They are rare and quite fatal. The average reported mortality rate of SJS is 1–5%, and that of TEN is 25–35% (6). If the patient is older or has a larger area of skin exfoliation, the mortality rate will be higher. Once SJS develops to TEN, more than 50% of surviving patients suffer from long-term sequelae of the disease (7, 8).

Drugs with higher correlation with SJS were sulfanilamide antibiotics, allopurinol, certain anti-epileptic drugs and nevirapine (9). Since 1957 (10), 30 years after SJS was first reported (11), studies (12–14) of NSAIDs-related SJS have been reported. Nevertheless, most of the evidence for NSAIDs-related SJS comes from case reports and clinical trials. Large sample analysis based on a database is also rare in recent years. Therefore, it is necessary to update our understanding and outline the risks and characteristics of adverse events after NSAIDs treatment for further prevention and management. Hence, we tried to investigate the FDA's Adverse Event Reporting System (FAERS) to evaluate and compare the relationship among acetaminophen, ibuprofen, aspirin, diclofenac, celecoxib, and serious skin adverse events in a large population. Moreover, the differences in onset time, mortality, and hospitalization rate among them were further investigated.

METHODS

Data Source

A retrospective pharmacovigilance study was conducted using data retrieved from the FAERS database from January 2004 to March 2021.

The FAERS is a public voluntary self-reporting database that provides information on adverse events and medication error reports submitted by a wide range of individuals, including physicians, consumers, and others, from all over the world. Information interchange codes for the FAERS database include demographic and administrative information (DEMO), the Medical Dictionary for Regulatory Activities (MedDRA) preferred terms (PTs) coded for the adverse event (REAC), drug information (DRUG), patient outcomes (OUTC), report sources (RPSR), therapy start dates and end dates for reported drugs (THER), and indications for use (INDI).

Adverse Event and Drug Identification

Adverse events were investigated by using the MedDRA (Version 24.0) Preferred Terms as follows: epidermal necrosis (10059284), epidermal necrolysis (10014986), Stevens-Johnson syndrome (10042033), toxic epidermal necrolysis (10044223), Stevens-Johnson reaction (10042029). Thus, the MICROMEDEX® (Index Nominum) was used like a dictionary. Acetaminophen, ibuprofen, aspirin, diclofenac, and celecoxib were defined as both brand and generic names in the DRUG file, and the role of the drug was identified as "primary suspected."

Data Mining

Based on the basic principles of Bayesian analysis and non-proportional analysis, we applied the reporting odds ratio (ROR), the proportional reporting ratio (PRR), the Bayesian confidence propagation neural network (BCPNN), and the multi-item gamma Poisson shrinker (MGPS) algorithms to investigate the association between NSAIDs and the adverse reactions. The equations and criteria for the four algorithms (15–23) are shown in **Table 1**. These algorithms were extracted to measure the strength of the association between drugs and adverse events, and if one of the four algorithms met the criteria, it should be considered a positive signal for SJS.

We calculated the onset time of SJS following acetaminophen, ibuprofen, aspirin, diclofenac, and celecoxib, respectively, which was defined as the interval between adverse event onset date and start date of the administration. Reports with incorrect input or incorrect data input were also excluded. In addition, mortality would be defined as the number of fatal events divided by the total number of NSAIDs-related SJS.

Statistical Analysis

Descriptive analysis was applied to summarize the clinical characteristics of SJS patients resulting in NSAIDs from the FAERS database. As the data were not normally distributed, non-parametric tests (the Dunn's multiple comparison test for dichotomous variables and the Kruskal-Wallis test when there were more than two subgroups of respondents) were used to compare the time to onset of NSAIDs-associated SJS. Pearson's chi-square test or Fisher's exact test was utilized to compare the mortality and hospitalization rates between different NSAIDs. The statistical significance was set at $p < 0.001$ with 95% confidence intervals. All statistical analyses were performed using GraphPad Prism 8 (GraphPad Software, CA, USA).

RESULTS

Disproportionality Analysis and Bayesian Analysis

From January 2004 to March 2021, a total of 1876 cases of SJS-related reports were recorded in the FAERS database. Four hundred and seventy five cases of SJS associated with

TABLE 1 | Summary of major algorithms used for signal detection.

Algorithms	Equation*	Criteria
ROR	$ROR = (a/b)/(c/d)$ $95\%CI = e^{\ln(ROR)\pm1.96(1/a+1/b+1/c+1/d)\text{^}0.5}$	95% CI > 1, N ≥ 2
PRR	$PRR = (a/(a+c))/(b/(b+d))$ $\chi^2 = \Sigma((O-E)^2/E)$; (O=a, E = (a+b)(a+c)/(a+b+c+d))	PRR ≥ 2, $\chi^2 \geq 4$, N ≥ 3
BCPNN	$IC = \log_2 a(a+b+c+d)/((a+c)(a+b))$ $IC025 = e^{\ln(IC)-1.96(1/a+1/b+1/c+1/d)\text{^}0.5}$	IC025 > 0
MGPS	$EBGM = a(a+b+c+d)/((a+c)(a+b))$ $EB05 = e^{\ln(EBGM)-1.64(1/a+1/b+1/c+1/d)\text{^}0.5}$	EB05 ≥ 2, N > 0

**a: number of reports containing both the suspect drug and the suspect adverse drug reaction. b: number of reports containing the suspect adverse drug reaction with other medications (except the drug of interest). c: number of reports containing the suspect drug with other adverse drug reactions (except the event of interest). d: number of reports containing other medications and other adverse drug reactions. ROR, reporting odds ratio; CI, confidence interval; N, the number of co-occurrences; PRR, proportional reporting ratio; χ^2, chi-squared; BCPNN, Bayesian confidence propagation neural network; IC, information component; IC025, the lower limit of the 95% two-sided CI of the IC; MGPS, multi-item gamma Poisson shrinker; EBGM, empirical Bayesian geometric mean; EB05, the lower 90% one-sided CI of EBGM.*

TABLE 2 | Signal detection for NSAIDs-associated Stevens-Johnson syndrome.

Drugs	*N*	ROR (95% two-sided CI)	PRR (χ^2)	IC (IC025)	EBGM (EBGM05)
APAP	475	4.65 (4.25,5.09)	4.62 (1324.31)	2.19 (2.00)	4.55 (4.22)
Ibuprofen	847	7.06 (6.59,7.56)	6.98 (4201.14)	2.76 (2.58)	6.78 (6.40)
Aspirin	173	2.75 (2.37,3.2)	2.74 (190.68)	1.45 (1.25)	2.73 (2.41)
Diclofenac	202	2.54 (2.21,2.92)	2.53 (186.26)	1.33 (1.16)	2.52 (2.24)
Celecoxib	179	2.54 (2.19,2.94)	2.53 (165.11)	1.33 (1.15)	2.52 (2.23)

NSAIDs, non-steroidal anti-inflammatory drugs; APAP, acetaminophen; ROR, reporting odds ratio; CI, confidence interval; PRR, proportional reporting ratio; χ^2, chi-squared; IC, information component; EBGM, empirical Bayesian geometric mean.

acetaminophen (APAP) as a suspicious drug, 847 cases associated with ibuprofen, 173 cases associated with aspirin, 202 cases associated with diclofenac, and 179 cases associated with celecoxib were identified. According to the standards of the four algorithms, the severe skin adverse reaction signals were detected for these five NSAIDs, respectively. As shown in **Table 2**, all of these five drugs had statistically significant ROR, PRR, information component (IC), and empirical Bayesian geometric mean (EBGM). Among them, ibuprofen had the highest association with SJS based on the highest ROR (ROR = 7.06, 95% two-sided CI = 6.59–7.56), PRR (PRR = 6.98, $\chi 2 = 4201.14$) and empirical Bayes geometric mean (EBGM = 6.78, 95% one-sided CI = 6.40). On the contrary, the lowest association with SJS was found in celecoxib.

Descriptive Analysis

The baseline clinical characteristics are summarized in **Table 3**. Except for the unspecified age, SJS was more likely to occur in young patients (<18 years old) treated with ibuprofen (51.77%) or acetaminophen (36.01%), while aspirin-associated SJS mostly occurred in elderly patients (75–84 years old) (25.63%). In terms of diclofenac and celecoxib, middle-aged patients (45–64 years old) accounted for 34.29 and 47.62% of reported cases respectively, accounting for the majority of the patients in their different age groups. Except for the unspecified data, females made up far more reports than males in the case of all NSAIDs except for acetaminophen, especially celecoxib (68.94 vs. 31.06%), while the proportion of females and males were almost equal in the case of acetaminophen (49.14 vs. 50.86%). As for acetaminophen, ibuprofen, and aspirin, nearly half of the reports were from Europe (43.74, 48.60, and 51.53%, respectively). Diclofenac-associated SJS was mainly reported from Asia (49.43%) and 85.63% of the reports of celecoxib-associated SJS were from North America. Except for celecoxib, other health-professional who were not the pharmacist or the physician accounted for the majority of the reported cases (acetaminophen: 55.82%, ibuprofen: 41.20%, aspirin: 46.54%, diclofenac: 57.23%). For celecoxib, physicians submitted 34.27% of reported cases, which was only lower than the number of cases reported by lawyers (36.36%).

Time to Onset of NSAIDs-Associated SJS

We described the time to onsets of SJS for NSAIDs in **Figure 1**. According to the data, the median onset time of celecoxib-associated SJS was 28 days [interquartile range (IQR) 5.75–490.75], which was significantly longer than that of APAP- (4 days, IQR 1.75–9.75), ibuprofen- (3 days, IQR 1–7) and

TABLE 3 | Clinical characteristics of patients with NSAIDs-associated Stevens-Johnson syndrome collected from the FAERS database (January 2004 to March 2021).

Characteristics	Reports (*N*, %)				
	Acetaminophen	Ibuprofen	Aspirin	Diclofenac	Celecoxib
Patient age (year)					
<18	130 (27.37)	337 (39.69)	21 (12.07)	12 (5.94)	0 (0.00)
18–44	120 (25.26)	218 (25.68)	30 (17.24)	52 (25.74)	15 (8.38)
45–64	48 (10.11)	39 (4.59)	31 (17.82)	60 (29.70)	40 (22.35)
65–74	24 (5.05)	19 (2.24)	27 (15.52)	30 (14.85)	12 (6.70)
75–84	34 (7.16)	30 (3.53)	41 (23.56)	10 (4.95)	14 (7.82)
>84	5 (1.05)	8 (0.94)	10 (5.75)	11 (5.45)	3 (1.68)
Unknown	114 (24.00)	198 (23.32)	14 (8.05)	27 (13.37)	95 (53.07)
Patient gender					
Female	172 (36.21)	427 (50.29)	102 (58.62)	106 (52.48)	111 (62.01)
Male	178 (37.47)	291 (34.28)	66 (37.93)	86 (42.57)	50 (27.93)
Unknown	125 (26.32)	131 (15.43)	6 (3.45)	10 (4.95)	18 (10.06)
Area					
Africa	16 (3.37)	4 (0.47)	7 (4.02)	2 (0.99)	0 (0.00)
Asia	168 (35.37)	70 (8.24)	60 (34.48)	87 (43.07)	11 (6.15)
Europe	199 (41.89)	398 (46.88)	84 (48.28)	61 (30.20)	6 (3.35)
Oceania	2 (0.42)	17 (2.00)	1 (0.57)	0 (0.00)	4 (2.23)
North America	67 (14.11)	308 (36.28)	11 (6.32)	24 (11.88)	137 (76.54)
South America	3 (0.63)	22 (2.59)	0 (0.00)	2 (0.99)	2 (1.12)
Unknown	20 (4.21)	30 (3.53)	11 (6.32)	26 (12.87)	19 (10.61)
Reporters					
Consumer	24 (5.05)	113 (13.31)	29 (16.67)	21 (10.40)	21 (11.73)
Lawyer	1 (0.21)	45 (5.30)	0 (0.00)	1 (0.50)	52 (29.05)
Pharmacist	14 (2.95)	39 (4.59)	4 (2.30)	6 (2.97)	4 (2.23)
Physician	147 (30.95)	214 (25.21)	52 (29.89)	40 (19.80)	49 (27.37)
Other health-professional	235 (49.47)	288 (33.92)	74 (42.53)	91 (45.05)	17 (9.50)
Unknown	54 (11.37)	150 (17.67)	15 (8.62)	43 (21.29)	36 (20.11)
Outcome event					
Congenital anomaly	0 (0.00)	0 (0.00)	0 (0.00)	0 (0.00)	1 (0.56)
Death	46 (9.73)	58 (6.87)	34 (19.65)	50 (25.00)	21 (11.80)
Disability	17 (3.59)	74 (8.77)	3 (1.73)	7 (3.50)	19 (10.67)
Hospitalization-initial or prolonged	320 (67.65)	669 (79.27)	84 (48.55)	117 (58.50)	84 (47.19)
Life-threatening	92 (19.45)	234 (27.73)	50 (28.9)	47 (23.50)	18 (10.11)
Other serious (Important medical event)	235 (49.68)	420 (49.76)	59 (34.1)	120 (60.00)	147 (82.58)
Required intervention to prevent permanent impairment/Damage	0 (0.00)	16 (1.90)	0 (0.00)	1 (0.50)	5 (2.81)

NSAIDs, non-steroidal anti-inflammatory drugs; FAERS, FDA Adverse Event Reporting System.

diclofenac-related SJS (3 days, IQR 0–21) (Dunn's multiple comparison test, $p < 0.001$). Meanwhile, the median onset time of aspirin-associated SJS was 17.5 days (IQR 7.25–28.75), which was also longer than that of the three drugs mentioned above (Dunn's multiple comparison test, $p < 0.001$). However, there was no significant difference between aspirin-related SJS and celecoxib-related SJS. In addition, the average time to onset of celecoxib-associated SJS (317.56 days) and aspirin-associated SJS (81.34 days) was significantly different from that of APAP (7.10 days), ibuprofen (26.33 days) and diclofenac (35.84 days) (Dunn's multiple comparison test, $p < 0.001$).

Fatality and Hospitalization Due to NSAIDs-Associated SJS

The rate of fatality and hospitalization due to SJS following NSAIDs were assessed to analyze the prognosis of NSAIDs-associated severe skin adverse reactions. The hospitalization rate of ibuprofen-associated SJS was 79.27%, ranking first among the five NSAIDs with absolute advantage (acetaminophen: 67.65%, diclofenac: 58.5%, celecoxib: 47.19%, aspirin: 48.55%) and there were significant differences between ibuprofen and the remaining four NSAIDs (Fisher's exact test, $p < 0.001$). However, the mortality rate of SJS caused by ibuprofen is 6.87%, which was significantly lower than that of aspirin-associated SJS (19.65%)

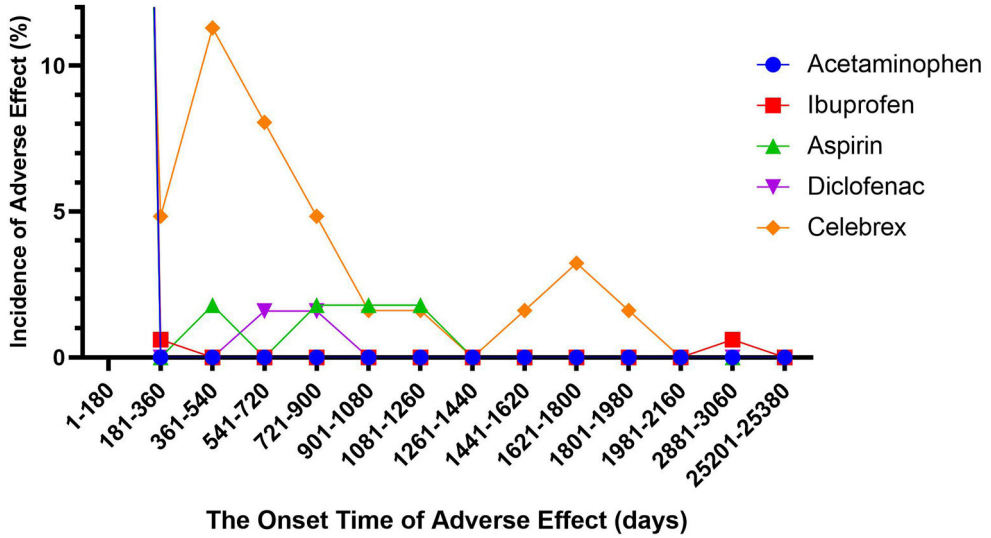

FIGURE 1 | Time to event onset of Stevens-Johnson syndrome following different non-steroidal anti-inflammatory drugs.

and diclofenac-associated SJS (25.00%) (Fisher's exact test, $p < 0.001$). There was no significant difference between SJS caused by aspirin and diclofenac.

DISCUSSION

To the best of our knowledge, this study is the largest collection based on the FAERS pharmacovigilance database from January 2004 to March 2021, describing the differences in the vulnerable population, onset time, and adverse outcomes of SJS following NSAIDs (acetaminophen, ibuprofen, aspirin, diclofenac, and celecoxib) in real-world practice. Non-steroidal anti-inflammatory drugs, especially the COX-2 specific inhibitors, were predominantly suspected of triggering SJS (24). However, most previous studies were based on case report series (25, 26), or only focused on a small sample of people in a specific area (27–29). There has been a previous study based on the FAERS database (30), but only some reports of S-NSAIDs in the 2 years after their marketing (up to March 2004) were studied. Therefore, they did not discuss the characteristics of SJS following NSAIDs (both selective and non-selective) from a more comprehensive perspective, nor did they compare SJS following these drugs among these drugs.

Current studies have identified NSAIDs as a suspected cause of SJS (25). Sequelae of Stevens-Johnson syndrome are rare. Reports of SJS caused by these five NSAIDs have only appeared since 2005, and the total number of reports so far is still small. Since there is no specific treatment other than to relieve symptoms, SJS can be life-threatening once it occurs (31). Non-steroidal anti-inflammatory drugs have been widely used for a long time, not only as prescription drugs but also as over-the-counter. Stevens-Johnson syndrome, as one of its serious skin adverse reactions, has a low incidence, but the pain brought by SJS and its sequelae to patients still cannot be ignored.

The mechanism of NSAIDs-associated SJS has not been determined so far. It is hypothesized that liver injury causes toxic retinoid compounds to overflow into the circulation, leading to an endogenous form of hypervitaminosis A and widespread cell apoptosis mediated by granular globulin, eventually manifesting as SJS/TEN (32). Meanwhile, NSAIDs are a leading cause of liver injury across the world (33). Based on the above two points, the reason why NSAIDs lead to SJS is that NSAIDs cause initial damage, which then leads to mitochondrial permeability transformation, and eventually leads to hepatocyte necrosis or apoptosis (34), which finally leads to SJS through the pathways mentioned above. It has also been found that the drug can induce keratinocytes to express the death receptor CD95 (Fas) and its ligand (Fas L), thus significantly increasing the expression of TNF-α, perforin and granzyme B, eventually leading to cell necrosis (35, 36). In addition, the most common drugs related to SJS are the sulfonamide antibiotics (5), so aspirin and celecoxib may be related to SJS due to its sulfonamide moieties.

According to epidemiological results, although all age groups may be affected, the main population still has different priorities. This may be associated with the difference in the population to which they apply. Celecoxib is not recommended for patients younger than 18 years old and therefore there is no data for this age group of patients with celecoxib-associated SJS. Because the World Health Organization (WHO) only recommends acetaminophen and ibuprofen as antipyretic drugs for children, children with fevers are more likely to be exposed to them than other age groups. In addition, because the livers of children are not fully developed and various drug-metabolizing enzymes are not yet complete, they are more likely to develop NSAIDS induced liver damage, which can lead to the progression of SJS. Thus, patients younger than 18 years old are more likely to have SJS. Although aspirin is an antipyretic analgesic drug, it is also often used to reduce the risk of myocardial infarction in patients with cardiovascular risk factors (37). Aging will lead

to the decline of liver function in patients (38), which provides an opportunity for the occurrence and development of SJS. At the same time, aspirin might accumulate in the body due to the decreased kidney function in older adults with chronic cardiovascular disease. Thus, aspirin-related SJS are more likely to occur in elder patients.

Based on the FAERS database, the median and average time to onset of severe skin adverse reactions for celecoxib and aspirin were significantly longer than those of APAP, ibuprofen, and diclofenac. However, there is no significant difference between celecoxib and aspirin, or among APAP, ibuprofen, and diclofenac. It may be less convincing to use selective inhibition of COX-2 directly as the cause of the difference in onset. Studies have found that the same patient groups are affected after the use of NS-NSAIDs and S-NSAIDs (25). In addition, aspirin is a non-selective COX inhibitor and celecoxib is a selective COX inhibitor, and the difference between the two does not make a significant difference. However, the median onset time of APAP- and ibuprofen-related SJS, both NSAIDs, is one-fourth to one-fifth that of aspirin-related SJS. From another perspective, we could infer the difference in onset time from the difference in their chemical structure. Aspirin and celecoxib contain sulfonamide moieties whereas the other three drugs do not. The most common drugs that cause SJS are sulfonamide antibiotics, whether it means that sulfa drugs can preserve the potential for serious skin adverse events for a longer period of time. All of this still requires future experiments or longer observations to prove.

According to current research, Stevens-Johnson syndrome usually means an adverse outcome (hospitalization or death). More than almost half of the patients with NSAIDs-associated SJS are likely to be hospitalized, especially ibuprofen (79.27%) and acetaminophen (67.65%). There were significant differences between ibuprofen and the remaining four NSAIDs (Fisher's exact test, $p < 0.001$). Again, this requires special attention in pediatric patients. The young age and short onset time, coupled with the lack of good treatment for SJS itself, may lead to more children being hospitalized. However, the mortality rate of SJS following ibuprofen is 6.87%, which was significantly lower than that of aspirin-associated SJS (19.65%) (Fisher's exact test, $p < 0.001$). This may be because aspirin affects mainly the elderly and the patients it treats are more likely to have cardiovascular disease risk factors and are more likely to die with poorer underlying health conditions. However, it should be noted that SJS itself lacks targeted treatments other than symptom relief, so caution should be exercised regardless of the mortality rate in this study.

Despite the advantages of real-world research and the data mining techniques in this study, inevitably, there are some limitations to this study. First, the signals obtained through Bayesian analysis and disproportionate analysis can only prove that there is a correlation between NSAIDs and SJS, but cannot prove the causal relationship between them. Therefore, the hypothesis generated by the disproportionation analysis needs to be further verified by more reliable methods. Second, FAERS is a spontaneous adverse drug event reporting system, and there may be arbitrariness in reporting. Although we can see the identity of the reporter, the omissions or errors in the report content caused by the recall bias cannot be avoided. For possible duplicate reports (different CASEID but overlapping data), we delete them based on event_dt, age, sex and reporter_country according to the method recommended by the FDA, but important reports may be hidden in the deleted data. Fourth, different drugs are approved at different times, which can lead to more adverse event reports for drugs that have been on the market for long. Take celecoxib and ibuprofen as examples, in the United States, celecoxib was approved for marketing in 2008, while ibuprofen had been on the market as early as 1974. The 34-year difference would bring about a big difference in the number of reports, especially when the start time of the report we selected is January 2004. Fifth, although we can see the statistics of the basic information of many patients, the basic disease status of the patients is not clear, which will bring many confounding factors and bring uncertainty to our analysis. For example, patients may already have underlying chronic conditions such as cardiovascular disease (especially for aspirin), or baseline liver insufficiency, which can affect skin adverse reactions. Although these drawbacks above do exist, the FAERS database can identify signals of NSAIDs and SJS, and further, describe the treatment of these 5 NSAIDs. Our study may provide a new basis for further clinical studies of well-organized NSAIDs-associated SJS.

DATA AVAILABILITY STATEMENT

The original contributions presented in the study are included in the article/supplementary material, further inquiries can be directed to the corresponding authors.

AUTHOR CONTRIBUTIONS

Q-hS analyzed and interpreted data, plotted figures, and wrote the manuscript draft. X-dY, NZ, Z-xZ, and X-yM participated in the interpretation of data. BZ designed and directed the research. Z-lL assisted in preparing this manuscript and providing constructive suggestions. All authors contributed to the article and approved the submitted version.

FUNDING

Project sponsored by Innovative Training Program for College Students, School of Medicine, Shanghai Jiaotong University (No. 1521Y424), and Science and Technology Commission of Shanghai Municipality (No. 21DZ2300700).

REFERENCES

1. Bindu S, Mazumder S, Bandyopadhyay U. Non-steroidal anti-inflammatory drugs (NSAIDs) and organ damage: a current perspective. *Biochem Pharmacol.* (2020) 180:114147. doi: 10.1016/j.bcp.2020.114147
2. Marjoribanks J, Ayeleke RO, Farquhar C, Proctor M. Nonsteroidal anti-inflammatory drugs for dysmenorrhoea. *Cochrane Database Syst Rev.* (2015) 2015:CD001751. doi: 10.1002/14651858.CD001751.pub3
3. Botting R, Ayoub SS. COX-3 and the mechanism of action of paracetamol/acetaminophen. *Prostaglandins Leukot*

Essent Fatty Acids. (2005) 72:85–7. doi: 10.1016/j.plefa.2004.10.005
4. Chandrasekharan NV, Dai H, Roos KL, Evanson NK, Tomsik J, Elton TS, et al. COX-3, a cyclooxygenase-1 variant inhibited by acetaminophen and other analgesic/antipyretic drugs: cloning, structure, and expression. *Proc Natl Acad Sci U S A.* (2002) 99:13926–31. doi: 10.1073/pnas.162468699
5. Harr T, French LE. Toxic epidermal necrolysis and stevens-johnson syndrome. *Orphanet J Rare Dis.* (2010) 5:39. doi: 10.1186/1750-1172-5-39
6. Harr T, French LE. Stevens-Johnson syndrome and toxic epidermal necrolysis. *Chem Immunol Allergy.* (2012) 97:149–66. doi: 10.1159/000335627
7. Yip LW, Thong BY, Lim J, Tan AW, Wong HB, Handa S, et al. Ocular manifestations and complications of Stevens-Johnson syndrome and toxic epidermal necrolysis: an Asian series. *Allergy.* (2007) 62:527–31. doi: 10.1111/j.1398-9995.2006.01295.x
8. Shanbhag SS, Hall L, Chodosh J, Saeed HN. Long-term outcomes of amniotic membrane treatment in acute stevens-johnson syndrome/toxic epidermal necrolysis. *Ocul Surf.* (2020) 18:517–22. doi: 10.1016/j.jtos.2020.03.004
9. Lerch M, Mainetti C, Terziroli Beretta-Piccoli B, Harr T. Current perspectives on stevens-johnson syndrome and toxic epidermal necrolysis. *Clin Rev Allergy Immunol.* (2018) 54:147–76. doi: 10.1007/s12016-017-8654-z
10. Vankos J, Pastinszky S. Ein fall von durch Phenylbutazon hervorgerufenem Stevens-Johnson Syndrom mit tödlichem Ausgange [A fatal case of Stevens-Johnson syndrome due to phenylbutazone]. *Z Haut Geschlechtskr.* (1957) 23:54–7.
11. Stevens AM, Johnson FC. A new eruptive fever associated with stomatitis and ophtalmia; report of two cases in children. *Am J Dis Children.* (1922) 24:526–33. doi: 10.1001/archpedi.1922.04120120077005
12. Angadi SS, Karn A. Ibuprofen induced Stevens-Johnson syndrome - toxic epidermal necrolysis in Nepal. *Asia Pac Allergy.* (2016) 6:70–3. doi: 10.5415/apallergy.2016.6.1.70
13. Bang D, Shah T, Thakker D, Shah Y, Raval AD. Drug-induced Stevens-Johnson syndrome: case series from tertiary care centre in Gujarat. *Pharmacoepidemiol Drug Saf.* (2012) 21:384–95. doi: 10.1002/pds.3212
14. Editorial Office. Erratum to ibuprofen induced Stevens-Johnson syndrome and liver injury in children: a case report. *Transl Pediatr.* (2021) 10:2881. doi: 10.21037/tp-21-430
15. van Puijenbroek EP, Bate A, Leufkens HG, Lindquist M, Orre R, Egberts AC, et al. A comparison of measures of disproportionality for signal detection in spontaneous reporting systems for adverse drug reactions. *Pharmacoepidemiol Drug Saf.* (2002) 11:3–10. doi: 10.1002/pds.668
16. Szumilas M. Explaining odds ratios. *J Can Acad Child Adolesc Psychiatry Aug.* (2010) 19:227–9.
17. Ooba N, Kubota K. Selected control events and reporting odds ratio in signal detection methodology. *Pharmacoepidemiol Drug Saf.* (2010) 19:1159–65. doi: 10.1002/pds.2014
18. Evans SJ, Waller PC, Davis S. Use of proportional reporting ratios (PRRs) for signal generation from spontaneous adverse drug reaction reports. *Pharmacoepidemiol Drug Saf.* (2001) 10:483–6. doi: 10.1002/pds.677
19. Hauben M, Madigan D, Gerrits CM, Walsh L, Van Puijenbroek EP. The role of data mining in pharmacovigilance. *Expert Opin Drug Saf Sep.* (2005) 4:929–48. doi: 10.1517/14740338.4.5.929
20. Noren GN, Bate A, Orre R, Edwards IR. Extending the methods used to screen the WHO drug safety database towards analysis of complex associations and improved accuracy for rare events. *Stat Med.* (2006) 25:3740–57. doi: 10.1002/sim.2473
21. Hauben M. A brief primer on automated signal detection. *Ann Pharmacother.* (2003) 37:1117–23. doi: 10.1345/aph.1C515
22. DuMouchel W. Bayesian data mining in large frequency tables, with an application to the FDA spontaneous reporting system. *Am Stat.* (1999) 53:177–90. doi: 10.1080/00031305.1999.10474456
23. Szarfman A, Machado SG, O'Neill RT. Use of screening algorithms and computer systems to efficiently signal higher-than-expected combinations of drugs and events in the US FDA's spontaneous reports database. *Drug Saf.* (2002) 25:381–92. doi: 10.2165/00002018-200225060-00001
24. Liotti L, Caimmi S, Bottau P, Bernardini R, Cardinale F, Saretta F, et al. Clinical features, outcomes and treatment in children with drug induced Stevens-Johnson syndrome and toxic epidermal necrolysis. *Acta Biomed.* (2019) 90:52–60. doi: 10.23750/abm.v90i3-S.8165
25. Ward KE, Archambault R, Mersfelder TL. Severe adverse skin reactions to nonsteroidal antiinflammatory drugs: a review of the literature. *Am J Health Syst Pharm.* (2010) 67:206–13. doi: 10.2146/ajhp080603
26. Roujeau JC. Clinical aspects of skin reactions to NSAIDs. *Scand J Rheumatol Suppl.* (1987) 65:131–4. doi: 10.3109/03009748709102191
27. Layton D, Marshall V, Boshier A, Friedmann P, Shakir SA. Serious skin reactions and selective COX-2 inhibitors: a case series from prescription-event monitoring in England. *Drug Saf.* (2006) 29:687–96. doi: 10.2165/00002018-200629080-00005
28. Wang YH, Chen CB, Tassaneeyakul W, Saito Y, Aihara M, Choon SE, et al. The medication risk of Stevens-Johnson syndrome and toxic epidermal necrolysis in asians: the major drug causality and comparison with the US FDA label. *Clin Pharmacol Ther.* (2019) 105:112–20. doi: 10.1002/cpt.1071
29. El-Nabarawy EA, Elmasry MF, El Lawindi MI, Tarek YA. An epidemiological and clinical analysis of cutaneous adverse drug reactions seen in a tertiary care outpatient clinic in cairo, Egypt. *Acta Dermatovenerol Croat.* (2018) 26:233–42.
30. La Grenade L, Lee L, Weaver J, Bonnel R, Karwoski C, Governale L, et al. Comparison of reporting of Stevens-Johnson syndrome and toxic epidermal necrolysis in association with selective COX-2 inhibitors. *Drug Saf.* (2005) 28:917–24. doi: 10.2165/00002018-200528100-00008
31. Ramos-Casals M, Brito-Zerón P, Bombardieri S, Bootsma H, De Vita S, Dörner T, et al. EULAR recommendations for the management of Sjögren's syndrome with topical and systemic therapies. *Ann Rheum Dis.* (2020) 79:3–18. doi: 10.1136/annrheumdis-2019-216114
32. Mawson AR, Eriator I, Karre S. Stevens-Johnson syndrome and toxic epidermal necrolysis (SJS/TEN): could retinoids play a causative role? *Med Sci Monit.* (2015) 21:133–43. doi: 10.12659/MSM.891043
33. Zoubek ME, Lucena MI, Andrade RJ, Stephens C. Systematic review: ibuprofen-induced liver injury. *Aliment Pharmacol Ther.* (2020) 51:603–11. doi: 10.1111/apt.15645
34. Russmann S, Jetter A, Kullak-Ublick GA. Pharmacogenetics of drug-induced liver injury. *Hepatology.* (2010) 52:748–61. doi: 10.1002/hep.23720
35. Nassif A, Bensussan A, Boumsell L, Deniaud A, Moslehi H, Wolkenstein P, et al. Toxic epidermal necrolysis: effector cells are drug-specific cytotoxic T cells. *J Allergy Clin Immunol.* (2004) 114:1209–15. doi: 10.1016/j.jaci.2004.07.047
36. Abe R, Shimizu T, Shibaki A, Nakamura H, Watanabe H, Shimizu H. Toxic epidermal necrolysis and Stevens-Johnson syndrome are induced by soluble Fas ligand. *Am J Pathol.* (2003) 162:1515–20. doi: 10.1016/S0002-9440(10)64284-8
37. Gaziano JM, Brotons C, Coppolecchia R, Cricelli C, Darius H, Gorelick PB, et al. Use of aspirin to reduce risk of initial vascular events in patients at moderate risk of cardiovascular disease (ARRIVE): a randomised, double-blind, placebo-controlled trial. *Lancet.* (2018) 392:1036–46. doi: 10.1016/S0140-6736(18)31924-X
38. Klotz U. Pharmacokinetics and drug metabolism in the elderly. *Drug Metab Rev.* (2009) 41:67–76. doi: 10.1080/03602530902722679

Conflict of Interest: The authors declare that the research was conducted in the absence of any commercial or financial relationships that could be construed as a potential conflict of interest.

frontiers | Frontiers in Pediatrics

ORIGINAL RESEARCH
published: 15 June 2022
doi: 10.3389/fped.2022.903507

Spina Bifida Occulta Is a Risk Factor for Spinal Cord Injury Without Fracture or Dislocation for Children Performing a Backbend During Dance

*Guoqing Liu[1], Wei Jiang[1], Xiang Tang[1], Shali Tan[2], Mingqiang Zhang[1], Liang Tao[1], Nong Xiao[1] and Yuxia Chen[1]**

[1] Department of Rehabilitation, National Clinical Research Center for Child Health and Disorders, Ministry of Education Key Laboratory of Child Development and Disorders, Chongqing Key Laboratory of Pediatrics, Children's Hospital of Chongqing Medical University, Chongqing, China, [2] Department of Pediatrics, The People's Hospital of Fengjie, Chongqing, China

OPEN ACCESS

Edited by:
Jian Gao,
Shanghai Children's Medical Center, China

Reviewed by:
Yanling Wu,
Yanbian University, China
Flavio Giordano,
University of Florence, Italy

***Correspondence:**
Yuxia Chen
chenyux666@163.com

Specialty section:
This article was submitted to Obstetric and Pediatric Pharmacology, a section of the journal Frontiers in Pediatrics

Received: 24 March 2022
Accepted: 16 May 2022
Published: 15 June 2022

Citation:
Liu G, Jiang W, Tang X, Tan S, Zhang M, Tao L, Xiao N and Chen Y (2022) Spina Bifida Occulta Is a Risk Factor for Spinal Cord Injury Without Fracture or Dislocation for Children Performing a Backbend During Dance. Front. Pediatr. 10:903507. doi: 10.3389/fped.2022.903507

Objective: This study aimed to explore the clinical features and outcomes of children with spinal cord injury (SCI) without fracture or dislocation.

Methods: The clinical data of children with SCI without fracture or dislocation in this retrospective study were collected in Chongqing, China (January 2010 to December 2021). We collected patient demographics at admission including age, gender, cause, level, and severity of the injury in admission and complications. Reports from radiologic imaging were reviewed to identify spina bifida occulta (SBO). Neurological function was evaluated using the American Spinal Injury Association (ASIA) Impairment Scale (AIS) for an SCI.

Results: A total of 74 children with SCI (male, 27%; female, 73%; male-to-female ratio, 1:2.7; average age, 5.7 years) were included. The main cause of injury was backbend during the dance (34 patients, 45.9%, including 2 patients who hugged back falling backward), followed by traffic accidents (17 patients, 23%). Children with backbend-related SCI were older than other children (6.9 vs. 4.9 years old, $P < 0.001$). When reviewing all radiological images, it was found that 20 (27%) patients with SCI had SBO. The proportion of SCI with SBO caused by backbend was considerably higher than those caused by non-backbend (41.2 vs. 15%, $P = 0.012$). The AIS were 22 (29.7%), 4 (5.4%), 8 (10.8%), 31 (41.9%), and 9 (12.2%) in A, B, C, D, and E, respectively. The prognosis was poorer in the backbend during dancing than other causes of injury ($p = 0.003$).

Conclusion: This study showed that backbend during the dance was the main cause of children's SCI without fracture or dislocation in Chongqing, China. The prognosis was poorer in those children than in other causes of injury. Meanwhile, we have established an association between SBO and SCI for children performing a backbend during the dance.

Keywords: spinal cord injury without fracture or dislocation, spina bifida occulta, risk factor, children, China

INTRODUCTION

Spinal cord injury without radiologic abnormality (SCIWORA) was defined as traumatic myelopathy without radiographic features of spinal fracture or dislocation, which was initially described by Pang and Wilberger in 1982 (1). Along with the development and popularity of MRI, real SCIWORA or without neuroimaging abnormality has become increasingly rare. Previous studies demonstrated the leading etiologies of spinal cord injury (SCI) without fracture or dislocation, including motor vehicle accidents, falls, sports, and child abuse in western countries (2). While that appeared different in China, dance injury has been supposed to be the main cause (3, 4). In 2019, Liang et al. (5) reported three cases of pediatric SCI caused by minor trauma and suggest that spina bifida occulta (SBO) might be a predisposing factor for SCI without fracture or dislocation.

Spina bifida is the term used to describe the failure of fusion of the neural folds during the neurulation phase of embryologic development, which has usually been divided into spina bifida cystica (SBC) and SBO (6). SBO has recently been linked with voiding dysfunction, constipation, or lower urinary tract abnormality (7, 8). The pathological changes in the core of SBO are tethered spinal cord, which has longitudinal traction damage to the spinal cord (6). Chronic spinal cord traction may play an important role in the mechanism of pediatric SCI following minor trauma.

Therefore, the aim of the present study was to determine the demographic of SCI without fracture or dislocation and to compare the prevalence of SBO between SCI following backbend during the dance and those without backbend. Furthermore, the study also assessed potential risk factors for the severity of the injury. Identification of risk factors for children attending dancing courses could be of value in risk assessment and prevention.

TABLE 1 | Clinical characteristics ($n = 74$).

Age (year), mean (SD)	5.8 (2.7)
Sex, *n* (%)	
Male	20 (27.0)
Female	54 (73.0)
Cause of injury, *n* (%)	
Back bend	34 (45.9)
Traffic accident	17 (23.0)
High fall	3 (4.1)
Low fall	15 (20.3)
Violence	2 (2.7)
Sports	3 (4.1)
MRI, *n* (%)	
Normal	9 (12.2)
Abnormal	65 (87.8)
Severity of the injury	
Complete	25 (33.8)
Incomplete	49 (66.2)
Complication in rehabilitation ($n = 54$), *n* (%)	
Neurogenic bladder	45 (83.3)
Osteopenia	26 (48.1)
Urinary Stone	6 (11.1)
Spasticity	14 (25.9)
Pressure ulcer/scald	7 (13.0)
Urinary tract infection	36 (66.7)
Progression at last follow up	
A	22 (29.7)
B	4 (5.4)
C	8 (10.8)
D	31 (41.9)
E	9 (12.2)

SD, standard deviation.

MATERIALS AND METHODS

Study Population

We retrospectively analyzed 74 children with SCI identified in the medical database at Children's Hospital of Chongqing Medical University from January 2010 to December 2021. Two independent researchers reviewed all medical records and radiological images to identify SCI. The inclusion criteria were as follows: (1) patients admitted with a diagnosis of traumatic spinal cord injury; (2) without fracture or dislocation of the spine; and (3) follow-up time >6 months. The exclusion criteria were as follows: (1) with any other neurologic diseases; (2) incomplete radiological data; and (3) with neoplasm, vascular malformation, and so on. The study was approved by the Ethics Committee of Children's Hospital of Chongqing Medical University (NO. 202249).

Measures and Definition

We collected patient demographics at admission including age, gender, cause, level, and severity of the injury in admission, and complications. Reports from radiologic imaging were reviewed to identify SBO, if present, and the length of lesions on a sagittal T2-Weighted magnetic resonance image (MRI). Neurological function was evaluated using the American Spinal Injury Association (ASIA) Impairment Scale (AIS) for a spinal cord injury, the severity of the injury was graded as A to E, while A represents a complete injury, and B through E represents incomplete injuries. Age was divided into two groups: 0–8 years and 9–18 years. Falling below 1 meter was classified as a low fall, and above 1 meter was classified as a high fall.

Statistical Analysis

Continuous variables were expressed as means ± *SD* and categorical variables as numbers and percentages. Differences in categorical variables were compared using Chi-square or Fisher's exact test between groups. The two means were compared with independent *t*-tests for normally distributed variables and the Mann-Whitney U test for nonnormally distributed variables. Univariate and multivariate logistic regression analyses were applied to assess the risk factors for the severity of the injury. A P-value of < 0.05 was considered statistically significant. Statistical analyses were performed using R software version 4.1.2 (Project for Statistical Computing).

TABLE 2 | Characteristics of SCI caused by backbend and non-backbend.

	Backbend $n = 34$	Non-backbend $n = 40$	*P*
Age, mean (SD)	6.9 (1.6)	4.9 (3.1)	<0.001
Sex			<0.001
Male	1 (2.9)	19 (47.5)	
Female	33 (97.1)	21 (52.5)	
Neurological level of injury			<0.001
Paraplegia	34 (100)	28 (70.0)	
Tetraplegia	0	12 (30.0)	
Severity of the injury			0.455
Complete	13 (38.2)	12 (30.0)	
Incomplete	21 (61.8)	28 (70.0)	
Length of lesion, Median (IQR)	7 (3, 9)	5 (3, 7.5)	0.268
SBO			0.012
Yes	14 (41.2)	6 (15.0)	
No	20 (58.8)	34 (85.0)	

SD, standard deviation; IQR, interquartile range; SBO, spina bifida occulta.

RESULTS

Patients Characteristics

Patients characteristics are summarized in **Table 1**. For those subjects, the average age range was 5.8 (2.7) years old, and the maximal age range was 15 years, while the minimum age range was 1.1 years. The main etiology of injury was backbend during dancing (34 patients, 45.9%, including 2 patients hugged back falling backward), followed by traffic accident (17 patients, 23%). Only very few injuries (3 patients, 4.1%) occur during sports activities. In total, 65 (87.8%) patients had various lesions determined by MRI. The most common type of complication was the neurogenic bladder, which occurred in 45 of 54 patients (83.3%) during the convalescent phase. Urinary tract infection (66.7%) and osteopenia (48.1%) were the second and third most common complications found in patients, respectively.

Patients Characteristics: Backbend vs. Non-backbend

Table 2 summarizes the demographic, injury, and MRI features of patients by backbend vs. non-backbend. The causes of injuries in patients by backbend were older than those caused by non-backbend (6.9 vs. 4.9 years old, $P < 0.001$). There was a proportional difference between males and females (female predominance), with a male-to-female ratio of 1:2.7. Injuries in patients caused by back bend were more likely to suffer from longer levels of lesions determined by MRI (7 vs. 5 vertebral). When reviewing all radiological images, we were surprised to find that there were 20 (27%) patients with SBO in all patients (**Figure 1**). The main types of SBO were simple lumbosacral spinal dysraphism (15 patients, 75%, including one patient who had combined sacral lumbarization) and fatty filum terminale (4 patients, 20%). The proportion of patients with SBO caused by backbend was considerably higher than those caused by non-backbend (41.2 vs. 15%, $P = 0.012$).

Risk Factors for Severity of the Injury

Univariate and multivariate logistic regression analyses were employed to analyze the risk factors that featured statistical differences between the complete SCI group and the incomplete SCI group. It was observed that sex, age, cause, and SBO are not the risk factors affecting the severity of the injury, as shown in **Table 3**.

Progression During the Last Follow-up

American Spinal Injury Association Impairment Scale grades and complications at the last follow-up were shown in **Table 4**. Final AIS grades were as follows: 22 A (29.7%), 4 B (5.4%), 8 C (10.8%), 31 D (41.9%), and 9 E (12.2%). The prognosis was poorer in the backbend during dancing than other causes of injury ($p = 0.003$). Complete injury in admission was also significantly associated with poorer neurologic recovery ($p < 0.001$). Although there was no statistical difference between SBO and normal, the proportion of patients with SBO caused by backbend was considerably higher than that caused by non-backbend (41.2 vs. 15%, $P = 0.012$).

DISCUSSION

There is a wide disparity in the incidence rates of SCI without fracture or dislocation across the world (9, 10), with the highest incidence in pediatrics subjects, which is largely explained by differences in spinal biomechanical specificities. Pediatrics show a great deformation capacity due to their disc and ligament elasticity and anatomic features, especially before 8 years of age (11, 12). Although some studies have investigated the pathogenesis of SCI caused by backbend during dance (13, 14), the underlying mechanisms remain incompletely understood.

Compared with previous studies in other countries, the obvious difference was the demographic factors, which were in accordance with the results of Zou et al. (4). The age of SCI for this study was younger than compared with other studies (5.8 vs. 9.78 years), besides, the male-to-female ratio was 1:2.7, indicating a slightly higher incidence of females compared with other countries in which the male-to-female ratio was 1.8–3.3:1 (2, 9). Alternatively, the incidence of paraplegia caused by thoracic or/and lumbar was higher (83.8%), this result reached 100% in patients with injuries caused by backbend during the dance, which was different from almost all of the previous studies as well (2, 9, 15). Road accidents (37%) and sports accidents (31%) were identified as the main causes of SCI by a systematic review (16). While backbend during the dance was the main cause of children SCI in China in the present study which is similar to the study by Zou et al. (4).

Previous literature suggested that children (particularly those younger than 8 years) have specific biomechanics of the vertebral column due to lack of uncus, anterior vertebral wall immaturity, and vertebral ligament elasticity (17). Under external force, vertebral displacement recaptures quickly, and damage to the spinal cord could occur at the same time. The present study identified that children younger than 8 years of age represented 82.4% of all children with SCI. Interestingly, demographic differences mentioned above were associated with the main cause. Attending dancing courses is a more common

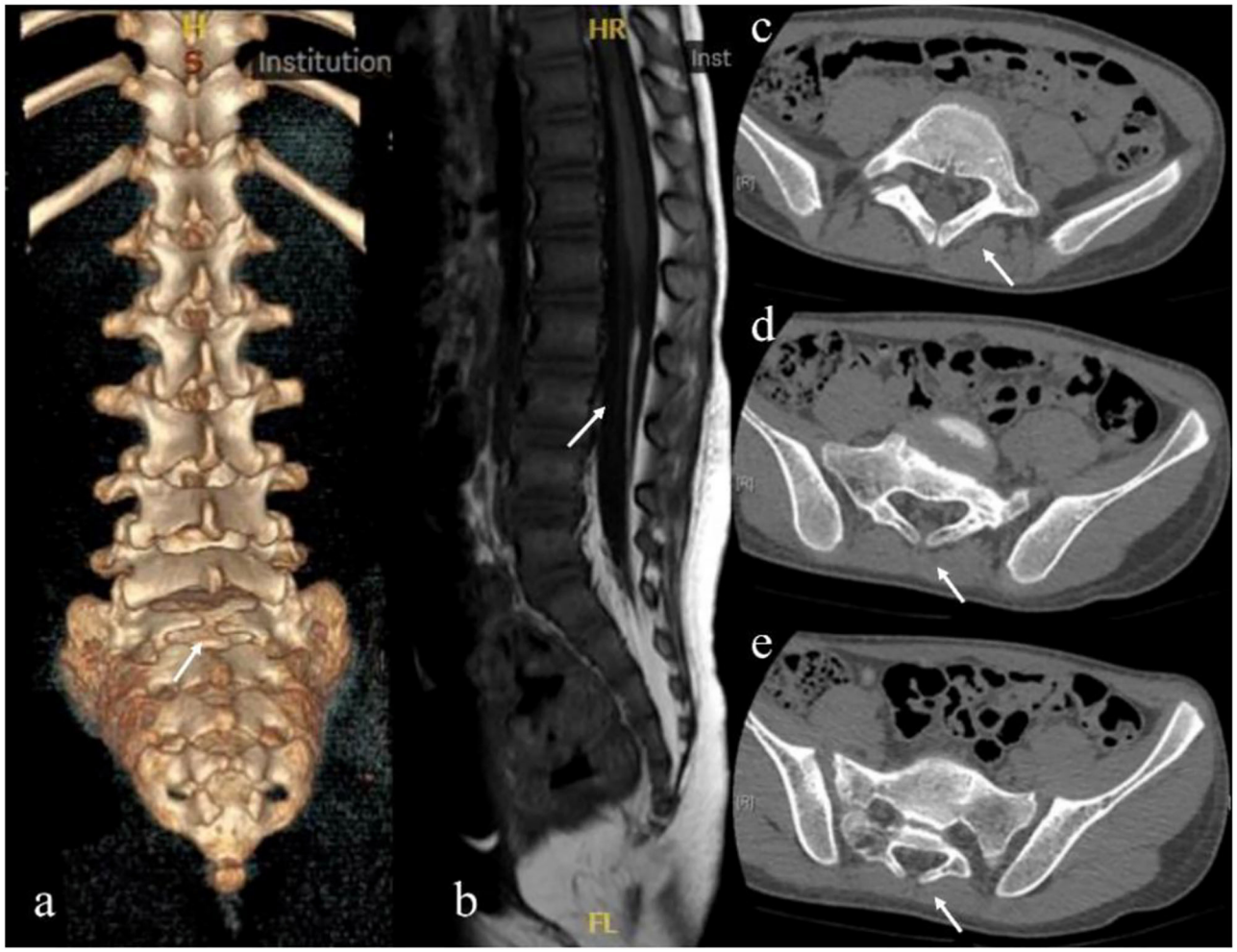

FIGURE 1 | Radiological images showing spina bifida occulta. **(a)** Sacral 1 spina bifida occulta. **(b)** Fatty filum terminale. **(c–e)** are from the same patient. **(c)** Sacral lumbarization and Lumbar 6 spina bifida occulta. **(d)** Sacral 1 spina bifida occulta. **(e)** Sacral 2 spina bifida occulta.

TABLE 3 | Univariate and multivariate logistic regression analysis of the severity of the injury.

Variables	Univariate			Multivariate		
	OR	95%CI	*P*	OR	95%CI	*P*
Sex (female/male)	0.689	0.238–1.995	0.493	0.443	0.119–1.651	0.225
Age (>8/≤8)	0.847	0.233–3.078	0.800	0.864	0.233–3.204	0.826
Cause (backbend/non-backbend)	1.444	0.549–3.800	0.456	2.368	0.690–8.131	0.171
SBO (yes/no)	0.789	0.261–2.390	0.676	0.682	0.211–1.201	0.522

OR, odds ratio; CI, confidence interval; SBO, spina bifida occulta.

phenomenon for girls, especially at the age of 4–8 years. The spinal cord has poor tolerance to traction compared with the spinal. When the amplitude of back extension continues to rise beyond the tolerance threshold of the spinal cord which is fixed in vertebral foramen by spinal nerve root passing through the corresponding intervertebral foramina, a spinal cord injury of the thoracic and/or lumbar will be triggered (13). However, we did not find that backbend during the dance was an independent risk factor for SCI without fracture or dislocation. This may be due to the small sample size. In the current study, there was a significant difference in the prognosis between the backbend and non-backbend ($P = 0.003$). This was potentially due to more patients with complete injuries which also served as a poor prognostic indicator of SCI in the group backbend.

TABLE 4 | Progression at last follow-up.

	AIS						P
	ALL (*n* = 74)	A (*n* = 22)	B (*n* = 4)	C (*n* = 8)	D (*n* = 31)	E (*n* = 9)	
Age							0.880
0–8 year	61 (82.4)	18 (81.8)	4 (100)	6 (75.0)	26 (83.9)	7 (77.8)	
9–18 year	13 (17.6)	4 (18.2)	0	2 (25.0)	5 (16.1)	2 (22.2)	
Sex							0.069
Male	20 (27.0)	3 (13.6)	3 (75.0)	3 (37.5)	10 (32.3)	1 (11.1)	
Female	54 (73.0)	19 (86.4)	1 (25.0)	5 (62.5)	21 (67.7)	8 (88.8)	
Etiology							0.003
Backbend	34 (45.9)	14 (63.6)	0	1 (12.5)	12 (38.7)	7 (77.8)	
Non-back bend	40 (54.1)	8 (36.4)	4 (100)	7 (87.5)	19 (61.3)	2 (22.2)	
Neurological level of injury							0.232
Paraplegia	62 (83.8)	21 (95.5)	4 (100)	7 (87.5)	23 (74.2)	7 (77.8)	
Tetraplegia	12 (16.2)	1 (4.5)	0	1 (12.5)	8 (25.8)	2 (22.2)	
Severity of the injury							<0.001
Complete	25 (33.8)	19 (86.4)	4 (100)	1 (12.5)	1 (3.2)	0	
Incomplete	49 (66.2)	3 (13.6)	0	7 (87.5)	30 (96.8)	9 (100)	
SBO							0.531
Yes	20 (27.0)	6 (27.3)	0	3 (37.5)	7 (22.6)	4 (44.4)	
No	54 (73.0)	16 (72.7)	4 (100)	5 (62.5)	24 (77.4)	5 (55.6)	

SD, standard deviation; IQR, interquartile range; SBO, spina bifida occulta.

Another important finding was that 20 (27%) patients with SBO observed in our study included simple lumbo-sacral spinal dysraphism, fatty filum terminale, and sacral lumbarization for the first time. Spina bifida is the term used to describe the failure of fusion of the neural folds during the neurulation phase of embryologic development, which is usually been divided into SBC and SBO (18). Previous literature has commonly believed that SBO is a failure of fusion of the vertebral arches that are covered by the skin and mostly does not involve the spinal cord. Based on their pathological characteristics, SBO is classified into different types, including simple lumbosacral spinal dysraphism, spinal cord lipoma, diastematomyelia, fatty filum terminale, intradural lipoma, and so on (19). The pathological changes in the core of spina bifida are tethered spinal cord, that has longitudinal traction damage to the spinal cord (18). Lipomas of the spinal cord and fatty myelomeningocele often have fat masses that compress the spinal cord laterally and may restrict the growth and extension of spinal cord nerve roots, leading to neurodevelopmental dysplasia (19). SBO is easily disregarded since it does not show any symptoms, and even in those who show symptoms, the symptoms tend to be limited to only bowel and bladder dysfunction. Meanwhile, the proportion of SCIWORA with SBO caused by backbend was considerably higher than that caused by non-backbend ($P = 0.012$). We hypothesized that there was a possible association between SBO and spinal cord abnormalities which could cause spinal cord damage more easily. The hypothesis is supported by Liang et al. (5), who reported three children with real SCIWORA caused by minor trauma. Although three patients had no signs of tethered cord syndrome prior, tight filum terminale was found during the operation. The filum terminale is a fibrous and viscoelastic band that connects the conus medullaris to the periosteum of the coccyx, and it is thought to fixate and stabilize the lower cord during abnormal cephalad and caudal traction, and also allow the conus to move during flexion and extension of the spine (20). The fatty filum terminale refers to a filum that is both >2 mm in diameter and contains a fat signal (21). The fat infiltration can cause stretching and tethering of the conus resulting in neurological symptoms. Identification of risk factors for children attending dancing courses could be of value in risk assessment and prevention. Although the direct evidence is still missing and the exact mechanism remains unclear, SBO might cause chronic spinal cord traction or underlying structures occurs resulting in a pediatric thoracic and lumber SCI following minor trauma.

This study still has some limitations. First, the study was retrospective, thus, our results need confirmation in a prospective study. Second, single-center research study with inevitable selection bias. Third, we were unable to assess the risk factors for backbend during dance and SCI without fracture or dislocation due to the lack of a control group. Although we looked for risk factors for complete SCI, it was observed that sex, age, cause, and SBO are not the risk factors affecting the severity of the injury. This may be due to the small sample size. Further studies with larger sample sizes are required for confirming the relationship. Finally, lack of pathologically confirmed patients. However, all of the patients were strictly screened with both comprehensive ASIA assessments and radiographic. SCI without fracture or dislocation is a disease that has low prevalence rates

but significant disability for children, and its poor prognosis severely influences the affected patients. It is important to prevent this disease. Therefore, scientific popularization should be strengthened to enhance the awareness of individuals who practice any activity that involves backbend. Children, particularly those younger than 8 years, should be encouraged to avoid prolonged, repetitive backbend of the spine to reduce the risk during the dance.

In summary, this study showed that backbend during the dance was the main cause of children's SCI without fracture or dislocation in China. The prognosis was poorer in those children than in other causes of injury. Meanwhile, we have established an association between SBO and SCI for children performing a backbend during the dance.

DATA AVAILABILITY STATEMENT

The raw data supporting the conclusions of this article will be made available by the authors, without undue reservation.

ETHICS STATEMENT

The studies involving human participants were reviewed and approved by the Ethics Committee of Children's Hospital of Chongqing Medical University. Written informed consent from the participants' legal guardian/next of kin was not required to participate in this study in accordance with the national legislation and the institutional requirements.

AUTHOR CONTRIBUTIONS

GL conceptualized and designed the study, carried out the initial analyses, and drafted the initial manuscript. ST, MZ, and LT designed the data collection instruments and collected data. XT coordinated and supervised data collection, assisted in the statistical analysis, and carried out the initial analyses. WJ coordinated and supervised data collection and critically reviewed the manuscript for important intellectual content. YC and NX conceptualized and designed the study, supervised data collection, and reviewed and revised the manuscript. All authors read and approved the final manuscript.

FUNDING

This work was supported by the Program for Technological Innovation and Application Development of Chongqing (cstc2019jscx-msxmX0197).

ACKNOWLEDGMENTS

We thank all of the participants for their help.

REFERENCES

1. Pang D, Wilberger JE. Spinal cord injury without radiographic abnormalities in children. *J Neurosurg.* (1982) 57:114–29. doi: 10.3171/jns.1982.57.1.0114
2. Knox J. Epidemiology of spinal cord injury without radiographic abnormality in children: a nationwide perspective. *J Child Orthop.* (2016) 10:255–60. doi: 10.1007/s11832-016-0740-x
3. Wang YJ, Zhou HJ, Wei B, Liu GL, Zheng Y, Zhang Y, et al. Clinical characteristics analysis of 120 cases of pediatric spinal cord injury without radiologic abnormality. *Zhonghua Yi Xue Za Zhi.* (2016) 96:122–5. doi: 10.3760/cma.j.issn.0376-2491.2016.02.010
4. Zou Z, Teng A, Huang L, Luo X, Wu X, Zhang H, et al. Pediatric Spinal Cord Injury without Radiographic Abnormality: The Beijing Experience. *Spine.* (2021) 46:E1083–8. doi: 10.1097/BRS.0000000000004030
5. Liang QC, Yang B, Song YH, Gao PP, Xia ZY, Bao N. Real spinal cord injury without radiologic abnormality in pediatric patient with tight filum terminale following minor trauma: a case report. *BMC Pediatr.* (2019) 19:513. doi: 10.1186/s12887-019-1894-8
6. Fidas A, MacDonald HL, Elton RA, McInnes A, Wild SR, Chisholm GD. Prevalence of spina bifida occulta in patients with functional disorders of the lower urinary tract and its relation to urodynamic and neurophysiological measurements. *BMJ.* (1989) 298:357–9. doi: 10.1136/bmj.298.6670.357
7. Yavuz A, Bayar G, Kilinc MF, Sariogullari U. The relationship between nocturnal enuresis and spina bifida occulta: a prospective controlled trial. *Urology.* (2018) 120:216–21. doi: 10.1016/j.urology.2018.07.038
8. Yuan Z, Cheng W, Hou A, Wang W, Zhang S, Liu D, et al. Constipation is associated with spina bifida occulta in children. *Clin Gastroenterol Hepatol.* (2008) 6:1348–53. doi: 10.1016/j.cgh.2008.07.009
9. Brauge D, Plas B, Vinchon M, Charni S, Di Rocco F, Sacko O, et al. Multicenter study of 37 pediatric patients with SCIWORA or other spinal cord injury without associated bone lesion. *Orthop Traumatol Surg Res.* (2020) 106:167–71. doi: 10.1016/j.otsr.2019.10.006
10. Piatt JH. Pediatric spinal injury in the US: epidemiology and disparities. *J Neurosurg Pediatr.* (2015) 16:463–71. doi: 10.3171/2015.2.PEDS1515
11. Rekate HL, Theodore N, Sonntag VK, Dickman CA. Pediatric spine and spinal cord trauma: State of the art for the third millennium. *Childs Nerv.* (1999) 15:743–50. doi: 10.1007/s003810050464
12. Kriss VM, Kriss TC. SCIWORA (spinal cord injury without radiographic abnormality) in infants and children. *Clin Pediatr.* (1996) 35:119–24. doi: 10.1177/000992289603500302
13. Ren J, Zeng G, Ma Y-J, Chen N, Chen Z, Ling F, et al. Pediatric thoracic SCIWORA after back bend during dance practice: a retrospective case series and analysis of trauma mechanisms. *Childs Nerv Syst.* (2017) 33:1191–8. doi: 10.1007/s00381-017-3407-0
14. Tong A-N, Zhang J-W, Zhou H-J, Tang H-H, Bai J-Z, Wang F-Y, et al. Ischemic damage may play an important role in spinal cord injury during dancing. *Spinal Cord.* (2020) 58:1310–6. doi: 10.1038/s41393-020-0503-x
15. Mohanty SP, Bhat NS, Singh KA, Bhushan M. Cervical spinal cord injuries without radiographic evidence of trauma: a prospective study. *Spinal Cord.* (2013) 51:815–8. doi: 10.1038/sc.2013.87
16. Boese CK, Oppermann J, Siewe J, Eysel P, Scheyerer MJ, Lechler P. Spinal cord injury without radiologic abnormality in children: a systematic review and meta-analysis. *J Trauma Acute Care Surg.* (2015) 78:874–82.. doi: 10.1097/TA.0000000000000579
17. Pang D. Spinal cord injury without radiographic abnormality in children, 2 decades later. *Neurosurgery.* (2004) 55:1325–42. doi: 10.1227/01.NEU.0000143030.85589.E6
18. Copp AJ, Adzick NS, Chitty LS, Fletcher JM, Holmbeck GN, Shaw GM. Spina bifida. *Nat Rev Dis Primer.* (2015) 1:15007. doi: 10.1038/nrdp.2015.7
19. Kumar A, Tubbs RS. Spina bifida: a diagnostic dilemma in paleopathology. *Clin Anat N Y N.* (2011) 24:19–33. doi: 10.1002/ca.21058
20. De Vloo P, Monea AG, Sciot R, van Loon J, Van Calenbergh F. The filum terminale: a cadaver study of anatomy, histology, and elastic properties. *World Neurosurg.* (2016) 90:565–73.e1. doi: 10.1016/j.wneu.2015.12.103

21. Badve CA, Khanna PC, Phillips GS, Thapa MM, Ishak GE. MRI of closed spinal dysraphisms. *Pediatr Radiol.* (2011) 41:1308–20. doi: 10.1007/s00247-011-2119-y

Conflict of Interest: The authors declare that the research was conducted in the absence of any commercial or financial relationships that could be construed as a potential conflict of interest.

Publisher's Note: All claims expressed in this article are solely those of the authors and do not necessarily represent those of their affiliated organizations, or those of the publisher, the editors and the reviewers. Any product that may be evaluated in this article, or claim that may be made by its manufacturer, is not guaranteed or endorsed by the publisher.

frontiers | Frontiers in Pharmacology

ORIGINAL RESEARCH
published: 16 June 2022
doi: 10.3389/fphar.2022.905879

The Correlation Between Busulfan Exposure and Clinical Outcomes in Chinese Pediatric Patients: A Population Pharmacokinetic Study

Xiaohuan Du[1,2†], Chenrong Huang[1,3†], Ling Xue[1,4†], Zheng Jiao[5], Min Zhu[5], Jie Li[6], Jun Lu[6], Peifang Xiao[6], Xuemei Zhou[6], Chenmei Mao[2], Zengyan Zhu[2], Ji Dong[1], Xiaoxue Liu[1], Zhiyao Chen[1], Shichao Zhang[1], Yiduo Ding[1], Shaoyan Hu[6] and Liyan Miao[1,3,7]**

[1]Department of Pharmacy, The First Affiliated Hospital of Soochow University, Suzhou, China, [2]Department of Pharmacy, The Children's Hospital of Soochow University, Suzhou, China, [3]Institute for Interdisciplinary Drug Research and Translational Sciences, College of Pharmaceutical Science, Soochow University, Suzhou, China, [4]Department of Pharmacology, University of the Basque Country (UPV/EHU), Leioa, Spain, [5]Department of Pharmacy, Shanghai Chest Hospital, Shanghai Jiao Tong University, Shanghai, China, [6]Department of Hematology and Oncology, The Children's Hospital of Soochow University, Suzhou, China, [7]National Clinical Research Center for Hematologic Diseases, The First Affiliated Hospital of Soochow University, Suzhou, China

OPEN ACCESS

Edited by:
Xiaoling Wang,
Capital Medical University, China

Reviewed by:
Li Zhiling,
Shanghai Jiao Tong University, China
Xujie Zhao,
St. Jude Children's Research Hospital, United States

***Correspondence:**
Liyan Miao
miaolysuzhou@163.com
Shaoyan Hu
hushaoyan@suda.edu.cn

†These authors have contributed equally to this work and share first authorship

Specialty section:
This article was submitted to Obstetric and Pediatric Pharmacology, a section of the journal Frontiers in Pharmacology

Received: 28 March 2022
Accepted: 31 May 2022
Published: 16 June 2022

Citation:
Du X, Huang C, Xue L, Jiao Z, Zhu M, Li J, Lu J, Xiao P, Zhou X, Mao C, Zhu Z, Dong J, Liu X, Chen Z, Zhang S, Ding Y, Hu S and Miao L (2022) The Correlation Between Busulfan Exposure and Clinical Outcomes in Chinese Pediatric Patients: A Population Pharmacokinetic Study. Front. Pharmacol. 13:905879. doi: 10.3389/fphar.2022.905879

Aims: The aims of the study were to 1) establish a population pharmacokinetic (Pop-PK) model for busulfan in Chinese pediatric patients undergoing hematopoietic stem cell transplantation (HSCT) and then estimate busulfan exposure and 2) explore the association between busulfan exposure and clinical outcomes.

Methods: A total of 128 patients with 467 busulfan concentrations were obtained for Pop-PK modeling using nonlinear mixed effect model (NONMEM) software. Sixty-three patients who received the 16-dose busulfan conditioning regimen were enrolled to explore the correlations between clinical outcomes and the busulfan area under the concentration–time curve (AUC) using the Cox proportional hazards regression model, Kaplan–Meier method and logistic regression.

Results: The typical values for clearance (CL) and distribution volume (V) of busulfan were 7.71 L h^{-1} and 42.4 L, respectively. The allometric normal fat mass (NFM) and maturation function (F*mat*) can be used to describe the variability in CL, and the fat-free mass (FFM) can be used to describe the variability in V. Patients with AUCs of 950–1,600 μM × min had 83.7% (95% CI: 73.3–95.5) event-free survival (EFS) compared with 55.0% (95% CI: 37.0–81.8) for patients with low or high exposure (p = 0.024). The logistic regression analysis results showed no association between transplant-related toxicities and the busulfan AUC (p > 0.05).

Conclusions: The variability in busulfan CL was related to the NFM and F*mat*, while busulfan V was related to the FFM. Preliminary analysis results suggested that a busulfan AUC of 950–1,600 μM × min was associated with better EFS in children receiving the 16-dose busulfan regimen.

Keywords: event-free survival, busulfan exposure, population pharmacokinetics, pediatric patients, hematopoietic stem cell transplantation

INTRODUCTION

Hematopoietic stem cell transplantation (HSCT) effectively treats many life-threatening malignant and nonmalignant diseases in pediatric patients (McCune and Holmberg, 2009). Busulfan is a bifunctional alkylating agent widely used in conditioning regimens in combination with cyclophosphamide (CTX), fludarabine and other chemotherapeutic drugs applied before HSCT. Busulfan is known for high variability in intra- and interindividual pharmacokinetics (PK) and pharmacodynamics (PD), especially in children (Nguyen et al., 2004; Booth et al., 2007; Bartelink et al., 2012; Savic et al., 2013; Long-Boyle et al., 2015; Marsit et al., 2020).

To identify relevant relationships between busulfan PK and potential covariates, population PK (Pop-PK) models have been established for different populations. Based on the Pop-PK model, weight-based initial dosing strategies were proposed by the United States FDA, and the European Medicines Agency (EMA) created in children (Nguyen et al., 2004; Booth et al., 2007). Except for body weight (Nguyen et al., 2004; Booth et al., 2007; Bartelink et al., 2012), other Pop-PK models have shown that age (Savic et al., 2013; McCune et al., 2014), body surface area (BSA) (Trame et al., 2011; Wang et al., 2015; Rhee et al., 2017), body composition (McCune et al., 2014; van Hoogdalem et al., 2020), coadministered drugs (such as fludarabine) (Ishiwata et al., 2018) were associated with busulfan clearance (CL). Notably, the influence of genetic polymorphisms in glutathione S-transferase (GST) enzymes, which mediate the metabolism of busulfan conjugation with glutathione, affect the degree of busulfan metabolism and may cause variability in busulfan PK (Yin et al., 2015; Ansari et al., 2017; Nava et al., 2017; Kim et al., 2019). *GSTA1*, the predominant enzyme in busulfan metabolism, was first introduced as one of the covariates into a Pop-PK model in children and adolescents (Nava et al., 2018). Recently, Yuan et al. (2021) also showed a lower CL of busulfan in patients with the *GSTA1* mutant genotype than in those with the wild-type in a Chinese pediatric population (Yuan et al., 2021).

However, the pediatric patients with these alternative Pop-PK models and dosing nomograms were mainly Caucasian (Nguyen et al., 2004; Booth et al., 2007; Trame et al., 2011; McCune et al., 2014; Nava et al., 2018; van Hoogdalem et al., 2020), Japanese (Nakamura et al., 2008; Ishiwata et al., 2018), and Korean (Rhee et al., 2017) populations. As we know, there are a few Pop-PK studies on busulfan in Chinese adults (Wu et al., 2017; Huang et al., 2019; Sun et al., 2020), and there are only two Pop-PK studies on busulfan in Chinese children (Yuan et al., 2021; Huang et al., 2022). A systemic external evaluation of 11 published models on busulfan using data from Chinese pediatric patients by Huang et al. (2022) showed that the model developed only from the Korean population (Rhee et al., 2017) was suitable for Chinese HSCT pediatric patients (Huang et al., 2022). Therefore, due to the differences in body size, dietary habits and genetic background of the populations included in different Pop-PK studies, continued Pop-PK studies in the Chinese pediatric population are warranted to establish a platform for individualized busulfan administration.

It is widely understood that systemic exposure to busulfan measured as the area under the concentration time curve (AUC) or average steady-state concentration (Css) has a certain correlation with clinical outcomes (Bartelink et al., 2016; Palmer et al., 2016). Subexposure (< AUC 900 μM × min or Css 600 ng ml^{-1}) results in higher rates of failure, graft rejection and disease relapse (Slattery et al., 1995; McCune et al., 2002; Bartelink et al., 2009). However, overexposure (>AUC 1500 μM × min or Css 900 ng ml^{-1}) is associated with an increased risk of transplant-related toxicities (TRTs), such as veno-occlusive disease (VOD), acute graft-versus-host disease (aGVHD) and transplantation-related mortality (Grochow et al., 1989; Dix et al., 1996; Ljungman et al., 1997; Andersson et al., 2002). In children, the target exposures recommended by the FDA and EMA dosage regimens are 900–1,350 ± 5% μM × min and 900–1,500 μM × min for 6-hourly intravenous (IV) busulfan administration, respectively (Palmer et al., 2016). Nevertheless, studies on the relationship between busulfan exposure and clinical outcomes in Chinese populations are still scarce (Yin et al., 2015), especially among children (Shao et al., 2022).

Hence, the aims of the current study were 1) to characterize the PK of IV busulfan in Chinese children using Pop-PK analysis; 2) to evaluate the associations between busulfan exposure (expressed as AUC) and clinical outcomes in patients receiving a 16-dose busulfan myeloablative regimen (four times daily for four consecutive days), and preliminarily explore the optimum busulfan therapeutic range.

MATERIALS AND METHODS

Patients and Treatment Regimens

This study was conducted with 128 pediatric patients who received busulfan from July 2018 to February 2021. Patients who received IV busulfan as part of the conditioning regimen for HSCT were included, and patients for whom busulfan PK data were not available due to blood collection difficulties were excluded. This study was approved by the Medical Ethics Committee of the Children's Hospital of Soochow University (Suzhou, China), and all patients/parents provided written informed consent.

Busulfan (Busulfex; Otsuka Pharmaceutical Co., Ltd.) dosage was 0.8 mg kg^{-1}–1.2 mg kg^{-1} based on the actual or adjusted body weight (for obese patients). The adjusted body weight was calculated using the following equation: adjusted body weight = (actual weight − standard weight) × 0.25 + standard weight. The standard weight refers to the standardized growth charts for height and weight of Chinese children and adolescents aged 0–18 years (Hui et al., 2009). The therapeutic dose strata of busulfan are summarized in **Supplementary Table S2**. Busulfan was administered four times daily over 2 to 4 consecutive days as a 2 h infusion *via* a central venous catheter. No dosage adjustments were performed during the whole therapy procedure.

The pretreatment regimen varied depending on the different underlying diseases and types of donors. Generally, busulfan was combined with either CTX, fludarabine (FLU), cladribine,

cytarabine, etoposide or anti-thymocyte globulin. Oral phenytoin was used on the busulfan infusion days as seizure prophylaxis, beginning the day before the initiation of busulfan treatment. Cyclosporine or tacrolimus and mycophenolate mofetil in combination with methotrexate were used for aGVHD prophylaxis. Heparin and alprostadil were used for VOD prophylaxis, and mesna was given to prevent hemorrhagic cystitis.

Busulfan Pharmacokinetic Analysis and Genotyping

PK blood samples were obtained from the peripheral vein or central venous line (not used to infuse busulfan) at 0, 2, and 4 h (prior to the next scheduled busulfan administration) after the end of the first dose of busulfan infusion. Additionally, samples were collected before the fifth infusion dose for 61 (47.7%) patients. The specific time of sampling was recorded. Two to three milliliters of whole blood were collected in EDTA tubes for each sample. The samples were centrifuged and stored at −80°C until analysis. Busulfan plasma concentrations were measured using optimized liquid chromatography–tandem mass spectrometry (Li-na et al., 2016). The calibration curve was linear over a concentration range of 0.1–10 μg ml^{-1} (r = 0.997), and the lower limit of quantitation was 0.1 μg ml^{-1}.

Blood samples for genotyping were withdrawn before the first busulfan infusion. DNA extraction was performed using the QIAamp DNA Blood Mini Kit (Qiagen, Germany), following the manufacturer's instructions. The genetic variants for *GSTA1* were determined at the following loci: rs3957357, rs3957356, rs11964968, rs4715333, and rs58912740. *GSTP1* was genotyped according to rs1695. Single-nucleotide polymorphisms (SNPs) in the *GSTA1* and *GSTP1* genes were separately genotyped using multiplex PCR and sequencing. A panel containing 6 target SNP sites was designed. Library preparation was performed using two-step PCR. Paired-end sequencing of the library was performed on HiSeq XTen sequencers (Illumina, San Diego, CA).

Population Pharmacokinetic Modeling

Pop-PK analysis was performed using nonlinear mixed effect model (NONMEM) software (version 7.3.0; Double Precision; ICON Development Solutions). The auxiliary software included Wings for NONMEM (Version 7.4.1, http://wfn.sourceforge.net), R packages (version 3.4.3, http://www.r-project.org) and Pirana (version 2.9.4, http://www.pirana-software.com). The ADVAN1 and TRAN2 subroutines and the first-order conditional estimation method with interaction (FOCE-I) were chosen to estimate parameters.

Busulfan pharmacokinetics were fitted using a one-compartment PK model with first-order elimination as the structural model. The estimated PK parameters included the CL and distribution volume (V). The between-subject (BSV) and between-occasion variability (BOV) were assessed using an exponential model (**Supplementary Equation S1**). Residual variability was described using a combined model with a proportional and additive model (**Supplementary Equation S2**).

The variability in CL and V was predicted using body size and composition with a theory-based allometric model and busulfan metabolism maturation upon CL was also evaluated as a maturation function (F*mat*), as proposed by McCune et al. (2014). Nine different models based on normal fat mass (NFM) scaling of CL were assessed using **Eq. 1** (**Table 1**). V was predicted using **Eq. 2**. The Akaike information criterion (AIC) and Bayesian information criterion (BIC) were estimated for these models using Pirana. Models with lower AIC and BIC values were considered superior models.

$$CL = CL_{STD} \times \left(\frac{NFM}{NFM_{STD}}\right)^{k1} \times Fmat \quad (1)$$

$$V = V_{STD} \times \frac{NFM}{NFM_{STD}} \quad (2)$$

where CL_{STD} and V_{STD} are the typical CL and V values scaled to those of an adult male with a body weight of 70 kg and a height of 176 cm. The standard NFM (NFM_{STD}) was calculated using **Supplementary Equations S3, S4**. The exponent k_1 was estimated in seven models, and in Model I and Model III, k_1 was fixed to a theory-based value of 3/4 (Holford and Anderson, 2017). F*mat* represents the maturation of CL based on postmenstrual age (PMA) using **Supplementary Equations S5, S6** and was fixed to 1, except in Model III.

Other potential covariates included the baseline disease (malignant vs. nonmalignant), hematological and biological indicators, genotype and daily dosage of coadministered drugs (including fludarabine, phenytoin and metronidazole), which were collected from the patients' medical records. The continuous covariates were introduced into the model as **Supplementary Equation S7**. The categorical covariates were introduced into the model as **Supplementary Equation S8**. All covariates were introduced into the basic model individually to identify the covariates with statistical significance for the busulfan PK parameters. The significance level was set to 0.05 (*df* = 1, change in objective function value (OFV) = 3.84). The analysis of potential covariates was further performed using a stepwise procedure based on the changes in OFV. During forward selection, the significance level was set to 0.01 (*df* = 1, change in OFV = 6.64). During backward elimination, the significance level was set to 0.001 (*df* = 1, change in OFV = 10.83).

The accuracy and robustness of the final model were evaluated using bootstrap methods, goodness-of-fit plots and prediction-corrected visual predictive checking (pc-VPC). Once the final Pop-PK model was established, it was used to provide estimates of individual busulfan AUC for subsequent evaluations of the relationships with transplantation outcomes.

Correlation Analysis Between Busulfan Area Under the Concentration–Time Curve and Clinical Outcomes

The main study endpoint was event-free survival (EFS), as calculated from the time of transplant until graft failure, relapse of disease, or death, whichever occurred first (Philippe et al., 2016). First, the busulfan AUC was taken as a continuous

TABLE 1 | Parameter estimates of the nine NFM-dependent CL candidate models.

Parameters	Model I	Model II	Model III	Model IV	Model V	Model VI	Model VII	Model VIII	Model IX
	3/4 Allometric model	Simple exponent model	3/4 Allometric and maturation function model	Age-cutoff separated model	Age-cutoff separated model	Weight-dependent exponent model	FFM-dependent exponent model	Age-dependent exponent model	PMA-dependent exponent model
Model description	CL×(NFM/56.1)$^{3/4}$	CL×(NFM/56.1)^{k1}	CL×(NFM/56.1)$^{3/4}$×F*mat*	CL×(NFM/56.1)^{k1}	CL×(NFM/56.1)^{k1}	CL×(NFM/56.1)^{k1}	CL×(NFM/56.1)^{k1}	CL×(NFM/56.1)^{k1}	CL×(NFM/56.1)^{k1}
OFV	−1305.01	−1306.7	−1307.41	−1308.2	−1308.25	−1313.41	−1311.72	−1310.33	−1310.09
AIC	−1291.01	−1290.7	−1289.41	−1288.2	−1288.25	−1291.41	−1289.72	−1288.33	−1288.09
BIC	−1261.98	−1257.53	−1252.1	−1246.73	−1246.78	−1245.8	−1244.11	−1242.72	−1242.48
CL_STD (L h^{-1})	7.5	7.98	7.71	21.3[a]/7.86[b]	11.7[c]/7.86[d]	7.79	7.87	7.73	7.74
V_STD (L)	42.4	42.4	42.4	42.4	42.4	42.4	42.4	42.4	42.4
RUV_PROP	0.131	0.131	0.13	0.13	0.131	0.13	0.13	0.13	0.13
RUV_ADD	0.0479	0.0479	0.048	0.0479	0.0477	0.0478	0.0477	0.0479	0.0479
F*fat*_CL	0.654	0.625	0.692	0.66	0.683	0.771	0.748	0.725	0.72
k_1	0.75	0.801	0.75	1.31[a]/0.783[b]	1.0[c]/0.785[d]		-	-	-
$k_1 = k_0$–*kmax*/{[1+ (Weight or FFM/k_{50})$^{-HILL}$]} or $k_1 = k_0$–*kmax*/{[1+ (Age or PMA/k_{50})$^{-HILL}$]}									
TM_{50}	-	-	31	-	-	-	-	-	-
k_0	-	-	-	-	-	0.938	0.985	0.838	0.832
kmax	-	-	-	-	-	0.169	0.205	0.0808	0.0731
k_{50}	-	-	-	-	-	8.46	5.85	1.4	115
HILL	-	-	2.03	-	-	964	365	285	1080
BSV_CL	0.237	0.235	0.234	0.234	0.233	0.229	0.23	0.231	0.231
BSV_V	0.24	0.24	0.24	0.241	0.24	0.241	0.241	0.241	0.241

[a]*Estimates for children ≤1 year of age.*
[b]*Estimates for children >1 year of age.*
[c]*Estimates for children ≤2 years of age.*
[d]*Estimates for children >2 years of age.*
*OFV, objective function value; AIC, akaike information criterion; BIC, bayesian information criterion; Clearance (CL_STD) and distribution volume (V_STD) estimates are standardized for an adult male with a bodyweight of 70 kg and a height of 176 cm (FFM_{STD} = 56.1 kg); RUV_PROP, proportional residual unidentified variability; RUV_ADD, additive residual unidentified variability; F*fat_CL*, fat fraction for CL; TM_{50}, postmenstrual age (PMA) when busulfan metabolism reaches 50% of adult levels;* kmax *is the maximum decrease of the exponent,* k_{50} *is the weight (Model VI and VII) or age (Model VIII and IX) at which a 50% decrease in the maximum decrease is attained; HILL, hill coefficient for maturation; BSV, between-subject variability, implicated in CL and V.*

variable, with a quadratic function to describe the correlation between log (AUC) and the log hazard of an event. The busulfan AUC range corresponding to a negative log hazard of an event was considered the optimum range. Second, the busulfan AUC was evaluated as a categorical variable (within or outside of the optimum range), together with age, weight, sex, disease type, donor source, and HLA disparity, using univariate and multivariate Cox proportional hazards regression models.

The secondary study endpoint was TRTs, including VOD, grade II–IV aGVHD, mucositis and hemorrhagic cystitis. VOD was diagnosed according to the modified Seattle criteria (Dignan et al., 2013), aGVHD was diagnosed and graded according to the Mount Sinai Acute GVHD International Consortium (MAGIC) criteria (Harris et al., 2016), and oral mucositis was evaluated and scored based on the ESMO Clinical Practice Guidelines (Peterson et al., 2015). The cumulative incidence of TRTs was evaluated with graft failure, relapse, and death as competing events. The correlation of TRTs incidence with the busulfan AUC was analyzed using logistic regression. All computations were conducted in R (version 4.1.0) with the *survival*, *survminer*, and *ezcox* R packages. $p < 0.05$ was regarded as significant.

RESULTS

Patient Characteristics

A total of 467 blood samples obtained from 128 enrolled patients were collected for Pop-PK model development. The patient characteristics and clinical laboratory results for the patients are summarized in **Supplementary Table S3**. Because samples for genotyping were not available from two patients, the *GSTA1* and *GSTP1* genotyping results were obtained for 126 patients and are summarized in **Supplementary Table S4**. Both the G*STA1* and *GSTP1* genetic frequencies for the patients were in Hardy–Weinberg equilibrium.

Population Pharmacokinetic Model Development

Among the nine various NFM-dependent CL models examined (**Table 1**), although the AIC value for the weight-dependent exponential model (Model VI) was the smallest, the larger HILL index value resulted in k_1 being approximately equal to 0.769, which was close to the fixed value for the allometric

TABLE 2 | Final Pop-PK model for busulfan: PK parameter estimates and bootstrap results.

Parameter	Original	Average	95% CIs		RSE (%)	Shrinkage (%)
CL_STD (L h^{-1})	7.71	7.90	7.30	9.44	10.6	
V_STD (L)	42.4	42.4	40.4	44.5	2.6	
RUV_PROP	0.130	0.130	0.092	0.164	13.7	
RUV_ADD (mg L^{-1})	0.048	0.046	0.016	0.065	26.2	
F*fat*_CL	0.692	0.702	0.196	1.301	38.7	
TM_{50} (weeks)	31.0	35.2	8.2	79.5	58.1	
HILL	2.03	2.97	0.44	9.92	81.1	
BSV_CL	0.234	0.229	0.195	0.265	7.9	8.24
BSV_V	0.240	0.238	0.191	0.287	10.1	15.9

*CI, confidence interval; RSE, relative standard error; Clearance (CL_STD) and distribution volume (V_STD) estimates are standardized for an adult male with a bodyweight of 70 kg and a height of 176 cm (FFM_{STD} = 56.1 kg); RUV_PROP, proportional residual unidentified variability; RUV_ADD, additive residual unidentified variability; F*fat*_CL, fat fraction for CL; TM_{50}, postmenstrual age when busulfan metabolism reaches 50% of adult levels; HILL, hill coefficient for maturation; BSV, between-subject variability, implicated in CL and V.*

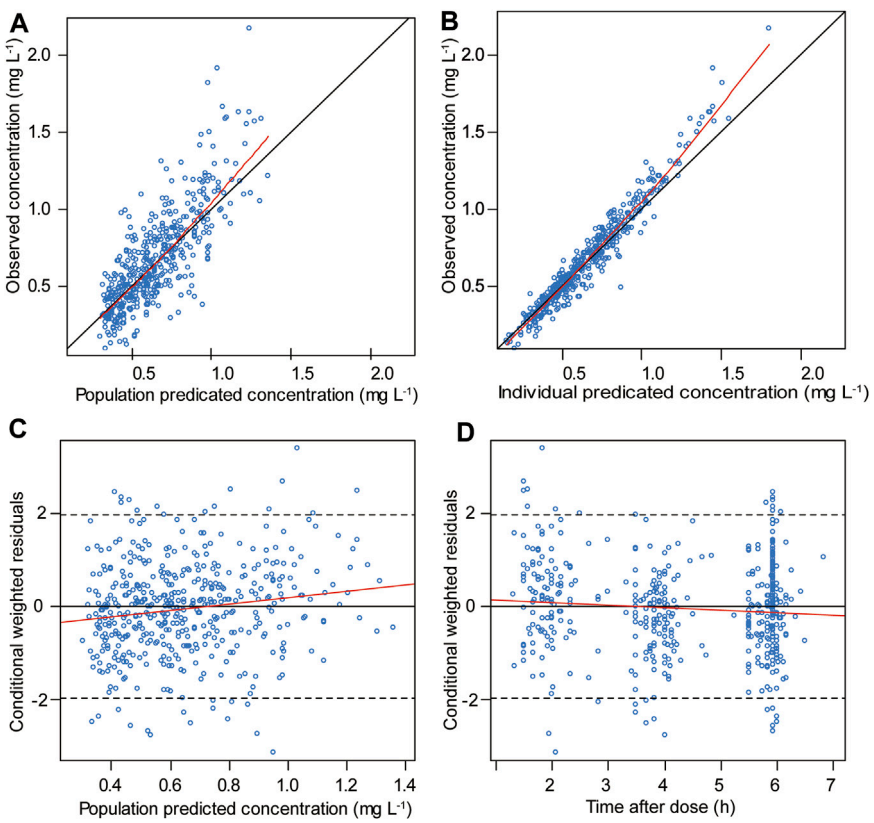

FIGURE 1 | Goodness-of-fit plots for the final model included the following: **(A)** observed vs. population predicted concentrations, **(B)** observed vs. individual predicted concentrations, **(C)** conditional weighted residuals vs. population predicted concentrations and **(D)** conditional weighted residuals vs. time after the first dose. The red line represents the fitted line.

exponent of 3/4 in Model III. Meanwhile, the F*mat* parameter introduced in Model III could better predict the effect of body size, physiological function, and body maturity on CL. Therefore, Model III was finally chosen as the basic structural model.

In the initial covariates screening process, the disease status (malignant or nonmalignant), *GSTA1,* and *GSTP1* gene polymorphisms had no statistical significance on the PK parameters of busulfan. During forward selection, the results showed that urea nitrogen (UREA) and γ-glutamyl transpeptidase (GGT) had statistical significance, but the correlation coefficient was 0.244 for UREA on CL and −0.1 for GGT on V, which was inconsistent with physiological function. Therefore, these two covariates were eliminated from the model, and then the final model was established. The potential covariate screening results are shown in **Supplementary Table S5**.

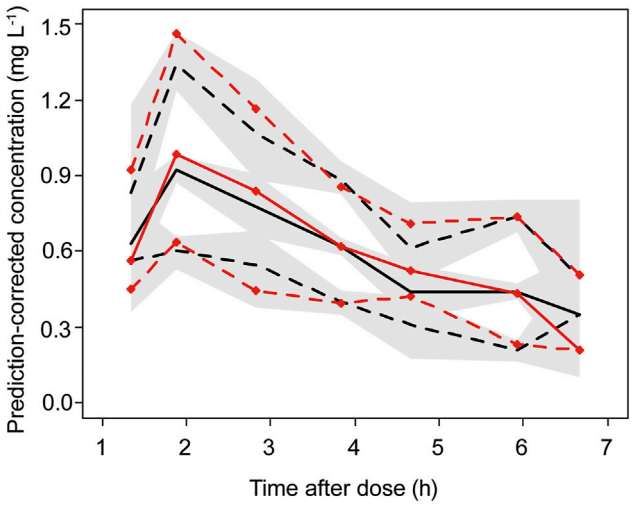

FIGURE 2 | Final model prediction-corrected visual prediction check (pc-VPC) of busulfan concentration. Observed (with symbols) and predicted 5th, 50th and 95th percentiles, with predicted 95% CIs (shaded regions). The red line represents the observed concentrations, and the black line represents the predicted concentrations.

The parameter estimates of the final model and bootstrap are summarized in **Table 2**. The final model indicated that the typical population estimates of CL and V were 7.71 L h^{-1} and 42.4 L, respectively. The value of the fraction of fat mass estimated for CL (F*fat*_CL) was 0.692, and that for V was zero. These values indicated that NFM and F*mat* were suitable covariates for explaining variability in CL, while FFM was the covariate for explaining variability in V. The BSV values for CL and V were 23.4% and 24.0%, respectively.

The goodness-of-fit plots for the final model are shown in **Figure 1**. The pc-VPC plot for the final model is shown in **Figure 2**.

Correlations Between the Busulfan Area Under the Concentration–Time Curve and Clinical Outcomes

To avoid the variation in busulfan exposure caused by different busulfan administration days, this part of the study only included patients received 16-dose busulfan myeloablative regimen (4 times daily over 4 days). The demographic and transplantation characteristics of the 63 patients are summarized in **Table 3**. The median busulfan AUC obtained from the Pop-PK model was 1,425.4 μM × min (range 691.5–2156.0 μM × min). With a median follow-up of 24.8 months (6.8–32.8 months), a total of 16 events occurred, including graft failure in 2 patients, disease relapse in 8 patients (four patients died) and 7 patient deaths (one with graft failure and six not related to relapse). The event summary information is listed in **Supplementary Table S6**.

TABLE 3 | Characteristics of patients treated with the 16-dose busulfan regimen (*n* = 63).

Demographic characteristics	Median (range)/number (%)
Follow-up (months)	24.8 (6.8–32.8)
Age (years)	2.5 (0.6–16.9)
Bodyweight (kg)	14.4 (7–63)
Busulfan AUC (μM × min)	1425.4 (691.5–2156.0)
Sex	
Male	44 (69.8%)
Female	19 (30.2%)
Diagnosis	
Malignant	50 (79.4%)
Acute myeloid leukemia (AML)	24 (38.1%)
Acute lymphoblastic leukemia (ALL)	22 (34.9%)
Myelodysplastic (MDS)	1 (1.6%)
Myeloproliferative neoplasms (MPN)	1 (1.6%)
Juvenile myelomonocytic leukemia (JMML)	2 (3.2%)
Nonmalignant	13 (20.6%)
Wiskott-Aldrich syndrome (WAS)	8 (12.7%)
Thalassemia	4 (6.3%)
Severe aplastic anemia (SAA)	1 (1.6%)
HLA disparity	
Matched	5 (7.9%)
Mismatched	58 (92.1%)
Cell source	
Umbilical cord blood	31 (49.2%)
Peripheral blood stem cell	12 (19.0%)
Bone marrow or peripheral blood stem cell and bone marrow combined	20 (31.7%)
Events	
Graft failure	2 (3.2%)
Disease relapse	8 (17.4%)
Death	11 (17.5%)

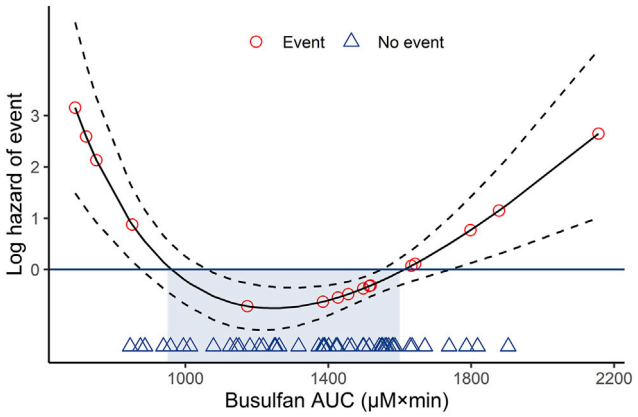

FIGURE 3 | Log hazard risk model for event-free survival calculated as a quadratic function. Dotted lines represent the 95% confidence intervals. AUC, area under the curve.

After HSCT, the estimated EFS was 74.5% (95% CI: 64.4–86.1) at 2 years. In the log hazard model, the estimated hazard of events as a function of busulfan AUC suggested the existence of an optimal interval. The model produced an optimum busulfan AUC of 950–1,600 μM × min, as shown in **Figure 3**.

In the univariate and multivariate Cox regression analyses, the busulfan AUC was identified as the only significant factor for EFS (hazard ratio (HR) 0.32, 95% CI: 0.12–0.86; $p = 0.02$), as shown by the forest map in **Figure 4**, while weight, sex, disease type, donor source, and HLA disparity did not affect EFS. Kaplan–Meier curves were used to compare the EFS of patients inside the optimum AUC interval with that of patients outside the interval. Patients with an AUC of 950–1,600 μM × min had 83.7% (95% CI: 73.3–95.5) EFS compared with 55.0% (95% CI: 37.0–81.8) for patients with low (<950 μM × min) or high (>1,600 μM × min) exposure ($p = 0.024$; **Figure 5**).

Grade II-IV aGVHD developed in 17 (27.0%) patients (grade II in 4 patients, grade III in 6 patients, and grade IV in 7 patients), with a cumulative incidence of 26.98% (95% CI: 15.9–38.1) at 100 days. In the absence of VOD, hepatotoxicity (serum bilirubin) of at least grade 2 until 30 days after transplantation was evaluated and graded according to the Common Terminology Criteria for Adverse Events (v5.0). Hepatotoxicity occurred in 18 patients (grade II in 17 patients and grade III in one patient). The cumulative incidences of hepatotoxicity, oral mucositis (in 10 patients) and hemorrhagic cystitis (in 3 patients) at 30 days posttransplantation were 28.6% (95% CI: 17.3–39.8), 15.9% (95% CI: 6.7–25.0), and 4.8% (95% CI: 0.00–10.1), respectively. The logistic regression analysis results showed no association between these toxicity complications and the busulfan AUC ($p > 0.05$, **Supplementary Figure S1**).

DISCUSSION

This study used Pop-PK analysis to characterize the relationships between busulfan exposure and clinical outcomes in Chinese pediatric patients with HSCT. With the developed Pop-PK model and using physiologically-based descriptions of body composition and theory-based allometric principles, CL for busulfan was estimated according to allometry NFM and F*mat*, and V was estimated according to FFM. Furthermore,

Covariate		Number of patients	Hazard ratio	Hazard ratio (95% CI)	P
Sex	Female	19		Reference	
	Male	44		1.35 (0.44, 4.20)	0.60
Age (year)	<3	32		Reference	
	>= 3	31		1.30 (0.49, 3.50)	0.60
Weight (kg)	< 15	32		Reference	
	>= 15	31		0.97 (0.36, 2.59)	0.95
Disease type	Malignant	50		Reference	
	Nonmalignant	13		0.24 (0.03, 1.79)	0.16
Donor source	BM/BM+PB	20		Reference	
	CB	31		0.95 (0.33, 2.73)	0.92
	PB	12		0.53 (0.11, 2.61)	0.43
HLA disparity	Match	5		Reference	
	Mismatch	58		1.46 (0.19, 11.05)	0.71
BU AUC (μM×min)	< 950 or >1600	20		Reference	
	950-1600	43		0.32 (0.12, 0.86)	0.02

FIGURE 4 | Forest plot of univariate Cox regression analysis for event-free survival ($n = 63$).

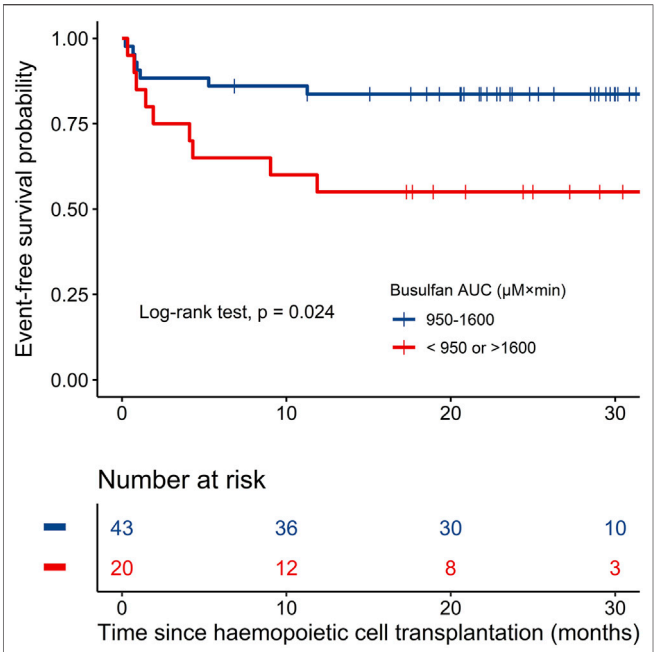

FIGURE 5 | Kaplan–Meier plots of event-free survival in the two groups based on busulfan AUC (n = 63).

the results demonstrated that an AUC of 950–1,600 μM × min was associated with better EFS in children receiving the 16-dose busulfan regimen before HSCT.

The typical population estimates for busulfan CL and V standardized for an adult patient weighing 70 kg were 7.71 L h^{-1} and 42.4 L in the final model, respectively. The estimated V was in good accordance with other reports (McCune et al., 2014; Rhee et al., 2017; Nava et al., 2018; Yuan et al., 2021). The estimated CL was slightly lower than that in prior studies from Korea (10.7 L h^{-1}) (Rhee et al., 2017), Caucasian (11.4 and 13.58 L h^{-1}) (McCune et al., 2014; Nava et al., 2018) and Chinese (11.08 L h^{-1}) (Yuan et al., 2021) pediatric patients. However, in a recently published study (Dunn et al., 2021), the typical CL for a 20 kg child was 1.14 L h^{-1}, which were reduced estimates compared to ours and prior studies. These discrepancies in CL might be due to published models contain various structural PK models, various covariates, different age distributions and ethnicities (Huang et al., 2022).

It is well-known that body weight, age and body surface area (BSA) have significant impacts on busulfan PK in pediatric patients (Nguyen et al., 2004; Booth et al., 2007; Trame et al., 2011; Bartelink et al., 2012; Savic et al., 2013; McCune et al., 2014; Wang et al., 2015; Rhee et al., 2017). NFM, a theory-based size descriptor that divides body weight into FFM and fat mass, was used to estimate the effect of body size and composition on busulfan PK in infants to adults (McCune et al., 2014; van Hoogdalem et al., 2020). In the present analysis, nine models were proposed to characterize the PK of busulfan by introducing the NFM parameter. In the final model, 69.2% fat mass in addition to FFM described CL for busulfan, whereas the F*fat* was zero for V. As proposed by McCune et al., the fraction of the fat mass was 50.9% for CL and 20.3% for V (McCune et al., 2014). The different fractions of fat mass may be caused by the different age distributions in the different study groups. In McCune et al. (2014) study, infant and adult patients were included, with a wide age range (0.1–65.8 years). All patients included in the present study were children, with an average age of 6.1 years (0.6–17 years). The maturation of CL is more appropriately described by PMA than by postnatal age because the maturation of CL begins before birth (Anderson and Holford, 2009). The PMA was calculated by adding postnatal age to gestational age. In the current study, the maturation of the busulfan CL reached 50% of adult values at 31 weeks of PMA, considering body composition, which was lower than in another study (TM_{50} = 45.7) (McCune et al., 2014). In our cohort, the actual gestational ages of the patients were recorded, whereas, in McCune et al. (2014) study, the values were assumed to be 40 weeks due to missing information. This might be the reason for the bias. In two recent Pop-PK studies of busulfan based on Chinese pediatric patients, BSA was considered one of the significant covariates for CL in the model developed by Yuan et al. (2021). Huang et al. (2022) conducted a systemic external evaluation of 11 published models of busulfan based on an independent dataset from 40 Chinese pediatric populations and similarly concluded that a model developed from the Korean population with BSA affecting CL as one of the covariates had the most satisfactory predictability for Chinese children (Huang et al., 2022). Based on children's growth and developmental characteristics, CL in the pediatric population should be investigated using models that account for the influences of body size, maturation, and organ function. Allometric scaling using an empiric power exponent of 3/4 is superior to scaling using BSA, which has already been described by Anderson and Holford (Anderson and Holford, 2009).

After including body composition and maturation in the model, several other potential covariates (including disease type, concomitant medications, hematological and biological indicators, and genetic variants of *GSTA1* or *GSTP1*) had no significant effect on busulfan PK. The guideline from the American Society for Blood and Bone Marrow Transplantation (ASBMT) stated that fludarabine, deferasirox, and metronidazole have an impact on IV busulfan CL. The effect of phenytoin on IV busulfan CL is unclear, although it is known to affect oral busulfan CL (Palmer et al., 2016). However, none of these three drugs were found to have an effect on IV busulfan PK in the present study. This finding was consistent with the results of a recent report, which showed that children with HSCT did not experience significant effects on busulfan CL when coadministered with drugs that could theoretically interfere with busulfan metabolism (Dunn et al., 2021). Busulfan is mainly metabolized and eliminated by the liver. Elevated alanine transaminase (ALT) and aspartate transaminase (AST) levels are indicative of potential liver damage, thus affecting the elimination of busulfan. Two cohorts of Asian pediatric patients showed that increased AST levels affected busulfan CL (Rhee et al., 2017; Yuan et al., 2021). However, ALT or AST enzymes were not found to be significant covariates with busulfan CL in

the present study, which is in line with another report on pediatric Fanconi anemia patients (van Hoogdalem et al., 2020). This might be explained by the fact that only a few cases (7 cases) of our children had both abnormally high ALT and AST levels. In the study by Bartelink et al. (2012), it was also shown that neither biochemical parameters nor blood counts could predict individual variability (Bartelink et al., 2012). The influence of GST gene polymorphisms on busulfan CL remains controversial (Kim et al., 2019). However, the present study and other modeling studies failed to incorporate the genetic variants of *GSTA1* and *GSTP1* as covariates into the final model (Zwaveling et al., 2008; Sun et al., 2020). Models established in pediatric populations could suggest that a validated pharmacogenetics-based Pop-PK model would be a beneficial tool for individualized busulfan administration (Nava et al., 2017; Nava et al., 2018; Yuan et al., 2021).

The AUC 900–1,350 μM × min or 900–1,500 μM × min has been widely used as a target busulfan exposure to improve clinical outcomes in children with HSCT (Bolinger et al., 2001; Ansari et al., 2014; Philippe et al., 2016). A recent report showed that Chinese children with a target exposure of 900–1,350 μM × min also had a better survival outcome (Shao et al., 2022). In the present study of 63 children on a 16-dose busulfan pretreatment regimen, we found that patients with an AUC of 950–1,600 μM × min achieved optimal EFS, which is slightly higher than the target exposure recommended by the FDA or EMA dosage regimens for children. A previous retrospective study conducted by Bartelink et al. (2009) suggested that a total AUC of 74–82 mg h L^{-1} (~AUC 1125–1,250 μM × min per dose) was associated with the highest EFS in children with malignant and nonmalignant diseases (Bartelink et al., 2009). A multicenter study from 15 different transplantation centers defined that the optimum cumulative AUCs of 78–101 mg h L^{-1} (~AUC 1225–1,575 μM × min per dose) predicted higher EFS in children and young adults than those in lower- and higher-exposure groups (Bartelink et al., 2016). This upper threshold of 1,575 μM × min is generally consistent with 1,600 μM × min in this study, showing that this threshold is safe and associated with low toxicity. Notably, Ansari et al. indicated that Css >600 ng ml^{-1} (~AUC >900 μM × min) was independently associated with lower EFS by multivariate analysis (Ansari et al., 2014). Benadiba et al. (2018) also observed reduced EFS in patients with Css >600 ng ml^{-1} compared with patients with Css <600 ng ml^{-1} in children with myeloid malignancies receiving unrelated umbilical cord blood transplantation (Benadiba et al., 2018). The differences in the optimal exposure of busulfan between these studies may be influenced by multiple factors, including age, donor source, disease diagnosis, and other myeloablative agents included in the preparative regimen (Bartelink et al., 2016; Shukla et al., 2020). Despite the bias, these findings suggest that busulfan exposure is strongly associated with clinical outcomes in children and that establishing an optimal target exposure is warranted.

No significant correlations between busulfan AUC and TRTs were identified in the current analysis. This is consistent with the findings reported in a recent study in a Chinese pediatric population. This literature showed that busulfan exposure could not be used to predict VOD, liver injury, grade II-IV aGVHD, hemorrhagic cystitis or oral mucositis after multivariate analyses (Shao et al., 2022). As early as 30 years ago, the busulfan AUC of 1,500 μM × min was considered the upper threshold because higher exposure was associated with an increased risk of VOD in adults (Grochow et al., 1989). For safety reasons, this threshold was also used in pediatric patients, although this correlation remains controversial according to previous studies using IV busulfan in children (Bartelink et al., 2009; Malär et al., 2011; Ansari et al., 2014; Philippe et al., 2016). Since all patients in the current cohort did not have VOD, the association between high busulfan exposure and VOD could not be established. A previous study done by Philippe et al. reported that all children who developed VOD had a busulfan AUC of <1,500 μM × min (Philippe et al., 2016). In another large cohort, also by Philippe et al. (2019), which specifically looked at the determinants of VOD, an increased risk of VOD was observed in children with a maximum busulfan concentration (Cmax) value of ≥1.88 ng ml^{-1} (Philippe et al., 2019). In addition to the high busulfan exposure, several other factors, such as underlying disease, genetic polymorphisms, iron overload, hepatic fibrosis or cirrhosis, influence the incidence of VOD (Dignan et al., 2013; Philippe et al., 2019). At present, the correlation between aGVHD and busulfan exposure is not clear, and conflicting results exist. Some studies have shown that higher busulfan exposure was associated with a higher incidence of grade II-IV aGVHD (Bartelink et al., 2009; Ansari et al., 2014); however, other researchers have found that the risk of aGVHD increased with low exposure (Russell et al., 2013). Similar to our study, some previous investigations found no association between busulfan exposure and grade II-IV aGVHD in children (Baker et al., 2000; Shao et al., 2022). Although a previous study showed a positive correlation between busulfan AUC and the severity of stomatitis in children (Michel et al., 2012), the correlation was not found in this study, which was also consistent with other studies (Bartelink et al., 2009; Ansari et al., 2014). Several studies have emphasized that the combined use of melphalan may increase the risk of stomatitis because melphalan is metabolized by the same enzyme system as busulfan (Bartelink et al., 2009; Michel et al., 2012). Although one study showed that the cumulative incidence of hemorrhagic cystitis was higher for patients with a Css >600 ng ml^{-1} compared to patients with Css <600 ng ml^{-1} (Benadiba et al., 2018), this correlation was not observed in our study and another study (Ansari et al., 2014). These differences may be explained by different populations and conditioning regimens. Other factors must be further studied to identify patients at risk for such toxicities.

However, the present study has several limitations. It included a limited number of patients from a single center. The predictive performance of the final Pop-PK model has yet to undergo external validation. Moreover, several other genetic covariates for busulfan PK have not been assessed in the present analysis, such as the *GSTM1*-null and CYP39A1 genotypes, which were found in association with busulfan PK (Ten Brink et al., 2013; Ansari et al., 2017). In addition, other factors might have affected clinical outcomes, such as the disease grading and remission status of malignant disease before transplantation, GVHD prophylaxis regimens before and after transplantation could

not be included in the present analysis (Bartelink et al., 2016). A multicenter trial is ongoing (ClinicalTrials.gov: NCT04786002), aiming to establish the optimal busulfan treatment window for myeloablative conditioning in Chinese pediatric patients and confirm our preliminary results.

CONCLUSION

In conclusion, the final Pop-PK model established in the current study shows that allometric FFM, F*fat* and F*mat* can describe the variability in busulfan CL in pediatric patients and that FFM can be used to describe the variability in V, while fat mass has no correlation with V. The result of the present study suggests that busulfan exposure (an AUC of 950–1,600 μM × min) was associated with better EFS in children receiving a 16-dose busulfan myeloablative conditioning regimen before HSCT. The performance of the present Pop-PK model and the preliminarily established target busulfan exposure need to be further validated in prospective studies with larger samples.

DATA AVAILABILITY STATEMENT

The original contributions presented in the study are included in the article/**Supplementary Material**, further inquiries can be directed to the corresponding authors.

ETHICS STATEMENT

The studies involving human participants were reviewed and approved by the Medical Ethics Committee of the Children's Hospital of Soochow University (Suzhou, China). Written informed consent to participate in this study was provided by the participants' legal guardian/next of kin.

AUTHOR CONTRIBUTIONS

XD, CH, LM, and SH designed and performed the study; CM and ZZ participated in the study design; XD, CH, and LX drafted the manuscript; LM and SH reviewed the manuscript; JL, JL, PX, and XZ enrolled patients and interpreted the medical results. LX performed the Pop-PK model; ZC and SZ helped with genetic typing; MZ and ZJ analyzed the data and interpreted the data. XD, JD, XL, and YD provided the reagents and measured the samples.

FUNDING

This study was supported by the Translational Research Grant of NCRCH (No. 2020WSC07), the Project of Science and Technology Development Plan of Suzhou City (No. SYSD2020186) and the Suzhou Health Talent Program (No. GSWS2019001).

ACKNOWLEDGMENTS

The authors gratefully thank the patients and their parents for consenting to participate in this study. We also thank the nurses and the medical staff of the Department of Hematology and Oncology of the Children's Hospital of Soochow University for their collaboration.

SUPPLEMENTARY MATERIAL

The Supplementary Material for this article can be found online at: https://www.frontiersin.org/articles/10.3389/fphar.2022.905879/full#supplementary-material

Supplementary Figure S1 | Logistic regression for the correlation of transplant-related toxicities with the busulfan AUC.

REFERENCES

Anderson, B. J., and Holford, N. H. (2009). Mechanistic Basis of Using Body Size and Maturation to Predict Clearance in Humans. *Drug Metab. Pharmacokinet.* 24 (1), 25–36. doi:10.2133/dmpk.24.25

Andersson, B. S., Thall, P. F., Madden, T., Couriel, D., Wang, X., Tran, H. T., et al. (2002). Busulfan Systemic Exposure Relative to Regimen-Related Toxicity and Acute Graft-Versus-Host Disease: Defining a Therapeutic Window for i.V. BuCy2 in Chronic Myelogenous Leukemia. *Biol. Blood Marrow Transpl.* 8 (9), 477–485. doi:10.1053/bbmt.2002.v8.pm12374452

Ansari, M., Curtis, P. H., Uppugunduri, C. R. S., Rezgui, M. A., Nava, T., Mlakar, V., et al. (2017). GSTA1 Diplotypes Affect Busulfan Clearance and Toxicity in Children Undergoing Allogeneic Hematopoietic Stem Cell Transplantation: a Multicenter Study. *Oncotarget* 8 (53), 90852–90867. doi:10.18632/oncotarget.20310

Ansari, M., Théoret, Y., Rezgui, M. A., Peters, C., Mezziani, S., Desjean, C., et al. (2014). Association between Busulfan Exposure and Outcome in Children Receiving Intravenous Busulfan before Hematopoietic Stem Cell Transplantation. *Ther. Drug Monit.* 36 (1), 93–99. doi:10.1097/FTD.0b013e3182a04fc7

Baker, K. S., Bostrom, B., DeFor, T., Ramsay, N. K., Woods, W. G., and Blazar, B. R. (2000). Busulfan Pharmacokinetics Do Not Predict Relapse in Acute Myeloid Leukemia. *Bone Marrow Transpl.* 26 (6), 607–614. doi:10.1038/sj.bmt.1702590

Bartelink, I. H., Boelens, J. J., Bredius, R. G., Egberts, A. C., Wang, C., Bierings, M. B., et al. (2012). Body Weight-dependent Pharmacokinetics of Busulfan in Paediatric Haematopoietic Stem Cell Transplantation Patients: towards Individualized Dosing. *Clin. Pharmacokinet.* 51 (5), 331–345. doi:10.2165/11598180-000000000-00000

Bartelink, I. H., Bredius, R. G., Belitser, S. V., Suttorp, M. M., Bierings, M., Knibbe, C. A., et al. (2009). Association between Busulfan Exposure and Outcome in Children Receiving Intravenous Busulfan before Hematologic Stem Cell Transplantation. *Biol. Blood Marrow Transpl.* 15 (2), 231–241. doi:10.1016/j.bbmt.2008.11.022

Bartelink, I. H., Lalmohamed, A., van Reij, E. M., Dvorak, C. C., Savic, R. M., Zwaveling, J., et al. (2016). Association of Busulfan Exposure with Survival and Toxicity after Haemopoietic Cell Transplantation in Children and Young Adults: a Multicentre, Retrospective Cohort Analysis. *Lancet Haematol.* 3 (11), e526–e536. doi:10.1016/s2352-3026(16)30114-4

Benadiba, J., Ansari, M., Krajinovic, M., Vachon, M. F., Duval, M., Teira, P., et al. (2018). Pharmacokinetics-adapted Busulfan-Based Myeloablative Conditioning before Unrelated Umbilical Cord Blood Transplantation for Myeloid Malignancies in Children. *PLoS One* 13 (4), e0193862. doi:10.1371/journal.pone.0193862

Bolinger, A. M., Zangwill, A. B., Slattery, J. T., Risler, L. J., Sultan, D. H., Glidden, D. V., et al. (2001). Target Dose Adjustment of Busulfan in Pediatric Patients

Undergoing Bone Marrow Transplantation. *Bone Marrow Transpl.* 28 (11), 1013–1018. doi:10.1038/sj.bmt.1703264

Booth, B. P., Rahman, A., Dagher, R., Griebel, D., Lennon, S., Fuller, D., et al. (2007). Population Pharmacokinetic-Based Dosing of Intravenous Busulfan in Pediatric Patients. *J. Clin. Pharmacol.* 47 (1), 101–111. doi:10.1177/0091270006295789

Dignan, F. L., Wynn, R. F., Hadzic, N., Karani, J., Quaglia, A., Pagliuca, A., et al. (2013). BCSH/BSBMT Guideline: Diagnosis and Management of Veno-Occlusive Disease (Sinusoidal Obstruction Syndrome) Following Haematopoietic Stem Cell Transplantation. *Br. J. Haematol.* 163 (4), 444–457. doi:10.1111/bjh.12558

Dix, S. P., Wingard, J. R., Mullins, R. E., Jerkunica, I., Davidson, T. G., Gilmore, C. E., et al. (1996). Association of Busulfan Area under the Curve with Veno-Occlusive Disease Following BMT. *Bone Marrow Transpl.* 17 (2), 225–230.

Dunn, A., Moffett, B. S., Ivaturi, V., and Gobburu, J. V. S. (2021). Characterization of Drug-Drug Interactions on the Pharmacokinetic Disposition of Busulfan in Paediatric Patients during Haematopoietic Stem Cell Transplantation Conditioning. *Brit J. Clin. Pharma* 88, 2223–2235. doi:10.1111/bcp.15151

Grochow, L. B., Jones, R. J., Brundrett, R. B., Braine, H. G., Chen, T. L., Saral, R., et al. (1989). Pharmacokinetics of Busulfan: Correlation with Veno-Occlusive Disease in Patients Undergoing Bone Marrow Transplantation. *Cancer Chemother. Pharmacol.* 25 (1), 55–61. doi:10.1007/bf00694339

Harris, A. C., Young, R., Devine, S., Hogan, W. J., Ayuk, F., Bunworasate, U., et al. (2016). International, Multicenter Standardization of Acute Graft-Versus-Host Disease Clinical Data Collection: A Report from the Mount Sinai Acute GVHD International Consortium. *Biol. Blood Marrow Transpl.* 22 (1), 4–10. doi:10.1016/j.bbmt.2015.09.001

Holford, N. H. G., and Anderson, B. J. (2017). Allometric Size: The Scientific Theory and Extension to Normal Fat Mass. *Eur. J. Pharm. Sci.* 109S, S59–S64. doi:10.1016/j.ejps.2017.05.056

Huang, H., Liu, M., Ren, J., Hu, J., Lin, S., Li, D., et al. (2022). Can Published Population Pharmacokinetic Models of Busulfan Be Used for Individualized Dosing in Chinese Pediatric Patients Undergoing Hematopoietic Stem Cell Transplantation? an External Evaluation. *J. Clin. Pharmacol.* 62 (5), 609–619. doi:10.1002/jcph.1992

Huang, J., Li, Z., Liang, W., Chen, B., Hu, J., and Yang, W. (2019). Accurate Prediction of Initial Busulfan Exposure Using a Test Dose with 2- and 6-Hour Blood Sampling in Adult Patients Receiving a Twice-Daily Intravenous Busulfan-Based Conditioning Regimen. *J. Clin. Pharmacol.* 59 (5), 638–645. doi:10.1002/jcph.1354

Hui, L., Cheng-ye, J., Xin-nan, Z., and Ya-qin, Z. (2009). Height and Weight Standardized Growth Charts for Chinese Children and Adolescents Aged 0 to 18 Years. *Chin. J. Pediatr.* 47 (5), 371–375. (in Chinese). doi:10.3760/cma.j.issn.0578-1310.2009.07.003

Ishiwata, Y., Nagata, M., Tsuge, K., Takahashi, H., Suzuki, S., Imai, K., et al. (2018). Population Pharmacokinetics of Intravenous Busulfan in Japanese Pediatric Patients with Primary Immunodeficiency Diseases. *J. Clin. Pharmacol.* 58 (3), 327–331. doi:10.1002/jcph.1027

Kim, M. G., Kwak, A., Choi, B., Ji, E., Oh, J. M., and Kim, K. (2019). Effect of Glutathione S-Transferase Genetic Polymorphisms on Busulfan Pharmacokinetics and Veno-Occlusive Disease in Hematopoietic Stem Cell Transplantation: A Meta-Analysis. *Basic Clin. Pharmacol. Toxicol.* 124 (6), 691–703. doi:10.1111/bcpt.13185

Li-na, Z., Ji, D., and Li-yan, M. (2016). Determination of Busulfan Concentration in Plasma by UPLC-MS-MS. *Anti Infect. Pharm.* 13 (6), 1216–1219. (in Chinese). doi:10.13493/j.issn.1672-7878.2016.06-004

Ljungman, P., Hassan, M., Békássy, A. N., Ringdén, O., and Oberg, G. (1997). High Busulfan Concentrations Are Associated with Increased Transplant-Related Mortality in Allogeneic Bone Marrow Transplant Patients. *Bone Marrow Transpl.* 20 (11), 909–913. doi:10.1038/sj.bmt.1700994

Long-Boyle, J. R., Savic, R., Yan, S., Bartelink, I., Musick, L., French, D., et al. (2015). Population Pharmacokinetics of Busulfan in Pediatric and Young Adult Patients Undergoing Hematopoietic Cell Transplant: a Model-Based Dosing Algorithm for Personalized Therapy and Implementation into Routine Clinical Use. *Ther. Drug Monit.* 37 (2), 236–245. doi:10.1097/ftd.0000000000000131

Malär, R., Sjöö, F., Rentsch, K., Hassan, M., and Güngör, T. (2011). Therapeutic Drug Monitoring Is Essential for Intravenous Busulfan Therapy in Pediatric Hematopoietic Stem Cell Recipients. *Pediatr. Transpl.* 15 (6), 580–588. doi:10.1111/j.1399-3046.2011.01529.x

Marsit, H., Philippe, M., Neely, M., Rushing, T., Bertrand, Y., Ducher, M., et al. (2020). Intra-individual Pharmacokinetic Variability of Intravenous Busulfan in Hematopoietic Stem Cell-Transplanted Children. *Clin. Pharmacokinet.* 59 (8), 1049–1061. doi:10.1007/s40262-020-00877-z

McCune, J. S., Bemer, M. J., Barrett, J. S., Scott Baker, K., Gamis, A. S., and Holford, N. H. (2014). Busulfan in Infant to Adult Hematopoietic Cell Transplant Recipients: a Population Pharmacokinetic Model for Initial and Bayesian Dose Personalization. *Clin. Cancer Res.* 20 (3), 754–763. doi:10.1158/1078-0432.CCR-13-1960

McCune, J. S., Gooley, T., Gibbs, J. P., Sanders, J. E., Petersdorf, E. W., Appelbaum, F. R., et al. (2002). Busulfan Concentration and Graft Rejection in Pediatric Patients Undergoing Hematopoietic Stem Cell Transplantation. *Bone Marrow Transpl.* 30 (3), 167–173. doi:10.1038/sj.bmt.1703612

McCune, J. S., and Holmberg, L. A. (2009). Busulfan in Hematopoietic Stem Cell Transplant Setting. *Expert Opin. Drug Metab. Toxicol.* 5 (8), 957–969. doi:10.1517/17425250903107764

Michel, G., Valteau-Couanet, D., Gentet, J. C., Esperou, H., Socié, G., Méchinaud, F., et al. (2012). Weight-based Strategy of Dose Administration in Children Using Intravenous Busulfan: Clinical and Pharmacokinetic Results. *Pediatr. Blood Cancer* 58 (1), 90–97. doi:10.1002/pbc.22959

Nakamura, H., Sato, T., Okada, K., Miura, G., Ariyoshi, N., Nakazawa, K., et al. (2008). Population Pharmacokinetics of Oral Busulfan in Young Japanese Children before Hematopoietic Stem Cell Transplantation. *Ther. Drug Monit.* 30 (1), 75–83. doi:10.1097/FTD.0b013e3181621cde

Nava, T., Kassir, N., Rezgui, M. A., Uppugunduri, C. R. S., Huezo-Diaz Curtis, P., Duval, M., et al. (2018). Incorporation of GSTA1 Genetic Variations into a Population Pharmacokinetic Model for IV Busulfan in Paediatric Hematopoietic Stem Cell Transplantation. *Br. J. Clin. Pharmacol.* 84 (7), 1494–1504. doi:10.1111/bcp.13566

Nava, T., Rezgui, M. A., Uppugunduri, C. R. S., Curtis, P. H., Théoret, Y., Duval, M., et al. (2017). GSTA1 Genetic Variants and Conditioning Regimen: Missing Key Factors in Dosing Guidelines of Busulfan in Pediatric Hematopoietic Stem Cell Transplantation. *Biol. Blood Marrow Transpl.* 23 (11), 1918–1924. doi:10.1016/j.bbmt.2017.07.022

Nguyen, L., Fuller, D., Lennon, S., Leger, F., and Puozzo, C. (2004). I.V. Busulfan in Pediatrics: a Novel Dosing to Improve Safety/efficacy for Hematopoietic Progenitor Cell Transplantation Recipients. *Bone Marrow Transpl.* 33 (10), 979–987. doi:10.1038/sj.bmt.1704446

Palmer, J., McCune, J. S., Perales, M. A., Marks, D., Bubalo, J., Mohty, M., et al. (2016). Personalizing Busulfan-Based Conditioning: Considerations from the American Society for Blood and Marrow Transplantation Practice Guidelines Committee. *Biol. Blood Marrow Transpl.* 22 (11), 1915–1925. doi:10.1016/j.bbmt.2016.07.013

Peterson, D. E., Boers-Doets, C. B., Bensadoun, R. J., Herrstedt, J., and Committee, E. G. (2015). Management of Oral and Gastrointestinal Mucosal Injury: ESMO Clinical Practice Guidelines for Diagnosis, Treatment, and Follow-Up. *Ann. Oncol.* 26 (Suppl. 5), v139–51. doi:10.1093/annonc/mdv202

Philippe, M., Goutelle, S., Guitton, J., Fonrose, X., Bergeron, C., Girard, P., et al. (2016). Should Busulfan Therapeutic Range Be Narrowed in Pediatrics? Experience from a Large Cohort of Hematopoietic Stem Cell Transplant Children. *Bone Marrow Transpl.* 51 (1), 72–78. doi:10.1038/bmt.2015.218

Philippe, M., Neely, M., Rushing, T., Bertrand, Y., Bleyzac, N., and Goutelle, S. (2019). Maximal Concentration of Intravenous Busulfan as a Determinant of Veno-Occlusive Disease: a Pharmacokinetic-Pharmacodynamic Analysis in 293 Hematopoietic Stem Cell Transplanted Children. *Bone Marrow Transpl.* 54 (3), 448–457. doi:10.1038/s41409-018-0281-7

Rhee, S. J., Lee, J. W., Yu, K. S., Hong, K. T., Choi, J. Y., Hong, C. R., et al. (2017). Pediatric Patients Undergoing Hematopoietic Stem Cell Transplantation Can Greatly Benefit from a Novel Once-Daily Intravenous Busulfan Dosing Nomogram. *Am. J. Hematol.* 92 (7), 607–613. doi:10.1002/ajh.24734

Russell, J. A., Kangarloo, S. B., Williamson, T., Chaudhry, M. A., Savoie, M. L., Turner, A. R., et al. (2013). Establishing a Target Exposure for Once-Daily Intravenous Busulfan Given with Fludarabine and Thymoglobulin before Allogeneic Transplantation. *Biol. Blood Marrow Transpl.* 19 (9), 1381–1386. doi:10.1016/j.bbmt.2013.07.002

Savic, R. M., Cowan, M. J., Dvorak, C. C., Pai, S. Y., Pereira, L., Bartelink, I. H., et al. (2013). Effect of Weight and Maturation on Busulfan Clearance in Infants and Small Children Undergoing Hematopoietic Cell Transplantation. *Biol. Blood Marrow Transpl.* 19 (11), 1608–1614. doi:10.1016/j.bbmt.2013.08.014

Shao, D. F., Li, J. H., Hu, T., Zhang, Z. X., Zhang, L., Li, J. J., et al. (2022). Clinical Outcomes of Individualized Busulfan-Dosing in Hematopoietic Stem Cell Transplantation in Chinese Children Undergoing with Therapeutic Drug Monitoring. *Bone Marrow Transpl.* 57 (3), 473–478. doi:10.1038/s41409-021-01545-x

Shukla, P., Goswami, S., Keizer, R. J., Winger, B. A., Kharbanda, S., Dvorak, C. C., et al. (2020). Assessment of a Model-Informed Precision Dosing Platform Use in Routine Clinical Care for Personalized Busulfan Therapy in the Pediatric Hematopoietic Cell Transplantation (HCT) Population. *Front. Pharmacol.* 11, 888. doi:10.3389/fphar.2020.00888

Slattery, J. T., Sanders, J. E., Buckner, C. D., Schaffer, R. L., Lambert, K. W., Langer, F. P., et al. (1995). Graft-rejection and Toxicity Following Bone Marrow Transplantation in Relation to Busulfan Pharmacokinetics. *Bone Marrow Transpl.* 16 (1), 31–42.

Sun, Y., Huang, J., Hao, C., Li, Z., Liang, W., Zhang, W., et al. (2020). Population Pharmacokinetic Analysis of Intravenous Busulfan: GSTA1 Genotype Is Not a Predictive Factor of Initial Dose in Chinese Adult Patients Undergoing Hematopoietic Stem Cell Transplantation. *Cancer Chemother. Pharmacol.* 85 (2), 293–308. doi:10.1007/s00280-019-04001-2

Ten Brink, M. H., Swen, J. J., Böhringer, S., Wessels, J. A., van der Straaten, T., Marijt, E. W., et al. (2013). Exploratory Analysis of 1936 SNPs in ADME Genes for Association with Busulfan Clearance in Adult Hematopoietic Stem Cell Recipients. *Pharmacogenet Genomics* 23 (12), 675–683. doi:10.1097/fpc.0000000000000007

Trame, M. N., Bergstrand, M., Karlsson, M. O., Boos, J., and Hempel, G. (2011). Population Pharmacokinetics of Busulfan in Children: Increased Evidence for Body Surface Area and Allometric Body Weight Dosing of Busulfan in Children. *Clin. Cancer Res.* 17 (21), 6867–6877. doi:10.1158/1078-0432.Ccr-11-0074

van Hoogdalem, M. W., Emoto, C., Fukuda, T., Mizuno, T., Mehta, P. A., and Vinks, A. A. (2020). Population Pharmacokinetic Modelling of Busulfan and the Influence of Body Composition in Paediatric Fanconi Anaemia Patients. *Br. J. Clin. Pharmacol.* 86 (5), 933–943. doi:10.1111/bcp.14202

Wang, Y., Kato, K., Le Gallo, C., Armstrong, E., Rock, E., and Wang, X. (2015). Dosing Algorithm Revisit for Busulfan Following IV Infusion. *Cancer Chemother. Pharmacol.* 75 (3), 505–512. doi:10.1007/s00280-014-2660-0

Wu, X., Xie, H., Lin, W., Yang, T., Li, N., Lin, S., et al. (2017). Population Pharmacokinetics Analysis of Intravenous Busulfan in Chinese Patients Undergoing Hematopoietic Stem Cell Transplantation. *Clin. Exp. Pharmacol. Physiol.* 44 (5), 529–538. doi:10.1111/1440-1681.12735

Yin, J., Xiao, Y., Zheng, H., and Zhang, Y. C. (2015). Once-daily i.V. BU-Based Conditioning Regimen before Allogeneic Hematopoietic SCT: a Study of Influence of GST Gene Polymorphisms on BU Pharmacokinetics and Clinical Outcomes in Chinese Patients. *Bone Marrow Transpl.* 50 (5), 696–705. doi:10.1038/bmt.2015.14

Yuan, J., Sun, N., Feng, X., He, H., Mei, D., Zhu, G., et al. (2021). Optimization of Busulfan Dosing Regimen in Pediatric Patients Using a Population Pharmacokinetic Model Incorporating GST Mutations. *Pharmgenomics Pers. Med.* 14, 253–268. doi:10.2147/PGPM.S289834

Zwaveling, J., Press, R. R., Bredius, R. G., van Derstraaten, T. R., den Hartigh, J., Bartelink, I. H., et al. (2008). Glutathione S-Transferase Polymorphisms Are Not Associated with Population Pharmacokinetic Parameters of Busulfan in Pediatric Patients. *Ther. Drug Monit.* 30 (4), 504–510. doi:10.1097/FTD.0b013e3181817428

Conflict of Interest: The authors declare that the research was conducted in the absence of any commercial or financial relationships that could be construed as a potential conflict of interest.

The reviewer LZ declared a shared parent affiliation with the authors ZJ and MZ to the handling editor at the time of review.

Publisher's Note: All claims expressed in this article are solely those of the authors and do not necessarily represent those of their affiliated organizations, or those of the publisher, the editors and the reviewers. Any product that may be evaluated in this article, or claim that may be made by its manufacturer, is not guaranteed or endorsed by the publisher.

frontiers | Frontiers in Pharmacology

ORIGINAL RESEARCH
published: 27 June 2022
doi: 10.3389/fphar.2022.903488

A Multi-Centre Prospective Study of the Efficacy and Safety of Alglucosidase Alfa in Chinese Patients With Infantile-Onset Pompe Disease

Diqi Zhu[1†], Jiacong Zhu[1,2†], Wenjuan Qiu[3†], Benzhen Wang[4], Lin Liu[5], Xiaodan Yu[6], Zhenheng Ou[5], Guangsong Shan[4], Jian Wang[7], Bin Li[8], Xiaokang Chen[8], Cong Liu[5], Zipu Li[4]* and Lijun Fu[1,9]**

[1]Department of Cardiology, Shanghai Children's Medical Center, Shanghai Jiao Tong University School of Medicine, Shanghai, China, [2]Department of Pediatrics, The Second Hospital of Jiaxing, Jiaxing, China, [3]Department of Pediatric Endocrinology and Genetic Metabolism, Xinhua Hospital, Shanghai Institute of Pediatric Research, Shanghai Jiao Tong University School of Medicine, Shanghai, China, [4]Heart Center, Women and Children's Hospital, Qingdao University, Qingdao, China, [5]Department of Pediatric Cardiology, Shenzhen Children's Hospital, Shenzhen, China, [6]Department of Developmental and Behavioral Pediatrics, Shanghai Children's Medical Center, Shanghai Jiao Tong University School of Medicine, Shanghai, China, [7]Research Division of Birth Defects, Institute of Pediatric Translational Medicine, Shanghai Children's Medical Center, Shanghai Jiao Tong University School of Medicine, Shanghai, China, [8]Medical Department, Sanofi Investment Co., Ltd., Shanghai, China, [9]Shanghai Clinical Research Center for Rare Pediatric Disease, Shanghai, China

OPEN ACCESS

Edited by:
Yang Zhou,
Brown University, United States

Reviewed by:
Shiwei Yang,
Children's Hospital of Nanjing Medical University, China
Bo Han,
Shandong Provincial Hospital, China

***Correspondence:**
Lijun Fu
13671933379@163.com
Zipu Li
apuqd@sina.com
Cong Liu
szliucong@163.com

[†]These authors have contributed equally to this work

Specialty section:
This article was submitted to Obstetric and Pediatric Pharmacology, a section of the journal Frontiers in Pharmacology

Received: 25 March 2022
Accepted: 05 May 2022
Published: 27 June 2022

Citation:
Zhu D, Zhu J, Qiu W, Wang B, Liu L, Yu X, Ou Z, Shan G, Wang J, Li B, Chen X, Liu C, Li Z and Fu L (2022) A Multi-Centre Prospective Study of the Efficacy and Safety of Alglucosidase Alfa in Chinese Patients With Infantile-Onset Pompe Disease. Front. Pharmacol. 13:903488. doi: 10.3389/fphar.2022.903488

Background: A high prevalence of infantile-onset Pompe disease (IOPD) in the Chinese population has been noted, but there are currently no reported clinical trials of enzyme replacement therapy (ERT) for IOPD in this population**.** The purpose of this study was to evaluate the efficacy and safety of alglucosidase alfa in Chinese patients with IOPD.

Materials and Methods: A multicentre, single-arm, prospective, open-label clinical trial was performed at 4 sites in China. Eligible Chinese subjects with IOPD received an infusion of alglucosidase alfa at a dose of 20 mg/kg every 2 weeks for up to 52 weeks. The primary endpoints of clinical efficacy were the survival rate and changes in the left ventricular mass index (LVMI). The safety assessment was based on the incidence of adverse events (AEs).

Results: A total of 10 eligible subjects were enrolled in the study. The mean age at the start of ERT was 5.36 ± 1.56 months. Nine subjects had survived after 52 weeks of treatment. One subject discontinued the study and died after mechanical ventilation was withdrawn. The intent-to-treat analysis demonstrated that the survival rate was 90.0% (95% confidence interval: 55.5–99.7%). The mean LVMI at week 52 was 70.59 ± 39.93 g/m^2 compared to that of 298.02 ± 178.43 g/m^2 at baseline, with a difference of -227.60 ± 155.99 g/m^2. All subjects had left ventricular mass (LVM) Z scores >10 at baseline, and eight subjects (80%) achieved Z scores <5 at week 52. No treatment-related AEs were observed, and no AEs led to the discontinuation of treatment.

Abbreviations: AEs, Adverse events; CRIM, Cross-reactive immunologic material; ERT, Enzyme replacement therapy; GAA, Acid alpha-glucosidase; ITT, Intent-to-treat; IOPD, Infantile-onset Pompe disease; LOPD, Late-onset Pompe disease; LVMI, Left ventricular mass index; LVM, Left ventricular mass; rhGAA, Recombinant human GAA; SAEs, Serious treatment-emergent adverse events; TEAEs, Treatment-emergent adverse events; ITI, Immune tolerance induction,

Conclusions: This clinical trial is the first study of ERT for IOPD in China, indicating that alglucosidase alfa has favourable efficacy and safety for the treatment of Chinese patients with IOPD (ClinicalTrials.gov number, NCT03687333).

Keywords: Pompe disease, glycogen storage disease type II, enzyme replacement therapy, alglucosidase alfa, survival rate, left ventricular mass index

INTRODUCTION

Pompe disease, also called acid maltase deficiency or type II glycogen storage disease, is a rare, autosomal recessive, but lethal metabolic myopathy caused by mutations in the gene coding for acid alpha-glucosidase (GAA), the enzyme that decomposes glycogen in the lysosome (Kohler et al., 2018). With GAA deficiency, a lysosomal accumulation of glycogen develops in multiple tissues, with skeletal and cardiac muscles being the most severely affected.

Two categories of Pompe disease, namely, infantile-onset Pompe disease (IOPD) and late-onset Pompe disease (LOPD), are recognized according to the age of symptom onset and the occurrence of cardiomyopathy. Classic IOPD is the most severe form of Pompe disease, which is characterized by an age of onset of less than 12 months, rapidly progressive hypertrophic cardiomyopathy and respiratory distress (Kishnani et al., 2006b; van den Hout et al., 2003). Most untreated IOPD patients cannot survive beyond 1 year of age (Kishnani et al., 2006b). In contrast, LOPD manifests after 12 months of age and generally lacks significant cardiac involvement. The incidence of Pompe disease appears to vary by ethnicity and geographic region. The estimated frequency of IOPD is approximately 1 in 100,000; higher frequencies of the infantile-onset form have been reported in some populations, including African Americans (approximately 1 in 14,000) and persons with Chinese ancestry (1 in 50,000 to 1 in 40,000) (Hirschhorn R, 2001).

Enzyme replacement therapy (ERT) using recombinant human GAA (rhGAA) has changed the natural course of Pompe disease. The lifespan of infants with IOPD has been significantly extended. Sustained and striking cardiac improvement has been observed in the majority of patients(Kishnani et al., 2007). The safety and efficacy of alglucosidase alfa have been demonstrated in a number of clinical trials (Kohler et al., 2018); however, these trials did not include Chinese patients.

rhGAA has been approved in the USA and Europe since 2006, and in China since 2015, since the National Medical Products Administration in China considered it to be urgently needed in clinical practice. Here, we report the results of a multicentre prospective study of alglucosidase alfa in China, which was the first clinical trial to evaluate the efficacy and safety of alglucosidase alfa in Chinese patients with IOPD.

MATERIALS AND METHODS

Study Design

This study was conducted in accordance with consensus ethics principles derived from international ethics guidelines, including the Declaration of Helsinki, the International Conference on Harmonization guidelines for Good Clinical Practice, and all applicable laws, rules, and regulations. The protocol and its amendments were reviewed and approved by independent ethics committees and/or institutional review boards.

This was a multicentre, single-arm, prospective, open-label clinical trial to assess the efficacy and safety of a 52-week treatment with alglucosidase alfa (Myozyme®) in subjects with IOPD at 4 sites (Shanghai Children's Medical Center, Xinhua Hospital Affiliated to Shanghai Jiao Tong University School of Medicine, Shenzhen Children's Hospital, and Qingdao Women and Children's Hospital) in China. The eligible subjects with IOPD received an infusion of alglucosidase alfa at a dose of 20 mg/kg every 2 weeks for up to 52 weeks. Subjects received treatment with alglucosidase alfa for 52 weeks or withdrew due to intolerable side effects of the study drug or death, whichever came first. Since GAA protein levels are unable to be detected in China, a negative cross-reactive immunologic material (CRIM) status was rapidly inferred by gene mutation analysis. Any patient who carried 2 predicted null alleles was considered CRIM-negative (Bali et al., 2012). The null allele is a nonsense or frameshift mutation resulting in a premature termination codon in any exon but the last or multiexon deletion. If a patient had at least one missense mutation, he or she was considered CRIM-positive. For patients whose CRIM status was inferred to be negative by gene mutation, an immune tolerance induction (ITI) regimen including rituximab, methotrexate, and intravenous immune globulin was recommended concomitantly with ERT (Mendelsohn et al., 2009; Messinger et al., 2012; Banugaria et al., 2013; Kazi et al., 2017).

IOPD is a rapidly fatal disorder, and several clinical trials have shown that treatment with alglucosidase alfa can improve survival, cardiac and respiratory function, growth, and motor development in severely affected infants(Kishnani et al., 2007; Nicolino et al., 2009; Kishnani et al., 2006b). It was considered unethical to include a placebo group as part of the study design. Thus, no control group was applied for this study.

Patients

All eligible patients had a confirmed diagnosis of IOPD with the documented onset of Pompe disease symptoms up to 12 months of age (corrected for gestation if born before 40 weeks) and a diagnosis of Pompe disease confirmed by GAA enzyme deficiency from any tissue source and *GAA* gene mutations. The pathogenicity of mutations was determined according to the Pompe disease *GAA* variant

database (https://www.pompevariantdatabase.nl). The exclusion criteria were patients who had previously been treated with GAA, patients who were participating in another clinical study using any investigational therapy, patients with conditions/situations such as clinical signs of cardiac failure with a left ventricular ejection fraction (LVEF) < 40%, respiratory insufficiency (O_2 saturation <90% or CO_2 partial pressure >55 mm Hg [venous] or >40 mm Hg [arterial] in room air or with any ventilator use), patients who were dependent on invasive or noninvasive ventilator support, patients with major congenital anomalies or clinically significant intercurrent organic diseases unrelated to Pompe disease, patients who were not suitable for participation, regardless of the reason, as judged by the investigator, including those with medical or clinical conditions, and patients who were potentially at risk of noncompliance with the study procedures. The dates for the first eligible subject enrolled and last eligible subject to complete the study were December 4, 2018, and December 30, 2020, respectively.

Assessments of Clinical Efficacy

The primary endpoints of clinical efficacy were the survival rates and changes from baseline in the left ventricular mass index (LVMI) at 52 weeks of treatment. The secondary endpoints were survival free of invasive ventilator use at 52 weeks of treatment; survival free of any ventilator use at 52 weeks of treatment; physical growth (change from baseline at week 52 regarding length and weight); the number of motor development milestones achieved at week 52 and changes from baseline; changes from baseline in the GESELL Developmental Scale score at week 52; and the proportion of subjects with signs and/or symptoms of cardiac failure at week 52.

Safety Assessments

Safety was evaluated in terms of adverse events (AEs) reported by the caregiver or noted by the investigator. Clinical and laboratory safety assessments included clinical haematology, chemistry, and urinalysis assessments. Other safety endpoints included vital signs (body temperature, heart rate, respiratory rate, and blood pressure), physical examinations, and electrocardiograms.

Statistical Analysis

Available clinical parameters and demographics were described. Efficacy and safety were analysed in the intent-to-treat (ITT) population defined as all patients treated with alfa glucosidase. At the end of the study, the proportion of subjects who were alive was calculated, and the changes in LVMI and LVM Z scores from baseline were analysed. The number of subjects who were alive independent of an invasive ventilator or any ventilator, physical growth, the number of motor development milestones achieved, motor development gains (GESELL Developmental Scale), and the proportion of patients with signs/symptoms of heart failure at each visit were calculated or statistically described. The safety assessment was based on the incidence of AEs.

RESULTS

Patient Characteristics

A total of 10 subjects were enrolled in the study, and all subjects (100.0%) were included in the ITT population and safety population. The mean age at the start of ERT was 5.36 ± 1.56 (range from 1.5 to 7.4) months. Of the 10 subjects, four (40.0%) were male and six (60.0%) were female; all subjects were predominantly of Asian descent (100.0%), and nine subjects (90.0%) were of Han nationality. Seven subjects (70%) had a medical history other than IOPD, and one subject (10%) had a surgical history. The average length and weight of all subjects were 65.16 ± 6.31 cm and 5.76 ± 1.02 kg, respectively. The mean age at disease onset was 4.2 ± 1.48 months. Various *GAA* gene mutations were found in the subjects, including missense, nonsense, insertion, splicing, and duplication mutations. The most frequent mutation observed in our study was c.1935C > A, with four out of ten patients having this mutation. Nine subjects (90%) had a CRIM-positive status, and one (10%) subject had a negative status. The mean LVMI and LVEF were 298.02 ± 178.43 g/m^2 and 57.97 ± 13.32%, respectively. No subject was dependent on a ventilator at the beginning of this study. The baseline characteristics of the study subjects are shown in **Table 1**.

Efficacy

Survival Rate and Ventilator Independence

In the ITT population, among all 10 patients, nine subjects survived, and one subject died. The survival rate was 90.0%, and the 95% confidence interval (CI) was 55.5–99.7%. The subject who died (Patient 0101 in **Table 1**) was the only CRIM-negative subject in this study. She suffered from respiratory failure and received invasive mechanical ventilation for nearly one month. She was withdrawn from the study when her family members signed to stop all treatment and died after mechanical ventilation was withdrawn.

Invasive or noninvasive ventilator dependency was continuously monitored during this study. In the ITT population, one subject (Patient 0101 in **Table 1**) used an invasive ventilator during this study, as described above. Another subject had been supported temporarily by a noninvasive ventilator at week 2. The remaining eight subjects did not use any ventilators. At the end of the study, all nine survivors were free from the use of any ventilators. Thus, the survival rate was 100% (n = 9; 95% CI: 66.4–100%) in the subjects who did not use any invasive ventilators and 100% (n = 8; 95% CI: 63.1–100%) in the subjects who did not use any ventilators at week 52 (**Table 2**).

Cardiac Improvement

At baseline, all 10 subjects (100%) were found to have left ventricular hypertrophy (abnormally elevated LVMI scores and LVM Z scores >2). The mean LVMI of the subjects decreased steadily from baseline over the study period. The mean LVMI was 70.59 ± 39.93 g/m^2 at week 52 compared to that of 298.02 ± 178.43 g/m^2 at baseline, and the difference was

TABLE 1 | Baseline characteristics of 10 Chinese patients with infantile-onset Pompe disease.

Patient	[a]Age (months)	Sex	Ethnicity	Length (cm)	Weight (kg)	Onset Age (months)	[b]Medical/ Surgical History	GAA Gene mutations	[c]CRIM Status	[d]GAA Activity (Normal Reference Range)	LVMI (g/m^2)	LVEF (%)	Ventilator use
0101	6.1	F	Han	70.5	6.3	5	Yes	c.258dupC, p.Asn87Glnfs*9(het) c.1987C > T, p.Gln663*(het)	–	1.12 (2.88–98.02 μmol/L/h)	296.5	76.7	No
0102	1.5	F	Han	55	3.9	1	No	c.1802C > T, p.Ser601Leu(het) c.1822C > T, p.Arg608*(het)	+	0.76 (2.88–98.02 μmol/L/h)	79.0	63.9	No
0103	5.8	F	Han	58	5.0	4	No	c.1935C > A, p.Asp645Glu (het) c.2662G > T, p.Glu888*(het)	+	1.05 (2.88–98.02 μmol/L/h)	291.1	61.1	No
0104	7	F	She	64	6.2	6	Yes	c.1432G > A, p.Gly478Arg(het) c.1935C > A, p.Asp645Glu(het)	+	0.37 (2.88–98.02 μmol/L/h)	745.5	49.2	No
0105	5.9	F	Han	65.6	4.6	5	Yes	c.1832G > A, p.Gly611Asp(het) c.1935C > A, p.Asp645Glu(het)	+	1.10 (2.88–98.02 μmol/L/h)	298.8	41.1	No
0106	5.5	M	Han	77	6.6	4	No	c.796C > T, p.Pro266Ser(het) c.1562A > T, p.Glu521Val(het)	+	0.03 (2.88–98.02 μmol/L/h)	228.4	45.2	No
0302	5.4	M	Han	65	6.3	4	Yes	c.1935C > A, p.Asp645Glu(het) c.2662G > T, p.Glu888*(het)	+	6.8 (24.8–93.0 nmol/g/min)	361.9	79.8	No
0303	4.8	M	Han	64.5	7.0	4	Yes	c.1082C > T, p.Pro361Leu(het) c.1942G > A, p.Gly648Ser(het)	+	2.06 (>14nmol/1 h/mg)	140.3	58.7	No
0401	7.4	M	Han	70	6.5	6	Yes	c.1121G > A, p.Cys374Tyr(het) c.1935C > A, p.Asp645Glu(het)	+	2.4 (62.3–301.7 nmol/h/mgPr)	231.8	44.0	No
0403	4.2	F	Han	62	5.2	3	Yes	c.859-2A > T, p.?(het) c.1861T > G, p.Trp621Gly(het)	+	0.7 (62.3–301.7 nmol/h/mgPr)	306.9	60.0	No

F, female; M, male; w/s, with support.

[a]*Age at first infusion.*

[b]*Other than IOPD.*

[c]*CRIM status was predicted by* GAA *gene mutations.*

[d]*All patients had GAA enzyme test results below the lower limit of the normal reference range.*

Due to the different GAA enzyme detection methods used in the medical center of each patient, the normal reference value range and numerical unit of each patient in the table are different. LVEF: left ventricular ejection fraction. LVMI: left ventricular mass index.

TABLE 2 | Survival under different ventilation conditions at week 52.

	Free of Any Ventilator use (*n* = 8)	Free of Invasive Ventilator use (*n* = 9)
Survival, n (%)	8 (100%)	9 (100%)
95% confidence interval	(63.1%, 100%)	(66.4%, 100%)

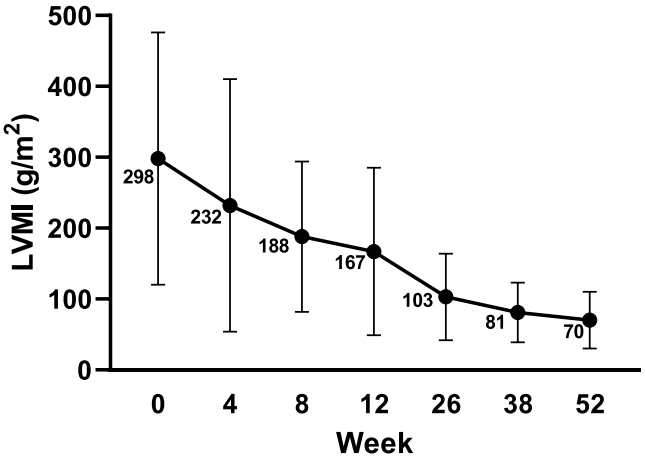

FIGURE 1 | LVMI changes from baseline echocardiography by visit. Data are presented as the mean ± SD. LVMI: left ventricular mass index.

−227.60 ± 155.99 g/m^2 (**Figure 1**). The Z score of the LVM also improved gradually. The mean LVM Z score was 16.63 ± 5.17 at baseline and 4.30 ± 2.78 at week 52 (**Figure 2**). Compared to 100% of subjects with LVM Z scores >10 at baseline, eight subjects (80%) had LVM Z scores <5, with one subject (10.0%) having an LVM Z score <2 at week 52. Before she passed away, the LVM Z score of the subject who died decreased from 12.22 at baseline to 8.90 at week 8, suggesting the effect of the treatment.

During the study, two subjects (20.0%) at week 4 and one subject (10.0%) at week 8 had signs and/or symptoms of cardiac failure. No subject exhibited any signs and/or symptoms of cardiac failure at week 52.

Physical Growth and Other Developments

Overall, the length and weight of the subjects increased in this study. The mean baseline length and weight were 65.16 ± 6.31 cm and 5.76 ± 1.02 kg, respectively. At week 52, the differences in length and weight from baseline were 12.66 ± 4.68 cm and 2.69 ± 0.75 kg, respectively. Age-equivalent weight and length values were also analysed. At baseline, nine (9/10, 90.0%) and seven (7/10, 70.0%) patients had lengths/weights above or equal to the 3rd percentile of their age-appropriate lengths/weights, respectively. At week 52, there were seven subjects (7/10, 70%) whose length was greater than or equal to the 3rd percentile. In terms of weight, five subjects (5/10, 50%) reached standard weight-for-age percentiles.

In the ITT population, all subjects obtained new motor development milestones during the treatment. At baseline, six subjects (6/10, 60%) presented at least one of the following motor development milestones: five subjects could hold their head up, one subject could bear weight on their legs, one subject could roll, and one subject could sit with support. At week 52, all nine survivors achieved one or more motor development milestones: all subjects could hold their head up and sit with support, eight subjects could roll over, seven subjects could sit without support, three subjects could bear weight on their legs, three subjects could walk with support, two subjects could pull to stand, one subject could walk without support, and one subject could walk up steps. No subject ever learned to run or walk down steps during the treatment period. At baseline, the number of motor development milestones achieved was 0.8 ± 0.92, compared to that of 4.8 ± 1.99 at week 52, with a difference of 3.9 ± 1.62.

The measured mature month ages for motor, adaptive (cognitive), language, and personal-social behaviours based on the GESELL Developmental Scale increased during the

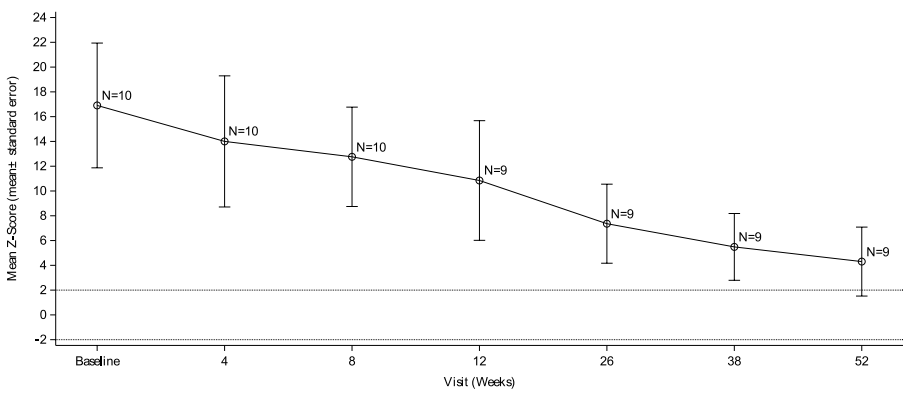

FIGURE 2 | LVM Z score changes from baseline echocardiography by visit. Data are presented as the mean ± SD. LVM: left ventricular mass.

trial. The mean changes from baseline were 5.87 ± 3.68, 8.50 ± 3.26, 6.82 ± 3.05, and 8.73 ± 3.11 at week 52, respectively.

Safety

In the safety population, at least one AE was reported for each subject. All AEs identified in this study were treatment-emergent adverse events (TEAEs), and at least one serious treatment emergent adverse event (SAE) was reported for nine subjects (90%). The most commonly reported SAEs (≥20%) were pneumonitis (60.0%; n = 6), followed by pneumonia (30.0%; n = 3), respiratory tract infection (20.0%; n = 2), gastroenteritis rotavirus (20.0%; n = 2) and bronchitis (20.0%; n = 2). No SAEs were related to the study drug, and the outcome of most SAEs was recovered or resolved. No SAEs led to discontinuation from the study. The infusion-associated reactions, such as rash, fever, and urticaria, were not common. In our study, one subject (Patient 0101 in **Table 1**) with a predicted CRIM-negative status had an AE (asphyxia) leading to death, which was unrelated to the study drug.

DISCUSSION

In this first clinical trial for Chinese patients with IOPD, we report that 90.0% (9/10) of the patients who received alglucosidase alfa at a dose of 20 mg/kg every 2 weeks from the age of 1.5–7.4 (5.36 ± 1.56) months had survived after 52 weeks of treatment. In contrast, a multinational study of the natural course of IOPD showed that just a few percent (25.7%) of patients without treatment are able to survive beyond one year of age (Kishnani et al., 2006a). In our previous study of the clinical course of IOPD, 17 untreated Chinese patients died at a median age of 8.2 months. Only two of them survived beyond one year of age (Fu et al., 2014). Chen *et al* investigated the clinical outcomes of 25 Chinese patients with IOPD. Only one patient receiving ERT survived beyond the age of two years. Of the remaining 24 patients who were not treated with ERT, all but one patient died at a median age of 8.3 months (Chen et al., 2017). Our current study clearly demonstrated the ability of alglucosidase alfa to change the natural course of disease in Chinese IOPD patients and extend their lifespans. This finding is similar to the results of a US clinical trial of ERT for IOPD in which a 52-week alglucosidase alfa treatment reduced the risk of death by 99% compared to the untreated historic cohort (Kishnani et al., 2007).

Cardiac and respiratory failure is the main cause of death in the absence of treatment for IOPD patients. Most subjects (90%) in this study survived independent of the use of invasive ventilators and any other ventilators after 52 weeks of treatment, although one subject needed a noninvasive ventilator and one subject needed an invasive ventilator during the study. The ventilator-free survival rate by the end of the 52-week treatment period was higher than that (66.7%) in the US clinical trial mentioned above (Kishnani et al., 2007). In our trial, a remarkable improvement in cardiac status was observed after ERT therapy. One hundred percent of the surviving subjects had no symptoms or signs of cardiac failure at the end of the clinical trial, which likely contributed to the increased survival rates observed in this study. Moreover, the mean LVMI and LVM Z scores of the ITT population gradually decreased during treatment. Eight subjects (80%) achieved an LVM Z score <5, and one subject (10%) had a Z score <2 after 52 weeks of alglucosidase alfa administration. In comparison, Nicolino *et al* reported that more than half of IOPD patients (57%, 12/21) attained a normal LVM score (Z score <2) with a median treatment duration of 120 weeks (Nicolino et al., 2009). The difference in the regression of cardiac hypertrophy observed in the two studies may be attributed to the different durations of ERT therapy. Long-term alglucosidase alfa treatment will lead to further improvements in left ventricular hypertrophy in patients with IOPD.

For untreated IOPD patients, physical growth and motor development are severely delayed, and major developmental milestones, such as rolling over, sitting or standing, are not generally achieved. Among the 18 patients in the US clinical trial, 15 maintained normal physical growth, 13 had consistent motor and functional gains, and all acquired cognitive, language, and personal/social development skills during the 52-week treatment period (Kishnani et al., 2007). In our study, a total of 3.9 ± 1.62 motor development milestones were achieved at 52 weeks compared with the baseline. At week 52, the length and weight of the patients increased from baseline by 12.66 ± 4.67 cm and 2.69 ± 0.75 kg, respectively. Seven subjects (70%) and five subjects (50%) remained in percentiles greater than or equal to the 3rd percentile at the end of the study. Although our findings for length and weight were lower than those of previous studies, the length and weight of the subjects showed the same increasing trends as those reported in the published literature (Kishnani et al., 2007; Nicolino et al., 2009). In this study, the GESELL Developmental Scale was used to evaluate the functional skills of IOPD patients, which indicated remarkable progress in comprehensive development after alglucosidase alfa treatment. Taken together, the secondary points achieved in our study were similar to those of the US clinical trial.

At least one TEAE was observed for each subject in this study, such as vomiting, otitis media, pneumonia, and upper respiratory tract infection. However, the majority of AEs reported in previous studies were related to rhGAA intravenous infusion, such as rash, fever, and urticaria (Kishnani et al., 2007; Nicolino et al., 2009), which were not common in our study. This might be attributed to the pretreatment with 5 mg of dexamethasone 30 min prior to the infusion of alglucosidase alfa in the majority of patients in our cohort. No treatment related TEAEs were observed in our study, and no AEs led to the discontinuation of treatment, indicating the good tolerability and good safety of alglucosidase alfa administration. One patient died in our study; this patient was predicted to have a CRIM-negative status. Owing to a complete inability to generate native enzymes, CRIM-negative patients are more likely to develop high and sustained anti-rhGAA IgG antibody titers, rendering ERT ineffective (Kishnani et al., 2010; Banugaria et al., 2011; Berrier et al., 2015). Identifying CRIM status is crucial before initiating ERT because ITI has been found to be effective in CRIM-negative patients before or shortly after the start of ERT (Bali et al., 2012). A patient is designated to be CRIM-negative if the GAA protein is undetectable (Kishnani et al., 2010). Unfortunately, CRIM status cannot be tested in China. Bali *et al.* determined that types of *GAA* gene mutations are well associated with the levels of GAA protein. Most CRIM-negative patients have two null alleles (frame shift,

nonsense, and multiexon deletions), resulting in the lack of production of the GAA protein (Bali et al., 2012). The only patient (Patient 0101 in **Table 1**) who died in this study had a frameshift mutation (c.258dupC, p. Asn87Glnfs*9) and a nonsense mutation (c.1987C > T, p. Gln663*) in the *GAA* gene, causing two null alleles. This patient's CRIM status was accordingly predicted to be negative. ITI with methotrexate, rituximab, and intravenous immunoglobulin was administered for this patient, followed by ERT. However, ERT did not produce the expected effects in this patient. Very recently, Li *et al* reported that in CRIM-negative IOPD patients treated with ITI + ERT, the clinical outcomes of the early group (treatment initiation at age ≤4 weeks) were much better than those of the intermediate group (treatment initiation at age >4 and ≤15 weeks) and late group (treatment initiation at age >15 weeks) (Li et al., 2021). In the intermediate group and late group, 66% (10/15) of the patients needed a breathing device during the treatment. This investigation indicates that the age at ITI + ERT treatment initiation markedly impacts the clinical outcomes of CRIM-negative IOPD patients. The CRIM-negative patient in our study was older than 15 weeks at initial treatment, which might be the reason why the patient did not achieve the expected outcome even after receiving ITI + ERT therapy. This highlights the significance of the early recognition of IOPD patients and the early application of ITI + ERT in CRIM-negative patients.

Since it received approval in Europe and the USA in 2006, alglucosidase alfa has shown good efficacy, safety, and tolerability in IOPD patients. However, data to evaluate the efficacy, safety, and tolerability of alglucosidase alfa for Chinese IOPD patients were not available until the current study was performed. Our clinical trial is the first study of ERT in China, and it demonstrated that alglucosidase alfa has favourable efficacy and safety for treating Chinese patients with IOPD.

DATA AVAILABILITY STATEMENT

The original contributions presented in the study are included in the article/Supplementary materials, further inquiries can be directed to the corresponding authors.

ETHICS STATEMENT

The studies involving human participants were reviewed and approved by Institutional Review Board of Shanghai Children's Medical Center Affiliated to Shanghai Jiao Tong University School of Medicine, Xinhua Hospital Ethics Committee Affiliated to Shanghai Jiaotong University School of Medicine, Ethics Committee Affiliated to Qingdao Women and Children's Hospital, and Ethics Committee Affiliated to Shenzhen children's Hospital Medical. Written informed consent to participate in this study was provided by the participants' legal guardian/next of kin. Written informed consent was obtained from the minor(s)' legal guardian/next of kin for the publication of any potentially identifiable images or data included in this article.

AUTHOR CONTRIBUTIONS

DZ participated in writing the manuscript; WQ participated in enzyme activity assessment; DZ, JZ, BW, LL, ZO, and GS participated in enzyme replacement therapy. XY participated in performing the Gesell Developmental Scale Test. JW participated in the molecular genetic studies; LF, ZL, and CL recruited the patients and designed the study. BL and XC participated in the study design and coordinated the study centres. All authors read and approved the final manuscript.

FUNDING

This study was sponsored by Sanofi. Editorial support for this publication was provided by SunHealth (Beijing) Ltd, funded by Sanofi.

ACKNOWLEDGMENTS

We acknowledge the valuable contributions of all members and sites in this clinical trial. We thank Sanofi for providing statistical advice and assistance with writing.

REFERENCES

Bali, D. S., Goldstein, J. L., Banugaria, S., Dai, J., Mackey, J., Rehder, C., et al. (2012). Predicting Cross-Reactive Immunological Material (CRIM) Status in Pompe Disease Using GAA Mutations: Lessons Learned from 10 Years of Clinical Laboratory Testing Experience. *Am. J. Med. Genet. C Semin. Med. Genet.* 160C, 40–49. doi:10.1002/ajmg.c.31319

Banugaria, S. G., Prater, S. N., Ng, Y. K., Kobori, J. A., Finkel, R. S., Ladda, R. L., et al. (2011). The Impact of Antibodies on Clinical Outcomes in Diseases Treated with Therapeutic Protein: Lessons Learned from Infantile Pompe Disease. *Genet. Med.* 13, 729–736. doi:10.1097/GIM.0b013e3182174703

Banugaria, S. G., Prater, S. N., Patel, T. T., Dearmey, S. M., Milleson, C., Sheets, K. B., et al. (2013). Algorithm for the Early Diagnosis and Treatment of Patients with Cross Reactive Immunologic Material-Negative Classic Infantile Pompe Disease: A Step towards Improving the Efficacy of ERT. *PLoS One* 8, e67052. doi:10.1371/journal.pone.0067052

Berrier, K. L., Kazi, Z. B., Prater, S. N., Bali, D. S., Goldstein, J., Stefanescu, M. C., et al. (2015). CRIM-Negative Infantile Pompe Disease: Characterization of Immune Responses in Patients Treated with ERT Monotherapy. *Genet. Med.* 17, 912–918. doi:10.1038/gim.2015.6

Chen, X., Liu, T., Huang, M., Wu, J., Zhu, J., Guo, Y., et al. (2017). Clinical and Molecular Characterization of Infantile-Onset Pompe Disease in Mainland Chinese Patients: Identification of Two Common Mutations. *Genet. Test. Mol. Biomarkers* 21, 391–396. doi:10.1089/gtmb.2016.0424

Fu, L., Qiu, W., Yu, Y., Guo, Y., Zhao, P., Zhang, X., et al. (2014). Clinical and Molecular Genetic Study of Infantile-Onset Pompe Disease in Chinese Patients: Identification of 6 Novel Mutations. *Gene* 535, 53–59. doi:10.1016/j.gene.2013.10.066

Hirschhorn R, R. A. (2001). "Glycogen Storage Disease Type II: Acid α-Glucosidase (Acid Maltase) Deficiency," in *The Metabolic and Molecular Bases of Inherited Diseases*. 8th ed. (New York, NY: McGraw-Hill).

Kazi, Z. B., Desai, A. K., Berrier, K. L., Troxler, R. B., Wang, R. Y., Abdul-Rahman, O. A., et al. (2017). Sustained Immune Tolerance Induction in Enzyme Replacement Therapy-Treated CRIM-Negative Patients with Infantile Pompe Disease. *JCI Insight* 2, e94328. doi:10.1172/jci.insight.94328

Kishnani, P. S., Corzo, D., Nicolino, M., Byrne, B., Mandel, H., Hwu, W. L., et al. (2007). Recombinant Human Acid [Alpha]-Glucosidase: Major Clinical Benefits in Infantile-Onset Pompe Disease. *Neurology* 68, 99–109. doi:10.1212/01.wnl.0000251268.41188.04

Kishnani, P. S., Goldenberg, P. C., Dearmey, S. L., Heller, J., Benjamin, D., Young, S., et al. (2010). Cross-Reactive Immunologic Material Status Affects Treatment Outcomes in Pompe Disease Infants. *Mol. Genet. Metab.* 99, 26–33. doi:10.1016/j.ymgme.2009.08.003

Kishnani, P. S., Hwu, W. L., Mandel, H., Nicolino, M., Yong, F., Corzo, D., et al. (2006a). A Retrospective, Multinational, Multicenter Study on the Natural History of Infantile-Onset Pompe Disease. *J. Pediatr.* 148, 671–676. doi:10.1016/j.jpeds.2005.11.033

Kishnani, P. S., Nicolino, M., Voit, T., Rogers, R. C., Tsai, A. C., Waterson, J., et al. (2006b). Chinese Hamster Ovary Cell-Derived Recombinant Human Acid Alpha-Glucosidase in Infantile-Onset Pompe Disease. *J. Pediatr.* 149, 89–97. doi:10.1016/j.jpeds.2006.02.035

Kohler, L., Puertollano, R., and Raben, N. (2018). Pompe Disease: From Basic Science to Therapy. *Neurotherapeutics* 15, 928–942. doi:10.1007/s13311-018-0655-y

Li, C., Desai, A. K., Gupta, P., Dempsey, K., Bhambhani, V., Hopkin, R. J., et al. (2021). Transforming the Clinical Outcome in CRIM-Negative Infantile Pompe Disease Identified via Newborn Screening: the Benefits of Early Treatment with Enzyme Replacement Therapy and Immune Tolerance Induction. *Genet. Med.* 23, 845–855. doi:10.1038/s41436-020-01080-y

Mendelsohn, N. J., Messinger, Y. H., Rosenberg, A. S., and Kishnani, P. S. (2009). Elimination of Antibodies to Recombinant Enzyme in Pompe's Disease. *N. Engl. J. Med.* 360, 194–195. doi:10.1056/NEJMc0806809

Messinger, Y. H., Mendelsohn, N. J., Rhead, W., Dimmock, D., Hershkovitz, E., Champion, M., et al. (2012). Successful Immune Tolerance Induction to Enzyme Replacement Therapy in CRIM-Negative Infantile Pompe Disease. *Genet. Med.* 14, 135–142. doi:10.1038/gim.2011.4

Nicolino, M., Byrne, B., Wraith, J. E., Leslie, N., Mandel, H., Freyer, D. R., et al. (2009). Clinical Outcomes After Long-Term Treatment with Alglucosidase Alfa in Infants and Children with Advanced Pompe Disease. *Genet. Med.* 11, 210–219. doi:10.1097/GIM.0b013e31819d0996

Van Den Hout, H. M., van Diggelen, O. P., Smeitink, J. A., Poll-The, B. T., et al. (2003). The Natural Course of Infantile Pompe's Disease: 20 Original Cases Compared with 133 Cases from the Literature. *Pediatrics* 112, 332–340. doi:10.1542/peds.112.2.332

Conflict of Interest: BL and XC were employed by the company Sanofi Investment Co., Ltd.

The remaining authors declare that the research was conducted in the absence of any commercial or financial relationships that could be construed as a potential conflict of interest.

Publisher's Note: All claims expressed in this article are solely those of the authors and do not necessarily represent those of their affiliated organizations, or those of the publisher, the editors and the reviewers. Any product that may be evaluated in this article, or claim that may be made by its manufacturer, is not guaranteed or endorsed by the publisher.

frontiers | Frontiers in Pharmacology

ORIGINAL RESEARCH
published: 20 July 2022
doi: 10.3389/fphar.2022.935627

Signal Detection of Pediatric Drug–Induced Coagulopathy Using Routine Electronic Health Records

Xiaolu Nie[1,2,3‡], Yuncui Yu[4‡], Lulu Jia[4], Houyu Zhao[2], Zhenping Chen[5], Liqiang Zhang[6], Xiaoling Cheng[4], Yaqi Lyu[7], Wang Cao[4], Xiaoling Wang[4†] and Xiaoxia Peng[1,3*†]*

[1]Center for Clinical Epidemiology and Evidence-based Medicine, National Center for Children's Health, Beijing Children's Hospital, Capital Medical University, Beijing, China, [2]Department of Epidemiology and Biostatistics, School of Public Health, Peking University, Beijing, China, [3]Hainan Institute of Real World Data, Qionghai, China, [4]Department of Pharmacy, Beijing Children's Hospital, Capital Medical University, National Center for Children's Health, Beijing, China, [5]Hematologic Disease Laboratory, National Center for Children's Health, Beijing Pediatric Research Institute, Beijing Children's Hospital, Capital Medical University, Beijing, China, [6]Hematology Center, National Center for Children's Health, Beijing Children's Hospital, Capital Medical University, Beijing, China, [7]Department of Medical Record Management, Beijing Children's Hospital, Capital Medical University, National Center for Children's Health, Beijing, China

OPEN ACCESS

Edited by:
Catherine M. T. Sherwin,
Wright State University, United States

Reviewed by:
Nan Li,
Peking University Third Hospital, China
Haibo Song,
National Center for ADR Monitoring, China, China

***Correspondence:**
Xiaoling Wang
eyjdb6380@163.com
Xiaoxia Peng
pengxiaoxia@bch.com.cn

†These authors have contributed equally to this work and share senior authorship

‡These authors have contributed equally to this work and share first authorship

Specialty section:
This article was submitted to Obstetric and Pediatric Pharmacology, a section of the journal Frontiers in Pharmacology

Received: 04 May 2022
Accepted: 16 June 2022
Published: 20 July 2022

Citation:
Nie X, Yu Y, Jia L, Zhao H, Chen Z, Zhang L, Cheng X, Lyu Y, Cao W, Wang X and Peng X (2022) Signal Detection of Pediatric Drug–Induced Coagulopathy Using Routine Electronic Health Records. Front. Pharmacol. 13:935627. doi: 10.3389/fphar.2022.935627

Background: Drug-induced coagulopathy (DIC) is a severe adverse reaction and has become a significantly increased clinical problem in children. It is crucial to the detection of the DIC safety signal for drug post-marketing scientific supervision purposes. Therefore, this study aimed to detect potential signals for DIC in children using the routine electronic medical record (EMR) data.

Methods: This study extracted EMR data from Beijing Children's Hospital between 2009 and 2020. A two-stage modeling method was developed to detect the signal of DIC. We calculated the crude incidence by mining cases of coagulopathy to select the potential suspected drugs; then, propensity score-matched retrospective cohorts of specific screened drugs from the first stage were constructed and estimated the odds ratio (OR) and 95% confidence interval (CI) using conditional logistic regression models. The current literature evidence was used to assess the novelty of the signal.

Results: In the study, from a total of 340 drugs, 22 drugs were initially screened as potentially inducing coagulopathy. In total, we identified 19 positive DIC associations. Of these, potential DIC risk of omeprazole (OR: 2.23, 95% CI: 1.88–2.65), chlorpheniramine (OR:3.04, 95% CI:2.56–3.60), and salbutamol sulfate (OR:1.36, 95% CI:1.07–1.73) were three new DIC signals in both children and adults. Twelve associations between coagulopathy and drugs, meropenem (OR: 3.38, 95% CI: 2.72–4.20), cefoperazone sulbactam (OR: 2.80, 95% CI: 2.30–3.41), fluconazole (OR: 2.11, 95% CI: 1.71–2.59), voriconazole (OR: 2.82, 95% CI: 2.20–3.61), ambroxol hydrochloride (OR: 2.12, 95% CI: 1.74–2.58), furosemide (OR: 2.36, 95% CI: 2.08–2.67), iodixanol (OR: 2.21, 95% CI: 1.72–2.85), cefamandole (OR: 1.82, 95% CI: 1.56–2.13), ceftizoxime (OR: 1.95, 95% CI: 1.44–2.63), ceftriaxone (OR: 1.95, 95% CI: 1.44–2.63), latamoxef sodium (OR: 1.76, 95% CI: 1.49–2.07), and sulfamethoxazole (OR: 1.29, 95% CI: 1.01–1.64), were considered as new signals in children.

Conclusion: The two-stage algorithm developed in our study to detect safety signals of DIC found nineteen signals of DIC, including twelve new signals in a pediatric population. However, these safety signals of DIC need to be confirmed by further studies based on population study and mechanism research.

Keywords: drug-induced coagulopathy, children, signal detection, electronic health records, post-marketing pharmacovigilance, drug scientific supervision

1 INTRODUCTION

Drug-induced coagulopathy (DIC) is an adverse drug reaction (ADR) that manifests as derangement of hemostasis and is a significantly under-recognized clinical problem, especially in surgical patients (Peralta et al., 2019); 7.2 out of 100 patients taking anticoagulants require management for DIC (Nalezinski, 2022). The prothrombin time (PT) or the activated partial thromboplastin time (APTT) is usually longer than the upper limits of normal (Hiensch and Lee, 2021); therefore, DIC can often lead to abrupt and excessive bleeding complications and even death (Hiensch and Lee, 2021). Early identification and timely correction of DIC in surgical patients or emergency department patients with significant bleeding are paramount to prevent death and other consequences of hemorrhage (Liu et al., 2019). It has been reported that many kinds of medications, including vitamin K antagonists, direct oral anticoagulants, and antibiotics, could lead to DIC in the adult population (Zengotita and Holt, 1986; Hall and Carson, 2012; Liu et al., 2019). However, the current pediatric drug safety landscape, including clinical trials, is limited as it rarely includes children and relies on extrapolation from adults. Children have immature organ function and a different spectrum of diseases compared with adults, and it is proposed that pediatric drug safety should comprehensively consider children's systems biology (Giangreco et al., 2022). Hence, accurate methods for post-marketing drug safety surveillance and signal detection of DIC in children are urgently needed.

Considering the limitation of the passive surveillance system using spontaneous reporting system databases such as the FDA Adverse Event Reporting System (FAERS) and EudraVigilance, ADR active surveillance using real-world data (RWD), electronic medical records (EMR) for instance, has opened a new era in pharmacovigilance (Lee et al., 2020). The depth and breadth of clinical data within EHR systems paired with innovative data-mining methods can be leveraged to detect novel drug safety signal, especially the off-label drug use that often occur in pediatric patients (Rudin et al., 2020). Several studies have been conducted to develop methods for detecting signals of hematological disorders using RWD databases (Fuzier et al., 2013; Nie et al., 2021). However, these studies mainly focused on adult patients, and, to date, little is known about children.

This study aimed to develop a two-stage procedure to detect signals of DIC in the child population using EMR data and provide candidate drugs for further precise drug monitoring and precision medicine in pediatrics.

2 METHOD

The study was conducted in accordance with the Declaration of Helsinki. The protocol was approved by the Institutional Review Board (IRB) of Beijing Children's Hospital, Capital Medical University (approval number: 2018-129), with a waiver of informed consent. All the data we used have been de-identified to protect patient privacy and confidentiality. This study was reported critically according to the RECORD-PE statement.

2.1 Data Sources

This retrospective cohort study was conducted using data on hospitalized patients in Beijing Children's Hospital (BCH) longitudinal inpatient database from 1 January 2009 to 31 December 2020, which has been described previously (Nie et al., 2021). These data encompassed health information including medical orders of doctors, diagnosis records from hospital information systems, laboratory tests from laboratory information systems, and drug prescriptions. If a person with the same patient ID had multiple hospital admissions, we identified these records as different records. Therefore, there were approximately 5,75,965 records of inpatients under 18 years of age.

2.2 Study Population Identification

Eligible participants were hospitalized patients aged 28 days to 18 years old and had at least two times laboratory test records of any of the two kinds of main coagulation function index for PT or APTT as well as drug prescriptions in the data warehouse. Considering the temporal relationship between suspected drug and coagulopathy events is important for safety signal identification, patients whose initial PT or APTT index at the beginning of the study was out of reference interval (i.e., PT > 12.5 s or PT < 9.4 s APTT > 38.4 s or APTT < 25.1 s) were excluded.

2.3 Laboratory Criterion of DIC

The laboratories of BCH are certified and accredited under the appropriate International Organization for Standardization standards. According to the definition of coagulopathy in the published Mount Sinai Expert Guides: Critical Care in 2021 (3), the reference interval of pediatric coagulation parameters (Jiang et al., 2015), and the method of the IHI Global ADR Trigger Tool (Griffin and Resar, 2009), the trigger of pediatric DIC in this study was defined as PT longer than 12.5 s or APTT longer than 38.4 s after administration of a particular medicine within the appropriate therapeutic dose range.

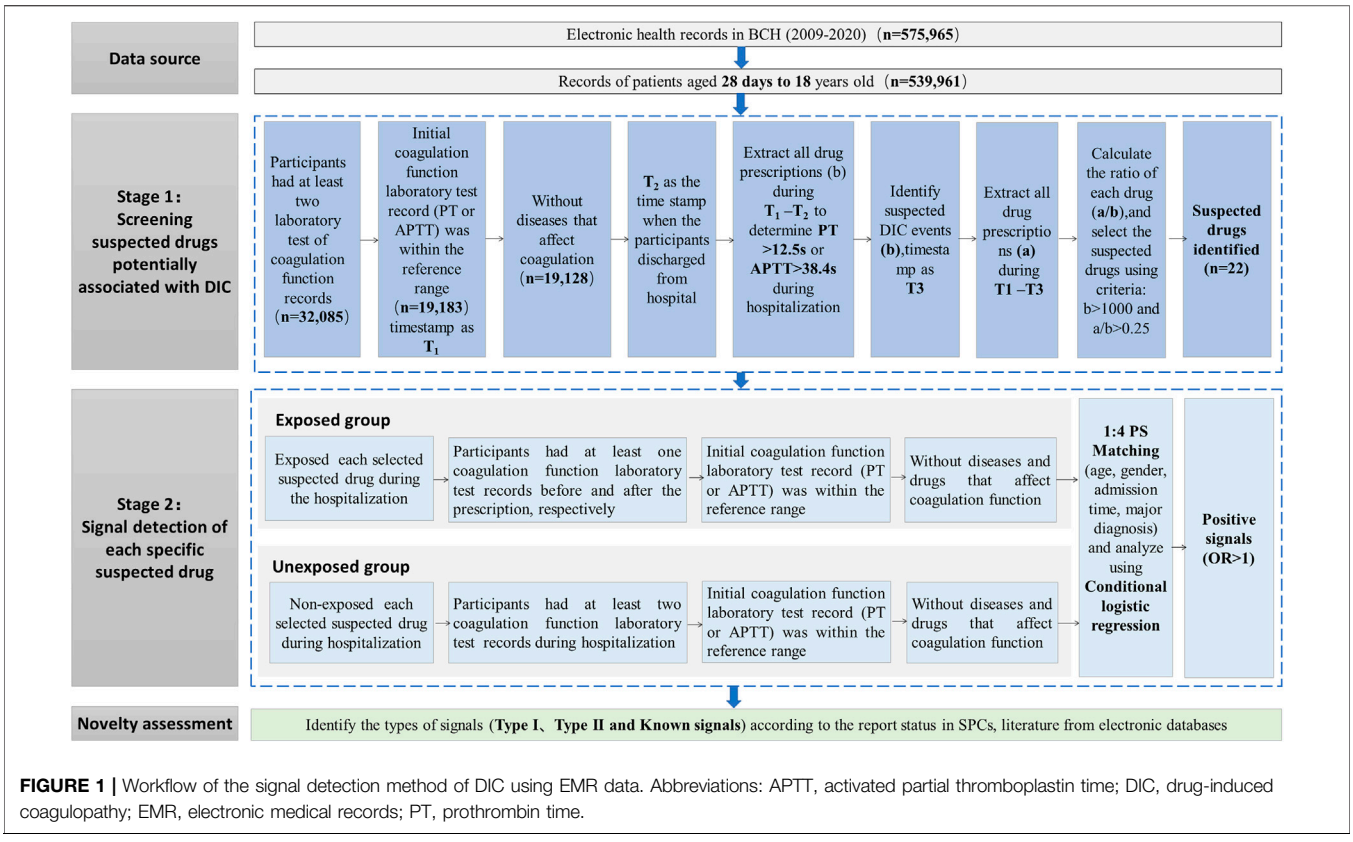

FIGURE 1 | Workflow of the signal detection method of DIC using EMR data. Abbreviations: APTT, activated partial thromboplastin time; DIC, drug-induced coagulopathy; EMR, electronic medical records; PT, prothrombin time.

2.4 Development of a Two-Stage Signal Detection Model

The overall workflow of this study was shown in **Figure 1**. All the involved drugs were unified with generic names and mapped with Anatomical Therapeutic Chemical (ATC) code. If a patient was prescribed more than two drugs in one record, we counted the number of users for each drug, respectively. Duplicate prescriptions of the same drug in each admission were counted only once.

2.4.1 Stage 1: Screening Suspected Drugs Potentially Associated With DIC

To identify suspected drugs potentially associated with DIC for further association analysis, we developed a workflow containing three main steps (see Stage 1 part in **Figure 1**). The main steps were as follows:

2.4.1.1 Identification of the scope for initial calculation of the number of drug users

Considering the confounding by indication, we excluded the records of patients containing a diagnosis of diseases that may affect coagulation function (shown in **Supplementary Table S1**). The remaining hospitalization records were defined as Group 1. The time when a patient in Group 1 obtained an initial normal result of PT or APTT after admission to the hospital was signed as timestamp 1 (T_1), and the time for discharge of each hospitalization of every involved patient was labeled as timestamp 2 (T_2). We calculated the number of drug users (b) during the period of T_1-T_2. Considering the temporal relationship between drugs and adverse reactions, we calculated the number of each kind of medication separately if a patient administered some kinds of medications at one hospitalization record before the predefined trigger of coagulopathy occurred.

2.4.1.2 Detection of the number of potential DIC events

The hospitalization records of patients in Group 1, which were potential DIC events during T_1-T_2 according to the definition of DIC trigger, were included in Group 2. We labeled the time of PT longer than 12.5 s or APTT longer than 38.4 s as timestamp 3 (T_3). Then, the number of users for each medicine in Group 2 who were identified by the DIC trigger (a) during the period of T_1-T_3 was calculated.

2.4.1.3 Calculation of the crude ratio of potential DIC events

The ratio a/b for each drug was calculated. The suspected drug met the following criteria and was selected for further association analysis: (Peralta et al., 2019) set the threshold of a/b ratio according to the range of a/b values of solvents for intravenous infusions, such as normal saline and glucose injection, which can be regarded as the value of background since it is well known that normal saline and glucose injection have no effect on DIC; (Nalezinski, 2022) number of total users (b) >1,000, ensuring sufficient sample size and adequate power. Considering the a/b values of solvents for intravenous infusions, such as normal saline and glucose injection, ranged from 0.125 to 0.243, which can be regarded as the value of background since it is well known that normal saline and glucose injection have no effect on DIC, we set the screening threshold value of a/b ratio for suspected drugs as 0.250.

2.4.2 Stage 2: Signal Detection of Suspected Drug

According to the aforementioned screening procedure of suspected drugs, we conducted a series of retrospective propensity score-matched cohort studies to detect the association between suspected drugs and DIC by comparing differences in coagulopathy event rates between the exposed and unexposed groups. Each suspected drug detected from Stage 1 was considered as an exposure and was examined in a cohort study according to the following procedures. The overall main framework is displayed in Stage 2 part in **Figure 1**.

2.4.2.1 Algorithm defined exposed group

The eligible participants were required to be prescribed a specific screened drug after admission to BCH and had at least one PT or APTT result before and after taking the specific suspected drug, respectively. The date of initial prescription of a specific drug was considered the index time for the corresponding participant, and eligible participants should have an initial PT result within 9.4–12.5 s or an initial APTT result within 25.1–38.4 s before the index time. To accurately assess the drug-coagulopathy associations, patients who were diagnosed with diseases that may affect coagulopathy function (shown in **Supplementary Table S1**) or received prescriptions of anticoagulation (shown in **Supplementary Table S2**) (Hiensch and Lee, 2021) before the first abnormal test of coagulation index PT or APTT were also excluded.

2.4.2.2 Algorithm defined unexposed group

The patients without prescriptions of specific suspected drugs were initially selected for the unexposed group. Among them, we chose the participants with at least two records of laboratory results of PT or APTT tests from admission to discharge and had an initial result of PT or APTT within the reference interval (PT: 9.4–12.5 s; APTT: 25.1–38.4 s). For the same selection considerations as the exposure group, we excluded patients diagnosed with potential coagulopathy diseases or who had prescriptions of agents which affect the coagulation function.

2.4.2.3 Follow-up of the cohort

Follow-up of each cohort ended until the first occurrence of the following events: the library index of PT > 12.5 s or APTT > 38.4 s after administration, discharged from hospital, or until 31 December 2020.

2.4.2.4 Propensity score matching

Given that some important variables (such as age, gender, and underlying diseases) may be imbalanced between two compared groups of this observational study, the propensity score matching method was conducted to balance the baseline characteristics of each screened suspected drug group and the unexposed group. We calculated propensity scores for the initial prescription of a specific suspected drug using the logistic regressions. The variables included in the model included age, gender, admission time, and major diagnosis (based on the classification in ICD-10). Patients with missing values for age, gender, and admission date were excluded from the analysis. For a particular suspected drug, the records from the exposed group were matched 1:4 to those of the unexposed group using the caliper matching method (caliper equaled 0.1).

2.4.2.5 Signal detection

We compared the OR of DIC in each specific suspected drug cohort with the corresponding unexposed group cohorts using conditional logistic regression models. The odds ratio (OR) and its 95% confidence interval (CI) were estimated to assess the association between specific suspected drugs and the incidence of coagulopathy events. The signal of DIC was positive if the lower limit of the 95% CI of OR was greater than 1.0; otherwise, it was regarded as a negative signal.

2.5 Signal Novelty Assessment

One of the important steps in assessing adverse drug reactions is the evaluation of biological mechanisms. Since there was no recognized gold standard for evaluating the relevance of the DIC association, we performed a manual review of the summary of product characteristics (SPCs) included in the Drugs@FDA: FDA-approved drugs, Micromedex, the specification of drugs in China (https://www.yaozh.com/), and electronic literature databases, including PubMed, Embase, and China National Knowledge Infrastructure and Wanfang Database. We applied a combination of keywords and mesh words of generic names for each positive signal drug and adverse event, such as "coagulopathy," "coagulation defects," "coagulation disorders," "coagulation dysfunction," "hypocoagulability," and "hypoprothrombinemia." According to the report status in SPCs and literature from electronic databases, we defined two types of new DIC signals for children: 1) the specific drug DIC signal had never been reported in the summary of product characteristics or in the literature; 2) the specific drug signal had been reported in the literature about adults, but no reports about children could be found in the literature.

2.6 Statistical Analysis

The primary association analysis was conducted by conditional logistic regression and the propensity score matching method. To evaluate the robustness of the primary results, we also performed sensitivity analyses using unconditional logistic regression and the propensity score regression method other than matching in the primary analysis.

All p values were 2-sided, and $p < 0.05$ was considered significant for all tests. MySQL software version 14.14 (Oracle, California, United States) was used as the database management system to extract the required data from BCH's EMR database. Data were processed and summarized using the pandas v1.2.2 model in Python 3.7. R 3.5.2 software (R Foundation for Statistical Computing, Vienna, Austria. ISBN 3-900051-00-3) was used for statistical analysis, and SAS 9.4 TS Level M5 (SAS Institute Inc., Cary, NC, United States) was used for the forest plot demonstrating the results of association analysis.

3 RESULTS

3.1 Selection of Suspected Drugs

After combining drugs with the same ingredients as ATC but different dosages and forms, 340 drugs remained. Among these

TABLE 1 | Suspected drugs associated with coagulopathy in the pediatric population.

Drug name	Pharmacological classification	ATC code	Number of DIC events (a)	Total number of usages (b)	Ratio (a/b)
Acetaminophen	Antipyretic	N02BE01	750	1,569	0.478
Meropenem	Beta-lactam antibiotic	J01DH02	1,090	2,366	0.461
Phenobarbital	Sedative-hypnotic	N03AA02	535	1,196	0.447
Cefoperazone sulbactam	Beta-lactam antibiotic	J01DD12	1,382	3,098	0.446
Fluconazole	Antifungal drug	J02AC01	1,002	2,335	0.429
Voriconazole	Antifungal drug	J02AC03	772	1,800	0.429
Ambroxol hydrochloride	Expectorant	R05CB06	2,532	5,940	0.426
Salbutamol sulfate	Asthmatic	R03AC02	1,220	3,090	0.395
Vancomycin	Polypeptide antibiotic	J01XA01	1,781	4,599	0.387
Ribavirin	Antiviral agent	J05AP01	429	1,150	0.373
Furosemide	Diuretic	C03CA01	3,345	9,161	0.365
Iodixanol	Contrast agent	V08AB09	381	1,072	0.355
Nifedipine	Calcium channel blocker	C08CA05	422	1,205	0.350
Chlorpheniramine	Antihistaminic	R06AB04	1,419	4,160	0.341
Cefamandole	Cephalosporin	J01DC03	2,355	7,066	0.333
Ibuprofen	Antipyretic	M01AE01	2,832	8,524	0.332
Ceftizoxime	Cephalosporin	J01DD07	496	1,511	0.328
Omeprazole	Mucosal protective agent	A02BC01	1,206	3,704	0.326
Ceftriaxone	Cephalosporin	J01DD04	529	1,700	0.311
Cetirizine	Antihistaminic	R06AE07	508	1,664	0.305
Latamoxef sodium	Beta-lactam antibiotic	J01DD06	1,851	6,192	0.299
Sulfamethoxazole	Sulfonamides and trimethoprim	J01EE01	1,010	3,917	0.258

DIC, drug-induced coagulopathy; ATC, anatomical therapeutic chemical.

drugs, 101 satisfied the screening criteria that the total number of drug users was >1,000. Then, the a/b crude ratio was calculated. Considering the a/b values of solvents for intravenous infusions, such as normal saline and glucose injection, ranged from 0.125 to 0.243, which can be regarded as the value of background since it is well known that normal saline and glucose injection have no effect on DIC, we set the screening threshold value of a/b ratio as 0.250. Twenty-two drugs were considered suspected drugs and chosen for DIC signal detection in Stage 2. These were acetaminophen, meropenem, phenobarbital, cefoperazone sodium sulbactam sodium, fluconazole, voriconazole, ambroxol hydrochloride, salbutamol sulfate, vancomycin, ribavirin, furosemide, iodixanol, nifedipine, chlorpheniramine, cefamandole, ibuprofen, ceftizoxime, omeprazole, ceftriaxone, cetirizine, latamoxef sodium, and sulfamethoxazole. The selected suspected drugs are shown in **Table 1**.

3.2 Association of Suspected Drugs and Coagulopathy

The results of data extraction for the suspected drugs for each step are presented in **Supplementary Table S3**. For detection of the DIC signals, the median number of patients enrolled in the drug exposure groups was 492 [interquartile range (IQR): 345–826] ranging from 183 (phenobarbital) to 2,182 (furosemide), and the median number of patients enrolled in the comparison groups was 6,646 (IQR: 5,923–7,155) ranging from 4,394 (furosemide) to 7,294 (phenobarbital). The basic clinical information between two groups of each drug before and after PS matching is given in **Supplementary Table S4**, respectively.

Of the 22 suspected drugs, 19 showed a positive signal, including 10 anti-infective drugs (meropenem, cefoperazone sulbactam, fluconazole, voriconazole, vancomycin, cefamandole, ceftizoxime, ceftriaxone, latamoxef sodium, and sulfamethoxazole, all OR > 1.00, $p < 0.001$, see details in **Figure 2**), two antipyretics (acetaminophen, OR: 3.55, 95% CI: 2.75–4.59, $p < 0.001$; ibuprofen, OR: 2.06, 95% CI: 1.81–2.34, $p < 0.001$), one sedative-hypnotic (phenobarbital, OR: 1.99, 95% CI: 1.41–2.82, $p < 0.001$), one expectorant (ambroxol hydrochloride, OR: 2.12, 95% CI: 1.74–2.58, $p < 0.001$), one asthmatics (salbutamol sulfate, OR: 1.36, 95% CI: 1.07–1.73, $p < 0.001$), one diuretics (furosemide, OR: 2.36, 95% CI: 2.08–2.67, $p < 0.001$), one contrast agent (iodixanol, OR: 2.21, 95% CI: 1.72–2.85, $p < 0.001$), one antihistaminic (chlorpheniramine, OR: 3.04, 95% CI: 2.56–3.60, $p < 0.001$), and one mucosal protective agent (omeprazole, OR: 2.23, 95% CI: 1.88–2.65, $p < 0.001$). The remaining three drugs (ribavirin, nifedipine, and cetirizine) were found to be not associated with DIC. The detailed results of all the 22 drugs-DIC associations are shown in **Figure 2**.

Results from sensitivity analyses also showed the same results for each drug with the primary analysis conducted by the propensity score matching method. Nineteen drugs were potentially associated with DIC, and three drugs were not statistically associated with DIC (**Supplementary Table S5**).

3.3 Signal Novelty Evaluation

The novelty of 19 positive DIC signals observed in Stage 2 was further evaluated through SPCs and current literature (**Table 2**). Three drugs, namely salbutamol sulfate, chlorpheniramine, and omeprazole, were found to be new DIC type I signals, as the coagulopathy event had never been reported in the literature,

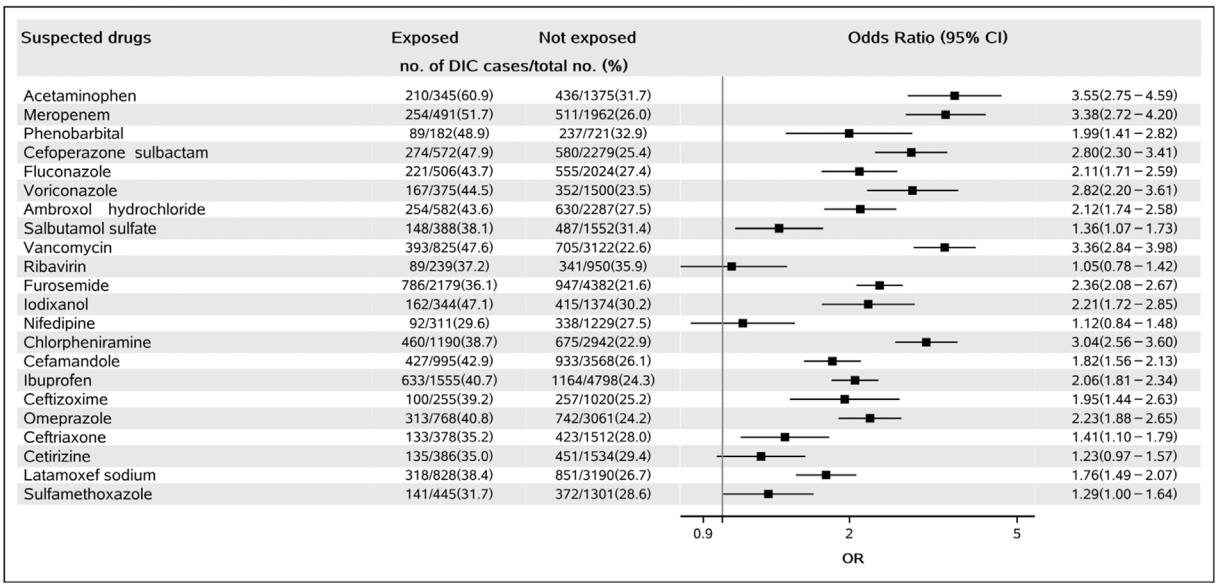

FIGURE 2 | Forest plot for the association of suspected drugs and DIC. Abbreviations: DIC, drug-induced coagulopathy.

TABLE 2 | The novelty of the positive signals of DIC.

Suspected drugs	Literature of PubMed/ Embase[a]		Literature of Chinese database (CNKI/Wangfang)[a]		SPCs[b]	Signal type[c]
	Adults	Children	Adults	Children		
Acetaminophen	√	√	√	×	√	Known
Meropenem	√	×	√	×	×	II
Phenobarbital	√	√	×	×	×	Known
Cefoperazone sulbactam	√	×	√	×	√	II
Fluconazole	√	×	√	×	√	II
Voriconazole	√	×	√	×	×	II
Ambroxol hydrochloride	×	×	√	×	×	II
Salbutamol sulfate	×	×	×	×	×	I
Vancomycin	√	×	×	√	×	Known
Furosemide	√	×	×	×	×	II
Iodixanol	√	×	√	×	×	II
Chlorpheniramine	×	×	×	×	√	I
Cefamandole	√	×	√	×	×	II
Ibuprofen	√	√	√	√	√	Known
Ceftizoxime	√	×	×	×	×	II
Omeprazole	×	×	×	×	×	I
Ceftriaxone	√	×	√	×	×	II
Latamoxef sodium	√	×	√	×	×	II
Sulfamethoxazole	√	×	×	×	×	II

DIC, drug-induced coagulopathy; SPCs, summary of product characteristics.

[a]Literature reviewed: 1) PUBMED: https://pubmed.ncbi.nlm.nih.gov; 2) Embase: https://www.embase.com; 3) Wanfang: https://www.wanfangdata.com.cn/index.html; 4) CNKI: https://www.cnki.net.

[b]SPCs reviewed: 1) Micromedex: https://www.ibm.com/watson-health/learn/micromedex; 2) FDA website: https://www.fda.gov/; (3) Drug instructions: https://www.yaozh.com/.

[c]Signal type I: The specific drug-DIC signal had never been reported in the summary of product characteristics or in the literature; II: the specific DIC signal had been reported in the literature about adults, but no reports about children could be found in the literature; known: the specific drug-DIC association had been reported.

neither in children nor adults. In addition, twelve drugs, namely meropenem, cefoperazone sulbactam, fluconazole, voriconazole, ambroxol hydrochloride, furosemide, iodixanol, cefamandole, ceftizoxime, ceftriaxone, latamoxef sodium, and sulfamethoxazole, were considered new signals for type II DIC. Coagulation disorders associated with these 12 drugs have not been found in pediatric patients but have been reported in adults. The remaining four drugs have been reported to be associated with coagulation dysfunction in both adult and pediatric patients.

4 DISCUSSION

Early recognition of the cause of coagulation disorder is critical to making appropriate treatment and saving patients' lives. Drug-induced coagulopathy is a type of acquired coagulopathy that has been associated with some medications and can lead to devastating consequences for the patient, especially for critically ill patients (Levi and Schultz, 2010). Often, the cause of DIC is not recognized in a timely manner, resulting in recurrent coagulation disorders and inappropriate treatments. Drug-induced coagulopathy and bleeding have similar principles of management including protocols calling for early diagnosis and timely reversal of coagulopathy with antidotes (Nalezinski, 2022). Greater publicity will increase awareness and suspicion of DIC among pediatricians and improve clinicians' ability to evaluate, accurately diagnose, and manage patients who present with unexpected coagulopathy (Nalezinski, 2022) because a delay in recognition can lead to significant morbidity and mortality; clinical criteria such as the Naranjo Adverse Drug Reaction Probability Scale were used to help determine the risk of DIC, which was less efficient. By contrast, our algorithm based on EMR data could be a referential experience to provide more clues for pediatric drug post-marketing pharmacovigilance. We found nineteen positive signals of DIC, including twelve new signals in a pediatric population. Considering the precision medicine in pediatrics, when children are treated with such drugs, health professionals should be aware of the potential coagulation disorder risk and monitor coagulation parameters during clinical therapy with these suspected drugs, particularly the need to monitor AT and APTT. In addition, these drugs may be the suspected drugs for post-marketing surveillance and regulation, which could be the candidate target drugs for further signal validation studies.

4.1 New Signals of DIC

Using our established two-stage algorithm, the association of omeprazole, salbutamol sulfate, and chlorpheniramine with DIC was found to be a potential three new type I positive signals in this study for the first time. Although there have been no published reports about these potential drug-coagulopathy event pairs neither in pediatrics nor in adults, some other clues could indicate these potential associations might exist. FDA has initiated two phase IV clinical studies about omeprazole and coagulopathy, one is focused on coagulopathy and drugs of ingredients of omeprazole, and another is about omeprazole and coagulopathy (eHealthMe, 2022; eHealthMe) using real-world post-marketing data. With real-world medical big data and proven AI algorithms, eHealthMe provides a platform for everyone to run phase IV clinical trials. According to the latest updated data on 21 April 2022, 4,63,527 people reported having side effects when taking drugs with ingredients of omeprazole. Among them, 850 people (0.18%) had coagulopathy. Similar post-marketing safety reports on salbutamol sulfate could be searched in the SIDER 4.1 database (Resource), which contains available information including side effect frequency, drug, and side effect classifications as well as links to further information on marketed medicines and their recorded adverse drug reactions. The information is extracted from public documents and package inserts. Considering the new signal of chlorpheniramine, the adverse effects listed in its SPCs include drowsiness, thirst, polyuria, sore throat, drowsiness, weakness, palpitations, ecchymosis of the skin, and bleeding tendency. A rare case report suggested that acquired hemophilia due to factor VIII inhibitor(s) should be considered in the appropriate setting when patients present with unexplained and even minor bleeding while on treatment with acetaminophen or chlorpheniramine alone or combined (Famularo et al., 2004). Since this rare case was unclear whether exposure to those compounds triggered an autoimmune response against factor VIII although there has been no clinical or laboratory evidence in this patient of liver dysfunction, which ruled out the hypothesis of factor VIII coagulopathy caused by acetaminophen-induced impairment of liver metabolism. The use of the Naranjo Probability Scale indicated a possible relationship between acquired hemophilia and exposure to acetaminophen and chlorpheniramine therapy in this patient. Further investigations about the potential association between chlorpheniramine and coagulopathy are still needed. It should be noted that general ADR was defined as "an appreciably harmful or unpleasant reaction, resulting from an intervention related to the use of a medicinal product" (Edwards and Aronson, 2000), which includes drug side effects and toxic effects (toxicity), allergic reactions, diathesis, double infection induced by anti-infection drugs, dependency, and carcinogenic, teratogenic and mutagenic effects, etc. Considering overdose drug use is more common in children's clinical practice, further mechanism search is urgent to validate type I DIC signals detected in our studies.

Other twelve drug-DIC associations (meropenem, cefoperazone sulbactam, fluconazole, voriconazole, ambroxol hydrochloride, furosemide, iodixanol, cefamandole, ceftizoxime, ceftriaxone, latamoxef sodium, and sulfamethoxazole) were identified as potentially new type II signals in children. Among them, cefamandole, ceftizoxime, and ceftriaxone are cephalosporins, while cefoperazone sulbactam is a compound preparation of cephalosporin. Latamoxef sodium belongs to the β-Lactam family of antibiotics, and its antibacterial spectrum and antibacterial action are like that of the third-generation cephalosporin. Cephalosporins that contain the N-methylthiotetrazole side chain (NMTT-cephalosporin) have been reported to be associated with coagulation-related adverse events, especially hypoprothrombinemia or PT prolongation in patients with underlying clinical conditions at risk for bleeding (Park et al., 2019). Due to the chemical structure of the NMTT, this side chain interferes with vitamin K metabolism and results in a decrease in prothrombin synthesis and a corresponding decrease in thrombin synthesis. Hypoprothrombinemia is characterized by a deficiency of the clotting factor prothrombin and presents an elevated PT level and a prolonged APTT (Agnelli et al., 1986). Some adult case reports have documented cephalosporin-induced acute coagulopathy (Chang, 1983; Haubenstock et al., 1983; Cuxart et al., 1987; Nichols et al., 1987; Li et al., 2017; Hu, 2019; Wang et al., 2020; Li et al., 2021) but few about the pediatric population. The incidence of vitamin K-dependent

coagulopathy associated with NMTT-containing antibiotics was shown to range from 2.2 to 19% while the incidence of bleeding associated with non-NMTT-containing antibiotics such as sulfamethoxazole (SMX) and meropenem was shown to range from 0 to 4% (Shevchuk and Conly, 1990; Cook and Ponte, 1994; Fotouhie et al., 2016; Furumi et al., 2019; Guo et al., 2022). Therefore, treatment with antibiotics, including non-NMTT-containing antibiotics and cephalosporins, should be remembered as potential causes of vitamin K deficiency. The liver is the main synthesis site of most coagulation factors (factor II, V, VII, IX, XII, fibrinogen, and fibrinolytic progenitor) and inhibitory proteins (α2 anti-fibrinolytic enzyme, antithrombin, protein C, protein S, etc.). Oral azole antifungal medications including fluconazole and voriconazole could affect liver function to reduce vitamin K absorption and result in deficiency of vitamin K-dependent factors II, VII, X, and IX (Lo Re et al., 2016). There had been some adults case reports about the coagulopathy events induced by ambroxol hydrochloride (Hu et al., 2003), furosemide (Hilden and Amris, 1968; Averina and Alieva, 1972), and iodixanol (Bai et al., 2021), but few of them tried to explain the mechanism of drug adverse reaction. Although our results were the first to show that these aforementioned twelve type II signal drugs might be associated with adverse coagulopathy in children, these findings will need further investigation to be confirmed and explained.

4.2 Strength and Limitation

Strengths of this study are its large size and longitudinal integrated multi-source data from the hospital information systems, biochemical laboratory, and drug prescription records with detailed clinical data. The inadequacy of the spontaneous reporting system (SRS) has led many countries to implement pharmacovigilance systems to enhance their risk management capacity. Compared with the proposed tool with those based on the SRS, the active surveillance based on the routinely collected data integration is an effective approach for pharmacovigilance, which can detect previously unrecognized adverse drug signals in the real practice immediately, as well as provide more detailed information about symptoms, signs, diagnosis, timing sequence, and medication to analyze the potential association for drug-ADR pairs. Also of note, Yoon et al. (2012) established a series of electronic health record (EHR)-based pharmacovigilance methods called the BASE, CLEAR, and MetaLAB for laboratory abnormalities (Lee et al., 2017). Our study used a two-stage data-driven drug screening and PS matching method to detect children's DIC signals. It is important to realize that this is a tool to assist with detection but does not ensure the identification of ADRs. In comparison with the CLEAR method, our 2-stage designed approach has several advantages. In the process of selecting the drugs suspected to cause DIC, we assessed the potentialities by computing the crude incidence of ADEs in drug users. This crucial additional step increased the efficiency and speed of subsequent steps. In addition, more complicated confounders, such as relevant diagnoses with clear competing causes and medications that may affect the level of relevant laboratory indicators and induce confounding by indication, were excluded to enhance the reliability and accuracy of the results. These results suggested that our method is a valuable tool to facilitate earlier signal detection using routinely collected EMR data.

This study also had some limitations inherent to hospital-based retrospective observational data; hence, there is always a chance of unmeasured residual confounding. The signal detection using our method was dependent on the time for measurement of PT or APTT, and the sequence relationship between these signals and the actual occurrence of DIC may be inverted due to the possible delayed detection. Dose-related effects and possible residual confounders, such as those not controlled, lead to potential bias. Third, since our study is only based on EMR data from a single-center and coagulation tests are not routine laboratory tests, the sample size of exposure to both specific drugs and PT/APTT tests, such as phenobarbital, was small and limited, which could lead to poor representation of results. Therefore, the external data validation and distributed signal detection method based on multi-center EMR data should be further discussed in the future.

After two decades of implementation of the drug-related adverse reaction reporting system, China has formally implemented a pharmacovigilance system with the pharmacovigilance quality management standards and a series of supporting technical documents created to improve the safety of medication given to patients (Song et al., 2022). Since the development of children's medicine cannot meet clinical needs, potential off-label drug use may occur in children, and this risk should not be ignored (Moore-Hepburn and Rieder, 2021). Access to high-quality data from multiple sources will lead to more comprehensive and scientific risk assessment and the generation of reliable scientific evidence for drug safety regulatory decisions. China has improved its spontaneous reporting system by installing the China Hospital Pharmacovigilance System (CHPS) module in hospital information systems (HIS) of some sentinel tertiary hospitals. The main function of the CHPS module is to automatically capture most of the information needed for the ADR report form from the hospital's HIS system, which will lead to significant time savings for HCPs completing ADR reports and reduce the omission of important information during the filing process. On the other hand, bringing together a wealth of real-world data to build new pharmacovigilance systems has proven the possibility of successfully detecting and assessing safety signals and effectively enhancing pharmacovigilance capabilities. At present, we have developed an automated program based on this algorithm. Furthermore, in the next step, more attention will be paid to integrating these multiple modules into a drug safety monitoring platform to support quick-response tools for pediatric clinicians and pharmacists in multi-center hospitals through a common data model (CDM), just like the Sentinel Initiative of FDA. Future research will also focus on tighter integration of the structured data and clinical narratives in EMR data to improve the accuracy and scalability of the method.

5 CONCLUSION

In this study, we developed a two-stage designed pharmacovigilance method to explore potentially DIC signals using routine EMR data.

Fifteen positive signals of DIC, including twelve new signals in children, were detected. Our work promotes the application of EMR datasets in pharmacovigilance and precision medicine in pediatrics.

DATA AVAILABILITY STATEMENT

The original contributions presented in the study are included in the article/**Supplementary Material**; further inquiries can be directed to the corresponding authors.

ETHICS STATEMENT

The studies involving human participants were reviewed and approved by the Institutional Ethics Committee of Beijing Children's Hospital in China (approval number: 2018-129). Written informed consent for participation was not provided by the participants' legal guardians/next of kin because this study was with a waiver of informed consent.

AUTHOR CONTRIBUTIONS

All the authors were involved in the study. Conceptualization, XN, YY, XP, and XW; data extraction, XN, LJ, and YY; methodology, XN, YY, and XP; project administration, ZC, LZ, XC, and YL; quality control: WC and XW; formal analysis, XN; writing—original draft, XN and YY; writing—review and editing, XW and XP. Supervision, XW and XP; funding acquisition, XN, YY, and XP. All authors approved the final version of the manuscript. All authors have read and agreed to the published version of the manuscript.

FUNDING

This work was supported by the Hainan Free Trade Port Boao Hope City Real-World Study Project (HNLC2022RWS015, HNLC2022RWS010); The Special Fund of the Pediatric Medical Coordinated Development Center of Beijing Hospitals Authority (No. XTCX201812); The National Natural Science Foundation of China (No. 72174128, 82102688); Cooperation project of China Society for Drug Regulation (DRM2021004).

SUPPLEMENTARY MATERIAL

The Supplementary Material for this article can be found online at: https://www.frontiersin.org/articles/10.3389/fphar.2022.935627/full#supplementary-material

REFERENCES

Agnelli, G., Del Favero, A., Parise, P., Guerciolini, R., Pasticci, B., Nenci, G. G., et al. (1986). Cephalosporin-induced Hypoprothrombinemia: Is the N-Methylthiotetrazole Side Chain the Culprit? *Antimicrob. Agents Chemother.* 29 (6), 1108–1109. eng. Epub 1986/06/01Cited in: Pubmed; PMID 3729364. doi:10.1128/aac.29.6.1108

Averina, R. I., and Alieva, Z. M. (1972). Effect of Furosemide on the Blood Coagulation. *Sov. Med.* 35 (8), 115–118. Vliianie furosemida na svertyvaemost' krovi. rus. Epub 1972/08/01. Cited in: Pubmed; PMID 5070527.

Bai, J., Liu, Z., Ma, Y., Xue, X., Lu, Y., Yang, L., et al. (2021). Anaphylactic Shock Induced by Iodoxanol Contrast Agent in CT Examination: a Case Report. *Qinghai J. Med.* 51 (07), 60–62.

Chang, J. C. (1983). Acquired Coagulopathy Owing to Parenteral Cefamandole: Renal Failure as a Predisposing Factor. *Ann. Clin. Lab. Sci.* 13 (5), 418–424. eng. Epub 1983/09/01. Cited in: Pubmed; PMID 6638932.

Cook, D. E., and Ponte, C. D. (1994). Suspected Trimethoprim/sulfamethoxazole-Induced Hypoprothrombinemia. *J. Fam. Pract.* 39 (6), 589–591. eng. Epub 1994/12/01. Cited in: Pubmed; PMID 7798864.

Cuxart, M., Nogues, X., Cuevas, X., and Aubia, J. (1987). Coagulation Disorders Associated with Cefamandole: Presentation of 2 Cases. *Med. Clin. Barc.* 89 (4), 173–174. Trastornos de coagulación asociados al cefamandol: presentación de dos casos. spa. Epub 1987/06/20. Cited in: Pubmed; PMID 3626671.

Edwards, I. R., and Aronson, J. K. (2000). Adverse Drug Reactions: Definitions, Diagnosis, and Management. *Lancet* 356 (9237), 1255–1259. eng. Epub 2000/11/10Cited in: Pubmed; PMID 11072960. doi:10.1016/s0140-6736(00)02799-9

eHealthMe *Coagulopathy and Drugs of Ingredients of Omeprazole - a Phase IV Clinical Study of FDA Data*.

eHealthMe. 2022. Omeprazole and Coagulopathy - a Phase IV Clinical Study of FDA Data. [cited 2022 04-22]. Available from: https://www.ehealthme.com/ds/omeprazole/coagulopathy/.

Famularo, G., De Maria, S., Minisola, G., and Nicotra, G. C. (2004). Severe Acquired Hemophilia with Factor VIII Inhibition Associated with Acetaminophen and Chlorpheniramine. *Ann. Pharmacother.* 38 (9), 1432–1434. eng. Epub 2004/07/22Cited in: Pubmed; PMID 15266042. doi:10.1345/aph.1E100

Fotouhie, A., Desai, H., Parsa, N. A., and King, S. (2016). Gastrointestinal Bleeding Secondary to Trimethoprim-Sulfamethoxazole-Induced Vitamin K Deficiency. *BMJ Case Rep.* 2016, 2016. eng. Epub 2016/06/09Cited in: Pubmed; PMID 27268289. doi:10.1136/bcr-2016-214437

Furumi, Y., Shimizu, S., Ogawa, Y., Hirose, D., Takada, Y., Kanetaka, H., et al. (2019). A Suspicious Case of Coagulation Disorder Caused by Vitamin K Deficiency Associated with Fasting and Antibiotics. *Nihon Ronen Igakkai Zasshi* 56 (2), 204–208. jpn. Epub 2019/05/17Cited in: Pubmed; PMID 31092787. doi:10.3143/geriatrics.56.204

Fuzier, R., Serres, I., Guitton, E., Lapeyre-Mestre, M., and Montastruc, J. L. (2013). Adverse Drug Reactions to Gabapentin and Pregabalin: a Review of the French Pharmacovigilance Database. *Drug Saf.* 36 (1), 55–62. doi:10.1007/s40264-012-0006-6

Giangreco, N. P., Elias, J. E., and Tatonetti, N. P. (2022). No Population Left behind: Improving Paediatric Drug Safety Using Informatics and Systems Biology. *Brit J. Clin. Pharma* 88, 1464–1470. eng. Epub 2020/12/18Cited in: Pubmed; PMID 33332641. doi:10.1111/bcp.14705

Griffin, F. A., and Resar, R. K. (2009). "IHI Global Trigger Tool for Measuring Adverse Events," in *IHI Innovation Series White Paper*. Second Edition (Cambridge, Massachusetts: Institute for Healthcare Improvement).

Guo, M., Liang, J., Li, D., Zhao, Y., Xu, W., Wang, L., et al. (2022). Coagulation Dysfunction Events Associated with Tigecycline: a Real-World Study from FDA Adverse Event Reporting System (FAERS) Database. *Thromb. J.* 20 (1), 12. eng. Epub 2022/03/07Cited in: Pubmed; PMID 35248072. doi:10.1186/s12959-022-00369-z

Hall, A. B., and Carson, B. C. (2012). Reversal of Warfarin-Induced Coagulopathy: Review of Treatment Options. *J. Emerg. Nurs.* 38 (1), 98–101. eng. Epub 2011/04/09Cited in: Pubmed; PMID 21474171. doi:10.1016/j.jen.2010.12.015

Haubenstock, A., Schmidt, P., Zazgornik, J., Balcke, P., and Kopsa, H. (1983). Hypoprothrombobinaemic Bleeding Associated with Ceftriaxone. *Lancet* 1 (8335), 1215–1216. eng. Epub 1983/05/28Cited in: Pubmed; PMID 6134007. doi:10.1016/s0140-6736(83)92487-x

Hiensch, R. J. T., and Lee, A. (2021). "Coagulopathy and Thrombocytopenia," in *Mount Sinai Expert Guides: Critical Care* (New Jersey: Wiley), 561–574. doi:10.1002/9781119293255.ch56

Hilden, M., and Amris, C. J. (1968). Coagulation and Fibrinolytic Studies in Normal Individuals during Diuretic Treatment with Furosemide. *Scand. J. Haematol.* 5 (1), 75–80. eng. Epub 1968/01/01Cited in: Pubmed; PMID 5665820. doi:10.1111/j.1600-0609.1968.tb01720.x

Hu, D., Xi, F., and Shou, J. (2003). Coagulopathy and Henoch Purpura Induced by Ambroxol Tablets: a Case Report. *Chin. J. Clin. Pharm.* (06), 378. doi:10.3969/j.issn.1007-4406.2003.06.023

Hu, H. R. (2019). Fatal Vitamin K-Dependent Coagulopathy Associated with Cefoperazone/Sulbactam: A Case Report. *Drug Saf. Case Rep.* 6 (1), 6. eng. Epub 2019/06/16Cited in: Pubmed; PMID 31201572. doi:10.1007/s40800-019-0100-0

Jiang, Z., Shen, K., and Shen, Y. (2015). *Zhu Futang Practice of Pediatrics* (Beijing: People's Medical Publishing House). (ed E, editor.).

Lee, G. M., Romero, J. R., and Bell, B. P. (2020). Postapproval Vaccine Safety Surveillance for COVID-19 Vaccines in the US. *JAMA* 324 (19), 1937–1938. doi:10.1001/jama.2020.19692

Lee, S., Choi, J., Kim, H. S., Kim, G. J., Lee, K. H., Park, C. H., et al. (2017). Standard-based Comprehensive Detection of Adverse Drug Reaction Signals from Nursing Statements and Laboratory Results in Electronic Health Records. *J. Am. Med. Inf. Assoc.* 24 (4), 697–708. eng. Epub 2017/01/15Cited in: Pubmed; PMID 28087585. doi:10.1093/jamia/ocw168

Levi, M., and Schultz, M. (2010). Coagulopathy and Platelet Disorders in Critically Ill Patients. *Minerva Anestesiol.* 76 (10), 851–859. eng. Epub 2010/10/12. Cited in: Pubmed; PMID 20935621.

Li, L., Chen, D., Wang, C., Li, T., Zhang, X., Dong, H., et al. (2017). A Case of Coagulopathy Aggravated by Cephalosporin. *Her. Med.* 36 (3), 346–347. doi:10.3870/j.issn.1004-0781.2017.03.024

Li, Y., Wei, X., Zhang, L., Liao, H., Peng, F., Li, Y., et al. (2021). Coagulopathy and Liver Dysfunction in Young Male Patients with Cefoperazone Sulbactam Sodium. *Chin. Remedies Clin.* 21 (13), 2363–2364. doi:10.11655/zgywylc2021.13.062

Liu, J., Liu, Y., Liu, S., Zhang, Q., Zheng, J., Niu, Y., et al. (2019). Hypocoagulation Induced by Broad-Spectrum Antibiotics in Extensive Burn Patients. *Burns Trauma* 7, 13. eng. Epub 2019/05/07Cited in: Pubmed; PMID 31058197. doi:10.1186/s41038-019-0150-7

Lo Re, V., 3rd, Carbonari, D. M., Lewis, J. D., Forde, K. A., Goldberg, D. S., Reddy, K. R., et al. (2016). Oral Azole Antifungal Medications and Risk of Acute Liver Injury, Overall and by Chronic Liver Disease Status. *Am. J. Med.* 129 (3), 283–e5. e5. eng. Epub 2015/11/26Cited in: Pubmed; PMID 26597673. doi:10.1016/j.amjmed.2015.10.029

Moore-Hepburn, C., and Rieder, M. (2021). Paediatric Pharmacotherapy and Drug Regulation: Moving Past the Therapeutic Orphan. *Br. J. Clin. Pharmacol.*, 1–8. [Online ahead of print]. doi:10.1111/bcp.14769

Nalezinski, S. (2022). Methods to Correct Drug-Induced Coagulopathy in Bleeding Emergencies: A Comparative Review. *Lab. Med.* 24, 1–10. [Online ahead of print]. doi:10.1093/labmed/lmab115

Nichols, R. L., Wikler, M. A., McDevitt, J. T., Lentnek, A. L., and Hosutt, J. A. (1987). Coagulopathy Associated with Extended-Spectrum Cephalosporins in Patients with Serious Infections. *Antimicrob. Agents Chemother.* 31 (2), 281–285. eng. Epub 1987/02/01Cited in: Pubmed; PMID 3471181. doi:10.1128/aac.31.2.281

Nie, X., Jia, L., Peng, X., Zhao, H., Yu, Y., Chen, Z., et al. (2021). Detection of Drug-Induced Thrombocytopenia Signals in Children Using Routine Electronic Medical Records. *Front. Pharmacol.* 2021, 3116. doi:10.3389/fphar.2021.756207

Park, G. H., Kim, S., Kim, M. S., Yu, Y. M., Kim, G. H., Lee, J. S., et al. (2019). The Association Between Cephalosporin and Hypoprothrombinemia: A Systematic Review and Meta-Analysis. *Int. J. Environ. Res. Public Health* 16 (20), 16. eng. Epub 2019/10/19Cited in: Pubmed; PMID 31623191. doi:10.3390/ijerph16203937

Peralta, R., Thani, H. A., and Rizoli, S. (2019). Coagulopathy in the Surgical Patient: Trauma-Induced and Drug-Induced Coagulopathies. *Curr. Opin. Crit. Care* 25 (6), 668–674. eng. Epub 2019/10/02Cited in: Pubmed; PMID 31574017. doi:10.1097/mcc.0000000000000676

Resource, S. S. E.(2015). Salbutamol. SIDER 4.1: SIDER Effect Resource. Available from: http://sideeffects.embl.de/drugs/2083/ (Accessed April 22, 2022).

Rudin, R. S., Friedberg, M. W., Shekelle, P., Shah, N., and Bates, D. W. (2020). Getting Value From Electronic Health Records: Research Needed to Improve Practice. *Ann. Intern Med.* 172 (11 Suppl. l), S130–s136. eng. Epub 2020/06/02Cited in: Pubmed; PMID 32479182. doi:10.7326/m19-0878

Shevchuk, Y. M., and Conly, J. M. (1990). Antibiotic-associated Hypoprothrombinemia: a Review of Prospective Studies, 1966-1988. *Rev. Infect. Dis.* 12 (6), 1109–1126. eng. Epub 1990/11/01. Cited in: Pubmed; PMID 2267487. doi:10.1093/clinids/12.6.1109

Song, H., Pei, X., Liu, Z., Shen, C., Sun, J., Liu, Y., et al. (2022). Pharmacovigilance in China: Evolution and Future Challenges. *Brit J. Clin. Pharma*. eng. Epub 2022/02/16Cited in: Pubmed; PMID 35165914. doi:10.1111/bcp.15277

Wang, W., Liu, Y., Yu, C., Tan, J., Xiong, W., Dong, D., et al. (2020). Cefoperazone-sulbactam and Risk of Coagulation Disorders or Bleeding: a Retrospective Cohort Study. *Expert Opin. Drug Saf.* 19 (3), 1–13. [Online ahead of print]. doi:10.1080/14740338.2020.1713090

Yoon, D., Park, M. Y., Choi, N. K., Park, B. J., Kim, J. H., and Park, R. W. (2012). Detection of Adverse Drug Reaction Signals Using an Electronic Health Records Database: Comparison of the Laboratory Extreme Abnormality Ratio (CLEAR) Algorithm. *Clin. Pharmacol. Ther.* 91 (3), 467–474. eng. Epub 2012/01/13Cited in: Pubmed; PMID 22237257. doi:10.1038/clpt.2011.248

Zengotita, H. E., and Holt, R. J. (1986). Neuroleptic Drug-Induced Coagulopathy: Mechanism of Reaction and Duration of Effect. *J. Clin. Psychiatry* 47 (1), 35–37. eng. Epub 1986/01/01. Cited in: Pubmed; PMID 3941056.

Conflict of Interest: The authors declare that the research was conducted in the absence of any commercial or financial relationships that could be construed as a potential conflict of interest.

frontiers | Frontiers in Pharmacology

ORIGINAL RESEARCH
published: 26 July 2022
doi: 10.3389/fphar.2022.933739

Population Pharmacokinetics of Cyclosporine in Chinese Pediatric Patients With Acquired Aplastic Anemia

Xuan Gao[1†], Zhu-Li Bian[2†], Xiao-Hong Qiao[2†], Xiao-Wen Qian[3], Jun Li[3], Guo-Mei Shen[1], Hui Miao[3], Yi Yu[3], Jian-Hua Meng[3], Xiao-Hua Zhu[3], Jun-Ye Jiang[3], Jun Le[3], Ling Yu[3], Hong-Sheng Wang[3] and Xiao-Wen Zhai[3]**

[1]Outpatient and Emergency Management Office, National Children's Medical Center, Children's Hospital of Fudan University, Shanghai, China, [2]Department of Pediatrics, Tongji Hospital, School of Medicine, Tongji University, Shanghai, China, [3]Department of Hematology and Oncology, National Children's Medical Center, Children's Hospital of Fudan University, Shanghai, China

OPEN ACCESS

Edited by:
Yang Zhou,
Brown University, United States

Reviewed by:
Wei Zhao,
Shandong University, China
Jignesh D. Dalal,
Case Western Reserve University, United States

***Correspondence:**
Xiao-Wen Zhai
xwzhai@fudan.edu.cn
Hong-Sheng Wang
honswang@hotmail.com

[†]These authors have contributed equally to this work and share first authorship

Specialty section:
This article was submitted to Obstetric and Pediatric Pharmacology, a section of the journal Frontiers in Pharmacology

Received: 01 May 2022
Accepted: 22 June 2022
Published: 26 July 2022

Citation:
Gao X, Bian Z-L, Qiao X-H, Qian X-W, Li J, Shen G-M, Miao H, Yu Y, Meng J-H, Zhu X-H, Jiang J-Y, Le J, Yu L, Wang H-S and Zhai X-W (2022) Population Pharmacokinetics of Cyclosporine in Chinese Pediatric Patients With Acquired Aplastic Anemia. Front. Pharmacol. 13:933739. doi: 10.3389/fphar.2022.933739

Cyclosporine (CsA) is a component of the first-line treatment for acquired aplastic anemia (acquired AA) in pediatric patients. This study aimed to develop a population pharmacokinetic (PK) model of CsA in Chinese pediatric patients with acquired AA to inform individual dosage regimens. A total of 681 CsA whole blood concentrations and laboratory data of 157 pediatric patients with acquired AA were retrospectively collected from two hospitals in Shanghai. A nonlinear mixed-effect model approach was used to build the population PK model. Potential covariate effects of age, body weight, and biochemical measurements (renal and liver functions) on CsA PK disposition were evaluated. Model fit was assessed using the basic goodness of fit and a visual predictive check. The CsA concentration data were accurately described using a two-compartment disposition model with first-order absorption and elimination. Body weight value was implemented as a fixed allometric function on all clearance and volume of distribution parameters. Total bilirubin level was identified as a significant covariate on apparent clearance (CL/F), with a 1.07% reduction per 1 nmol/L rise in total bilirubin level. The final estimates for CL/F and central volume (Vc/F) were 29.1 L/h and 325 L, respectively, for a typical 28 kg child. Other covariates (e.g., gender, age, albumin, hemoglobin, hematocrit, serum creatinine, and concomitant medication) did not significantly affect the PK properties of CsA. This population PK model, along with a maximum a *posteriori* Bayesian approach, could estimate individual PK parameters in pediatric patients with acquired AA to conduct individual CsA therapy.

Keywords: cyclosporine, population pharmacokinetics, NONMEM, acquired aplastic anemia, pediatric patients

INTRODUCTION

Acquired aplastic anemia (acquired AA) is a rare heterogeneous disorder characterized by peripheral pancytopenia and bone marrow aplasia or hypoplasia. Most patients with acquired AA (70–80%) are idiopathic because their primary etiology remains unknown (Marsh et al., 2009; Shallis et al., 2018). The annual incidence of acquired AA in Asians is 2- to 3-fold higher than that in the Western

population, which has been reported to be approximately 2–2.3 patients per million (Issaragrisil et al., 1991; Montane et al., 2008; Young and Kaufman, 2008). The median age at disease diagnosis among children is around 9 years (Jeong et al., 2011). Acquired AA diagnosis was divided into three subtypes according to the related clinical guidance (Camitta et al., 1975; Camitta et al., 1976; Bacigalupo et al., 1988; Brodsky and Jones, 2005), including nonsevere AA (NSAA), severe AA (SAA), and very severe AA (vSAA). As per current clinical guidelines, immunosuppressive therapy (IST) using antithymocyte globulin (ATG) combined with cyclosporine A (CsA) is the standard first-line treatment for patients with SAA or vSAA without a suitable donor and for those with NSAA who are transfusion-dependent or experienced bleeding (Speck et al., 1977; Bacigalupo et al., 1988; Marsh et al., 1999; Rosenfeld et al., 2003; Viollier et al., 2005; Yoshida and Kojima, 2018). The overall survival rate of patients treated with IST was reported to be 68–90%, and the response rate ranged from 58 to 90% (Frickhofen et al., 1991; Rosenfeld et al., 1995; Frickhofen and Rosenfeld, 2000; Rosenfeld et al., 2003; Führer et al., 2005; Locasciulli et al., 2007; Pongtanakul et al., 2008; Saracco et al., 2008; Deyell et al., 2011; Samarasinghe et al., 2012; Dufour et al., 2015).

CsA, a classic calcineurin inhibitor, has been widely used in IST for decades (Yoshida and Kojima, 2018). CsA is mainly metabolized *via* cytochrome P450 isoenzymes (CYP) 3A4 and 3A5 in the liver and is also a substrate of P-glycoprotein (Kronbach et al., 1988; Aoyama et al., 1989; von Richter et al., 2004; Wojnowski, 2004; Patel and Wairkar, 2019). CsA has been reported to have high variability in its pharmacokinetic (PK) disposition (Ptachcinski et al., 1986), especially for oral dosing (Lindholm et al., 1988; Patel and Wairkar, 2019). CsA has a narrow therapeutic window for immunosuppressive purposes, usually with a whole blood trough concentration of 100–200 ng/ml for clinical indications (Marsh et al., 2009; Jain et al., 2019). Suboptimal concentration results in an insufficient clinical response, and high exposure raises patient safety concerns. The serious adverse effects included dyslipidemia, posttransplant diabetes mellitus, hypertension, intermittent renal hypoperfusion, and both reversible acute toxicity and irreversible tubulointerstitial fibrosis (Dunn et al., 2001; Olyaei et al., 2001). Its effects are different in children compared to adults because of the developmental processes, and the ontogeny of enzymes and body size could affect the disposition of the drug in the body. Thus, according to clinical guidelines, routine therapeutic drug monitoring (TDM) is strongly recommended for CsA, particularly in pediatric patients.

Population PK properties of CsA in pediatric patients have been investigated in several clinical trials, mainly targeting stem cell transplantation, posttransplantation, and nephrotic syndrome conditions (Irtan et al., 2007; Willemze et al., 2008; Kim et al., 2015; Li et al., 2019; Zhao et al., 2022). To date, population PK analysis of CsA in children with acquired AA has seldom been reported (Ni et al., 2013). Considering the remarkable difference in the physiopathology between transplantation and acquired AA, PK extrapolation across indications would have high uncertainties. This study aimed to establish a population model to characterize the PK of CsA in Chinese pediatric patients with acquired AA and to explore the potential covariate effects. The proposed population PK model can provide guidance for individual CsA therapy in pediatric patients with acquired AA.

MATERIALS AND METHODS

Study Population

The eligibility criteria for the study population were pediatric patients (≤18 years old) diagnosed with acquired AA who received CsA treatment at two hospitals in Shanghai (Children's Hospital of Fudan University and Tongji Hospital of Tongji University) from January 2014 to December 2021. The diagnosis of acquired AA was based on several critical criteria (e.g., peripheral blood investigations, bone marrow smear, and biopsy) and excluded other disease conditions such as autoimmune disease, congenital bone marrow failure, acute myeloid leukemia, acute lymphoblastic leukemia, myelodysplastic syndrome, and other malignant hematological tumors. Patients with acquired AA who received stem cell transplantation were also excluded from this study. The study protocol and the data collection were approved by the hospital's research ethics committee.

Acquired Aplastic Anemia Treatment Protocol

The acquired AA treatment regimen was in accordance with the suggestions in the clinical guidance, including IST-containing treatment (e.g., ATG + CsA, CsA + androgen, or CsA monotherapy) and supportive care measures (transfusions, protective isolation, antibiotics, and others). The initial oral dosing regimen of CsA was 5 mg/kg/day orally, twice daily. In general, the dose was adjusted from 5 to 8 mg/kg/day and could even to 10 mg/kg/day, depending on CsA concentration, to ensure that the concentration is within the therapeutic window. As per a clinical guideline for childhood acquired AA in China (The Society of Pediatrics, 2014), it was recommended that the therapeutic windows for CsA be 100–200 ng/ml and 300–400 ng/ml for trough and peak concentration, respectively. The first whole blood concentration of CsA at a steady state was monitored after 2 weeks of administration, and then every 3–6 months afterward, if indicated. The dose was reduced only after the concentration was maintained at these levels for at least 12 months. The dose was tapered slowly (e.g., 10–20% of the original dosage was tapered once every 3 months). The clinical physician closely monitored the complete blood count, liver and renal functions, and whole blood CsA concentration at each time of dose adjustment and carefully reduced the amount if there was any fluctuation. All treatments were in accordance with the diagnosis and treatment recommendations of the pediatric society of the Chinese Medical Association.

Pharmacokinetic Sampling and Measurement

For TDM purposes, only sparse whole blood samples were routinely collected for CsA concentration measurement according to clinical practice in the two study hospitals. The PK samples were collected at or around the peak (2–4 h postdosing) and predose (within 1 h prior to dosing). CsA whole blood concentrations were determined using an Emit® 2000 Cyclosporine Specific assay (6R079UL; Siemens Healthcare Diagnostics, Inc., Newark, NJ, United States) in accordance with the procedures in the manual.

Data Collection

All relevant clinical data for the present population PK analysis were collected from patients' medical records in the hospital information system. The data mainly contained: 1) Demographic data (gender, age at treatment, and body weight at treatment); 2) laboratory tests, including but not limited to complete blood count (red blood cell, white blood cell, platelets, hemoglobin [Hb], hematocrit [HCT]), liver function (aspartate transaminase [AST], alanine transaminase [ALT], alkaline phosphatase [ALP], direct bilirubin, total bilirubin [TBIL]), and renal function (serum creatinine [SCr] levels); 3) concomitant medications (e.g., granulocyte colony-stimulating factor, rabbit ATG [r-ATG], glucocorticoids, and testosterone undecanoate) during the therapy; and 4) PK data, such as the date and time of CsA administration, and CsA concentration readout.

Population Pharmacokinetic Analysis Approach

Population PK analysis was conducted using a nonlinear mixed-effect modeling approach using NONMEM® software (version 7.4, ICON Development Solutions, Ellicott City, MD, United States) with a gFortran compiler (version 4.6.0). PsN (version 4.6.0) and the R language (version 3.4.0) were used to summarize and visualize the modeling outputs. First-order conditional estimation with the η-ε interaction algorithm (FOCE-I) was utilized throughout the model-building procedures. Discrimination between hierarchical models was based on the objective function value (OFV), which was proportional to twice the log-likelihood (-2LL). A decrease in OFV (ΔOFV) of 3.84 was considered a statistically significant improvement in model fitting ($p < 0.05$) between the two hierarchical models after the inclusion of one additional parameter ($df = 1$).

CsA concentrations were logarithmically converted for modeling analysis. A base model was selected without any covariates capable of appropriately capturing the concentration–time data. During the base model selection stage, all possible structural compartments (i.e., one- and two-compartment disposition models) were investigated.

Interindividual variability (IIV) was modeled as an exponential function on all PK parameters, where applicable (**Eq. 1**).

$$\theta_i = \theta \bullet \exp\left(\eta_{i,\theta}\right) \tag{1}$$

where θ_i is the individual PK parameter estimate for the ith individual patient, θ is the population estimate of the investigated PK parameter, and $\eta_{i,\theta}$ is the IIV of the investigated PK parameter, which is assumed to follow a normal distribution with a zero mean and variance ω^2. The residual variability, assumed to be normally distributed with zero mean and variance σ^2, was modeled with an additive error on the natural log-transformed concentrations, which was approximately equal to an exponential residual error on an arithmetic scale.

Covariate Modeling

Body weight was implemented in the model as a simultaneous inclusion of an allometric function for all clearance and distribution volume parameters (**Eqs 2**, **3**, respectively).

$$CL_i = CL_{typical} \cdot \left(\frac{BW_i}{BW_{median}}\right)^{0.75} \cdot \exp\left(\eta_{i,CL}\right), \tag{2}$$

$$V_i = V_{typical} \cdot \left(\frac{BW_i}{BW_{median}}\right) \cdot \exp\left(\eta_{i,V}\right), \tag{3}$$

where BW_i is the individual body weight for the i^{th} individual and BW_{median} is the median body weight of the study population (28 kg).

In addition to body weight, other potential covariates, such as age, gender, laboratory tests of liver and renal function, and concomitant drugs, were investigated for all model parameters, except absorption-rate constant, using a forward selection ($p = 0.05$) and followed a strict backward elimination ($p = 0.01$) procedure.

Model Evaluation

Basic goodness-of-fit plots, such as the conditional weighted residue versus population prediction, conditional weighted residue versus time, observation versus population prediction, and individual prediction, were used to evaluate systematic discrepancies and model misspecification if it exists. The sampling importance resampling approach was employed to derive parameter uncertainties for the final population PK model with the options of sample = 2,000 and resample = 1,000. The overall predictive performance of the final population PK model was evaluated using prediction-corrected visual predictive checks [(Bergstrand et al., 2011), n = 1,000 simulations].

In Silico Simulation

Based on the final population PK model, *in silico* simulations were conducted according to different clinical scenarios, such as body weight, significant covariates, and dosing regimens (n = 1,000 for each scenario). The simulated PK exposure parameters (e.g., trough concentration) for each scenario were summarized and visualized.

TABLE 1 | Demographic data of children with acquired aplastic anemia.

Variable	Value
Patient numbers	157
Age (years) [median (range)]	7.8 (1.5, 18.8)
Bodyweight (kg) [median (range)]	27.5 (12.0, 91.0)
The severity of AA, *n* (%)	
NSAA	94 (59.9)
SAA	40 (25.4)
vSAA	21 (13.4)
Biochemistry tests [median (range)]	
White blood cell (10^9/L)	3.97 (0.26, 12.10)
Hb (g/ml)	85 (48.2, 150)
Neutrophil (%)	34.4 (1.1, 83.0)
Blood urea nitrogen (mmol/L)	5.10 (1.10, 16.30)
Total protein (g/L)	66.8 (45.5, 86.6)
Albumin (g/L)	40.3 (25.8, 48.4)
ALT	13.0 (1.0, 209.9)
AST	21.0 (8.0, 91.3)
Total bilirubin (μmol/L)	10.90 (4.00, 70.00)
Direct bilirubin (μmol/L)	2.50 (0.30, 39.50)
Serum creatine (μmol/L)	40.0 (16.0, 127.0)
Concomitant medications, *n* (%)	
Testosterone undecanoate	111 (70.7)
Prednisone	24 (15.3)
Methylprednisolone	47 (29.9)
Prednisolone	2 (1.3)
Dexamethasone	1 (0.6)
r-ATG	47 (29.9)
Granulocyte colony-stimulating factor	27 (17.2)

Note: The continuous variables were presented as median (range). NSAA, nonsevere aplastic anemia; SAA, severe aplastic anemia; vSAA, very severe aplastic anemia; Hb, hemoglobin; ALT, alanine transaminase; AST, aspartate transaminase; r-ATG, rabbit anti-thymocyte globulin.

RESULTS

In total, 681 whole blood CsA concentrations of samples from 157 pediatric patients were included in the current population PK modeling analysis. The basic demographic characteristics of patients are presented in **Table 1**. Overall, the baseline demographic data of the patients were comparable between the two hospitals.

A one-compartment model with first-order absorption and elimination processes offered an OFV of 299.011. Utilizing a two-compartment model indicated a significant improvement in the model fit (ΔOFV = −249.597). However, the peripheral volume of distribution estimate was implausible (6350 L); therefore, this parameter and intercompartment clearance were fixed at 496 and 5 L/h, respectively, according to the reported literature value (Eljebari et al., 2012). This model still resulted in a superior model fit compared with the one-compartment model (ΔOFV = −136.676).

Body weight implemented as an allometric function on all clearance and volume of distribution parameters in the model did not lead to a worse model (ΔOFV = −1.363).

Further inclusion of albumin (ALB) on clearance with a linear function resulted in a significant decrease in OFV (ΔOFV = −11.425). However, the parameter estimate had poor precision (RSE = 56%); therefore, ALB was not retained in the model. Inclusion of TBIL on clearance in a linear manner led to a significant improvement in the model fit (ΔOFV = −8.762) with a good precision of estimate (RSE = 20.4%) and therefore was retained in the model. Other covariates had no statistically significant effects on PK parameters.

The final parameter estimates had a good precision (RSE<30%) and confirmed the stability of the model (**Table 2**). The basic goodness-of-fit diagnostic plots (**Figure 1**) did not show any evident systematic discrepancies. Overall, the predictive-corrected visual predictive checks showed good consistency between the model-predicted and observed CsA concentration versus time profiles, although the maximum concentrations were slightly underestimated (**Figure 2**).

In Silico Simulation

After orally administering a 5 mg/kg daily dose of CsA, the model predicted a trough concentration at a steady state by body weight and TBIL levels, as shown in **Figure 3**. Considering the proposed dosing regimen, the exposure in pediatric patients with low body weight bands (<30 kg) was below the therapeutic windows (100–200 ng/ml), suggesting that an increase in dosage must be considered to achieve sufficient exposure. Moreover, pediatric patients with higher TBIL levels appeared to have higher exposure, and dose reduction in these patients was deemed necessary.

DISCUSSION

This is a pooled population PK analysis of CsA in pediatric patients with acquired AA in two study hospitals. The proposed population PK model could accurately describe the PK properties of CsA in the target population, and TBIL could affect clearance.

As CsA has high variability in PK profiles, routine TDM is mandatory in clinical practice for individual therapy. The population PK approach combined with Bayesian estimates for individual PK parameters offers a powerful tool to achieve this purpose. Regarding the structural model in population analyses for CsA, the one-compartment deposition model was commonly used for sparse PK data (Xiaoli and Qiang, 2009; Ni et al., 2013; Li et al., 2019; Albitar et al., 2020). The current modeling analysis using CsA trough and peak concentrations suggested an appropriate two-compartment disposition model, which was consistent with several published CsA population analyses (Wilhelm et al., 2012; Okada et al., 2017). In the current investigation, the apparent clearance (CL/F) estimate for a typical 28 kg child was 29.1 L/h, which was higher than that reported in a previous study including 102 children with AA (15.1 L in a child weighing 29.8 kg) (Ni et al., 2013). The discrepancy in CL/F might be attributed to the difference in sampling strategy (trough and peak concentrations in our study) and the sequential utilization of different structural models. However, the CL/F estimate in the present study was within

TABLE 2 | Pharmacokinetic parameter estimates from the final population model of cyclosporine A in children with acquired aplastic anemia.

Parameters	NM estimates	SIR median (95%CI)	CV for IIV	SIR median (95%CI)	Shrinkage (%)
Ka (/h)	1.26 (20.9)	1.27 (0.78–2.02)	—	—	—
CL/F (L/h)	29.1 (3.8)	29.0 (26.9–31.2)	28.0 (24.9)	28.7 (20.9–35.7)	34.7
V_C/F (L)	325 (15.7)	319 (273–398)	62.1 (29.3)	62.1 (48.7–77.3)	43.6
Q/F (L/h)	3.1 FIX	—	—	—	—
V_P/F—(L)	262 FIX	—	—	—	—
TBIL on CL (%)	−1.07 (20.4)	−1.05 (−1.50 to −0.50)	—	—	—
σ	0.348 (10.1)	0.348 (0.356–0.393)	—	—	—

Ka is the first-order absorption-rate constant. CL/F represents the apparent elimination clearance. V_C/F is the apparent central volume of the distribution. Q/F is the apparent intercompartmental clearance. V_P/F is the apparent peripheral volume of the distribution. σ is the additive residue error on the logarithmic scale. Population estimates in Table 2 are given for a "typical" child with a body weight of 28 kg. Body weight was implemented as a fixed allometric function on all clearance and volume of distribution parameters using a power coefficient of 0.75 and 1.0, respectively. The coefficient of variation for interindividual variability (IIV) was calculated as 100 × ($e^{variance}$)$^{1/2}$. The relative standard error (%RSE) was calculated as 100 × (standard deviation/mean). The total bilirubin (TBIL) was implemented on the CL as a linear function (CL = $CL_{typical}$ × ((TBIL-10.65) × −0.0107)). SIR: Sampling importance resampling approach. The uncertainty was derived from the SIR with 2,000 samples and 1,000 resamples.

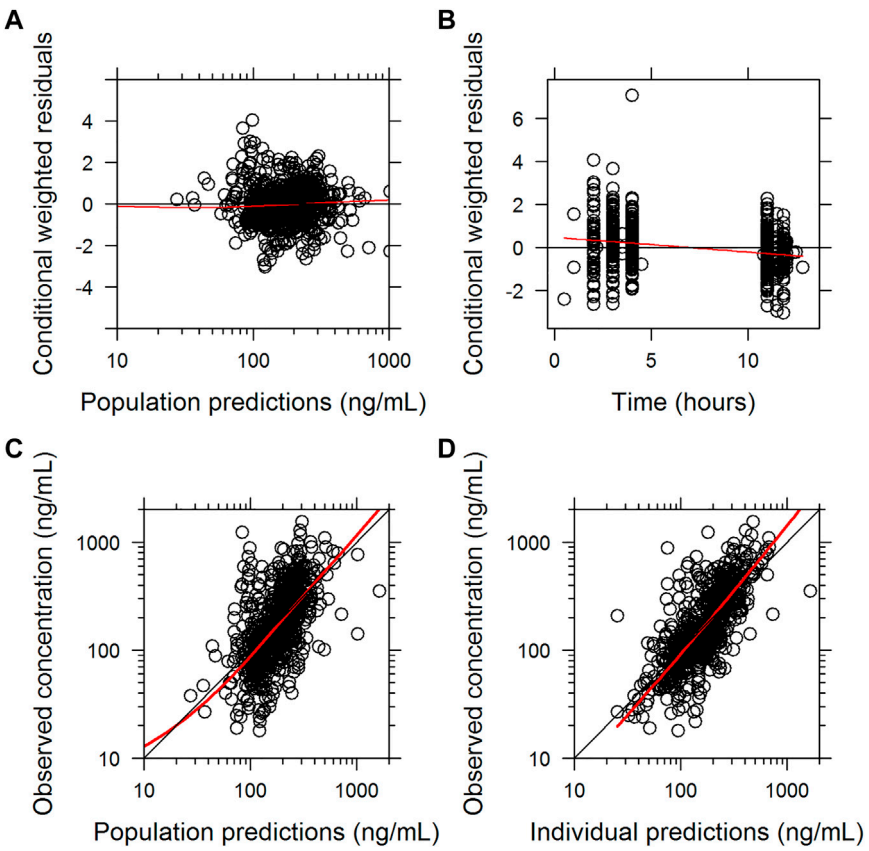

FIGURE 1 | Basic goodness of fit of the final population pharmacokinetic model of cyclosporine A. **(A)** conditionally weighted residuals vs. population-predicted concentrations**. (B)** conditionally weighted residuals vs. time. **(C)** observed plasma concentrations vs. population-predicted concentrations. **(D)** observed plasma concentrations vs. individually predicted concentrations; solid red lines represent locally weighted least-squares regressions.

the range of that of published population PK models for pediatric patients receiving transplantation. The CL/F was 23.1 L/h in 98 pediatric renal transplant patients weighing 35.2 kg (Irtan et al., 2007) and 29.3 L/h in 17 pediatric patients receiving stem cell transplantation with an average body weight of 32.4 kg (Willemze et al., 2008). In the present study, the central volume (Vc/F) estimate was 325 L for a typical 28 kg child, which was higher than that reported in a previous pediatric AA study (89.1 L for a 29.8 kg child) (Ni et al., 2013), pediatric patients who received renal transplants (70.3 L for a 35.2 kg child) (Irtan et al., 2007), and pediatric patients who received stem cell transplantation (42.7 L for a 32.4 kg child)

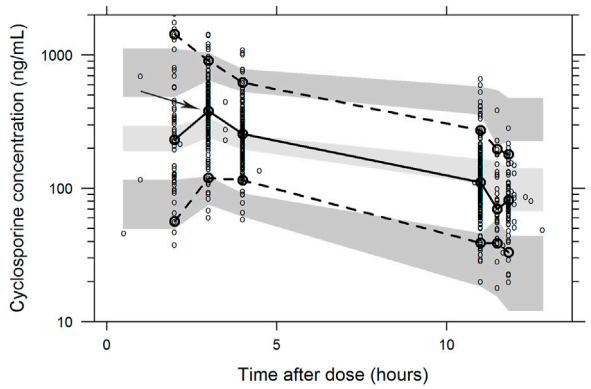

FIGURE 2 | Visual predictive check of the final population pharmacokinetic model of cyclosporine A. The visual predictive check was based on 1,000 stochastic simulations. Open circles are the observations and solid lines represent the 5th, 50th, and 95th percentiles of the observed data. The shaded areas represent 95% prediction intervals around the simulated 5th, 50th, and 95th percentiles. The Cmax was slightly underestimated.

(Willemze et al., 2008) and lower than that reported in a recent study of Chinese pediatric patients with nephrotic syndrome (2320 L for a typical 25 kg child) (Zhao et al., 2022). The Vc/F estimate was still within the range of reported values from literature. Moreover, the total V/F (Vc + Vp) normalized to a 70 kg adult was 1,468 L, which was similar to those reported in some studies with adult patients (1,080 and 1,010 L for Chinese adults (Zhou et al., 2012; Wang et al., 2022), and 1,990 L for Korean adults (Ji et al., 2011)).

Considering the principles of allometry in pediatrics, the body weight was highly suggested to be included in the model (Holford et al., 2013). Fanta et al. (2007) conducted a population PK analysis for 162 pediatric patients before a transplant and found that young patients (<8 years) had approximately 25% higher body weight normalized clearance than older children. In a population PK study of pediatric patients with acquired AA, the body weight was found to correlate with CL/F and V/F (Ni et al., 2013). In the present study, we applied the body weight value in all the clearance and volume parameters as an allometric function with the fixed exponent of 0.75 and 1.0, respectively, which did not result in a poor model. In addition, a few studies included body surface area (BSA) (Okada et al., 2017) in the model; however, this variable was not investigated in the present study since some height data were missing, and we were unable to calculate the BSA.

Since CsA undergoes liver metabolism and renal elimination, laboratory tests for liver and renal function show that PK disposition is seemingly affected in the body. Fanta et al. (2007) suggested that total plasma cholesterol level was correlated with CL/F in pediatric patients undergoing renal transplantation, with a 5.4% reduction per 1 mmol/L increase in cholesterol level. A population PK analysis of Chinese patients who underwent allogeneic hematopoietic stem cell transplantation showed that the plasma albumin level was inversely correlated with CL/F, with a 2.89% drop per 1 g/L increase in albumin level (Zhou et al., 2012). In the present study, total plasma cholesterol level was not routinely measured during outpatient visits; therefore, this covariate was not investigated. Moreover, we had a similar finding on the albumin covariate, but considering the poor precision of the estimate (>50%), the albumin value was removed from the final model. We identified TBIL as a significant covariate on CL/F, with a 1.07% reduction per 1 nmol/L rise in TBIL. Several studies on patients with transplantation have reported that TBIL, a biomarker of liver function, was relevant to CL/F (Wu et al., 2005; Ji et al., 2011). This finding suggested that dose adjustment may be required in patients with elevated TBIL levels.

Ni et al. (2013) found that SCr levels were a significant covariate on CL/F in pediatric patients with AA, with an 8.1% decrease per 1 μmol/L increase in SCr. Fanta et al. (2007)

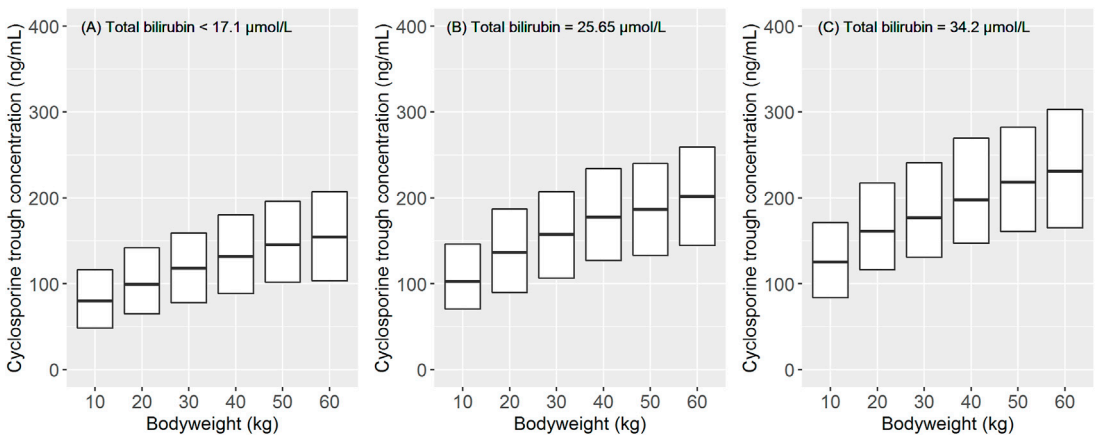

FIGURE 3 | Impact of body weight and total bilirubin level on the pharmacokinetic exposure at steady state after the oral administration of cyclosporine A (5 mg/kg/d). The data of 1,000 children were used for the simulation for each body weight band. The simulation was stratified by different total bilirubin levels: **(A)** the normal level (<17.1 μmol/L). **(B)** and **(C)** 1.5 and 2 times the upper limits of the normal level (25.65 and 34.2 μmol/L), respectively. The total simulated exposure was presented as median values (25th–75th percentiles).

indicated that SCr levels were significantly correlated with CL/F in children undergoing renal transplantation, although the covariate effect size was small. A population PK analysis of CsA in Chinese pediatric patients receiving hematopoietic stem cell transplantation suggested a nonlinear relationship between estimated glomerular filtration rates and CL/F, with an exponent of 0.545 in power function (Li et al., 2019). In the present study, we did not identify a significant effect of SCr levels; the most likely explanation was that the majority of children had normal renal functions during the treatment period. Moreover, CsA was highly bound to erythrocytes and plasma proteins, and its distribution in the blood was reported to be approximately 41–58% in erythrocytes (Han et al., 2013). HCT was considered a significant covariate in a few previous studies (Wu et al., 2005; Yin et al., 2006; Fanta et al., 2007; Zhou et al., 2012). However, we did not find such a relationship in this study. Considering transfusion was needed in some patients, the relationship between Hb and Vc/F has been assessed with no statistical significance in the present study. However, a power relationship was suggested, with the exponent estimate of 0.159. Again, the Vc/F estimate was 290 L for a typical child with a Hb level of 85 g/L. The impact of Hb on Vc/F was not substantial.

Concomitant drugs, such as anabolic steroids (Ni et al., 2013) and triazole antifungal agents (Zhou et al., 2012; Li et al., 2019; Ling et al., 2021), have been reported to affect CsA PK exposure. Children undergoing IST often receive steroids as a concomitant drug (Ettenger, 1998; Benfield et al., 1999; Clucas et al., 2019). In theory, steroids could reduce CYP450 3A metabolism in CsA *via* competitive inhibition (Nakamura et al., 2002). The effects of steroids (methylprednisolone, prednisolone, or prednisone) on CsA PK exposure were further assessed in adult patients (Lam et al., 2008). In the present study, five types of steroids (**Table 1**) were comedicated with CsA in the treatment; however, the most frequently used steroids (testosterone, prednisone, and methylprednisolone) did not significantly influence CL/F according to the modeling analysis. Moreover, only a few patients (<5%) received triazole antifungal agent treatment, and its effect on CL/F was not further investigated.

This study has several limitations. 1) The CsA data were retrospectively collected from two centers, and a prospective clinical study would improve the data accuracy. 2) Enzyme polymorphisms have been demonstrated to contribute to the PK variability in CsA. However, relevant CYP3A and ABCB1 polymorphisms were not detected in this study, which may reduce the chance of finding polymorphism-related covariates. 3) In the present study, only two covariates were included in the final model; other significant covariates such as albumin were not retained due to the poor precision of parameter estimation. This model should, in the future, be updated with emerging data, which will allow the assessment of the covariates in a broader population and improve the goodness of fit accordingly, especially for population/individual predictions versus observation plots.

CONCLUSION

In this study, we developed a population PK model to describe the PK property of CsA in Chinese pediatric patients with acquired AA. Body weight and TBIL level were significant covariates for the PK disposition of CsA. The proposed model could inform precision medicine in CsA therapy for pediatric patients with acquired AA.

DATA AVAILABILITY STATEMENT

The original contributions presented in the study are included in the article/Supplementary Materials; further inquiries can be directed to the corresponding authors.

ETHICS STATEMENT

The studies involving human participants were reviewed and approved by the Research Ethics Committee of the Children's Hospital of Fudan University. Written informed consent to participate in this study was provided by the participants' legal guardian/next of kin.

AUTHOR CONTRIBUTIONS

X-WZ and H-SW conceived and designed the study. XG, Z-LB, X-HQ, X-WQ, JL, G-MS, HM, YY, J-HM, X-HZ, J-YJ, JL, and LY collected the data, whereas X-WZ and H-SW evaluated the data. XG, Z-LB, and X-HQ built the model and wrote the manuscript. X-WZ and H-SW have reviewed and edited the manuscript. All the authors have read and approved the final manuscript.

FUNDING

This work was supported by the Science and Technology Commission of Shanghai Municipality (21Y31900302) and Cyrus Tang Foundation (ZSBK0070).

ACKNOWLEDGMENTS

We would like to pay our sincere and kind respect to pediatric patients for their participation, to the doctors and nurses at the Children's Hospital of Fudan University and Tongji Hospital of Tongji University for taking care of the patients, and to the lab and the Department of Pharmacy for measurements.

REFERENCES

Albitar, O., Ballouze, R., Harun, S. N., Mohamed Noor, D. A., and Sheikh Ghadzi, S. M. (2020). Population Pharmacokinetic Modeling of Cyclosporine Among Malaysian Renal Transplant Patients: An Evaluation of Methods to Handle Missing Doses in Conventional Drug-Monitoring Data. *J. Clin. Pharmacol.* 60, 1474–1482. doi:10.1002/jcph.1670

Aoyama, T., Yamano, S., Waxman, D. J., Lapenson, D. P., Meyer, U. A., Fischer, V., et al. (1989). Cytochrome P-450 hPCN3, a Novel Cytochrome P-450 IIIA Gene Product that Is Differentially Expressed in Adult Human Liver. cDNA and Deduced Amino Acid Sequence and Distinct Specificities of cDNA-Expressed hPCN1 and hPCN3 for the Metabolism of Steroid Hormones and Cyclosporine. *J. Biol. Chem.* 264, 10388–10395. doi:10.1016/s0021-9258(18)81632-5

Bacigalupo, A., Hows, J., Gluckman, E., Nissen, C., Marsh, J., Van Lint, M. T., et al. (1988). Bone Marrow Transplantation (BMT) versus Immunosuppression for the Treatment of Severe Aplastic Anaemia (SAA): a Report of the EBMT SAA Working Party. *Br. J. Haematol.* 70, 177–182. doi:10.1111/j.1365-2141.1988.tb02460.x

Benfield, M. R., Stablein, D., and Tejani, A. (1999). Trends in Immunosuppressive Therapy: a Report of the North American Pediatric Renal Transplant Cooperative Study (NAPRTCS). *Pediatr. Transpl.* 3, 27–32. doi:10.1034/j.1399-3046.1999.00001.x

Bergstrand, M., Hooker, A. C., Wallin, J. E., and Karlsson, M. O. (2011). Prediction-corrected Visual Predictive Checks for Diagnosing Nonlinear Mixed-Effects Models. *Aaps J.* 13, 143–151. doi:10.1208/s12248-011-9255-z

Brodsky, R. A., and Jones, R. J. (2005). Aplastic Anaemia. *Lancet* 365, 1647–1656. doi:10.1016/s0140-6736(05)66515-4

Camitta, B. M., Rappeport, J. M., Parkman, R., and Nathan, D. G. (1975). Selection of Patients for Bone Marrow Transplantation in Severe Aplastic Anemia. *Blood* 45, 355–363. doi:10.1182/blood.v45.3.355.bloodjournal453355

Camitta, B. M., Thomas, E. D., Nathan, D. G., Santos, G., Gordon-Smith, E. C., Gale, R. P., et al. (1976). Severe Aplastic Anemia: a Prospective Study of the Effect of Early Marrow Transplantation on Acute Mortality. *Blood* 48, 63–70. doi:10.1182/blood.V48.1.63.63

Clucas, D. B., Fox, L. C., Wood, E. M., Hong, F. S., Gibson, J., Bajel, A., et al. (2019). Revisiting Acquired Aplastic Anaemia: Current Concepts in Diagnosis and Management. *Intern Med. J.* 49, 152–159. doi:10.1111/imj.14140

Deyell, R. J., Shereck, E. B., Milner, R. A., and Schultz, K. R. (2011). Immunosuppressive Therapy without Hematopoietic Growth Factor Exposure in Pediatric Acquired Aplastic Anemia. *Pediatr. Hematol. Oncol.* 28, 469–478. doi:10.3109/08880018.2011.568043

Dufour, C., Pillon, M., Sociè, G., Rovò, A., Carraro, E., Bacigalupo, A., et al. (2015). Outcome of Aplastic Anaemia in Children. A Study by the Severe Aplastic Anaemia and Paediatric Disease Working Parties of the European Group Blood and Bone Marrow Transplant. *Br. J. Haematol.* 169, 565–573. doi:10.1111/bjh.13297

Dunn, C. J., Wagstaff, A. J., Perry, C. M., Plosker, G. L., and Goa, K. L. (2001). Cyclosporin: an Updated Review of the Pharmacokinetic Properties, Clinical Efficacy and Tolerability of a Microemulsion-Based Formulation (Neoral)1 in Organ Transplantation. *Drugs* 61, 1957–2016. doi:10.2165/00003495-200161130-00006

Eljebari, H., Gaies, E., Fradj, N. B., Jebabli, N., Salouage, I., Trabelsi, S., et al. (2012). Population Pharmacokinetics and Bayesian Estimation of Cyclosporine in a Tunisian Population of Hematopoietic Stem Cell Transplant Recipient. *Eur. J. Clin. Pharmacol.* 68, 1517–1524. doi:10.1007/s00228-012-1275-9

Ettenger, R. B. (1998). New Immunosuppressive Agents in Pediatric Renal Transplantation. *Transpl. Proc.* 30, 1956–1958. doi:10.1016/s0041-1345(98)00493-x

Fanta, S., Jönsson, S., Backman, J. T., Karlsson, M. O., and Hoppu, K. (2007). Developmental Pharmacokinetics of Ciclosporin-Aa Population Pharmacokinetic Study in Paediatric Renal Transplant Candidates. *Br. J. Clin. Pharmacol.* 64, 772–784. doi:10.1111/j.1365-2125.2007.03003.x

Frickhofen, N., Kaltwasser, J. P., Schrezenmeier, H., Raghavachar, A., Vogt, H. G., Herrmann, F., et al. (1991). Treatment of Aplastic Anemia with Antilymphocyte Globulin and Methylprednisolone with or without Cyclosporine. The German Aplastic Anemia Study Group. *N. Engl. J. Med.* 324, 1297–1304. doi:10.1056/nejm199105093241901

Frickhofen, N., and Rosenfeld, S. J. (2000). Immunosuppressive Treatment of Aplastic Anemia with Antithymocyte Globulin and Cyclosporine. *Semin. Hematol.* 37, 56–68. doi:10.1016/s0037-1963(00)90030-1

Führer, M., Rampf, U., Baumann, I., Faldum, A., Niemeyer, C., Janka-Schaub, G., et al. (2005). Immunosuppressive Therapy for Aplastic Anemia in Children: a More Severe Disease Predicts Better Survival. *Blood* 106, 2102–2104. doi:10.1182/blood-2005-03-0874

Han, K., Pillai, V. C., and Venkataramanan, R. (2013). Population Pharmacokinetics of Cyclosporine in Transplant Recipients. *AAPS J.* 15, 901–912. doi:10.1208/s12248-013-9500-8

Holford, N., Heo, Y. A., and Anderson, B. (2013). A Pharmacokinetic Standard for Babies and Adults. *J. Pharm. Sci.* 102, 2941–2952. doi:10.1002/jps.23574

Irtan, S., Saint-Marcoux, F., Rousseau, A., Zhang, D., Leroy, V., Marquet, P., et al. (2007). Population Pharmacokinetics and Bayesian Estimator of Cyclosporine in Pediatric Renal Transplant Patients. *Ther. Drug Monit.* 29, 96–102. doi:10.1097/FTD.0b013e3180310f9d

Issaragrisil, S., Sriratanasatavorn, C., Piankijagum, A., Vannasaeng, S., Porapakkham, Y., Leaverton, P. E., et al. (1991). Incidence of Aplastic Anemia in Bangkok. The Aplastic Anemia Study Group. *Blood* 77, 2166–2168. doi:10.1182/blood.v77.10.2166.bloodjournal77102166

Jain, R., Trehan, A., Bansal, D., and Varma, N. (2019). Aplastic Anemia in Children: How Good Is Immunosuppressive Therapy? *Pediatr. Hematol. Oncol.* 36, 211–221. doi:10.1080/08880018.2019.1621970

Jeong, D. C., Chung, N. G., Kang, H. J., Koo, H. H., Kook, H., Kim, S. K., et al. (2011). Epidemiology and Clinical Long-Term Outcome of Childhood Aplastic Anemia in Korea for 15 Years: Retrospective Study of the Korean Society of Pediatric Hematology Oncology (KSPHO). *J. Pediatr. Hematol. Oncol.* 33, 172–178. doi:10.1097/MPH.0b013e31820826a8

Ji, E., Kim, M. Y., Yun, H. Y., Kim, K. I., Kang, W., Kwon, K. I., et al. (2011). Population Pharmacokinetics of Cyclosporine in Korean Adults Undergoing Living-Donor Kidney Transplantation. *Pharmacotherapy* 31, 574–584. doi:10.1592/phco.31.6.574

Kim, M. G., Kim, I. W., Choi, B., Han, N., Yun, H. Y., Park, S., et al. (2015). Population Pharmacokinetics of Cyclosporine in Hematopoietic Stem Cell Transplant Patients: Consideration of Genetic Polymorphisms. *Ann. Pharmacother.* 49, 622–630. doi:10.1177/1060028015577798

Kronbach, T., Fischer, V., and Meyer, U. A. (1988). Cyclosporine Metabolism in Human Liver: Identification of a Cytochrome P-450III Gene Family as the Major Cyclosporine-Metabolizing Enzyme Explains Interactions of Cyclosporine with Other Drugs. *Clin. Pharmacol. Ther.* 43, 630–635. doi:10.1038/clpt.1988.87

Lam, S., Partovi, N., Ting, L. S., and Ensom, M. H. (2008). Corticosteroid Interactions with Cyclosporine, Tacrolimus, Mycophenolate, and Sirolimus: Fact or Fiction? *Ann. Pharmacother.* 42, 1037–1047. doi:10.1345/aph.1K628

Li, T. F., Hu, L., Ma, X. L., Huang, L., Liu, X. M., Luo, X. X., et al. (2019). Population Pharmacokinetics of Cyclosporine in Chinese Children Receiving Hematopoietic Stem Cell Transplantation. *Acta Pharmacol. Sin.* 40, 1603–1610. doi:10.1038/s41401-019-0277-x

Lindholm, A., Henricsson, S., Lind, M., and Dahlqvist, R. (1988). Intraindividual Variability in the Relative Systemic Availability of Cyclosporin after Oral Dosing. *Eur. J. Clin. Pharmacol.* 34, 461–464. doi:10.1007/bf01046702

Ling, J., Yang, X. P., Dong, L. L., Jiang, Y., Zou, S. L., Hu, N., et al. (2021). Population Pharmacokinetics of Ciclosporin in Allogeneic Hematopoietic Stem Cell Transplant Recipients: C-reactive Protein as a Novel Covariate for Clearance. *Clin. Pharm. Ther.* 47, 483–492. doi:10.1111/jcpt.13569

Locasciulli, A., Oneto, R., Bacigalupo, A., Socié, G., Korthof, E., Bekassy, A., et al. (2007). Outcome of Patients with Acquired Aplastic Anemia Given First Line Bone Marrow Transplantation or Immunosuppressive Treatment in the Last Decade: a Report from the European Group for Blood and Marrow Transplantation (EBMT). *Haematologica* 92, 11–18. doi:10.3324/haematol.10075

Marsh, J., Schrezenmeier, H., Marin, P., Ilhan, O., Ljungman, P., Mccann, S., et al. (1999). Prospective Randomized Multicenter Study Comparing Cyclosporin Alone versus the Combination of Antithymocyte Globulin and Cyclosporin for Treatment of Patients with Nonsevere Aplastic Anemia: A Report from the European Blood and Marrow Transplant (EBMT) Severe Aplastic Anaemia Working Party. *Blood* 93, 2191–2195. doi:10.1182/blood.V93.7.2191

Marsh, J. C. W., Ball, S. E., Cavenagh, J., Darbyshire, P., Dokal, I., Gordon-Smith, E. C., et al. (2009). Guidelines for the Diagnosis and Management of Aplastic Anaemia. *Br. J. Haematol.* 147, 43–70. doi:10.1111/j.1365-2141.2009.07842.x

Montané, E., Ibáñez, L., Vidal, X., Ballarín, E., Puig, R., García, N., et al. (2008). Epidemiology of Aplastic Anemia: a Prospective Multicenter Study. *Haematologica* 93, 518–523. doi:10.3324/haematol.12020

Nakamura, H., Nakasa, H., Ishii, I., Ariyoshi, N., Igarashi, T., Ohmori, S., et al. (2002). Effects of Endogenous Steroids on CYP3A4-Mediated Drug Metabolism by Human Liver Microsomes. *Drug Metab. Dispos.* 30, 534–540. doi:10.1124/dmd.30.5.534

Ni, S. Q., Zhao, W., Wang, J., Zeng, S., Chen, S. Q., Jacqz-Aigrain, E., et al. (2013). Population Pharmacokinetics of Ciclosporin in Chinese Children with Aplastic Anemia: Effects of Weight, Renal Function and Stanozolol Administration. *Acta Pharmacol. Sin.* 34, 969–975. doi:10.1038/aps.2013.9

Okada, A., Ushigome, H., Kanamori, M., Morikochi, A., Kasai, H., Kosaka, T., et al. (2017). Population Pharmacokinetics of Cyclosporine A in Japanese Renal Transplant Patients: Comprehensive Analysis in a Single Center. *Eur. J. Clin. Pharmacol.* 73, 1111–1119. doi:10.1007/s00228-017-2279-2

Olyaei, A. J., De Mattos, A. M., and Bennett, W. M. (2001). Nephrotoxicity of Immunosuppressive Drugs: New Insight and Preventive Strategies. *Curr. Opin. Crit. Care* 7, 384–389. doi:10.1097/00075198-200112000-00003

Patel, D., and Wairkar, S. (2019). Recent Advances in Cyclosporine Drug Delivery: Challenges and Opportunities. *Drug Deliv. Transl. Res.* 9, 1067–1081. doi:10.1007/s13346-019-00650-1

Pongtanakul, B., Das, P. K., Charpentier, K., and Dror, Y. (2008). Outcome of Children with Aplastic Anemia Treated with Immunosuppressive Therapy. *Pediatr. Blood Cancer* 50, 52–57. doi:10.1002/pbc.21377

Ptachcinski, R. J., Venkataramanan, R., and Burckart, G. J. (1986). Clinical Pharmacokinetics of Cyclosporin. *Clin. Pharmacokinet.* 11, 107–132. doi:10.2165/00003088-198611020-00002

Rosenfeld, S., Follmann, D., Nunez, O., and Young, N. S. (2003). Antithymocyte Globulin and Cyclosporine for Severe Aplastic Anemia: Association between Hematologic Response and Long-Term Outcome. *Jama* 289, 1130–1135. doi:10.1001/jama.289.9.1130

Rosenfeld, S. J., Kimball, J., Vining, D., and Young, N. S. (1995). Intensive Immunosuppression with Antithymocyte Globulin and Cyclosporine as Treatment for Severe Acquired Aplastic Anemia. *Blood* 85, 3058–3065. doi:10.1182/blood.v85.11.3058.bloodjournal85113058

Samarasinghe, S., Steward, C., Hiwarkar, P., Saif, M. A., Hough, R., Webb, D., et al. (2012). Excellent Outcome of Matched Unrelated Donor Transplantation in Paediatric Aplastic Anaemia Following Failure with Immunosuppressive Therapy: a United Kingdom Multicentre Retrospective Experience. *Br. J. Haematol.* 157, 339–346. doi:10.1111/j.1365-2141.2012.09066.x

Saracco, P., Quarello, P., Iori, A. P., Zecca, M., Longoni, D., Svahn, J., et al. (2008). Bone Marrow Failure Study Group of the, ACyclosporin A Response and Dependence in Children with Acquired Aplastic Anaemia: a Multicentre Retrospective Study with Long-Term Observation Follow-Up. *Br. J. Haematol.* 140, 197–205. doi:10.1111/j.1365-2141.2007.06903.x

Shallis, R. M., Ahmad, R., and Zeidan, A. M. (2018). Aplastic Anemia: Etiology, Molecular Pathogenesis, and Emerging Concepts. *Eur. J. Haematol.* 101, 711–720. doi:10.1111/ejh.13153

Speck, B., Gluckman, E., Haak, H. L., and Van Rood, J. J. (1977). Treatment of Aplastic Anaemia by Antilymphocyte Globulin with and without Allogeneic Bone-Marrow Infusions. *Lancet* 2, 1145–1148. doi:10.1016/s0140-6736(77)91537-9

The Society of Pediatrics, C. M. A. (2014). Recommendations on Diagnosis and Treatment for Childhood Acquired Aplastic Anemia. *Chin. J. Pediatr.* 52, 103–106. doi:10.3760/cma.j.issn.0578-1310.2014.02.006

Viollier, R., Passweg, J., Gregor, M., Favre, G., Kühne, T., Nissen, C., et al. (2005). Quality-adjusted Survival Analysis Shows Differences in Outcome after Immunosuppression or Bone Marrow Transplantation in Aplastic Anemia. *Ann. Hematol.* 84, 47–55. doi:10.1007/s00277-004-0930-3

Von Richter, O., Burk, O., Fromm, M. F., Thon, K. P., Eichelbaum, M., and Kivistö, K. T. (2004). Cytochrome P450 3A4 and P-Glycoprotein Expression in Human Small Intestinal Enterocytes and Hepatocytes: a Comparative Analysis in Paired Tissue Specimens. *Clin. Pharmacol. Ther.* 75, 172–183. doi:10.1016/j.clpt.2003.10.008

Wang, D. D., He, S. M., Yang, Y., Mao, Y. Z., Yin, D., Zheng, Z. Q., et al. (2022). Effects of Cimetidine on Ciclosporin Population Pharmacokinetics and Initial Dose Optimization in Aplastic Anemia Patients. *Eur. J. Pharm. Sci.* 174, 106183. doi:10.1016/j.ejps.2022.106183

Wilhelm, A. J., De Graaf, P., Veldkamp, A. I., Janssen, J. J., Huijgens, P. C., and Swart, E. L. (2012). Population Pharmacokinetics of Ciclosporin in Haematopoietic Allogeneic Stem Cell Transplantation with Emphasis on Limited Sampling Strategy. *Br. J. Clin. Pharmacol.* 73, 553–563. doi:10.1111/j.1365-2125.2011.04116.x

Willemze, A. J., Cremers, S. C., Schoemaker, R. C., Lankester, A. C., Den Hartigh, J., Burggraaf, J., et al. (2008). Ciclosporin Kinetics in Children after Stem Cell Transplantation. *Br. J. Clin. Pharmacol.* 66, 539–545. doi:10.1111/j.1365-2125.2008.03217.x

Wojnowski, L. (2004). Genetics of the Variable Expression of CYP3A in Humans. *Ther. Drug Monit.* 26, 192–199. doi:10.1097/00007691-200404000-00019

Wu, K. H., Cui, Y. M., Guo, J. F., Zhou, Y., Zhai, S. D., Cui, F. D., et al. (2005). Population Pharmacokinetics of Cyclosporine in Clinical Renal Transplant Patients. *Drug Metab. Dispos.* 33, 1268–1275. doi:10.1124/dmd.105.004358

Xiaoli, D., and Qiang, F. (2009). Population Pharmacokinetic Study of Cyclosporine in Patients with Nephrotic Syndrome. *J. Clin. Pharmacol.* 49, 782–788. doi:10.1177/0091270009337132

Yin, O. Q., Lau, S. K., and Chow, M. S. (2006). Population Pharmacokinetics of Cyclosporine in Chinese Cardiac Transplant Recipients. *Pharmacotherapy* 26, 790–797. doi:10.1592/phco.26.6.790

Yoshida, N., and Kojima, S. (2018). Updated Guidelines for the Treatment of Acquired Aplastic Anemia in Children. *Curr. Oncol. Rep.* 20, 67. doi:10.1007/s11912-018-0716-8

Young, N. S., and Kaufman, D. W. (2008). The Epidemiology of Acquired Aplastic Anemia. *Haematologica* 93, 489–492. doi:10.3324/haematol.12855

Zhao, Y., He, H., Zang, Y., Zhao, L., and Wang, X. (2022). Population Pharmacokinetics and Dose Simulation of Cyclosporine in Chinese Children with Nephrotic Syndrome: Effects of Weight and Total Cholesterol. *Int. J. Clin. Pharmacol. Ther.* 60, 87–96. doi:10.5414/cp203921

Zhou, H., Gao, Y., Cheng, X. L., and Li, Z. D. (2012). Population Pharmacokinetics of Cyclosporine A Based on NONMEM in Chinese Allogeneic Hematopoietic Stem Cell Transplantation Recipients. *Eur. J. Drug Metab. Pharmacokinet.* 37, 271–278. doi:10.1007/s13318-012-0087-8

Conflict of Interest: The authors declare that the research was conducted in the absence of any commercial or financial relationships that could be construed as potential conflicts of interest.

Publisher's Note: All claims expressed in this article are solely those of the authors and do not necessarily represent those of their affiliated organizations or those of the publisher, the editors, and the reviewers. Any product that may be evaluated in this article, or claim that may be made by its manufacturer, is not guaranteed or endorsed by the publisher.

frontiers | Frontiers in Pharmacology

TYPE Original Research
PUBLISHED 11 August 2022
DOI 10.3389/fphar.2022.955809

OPEN ACCESS

EDITED BY
Yang Zhou,
Brown University, United States

REVIEWED BY
Zhixin Zhang,
China-Japan Friendship Hospital, China
Huiwen Zhang,
Xinhua Hospital, China

*CORRESPONDENCE
Junfen Fu,
fjf68@zju.edu.cn
Shaoqing Ni,
chnsq@zju.edu.cn

†These authors have contributed equally to this work and share first authorship

SPECIALTY SECTION
This article was submitted to Obstetric and Pediatric Pharmacology, a section of the journal Frontiers in Pharmacology

RECEIVED 29 May 2022
ACCEPTED 13 July 2022
PUBLISHED 11 August 2022

CITATION
Jiang Z, Chen X, Dong G, Lou Y, Zhang J, Cheng X, Pan J, Liao W, Wu J, Huang X, Jin X, Liu D, Zeng T, Zhu S, Dong Q, Luo X, Lan D, Cao L, Zhang X, Liu J, Dai M, Zhang M, Liu L, Dong J, Zhao D, Ni S and Fu J (2022), Short-term efficacy and safety of a lower dose of polyethylene glycol recombinant human growth hormone in children with growth hormone deficiency: A randomized, dose-comparison study. *Front. Pharmacol.* 13:955809. doi: 10.3389/fphar.2022.955809

Short-term efficacy and safety of a lower dose of polyethylene glycol recombinant human growth hormone in children with growth hormone deficiency: A randomized, dose-comparison study

Zhouhong Jiang[1†], Xuefeng Chen[2†], Guanping Dong[2], Yin Lou[1], Jianping Zhang[3], Xinran Cheng[4], Jiayan Pan[5], Wei Liao[6], Jinzhun Wu[7], Xiaodong Huang[8], Xianjiang Jin[9], Deyun Liu[10], Ting Zeng[11], Shunye Zhu[12], Qin Dong[13], Xiaoming Luo[14], Dan Lan[15], Lizhi Cao[16], Xingxing Zhang[17], Jing Liu[18], Mingjuan Dai[19], Manyan Zhang[20], Li Liu[21], Junhua Dong[22], Dongmei Zhao[23], Shaoqing Ni[24,25]* and Junfen Fu[2,26]*

[1]Department of Pharmacy, The Children's Hospital, Zhejiang University School of Medicine, National Clinical Research Center for Child Health, Hangzhou, China, [2]Department of Endocrinology, The Children's Hospital, Zhejiang University School of Medicine, National Clinical Research Center for Child Health, Hangzhou, China, [3]Department of Pediatrics, Ningbo Women's and Children's Hospital, Ningbo, China, [4]Department of Pediatric Endocrine Genetics and Metabolism, Chengdu Women's and Children's Center Hospital, Chengdu, China, [5]Department of Pediatrics, Wuhu First People's Hospital, Wuhu, China, [6]Department of Pediatrics, First Affiliated Hospital of Army Medical University (Third Military Medical University), Chongqing, China, [7]Department of Pediatrics, The First Affiliated Hospital of Xiamen University, Xiamen, China, [8]Department of Endocrinology and Genetics, Shanghai Children's Medical Center, Shanghai Jiaotong University School of Medicine, Shanghai, China, [9]Department of Genetics and Endocrinology, The Second Affiliated Hospital and Yuying Children's Hospital of Wenzhou Medical University, Wenzhou, China, [10]Department of Pediatrics, The Second Affiliated Hospital of Anhui Medical University, Hefei, China, [11]Department of Child Health Care, Liuzhou Maternity and Child Healthcare Hospital, Liuzhou, China, [12]Department of Pediatrics, The Third Affiliated Hospital of Sun Yat-Sen University, Guangzhou, China, [13]Department of Pediatrics, Zhejiang Provincial Hospital of Chinese Medicine, Hangzhou, China, [14]Department of Pediatrics, Zhejiang Provincial People's Hospital, People's Hospital of Hangzhou Medical College, Hangzhou, China, [15]Department of Pediatrics, The First Affiliated Hospital of Guangxi Medical University, Nanning, China, [16]Department of Pediatrics, Xiangya Hospital, Central South University, Changsha, China, [17]Department of Pediatrics, The Second Xiangya Hospital, Central South University, Changsha, China, [18]Department of Pediatrics, Changchun Children's Hospital, Changchun, China, [19]Department of Pediatrics, Hangzhou First People's Hospital, Hangzhou, China, [20]Department of Pediatrics, Shaoxing Second Hospital, Shaoxing, China, [21]Department of Genetics and Endocrinology, Guangzhou Women and Children's Medical Center, Guangzhou, China, [22]Department of Pediatrics, Qilu Hospital of Shandong University, Jinan, China, [23]Pediatric Research Institute, Qilu Children's Hospital of Shandong University, Jinan, China, [24]National Clinical Trial Institute, The Children's Hospital, Zhejiang University School of Medicine, National Clinical Research Center for Child Health, Hangzhou, China, [25]Research Center for Clinical Pharmacy, Zhejiang University, Hangzhou, China, [26]The Children's Hospital, Zhejiang University School of Medicine, National Clinical Research Center for Child Health, Hangzhou, China

Abbreviations: AE, adverse event; BA, bone age; CA, chronological age; GH, growth hormone; GHD, growth hormone deficiency; Ht, height; HV, height velocity; IGF-1, insulin-like growth factor-1; mITT, modified intention-to-treat; PEG-rhGH, polyethylene glycol-recombinant human growth hormone; rhGH, recombinant human growth hormone; SD, standard deviation; SDS, standard deviation score; SS, safety set.

Objective: Polyethylene glycol recombinant human growth hormone (PEG-rhGH, Jintrolong®) is the first long-acting rhGH preparation that is approved to treat children with growth hormone deficiency (GHD) in China. Clinical experience with dose selections of PEG-rhGH is scarce. The present study compared the efficacy and safety of a lower dose to increase dosing regimens of PEG-rhGH treatment.

Methods: A multicenter, randomized, open-label, dose-comparison clinical study was conducted to compare the improvements in the height standard deviation score (Ht SDS), height velocity (HV), insulin-like growth factor-1 (IGF-1) SDS, and safety profiles of children with GHD who are treated with 0.2 mg/kg/week of PEG-rhGH dose or 0.14 mg/kg/week for 26 weeks.

Results: Ht SDS, HV, and IGF-1 SDS increased significantly after PEG-rhGH treatment in the two dose groups ($p < 0.05$). The improvements of Ht SDS, HV, and IGF-1 SDS were more significant in the high-dose group than in the low-dose group ($p < 0.05$). Ht SDS improvement in low-dose group was not non-inferiority to that in the high-dose group ($p = 0.2987$). The incidences of adverse events were comparable between the two groups.

Conclusion: The improvements of Ht SDS, HV, and IGF-1 SDS were more significant in the high-dose group than in the low-dose group ($p < 0.05$). PEG-rhGH at the dose of 0.14 mg/kg/week was effective and safe for children with GHD.

Clinical Trial Registration: clinicaltrials.gov, identifier NCT02908958.

KEYWORDS

PEG-rhGH, GHD, IGF-1, dose, children

Introduction

Recombinant human growth hormone (rhGH) has been used to treat growth hormone deficiency (GHD) in children for over 30 years with the aim of promoting linear growth (Richmond and Rogol, 2016; Collett-Solberg et al., 2019). The efficacy and safety of rhGH therapy has been demonstrated in many clinical trials (Shih et al., 1994; Peterkova et al., 2007; Slattery et al., 2014; Swerdlow et al., 2015; Rhie et al., 2019; Pfäffle et al., 2020; Backeljauw et al., 2021; Coutant et al., 2021). However, daily rhGH injections lead to poor adherence and decreased effectiveness. A recent meta-analysis reported that up to 71% of patients with GHD and their families were non-adherent to the prescribed treatment (Graham et al., 2018). As a result, several long-acting formulations of rhGH have been developed to reduce the frequency of administrations (Saenger and Mejia-Corletto, 2016; Miller et al., 2020).

Jintrolong® (GeneScience Pharmaceuticals, Changchun, China), a polyethylene glycol rhGH (PEG-rhGH), is the first commercial long-acting rhGH preparation approved in China. Compared to daily rhGH, PEG-rhGH has a longer T_{max} and $t_{1/2}$ and slower plasma clearance, which allows for weekly injection (Hou et al., 2016). Clinical studies have demonstrated the non-inferior efficacy and safety of PEG-rhGH compared to daily rhGH at an equivalent dose for the treatment of GHD (Luo et al., 2017; Qiao et al., 2019; Sun et al., 2021; Wang et al., 2021; Du et al., 2022). Notably, in a Phase III trial, PEG-rhGH treatment at 0.2 mg/kg/week was associated with greater increases in most of the efficacy endpoints, including height velocity (HV), height (Ht) standard deviation score (SDS), and insulin-like growth factor-1 (IGF-1) SDS, compared to daily rhGH dosing of 0.25 mg/kg/week (Luo et al., 2017). IGF-I has an effect on cell proliferation, and its increased serum concentration might be associated with an increased risk of common cancers (Renehan et al., 2004; Pfäffle, 2015). The change in the area under the concentration curve of IGF-1 after 7 days of PEG-rhGH injection at a dose of 0.2 mg/kg was 1.3 folds larger than that of rhGH at 0.25 mg/kg/week in a Phase I clinical trial ($p = 0.059$) (Hou et al., 2016). These results suggest that PEG-rhGH can be administrated at a lower dose to achieve comparable efficacy and safety.

Clinical experience with dose selections of PEG-rhGH is scarce. A PEG-rhGH dose of 0.14 mg/kg/week is equivalent to a daily rhGH dose of 0.12 IU/kg/d, which is within the recommended dose range for children with GHD. In addition, results of an animal study reported that in rats, a single PEG-rhGH dose of 0.14 mg/kg/week showed the same expected linear growth as a daily rhGH dose of 0.25 mg/kg/week (Zhang et al., 2012). Taken together, the present study aimed to compare the efficacy and safety of PEG-rhGH treatment at a dose of 0.14 mg/kg/week to 0.2 mg/kg/week in children with GHD.

Materials and methods

Study design and participants

This study was a multicenter, randomized, open-label, parallel-group, dose-comparison clinical trial that took place at 22 medical centers in China for 26 weeks. The study protocol was reviewed and approved by the Ethics Committee of the Children's Hospital, Zhejiang University School of Medicine and other participating centers. The parents or legal guardians of all participating children signed informed consents. The study was conducted in accordance with the principles of the Declaration of Helsinki and the International Conference on Harmonization Good Clinical Practice guidelines.

Eligible participants were prepubertal GHD patients (Tanner stage 1) aged at 3 years or older who had not received any GH treatment for 6 months. GHD was diagnosed using the following criteria: 1) height below -2SD or the third percentile of the normal growth curve for children of the same chronological age (CA) and sex in China (Hui et al., 2009); 2) HV ≤ 5 cm/year; 3) serum GH peak <10 μg/L in two different GH stimulation tests (stimulation with insulin, L-dopa, glucagon, arginine, or clonidine); and 4) bone age (BA) below 10 years for boys and 9 years for girls, with a minimum of a 1 year delay compared to the CA. Key exclusion criteria included renal or hepatic impairment; positive results for hepatitis B virus test, hypersensitivity of the study drug, serious cardiopulmonary, hematologic diseases, systemic infections or immunocompromising disorder, familial history of malignant tumor, diabetes, and other abnormal growth syndromes (i.e., Turners, constitutional delay of puberty, Laron Syndrome, growth hormone receptor deficiency). Those who had participated in other clinical trials within the 3 months prior to enrollment were also excluded.

Randomisation and masking

Patients were randomly assigned in a 1:1 ratio to randomized blocks (6 people per block) using a computer-generated random sequence to receive a PEG-rhGH dose of 0.14 mg/kg/week or 0.2 mg/kg/week. The study medicines and participant numbers were assigned in the forms of block multiples to each center. Each participant was assigned a unique medicine number. The investigators and parents/guardians were not masked to treatment allocation.

Procedures

PEG-rhGH was subcutaneously injected at a fixed time of the day by patients or their parents/guardians, who were able to administrate PEG-rhGH after training. The injection sites could be the lateral upper arm, lateral thigh, or the abdomen except the periumbilical area; the two injection sites were to be more than 2 cm apart. Each administration date and time was carefully recorded on diary cards. The treatments lasted for 26 weeks, and three follow-up visits were scheduled at week 4, 13, and 26 (± 5 days) after treatment initiation. At each visit, height and body weight were measured by designated personnel at each center. Blood samples were collected for blood routine tests, blood biochemistry, blood lip, blood glucose, thyroid function, serum IGF-1 concentration and anti-drug antibodies. Pituitary magnetic resonance imaging and electrocardiography were performed at each center. BA radiography was performed using the Tanner-Whitehouse three method at baseline and at week 26. Participants were not to use other medicines that may affect the efficacy of PEG-rhGH, such as gonadotropin-releasing hormone analogs, androgens, anabolic hormones, or other drugs that affect growth and development.

Outcomes

The primary efficacy outcome was the Ht SDS at week 26 after PEG-rhGH treatment. Secondary outcomes included HV and IGF-1 SDS at week 26 after PEG-rhGH treatment. Ht SDS and IGF-1 SDS were defined as the SD scores at each visit, based on the same CA and sex. HV was calculated as the height change per year. Safety was assessed by monitoring the adverse events (AEs), clinical symptoms, and laboratory tests at each visit. AEs were recorded, irrespective of their causal relationship to the treatment.

Statistical analysis

A sample size of at least 191 per group was needed to achieve a power of 90% with an α level of 0.025 for a non-inferiority margin of −20% in Ht SDS change (Sun et al., 2021). We assumed a dropout rate of 20% and to guarantee the robustness of the results, a total of 900 patients were planned to recruit.

Efficacy analysis was performed at week 26 in the modified intention-to-treat (mITT) and per-protocol populations. The mITT population included all randomized patients who received at least one injection of PEG-rhGH and completed at least one follow-up visit. The per-protocol population comprised of all randomized patients from the mITT population who completed all follow-up visits and had no major protocol deviations. Safety analysis was performed on the safety set (SS), which included all randomized patients who received at least one injection and safety record.

Continuous variables are presented as mean ± SD and categorical variables are presented as frequency and percentage. To assess the changes in PEG-rhGH treatment before and after with-in groups, continuous variables were statistically analyzed by paired *t*-test if they were normally

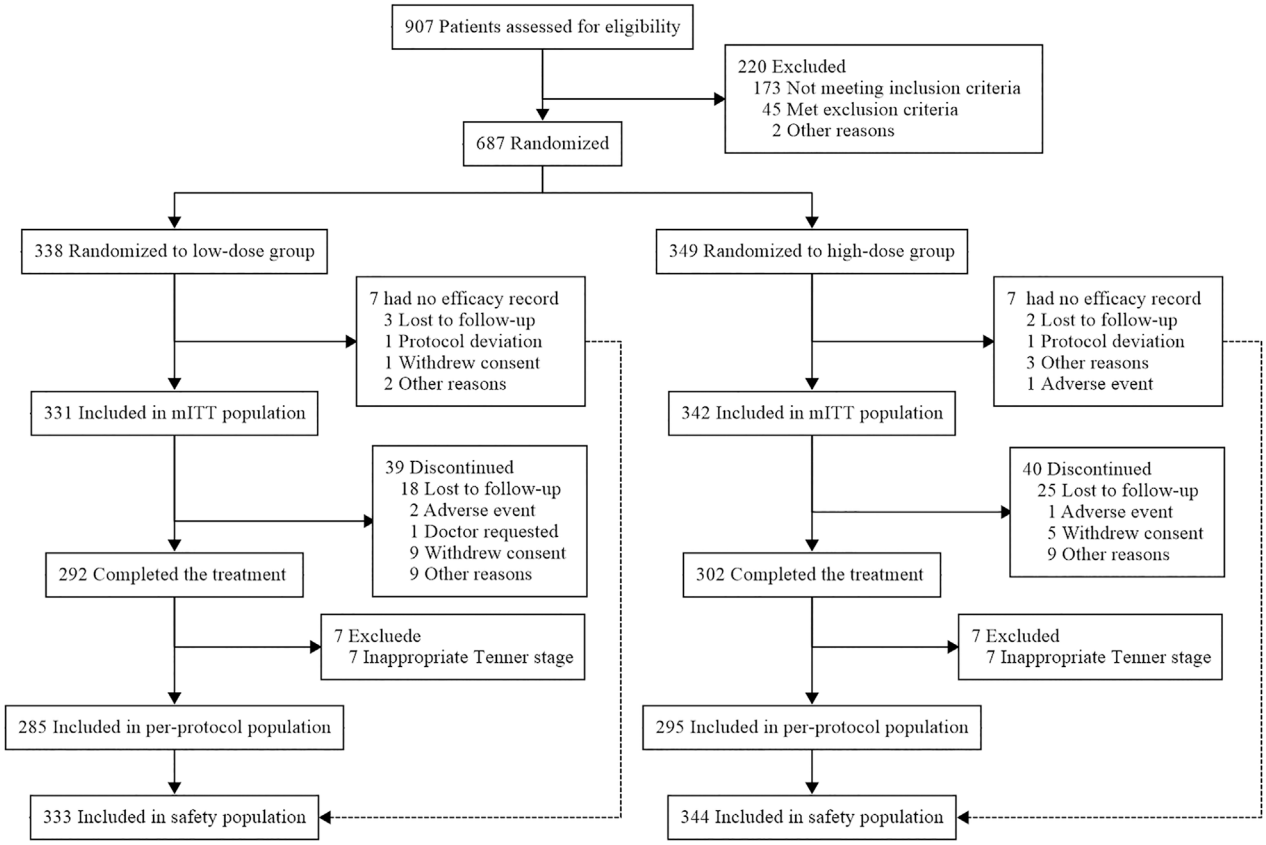

FIGURE 1
Patient flow diagram.

distributed and homogeneous; otherwise, a Wilcoxon rank-sum test was used. Missing data were imputed using the last-observation-carried-forward method. Changes between the two groups were analyzed by covariance (ANCOVA) with baseline as the covariate, taking the center effect into consideration. A chi-squared (χ^2) test was used to compare enumeration data and ratios. Results were considered significant at $p < 0.05$. The non-inferiority of 0.14–0.2 mg/kg/week would be accepted if the lower limit of the two-sided 95% CI for the difference between the two dose groups was greater than the non-inferiority margin. All statistical analyses were performed using SAS (version 9.4, SAS Institute Inc. Cary, NC).

Results

Patient characteristics

Between October 2014 and December 2017, 907 patients were screened and 687 patients were randomly assigned to receive 0.14 mg/kg/week of PEG-rhGH (n = 338) or 0.2 mg/kg/week (n = 349) (Figure 1). Seven patients in each group had no efficacy records and were not included in the mITT population. A total of 594 patients completed all follow-up visits, and seven patients in each group were excluded during data verification due to puberty. Finally, 285 patients in the low-dose group and 295 in the high-dose group were included in the per-protocol population. Since the results of the efficacy analysis of the per-protocol population were similar to those of the mITT population, only the mITT results are presented.

The demographic and baseline characteristics of the study population were comparable between the treatment groups (Table 1). All the patients were preadolescents, and BA/CA indicated retardation of bone maturation. All subjects were negative for Anti-GH antibodies.

Efficacy assessment

After PEG-rhGH treatment, the mean Ht SDS increased significantly in both dose groups at each assessment (Figure 2A).

TABLE 1 Demographic and clinical characteristics at baseline (mITT).

Characteristics	Low-dose group (N = 331)	High-dose group (N = 342)	p value
Male/Female	235/96	224/118	0.1256
CA, year	7.48 ± 2.48	7.48 ± 2.47	0.9739
BA, year	5.31 ± 2.27	5.36 ± 2.23	0.7979
BA/CA	0.69 ± 0.13	0.70 ± 0.12	0.7575
Height, cm	111.26 ± 12.30	111.51 ± 12.64	0.7929
Weight, kg	19.71 ± 5.50	19.62 ± 5.54	0.8367
BMI, kg/m^2	15.65 ± 1.85	15.48 ± 1.75	0.2273
Peak GH, ng/mL	5.92 ± 2.63	5.99 ± 2.54	0.7270
HV, cm/year	2.31 ± 1.54	2.44 ± 1.48	0.2746
Ht SDS	−2.68 ± 0.85	−2.66 ± 0.72	0.7271
IGF-1, ng/mL	120.43 ± 70.82	113.32 ± 60.93	0.2193
IGF-1 SDS	−1.15 ± 1.48	−1.10 ± 1.46	0.6398

CA, chronological age; BA, bone age; BMI, body mass index; Ht, height; HV, height velocity; IGF-1, insulin-like growth factor-1.

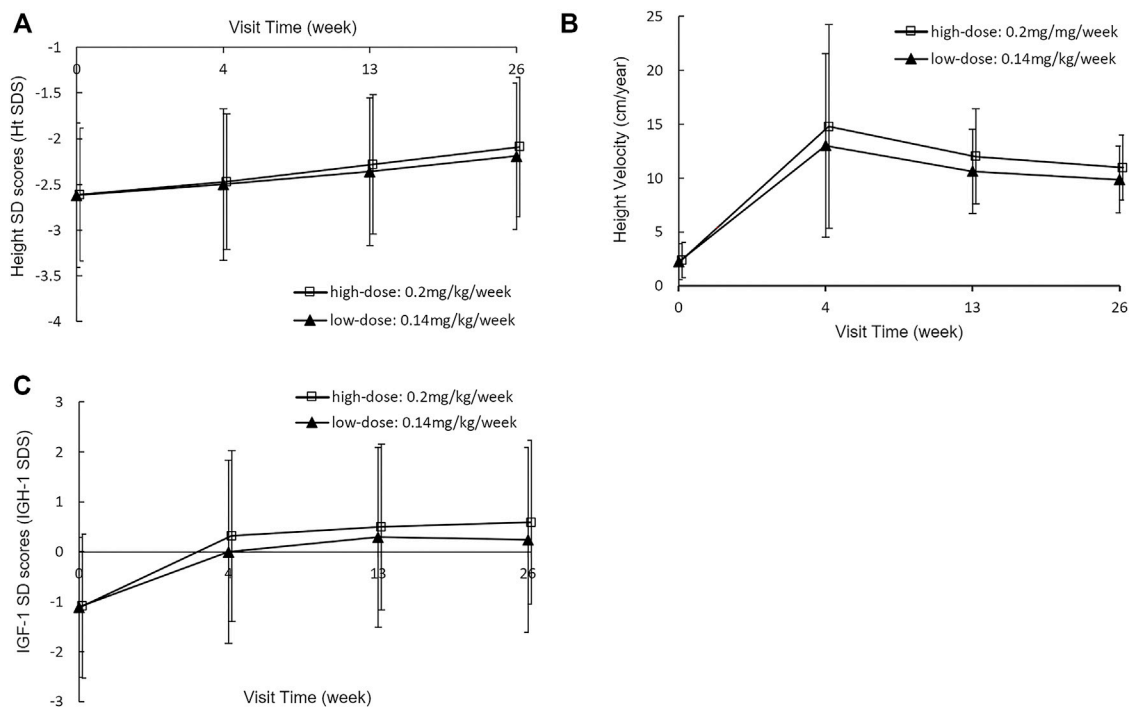

FIGURE 2
Height SDS **(A)**, Height velocity **(B)** and IGF-1 SDS **(C)** at baseline and week 4, 13 and 26 with a PEG-rhGH dose of 0.14 mg/kg/week or 0.2 mg/kg/week.

It increased from −2.68 ± 0.85 at baseline to −2.25 ± 0.72 at week 26 ($p < 0.0001$) in the low-dose group and from −2.66 ± 0.72 to −2.14 ± 0.75 ($p < 0.0001$) in the high-dose group. At each visit, the mean increments of Ht SDS in the low-dose group and the high-dose group were 0.12 ± 0.12 vs. 0.14 ± 0.13 ($p = 0.1302$) at week 4, 0.27 ± 0.19 vs. 0.32 ± 0.18 ($p = 0.0008$) at week 13, and 0.42 ± 0.28 vs. 0.51 ± 0.25 ($p < 0.0001$) at week 26, respectively. This suggests that the improvement of Ht SDS is dose-dependent, and the high dose had a more significant improvement in linear growth than the low dose. The lower limit of 95% CI of the Ht SDS change difference

TABLE 2 Blood glucose and lipid indexes during PEG-rhGH treatment (SS).

Index	Visit point, week	Low-dose group (N = 333)	High-dose group (N = 344)
FPG, mmol/L	0	4.73 ± 0.54	4.80 ± 0.60
	26	4.76 ± 0.52	4.82 ± 0.46
INS1, mIU/L	0	5.71 ± 4.87	5.97 ± 4.95
	26	6.28 ± 5.36	6.28 ± 4.66
HbA1c, %	0	5.35 ± 0.37	5.30 ± 0.87
	26	5.37 ± 0.35	5.32 ± 0.39
TC, mmol/L	0	4.34 ± 0.81	4.32 ± 0.81
	26	4.45 ± 0.89	4.38 ± 0.90
TG, mmol/L	0	0.79 ± 0.35	0.81 ± 0.44
	26	0.80 ± 0.37	0.80 ± 0.36
HDL, mmol/L	0	1.55 ± 0.33	1.54 ± 0.32
	26	1.55 ± 0.33	1.54 ± 0.38
LDL, mmol/L	0	2.38 ± 0.71	2.35 ± 0.67
	26	2.41 ± 0.70	2.37 ± 0.72

FPG, fasting blood glucose; HbA1c, glycosylated hemoglobin; INS1, fasting insulin; TC, total cholesterol; TG, triglyceride; HDL, high-density lipoprotein; LDL, low-density lipoprotein.

was −0.13, which was below the margin of −0.10. Thus, non-inferiority of Ht SDS change was not established (p = 0.2987).

HV increased rapidly in the first 4 weeks of PEG-rhGH treatment in both groups and then decreased slowly (Figure 2B). Similar effects of PEG-rhGH were observed in the HV as was observed in the Ht SDS. HV increased at a rate of 10.89 ± 8.05 cm/year in the low-dose group and 11.91 ± 8.83 cm/year in the high-dose group at week 4 (p = 0.1163). Then the increments decreased to 8.58 ± 4.30 cm/year in the low-dose group and 9.39 ± 8.97 cm/year in the high-dose group at week 13 (p = 0.0108), and 7.73 ± 3.53 cm/year and 8.46 ± 2.99 cm/year at week 26 (p = 0.0042). The low-dose group met the non-inferiority compared with the high-dose group, with a lower limit of 95% CI of −1.22 within the non-inferiority margin (p < 0.0001).

The mean IGF-1 SDS values also increased significantly (Figure 2C). In the low-dose group, it increased from -1.15 ± 1.48 at baseline to 0.06 ± 1.89, 0.20 ± 1.78, and 0.19 ± 1.82 at week 4, 13, and 26, respectively. And in the high-dose group, it increased from -1.10 ± 1.46 at baseline to 0.26 ± 1.74, 0.45 ± 1.68, and 0.57 ± 1.68 at week 4, 13, and 26, respectively. There were no significant increases of IGF-1 SDS at week 13 and 26 from baseline between two groups (p = 0.9508 in the low-dose group and p = 0.3766 in the high-dose group).

Safety

A total of 677 patients were concluded for the Safety analysis: 333 in the low-dose group and 344 in the high-dose group. Anti-GH antibodies were tested for patients at week 13 and week 26 after treatments initiation. No positive anti-drug antibodies were detected in both two groups. There were no statistical differences in the incidence of AEs and SAEs between the two groups (AEs: 50.5% vs. 53.9%, p = 0.3963; SAEs: 1.2% vs. 1.7%, p = 0.7525). The most common AEs were upper respiratory tract infections, followed by cough and fever in both the low-dose group (31.5%, 8.7%, and 7.8%) and the high-dose group (33.5%, 8.9%, and 6.5%). 33 in the low-dose group and 31 in the high-dose group were considered to be PEG-rhGH-related (p = 0.6896). All SAEs were not PEG-rhGH-related except for one case of Henoch-Schonlein purpura in the low-dose group, where the correlation with PEG-rhGH was not identifiable.

During PEG-rhGH treatment, no statistical changes were found in blood glucose and lipid indexes including fasting blood glucose, fasting insulin, glycosylated hemoglobin, total cholesterol, triglycerides, high-density lipoprotein, low-density lipoprotein (p > 0.05) (Table 2).

Discussion

Jintrolong® is the first long-acting rhGH preparation approved by the Center for Drug Evaluation of China. Based on the results of the present study, PEG-rhGH is effective and safe at a lower dose of 0.14 mg/kg/week for improving Ht SDS, HV and IGF-1 SDS in children with GHD; non-inferiority of Ht SDS at the dose of 0.14 mg/kg/week was not established after 26 weeks of treatment.

The GH/IGF-1 axis is critical for growth regulation (Balhara et al., 2012). GH induces bone growth by stimulating the production of IGF-1 in the liver, which in turn regulates GH secretion and stimulates longitudinal bone growth in the growth plate (Balhara et al., 2012; Wu et al., 2015). After 26 weeks of PEG-rhGH treatment, significant increases in Ht SDS and HV were observed in both dose groups, as expected. The incremental

changes in Ht SDS and HV in the high-dose group at week 26 yielded similar results as were reported in a Phase IV clinical trial and another single-center, nonrandomized cohort study of Jintrolong® at the same dose of 0.2 mg/kg/week (Qiao et al., 2019; Sun et al., 2021), but were less than the results from the Phase III clinical trial of Jintrolong® (Luo et al., 2017). Changes in Ht SDS were negatively correlate with age, baseline IGF-1, and peak GH levels (Sun et al., 2021). The mean peak GH level and mean value of IGF-1 SDS were lower in the Phase III clinical trial, which may explain the differences in growth responses in different clinical trials. Attempts have been made to extend the dosing interval of PEG-rhGH, however, changes of both Ht SDS and HV failed the non-inferiority test to weekly administration of PEG-rhGH or daily administration of rhGH (Sun et al., 2021). There were also some clinical trials that use the HV improvement as the primary efficacy outcome with the non-inferiority margin of −2 cm (Luo et al., 2017; Czepielewski et al., 2019). Although the non-inferiority was not established in terms of improving Ht SDS change, our results demonstrated that the dose of 0.14 mg/kg/week was non-inferior to the dose of 0.2 mg/kg/week in improving HV of children with GHD. Meanwhile, the efficacy of PEG-rhGH treatment at 0.14 mg/kg/week were consistent with the conventional dose of rhGH treatment in previous studies (Xue et al., 2016; Deal et al., 2018; Czepielewski et al., 2019). These results suggest that the PEG-rhGH dose of 0.14 mg/kg/week could be considered as a low dose option to attain an optimistic efficacy, which would reduce both adverse reactions and the treatment costs.

The serum IGF-1 level is an important parameter for monitoring GH treatment. It has been reported that children whose rhGH doses were adjusted maintain serum IGF-1 levels in the upper normal range (+ 1.5- + 2.5 SD) gained better improvement in growth response compared to children with IGF-I levels in the mid-normal range (Cecconi et al., 2004; Cohen et al., 2007; Pfäffle, 2015). Similar to Ht SDS and HV, IGF-1 SDS was significantly elevated during the 26 weeks and showed dose-dependent changes. Notably, the IGF-1 SDS rapidly increased at week four and reached a plateau at week 13 in the low-dose group but continued to increase slightly in the next 5 months in the high-dose group, although no significant differences observed ($p > 0.05$). The trends were different from the Phase III clinical trial of Jintrolong®, in which IGF-1 SDS reached a plateau at around week 13 and then gradually decreased with the same dose of 0.2 mg/kg/week (Luo et al., 2017). This difference may be attributed to the huge inter-individual variation in IGF-1 levels which are influenced by sex, age, body weight, nutritional status, and puberty stage and so on (Liu et al., 2019; Witkowska-Sędek et al., 2019; Papathanasiou et al., 2021). The previously mentioned cohort study reported that IGF-1 SDS in the PEG-rhGH group reached the upper limit of the normal range (0.96 ± 1.39) during the first 6 months and continued to increase over the next 18 months (Qiao et al., 2019). Considering the risks associated with IGF-1, the question of whether a high dose of PEG-rhGH leads to a supraphysiological level of IGF-1 requires long-term follow-up.

GH activates insulin-sensitive lipase, promotes fat decomposition, inhibits glucose uptake and utilization in skeletal muscles and adipose tissue, reduces glucose consumption, and increases blood glucose levels (Weber et al., 2017). It has been observed that the blood glucose and lipid levels decrease after rhGH treatment (Ciresi et al., 2007; Slattery et al., 2014; Kubo et al., 2017), while other clinical trials have not found significant changes in glucose metabolism after rhGH treatment (Czepielewski et al., 2019). A recent meta-analysis revealed a favorable role of rhGH therapy in lipid metabolism, which might depend on the duration of the intervention; however, the role of rhGH in glucose metabolism was not significant (Yuan et al., 2021). For instance, an increase in HbA1c level was observed after 1 year of rhGH therapy in a retrospective study of 101 pediatric patients with GHD (Pellegrin et al., 2019). For PEG-rhGH, improvements in lipid profiles (Hou et al., 2016) and non-significant changes in lipid metabolism (Wang et al., 2021) have been reported; however, none of them exert an unfavorable effect on glucose metabolism (Hou et al., 2016; Qiao et al., 2019; Wang et al., 2021). In our study, no significant changes were found in glucose or lipid metabolism after 26 weeks of PEG-rhGH treatment in children with GHD, regardless of PEG-rhGH dose. Our metabolomics analysis had revealed a strong association between fatty acids metabolism and the clinical efficacy of PEG-rhGH therapy, which would likely to be involved in fatty acid metabolism and energy metabolism (Li et al., 2022). Long-term follow-up is needed to confirm the effects of PEG-rhGH treatment on glucose and lipid metabolism.

Although the short-term efficacy and safety of PEG-rhGH treatment has been proven in clinical trials, introduction of a modified PEG molecule may cause new side effects (Lal and Hoffman, 2018). In addition, long-term elevated GH levels produced by PEG-rhGH treatment may induce iatrogenic acromegaly, neoplasia and glucose intolerance (Yuen et al., 2021). Therefore, every centimeter gained from PEG-rhGH treatment comes with a certain amount of risk. Moreover, despite the reduced frequency of injections, the cumulative cost of long-term treatment with PEG-rhGH remains high. Further pharmacoeconomic evaluations are needed to determine the correct cost and risk-benefit ratio.

Our study has some limitations. First, the pharmacokinetic and pharmacodynamic profiles of 0.14 mg/kg/week dosing have not been evaluated in order to explain the differences in the IGF-1 responses between the two PEG-rhGH doses. Second, serum IGF-1 levels increased steadily after PEG-rhGH injection and reached to a peak concentration after 2 days (Hou et al., 2016). However, for the convenience of patients and their parents, the follow-up visit was not strictly set for the second day after dosing according to the study protocol, which might introduce some error in the accuracy of the IGF-1 SDS.

In conclusion, there were significant increases in Ht SDS, HV, and IGF-1 SDS at week 26 after PEG-rhGH treatment in both dose groups. Ht SDS improvement with treatment using 0.14 mg/kg/week of PEG-rhGH was not non-inferiority to that at the standard dose of 0.2 mg/kg/week. Additionally, there were no significant changes in glucose or lipid metabolism after PEG-rhGH treatment at the different doses. Furthermore, a longer follow-up period is needed to assess the long-term efficacy and safety of lower doses of PEG-rhGH to optimize the therapeutic dose of PEG-rhGH.

Data availability statement

The original contributions presented in the study are included in the article/Supplementary Material, further inquiries can be directed to the corresponding authors.

Ethics statement

The studies involving human participants were reviewed and approved by the Ethics Committee of the Children's Hospital, Zhejiang University School of Medicine, Ningbo Women&Children's Hospital, Chengdu Women's and Children's Center Hospital, Wuhu First People's Hospital, First Affiliated Hospital of Army Medical University (Third Military Medical University), the First Affiliated Hospital of Xiamen University, Shanghai Children's Medical Center, Shanghai Jiaotong University School of Medicine, the Second Affiliated Hospital&Yuying Children's Hospital of Wenzhou Medical University, the Second Affiliated Hospital of Anhui Medical University, Liuzhou Maternity and Child Healthcare Hospital, the Third Affiliated Hospital of Sun Yat-Sen University, Zhejiang Hospital of TCM, Zhejiang Provincial People's Hospital, People's Hospital of Hangzhou Medical College, the First Affiliated Hospital of Guangxi Medical University, Xiangya Hospital, Central South University, the Second Xiangya Hospital, Central South University, Changchun Children's Hospital, Hangzhou First People's Hospital, Shaoxing Second Hospital, Guangzhou Women and Children's Medical Center, Qilu Hospital of Shandong University, Qilu Children's Hospital of Shandong University. Written informed consent to participate in this study was provided by the participants' legal guardian/next of kin.

Author contributions

JF is the principal investigator of the study. XC, JZ, XC, JP, WL, JW, XH, XJ, DL, TZ, SZ, QD, XL, DL, LC, XZ, JL, MD, MZ, LL, JD, and DZ are site investigators and conducted the study in each participating center. JF conceived the study design, managed the study, and coordinated the study. SN helped with study design, management and coordination. ZJ drafted this manuscript. ZJ and XC analyzed the data. ZJ, GD, and YL collected the data. JF provided final approval to the submitted version. All authors contributed to the article and approved the submitted version.

Funding

This research was s supported by the National Natural Science Foundation of China Grant No. 81573516.

Conflict of interest

The authors declare that the research was conducted in the absence of any commercial or financial relationships that could be construed as a potential conflict of interest.

Publisher's note

All claims expressed in this article are solely those of the authors and do not necessarily represent those of their affiliated organizations, or those of the publisher, the editors and the reviewers. Any product that may be evaluated in this article, or claim that may be made by its manufacturer, is not guaranteed or endorsed by the publisher.

References

Backeljauw, P., Miller, B. S., Levy, R., Mccormick, K., Zouater, H., Zabransky, M., et al. (2021). PATRO children, a multi-center, non-interventional study of the safety and effectiveness of Omnitrope(®) (somatropin) treatment in children: Update on the United States cohort. *J. Pediatr. Endocrinol. Metab.* 34 (4), 431–440. doi:10.1515/jpem-2020-0360

Balhara, B., Misra, M., and Levitsky, L. L. (2012). Recombinant human IGF-1 (insulin-like growth factor) therapy: Where do we stand today? *Indian J. Pediatr.* 79 (2), 244–249. doi:10.1007/s12098-011-0608-5

Cecconi, E., Gasperi, M., Bogazzi, F., Grasso, L., Genovesi, M., Marcocci, C., et al. (2004). Improvement of growth hormone deficiency in patients with primary hyperparathyroidism after parathyroidectomy: Results of a prospective study. *J. Clin. Endocrinol. Metab.* 89 (3), 1213–1216. doi:10.1210/jc.2003-031595

Ciresi, A., Amato, M. C., Criscimanna, A., Mattina, A., Vetro, C., Galluzzo, A., et al. (2007). Metabolic parameters and adipokine profile during GH replacement therapy in children with GH deficiency. *Eur. J. Endocrinol.* 156 (3), 353–360. doi:10.1530/eje.1.02343

Cohen, P., Rogol, A. D., Howard, C. P., Bright, G. M., Kappelgaard, A., Rosenfeld, R. G., et al. (2007). Insulin growth factor-based dosing of growth hormone therapy in children: A randomized, controlled study. *J. Clin. Endocrinol. Metab.* 92 (7), 2480–2486. doi:10.1210/jc.2007-0204

Collett-Solberg, P. F., Jorge, A., Boguszewski, M., Miller, B. S., Choong, C., Cohen, P., et al. (2019). Growth hormone therapy in children; research and practice - a review. *Growth Horm. IGF Res.* 44, 20–32. doi:10.1016/j.ghir.2018.12.004

Coutant, R., Bosch Muñoz, J., Dumitrescu, C. P., Schnabel, D., Sert, C., Perrot, V., et al. (2021). Effectiveness and overall safety of NutropinAq® for growth hormone deficiency and other paediatric growth hormone disorders: Completion of the international cooperative growth study, NutropinAq® European registry (iNCGS). *Front. Endocrinol.* 12, 676083. doi:10.3389/fendo.2021.676083

Czepielewski, M. A., Garret, Q., Vencio, S., Rassi, N., Felicio, J. S., Faria, M. S., et al. (2019). Efficacy and safety of a biosimilar recombinant human growth hormone (r-hGH cristalia) compared with reference r-hGH in children with growth hormone deficiency (ceres study): A randomized, multicentric, investigator-blind, phase 3 trial. *Growth Horm. IGF Res.* 48-49, 29–35. doi:10.1016/j.ghir.2019.07.003

Deal, C., Kirsch, S., Chanoine, J. P., Lawrence, S., Cummings, E., Rosolowsky, E. T., et al. (2018). Growth hormone treatment of Canadian children: Results from the Genesis phase IV prospective observational study. *CMAJ Open* 6 (3), E372–E383. doi:10.9778/cmajo.20180020

Du, H., Wu, D., Yi, P., Bai, X., Luo, Y., Yang, H., et al. (2022). Evaluation of efficacy and safety of long-acting PEGylated recombinant human growth hormone (Jintrolong) for patients with growth hormone deficiency. *J. Pediatr. Endocrinol. Metab.* 35 (4), 511–517. doi:10.1515/jpem-2021-0735

Graham, S., Weinman, J., and Auyeung, V. (2018). Identifying potentially modifiable factors associated with treatment non-adherence in paediatric growth hormone deficiency: A systematic review. *Horm. Res. Paediatr.* 90 (4), 221–227. doi:10.1159/000493211

Hou, L., Chen, Z. H., Liu, D., Cheng, Y. G., and Luo, X. P. (2016). Comparative pharmacokinetics and pharmacodynamics of a PEGylated recombinant human growth hormone and daily recombinant human growth hormone in growth hormone-deficient children. *Drug Des. devel. Ther.* 10, 13–21. doi:10.2147/DDDT.S93183

Hui, L., Cheng, J., Xin, Z., and Zhang, Y. Q. (2009). Height and weight standardized growth charts for Chinese children and adolescents aged 0 to 18 years. *Chin. J. PED* 47 (7), 487–492.

Kubo, T., Furujo, M., Takahashi, K., Hyodo, Y., Tsuchiya, H., Hattori, M., et al. (2017). Effects of growth hormone treatment on lipid profiles. *Indian J. Pediatr.* 85 (4), 261–265. doi:10.1007/s12098-017-2509-8

Lal, R. A., and Hoffman, A. R. (2018). Long-acting growth hormone preparations in the treatment of children. *Pediatr. Endocrinol. Rev.* 16, 162–167. doi:10.17458/per.vol16.2018.lh.longactingghpreparation

Li, J., Pan, W., Qian, J., Ni, Y., Fu, J., and Ni, S. (2022). Metabolomic differential compounds reflecting the clinical efficacy of polyethylene glycol recombinant human growth hormone in the treatment of childhood growth hormone deficiency. *Front. Pharmacol.* 13, 864058. doi:10.3389/fphar.2022.864058

Liu, H. J., Wang, L. H., and Chen, L. (2019). Evaluation of safety and efficacy of growth hormone therapy by IGF-1 Z score in children with short stature. *Adv. Ther.* 36 (9), 2374–2383. doi:10.1007/s12325-019-01021-5

Luo, X., Hou, L., Liang, L., Dong, G., Shen, S., Zhao, Z., et al. (2017). Long-acting PEGylated recombinant human growth hormone (Jintrolong) for children with growth hormone deficiency: Phase II and phase III multicenter, randomized studies. *Eur. J. Endocrinol.* 177 (2), 195–205. doi:10.1530/EJE-16-0905

Miller, B. S., Velazquez, E., and Yuen, K. (2020). Long-acting growth hormone preparations - current status and future considerations. *J. Clin. Endocrinol. Metab.* 105 (6), e2121–e2133. doi:10.1210/clinem/dgz149

Papathanasiou, T., Agersø, H., Damholt, B. B., Højby, R. M., and Kildemoes, R. J. (2021). Population pharmacokinetics and pharmacodynamics of once-daily growth hormone Norditropin(®) in children and adults. *Clin. Pharmacokinet.* 60, 1217–1226. doi:10.1007/s40262-021-01011-3

Pellegrin, M. C., Michelon, D., Faleschini, E., Germani, C., Barbi, E., and Tornese, G. (2019). Glucose metabolism evaluated by glycated hemoglobin and insulin sensitivity indices in children treated with recombinant human growth hormone. *J. Clin. Res. Pediatr. Endocrinol.* 11 (4), 350–357. doi:10.4274/jcrpe.galenos.2019.2019.0281

Peterkova, V., Arslanoglu, I., Bolshova-Zubkovskaya, E., Romer, T., Zdravkovic, D., Kratzsch, J., et al. (2007). A randomized, double-blind study to assess the efficacy and safety of valtropin, a biosimilar growth hormone, in children with growth hormone deficiency. *Horm. Res.* 68 (6), 288–293. doi:10.1159/000105494

Pfäffle, R., Bidlingmaier, M., Kreitschmann-Andermahr, I., Land, C., Partsch, C. J., Schwab, K. O., et al. (2020). Safety and effectiveness of Omnitrope®, a biosimilar recombinant human growth hormone: More than 10 Years' experience from the PATRO children study. *Horm. Res. Paediatr.* 93 (3), 154–163. doi:10.1159/000508190

Pfäffle, R. (2015). Hormone replacement therapy in children: The use of growth hormone and IGF-I. *Best. Pract. Res. Clin. Endocrinol. Metab.* 29 (3), 339–352. doi:10.1016/j.beem.2015.04.009

Qiao, Y., Wang, Z., Han, J., and Li, G. (2019). Use of PEGylated recombinant human growth hormone in Chinese children with growth hormone deficiency: A 24-month follow-up study. *Int. J. Endocrinol.* 2019, 1–7. doi:10.1155/2019/1438723

Renehan, A. G., Zwahlen, M., Minder, C., O'Dwyer, S. T., Shalet, S. M., and Egger, M. (2004). Insulin-like growth factor (IGF)-I, IGF binding protein-3, and cancer risk: Systematic review and meta-regression analysis. *Lancet* 363 (9418), 1346–1353. doi:10.1016/S0140-6736(04)16044-3

Rhie, Y. J., Yoo, J. H., Choi, J. H., Chae, H. W., Kim, J. H., Chung, S., et al. (2019). Long-term safety and effectiveness of growth hormone therapy in Korean children with growth disorders: 5-year results of LG growth study. *PLoS One* 14 (5), e0216927. doi:10.1371/journal.pone.0216927

Richmond, E., and Rogol, A. D. (2016). Treatment of growth hormone deficiency in children, adolescents and at the transitional age. *Best. Pract. Res. Clin. Endocrinol. Metab.* 30 (6), 749–755. doi:10.1016/j.beem.2016.11.005

Saenger, P. H., and Mejia-Corletto, J. (2016). Long-acting growth hormone: An update. *Endocr. Dev.* 30, 79–97. doi:10.1159/000439333

Shih, K. C., Ho, L. T., Kuo, H. F., Chang, T. C., Liu, P. C., Chen, C. K., et al. (1994). Linear growth response to recombinant human growth hormone in children with growth hormone deficiency. *Zhonghua Yi Xue Za Zhi (Taipei)* 54(1), 7–13.

Slattery, M., Bredella, M. A., Stanley, T., Torriani, M., and Misra, M. (2014). Effects of recombinant human growth hormone (rhGH) administration on body composition and cardiovascular risk factors in obese adolescent girls. *Int. J. Pediatr. Endocrinol.* 2014 (1), 22. doi:10.1186/1687-9856-2014-22

Sun, C., Lu, B., Liu, Y., Zhang, Y., Wei, H., Hu, X., et al. (2021). Reduced effectiveness and comparable safety in biweekly vs. Weekly PEGylated recombinant human growth hormone for children with growth hormone deficiency: A phase IV non-inferiority threshold targeted trial. *Front. Endocrinol.* 12, 779365. doi:10.3389/fendo.2021.779365

Swerdlow, A. J., Cooke, R., Albertsson-Wikland, K., Borgstrom, B., Butler, G., Cianfarani, S., et al. (2015). Description of the SAGhE cohort: A large European study of mortality and cancer incidence risks after childhood treatment with recombinant growth hormone. *Horm. Res. Paediatr.* 84 (3), 172–183. doi:10.1159/000435856

Wang, C., Huang, H., Zhao, C., Zhao, J., Xiong, R., Jin, R., et al. (2021). The impact of pegylated recombinant human growth hormone replacement therapy on glucose and lipid metabolism in children with growth hormone deficiency. *Ann. Palliat. Med.* 10 (2), 1809–1814. doi:10.21037/apm-20-871

Weber, M. M., Biller, B. M., Pedersen, B. T., Pournara, E., Christiansen, J. S., Hoybye, C., et al. (2017). The effect of growth hormone (GH) replacement on blood glucose homeostasis in adult nondiabetic patients with GH deficiency: Real-life data from the NordiNet® international outcome study. *Clin. Endocrinol.* 86 (2), 192–198. doi:10.1111/cen.13256

Witkowska-Sędek, E., Rumińska, M., Majcher, A., and Pyrżak, B. (2019). Gender-dependent growth and insulin-like growth factor-1 responses to growth hormone therapy in prepubertal growth hormone-deficient children. *Adv. Exp. Med. Biol.* 1133, 65–73. doi:10.1007/5584_2018_284

Wu, S., Yang, W., and De Luca, F. (2015). Insulin-like growth factor-independent effects of growth hormone on growth plate chondrogenesis and longitudinal bone growth. *Endocrinology* 156 (7), 2541–2551. doi:10.1210/en.2014-1983

Xue, Y., Gao, Y., Wang, S., and Wang, P. (2016). An examination of the effects of different doses of recombinant human growth hormone on children with growth hormone deficiency. *Exp. Ther. Med.* 11 (5), 1647–1652. doi:10.3892/etm.2016.3091

Yuan, Y., Zhou, B., Liu, S., Wang, Y., Wang, K., Zhang, Z., et al. (2021). Meta-analysis of metabolic changes in children with idiopathic growth hormone deficiency after recombinant human growth hormone replacement therapy. *Endocrine* 71 (1), 35–46. doi:10.1007/s12020-020-02435-w

Yuen, K., Miller, B. S., Boguszewski, C. L., and Hoffman, A. R. (2021). Usefulness and potential pitfalls of long-acting growth hormone analogs. *Front. Endocrinol.* 12, 637209. doi:10.3389/fendo.2021.637209

Zhang, Z. X., Liu, Y. K., Pan, H., Pan, L., Zhang, Q., Su, H. M., et al. (2012). The effect of polyethylene glycol recombinant human growth hormone on growth and glucose metabolism in hypophysectomized rats. *Growth Horm. IGF Res.* 22 (1), 30–35. doi:10.1016/j.ghir.2011.12.002

frontiers | Frontiers in Pediatrics

TYPE Original Research
PUBLISHED 16 August 2022
DOI 10.3389/fped.2022.956660

OPEN ACCESS

EDITED BY
Jian Gao,
Shanghai Children's Medical Center, China

REVIEWED BY
Michelle Seiler,
University Children's Hospital Zurich, Switzerland
Jijian Zheng,
Shanghai Children's Medical Center, China

*CORRESPONDENCE
Jianmin Zhang
zhangjianmin@bch.com.cn

SPECIALTY SECTION
This article was submitted to Obstetric and Pediatric Pharmacology, a section of the journal Frontiers in Pediatrics

RECEIVED 30 May 2022
ACCEPTED 25 July 2022
PUBLISHED 16 August 2022

CITATION
Cui X, Zhang J, Gao Z, Sun L and Zhang F (2022) A randomized, double-blinded, placebo-controlled, single dose analgesic study of preoperative intravenous ibuprofen for tonsillectomy in children.
Front. Pediatr. 10:956660.
doi: 10.3389/fped.2022.956660

A randomized, double-blinded, placebo-controlled, single dose analgesic study of preoperative intravenous ibuprofen for tonsillectomy in children

Xiaohuan Cui, Jianmin Zhang*, Zhengzheng Gao, Lan Sun and Fuzhou Zhang

Department of Anesthesiology, National Center for Children's Health, Beijing Children's Hospital, Capital Medical University, Beijing, China

Purpose: Tonsillectomy is a recognized treatment for children with tonsil hypertrophy and results in significant postoperative oropharyngeal pain. Fentanyl and other morphine-like analgesics are widely used as perioperative analgesia but are associated with side effects such as vomiting, nausea, and respiratory depression. As the least toxic non-steroidal anti-inflammatory drug, ibuprofen may be effective and safe for pain control after tonsillectomy. We aimed to explore whether the addition of intravenous (IV) ibuprofen administered at induction can reduce the need for early postoperativeanalgesics.

Study design and methods: This randomized, double-blind, controlled clinical trial enrolled 95 pediatric patients who underwent tonsillectomy. Participants aged 6 months to 12 years were randomly assigned to either the experimental and control groups (1:1). The children were premedicated 15 min before surgery with IV ibuprofen 10 mg kg^{-1} or placebo (normal saline). Pain was scored at 15, 30, and 120 min after extubation, and IV fentanyl (0.5 mcg kg^{-1}) was administered when the Faces, Legs, Activity, Cry, and Consolability (FLACC) Scale was $\geq$7 and deemed appropriate by the nursing staff in the post-anesthesia care unit (PACU). The visual analog scale was used as a supplementary evaluation for older children ($\geq$7 years old) who were awake and could self-report pain. The primary outcome variable was the number of patients who received postoperative analgesia.

Results: The requirement for rescue fentanyl was reduced by 18% with the addition of IV ibuprofen ($P = 0.043$). There were no signficant differences in the amount of fentanyl administered postoperatively ($P = 0.127$). Compared with the placebo group, the number of children who needed more than one dose of rescue fentanyl decreased in the experimental group, but the differences were not significant ($P = 0.056$). There were no significant differences between the groups in terms of operative blood loss ($P = 0.978$), vomiting, or postoperative bleeding ($P = 0.474$).

Conclusion: It is safe to administer IV ibuprofen 15 min before tonsillectomy, and it can significantly reduce the need for rescue fentanyl. IV ibuprofen

should be considered as an important part of the multimodal approach for postoperative analgesia in children.

Clinical trial registration: Chictr.org.cn, identifier: ChiCTR2100044508.

KEYWORDS

postoperative pain, pediatric pain management, intravenous ibuprofen, tonsillectomy, non-steroidal anti-inflammatory drug

Introduction

Almost all children undergoing tonsillectomy experience considerable long-term pain and are afraid to swallow or eat because of severe throat pain. Adequate postoperative pain management in children remains challenging for several reasons, wherein the most essential is the lack of choices in pediatric analgesic drugs. Morphine-like analgesics such as fentanyl and sufentanil are widely used but are associated with a considerable incidence of nausea and vomiting. In addition, for children with obstructive sleep apnea syndrome, the above drugs may even increase the incidence of postoperative respiratory depression (1).

Non-steroidal anti-inflammatory drugs (NSAIDs) are an important component of multimodal pain management because of their anti-inflammatory effects (2). In addition, they are opioid-sparing and do not cause respiratory or central nervous system depression, making them an effective and safe option for children. However, there are some limiting factors in the use of NSAIDs for pediatric pain management. First, only a few NSAIDs are approved for perioperative analgesia in children, and "off-label" use is common in many clinical settings. Second, NSAIDs may interfere with platelet aggregation, thereby increasing the risk of bleeding. Third, most NSAIDs approved for children come in oral dosage forms and may increase preoperative gastric volume. Despite some concerns of postoperative bleeding, a previous study has shown that ibuprofen, a reversible NSAID, shows a good safety profile (3), and the American Academy of Otolaryngology-Head and Neck Surgery has specifically stated that "ibuprofen can be used safely for pain control after surgery" (4). Recently, long-awaited intravenous (IV) ibuprofen for pediatric analgesia has been approved by several countries, providing more options for postoperative analgesia management in children.

This randomized, double-blinded, placebo-controlled, single dose clinical trial evaluated whether IV ibuprofen used at the induction of pediatric tonsillectomy can reduce the use of postoperative analgesics and achieve an ideal analgesic effect.

Abbreviations: AE, Adverse events; COX, cyclooxygenase; FLACC, Faces, Legs, Activity, Cry, and Consolability; IV, intravenous; NSAID, non-steroidal anti-inflammatory drug; PACU, post-anesthesia care unit.

Materials and methods

The study strictly adhered to the Helsinki guidelines, and all the guardians signed informed consent before enrollment.

The inclusion criteria were: (1) age between 6 months and 12 years; (2) American Society of Anesthesiologists physical status classification I–III; and (3) scheduled for tonsillectomy with/without adenoidectomy.

The exclusion criteria were as follows: (1) use of analgesics such as NSAIDs, tramadol, or local anesthetics 24 h before study drug administration; (2) history of severe allergic illness or hypersensitive to any of the medications in the study; (3) significant cognitive impairment; (4) history of gastrointestinal diseases or active bleeding; (5) history of serious cardiovascular diseases; (6) dehydration or abnormal renal function; (7) active asthma; and (8) obstructive sleep apnea (obstructive apnea-hypopnea index >10 times per h). Children over seven years of age were familiarized with the Oucher visual analog pain (VAS) scale upon enrollment in the study.

After the assignment, participants were randomly assigned to two groups in a 1:1 ratio: the IV ibuprofen and placebo groups. Children in the first group were given a single dose of 10 mg kg^{-1} (maximum 400 mg) IV ibuprofen. In contrast, children in the other group were administered volume-matched normal saline at induction of anesthesia. The investigators, patients, surgeons, and nurses in the post-anesthesia care unit (PACU) were blinded to the intervention assignments.

Standard perioperative care was set in this study. After the children entered the operating room, monitoring including oxygen saturation, blood pressure, bispectral index, and electrocardiogram, would be established. Experimental fluid was administered before induction. General anesthesia was induced with 2 mcg kg^{-1} fentanyl, 2–3 mg kg^{-1} propofol, 0.1 mg kg^{-1} cisatracurium, and 0.5 mg kg^{-1} dexamethasone. The experimental fluid was prepared by a pharmacist and administered for 15 min. Lidocaine cream was applied to the tracheal catheters, and endotracheal intubation was performed after spontaneous ventilation had disappeared. Anesthesia was maintained with propofol 10 mg·kg^{-1}·h^{-1} and remifentanil (0.3–0.4 mcg·kg^{-1}·min^{-1}) at the beginning and was adjusted to maintain the bispectral index monitor at 40–60. Systolic

blood pressure change was maintained within 20% of the baseline values.

A fully trained team performed all surgeries. The procedure was initiated at least 15 min after the experimental fluid was administered, and tonsillectomy was performed using only low-temperature plasma ablation. At the end of the surgery, 0.1 mg kg^{-1} tropisetron was administered to all children to prevent postoperative nausea and vomiting. The operating time was defined as the time interval between placement and removal of the mouthpiece. The children were extubated when adequate spontaneous breathing was observed, and they were transferred to the PACU.

In the PACU, nurses would console the patients and evaluate how well they were waking up. At 15 and 30 min after surgery, all children were assessed using the Faces, Legs, Activity, Cry, and Consolability (FLACC) scale. For children over seven years of age who were awake enough to describe pain, the VAS scores were used as a supplement. Rescue fentanyl (0.5 mcg kg^{-1}) was administered when the FLACC was ≥7, or the VAS was ≥70 mm. The nurses monitored the children intensively and reassessed them every 5 min. If the pain score persisted above 7, fentanyl injections were re-administered.

After returning to the ward, the children were discharged with cold compresses to the neck. They watched cartoons and drank normal-temperature water as soon as possible. Oral ibuprofen was allowed to be used as needed for at least 4 h after surgery. The incidence of vomiting, infusion site discomfort, and postoperative bleeding was followed up for 24 h.

The primary outcome variable was the number of children who received rescue fentanyl. Additional endpoints included the number of children who received repeat rescue fentanyl, weight-based postoperative fentanyl dose, intraoperative blood loss, pain scores at 15, 30, and 120 min after the surgery, the incidence of postoperative nausea and vomiting, and postoperative hemorrhage.

Data with a normal distribution are presented as the mean ± standard deviation, and the differences among groups were compared using the independent sample *t*-test (Student's *t*-test).

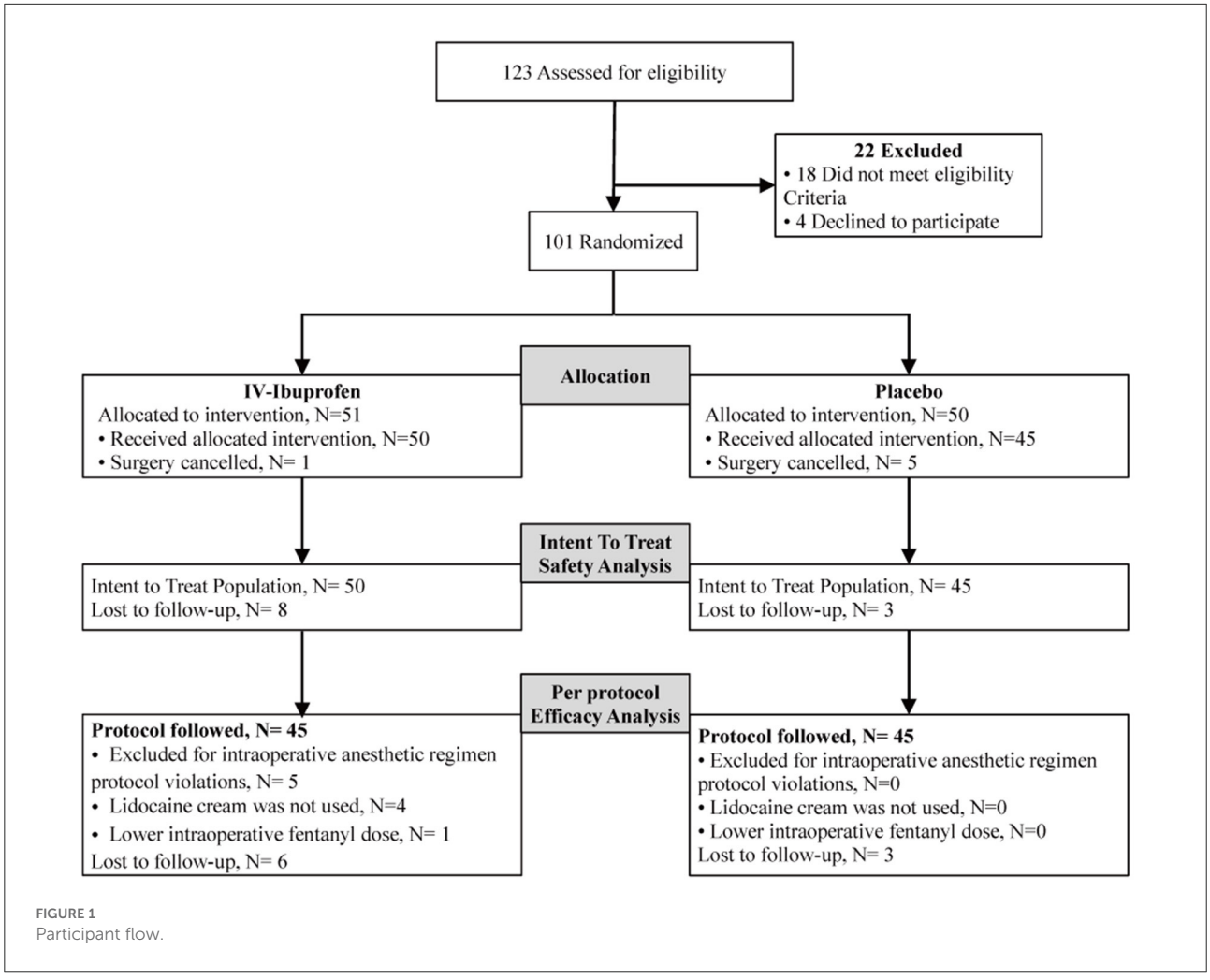

FIGURE 1
Participant flow.

Non-normally distributed data are expressed as the median (interquartile range), and the Mann–Whitney *U*-test was used to compare the differences. Categorical data were reported as numbers (percentages) and compared using the chi-square test or Fisher's exact test. Two-tailed *P*-values < 0.05 was considered statistically significant. Statistical analyses were performed using the SPSS statistical package (version 25.0; IBM SPSS Inc., Chicago, IL, USA).

A sample size of 80 participants was calculated using PASS 15.0 (NCSS PASS, UT, USA) to provide at least 80% power and a 0.05 significance level to detect a 30% reduction in the number of patients who needed supplementary fentanyl (5). Ninety patients were required to enroll, considering a 10% loss to follow-up rate.

Results

A total of 123 children were screened, and 95 children were enrolled from March 19 to June 16, 2021. The flowchart diagram is illustrated in Figure 1. The distribution of the patient and surgical characteristics were not significantly different between the two groups (Table 1).

Of the 95 children recruited, five were excluded because of protocol violations. Ninety children were eligible for efficacy (45 in the experimental group and 45 in the placebo group) (Figure 1). In the IV ibuprofen group, the number of children who received postoperative fentanyl was significantly lower than that in the placebo group [6 of 45 (13%) vs. 14 of 45 (31%), respectively, $P = 0.043$]. In addition, the pain scores of the two groups decreased with time after surgery, and significant differences were observed at 15 ($P = 0.06$) and 30 min ($P = 0.08$) (Figure 2). Although there were no significant differences in the amount of the supplementary fentanyl dose and the number of children receiving repeat rescue fentanyl, all five patients in the placebo group needed repeat fentanyl (Table 2).

Adverse events (AEs) are listed in Table 3. A total of 21 (22%) patients had AEs, wherein the most common AEs were infusion site discomfort (12%) and vomiting (4.2%). There were no differences between the two groups in surgical blood loss, perioperative bleeding, vomiting, infusion site discomfort, or reoperation rate.

Tonsillar fossa hemorrhage was noted in one patient in the placebo group. He experienced nausea after leaving the PACU, spitting out ∼5 ml of bloody saliva. An ear, nose, and throat specialist examined the patient and did not observe active bleeding. Therefore, he did not undergo resurgery, and the bleeding ended ∼10 mins later.

TABLE 1 Demographics.

	IV-Ibuprofen, $N = 50$	Placebo, $N = 45$
Gender		
Female	21 (42%)	19 (42%)
Male	29 (58%)	26 (58%)
P-value		0.456
Age (years)		
Mean (SD)	6.1 (2.45)	6.5 (2.39)
Median	5.8	6.3
P-value		0.344
Height (cm)		
Mean (SD)	116.9 (23.30)	122.0 (15.24)
Median	116.5	120.0
P-value		0.186
Body weight (kg)		
Mean (SD)	26.0 (13.84)	26.9 (10.48)
Median	21.5	24.0
P-value		0.211
BMI (kg/m2)		
Mean (SD)	17.1 (3.87)	17.4 (3.55)
Median	16.6	16.6
P-value		0.514
Operation duration (min)		
Mean (SD)	33.0 (11.08)	33.3 (13.97)
Median	30.5	29.0
P-value		0.638
Operation type		
tonsillectomy	7 (14%)	7 (16%)
adenotonsillectomy	43 (86%)	38 (84%)
P-value		0.437
Types of tonsils		
Intracapsular	23 (46%)	20 (44%)
Extracapsular	27 (54%)	25 (56%)
P-value		0.446

Discussion

Pain management after surgery in children remains challenging in many countries, mainly because of the following factors: first, the difficulty in pain assessment for children, especially in the early postoperative period; second, morphine-like analgesics, the essential component of pediatric postoperative pain treatment, may lead to several serious complications such as respiratory depression, sedation, and potentially apnea; and third, many NSAIDs are not authorized for pediatric use (6). Several studies have shown that pain management in children is usually inadequate (7–9). The precise use of drugs to achieve better analgesic effects is a common goal of pediatric anesthesiologists.

This was the first clinical trial evaluating the efficacy and safety of preoperative IV ibuprofen use in pediatric tonsillectomy in an Asian population. The analgesic activity of ibuprofen is related to its anti-inflammatory effects, and

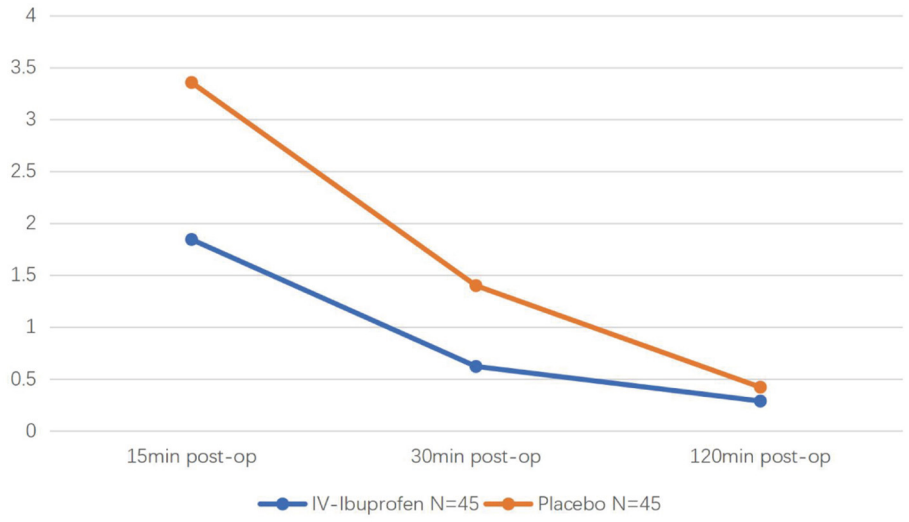

FIGURE 2
The Faces, Legs, Activity, Cry, and Consolability (FLACC) scale during the 2 h postoperative period of two groups.

TABLE 2 Postoperative analgesic requirements and intraoperative blood lose.

	Intent to treat		Efficacy evaluable	
	Ibuprofen ($n = 50$)	**Placebo ($n = 45$)**	**Ibuprofen ($n = 45$)**	**Placebo ($n = 45$)**
Number (%) of patients who received supplementary fentanyl				
0 dose supplementary fentanyl	40 (80%)	31 (69%)	39 (87%)	31 (69%)
≥1 dose supplementary fentanyl	10 (20%)	14 (31%)	6 (13%)	14 (31%)
P-value		0.139		0.043
Number (%) of patients who received				
≤1 dose supplementary fentanyl	50 (100%)	40 (89%)	45 (100%)	40 (89%)
>1 dose supplementary fentanyl	0 (0%)	5 (11%)	0 (0%)	5 (11%)
P-value*(Fisher)		0.021		0.056
Supplementary Fentanyl dose ($\mu g\ kg^{-1}$)				
Mean (SD)	0.10 (0.20)	0.23 (0.39)	0.07 (0.17)	0.23 (0.39)
Median	0	0	0	0
P-value		0.128		0.127
Surgical blood loss (ml)				
Mean (SD)	9.26 (2.11)	9.00 (2.67)	9.18 (2.21)	9.00 (2.67)
Median	10	10	10	10
P-value		0.781		0.978

it can reduce the levels of cyclooxygenase (COX)-1 and COX-2-derived proteinoids in the blood (10). IV ibuprofen exerts its effects within 15 min, reaches the maximum concentration in 30 min (T_{max}), and is metabolized by half in ~2 h. Therefore, for the pharmacology and pharmacokinetics analysis, we designed the study to determine whether IV ibuprofen used at least 15 min before surgery decreased the number of patients who received rescue fentanyl. The pain scores at 15 and 30 min were significantly lower in the IV ibuprofen group than in the placebo group. In addition, the number of children who needed rescue analgesia showed a significant reduction in the IV ibuprofen group. This indicates that IV ibuprofen has a preventive inhibitory effect on postoperative pain and is consistent with previous NSAID

TABLE 3 Adverse events.

	Placebo ($N = 45$) No. of events	IV-Ibuprofen ($N = 50$) No. of events	*P*-value
Vomiting	3	1	0.536
Infusion site discomfort	5	6	0.892
Postoperative bleeding	1	0	0.474
Headache	0	0	—
stomachache	1	0	0.474
Rash erythematous	2	2	0.686
Hypoxia	0	0	—

*One patient in the placebo group experienced a bleeding-related adverse event but didn't need reoperation.

studies. Moreover, the number of children who required repeated rescue fentanyl and the weight-based amount of fentanyl in the two groups were similar. Notably, the cases requiring a second dose of rescue fentanyl were all from the placebo group [0 of 45 (0%) vs. 5 of 45 (11%), respectively, $P = 0.056$]; a larger sample size might lead to further results.

In children treated with preoperative IV ibuprofen, intraoperative or postoperative bleeding was not noted. Although there are concerns regarding the association between ibuprofen and perioperative hemorrhage, recent studies have shown that ibuprofen is safe for children undergoing tonsillectomy (11, 12). A meta-analysis involving 36 studies demonstrated no increased risk of bleeding in patients using NSAIDs after tonsillectomy (13). Similarly, a study including 6014 children found that when age is controlled, the incidence of post-tonsillectomy hemorrhage among patients treated with ibuprofen was not statistically increased compared to patients treated with codeine (14).

This trial's efficacy and safety findings are consistent with the postulate before the study and with those of several previous studies (1, 4, 6). This could provide more evidence for pediatric anesthesiologists to precisely manage postoperative pain in children and may reduce fentanyl dosage during induction.

Analgesia after tonsillectomy in children is a multi-pronged approach that includes pharmaceutical and non-pharmaceutical methods. During the first 15 min after awakening, it is difficult to differentiate between emergence delirium and pain in clinical practice (15). Therefore, nurses in the PACU console the children first when they cannot identify the cause of unsettling behavior. Other non-pharmaceutical measures, such as postoperative honey, ice lollipop, early drinking of water, and distraction, can also effectively relieve postoperative pain (2, 16). Rescue fentanyl was administered only to those who experienced severe pain (FLACC $\geq$7) to decrease the risk of opioid toxicity. The significant decrease in pain scores 2 h after surgery was associated with multimodal analgesic measures, including neck cold compression, early drinking, and watching cartoons. The pain scores were similar in the two groups 2 h after surgery, suggesting that ibuprofen was largely metabolized, which is consistent with the metabolic characteristics of ibuprofen.

An appropriate scale is essential for establishing baseline discomfort and measuring the response to treatment. In previous studies, different scales have been used to measure postoperative pain after tonsillectomy in children (1, 17–21). During the recovery period, children of all ages may not yet be able to express and quantify the degree of their pain; therefore, an observational tool seems more reliable. Voepel-Lewis et al. (22) conducted 73 observations on 29 ill adults and eight children to evaluate the reliability and validity of the FLACC. They found that "it can be used across populations of patients and settings, and the scores are comparable to those of the commonly used 0-to-10 number rating scale." Pain assessment and management have become topics of interest (23), and further research is necessary to improve pain assessment in children after surgery.

The main limitation of this study was the anesthetic regimen containing fentanyl and remifentanil. This regimen has been used in our institution for years, and we retained it to reduce unnecessary exposure to postoperative pain. However, this may have clouded observations of the true effects of IV ibuprofen, which is more effective than the experimental results. Moss et al. (1) used less fentanyl in the induction period and maintained it with sevoflurane; significant reductions were observed in the doses of postoperative fentanyl, weight-based rescue fentanyl, and the number of patients who received more than one dose of fentanyl. Another limitation was the lack of age groups. In our study, infants younger than 6 months were excluded because previous research has shown that infants younger than 3–6 months metabolize analgesic medication differently than older children (24). The development of the nervous system in different stages of childhood may affect the way the body copes with pain and interventions. Previous studies suggested that postoperative pain is more severe in older children (25, 26). A large sample size with exact age stratification may have clarified the effects of IV ibuprofen more accurately and led to a more precise analgesic regimen for children. Third, this study only assessed the risk of postoperative bleeding in the first 24 h, which means that late bleeding events may have been missed. We intended to design a further study with an extended follow-up time of 14 days to observe possible bleeding caused by ibuprofen.

In conclusion, IV ibuprofen has a preventive inhibitory effect on pediatric postoperative pain and does not increase perioperative bleeding.

Data availability statement

The raw data supporting the conclusions of this article will be made available by the authors, without undue reservation.

Ethics statement

The studies involving human participants were reviewed and approved by the Clinical Research Ethics Committee of Beijing Children's Hospital. Written informed consent to participate in this study was provided by the participants' legal guardian/next of kin.

Author contributions

XC and ZG designed the study. XC analyzed the data and wrote the paper. LS and FZ participated in the interpretation of data. JZ directed the research and offered some suggestions. All authors contributed to the article and approved the submitted version.

Conflict of interest

The authors declare that the research was conducted in the absence of any commercial or financial relationships that could be construed as a potential conflict of interest.

Publisher's note

All claims expressed in this article are solely those of the authors and do not necessarily represent those of their affiliated organizations, or those of the publisher, the editors and the reviewers. Any product that may be evaluated in this article, or claim that may be made by its manufacturer, is not guaranteed or endorsed by the publisher.

References

1. Moss JR, Watcha MF, Bendel LP, McCarthy DL, Witham SL, Glover CD. A multicenter, randomized, double-blind placebo-controlled, single dose trial of the safety and efficacy of intravenous ibuprofen for treatment of pain in pediatric patients undergoing tonsillectomy. *Paediatr Anaesth.* (2014) 24:483–9. doi: 10.1111/pan.12381

2. Aldamluji N, Burgess A, Pogatzki-Zahn E, Raeder J, Beloeil H, PROSPECT Working Group collaborators*. PROSPECT guideline for tonsillectomy: systematic review and procedure-specific postoperative pain management recommendations. *Anaesthesia*. (2021) 76:947–61. doi: 10.1111/anae.15299

3. Poddighe D, Brambilla I, Licari A, Marseglia GL. Ibuprofen for pain control in children: new value for an old molecule. *Pediatr Emerg Care.* (2019) 35:448–53. doi: 10.1097/PEC.0000000000001505'

4. Baugh RF, Archer SM, Mitchell RB, Rosenfeld RM, Amin R, Burns JJ, et al. Clinical practice guideline: tonsillectomy in children. *Otolaryngol Head Neck Surg.* (2011) 144:S1–30. doi: 10.1177/0194599810389949

5. Pickering AE, Bridge HS, Nolan J, Stoddart PA. Double-blind, placebo-controlled analgesic study of ibuprofen or rofecoxib in combination with paracetamol for tonsillectomy in children. *Br J Anaesth.* (2002) 88:72–7. doi: 10.1093/bja/88.1.72

6. Kokki H. Nonsteroidal anti-inflammatory drugs for postoperative pain: a focus on children. *Paediatr Drugs.* (2003) 5:103–23. doi: 10.2165/00128072-200305020-00004

7. Rømsing J, Walther-Larsen S. Postoperative pain in children: a survey of parents' expectations and perceptions of their children's experiences. *Paediatr Anaesth.* (1996) 6:215–8. doi: 10.1111/j.1460-9592.1996.tb00431.x

8. Wilson CA, Sommerfield D, Drake-Brockman TFE, Lagrange C, Ramgolam A, von Ungern-Sternberg BS. A prospective audit of pain profiles following general and urological surgery in children. *Paediatr Anaesth.* (2017) 27:1155–64. doi: 10.1111/pan.13256

9. Sng QW, He HG, Wang W, Taylor B, Chow A, Klainin-Yobas P, et al. A meta-synthesis of children's experiences of postoperative pain management. *Worldviews Evid Based Nurs.* (2017) 14:46–54. doi: 10.1111/wvn.12185

10. Rainsford KD. Ibuprofen: pharmacology, efficacy and safety. *Inflammopharmacology.* (2009) 17:275–342. doi: 10.1007/s10787-009-0016-x

11. Michael A, Buchinsky FJ, Isaacson G. Safety of preoperative ibuprofen in pediatric tonsillectomy. *Laryngoscope.* (2018) 128:2415–8. doi: 10.1002/lary.27241

12. Patel NK, Shah SJ, Lee NK, Cao Q, Yang CJ. Intraoperative intravenous ibuprofen use is not associated with increased post-tonsillectomy bleeding. *Int J Pediatr Otorhinolaryngol.* (2020) 133:109965. doi: 10.1016/j.ijporl.2020.109965

13. Riggin L, Ramakrishna J, Sommer DD, Koren GA. A 2013 updated systematic review & meta-analysis of 36 randomized controlled trials; no apparent effects of non-steroidal anti-inflammatory agents on the risk of bleeding after tonsillectomy. *Clin Otolaryngol.* (2013) 38:115–29. doi: 10.1111/coa.12106

14. Pfaff JA, Hsu K, Chennupati SK. The use of ibuprofen in posttonsillectomy analgesia and its effect on posttonsillectomy hemorrhage rate. *Otolaryngol Head Neck Surg.* (2016) 155:508–13. doi: 10.1177/0194599816646363

15. Ferland CE, Vega E, Ingelmo PM. Acute pain management in children: challenges and recent improvements. *Curr Opin Anaesthesiol.* (2018) 31:327–32. doi: 10.1097/ACO.0000000000000579

16. Sng QW, Taylor B, Liam JL, Klainin-Yobas P, Wang W, He HG. Postoperative pain management experiences among school-aged children: a qualitative study. *J Clin Nurs.* (2013) 22:958–68. doi: 10.1111/jocn.12052

17. Alghamdi F, Roth C, Jatana KR, Elmaraghy CA, Rice J, Tobias JD, et al. Opioid-sparing anesthetic technique for pediatric patients undergoing adenoidectomy: a pilot study. *J Pain Res.* (2020) 13:2997–3004. doi: 10.2147/JPR.S281275

18. Harley EH, Dattolo RA. Ibuprofen for tonsillectomy pain in children: efficacy and complications. *Otolaryngol Head Neck Surg.* (1998) 119:492–6. doi: 10.1016/S0194-5998(98)70107-X

19. Kelly LE, Sommer DD, Ramakrishna J, Hoffbauer S, Arbab-Tafti S, Reid D, et al. Morphine or ibuprofen for post-tonsillectomy analgesia: a randomized trial. *Pediatrics.* (2015) 135:307–13. doi: 10.1542/peds.2014-1906

20. Moss JR, Cofer S, Hersey S, Goudy S, Werkhaven J, Swanson E, et al. Comparison of clonidine, local anesthetics, and placebo for pain reduction in pediatric tonsillectomy. *Arch Otolaryngol Head Neck Surg.* (2011) 137:591–7. doi: 10.1001/archoto.2011.45

21. Viitanen H, Tuominen N, Vääräniemi H, Nikanne E, Annila P. Analgesic efficacy of rectal acetaminophen and ibuprofen alone or in combination for paediatric day-case adenoidectomy. *Br J Anaesth.* (2003) 91:363–7. doi: 10.1093/bja/aeg196

22. Voepel-Lewis T, Zanotti J, Dammeyer JA, Merkel S. Reliability and validity of the face, legs, activity, cry, consolability behavioral tool in assessing acute pain in critically ill patients. *Am J Crit Care.* (2010) 19:55–61; quiz 62. doi: 10.4037/ajcc2010624

23. Gaglani A, Gross T. Pediatric pain management. *Emerg Med Clin North Am.* (2018) 36:323–34. doi: 10.1016/j.emc.2017.12.002

24. Friedrichsdorf SJ. Multimodal pediatric pain management (part 2). *Pain Manag.* (2017) 7:161–6. doi: 10.2217/pmt-2016-0051

25. Sowder JC, Gale CM, Henrichsen JL, Veale K, Liljestrand KB, Ostlund BC, et al. Primary caregiver perception of pain control following pediatric adenotonsillectomy: a cross-sectional survey. *Otolaryngol Head Neck Surg.* (2016) 155:869–75. doi: 10.1177/0194599816661715

26. Elinder K, Söderman AC, Stalfors J, Knutsson J. Factors influencing morbidity after paediatric tonsillectomy: a study of 18,712 patients in the national tonsil surgery register in sweden. *Eur Arch Otorhinolaryngol.* (2016) 273:2249–56. doi: 10.1007/s00405-016-4001-x

frontiers | Frontiers in Pharmacology

TYPE Clinical Trial
PUBLISHED 17 August 2022
DOI 10.3389/fphar.2022.916017

OPEN ACCESS

EDITED BY
Samuel Seward,
Icahn School of Medicine at Mount Sinai, United States

REVIEWED BY
Stanislas Grassin-Delyle,
Université de Versailles Saint-Quentin-en-Yvelines, France
Herm Jan Brinkman,
Sanquin Research, Netherlands

*CORRESPONDENCE
Tianlong Wang,
w_tl5595@hotmail.com

†These authors have contributed equally to this work

SPECIALTY SECTION
This article was submitted to Obstetric and Pediatric Pharmacology, a section of the journal Frontiers in Pharmacology

RECEIVED 08 April 2022
ACCEPTED 27 July 2022
PUBLISHED 17 August 2022

CITATION
Zhang T, Feng H, Xiao W, Li J, Liu Q, Feng X, Qi D, Fan X, Shan Y, Yu T, Zhao G and Wang T (2022), Prophylactic administration of tranexamic acid combined with thromboelastography-guided hemostatic algorithm reduces allogeneic transfusion requirements during pediatric resective epilepsy surgery: A randomized controlled trial. *Front. Pharmacol.* 13:916017. doi: 10.3389/fphar.2022.916017

Prophylactic administration of tranexamic acid combined with thromboelastography-guided hemostatic algorithm reduces allogeneic transfusion requirements during pediatric resective epilepsy surgery: A randomized controlled trial

Ting Zhang[1†], Hua Feng[1†], Wei Xiao[1], Jingsheng Li[1], Qinghai Liu[1], Xuexin Feng[1], Dezhou Qi[1], Xiaotong Fan[2], Yongzhi Shan[2], Tao Yu[3], Guoguang Zhao[2] and Tianlong Wang[1*]

[1]Department of Anesthesiology, Xuanwu Hospital, Capital Medical University, Beijing, China, [2]Department of Neurosurgery, Xuanwu Hospital, Capital Medical University, Beijing, China, [3]Department of Functional Neurosurgery, Xuanwu Hospital, Capital Medical University, Beijing, China

Background: Intraoperative bleeding and allogeneic transfusion remain common problems in pediatric resective epilepsy surgery. Tranexamic acid (TXA) is a widely recommended antifibrinolytic drug that reduces blood loss and transfusion requirements for bleeding patients. Thromboelastography (TEG)-guided hemostatic algorithm is commonly used in bleeding management. This trial was designed to validate the efficacy of a multimodal coagulation therapy involving continuous TXA infusion with TEG-guided hemostatic algorithm in reducing allogeneic exposure risk in pediatric resective epilepsy surgery.

Methods: Eighty-three children undergoing resective epilepsy surgery were randomized into a treatment group (Group T; n = 42) and a control group (Group C; n = 41). Group T received prophylactic TXA (10 mg/kg followed by 5 mg/kg/h) with TEG-guided hemostatic algorithm, whereas Group C received conventional coagulation management. The primary outcome was allogeneic transfusion rate during surgery, and the secondary outcomes were intraoperative blood loss, incidence of postoperative seizures, and thromboembolic events during hospitalization.

Results: The incidence of intraoperative allogeneic transfusion reduced by 34.7% with the use of a multimodal coagulation therapy (19.0% in Group T vs. 53.7% in Group C; RR 0.355, 95% CI 0.179–0.704; p = 0.001). This was mainly triggered by a significant reduction (44.1%) in intraoperative plasma transfusion (7.1% in Group T vs. 51.2% in Group C; RR 0.139, 95% CI 0.045–0.432; p = 0.000). The risk of intraoperative RBC transfusion was lower in Group T than in Group C, but the difference was not statistically significant (14.3% in Group T vs.

29.3% in Group C; RR 0.488, 95% CI 0.202–1.177; $p = 0.098$). No platelets were transfused in both groups. Further, 19 (45.2%) patients in Group T received fibrinogen concentrates guided by TEG data, whereas 1 (2.4%) patient in Group C received fibrinogen concentrates empirically. There were no significant differences in estimated blood loss and postoperative seizures between the two groups, and no thromboembolic events were observed after surgery.

Conclusion: Prophylactic administration of TXA combined with TEG-guided hemostatic algorithm can be an effective multimodal coagulation strategy for reducing allogeneic transfusion requirements during pediatric resective epilepsy surgery.

Clinical Trial Registration: www.chictr.org.cn/index.aspx, identifier ChiCTR1800016188.

KEYWORDS

tranexamic acid, antifibrinolytics, thromboelastography, epilepsy surgery, pediatric anesthesia, transfusion, blood loss, coagulation therapy

Introduction

Studies have shown that surgical treatment is valuable for certain children with medically intractable epilepsy (Sperling et al., 2016; Dwivedi et al., 2017). However, considerable blood loss and coagulation disorders are important risk factors that can compromise the safety of pediatric resective epilepsy surgery (Thudium et al., 2014). Children are associated with low absolute blood volume and relatively larger head-to-body ratio (Livingston and Lee, 2000), which made pediatric intracranial surgeries at high risk of intraoperative bleeding. Moreover, preoperative exposure to antiepileptic drugs (AEDs) could cause coagulation disorders, including thrombocytopenia, platelet dysfunction, hypofibrinogenemia, or acquired von Willebrand disease (Finsterer et al., 2001; Gerstner et al., 2006; Pan et al., 2007). In addition, extensive tissue injury during surgery can produce large amounts of tissue activators that activate plasmin from plasminogen, leading to hyperfibrinolysis. The acquired coagulopathy can aggravate intraoperative bleeding and increase allogeneic transfusion requirements (Goobie and Haas, 2014). Therefore, significant efforts should be made to optimize coagulation function and reduce the exposure to allogeneic products during pediatric resective epilepsy surgery.

No standard strategies have been previously recommended to optimize hemostatic systems for pediatric epilepsy surgery, and clinical transfusion practice is primarily based on a combination of subjective bleeding assessment and standard laboratory tests. Given that timely laboratory values cannot be obtained during surgery, allogeneic blood products, especially plasma and platelets, have usually been transfused at the discretion of the attending surgeon and anesthesiologist when significant blood loss was expected or occurred. This empirical transfusion strategy may lead to allogeneic blood abuse and waste and place patients at high risk for transfusion-related adverse outcomes (Stainsby et al., 2008; Lavoie, 2011).

Tranexamic acid (TXA) is an antifibrinolytic drug that competitively inhibits the conversion of plasminogen to plasmin, thereby blocking the proteolytic action of plasmin on fibrin clot, and as such inhibiting fibrinolysis during surgery (McCormack, 2012). Strong evidence has shown that prophylactic TXA use can reduce blood loss and transfusion requirements in surgeries for pediatric scoliosis, cardiac, and craniosynostosis without apparent morbidity or mortality (Dadure et al., 2011; Goobie et al., 2011; Pasquali et al., 2012; McNicol et al., 2016; Goobie et al., 2018). However, few studies have explored the role of TXA in pediatric resective epilepsy surgery.

Thromboelastography (TEG) is a point-of-care test that can be conducted in a relatively short period (15–30 min) and provides a comprehensive, graphical, and numerical evaluation of the patient's clotting system. TEG can be used to guide transfusion practice during coagulation management, thus reducing the requirement of blood transfusion and improving surgical outcomes (Wikkelso et al., 2016). There is growing evidence supporting the use of TEG to manage surgical bleeding (Wikkelso et al., 2016; Feng et al., 2019; Spahn et al., 2019). However, such evidence has been primarily based on elective cardiac surgery, with limited studies investigating TEG-guided transfusion in craniotomies, especially for children.

In our center, we use a combination of continuous TXA infusion with TEG-guided coagulation management during hemispherectomy; this seems to have reduced the amount of blood loss and subsequent allogeneic transfusion requirements in our cases without promoting clinical complications involving thrombotic events and seizures (Xiao et al., 2016). Therefore, this clinical trial was conducted to assess the efficacy of the multimodal coagulation therapy during pediatric epilepsy surgery. We hypothesized that prophylactic administration of TXA combined with TEG-guided hemostatic algorithm would reduce allogeneic transfusion requirements during pediatric resective epilepsy surgery.

Materials and methods

Research design

This single-center, prospective, randomized, controlled clinical trial was conducted at Xuanwu Hospital of Capital Medical University (Beijing, China) from June 2018 to November 2021. The research was approved by the Ethics Committee of Xuanwu Hospital of Capital Medical University [LYS(2018)103] and registered at the Chinese Clinical Trial Registry (www.chictr.org.cn/index.aspx; identifier ChiCTR1800016188). All experimental procedures were conducted in accordance with the Declaration of Helsinki. Written informed consent was obtained from the patient's parents or legally authorized representatives before enrollment into the study.

Participants

Patients meeting the following inclusion criteria were included: 1) diagnosis of symptomatic epilepsy, 2) scheduled for elective resection of epileptic focus, 3) aged 1–12 years, 4) body weight ≤40 kg, 5) American Society of Anesthesiologists physical status classification of I or II, and 6) provided written informed consent. The exclusion criteria were as follows: 1) accompanied with liver diseases, 2) accompanied with kidney diseases, 3) accompanied with hematological diseases, 4) family history of hemorrhagic diseases, 5) history of craniotomy, and 6) allergies to tranexamic acid. Patients with a duration of surgery of <3 or >8 h were excluded from analysis given that surgical procedures and consecutive blood loss might differ considerably.

Randomization and blinding

Enrolled patients were randomized into the treatment group (Group T) or control group (Group C) in a 1:1 ratio using a random digit table provided by a biostatistician at our center *via* SAS software (version 8.02; SAS Institute Inc., Cary, NC, United States). Allocation concealment was ensured by prepackaging the grouping information from the random digit table in sequentially numbered sealed opaque envelopes. The envelopes were kept by a nurse from the postanesthesia care unit who was blinded to this study. When a patient satisfied the inclusion criteria, the nurse opened the corresponding envelope and assigned the patient to the corresponding group. The patients, neurosurgeons, and the outcome assessor (a trained investigator, who collected postoperative data from the Electronic Medical Record System of our center), were all blinded to the group assignment.

Surgery and anesthesia

All surgical procedures were performed by one of two functional neurosurgeons who had >20 years of experience at our center. Anesthesia management in Group T was performed by a specific anesthesiologist who had been trained to conduct hemostatic strategies according to the protocol. The anesthesiologists who cared for the patients in Group C were assigned randomly according to the arrangement at our department.

All patients received general anesthesia as routinely practiced at our center. The following parameters were consistently monitored: electrocardiography, pulse oximetry, invasive blood pressure (IBP), bispectral index (BIS), nasopharyngeal temperature, partial pressure of end-tidal CO_2 ($P_{ET}CO_2$), and urine output. Patients were induced via intravenous propofol (2–3 mg/kg), sufentanil (0.3–0.5 μg/kg), and rocuronium (0.6–1 mg/kg). Thereafter, the patients were intubated and ventilated while maintaining the $P_{ET}CO_2$ at 30–35 mmHg. When venous access was difficult in the conscious state, intramuscular ketamine (5–7 mg/kg) or sevoflurane administration through inhalation was conducted before induction. Arterial cannulation and central venous puncture were conducted after anesthesia induction. Total intravenous anesthesia was achieved via continuous infusion of propofol (6–10 mg/kg/h) and remifentanil (0.2–0.4 μg/kg/min), which was titrated to maintain a BIS value within 40–60, as well as heart rate and IBP within 20% of baseline. A crystalloid-based fluid was administered to compensate for the preoperative fasting period, basic physiological requirement and intraoperative blood loss, and to maintain hemodynamic stability and urine output of ≥1 ml/kg/h. Moreover, intraoperative heating devices were utilized as necessary to maintain a nasopharyngeal temperature of ≥36°C. Similarly, pH values and plasma calcium levels were optimized to their normal ranges during surgery. Blood salvage was used intraoperatively to collect autologous blood from the surgical site, immediately returning the recovered red blood cells to the patients in real time. To relieve postoperative pain, sufentanil (0.1–0.15 μg/kg) was administered intravenously 30 min before the end of the surgery, and local infiltration with 0.25% ropivacaine (≤1 ml/kg) was performed prior to scalp closure. All patients were extubated at the end of surgery.

Blood-gas analysis (ABL800, Radiometer Medical Aps, Bronshoj, Denmark) was performed at four time points [prior to incision (T1), during the cutting of the dura mater (T2), during suturing of the dura mater (T3), and after scalp closure (T4)], or more frequently as indicated. Red blood cells (RBC) were administered at a target level of 10 g/dl when hemoglobin concentrations obtained from the blood-gas analysis dropped to <8 g/dl. The amount of RBC administered was calculated as follows: amount of RBC (ml) = body weight (kg) × desired increment in hemoglobin concentration (g/dl) × 5 (Morley, 2009).

Hemostatic strategies in group T

After induction of anesthesia before the surgical incision, an initial bolus of TXA (10 mg/kg) (Changchun Tiancheng Company, Changchun, China) was infused intravenously in 15 min, followed

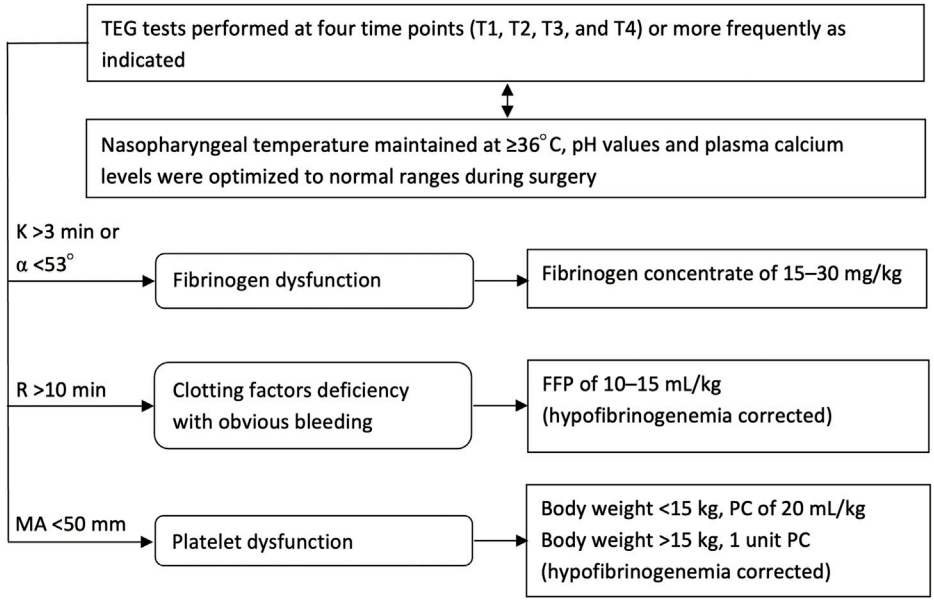

FIGURE 1
Flow chart for the TEG-guided hemostatic algorithm. TEG, thromboelastography; T1, prior to incision; T2, cutting of the dura mater; T3, suturing of the dura mater; T4, after scalp closure; K, coagulation time; α angle, angle of divergence; R, reaction time to clot formation; MA, maximum amplitude of clot strength; FFP, fresh frozen plasma; PC, platelet apheresis concentrate.

by a continuous infusion at 5 mg/kg/h until the end of the scalp closure. If the cumulative dose of TXA reached 1 g before the end of surgery, the infusion would be stopped.

We employed kaolin-activated TEG analysis (TEG-5000, Haemoscope Corporation, Illinois, United States) to monitor the patient's coagulation status and guide coagulation component supplementation. All the analyses were performed by an adequately trained anesthesiologist according to standard operating procedures. Whole blood samples for TEG analysis were obtained through a port located at the hub of the arterial catheter near the entry site. Dead space blood, up to 10 ml, was removed to avoid heparin contamination by the arterial flush solution. The collected samples were drawn into 1.8 ml vacutainers containing buffered sodium citrate (0.109 M, 3.2%). At 15 min after obtaining the samples, 1 ml of citrated whole blood was placed into a vial with a kaolin activator (#6300, Haemonetics Corporation) and mixed thoroughly by inversion 5 times. Then, 340 µl of citrated kaolin-activated blood was transferred to a 37°C warmed clear cup containing 20 µl of 0.2 M $CaCl_2$ for analysis. The TEG analyzer was allowed to run until LY30 (lysis at 30 min; percentage reduction in the maximal amplitude of the TEG tracing after 30 min) could be determined. The specific TEG parameters that were measured included reaction time (R), coagulation time (K), α angle, maximal amplitude (MA), and LY30.

TEG tests were conducted at four time points (similar to that for blood-gas analysis), and additional tests could be performed at any time if necessary, such as if ongoing bleeding had occurred. The TEG-guided hemostatic algorithm is presented in Figure 1. Fibrinogen concentrate (Shanghai RAAS Blood Products Co., Ltd., Shanghai, China) was administered at 15–30 mg/kg when signs of fibrinogen dysfunction (K time >3 min or α angel <53°) were observed. Repeated fibrinogen concentrate was administrated if necessary. After hypofibrinogenemia had been corrected, fresh frozen plasma (FFP) of 10–15 ml/kg was transfused if R time was >10 min with obvious bleeding at the surgical sites, and platelet apheresis concentrate (PC) was administered when MA value was <50 mm. The dose of PC was 20 ml/kg if body weight was <15 kg, otherwise, 1 unit. Generally, supplementation of coagulation components was conducted only if relevant bleeding was observed, but not due to abnormal TEG results without signs of bleeding.

Conventional hemostatic strategies in group C

Neither TXA nor TEG tests were performed. Hemostatic strategies were selected in accordance with routine practice at our center. Coagulation components were transfused guided by standard coagulation tests, which could be performed at any time as indicated. When prothrombin time (PT) or activated partial thromboplastin time (APTT) prolonged >1.5 times normal, or plasma fibrinogen concentration ranged 1.5–2.0 g/

L, FFP of 10–15 ml/kg was administered. Fibrinogen concentrate of 15–30 mg/kg was infused if plasma fibrinogen level was <1.5 g/L. Platelets were transfused if the platelet count dropped to $<100 \times 10^9$/L. If laboratory coagulation values could not be promptly obtained, hemostatic products were transfused empirically in selected patients mainly depending on signs of microvascular bleeding as well as the patient's hemodynamic parameters and consultant anesthesiologist's experience.

Postoperative management

Postoperative bleeding management was performed at the discretion of the consultant neurosurgical team. Generally, transfusion strategies were selected according to signs of clinical anemia or bleeding and abnormal laboratory values. After surgery, the neurosurgeons made ward rounds twice a day, and examined the patients for symptoms and signs of complications, until the patients were discharged. Side effects, including thrombotic events (e.g., deep vein thrombosis or pulmonary embolism) and seizures, were noted in the Electronic Medical Record System.

Data collection

Demographic and baseline laboratory data, including age, height, weight, hemoglobin concentration, platelet count, PT, APTT, international normalized ratio (INR), and plasma fibrinogen level, were preoperatively obtained. Surgical data from both groups, such as type of resection, duration of surgery and anesthesia, infusion volume and urine output as well as TEG parameters (R, K, α angle, MA, and LY30) in Group T and standard coagulation parameters in Group C were collected during surgery. Intraoperative blood loss was estimated using standard clinical variables (blood in cell-savers and suction containers and sponge weight). Hemoglobin concentration and platelet count on the first day after surgery, blood products (including RBC, plasma, and platelets) transfused perioperatively, fibrinogen concentrate supplementation, length of hospital stay after surgery, and postoperative complications (including thromboembolic events and seizures) were recorded.

Outcome measures

The primary outcome was allogeneic transfusion rate during surgery, defined as transfusion of any allogeneic blood product, including RBC, plasma, or platelets. The secondary outcomes included intraoperative blood loss, incidence of postoperative seizures, and postoperative thromboembolic events during hospitalization.

Sample size calculation

Sample size was calculated according to the incidence of allogeneic transfusion during surgery. In our pilot study ($n = 32$), the allogeneic transfusion rates were 37.50% and 68.75% in Groups T and C, respectively. The sample size software PASS 11 (NCSS, Caseville, Utah, United States) estimated that a total of 39 cases was required for each group to detect a significant change in the allogeneic transfusion incidence, with a type I error $\alpha = 0.05$ and type II error $\beta = 0.2$. Considering a withdrawal rate of 10%, the target sample size for each group was 43.

Statistical analyses

The groups T and C were compared with respect to demographics, baseline characteristics, transfusion requirements, and intraoperative and postoperative outcomes. All continuous variables were tested for normality using the Shapiro–Wilk test. Normally distributed data are presented as mean ± standard deviation (SD), and non-normally distributed data as median [25%–75% interquartile range (IQR)]. Continuous data with a normal distribution, such as age, height, preoperative platelet count, PT, INR, duration of surgery and anesthesia, postoperative hemoglobin level, and delta hemoglobin concentration (preoperative to postoperative day 1), were compared between groups by the independent-samples *t*-test. Intragroup comparisons of hemoglobin concentration between baseline and follow-up were analyzed using paired-samples *t*-test. Continuous data not conforming to a normal distribution, including weight, preoperative APTT, infusion volume, urine output, estimated blood loss, postoperative platelet count, and length of hospital stay after surgery, were compared between groups with the Mann–Whitney *U*-test. The Wilcoxon signed-rank test was applied to compare TEG values at different time points in Group T. Categorical variables, such as preoperative anemia (hemoglobin concentration <12 g/dl), preoperative hypofibrinogenemia (plasma fibrinogen concentration <2.0 g/L), type of extensive resection (hemispherectomy), allogeneic transfusion, fibrinogen concentrate administration, postoperative seizures and thromboembolic events, are expressed as N [percentages (%)] and compared between groups using the Pearson chi-square or continuity correction test as indicated. The relative risk (RR) and 95% confidence intervals (CI) between the two groups were calculated for data of allogeneic transfusion and postoperative seizures.

All statistical analyses were performed using SPSS software (version 20.0; SPSS Inc., Chicago, IL, United States), with a p value of <0.05 indicating statistical significance.

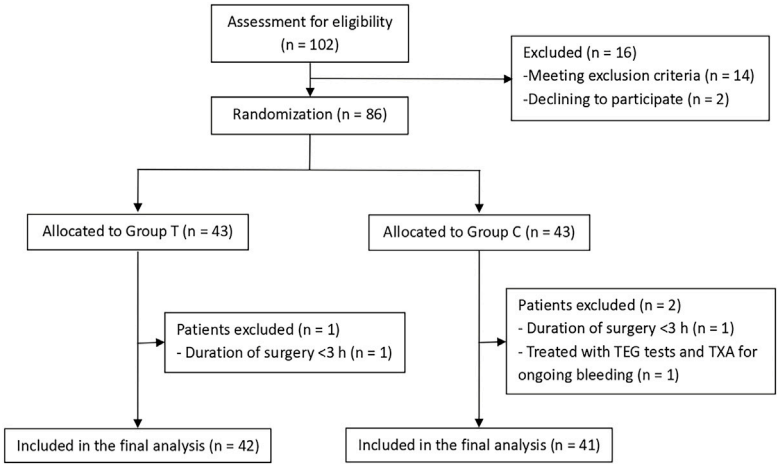

FIGURE 2
Flow chart of the study. TEG, thromboelastography; TXA, tranexamic acid.

TABLE 1 Demographic and baseline characteristics of the two groups.

Parameter	Group T (n = 42)	Group C (n = 41)	p value
Age[a] (years)	6.08 ± 2.65	6.89 ± 3.00	0.194
Height[a] (cm)	113.80 ± 16.01	121.21 ± 18.46	0.054
Weight[b] (kg)	20.50 (18.75–26.00)	25.00 (18.75–29.50)	0.179
Preoperative anemia[c&] [N (%)]	14 (33.3)	10 (24.4)	0.369
Preoperative laboratory values			
Platelets[a] (10^9/L)	273.17 ± 75.65	295.63 ± 84.26	0.205
PT[a] (s)	13.24 ± 0.66	13.25 ± 0.76	0.970
APTT[b] (s)	40.50 (36.55–44.03)	41.20 (36.45–44.40)	0.881
INR[a]	1.01 ± 0.07	1.01 ± 0.07	0.946
Preoperative hypofibrinogenemia[c&] [N (%)]	15 (35.7)	13 (31.7)	0.699
Hemispherectomies[c#] [N (%)]	3 (7.1)	2 (4.9)	1.000
Surgery duration[a] (min)	282.60 ± 58.70	283.07 ± 73.75	0.974
Anesthesia duration[a] (min)	394.48 ± 74.61	367.32 ± 79.01	0.111

[a]The values are given as mean ± SD, with groups compared by the independent-samples t-test.
[b]The values are given as median (25%–75% IQR), with groups compared by the Mann–Whitney U-test.
[c]The values are given as N (%), with groups compared by the [&]Pearson chi-square test, or [#]continuity correction test.
PT, prothrombin time; APTT, activated partial thromboplastin time; INR, international normalized ratio.

Results

Demographic and baseline characteristics

A total of 102 patients were assessed for eligibility, and 16 patients were excluded prior to randomization. The 86 patients who satisfied the inclusion criteria were randomly and equally assigned to Groups T and C, with each group comprising 43 patients. One patient in each group was excluded from the analysis for having <3 h duration of surgery, whereas another patient in Group C was excluded due to TEG and TXA treatment for ongoing bleeding. Finally, 83 patients were included in the analysis (42 in Group T and 41 in Group C) (Figure 2).

Demographic and baseline characteristics of both groups are summarized in Table 1. Baseline parameters, such as age,

TABLE 2 Transfusion of blood products and fibrinogen concentrate.

Parameter	Group T (n = 42) [N (%)]	Group C (n = 41) [N (%)]	RR (95% CI)	p value
Risk of allogeneic transfusion[a]				
Intraoperative	8 (19.0)	22 (53.7)	**0.355 (0.179–0.704)**	**0.001**
Total[b]	13 (31.0)	23 (56.1)	**0.552 (0.326–0.934)**	**0.021**
Risk of RBC transfusion[a]				
Intraoperative	6 (14.3)	12 (29.3)	0.488 (0.202–1.177)	0.098
Total[b]	11 (26.2)	15 (36.6)	0.716 (0.374–1.369)	0.307
Risk of plasma transfusion[a]				
Intraoperative	3 (7.1)	21 (51.2)	**0.139 (0.045–0.432)**	**0.000**
Total[b]	8 (19.0)	22 (53.7)	**0.355 (0.179–0.704)**	**0.001**
Total platelets transfusion[b]	0 (0)	0 (0)	NA	NA
Fibrinogen concentrate infusion[a]	19 (45.2)	1 (2.4)	**18.548 (2.601–132.243)**	**0.000**

The values are given as N (%).
[a]Pearson chi-square test used to compare groups. Boldface type indicates statistical significance.
[b]Total includes intraoperative and postoperative transfusion.
RR, relative risk; CI, confidence interval; RBC, red blood cells; NA, not applicable.

height, weight, preoperative laboratory values, percentage of hemispherectomies, duration of surgery and anesthesia, were comparable between both groups. Mean preoperative hemoglobin values were 12.35 ± 0.91 and 12.79 ± 0.99 g/dl in Groups T and C, respectively, with no difference in preoperative anemia (hemoglobin concentration <12 g/dl) between both groups (p = 0.369) (Table 1). Moreover, 15 (35.7%) and 13 (31.7%) patients in Groups T and C had hypofibrinogenemia (plasma fibrinogen level <2.0 g/L) preoperatively, with no difference with regard to the percentage of preoperative hypofibrinogenemia between the two groups (p = 0.699) (Table 1).

Transfusion requirements

The requirements of allogeneic transfusion in Group T were significantly lower than that in Group C: intraoperative requirements (19.0% vs. 53.7%; RR 0.355, 95% CI 0.179–0.704; p = 0.001) and total perioperative requirements (31.0% vs. 56.1%; RR 0.552, 95% CI 0.326–0.934; p = 0.021) (Table 2). The risks of RBC transfusion were lower in Group T than in Group C; however, the differences were not statistically significant. Intraoperative and total risks of plasma exposure were significantly lower in Group T compared with Group C: intraoperative risks (7.1% vs. 51.2%; RR 0.139, 95% CI 0.045–0.432; p = 0.000) and total perioperative risks (19.0% vs. 53.7%; RR 0.355, 95% CI 0.179–0.704; p = 0.001) (Table 2). None of the patients in both groups required platelets transfusion. Further, 19 (45.2%) patients in Group T received fibrinogen concentrates guided by TEG data, whereas only 1 (2.4%) patient in Group C received fibrinogen concentrates because of a preoperative fibrinogen level of <1.5 g/L.

Surgical data and postoperative outcomes

Intra- and postoperative clinical outcomes and laboratory values are presented in Table 3. Accordingly, Group T intraoperatively received higher volumes of crystalloids than Group C. No significant differences were observed in terms of intraoperative colloid input, urine output, estimated blood loss, and postoperative values of hemoglobin and platelets in the groups. Postoperative hemoglobin levels decreased in both groups, with the reduction in hemoglobin from preoperative baseline to postoperative being comparable between both groups.

Both groups had comparable duration of hospital stay after surgery, with no thromboembolic events occurring in either group. Postoperative seizures of varying degrees occurred in four (9.5%) and five patients (12.2%) in Groups T and C, respectively, during their hospital stay, with no significant difference between the two groups (RR 0.781, 95% CI 0.225–2.705; p = 0.969) (Table 3).

Coagulation profile

TEG tests were administered for all 42 patients in Group T. TEG values showed that 13 (31.0%) patients in Group T had accompanying preoperative fibrinogen dysfunction (K > 3 min or α < 53° at T1) and in 6 other patients, fibrinogen dysfunction occurred later during the surgery. After fibrinogen dysfunction had been corrected, three patients exhibited clotting factors deficiency in the TEG tests.

TABLE 3 Intraoperative and postoperative clinical outcomes and laboratory values in both groups.

Parameter	Group T (n = 42)	Group C (n = 41)	p value
Intraoperative fluids[a]			
Crystalloid (ml)	1490 (1325–1713)	1000 (700–1200)	**0.000**
Colloid (ml)	0 (0–200)	0 (0–200)	0.643
Urine output[a] (ml)	850 (638–1093)	800 (500–1000)	0.247
Estimated blood loss[a] (ml)	100 (100–155)	100 (100–150)	0.792
Hemoglobin level on POD 1[b] (g/dl)	10.55 ± 1.31	10.58 ± 1.32	0.921
Delta hemoglobin[b] (g/dl) (preoperative to POD 1)	−1.84 ± 1.39	−2.21 ± 1.67	0.290
Platelet count on POD 1[a] (10^9/L)	233.00 (185.00–263.00)	226.00 (186.50–286.50)	0.672
Postoperative thrombotic events[c] [N (%)]	0 (0)	0 (0)	NA
Postoperative seizures[c] [N (%)]	4 (9.5)	5 (12.2)	0.969
Hospital stay after surgery[a] (days)	8.00 (7.00–11.25)	9.00 (7.50–11.00)	0.827

[a]The values are given as median (25%–75% IQR), with groups compared by the Mann–Whitney U-test. Boldface type indicates statistical significance.
[b]The values are given as mean ± SD, with groups compared by the independent-samples t-test.
[c]The values are given as N (%), with groups compared by the continuity correction test.
POD, postoperative day; NA, not applicable.

TABLE 4 TEG data in Group T.

TEG variable	T1	T2	T3	T4	p value	p value	p value
					T2 vs. T1	T3 vs. T1	T4 vs. T1
R (min)	8.20 (7.10–9.35)	7.85 (7.20–9.23)	7.45 (6.65–9.23)	6.30 (5.20–8.90)	0.757	0.576	**0.006**
K (min)	2.40 (1.95–3.00)	2.20 (1.80–2.53)	2.10 (1.80–2.73)	1.80 (1.60–2.50)	**0.017**	**0.004**	**0.010**
α angle (degrees)	60.60 (53.15–66.25)	63.50 (58.70–66.33)	62.25 (59.60–66.33)	65.10 (57.10–69.70)	**0.024**	**0.028**	**0.005**
MA (mm)	56.80 (52.25–60.60)	57.95 (55.38–61.60)	58.60 (53.58–61.60)	59.90 (56.40–63.00)	**0.030**	**0.025**	**0.009**
LY30 (%)	0.50 (0.10–1.50)	0.55 (0.00–1.00)	0.25 (0.00–0.80)	0.20 (0.00–0.80)	0.334	0.189	**0.021**

The values are given as median (25%–75% IQR). The p values are obtained using the Wilcoxon signed-rank test. Boldface type indicates statistical significance.
TEG, thromboelastography; R, reaction time to clot formation; K, coagulation time; α angle, angle of divergence; MA, maximum amplitude of clot strength; LY30, percentage lysis 30 min post-MA; T1, prior to incision; T2, cutting of the dura mater; T3, suturing of the dura mater; T4, after scalp closure.

TEG data for the four time points (mentioned above) are reported in Table 4. Median R values were higher for T1 (8.20 min) than for T2 (7.85 min), T3 (7.45 min), and T4 (6.30 min), with the difference between T1 and T4 being significant (Table 4). Median K values were also higher for T1 (2.40 min) than for T2 (2.20 min), T3 (2.10 min), and T4 (1.80 min), with differences reaching significance for all comparisons (Table 4). The median α angle values for T2 (63.50°), T3 (62.25°), and T4 (65.10°) were significantly higher than those for T1 (60.60°) ($p < 0.05$ for all), with similar findings observed for MA values (Table 4). Overall, changes in TEG values showed that the hemostatic system was enhanced over time during the surgery. LY30 values were significantly lower at T4 than at T1; however, all LY30 values were within normal limits, indicating that none of the patients in Group T developed hyperfibrinolysis. No intraoperative standard coagulation tests were performed in Group C.

Discussion

The present study demonstrated that allogeneic transfusion requirements during pediatric resective epilepsy surgery reduced by 34.7% (RR of 0.355) with the use of an intraoperative multimodal coagulation therapy. The total risk of perioperative allogeneic blood exposure in Group T was also reduced by 25.1% (RR of 0.552), and this did not translate to lower postoperative hemoglobin concentrations. Moreover, no changes in postoperative outcomes of seizures or thromboembolic events were observed between the two groups. These findings suggest that the prophylactic administration of TXA combined with TEG-guided goal-directed hemostatic algorithm is an effective multimodal coagulation strategy for reducing allogeneic transfusion requirements during pediatric resective epilepsy surgery.

TABLE 5 Interpretation of TEG-5000 parameters.

Main parameter	Definition	Coagulation correlation	References ranges
R	The time from initiation to initial fibrin formation, arbitrarily defined as the trace amplitude of 2 mm	Clotting factors	5–10 min
K	The time taken for the amplitude to increase from 2 to 20 mm	Fibrinogen	1–3 min
α angle	The angle formed between the midline and the tangent to the main body of the trace	Fibrinogen	53°–72°
MA	The amplitude at the widest point of the trace	Platelet (~80%) Fibrinogen (~20%)	50–70 mm
LY30	The percentage reduction in amplitude 30 min after MA is reached	Fibrinolysis	0%–8%

Reference ranges according to the manufacturer of TEG-5000, for kaolin-activated citrated and recalcified blood samples.
R, reaction time to clot formation; K, coagulation time; α angle, angle of divergence; MA, maximum amplitude of clot strength; LY30, percentage lysis 30 min post-MA.

TEG is a viscoelastic test that can provide timely clotting and fibrinolysis information in the operation theater and guide direct supplementation of indicated blood components for appropriate coagulopathy (Whiting et al., 2015). The interpretation of TEG-5000 parameters from the User's Manual is summarized in Table 5. TEG-guided component replacement has been described in a variety of previous reports on bleeding management (Walsh et al., 2011; Johansson et al., 2013; Christiaans et al., 2014; Kane et al., 2016; Sujka et al., 2018). The time to clot formation (R-time) was used as a guide for clotting factors, the speed of clot formation (K-time, or α angle) as an indication for fibrinogen level. It was reported that ~80% of the clot strength was due to platelet contribution, and the remainder was the contribution of fibrin network (Wegner and Popovsky, 2010). Therefore, in the presence of normal fibrinogen level, overall clot strength (MA) was used to assess platelet function (Tanaka et al., 2014).

In the current study, TEG data revealed that 13 (31.0%) patients in Group T had accompanying preoperative fibrinogen dysfunction and 6 other patients experienced fibrinogen dysfunction later during surgery. After fibrinogen dysfunction had been corrected, only three patients exhibited clotting factors deficiency. Our results demonstrated that fibrinogen dysfunction was the main coagulopathy in pediatric resective epilepsy surgery. This could have been due to preoperative AEDs administration, which can impair hemostatic system, including a decrease in fibrinogen (Gerstner et al., 2006). Consistent with the mentioned finding, our laboratory results showed that approximately 1/3 of all patients showed complications of preoperative hypofibrinogenemia. Another reason for fibrinogen dysfunction may be craniotomy and intraoperative bleeding, considering Levy et al.'s (2012) finding that fibrinogen was the first coagulation factor that achieved a critical low value during massive blood loss. Evidence has shown that fibrinogen deficiency could further aggravate perioperative bleeding after craniotomy (Adelmann et al., 2014). Therefore, fibrinogen supplementation is vital for reversing and maintaining hemostatic function for pediatric epilepsy patients. Guided by TEG values, patients accompanied with fibrinogen dysfunction in Group T received directed fibrinogen concentration replacement. Thereafter, the hemostatic system was obviously optimized, as evidenced by a reduction in the K time and increase in the α angle and MA value.

The currently recommended threshold for perioperative fibrinogen replacement is 1.5–2.0 g/L (Kozek-Langenecker et al., 2017). Regarding the risk of increased intraoperative bleeding, one patient in Group C received fibrinogen concentrate for preoperative plasma fibrinogen level of <1.5 g/L, whereas other patients with preoperative hypofibrinogenemia (plasma fibrinogen concentrations ranging 1.5–2.0 g/L) received plasma transfusion. Since laboratory coagulation values could only be obtained in a long period of >2 h at our center, no intraoperative standard coagulation tests were performed in Group C. Intraoperative plasma transfusion in Group C was performed at the discretion of the attending anesthesiologists, mainly depending on signs of recurrent bleeding from the wound margins. Overall, 21 (51.2%) patients in Group C were transfused plasma traditionally to correct abnormal coagulation function and control microvascular bleeding. Generally, plasma is primarily recommended to correct coagulation factor deficiencies (Kozek-Langenecker et al., 2017). Studies have shown that plasma transfusion alone is inadequate to correct hypofibrinogenemia (Kozek-Langenecker et al., 2017). Bolliger et al. (2010) found that a minimum FFP transfusion volume of 20–30 ml/kg should be administered before expecting a significant increase in plasma fibrinogen concentration, whereas the frequently recommended FFP dosage ranges 10–15 ml/kg (Goobie and Haas, 2014). Fibrinogen concentrate, associated with decreased immunogenic and infectious complications and rapid availability (Levy et al., 2012), has recently been recommended to correct hypofibrinogenemia among pediatric surgery cases (Kozek-Langenecker et al., 2017). In the present study, after directed fibrinogen concentration replacement, only three (7.1%) patients in Group T required plasma transfusion because of clotting factors deficiency. Therefore, with the implementation of TEG-guided hemostatic algorithm, the risk of intraoperative plasma exposure was greatly reduced (by 44.1%, RR of 0.139). Our results are in accordance with the findings of Ak et al. (2009) and Schaden et al.

(2012), where Ak et al. (2009) observed that a TEG-guided transfusion algorithm promoted a significant lower FFP exposure compared to physician-directed transfusion in patients undergoing elective coronary artery bypass grafting, and Schaden et al. (2012) reported a significant reduction in allogeneic transfusion after a viscoelastic testing-based coagulation strategy for bleeding burn patients. In addition, in the present study, as plasma transfusion was significantly reduced, more crystalloid was needed to replace and maintain intravascular volume in Group T (Table 3).

As an essential component of multimodal coagulation therapy, TXA has been the most widely recommended pharmacological agent for suppressing fibrinolysis and preventing perioperative bleeding in recent pediatric critical bleeding guidelines (Kozek-Langenecker et al., 2017; Goobie et al., 2019). However, only a few clinical trials are available on TXA administration for pediatric epilepsy surgery, which might be owing to the concern of side effects of TXA, particularly seizures. Evidence has suggested that TXA-associated seizures are dose-related, given that high TXA dosing schemes, such as 100 mg/kg or >2 g/d have been reportedly associated with seizures in high-risk patients who underwent cardiac surgery or those with pre-existing renal impairment (Murkin et al., 2010; Lin and Xiaoyi, 2016; Murao et al., 2021). Moreover, studies using low dosage regimens did not report increased risk of seizures in pediatric patients (Goobie et al., 2017; Faraoni et al., 2019; Murao et al., 2021). In our trial, we cautiously selected a lower dosage scheme (10 mg/kg loading dose followed by 5 mg/kg/h maintenance infusion) based on pharmacokinetic modeling in pediatric patients, which had been shown to produce stable and therapeutic TXA plasma concentrations (Goobie et al., 2013). We found no significant difference in the incidence of postoperative seizures between the two groups, which agree with the findings of Goobie et al. (2017) during pediatric craniofacial surgery. None of the patients in Group T developed a clinical thromboembolic event, which is consistent with the finding that appropriate TXA administration was not associated with increased risk of thrombotic events (Shakur et al., 2010; Shakur et al., 2017; Myles et al., 2017; Goobie and Faraoni, 2019; Roberts et al., 2019; Murao et al., 2021). These results indicate that the TXA dosage regimen we adopted could be well tolerated by pediatric epilepsy patients.

LY30 values, the gold standard in detecting hyperfibrinolysis (Haas et al., 2014), were all within normal ranges (<8%), demonstrating that no hyperfibrinolysis occurred in Group T. In addition, the LY30 values at T4 were significantly lower than that at T1, indicating that fibrinolysis was further inhibited by TXA administration. Our results confirmed that prophylactic TXA administration could be an effective coagulation therapy for pediatric epilepsy surgery.

Data regarding RBC transfusion in pediatric resective epilepsy surgery are scarce. Most studies were retrospective and reported risks of RBC exposure that varied from 30% to 51% (Manohar et al., 2011; Thudium et al., 2014; Vadera et al., 2015). In our study, the total perioperative RBC transfusion requirements were approximately 30%, which was comparable to the findings of Manohar et al. (2011) and Vadera et al. (2015) but significantly lower than the 51% reported by Thudium et al. (2014). An important reason underlying this might be the different settings of RBC transfusion trigger; this value was 8 g/dl in our trial and 9.5 g/dl in the study by Thudium et al. (2014). The restrictive hemoglobin threshold of 8 g/dl has been shown to be indicated and safe in pediatric craniotomies (Goobie and Haas, 2014). In our study, the requirements for RBC transfusion were lower in Group T than in Group C, which may confirm the efficacy of our multimodal coagulation therapy in reducing RBC exposure. Given that our sample size was calculated based on transfusion incidence of all allogeneic products, including RBC and plasma, more patients may be needed to achieve a statistical difference.

Pediatric resective epilepsy surgery has been associated with significant blood loss (Thudium et al., 2014). In our study, the median estimated blood loss (EBL) was 100 ml for both groups, which was lower than the value (150 ml) reported by Thudium et al. (2014). This may be because fewer complex surgeries (only three hemispherectomies in Group T vs. two in Group C) had been conducted in recent years at our center, given that hemispherectomies had a significantly higher EBL than single lobectomies (Manohar et al., 2011). In addition, advancements in microsurgical techniques and the extensive experience of our surgical team might also contribute to the decreased blood loss. No significant difference was observed in the EBL between the groups, perhaps due to two factors: 1) blood loss itself is difficult to evaluate accurately and 2) surgical and anesthesia techniques have been constantly refined given that the current study lasted for over 3 years, and blood loss in these surgical settings at our center has been lower than before; this suggests that a larger sample size might be needed to detect differences in blood loss.

The current study has several limitations. First, given that this coagulation management strategy is a bundled treatment protocol, the reduction in allogeneic transfusion in our study cannot be attributed to one specific treatment factor, and further studies separately evaluating the efficacy of TXA administration or TEG-guided hemostatic algorithm for pediatric resective epilepsy surgery are warranted. Second, no TEG analyses were performed in Group C; thus, we could not compare the difference in coagulation function between groups due to the lack of matching TEG values in Group C. Therefore, the conclusion that our multimodal coagulation therapy can activate the hemostatic system of pediatric epilepsy surgical patients should be interpreted with caution. Moreover, intracranial surgery itself could be combined with enhanced hemostatic system given that the injured brain could release tissue thromboplastin and activate the coagulation cascade (van der Sande et al., 1983). Third, although the recommended triggers of TEG parameters for coagulation therapy have increased over the last years, a universally accepted threshold for initiating clotting

factor infusion, as well as the dose required to reach the targeted level, are still missing, especially for pediatric craniotomies. This needs to be verified by future clinical trials. Finally, while no thromboembolic events or increased incidence of postoperative seizures were observed in our study, it was not powered to make conclusions on safety of the multimodal coagulation therapy. Future larger multicenter trials in pediatric epilepsy surgery would be required to confirm the safety profile.

In conclusion, this study demonstrated that fibrinogen dysfunction was the main coagulopathy during pediatric resective epilepsy surgery. As a multimodal coagulation therapy for pediatric resective epilepsy surgery, the prophylactic use of TXA combined with TEG-guided hemostatic algorithm can optimize hemostatic function and promote lower risk of allogeneic exposure compared to conventional coagulation management strategies.

Data availability statement

The original contributions presented in the study are included in the article/supplementary material, further inquiries can be directed to the corresponding author.

Ethics statement

The studies involving human participants were reviewed and approved by the Ethics Committee of Xuanwu Hospital, Capital Medical University. Written informed consent to participate in this study was provided by the participants' legal guardian/next of kin.

Author contributions

TZ, HF, and TW: study design. TZ, HF, WX, JL, QL, DQ, X-TF, YS, TY, and GZ: study performance. TZ, HF, and X-XF: data analysis. TZ and HF: manuscript writing. HF and TW: manuscript revision. All authors contributed to the article and approved the final version of the manuscript.

Funding

This work was supported by Beijing Municipal Administration of Hospitals Incubating Program (PX2018075) and Xuanwu Hospital Funding Support (HZ2021PYLJ019) of Capital Medical University.

Acknowledgments

We sincerely thank all participating colleagues in the Departments of Neurosurgery, Functional Neurosurgery, Anesthesiology and Operating Room of Xuanwu Hospital, Capital Medical University, for their cooperation. We wish to express special appreciation to Chunxiu Wang, Evidence-based Medical Center of Xuanwu Hospital, Capital Medical University, for her expert statistical guidance.

Conflict of interest

The authors declare that the research was conducted in the absence of any commercial or financial relationships that could be construed as a potential conflict of interest.

Publisher's note

All claims expressed in this article are solely those of the authors and do not necessarily represent those of their affiliated organizations, or those of the publisher, the editors and the reviewers. Any product that may be evaluated in this article, or claim that may be made by its manufacturer, is not guaranteed or endorsed by the publisher.

References

Adelmann, D., Klaus, D. A., Illievich, U. M., Krenn, C. G., Krall, C., Kozek-Langenecker, S., et al. (2014). Fibrinogen but not factor XIII deficiency is associated with bleeding after craniotomy. *Br. J. Anaesth.* 113 (4), 628–633. doi:10.1093/bja/aeu133

Ak, K., Isbir, C. S., Tetik, S., Atalan, N., Tekeli, A., Aljodi, M., et al. (2009). Thromboelastography-based transfusion algorithm reduces blood product use after elective CABG: a prospective randomized study. *J. Card. Surg.* 24 (4), 404–410. doi:10.1111/j.1540-8191.2009.00840.x

Bolliger, D., Gorlinger, K., and Tanaka, K. A. (2010). Pathophysiology and treatment of coagulopathy in massive hemorrhage and hemodilution. *Anesthesiology* 113 (5), 1205–1219. doi:10.1097/ALN.0b013e3181f22b5a

Christiaans, S. C., Duhachek-Stapelman, A. L., Russell, R. T., Lisco, S. J., Kerby, J. D., and Pittet, J. (2014). Coagulopathy after severe pediatric trauma. *Shock* 41 (6), 476–490. doi:10.1097/SHK.0000000000000151

Dadure, C., Sauter, M., Bringuier, S., Bigorre, M., Raux, O., Rochette, A., et al. (2011). Intraoperative tranexamic acid reduces blood transfusion in children undergoing craniosynostosis surgery: A randomized double-blind study. *Anesthesiology* 114 (4), 856–861. doi:10.1097/ALN.0b013e318210f9e3

Dwivedi, R., Ramanujam, B., Chandra, P. S., Sapra, S., Gulati, S., Kalaivani, M., et al. (2017). Surgery for Drug-Resistant epilepsy in children. *N. Engl. J. Med.* 377 (17), 1639–1647. doi:10.1056/NEJMoa1615335

Faraoni, D., Rahe, C., and Cybulski, K. A. (2019). Use of antifibrinolytics in pediatric cardiac surgery: where are we now? *Paediatr. Anaesth.* 29 (5), 435–440. doi:10.1111/pan.13533

Feng, H., Charchaflieh, J. G., Wang, T., and Meng, L. (2019). Transfusion in adults and children undergoing neurosurgery: the outcome evidence. *Curr. Opin. Anaesthesiol.* 32 (5), 574–579. doi:10.1097/ACO.0000000000000754

Finsterer, J., Pelzl, G., and Hess, B. (2001). Severe, isolated thrombocytopenia under polytherapy with carbamazepine and valproate. *Psychiatry Clin. Neurosci.* 55 (4), 423–426. doi:10.1046/j.1440-1819.2001.00885.x

Gerstner, T., Teich, M., Bell, N., Longin, E., Dempfle, C. E., Brand, J., et al. (2006). Valproate-associated coagulopathies are frequent and variable in children. *Epilepsia* 47 (7), 1136–1143. doi:10.1111/j.1528-1167.2006.00587.x

Goobie, S. M., and Faraoni, D. (2019). Tranexamic acid and perioperative bleeding in children: what do we still need to know? *Curr. Opin. Anaesthesiol.* 32 (3), 343–352. doi:10.1097/ACO.0000000000000728

Goobie, S. M., and Haas, T. (2014). Bleeding management for pediatric craniotomies and craniofacial surgery. *Paediatr. Anaesth.* 24 (7), 678–689. doi:10.1111/pan.12416

Goobie, S. M., Meier, P. M., Pereira, L. M., McGowan, F. X., Prescilla, R. P., Scharp, L. A., et al. (2011). Efficacy of tranexamic acid in pediatric craniosynostosis surgery: a double-blind, placebo-controlled trial. *Anesthesiol. (Philadelphia)* 114 (4), 862–871. doi:10.1097/ALN.0b013e318210fd8f

Goobie, S. M., Meier, P. M., Sethna, N. F., Soriano, S. G., Zurakowski, D., Samant, S., et al. (2013). Population pharmacokinetics of tranexamic acid in paediatric patients undergoing craniosynostosis surgery. *Clin. Pharmacokinet.* 52 (4), 267–276. doi:10.1007/s40262-013-0033-1

Goobie, S. M., Cladis, F. P., Glover, C. D., Huang, H., Reddy, S. K., Fernandez, A. M., et al. (2017). Safety of antifibrinolytics in cranial vault reconstructive surgery: A report from the pediatric craniofacial collaborative group. *Paediatr. Anaesth.* 27 (3), 271–281. doi:10.1111/pan.13076

Goobie, S. M., Zurakowski, D., Glotzbecker, M. P., McCann, M. E., Hedequist, D., Brustowicz, R. M., et al. (2018). Tranexamic acid is efficacious at decreasing the rate of blood loss in adolescent scoliosis surgery: a randomized placebo-controlled trial. *J. Bone Jt. Surg. Am.* 100 (23), 2024–2032. doi:10.2106/JBJS.18.00314

Goobie, S. M., Gallagher, T., Gross, I., and Shander, A. (2019). Society for the advancement of blood management administrative and clinical standards for patient blood management programs. 4Th edition (pediatric version). *Paediatr. Anaesth.* 29 (3), 231–236. doi:10.1111/pan.13574

Haas, T., Goobie, S., Spielmann, N., Weiss, M., and Schmugge, M. (2014). Improvements in patient blood management for pediatric craniosynostosis surgery using a ROTEM(®) -assisted strategy - feasibility and costs. *Paediatr. Anaesth.* 24 (7), 774–780. doi:10.1111/pan.12341

Johansson, P. I., Sorensen, A. M., Larsen, C. F., Windelov, N. A., Stensballe, J., Perner, A., et al. (2013). Low hemorrhage-related mortality in trauma patients in a Level I trauma center employing transfusion packages and early thromboelastography-directed hemostatic resuscitation with plasma and platelets. *Transfusion* 53 (12), 3088–3099. doi:10.1111/trf.12214

Kane, L. C., Woodward, C. S., Husain, S. A., and Frei-Jones, M. J. (2016). Thromboelastography-does it impact blood component transfusion in pediatric heart surgery? *J. Surg. Res.* 200 (1), 21–27. doi:10.1016/j.jss.2015.07.011

Kozek-Langenecker, S. A., Ahmed, A. B., Afshari, A., Albaladejo, P., Aldecoa, C., Barauskas, G., et al. (2017). Management of severe perioperative bleeding. *Eur. J. Anaesthesiol.* 34 (6), 332–395. doi:10.1097/EJA.0000000000000630

Lavoie, J. (2011). Blood transfusion risks and alternative strategies in pediatric patients. *Paediatr. Anaesth.* 21 (1), 14–24. doi:10.1111/j.1460-9592.2010.03470.x

Levy, J. H., Szlam, F., Tanaka, K. A., and Sniecienski, R. M. (2012). Fibrinogen and hemostasis: a primary hemostatic target for the management of acquired bleeding. *Anesth. Analg.* 114 (2), 261–274. doi:10.1213/ANE.0b013e31822e1853

Lin, Z., and Xiaoyi, Z. (2016). Tranexamic acid-associated seizures: a meta-analysis. *Seizure* 36, 70–73. doi:10.1016/j.seizure.2016.02.011

Livingston, E. H., and Lee, S. (2000). Percentage of burned body surface area determination in obese and nonobese patients. *J. Surg. Res.* 91 (2), 106–110. doi:10.1006/jsre.2000.5909

Manohar, C., Avitsian, R., Lozano, S., Gonzalez-Martinez, J., and Cata, J. P. (2011). The effect of antiepileptic drugs on coagulation and bleeding in the perioperative period of epilepsy surgery: the Cleveland Clinic experience. *J. Clin. Neurosci.* 18 (9), 1180–1184. doi:10.1016/j.jocn.2011.02.018

McCormack, P. L. (2012). Tranexamic acid: a review of its use in the treatment of hyperfibrinolysis. *Drugs* 72 (5), 585–617. doi:10.2165/11209070-000000000-00000

McNicol, E. D., Tzortzopoulou, A., Schumann, R., Carr, D. B., and Kalra, A. (2016). Antifibrinolytic agents for reducing blood loss in scoliosis surgery in children. *Cochrane Database Syst. Rev.* 9, CD006883. doi:10.1002/14651858.CD006883.pub3

Morley, S. L. (2009). Red blood cell transfusions in acute paediatrics. *Arch. Dis. Child. Educ. Pract. Ed.* 94 (3), 65–73. doi:10.1136/adc.2007.135731

Murao, S., Nakata, H., Roberts, I., and Yamakawa, K. (2021). Effect of tranexamic acid on thrombotic events and seizures in bleeding patients: a systematic review and meta-analysis. *Crit. Care* 25 (1), 380. doi:10.1186/s13054-021-03799-9

Murkin, J. M., Falter, F., Granton, J., Young, B., Burt, C., and Chu, M. (2010). High-dose tranexamic Acid is associated with nonischemic clinical seizures in cardiac surgical patients. *Anesth. Analg.* 110 (2), 350–353. doi:10.1213/ANE.0b013e3181c92b23

Myles, P. S., Smith, J. A., Forbes, A., Silbert, B., Jayarajah, M., Painter, T., et al. (2017). Tranexamic acid in patients undergoing Coronary-Artery surgery. *N. Engl. J. Med.* 376 (2), 136–148. doi:10.1056/NEJMoa1606424

Pan, C. F., Shen, M. Y., Wu, C. J., Hsiao, G., Chou, D. S., and Sheu, J. R. (2007). Inhibitory mechanisms of gabapentin, an antiseizure drug, on platelet aggregation. *J. Pharm. Pharmacol.* 59 (9), 1255–1261. doi:10.1211/jpp.59.9.0010

Pasquali, S. K., Li, J. S., He, X., Jacobs, M. L., O'Brien, S. M., Hall, M., et al. (2012). Comparative analysis of antifibrinolytic medications in pediatric heart surgery. *J. Thorac. Cardiovasc. Surg.* 143 (3), 550–557. doi:10.1016/j.jtcvs.2011.06.048

Roberts, I., Shakur-Still, H., Aeron-Thomas, A., Belli, A., Brenner, A., Chaudary, M. A., et al. (2019). Effects of tranexamic acid on death, disability, vascular occlusive events and other morbidities in patients with acute traumatic brain injury (CRASH-3): a randomised, placebo-controlled trial. *Lancet* 394 (10210), 1713–1723. doi:10.1016/S0140-6736(19)32233-0

Schaden, E., Kimberger, O., Kraincuk, P., Baron, D. M., Metnitz, P. G., and Kozek-Langenecker, S. (2012). Perioperative treatment algorithm for bleeding burn patients reduces allogeneic blood product requirements. *Br. J. Anaesth.* 109 (3), 376–381. doi:10.1093/bja/aes186

Shakur, H., Roberts, I., Bautista, R., Caballero, J., Coats, T., Dewan, Y., et al. (2010). Effects of tranexamic acid on death, vascular occlusive events, and blood transfusion in trauma patients with significant haemorrhage (CRASH-2): a randomised, placebo-controlled trial. *Lancet* 376 (9734), 23–32. doi:10.1016/S0140-6736(10)60835-5

Shakur, H., Roberts, I., Fawole, B., Chaudhri, R., El-Sheikh, M., Akintan, A., et al. (2017). Effect of early tranexamic acid administration on mortality, hysterectomy, and other morbidities in women with post-partum haemorrhage (WOMAN): an international, randomised, double-blind, placebo-controlled trial. *Lancet* 389 (10084), 2105–2116. doi:10.1016/S0140-6736(17)30638-4

Spahn, D. R., Bouillon, B., Cerny, V., Duranteau, J., Filipescu, D., Hunt, B. J., et al. (2019). The European guideline on management of major bleeding and coagulopathy following trauma: fifth edition. *Crit. Care* 23 (1), 98. doi:10.1186/s13054-019-2347-3

Sperling, M. R., Barshow, S., Nei, M., and Asadi-Pooya, A. A. (2016). A reappraisal of mortality after epilepsy surgery. *Neurology* 86 (21), 1938–1944. doi:10.1212/WNL.0000000000002700

Stainsby, D., Jones, H., Wells, A. W., Gibson, B., and Cohen, H. (2008). Adverse outcomes of blood transfusion in children: analysis of UK reports to the serious hazards of transfusion scheme 1996-2005. *Br. J. Haematol.* 141 (1), 73–79. doi:10.1111/j.1365-2141.2008.07022.x

Sujka, J., Gonzalez, K. W., Curiel, K. L., Daniel, J., Fischer, R. T., Andrews, W. S., et al. (2018). The impact of thromboelastography on resuscitation in pediatric liver transplantation. *Pediatr. Transpl.* 22 (4), e13176. doi:10.1111/petr.13176

Tanaka, K. A., Bader, S. O., and Görlinger, K. (2014). Novel approaches in management of perioperative coagulopathy. *Curr. Opin. Anaesthesiol.* 27 (1), 72–80. doi:10.1097/ACO.0000000000000025

Thudium, M. O., von Lehe, M., Wessling, C., Schoene-Bake, J. C., and Soehle, M. (2014). Safety, feasibility and complications during resective pediatric epilepsy surgery: a retrospective analysis. *BMC Anesthesiol.* 14, 71. doi:10.1186/1471-2253-14-71

Vadera, S., Griffith, S. D., Rosenbaum, B. P., Seicean, A., Kshettry, V. R., Kelly, M. L., et al. (2015). National trends and in-hospital complication rates in more than 1600 hemispherectomies from 1988 to 2010: a nationwide inpatient sample study. *Neurosurgery* 77 (2), 185–191. doi:10.1227/NEU.0000000000000815

van der Sande, J. J., Veltkamp, J. J., and Bouwhuis-Hoogerwerf, M. L. (1983). Hemostasis and intracranial surgery. *J. Neurosurg.* 58 (5), 693–698. doi:10.3171/jns.1983.58.5.0693

Walsh, M., Thomas, S. G., Howard, J. C., Evans, E., Guyer, K., Medvecz, A., et al. (2011). Blood component therapy in trauma guided with the utilization of the perfusionist and thromboelastography. *J. Extra. Corpor. Technol.* 43 (3), 162–167.

Wegner, J., and Popovsky, M. (2010). Clinical utility of thromboelastography: one size does not fit all. *Semin. Thromb. Hemost.* 36 (07), 699–706. doi:10.1055/s-0030-1265286

Whiting, P., Al, M., Westwood, M., Ramos, I. C., Ryder, S., Armstrong, N., et al. (2015). Viscoelastic point-of-care testing to assist with the diagnosis, management and monitoring of haemostasis: a systematic review and cost-effectiveness analysis. *Health Technol. Assess.* 19 (58), 1–228. doi:10.3310/hta19580

Wikkelso, A., Wetterslev, J., Moller, A. M., and Afshari, A. (2016). Thromboelastography (TEG) or thromboelastometry (ROTEM) to monitor haemostatic treatment versus usual care in adults or children with bleeding. *Cochrane Database Syst. Rev.* 8, CD007871. doi:10.1002/14651858.CD007871.pub3

Xiao, W., Fu, W., Wang, T., and Zhao, L. (2016). Prophylactic use of tranexamic acid combined with thrombelastogram guided coagulation management may reduce blood loss and allogeneic transfusion in pediatric hemispherectomy: case series. *J. Clin. Anesth.* 33, 149–155. doi:10.1016/j.jclinane.2016.02.040

frontiers | Frontiers in Pharmacology

TYPE Systematic Review
PUBLISHED 22 August 2022
DOI 10.3389/fphar.2022.897869

OPEN ACCESS

EDITED BY
Yang Zhou,
Brown University, United States

REVIEWED BY
Chun-Ju Lin,
China Medical University Hospital, Taiwan
Benedetto Falsini,
Catholic University of the Sacred Heart, Italy
Chiara Bianca Maria Platania,
University of Catania, Italy

*CORRESPONDENCE
Yu Di,
diyujsdxt@163.com

SPECIALTY SECTION
This article was submitted to Obstetric and Pediatric Pharmacology, a section of the journal Frontiers in Pharmacology

RECEIVED 16 March 2022
ACCEPTED 15 July 2022
PUBLISHED 22 August 2022

CITATION
Wang Z, Zhang Z, Wang Y and Di Y (2022), Effect of ranibizumab on retinopathy of prematurity: A meta-analysis.
Front. Pharmacol. 13:897869.
doi: 10.3389/fphar.2022.897869

Effect of ranibizumab on retinopathy of prematurity: A meta-analysis

Zhibin Wang[1], Zhaobo Zhang[2], Yue Wang[1] and Yu Di[1]*

[1]Department of Ophthalmology, Shengjing Hospital of China Medical University, Shenyang China, [2]Department of Cardiology, First Hospital of China Medical University, Shenyang, China

The primary objective of this study was to systematically evaluate the clinical efficacy of intravitreal ranibizumab injection in the treatment for retinopathy of prematurity (ROP) in infants. The MEDLINE (PubMed), Embase, China Biology Medicine disc, Cochrane Library, Web of Science, WanFang Data, CNKI, and CQVIP databases were searched to collect randomized controlled trials (RCTs) comparing the efficacy of ranibizumab with laser treatment in ROP. The retrieval time was from 2007, on which ranibizumab was approved until 12 January 2022. Data were extracted based on predetermined inclusion and exclusion criteria. Two investigators employed QUADAS-2 to independently assess the quality of all eligible original studies. Following quality evaluation, we also performed a meta-analysis using STATA v 15.1 and RevMan v 5.4 and funnel plots were used to detect publication bias. A total of five RCTs were included in the meta-analysis. In this study, the regression rate of retinal neovascularization was used as the index of therapeutic effectiveness. According to the results, the retinal neovascularization regression rate of the intravitreal ranibizumab injection group was statistically higher than that of the laser therapy group [risk ratio (RR) = 1.26, 95% confidence interval (CI): 1.18–1.35]; however, the incidence of adverse events, including recurrence and complications, was not different between them (RR = 0.73, 95%CI: 0.19–2.80). Therefore, intravitreal ranibizumab injection may be more clinically effective than laser therapy in the treatment for ROP. The safety and efficacy of ranibizumab in the long-term treatment for ROP needs further investigation.

Systematic Review Registration: https://www.crd.york.ac.uk/prospero/, CRD42022296387

KEYWORDS

laser therapy, meta-analysis, ranibizumab, randomized controlled trials, retinopathy of prematurity, review

Abbreviations: RNV, retinal neovascularization; ROP, retinopathy of prematurity.

1 Introduction

Retinopathy of prematurity (ROP) affects some preterm infants with low birth weight and exposure to high oxygen supplementation, which may lead to blindness in severe cases. Pathological progression of ROP begins at the immature stage of retinal vascular and neuronal development in preterm infants (stage I), followed by tissue ischemia leading to hypoxia-induced neovascularization (stage II) (Xu et al., 2018; Wang et al., 2019). Mild ROP resolves spontaneously with few sequelae, but severe ROP can lead to retinal detachment, severe visual impairment, and blindness. With constant developments in perinatal medicine the survival rate of preterm and low birth weight infants are improving. However, the incidence of ROP remains high, with approximately 28,300–45,600 infants being diagnosed annually with irreversible visual impairment due to ROP worldwide (Blencowe et al., 2013). Currently, cryotherapy, fusion laser photocoagulation, and vitreous injections are mostly used to reduce peripheral retinal neovascularization (RNV) (Marlow et al., 2021). Laser or cryotherapy is commonly used in children with lesions up until stage III, while vitrectomy or scleral buckling is often required following stage IV and onwards. Although laser therapy is standard, it can lead to extensive and permanent destruction of the retina and blood vessels, leading to the loss of peripheral vision (Rishi and Rishi, 2019). Vascular endothelial growth factor (VEGF) is of great significance in the occurrence and development of ROP. Usually, the VEGF concentration in the vitreous is high in children with ROP, which provides a theoretical basis for clinical anti-VEGF therapy (Sankar et al., 2018). The anti-VEGF monoclonal antibody, ranibizumab, can inhibit the expression of VEGF. This may control the intraocular neovascularization and subsequently achieve the goal of treatment of ROP (Mitchell et al., 2011; Aranda et al., 2019). This study aims to provide a basis for guiding clinical decision-making by exploring the effective rate and incidence of adverse events in the treatment of ROP, by comparing ranibizumab with laser therapy through a meta-analysis.

2 Materials and methods

2.1 Search strategy

Two researchers searched MEDLINE (PubMed), Embase, Chinese Biomedical Literature Database (CBM), The Cochrane Library, Web of Science, WanFang Data, CNKI, and VIP database for relative literature. Randomized controlled trials (RCTS) were conducted to compare ranibizumab with laser therapy in the treatment of ROP. The search time is set to build from database construction until to 12-01-2022. Subsequently, each reviewer manually re-evaluated whether the delivered literature fit the theme of the meta-analysis used in this study. English search terms included: ROP (MeSH terms), ROP (All Fields), Prematurity Retinopathies (All Fields), Prematurity Retinopathy (All Fields), Retrolental Fibroplasia (All Fields), Fibroplasia Retrolental (All Fields), Fibroplasias Retrolental (All Fields), and Retrolental Fibroplasias (All Fields). The above search terms are connected by OR, followed by AND with Ranibizumab (MeSH terms), RhuFab V2 (All Fields), V2 RhuFab (All Fields), and Lucentis (All Fields). Two researchers then conducted a review of all preliminary studies eligible for inclusion in the study to determine whether other relevant studies were included in the study.

2.2 Study selection and eligibility criteria

The inclusion criteria comprised of the following conditions: 1) The types of studies were a RCT; 2) The subjects were premature infants (gestational age <37 weeks) diagnosed with ROP by binocular indirect ophthalmoscope and retinal camera (RetCam); 3) The experimental group was given intravitreal injection of ranibizumab, and the control group was given laser treatment; 4) Outcome indicators were the number of effective treatment cases (including neovascularization subsided and bleeding decreased, additional lesions were alleviated, blood circulation was restored to the vascular occlusion area, and no intraocular infection and adverse events occurred) and the number of adverse events (including recurrence, high myopia, amblyopia, glaucoma, and other complications); 5) Published in English or Chinese. Exclusion criteria comprised of the following criteria: 1) The full text of the study was not available; 2) Literature on inconsistent interventions or outcome measures; 3) Non-Chinese or non-English literature; 4) Duplicate reports and studies without original data; 5) Literature without outcome indicators or where outcome indicators were not available.

2.3 Quality assessment

Cochrane literature quality evaluation tool was used to evaluate the quality of the included RCTS. The evaluation included whether random assignment was used, whether the assignment was hidden, whether blinding was used, whether the results were complete, whether the results were reported selectively, and whether there were other sources of bias. There are “low risk,” “high risk,” and “unclear” judgments for every project. Two researchers independently evaluated the quality of the five included studies.

2.4 Statistical analysis

RevMan v 5.3 and STATA v 16.0 software were used for statistical analysis. Dichotomous variables (response rate and incidence of adverse events) were analyzed by risk ratio (RR) and 95% confidence interval (CI). $p < 0.05$ indicated statistically

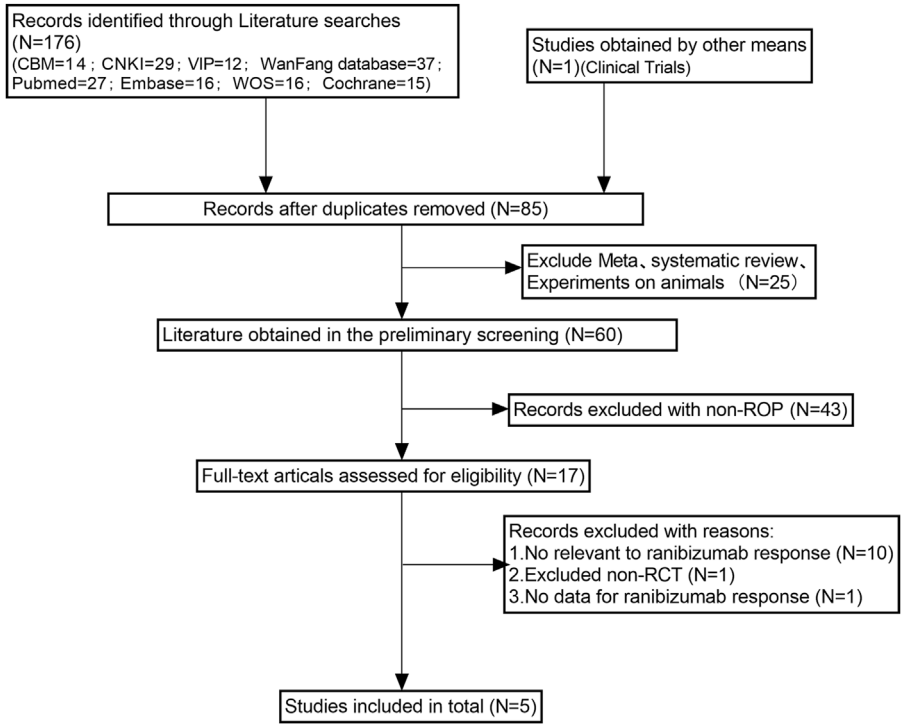

FIGURE 1
Literature screening process and results.

significant differences. The heterogeneity was determined by the chi-square test and I^2 to make a quantitative judgment. If no statistical heterogeneity among the results (I^2 <50%), the fixed effect model was used. If there were statistical heterogeneity (I^2 ≥50%), the random effects model for meta-analysis were used to find the source of the heterogeneity. For obvious clinical heterogeneity, we used subgroup analysis and sensitivity analysis, or only a descriptive analysis. Egger's method was used to test the publication bias. STATA 16.0 was used for meta regression to find the cause of heterogeneity.

3 Results

3.1 Characteristics of eligible literatures

The literature screening process and results are shown in Figure 1. We removed 92 duplicates from the original 177 articles retrieved from the databases. Subsequently, we excluded 68 unrelated articles and a variety of non-RCTs. Then, in order to further evaluate whether the remaining 17 studies met the conditions of our study, we obtained the full text of these 17 studies, and the results showed that 10 studies were not related to ranibizumab, one study had no data on ranibizumab response, and one study was a non-RCT study. Finally, we conducted quantitative analysis on five articles (Chen et al., 2018; Shi and Chen, 2018; Sun and Zhang, 2018; Stahl et al., 2019; Xin, 2021) that met the inclusion requirements.

3.2 The basic characteristics of the literature included in the study and the evaluation results of bias risk

Table 1 summarizes the relevant characteristics of the final five studies. The results of the quality evaluation chart made by the investigator with RevMan v 5.4 are shown in Figures 2, 3. All five eligible studies obtained moderate scores in the Quality assessment of Cochrane literature quality evaluation tool, indicating that the included RCTs have an overall medium risk of bias.

3.3 Meta-analysis

3.3.1 Effective rate

A total of five RCTs were included in the meta-analysis of this study (Chen et al., 2018; Shi and Chen, 2018; Sun and Zhang, 2018; Stahl et al., 2019; Xin, 2021). The effective rate tested for heterogeneity in all included studies delivered $I^2 = 0\%$ while the Q test showed $p = 0.53$, which indicated no heterogeneity among

TABLE 1 Basic characteristics of each study.

Included studies	Sample size (T/C, eye)	Correct gestational age (T/C, week)	Weight (T/C, kilogram)	Interventions		Follow-up time (month)	Outcome indicators
				T	C		
Xin (2021)	80/80	34.31 ± 1.31/34.18 ± 1.35	2.85 ± 0.43/ 2.84 ± 0.32	Ranibizumab	Laser therapy	6	①②
Shi,Y. J. (2018)	104/102	28.9 ± 1.30/28.93 ± 1.33	1.40 ± 0.20/ 1.39 ± 0.21	Ranibizumab	Laser therapy	1	①②
Chen L. F. (2018)	80/80	37.40 ± 1.75/36.93 ± 1.84	1.45 ± 0.20/ 1.42 ± 0.21	Ranibizumab	Laser therapy	1	①②
Sun.M. (2018)	40/40	30.1 ± 3.3/30.7 ± 3.5	1.53 ± 0.51/ 1.51 ± 0.40	Ranibizumab	Laser therapy	1	①②
Stahl (2019)	292/136	—	—	Ranibizumab	Laser therapy	6	①②

PS:T: Ranibizumab group; C: Laser group; ①Effective; ②Adverse events (include recurrency, complications).

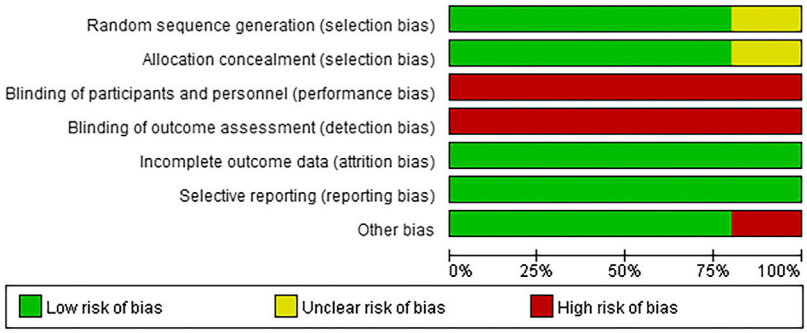

FIGURE 2
Risk assessment of bias in all included studies:risk of bias graph.

the literatures selected for this study (that is, heterogeneity does not have statistical significance). The fixed effect is selected to combine the effect size. The subsequent analysis indicates that the effective rate of ranibizumab injection was higher than that of laser therapy, and the difference was statistically significant [RR = 1.26, 95%CI (1.18, 1.35), z = 6.85, $p < 0.00001$] (Figure 4), which indicates that the efficacy of ranibizumab in the treatment of ROP was significantly better than treating with laser therapy alone, and the effective rate of intravitreal ranibizumab injection was 1.26 times that of laser treatment.

3.3.2 Adverse event rate

The adverse event rate tested for heterogeneity in all included studies delivered I^2 = 86.9% while the Q test showed p <0.00001, which suggested that the heterogeneity among the literature selected in this study was statistically significant. The adverse event rates were then further inspected at Labbe Plot and Galbraith Radial Plot (Figure 5). By graphical analysis, we concluded that there is a moderate heterogeneity among the literature in this study, and the effect size can be combined with random effect. The final result for the analysis of adverse event rates delivered RR = 0.73 [0.19, 2.80], meaning the number of adverse events in the intervention group were a total of 73% compared with those in the control group, but were not statistically significant (z = 0.46, $p = 0.65$) (Figure 6). This suggested that although ranibizumab could reduce the adverse events of ROP, there was no statistically significant difference in the incidence of adverse events between ranibizumab and the control measure (laser treatment).

3.3.3 Meta-regression

STATA16.0 was used for meta-regression analysis of the causes of heterogeneity in the incidence of adverse events. According to the number of weeks of corrected gestational age, the study was divided into three groups: 30–34 weeks, less than 30 weeks, and 34–36 weeks, respectively. Meta-regression was conducted using group (number of

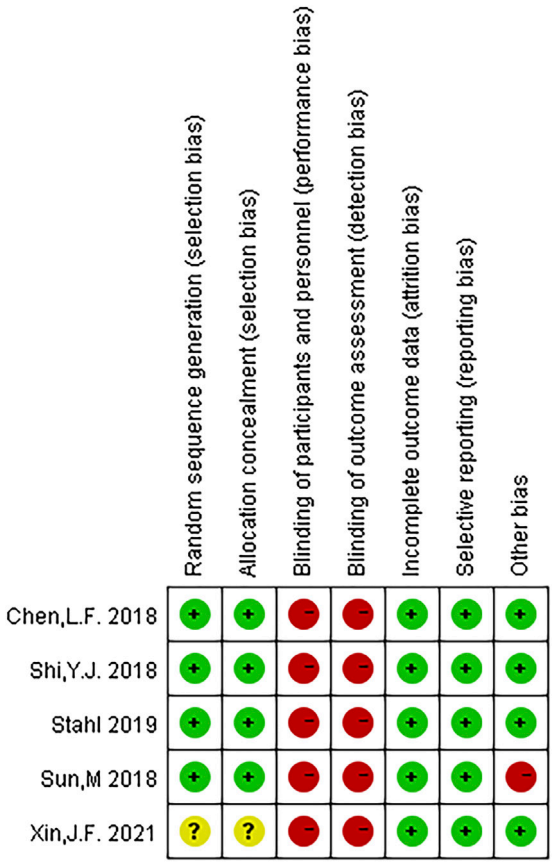

FIGURE 3
Risk assessment of bias in all included studies:risk of bias summary.

corrected gestational age) variables as covariate, and the results suggested that the number of corrected gestational age was the source of heterogeneity. However, due to the small number of RCTS included, subgroup studies cannot be carried out. Figure 7 shows the results of meta-regression.

3.4 Sensitivity analysis and publication bias

Sensitivity analysis was used to find out the heterogeneous causes, and sensitivity analysis was conducted on the five manuscripts used in this study. It was concluded that there was no study with a large impact on heterogeneity. Figure 8 clearly illustrates that deletion of any study did not result in a significant change in results, so the sensitivity analysis did not examine the source of heterogeneity. A funnel plot was used to investigate whether there was publication bias in the five manuscripts used in this study. To test the bias of treatment effectiveness we obtained funnel plot symmetry (Egger's test showed $p = 0.364$) and to test the bias of adverse events rate (Egger's test showed $p = 0.652$) we also obtained funnel plot symmetry (Figure 9). Therefore, we concluded that there was no publication bias, which indicated that the conclusion of this study was accurate and reliable.

4 Discussion

ROP is a secondary complication of prematurity generally due to oxygen supplementation in NICU, in preterm infants with severe pulmonary, brain or heart problems. It is more common in premature and low weight infants, which can lead to amblyopia, cataracts, retinal detachment, etc. This usually have serious effects on the quality of life of premature infants, such as impacts on their language, movement, and social adaptability, while bringing heavy burden to the family and society (Dogra et al., 2017). Because of its serious consequences, ROP has become the focus of ophthalmological research worldwide. The pathogenesis is actually clear, while the risk factor are not univocally identified. In the past, condensation and photocoagulation were usually used in the treatment of ROP, which mainly damage non-vascular structures in the retina of children, so as to reduce the oxygen consumption of retina metabolism, and then achieve the effect of reducing the neovascularization growth factor induced by ischemia and hypoxia, and finally achieve the purpose of

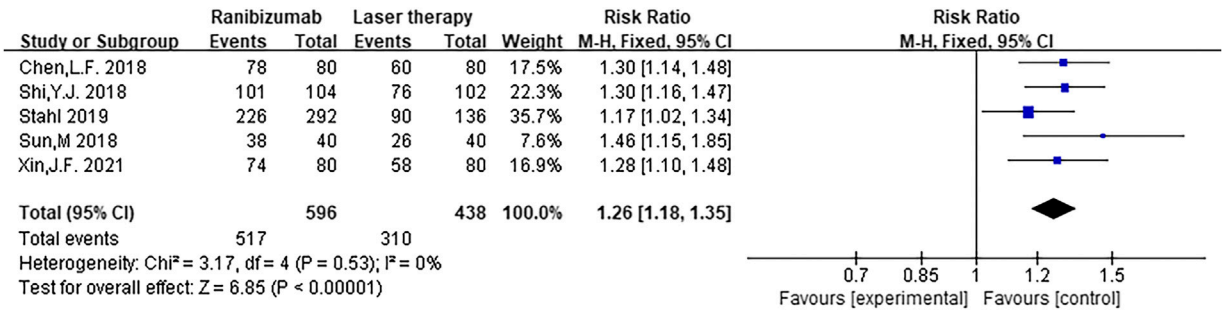

FIGURE 4
Forest plot: ranibizumab injection of retinopathy of prematurity (ROP) efficacy compared to laser treatment.

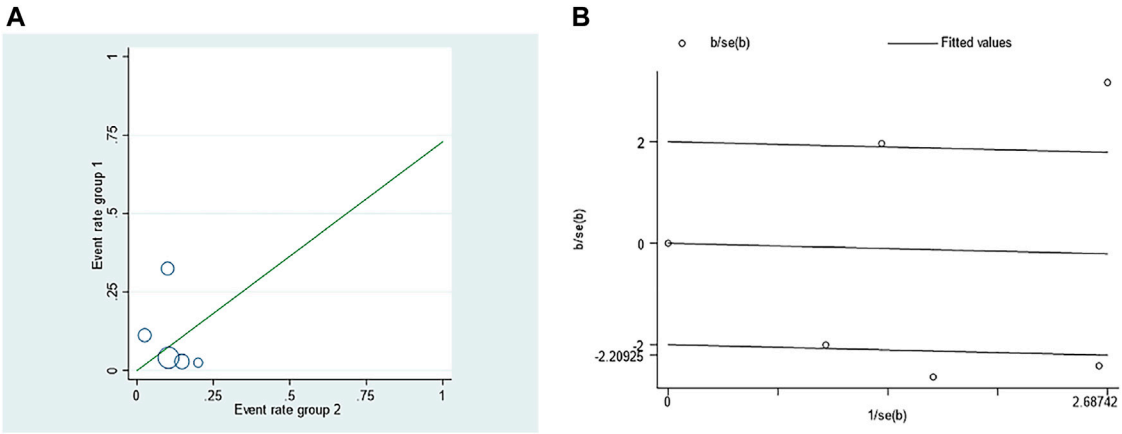

FIGURE 5
Investigation of the heterogeneity in the incidence of adverse events in retinopathy of prematurity (ROP) treated with ranibizumab and laser therapy: **(A)** Labbe Plot **(B)** Galbraith Radial Plot.

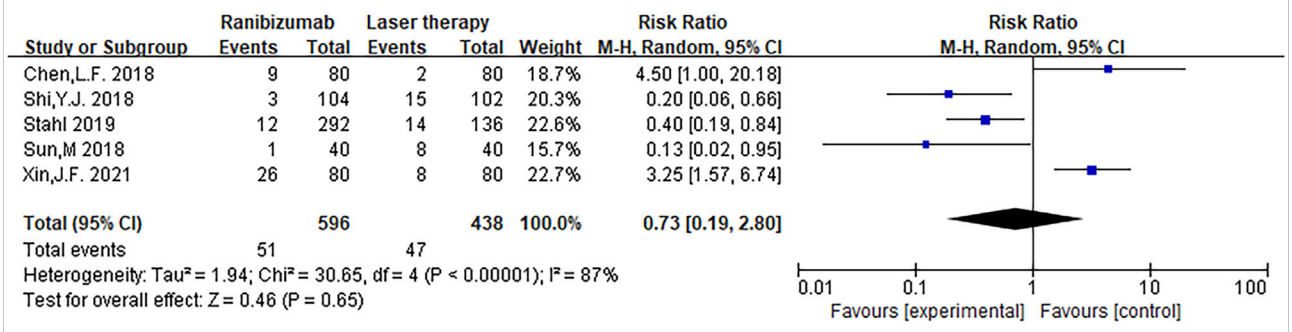

FIGURE 6
Forest plot: ranibizumab injection of retinopathy of prematurity (ROP) incidence of adverse events compared to laser treatment.

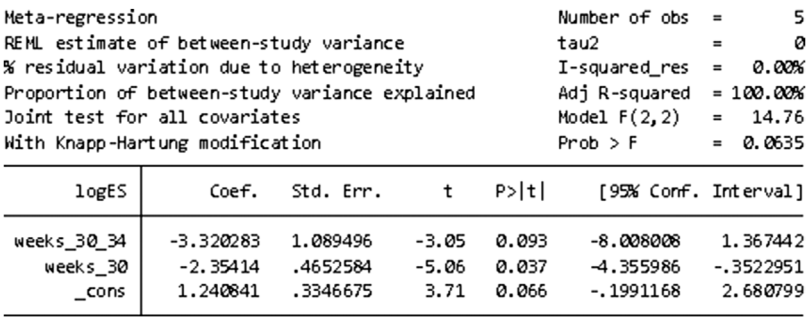

Meta-regression — Number of obs = 5
REML estimate of between-study variance — tau2 = 0
% residual variation due to heterogeneity — I-squared_res = 0.00%
Proportion of between-study variance explained — Adj R-squared = 100.00%
Joint test for all covariates — Model F(2,2) = 14.76
With Knapp-Hartung modification — Prob > F = 0.0635

logES	Coef.	Std. Err.	t	P>|t|	[95% Conf.	Interval]
weeks_30_34	-3.320283	1.089496	-3.05	0.093	-8.008008	1.367442
weeks_30	-2.35414	.4652584	-5.06	0.037	-4.355986	-.3522951
_cons	1.240841	.3346675	3.71	0.066	-.1991168	2.680799

FIGURE 7
Results of meta-regression to find the cause of heterogeneity in the incidence of adverse events.

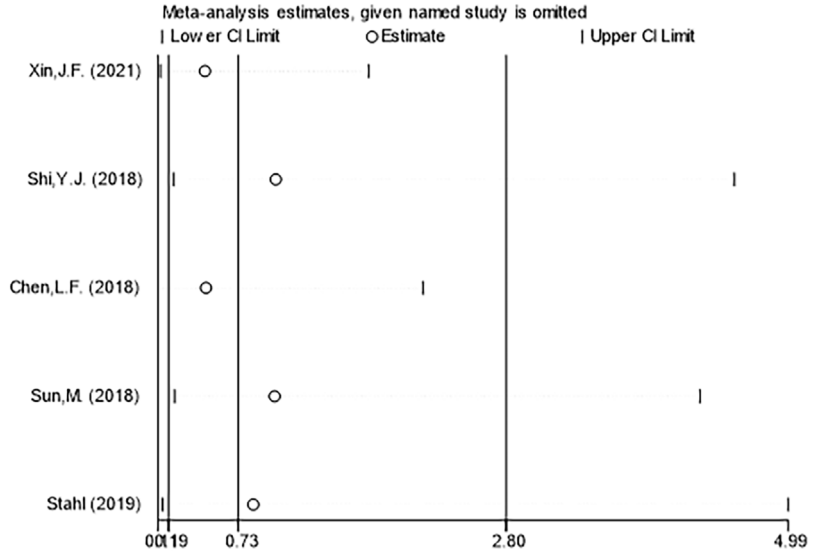

FIGURE 8
Sensitivity analysis of the incidence of adverse events between ranibizumab and laser therapy for retinopathy of prematurity (ROP).

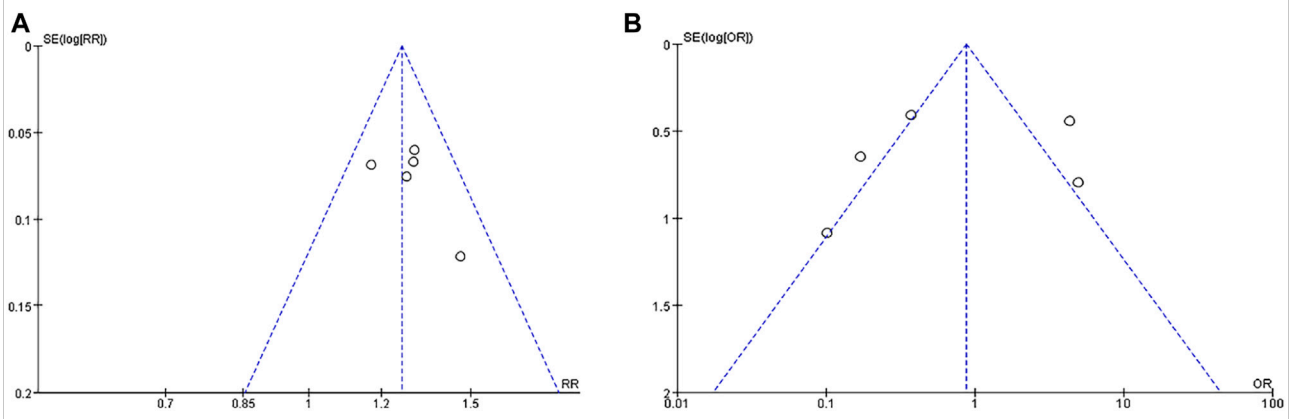

FIGURE 9
Funnel plot indicating publication bias for treatment effectiveness **(A)** and adverse events rate **(B)**.

inhibiting the development of RNV and controlling the disease of children (Ge et al., 2021). However, laser is often accompanied by a series of complications such as undertreatment, overtreatment (retinal burn, retinal hiatus, exudative retinal detachment), vitreous hemorrhage, corneal burn, as well as the high technical skill required of ophthalmologists, which limits its wide application in clinical practice. In recent years, a large number of studies have reported the efficacy and safety analysis of anti-VEGF (ranibizumab) treatment compared with laser therapy for ROP, with contrasting results (Hosseini et al., 2009; Mintz-Hittner et al., 2011; Lepore et al., 2014; Karkhaneh et al., 2016; Zhang et al., 2017; Stahl et al., 2019).

Intravitreal injection of anti-VEGF drugs has become the preferred treatment for ROP (Chiang, 2018). Ranibizumab is a recombinant humanized anti-VEGF antibody fragment (Fab), which is an inhibitor of angiogenesis (Itatani et al., 2018). It is also known that VEGF is an important factor in the development of neonatal retinopathy (Uemura et al., 2021), and the mechanism of action of ranibizumab is clear it blocks the VEGFR signaling by binding to VEGFA, which means intravitreal ranibizumab injection can inhibit the expression of VEGF, reduce the generation of RNV, and recast newly generated new blood vessels (Bhandari et al., 2020), so as to play an important role in the treatment of ROP and ensure the function of the retina, which has good clinical effect (Lee and

Shirley, 2021; Woo et al., 2021). The use of anti-VEGF drugs in the treatment of tissue damage is light, technically easy and quick to administer, and can safely treat critically ill patients presenting with refractive stroma turbidity (Sankar et al., 2018). In certain cases, anti-VEGF treatment even has more of the curative effect required for laser photocoagulation treatment (Stahl et al., 2019). Barry et al., 2021). At the turn of the century, it has been approved for the treatment of ocular neovascular diseases drugs. Furthermore, it can quickly penetrate the retina layer, has a small molecular weight, excludes segments of Fe, and has the advantage of diminished immune response (Dhoot and Kaiser, 2012; Jiang and Mieler, 2017). While anti-VEGF drugs have a distinct advantage in some cases (e.g., zone I disease or aggressive ROP), there are also disadvantages to this treatment, for example, after this treatment, the recurrence rate is still not low, which means anti-VEGF drugs do not effectively reduce the recurrence rate of the disease (Sankar et al., 2018), and often incomplete retinal vascularization, requiring vigilance and prolonged follow-up consultations (VanderVeen et al., 2017). According to the Cochrane review report, although the risk of early retinal dysstructure was reduced from 47.9% to 28.1%, and peripheral retinal ablation in early childhood was associated with a 13.6% reduction in the risk of visual impairment (Sankar et al., 2018). The treatment effect was remarkable, the recurrence rate was low, and the clinical application experience was extensive, which is still the current gold standard for ROP treatment. However, laser operation is more invasive than anti-VEGF intravitreal injections, and the general condition of patients may deteriorate after treatment (Anderson et al., 2014). Photocoagulation scarring affects peripheral visual field, and the high myopia rate increases after treatment (Anderson et al., 2014; VanderVeen et al., 2017; Yang et al., 2021).

This meta-analysis was conducted to evaluate the effective rate and incidence of adverse events in the treatment of ROP with ranibizumab and laser treatment. The results showed that the recovery rate in the ranibizumab group was higher than that in the laser therapy group, and the difference was statistically significant ($p < 0.05$), which suggests that the use of ranibizumab is clinically more effective in the treatment of ROP. There was no statistical difference in the incidence of adverse events between the two groups ($p > 0.05$), and the results may be biased due to the influence of follow-up time and follow-up indicators such as visual field assessment. Due to the small number of RCTs included, more high-quality clinical studies are needed for further verification. In addition, late recurrence of ROP represents a challenge during the follow-up phase and regular follow-ups should be emphasized. Otherwise, ROP recurrence will still occur in children with strabismus, amblyopia, retinal detachment and other complications. According to previous studies (Hartnett, 2017), follow-up of children with retinal vascularization or corrected gestational age of 45 weeks, no threshold lesions, retinal vessels have developed to zone 3 can be terminated if one of the above indications is met.

Shortcomings and prospects of this study: 1) The number of studies on some outcome indicators was small, and the outcome indicators were scattered; 2) The included indices were the number of cases and the number of researchers, and the results were inconsistent with the given parameters, requiring separate analysis; 3) The efficacy of different doses of ranibizumab may be different, and some studies have shown that 0.2 mg ranibizumab is more effective in the treatment of ROP (Stahl et al., 2019); 4) The treatment of ROP varies among different zones. Some studies have shown that anti-VEGF is more advantageous in the treatment of ROP zone I, but laser is better in the treatment of ROP zone II (Kuo et al., 2015). Because of the small number of studies and scattered outcome indicators, subgroup analysis was not feasible; 5) The study lacked comparisons with more established treatments such as vitreoretinal surgery; 6) Long-term effects on neurodevelopmental and functional ocular outcomes after treatment with ranibizumab or laser therapy were not included in this research.

Data availability statement

The raw data supporting the conclusion of this article will be made available by the authors, without undue reservation.

Author contributions

ZZ was responsible for conceptualization, data curation, formal analysis, funding acquisition, literature retrieval, methodology, project administration, resources, supervision, writing the original draft, and reviewing and editing the final draft. ZW was responsible for data curation, formal analysis, investigation, and resources. YW was responsible for data curation, formal analysis, investigation, and resources. YD was responsible for validation, writing—review and editing. Each researcher contributed to the meta-analysis and approved the submitted version.

Funding

Supported by the national natural science foundation of China (81600747), Foundation of Liaoning Province Education Administration (QNZR2020010), Project of Shenyang Science and Technology Department (21-173-9-52) and the 345 Talent Project o Shengjing Hospital of China Medical University.

Conflict of interest

The authors declare that the research was conducted in the absence of any commercial or financial relationships that could be construed as a potential conflict of interest.

Publisher's note

References

Anderson, M. F., Ramasamy, B., Lythgoe, D. T., and Clark, D. (2014). Choroidal thickness in regressed retinopathy of prematurity. *Eye (Lond)* 28 (12), 1461–1468. doi:10.1038/eye.2014.207

Aranda, J. V., Qu, J., Valencia, G. B., and Beharry, K. D. (2019). Pharmacologic interventions for the prevention and treatment of retinopathy of prematurity. *Semin. Perinatol.* 43 (6), 360–366. doi:10.1053/j.semperi.2019.05.009

Barry, G. P., Yu, Y., Ying, G. S., Tomlinson, L. A., Lajoie, J., Fisher, M., et al. (2021). Retinal detachment after treatment of retinopathy of prematurity with laser versus intravitreal anti-vascular endothelial growth factor. *Ophthalmology* 128 (8), 1188–1196. doi:10.1016/j.ophtha.2020.12.028

Bhandari, S., Nguyen, V., Fraser-Bell, S., Mehta, H., Viola, F., Baudin, F., et al. (2020). Ranibizumab or aflibercept for diabetic macular edema: Comparison of 1-year outcomes from the fight retinal blindness! Registry. *Ophthalmology* 127 (5), 608–615. doi:10.1016/j.ophtha.2019.11.018

Blencowe, H., Lawn, J. E., Vazquez, T., Fielder, A., and Gilbert, C. (2013). Preterm-associated visual impairment and estimates of retinopathy of prematurity at regional and global levels for 2010. *Pediatr. Res.* 74 (1), 35–49. doi:10.1038/pr.2013.205

Chen, L. F., Gao, H. S., and Wang, G. Q., Effects of intravitreal injection of ranibizumab on serum levels of vascular endothelial growth factor, insulin-like growth factor and glutamate in children with retinopathy of prematurity. *Maternal Child Health Care China*, 2018. 33(02): p. 349–352.

Chiang, M. F. (2018). How does the standard of care evolve? Anti-vascular endothelial growth factor Agents in retinopathy of prematurity treatment as an example. *Ophthalmology* 125 (10), 1485–1487. doi:10.1016/j.ophtha.2018.04.018

Dhoot, D. S., and Kaiser, P. K. (2012). Ranibizumab for age-related macular degeneration. *Expert Opin. Biol. Ther.* 12 (3), 371–381. doi:10.1517/14712598.2012.660523

Dogra, M. R., Katoch, D., and Dogra, M. (2017). An update on retinopathy of prematurity (ROP). *Indian J. Pediatr.* 84 (12), 930–936. doi:10.1007/s12098-017-2404-3

Ge, G., Zhang, Y., and Zhang, M. (2021). Pregnancy-induced hypertension and retinopathy of prematurity: A meta-analysis. *Acta Ophthalmol.* 99 (8), e1263–e1273. doi:10.1111/aos.14827

Hartnett, M. E. (2017). Advances in understanding and management of retinopathy of prematurity. *Surv. Ophthalmol.* 62 (3), 257–276. doi:10.1016/j.survophthal.2016.12.004

Hosseini, H., Khalili, M. R., and Nowroozizadeh, S. (2009). Intravitreal injection of bevacizumab (Avastin) for treatment of stage 3 retinopathy of prematurity in zone I or posterior zone II. *Retina* 29 (4), 562. doi:10.1097/IAE.0b013e31819a98a9

Itatani, Y., Kawada, K., Yamamoto, T., and Sakai, Y. (2018). Resistance to anti-angiogenic therapy in cancer-alterations to anti-VEGF pathway. *Int. J. Mol. Sci.* 19 (4), 1232. doi:10.3390/ijms19041232

Jiang, Y., and Mieler, W. F. (2017). Update on the use of anti-VEGF intravitreal therapies for retinal vein occlusions. *Asia. Pac. J. Ophthalmol.* 6 (6), 546–553. doi:10.22608/APO.2017459

Karkhaneh, R., Khodabande, A., Riazi-Eafahani, M., Roohipoor, R., Ghassemi, F., Imani, M., et al. (2016). Efficacy of intravitreal bevacizumab for zone-II retinopathy of prematurity. *Acta Ophthalmol.* 94 (6), e417–20. doi:10.1111/aos.13008

Kuo, H. K., Sun, I. T., Chung, M. Y., and Chen, Y. H. (2015). Refractive error in patients with retinopathy of prematurity after laser photocoagulation or bevacizumab monotherapy. *Ophthalmologica.* 234 (4), 211–217. doi:10.1159/000439182

Lee, A., and Shirley, M. (2021). Ranibizumab: A review in retinopathy of prematurity. *Paediatr. Drugs* 23 (1), 111–117. doi:10.1007/s40272-020-00433-z

Lepore, D., Quinn, G. E., Molle, F., Baldascino, A., Orazi, L., Sammartino, M., et al. (2014). Intravitreal bevacizumab versus laser treatment in type 1 retinopathy of prematurity: Report on fluorescein angiographic findings. *Ophthalmology* 121 (11), 2212–2219. doi:10.1016/j.ophtha.2014.05.015

Marlow, N., Stahl, A., Lepore, D., Fielder, A., Reynolds, J. D., Zhu, Q., et al. (2021). 2-year outcomes of ranibizumab versus laser therapy for the treatment of very low birthweight infants with retinopathy of prematurity (RAINBOW extension study): Prospective follow-up of an open label, randomised controlled trial. *Lancet. Child. Adolesc. Health* 5 (10), 698–707. doi:10.1016/S2352-4642(21)00195-4

Mintz-Hittner, H. A., Kennedy, K. A., and Chuang, A. Z. (2011). Efficacy of intravitreal bevacizumab for stage 3+ retinopathy of prematurity. *N. Engl. J. Med.* 364 (7), 603–615. doi:10.1056/NEJMoa1007374

Mitchell, P., Bandello, F., Schmidt-Erfurth, U., Lang, G. E., Massin, P., Schlingemann, R. O., et al. (2011). The RESTORE study: Ranibizumab monotherapy or combined with laser versus laser monotherapy for diabetic macular edema. *Ophthalmology* 118 (4), 615–625. doi:10.1016/j.ophtha.2011.01.031

Rishi, E., and Rishi, P. (2019). Macular hole following successful stage 4B/stage 5 retinopathy of prematurity surgery. *Indian J. Ophthalmol.* 67 (6), 971–973. doi:10.4103/ijo.IJO_719_18

Sankar, M. J., Sankar, J., Chandra, P., Bhat, V., and Srinivasan, R. (2018). Anti-vascular endothelial growth factor (VEGF) drugs for treatment of retinopathy of prematurity. *Cochrane Database Syst. Rev.* 1 (1), CD009734. doi:10.1002/14651858.CD009734.pub2

Shi, Y. J., and Chen, L. M. (2018). Effect of ranibizumab injection on serum VEGF and IGF-1 levels in children with retinopathy of prematurity. *Inn. Mong. Med. J.* 50 (10), 1235–1236.

Stahl, A., Lepore, D., Fielder, A., Fleck, B., Reynolds, J. D., Chiang, M. F., et al. (2019). Ranibizumab versus laser therapy for the treatment of very low birthweight infants with retinopathy of prematurity (RAINBOW): An open-label randomised controlled trial. *Lancet* 394 (10208), 1551–1559. doi:10.1016/S0140-6736(19)31344-3

Sun, M., and Zhang, Y. P., Clinical effect of vitreous injection of ranibizumab in the treatment of retinopathy of prematurity. *Contemp. Med.*, 2018. 24(19): p. 135–137.

Uemura, A., Fruttiger, M., D'Amore, P. A., De Falco, S., Joussen, A. M., Sennlaub, F., et al. (2021). VEGFR1 signaling in retinal angiogenesis and microinflammation. *Prog. Retin. Eye Res.* 84 (9), 100954. doi:10.1016/j.preteyeres.2021.100954

VanderVeen, D. K., Melia, M., Yang, M. B., Hutchinson, A. K., Wilson, L. B., and Lambert, S. R. (2017). Anti-vascular endothelial growth factor therapy for primary treatment of type 1 retinopathy of prematurity: A report by the American academy of ophthalmology. *Ophthalmology* 124 (5), 619–633. doi:10.1016/j.ophtha.2016.12.025

Wang, Z., Liu, C. H., Huang, S., and Chen, J. (2019). Wnt Signaling in vascular eye diseases. *Prog. Retin. Eye Res.* 70 (5), 110–133. doi:10.1016/j.preteyeres.2018.11.008

Woo, S. J., Veith, M., Hamouz, J., Ernest, J., Zalewski, D., Studnicka, J., et al. (2021). Efficacy and safety of a proposed ranibizumab biosimilar product vs a reference ranibizumab product for patients with neovascular age-related macular degeneration: A randomized alinical trial. *JAMA Ophthalmol.* 139 (1), 68–76. doi:10.1001/jamaophthalmol.2020.5053

Xin, J. F. (2021). Effect of intravitreal injection of ranibizumab on clinical efficacy and retinal functional development in children with retinopathy of prematurity. *Prog. Mod. Biomed.* 20 (01), 131–134.

Xu, Y., Lu, X., Hu, Y., Yang, B., Tsui, C. K., Yu, S., et al. (2018). Melatonin attenuated retinal neovascularization and neuroglial dysfunction by inhibition of HIF-1α-VEGF pathway in oxygen-induced retinopathy mice. *J. Pineal Res.* 64 (4), e12473. doi:10.1111/jpi.12473

Yang, X. Y., Cai, Y. T., and Li, Y., Interpretation of "clinical guidelines for anti-VEGF therapy in retinopathy of prematurity" by Japanese ophthalmology society. *Chin. J. Exp. Ophthalmol.*, 2021. 39(11): p. 1003–1009.

Zhang, G., Yang, M., Zeng, J., Vakros, G., Su, K., Chen, M., et al. (2017). Comparison of intravitreal injection of ranibizumab versus laser therapy for zone ii treatment-requiring retinopathy of prematurity. *Retina* 37 (4), 710–717. doi:10.1097/IAE.0000000000001241

frontiers | Frontiers in Pharmacology

TYPE Original Research
PUBLISHED 06 September 2022
DOI 10.3389/fphar.2022.925018

OPEN ACCESS

EDITED BY
Xiaoling Wang,
Beijing Children's Hospital, Capital Medical University, China

REVIEWED BY
Abad Khan,
University of Swabi, Pakistan
Ugo De Grazia,
IRCCS Carlo Besta Neurological Institute Foundation, Italy
Lateef Ahmad,
University of Swabi, Pakistan

*CORRESPONDENCE
Ya-Hui Hu,
huyahui324@163.com
Feng Chen,
cy.chen508@gmail.com

†Visiting graduate student from China Pharmaceutical University

SPECIALTY SECTION
This article was submitted to Obstetric and Pediatric Pharmacology, a section of the journal Frontiers in Pharmacology

RECEIVED 21 April 2022
ACCEPTED 01 August 2022
PUBLISHED 06 September 2022

CITATION
Zhao Y-T, Dai H-R, Li Y, Zhang Y-Y, Guo H-L, Ding X-S, Hu Y-H and Chen F (2022), Comparison of LC-MS/MS and EMIT methods for the precise determination of blood sirolimus in children with vascular anomalies. *Front. Pharmacol.* 13:925018. doi: 10.3389/fphar.2022.925018

Comparison of LC-MS/MS and EMIT methods for the precise determination of blood sirolimus in children with vascular anomalies

Yue-Tao Zhao[1,2†], Hao-Ran Dai[1,2†], Yue Li[1], Yuan-Yuan Zhang[1], Hong-Li Guo[1], Xuan-Sheng Ding[2], Ya-Hui Hu[1*] and Feng Chen[1*]

[1]Pharmaceutical Sciences Research Center, Department of Pharmacy, Children's Hospital of Nanjing Medical University, Nanjing, China, [2]School of Basic Medicine and Clinical Pharmacy, China Pharmaceutical University, Nanjing, China

Sirolimus (SRL) is a mammalian target of rapamycin (mTOR) inhibitor. The whole blood concentration of SRL is routinely monitored to tailor dosage and prevent toxicity. Currently, the enzyme multiplied immunoassay technique (EMIT) is often applied to perform therapeutic drug monitoring (TDM) of SRL, but the cross-reactivity with various metabolites is of great concern. A more specific method is required, such as liquid chromatography–tandem mass spectrometry (LC-MS/MS). However, no study on the method comparison of the EMIT and LC-MS/MS for the measurement of whole blood SRL concentration in children with vascular anomalies has been reported. This study developed a simple and sensitive LC-MS/MS assay for the determination of SRL. Meanwhile, consistency between LC-MS/MS and the EMIT was evaluated by linear regression and Bland–Altman analysis. Whole blood samples were deproteinized with methanol for erythrocyte lysis, and the resulting solution was injected into the LC-MS/MS system using the positive electrospray ionization mode. The multiple reaction monitoring transitions of *m/z* 931.7 → 864.6 and *m/z* 934.7 → 864.6 were used for SRL and SRL-d_3 as the internal standards, respectively. The analytes were separated on a C18 column with a gradient mobile phase (0.1 mM formic acid and 0.05 mM ammonium acetate in methanol/ultrapure water). Blood samples collected from children with vascular anomalies undergoing SRL therapy were tested by EMIT and by LC-MS/MS. The linear range of LC-MS/MS was 0.500–50.0 ng/ml and that of the EMIT was 3.50–30.0 ng/ml. A significant positive correlation between the two assays was established with a regression equation described as [***EMIT***] = 1.281 × [***LC–MS/MS***] + 2.450 (r = 0.8361). Bland–Altman plots showed a mean concentration overestimation of 4.7 ng/ml [95% CI: (–3.1, 12.6)] and a positive bias of 63.1% [95% CI: (–36.1, 162.3)] generated by the EMIT more than that of by LC-MS/MS. In conclusion, the two methods were closely correlated, indicating that switching between the two methods is feasible. Considering the overestimation nature of the EMIT assay, switching from the EMIT to the LC-MS/MS method deserves close attention and necessary re-evaluation for

the target therapeutic reference range, may be required when methods are switched within the same clinical laboratory or results are compared between different laboratories.

KEYWORDS

sirolimus, EMIT, LC-MS/MS, TDM, consistency, children, vascular anomalies

1 Introduction

Sirolimus (SRL) is a hydrophobic macrolide compound which was first isolated and developed as an antifungal drug (Sehgal, Baker et al., 1975; Vezina, Kudelski et al., 1975). Simultaneously, SRL exerts intensively immunosuppressive and antiproliferative activities due to its ability to inhibit the mammalian target of rapamycin (mTOR) (Sehgal 1995; Laplante and Sabatini, 2012). However, SRL has a narrow therapeutic window, and its clinical pharmacokinetics exhibits large intra- and inter-patient variability (Kahan, Napoli et al., 2000; Scott, Courter et al., 2013). Its side effects correlate closely to whole blood concentration; thus, the implementation of therapeutic drug monitoring (TDM) in whole blood samples for SRL is essential and beneficial to individualize dose regimens and ensure its efficacy and safety (Vogeser, Fleischer et al., 2002; Mano, Sato et al., 2011).

To routinely monitor the blood level of SRL, immunoassay methods have traditionally been involved (Sallustio, Noll et al., 2011). The enzyme multiplied immunoassay technique (EMIT) has been widely used for assaying endogenous and exogenous substances for a long time, and it is particularly useful in clinical TDM (Borgman, Hiemer et al., 2012). However, the EMIT shows poor specificity as it cannot distinguish the target analyte from its metabolite(s), which causes positive bias from true concentration values. Impressively, in our laboratory, where the EMIT assay has been applied to detect the whole blood SRL concentration for nearly 5 years for children with vascular anomalies, this method is still accompanied by some other weaknesses, including relatively high fluctuation of quality control (QC) samples and expensive reagent kit expenditure with a short validity period. Hence, more specific assays with better sensitivity and selectivity are required to alternatively measure the whole blood SRL concentration.

Liquid chromatography–tandem mass spectrometry (LC-MS/MS) has been widely applied for the analysis of low molecular weight molecules with the strengths of low interference, good selectivity, high degree of sensitivity, high throughput, and low costs per sample in terms of reagents (van den Ouweland and Kema, 2012). It allows the accurate determination of the target analyte(s) and/or its metabolites and ensures reliable results and superiority over other assays such as the EMIT (Nguyen, Duong et al., 2021). In clinical laboratories, the LC-MS/MS instrumentation provides great accuracy and is very suitable for routine TDM (Shipkova and Svinarov, 2016; Cui, Wang et al., 2020).

Recently, several LC-MS/MS methods with time-consuming solid-phase extraction, large sample size requirements or longer run time for each individual sample have been reported ((Salm, Taylor et al., 2000; Zochowska, Bartlomiejczyk et al., 2006; O'Halloran and Ilett, 2008; Morgan, Brown et al., 2014, Shi et al., 2016); Table 1). Some assays were suitable for routine TDM, but some others were not. Hence, the aims of this study were 1) to develop and validate an easy-to-use LC-MS/MS method for the analysis of SRL whole blood concentration; 2) to assess the method consistency between the newly validated LC-MS/MS and routine EMIT technique for SRL determination in our laboratory; and 3) to discuss the feasibility and necessity of the method switching from the EMIT to LC-MS/MS for routine SRL monitoring in clinical laboratories.

2 Materials and methods

2.1 Liquid chromatography–tandem mass spectrometry method

2.1.1 Chemicals, reagents, and materials

The reference material of SRL (purity: 95%, Lot No. 8-RTU-49-1, expiry date: 2023-04-09) and its isotopically labeled internal standard (IS), SRL-d_3 (technical grade, Lot No. 3-TKA-137-3, expiry date: 2023-10-08) were purchased from the Toronto Research Chemicals Inc. (Toronto, Canada). HPLC-grade methanol (MeOH) was bought from Merck KGaA (Darmstadt, Germany). ACS-grade formic acid (FA) and ammonium acetate (NH_4AC) were obtained from Tedia Company Inc. (Fairfield, OH, United States) and Sigma-Aldrich Co. LLC (Wilmington, United States), respectively. Ultrapure water (UPW) was generated from a Milli-Q water purification system (Millipore Corp., Bedford, MA, United States).

Chromatographic columns including Kinetex 1.7 μm C18 100 Å (50 mm × 2.1 mm), Luna 5 μm C18 100 Å (50 mm × 2.0 mm), Gemini 3 μm C18 110 Å (50 mm × 2.0 mm), Kinetex 2.6 μm C18 100 Å (50 mm × 2.1 mm), Kinetex 5 μm C18 100 Å (50 mm × 2.1 mm), and security guard cartridges C18 (4 mm × 2.0 mm) were purchased from the Phenomenex Inc. (Torrance, CA, United States).

TABLE 1 Comparison of this study with several previously published analytical methods for SRL.

Study	Method	Internal standard	Blood volume (μl)	Sample preparation	Elution	Column	Mobile phase	Linearity range (ng/ml)	Analytical time (min)	Accuracy (%)
Salm, Taylor et al. (2000)	HPLC-MS	32-O-desmethoxysirolimus	500	PPT by ACN and $ZnSO_4$, followed by SPE	Isocratic	Novapak C18 column (150 mm × 2.1 mm, 4 μm)	80% MeOH, 20% 50 mM NH_4AC, pH 5.1	0.2–100	10	94.4–104.4
Zochowska, Bartlomiejczyk et al. (2006)	HPLC-UV	Desmethoxyrapamycin	1500	PPT and extracted with 1-chlorobutan	Isocratic	Supelco RP C16-Amide column (150 mm × 4.6 mm, 5 μm)	60% ACN in water	3–50	15	NR
O'Halloran and Ilett (2008)	LC-MS/MS	Desmethoxyrapamycin Sirolimus-d_3	15	PPT by ACN and $ZnSO_4$	Gradient	Supelco C18 column (250 mm × 4.6 mm; 5 μm)	1 ml/L FA and 2 mM NH_4AC in MeOH and water	1–50	2.5	NR
Morgan, Brown et al. (2014)	LC-MS/MS	$^{13}C_2D_4$-everolimus	20	PPT by ACN and NH_4HCO_3 and $ZnSO_4$	Gradient	Waters Symmetry C18 column (50 mm × 2.1 mm, 3.5 μm)	2 mM NH_4AC and 0.1% FA in MeOH and water	1–49	6	90.7–113.16
Shi et al. (2016)	PS-MS/MS	Sirolimus-d_3	200	PPT by MeOH and dried	NR	NR	NR	LLOQ: 2	NR	NR
This study	LC-MS/MS	Sirolimus-d_3	100	PPT by MeOH	Gradient	Kinetex C18 column (50 mm × 2.1 mm, 1.7 μm)	0.1 mM FA and 0.05 mM NH_4AC in MeOH and water	0.5–50	3	88.7–111.8

Abbreviations: HPLC-MS, high-performance liquid chromatography–mass spectrometry; HPLC-UV, high-performance liquid chromatography–ultraviolet; LC-MS/MS, high-performance liquid chromatography–tandem mass spectrometry; PS-MS/MS, paper spray–tandem mass spectrometry; PPT, protein precipitation; ACN, acetonitrile; $ZnSO_4$, zinc sulfate; NH_4HCO_3, ammonium bicarbonate; MeOH: methanol; SPE, solid-phase extraction; NR, not reported; C18, octadecyl carbon chain; NH_4AC, ammonium acetate; FA, formic acid; LLOQ, lower limit of quantitation.

10.3389/fphar.2022.925018

TABLE 2 MRM transitions and conditions of SRL and SRL-d_3.

Compound	Transitions (*m/z*)	DP (V)	EP (V)	CE (V)	CXP (V)
SRL	931.7 → 864.6	24.0	5.00	23.0	21.0
SRL-d_3	934.7 → 864.6	17.0	8.00	26.0	30.0

Abbreviations: DP, declustering potential; EP, entrance potential; CE, collision energy; CXP, collision cell exit potential.

Cryopreserved human whole blood samples were supplied by the therapeutic drug monitoring lab (Children's Hospital of Nanjing Medical University, Nanjing, China), which were left-over samples from the clinical testing. The study was performed in accordance with the Helsinki Declaration, and the study protocol was approved by the Children's Hospital of Nanjing Medical University ethics committee (protocol number 202206114-1). This study aimed to evaluate the analytical consistency of the whole blood SRL levels generated by an EMIT assay and by an LC-MS/MS method, but no clinical and personal data were reported. Thus, the consent to participate is not applicable.

2.1.2 Liquid chromatography–tandem mass spectrometry conditions

This separation method was developed on a Jasper™ liquid chromatography system (AB Sciex Pte. Ltd., Singapore) with a binary pump (Sciex Dx™), an online degasser (Sciex Dx™), an auto-sampler (Sciex Dx™), and a column oven (Sciex Dx™). Liquid chromatographic (LC) separation was performed on a Kinetex C18 column, protected by a security guard C18 cartridge.

The mobile phase consisted of UPW (phase A) and MeOH (phase B), both containing 0.1 mM FA and 0.05 mM NH_4AC. A gradient elution with a flow rate at 0.4 ml/min was programmed as follows: 0–0.4 min, 50% phase B; 0.4–0.41 min, 50–90% phase B; 0.41–0.85 min, 90–100% phase B; 0.85–1.8 min, 100% phase B; 1.8–2.2 min, 100–50% phase B; 2.2–3.0 min, 50% phase B. The analytical run time was 3.0 min, and the LC flow was only directed into the MS between 1.0 and 3.0 min. The temperature for the column and auto-sampler was 50°C and 4°C, respectively.

MS detection of SRL and SRL-d_3 was conducted using a Triple Quad™ 4500MD system (AB Sciex Pte. Ltd., Singapore), equipped with an electrospray ionization (ESI) source. Quantification was operated in the positive ESI mode [ESI (+)], with multiple reaction monitoring (MRM) as the acquisition mode. The transitions and conditions are shown in Table 2. Other settings are as follows: curtain gas (CUR): 25 psi; collision-activated dissociation (CAD): 6 units; ion spray voltage: 5500 V; nebulizer gas (GS1): 40 psi; heater gas (GS2): 40 psi; ion source house temperature (TEM): 550°C. The LC-MS/MS system control and data analysis were performed using Analyst MD software (Version 1.6.3, AB Sciex Pte. Ltd., Singapore).

2.1.3 Preparation of solutions, calibration standards, and quality control samples

Stock solutions of SRL (1.00 mg/ml) and SRL-d_3 (1.00 mg/ml) were dissolved in MeOH. SRL stock solutions were further diluted with MeOH: H_2O (1:1; v/v) to prepare working solutions. All the stock solutions and working solutions were stored at −80°C before use.

Calibration standards and QC samples were prepared by spiking the working solutions into a blank matrix (human whole blood) at a ratio of 1: 20 to achieve serial concentrations of calibration standard samples. The calibration curve was prepared at 0.500, 1.00, 2.00, 5.00, 10.0, 30.0, and 50.0 ng/ml. The following QC samples with concentration levels were 0.500 ng/ml (lower limit of quantification QC, LLOQ QC), 1.50 ng/ml (low QC, LQC), 15.0 ng/ml (medium QC, MQC), and 40.0 ng/ml (high QC, HQC).

2.1.4 Sample preparation

The aliquot of 100 μl of the whole blood sample was pipetted into a 1.5-ml Eppendorf tube. An aliquot of 200 μl of MeOH containing IS (15 ng/ml of SRL-d_3) was added, followed by 300 μl of neat MeOH solvent. The mixture was vortexed for 10 min. After centrifugation at 12,000 rpm for 10 min at 4°C, 10 μl of the supernatant extract was injected into the LC-MS/MS system for analysis.

2.2 Method validation

The present method was optimized and validated using cryopreserved and fresh whole blood as matrices according to the Bioanalytical Method Validation Guidance for Industry published by the U.S. Food and Drug Administration (FDA) in 2018 (U.S. Food and Drug Administration, 2018).

2.2.1 Selectivity

Double blank samples from six different individual sources of the matrix were used to evaluate the selectivity of the analysis. The interference between the analyte and IS was assessed using human whole blood samples of zero blank containing IS and the upper limit of quantification (ULOQ) without IS.

2.2.2 Linearity and lower limit of quantification

Linearity of the LC-MS/MS assay was tested by analysis of all calibrators that were run in duplicate at the beginning and end of

each batch, with concentrations ranging from 0.500 to 50.0 ng/ml for SRL. The ratio of the standard peak area to the IS peak area was plotted against the ratio of the standard concentration/IS for constructing calibration curves, and a $1/x^2$ weighting factor was used for linear regression.

The LLOQ, defined as the lowest point of the calibration curve, should be within an acceptable range for method accuracy and precision, and the signal-to-noise ratio (S/N) should be no less than 5.

2.2.3 Accuracy and precision

Four concentration levels of QC samples (LLOQ QC, LQC, MQC, and HQC) in six replicates were assessed for determination of the intra-batch accuracy and precision. The inter-batch accuracy and precision were established by the repeat of the intra-batch validation procedure in three consecutive batches prepared on different days. Accuracy is expressed as a relative error (RE, %), and precision is expressed as the relative standard deviation (RSD, %).

2.2.4 Recovery and matrix effect

Recovery was tested by spiking equal amounts of SRL and IS into aliquots of blank whole blood before and after extraction. The experiment was performed using three concentration levels (LQC, MQC, and HQC) for SRL, and each was measured six times. The recovery was calculated from the signal intensity ratios of the samples spiked before preparation to the samples spiked after preparation. The matrix effect was evaluated using six different sets of extracted blank blood samples and methanol samples with equal volumes of the analyte and IS added by repeated measurements (n = 3). To determine the matrix effect, the mean peak area of the blank blood samples that were extracted and spiked with the analyte and IS at the designated concentration was compared to the mean peak area of matrix-free, methanol-enriched samples. The matrix effects of SRL and IS were calculated in the same way, and then the matrix effect was assessed by IS-normalized matrix factors.

2.2.5 Stability

The stability of the analyte in the matrix was determined by LQC and HQC samples in triplicates after being kept in various storage conditions: room temperature, −80°C, and five freeze–thaw cycles. The post-preparative stability was tested by reanalyzing the LQC and HQC samples stored in the auto-sampler (4°C).

2.3 Enzyme multiplied immunoassay technique assay

According to the package insert, the Emit® 2000 SRL Assay is a homogeneous enzyme immunoassay containing mouse monoclonal antibodies with a high specificity for SRL. This EMIT assay is based on a competition of SRL antibody binding sites. SRL in the sample competes with SRL in the enzyme reagent that is labeled with recombinant enzyme glucose 6-phosphate dehydrogenase (rG6PDH). Active (unbound) rG6PDH enzyme converts the oxidized nicotinamide adenine dinucleotide (NAD) in the antibody reagent to NADH, resulting in a kinetic absorbance change that can be measured spectrophotometrically. Enzyme activity decreases upon binding to the antibody, allowing SRL concentrations to be measured in terms of enzyme activity. The liquid assay reagent kit (Siemens Healthcare Diagnostics Inc., Newark, NJ, United States) contains antibody reagent 1, buffer reagent 2, and enzyme reagent 3.

2.3.1 Reagents

Emit® 2000 Sirolimus Calibrators (Lot No. P1; expiry date: 2022-03-02), Emit® 2000 Sirolimus Assay (Lot No. P1; expiry date: 2022-04-09), and Emit® 2000 Sirolimus Sample Pretreatment Reagent (Lot No. N2; expiry date: 2023-05-10) were obtained from the Siemens Healthcare Diagnostic Ltd. (Newark, NJ, United States). Controls of SRL (Lot No. 0336; expiry date: 2024-11-30) were supplied by Bio-Rad Laboratories Inc. (Irvine, United States).

2.3.2 Assay performance

Sample pretreatment is required for red blood cell lysis, SRL solubilization, and protein precipitation prior to measurement on the EMIT analyzer. This was accomplished by adding 50 µl of the sample pretreatment reagent (Siemens Healthcare Diagnostics Inc.) and 200 µl of MeOH to 200 µl of real whole blood samples, calibrators, or controls in micro-centrifuge tubes. The samples were then vortexed for 5 min, followed by standing at room temperature for another 2 min, and then centrifuged at 12,000 rpm for 5 min at 4°C. The resulting supernatant is decanted and measured on the analyzer.

The SRL assay was carried out for 20 min. The following instrument parameters were established: a pretreated sample (28 µl) was added to reagent 1 (120 µl) and reagent 2 (60 µl). Following a 130-s incubation at 37°C, reagent 3 (60 µl) was added. The reaction mixture was monitored at 340 nm, 106 s after the addition of reagent 3. Using SRL calibrators analyzed in duplicate, the data were fitted to a parametric logit mathematical equation. Sample results were calculated by the instrument from the stored calibration curve.

The whole blood SRL concentration was assayed using an automated enzyme immunoassay analyzer (SIEMENS, Munich, Germany). The calibration curve of the assay was prepared at 0.00, 3.00, 6.00, 12.0, 24.0, and 36.0 ng/ml. QC samples were accepted if the deviation did not

exceed ±15% to ensure the accuracy and precision of the EMIT method.

2.4 Comparison of sirolimus concentrations generated by liquid chromatography–tandem mass spectrometry and by the enzyme multiplied immunoassay technique

Post completing the routine SRL monitoring by the EMIT assay and reporting results to clinicians, the left-over whole blood specimens were determined again by the newly validated LC-MS/MS. All samples were collected between June and December 2021. These samples are routinely transported to our laboratory for monitoring the whole blood SRL levels in children with vascular anomalies. In brief, 114 blood samples were collected from 49 children at the Department of Orthopedics, Children's Hospital of Nanjing Medical University. The concentration results generated by LC-MS/MS and the EMIT were compared statistically.

2.5 Morphological examination of red blood cells

Blood smears were stained with Wright–Giemsa stain (Baso Diagnostics Inc., Zhuhai City, Guangdong Province, China). First, an aliquot of 0.5–0.8 ml solution A was dropped onto smears and stained for 1 min. Then, solution B was added to solution A (the volume of solution B was two to three times that of solution A). A ear washing bulb was used to make the liquid surface ripple by blowing out the breeze and mixing two solutions thoroughly. After staining for 4–10 min, the smears were rinsed. Dried smears were examined under a BX51 microscope (Olympus Corp., Tokyo, Japan), and images were collected through J D 801 series medical imaging workstation system software.

2.6 Statistical analysis

GraphPad Prism Software (version 8.3.0, CA, United States), Medcalc software (Ostend, Belgium), and Analyse-it Software (version 5.66, Leeds, United Kingdom) were used to statistically analyze all data. Linear regression analysis was performed by GraphPad to estimate the association between the assays. The Bland–Altman difference plot, which can be drawn by MedCalc software, is helpful in demonstrating the potential relationship between the differences and the magnitude of measurements exhibiting any systematic bias and in identifying possible outliers. Weighted Deming regression was performed by Analyse-it to complete the data comparison.

3 Results and Discussion

3.1 Optimization of the analytical method

3.1.1 Mass spectrometric parameter optimization

The majority of LC-MS/MS methods for measurement of SRL concentration have used ESI as the ion source (Koster, Dijkers et al., 2009; Ivanova, Artusi et al., 2011; Koster, Alffenaar et al., 2013; Yuan, Payto et al., 2014; Morgan, Nwafor et al., 2016). SRL did not readily protonate under ESI conditions because it is neutral, but SRL will preferentially form adducts with cations (e.g., Na^+, K^+, and NH_4^+) (Taylor 2004). Bogusz, Enazi et al. (2007) revealed the presence of the ammoniated adduct of SRL through syringe infusion experiments in the mobile phase in full scan mode. In line with Bogusz, Enazi et al. (2007), the ammonium adduct ions were confirmed for SRL and SRL-d_3 in this study. The MS/MS spectra of SRL and SRL-d_3 are shown in Figure 1A.

3.1.2 Mobile phase and gradient elution optimization

During initial method development, an attempt was made to optimize the mobile phase. Mobile phase selection is critical since it affects analyte selectivity and resolution. At first, MeOH was chosen as the organic phase because it was commonly used in our laboratory and was relatively economic and less toxic. No improvement in signal intensity or peak shape was found when ACN was alternatively tested as the mobile phase B. Thus, the mobile phase consisted of UPW (phase A) and MeOH (phase B). In addition to the properties of the target analyte and mobile phase composition, the solution environment is also critical for the sensitivity of ESI-based MS detection because of its key role in the nebulization and ionization process. The mobile phase modifiers (including the type and percentage of the organic solvent used and the type and concentration of the electrolyte added) affect the ionization efficiency and MS response of the target analytes (Li, Tian et al., 2012). In the current study, FA and NH_4AC were next examined for the candidate modifiers. Seven concentration levels of FA (0.008, 0.04, 0.1, 0.2, 0.5, 1, and 5 mM) were tested, and the optimal result appeared to be achieved with the 0.1 mM FA-modified mobile phase. Due to the $[M + NH_4]^+$ as the MRM transitions, eight concentration levels of NH_4AC (0.05, 0.1, 0.2, 0.5, 1, 2, 5, and 10 mM) were further examined, and the best result seemed to be achieved under the 0.05 mM NH_4AC. Collectively, the mobile phase contained 0.1 mM FA and 0.05 mM NH_4AC.

In the reversed-phase LC, method development often starts with a gradient elution separation. From such separation, it is likely to evaluate whether isocratic or gradient elution is appropriate for a given target analyte or more and test either the solvent strength for isocratic separations or the gradient

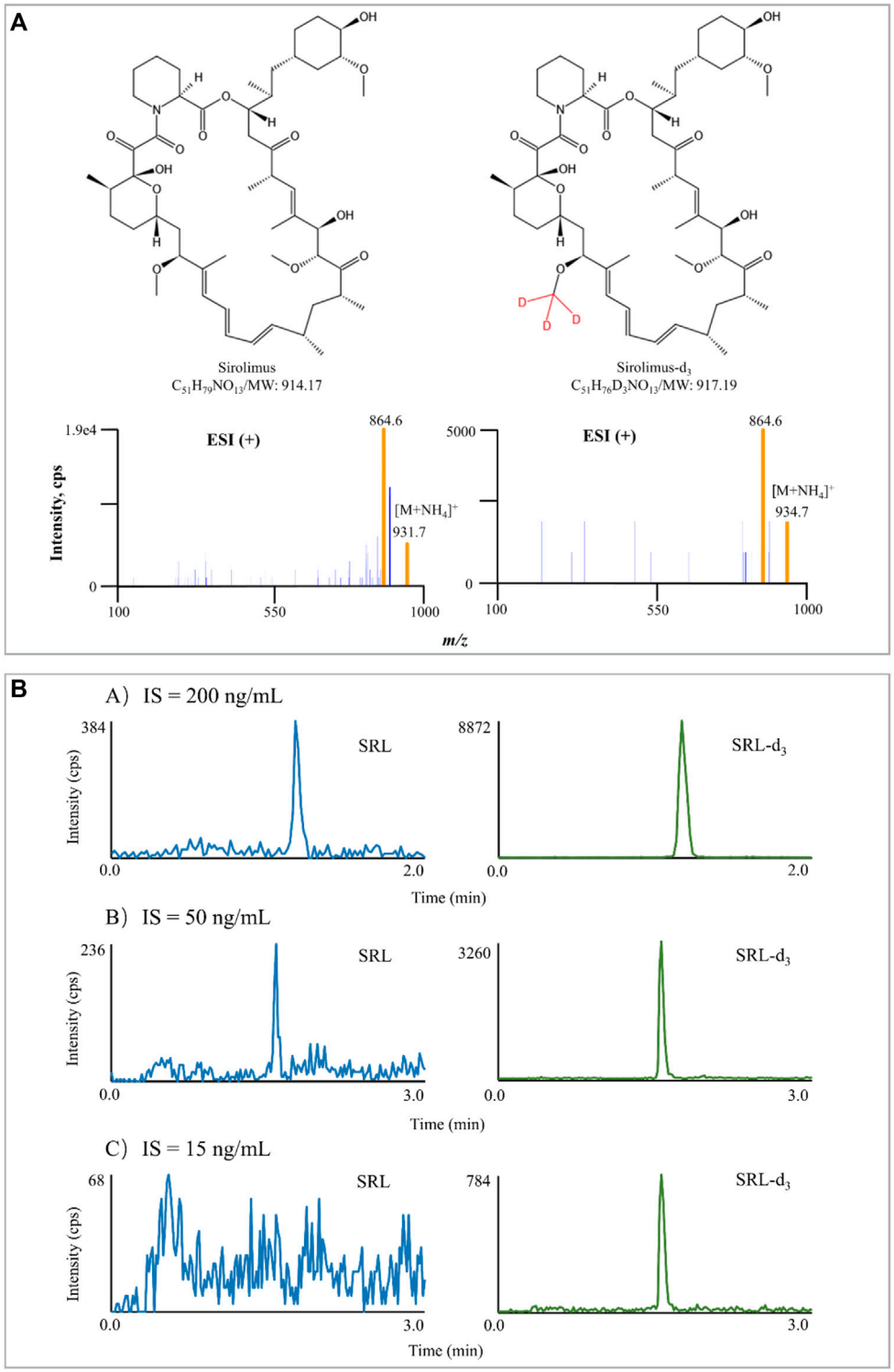

FIGURE 1
Typical MS/MS product ion spectra of SRL and SRL-d_3. The experiment was performed under *Manual Tune* mode by a syringe infusing the standard solution of SRL and SRL-d_3 (100 ng/ml) at a rate of 5 μl/min **(A)**. Interference of IS in blank samples spiked with IS only. The difference in chromatographic run time in **(A)** is due to the different gradient **(B)**.

range for gradient elution. Gradient elution is more attractive as it offers a favorable approach to significantly reduce the time required (Jandera, 2006). In this study, we found that SRL and SRL-d_3 were efficiently eluted at a high proportion of MeOH during the early stages of the experiments. The starting proportion of the UPW phase was 50%, and the MeOH percentage in the equivalent elution was examined from 80% to 100%. At last, the optimal elution ability and ionization efficiency were acquired when the organic phase proportion was 100%.

3.1.3 Selection of the chromatographic column

The particle size of a column packing affects the efficiency (theoretical plates) of a column. Smaller particle size helps optimize the performance of the LC-MS/MS method, attributing to shorter column lengths, higher optimum eluent velocities, and lower theoretical plate heights (Chen, Li et al., 2014). In addition, smaller particles can be used to enhance chromatographic resolution and decrease the analysis time (Nguyen, Guillarme et al., 2006). Therefore, in this study, we next investigated the influence of different columns on the performances of SRL and SRL-d_3 when other chromatographic conditions remained unchanged. The particle size varied from 1.7 to 5 μm, while the column length was fixed at 50 mm. Finally, the C18 column with a 50-mm length (2.1 mm ID) and 1.7-μm particle size in diameter (pore size, 100 Å) was selected, thereby achieving the optimal response and peak shape.

3.1.4 Internal standard concentration selection

In addition to the mobile phase used, chromatographic separation, and sample processing, the IS selection also contributes to the method performance (Valbuena, Shipkova et al., 2016). The IS compensates for those unavoidable assay variances and is widely used in quantitative LC-MS/MS bioanalysis for improving both the precision and accuracy of the assay (Lowes, Jersey et al., 2011). Ideally, a stable-isotope labeled chemical is preferred as it has exactly the same structure as the analyte and co-elutes with it (Fu, Barkley et al., 2020). In this study, SRL-d_3 was utilized, and the concentration of SRL-d_3 was initially set at 200 ng/ml, but the IS interfered seriously with SRL there. The SRL-d_3 concentration was subsequently reduced to 50 ng/ml, but the interference still existed. Interestingly, when the SRL-d_3 level was set at 15 ng/ml, the interference could be ignored and the MS response of the IS became stable (Figure 1B).

3.2 Sample cleanup optimization

SRL was distributed predominantly (about 95%) into red blood cells (RBCs), with only a small proportion of the drug being found in the plasma fraction (Stenton, Partovi et al., 2005). From the TDM standpoint, the preferred matrix for SRL measurement would be whole blood (Yatscoff, LeGatt et al., 1993). Optimum recovery of SRL from whole blood has proven to be problematic such as crosstalk interference and sacrificed recovery due to inappropriate clean-up methods in the past when compared with other common immunosuppressant drugs (Morgan, Brown et al., 2014). Therefore, the ability to lyse RBCs of the cleanup method can affect the results of concentration measurement. Therefore, in this study, we investigated the efficiency of the sample processing method on RBC lysis. Cryopreserved whole blood and fresh whole blood were treated in different ways and then stained with Wright–Giemsa stain to observe the RBC morphology under a microscope. Handling methods for whole blood samples include 1) spiking the working solution only, 2) up-and-down mixing after the addition of MeOH, and 3) vortexing for 10 min after the addition of MeOH. The results showed that up-and-down mixing after the addition of the precipitant was sufficient to lyse RBCs in fresh whole blood. The cells in the cryopreserved whole blood which has been cryopreserved for a long time showed a lysis state even after only spiking handling (Figure 2). Therefore, the sample cleanup method in this study was capable of lysing RBCs.

3.3 Liquid chromatography–tandem mass spectrometry method validation

3.3.1 Selectivity

There was only negligible interference in all double blank samples at the retention time of SRL. Good selectivity was confirmed between SRL and SRL-d_3.

3.3.2 Linearity and lower limit of quantification

The MS response was linear across the calibration range for SRL with a correlation coefficient no less than 0.990. The S/N of the LLOQ of SRL was > 5.

3.3.3 Accuracy and precision

The accuracy and precision results are summarized in Table 3. Both intra- and inter-batch accuracy and precision were acceptable (LLOQ QC: RE and RSD are < 20%, and others: RE and RSD are < 15%).

3.3.4 Recovery and matrix effect

The extraction recovery, measured at three different concentrations over the whole calibration range (n = 6 for each individual concentration level), was adequate. The post-extraction addition tests show that ion suppression or ion enhancement was not a problem with the present method (Table 4).

3.3.5 Stability

The stability of SRL in human whole blood at room temperature, at 4°C in the auto-sampler, and at −80°C for the long term and after five freeze–thaw (−80°C) cycles were acceptable as shown in Table 5.

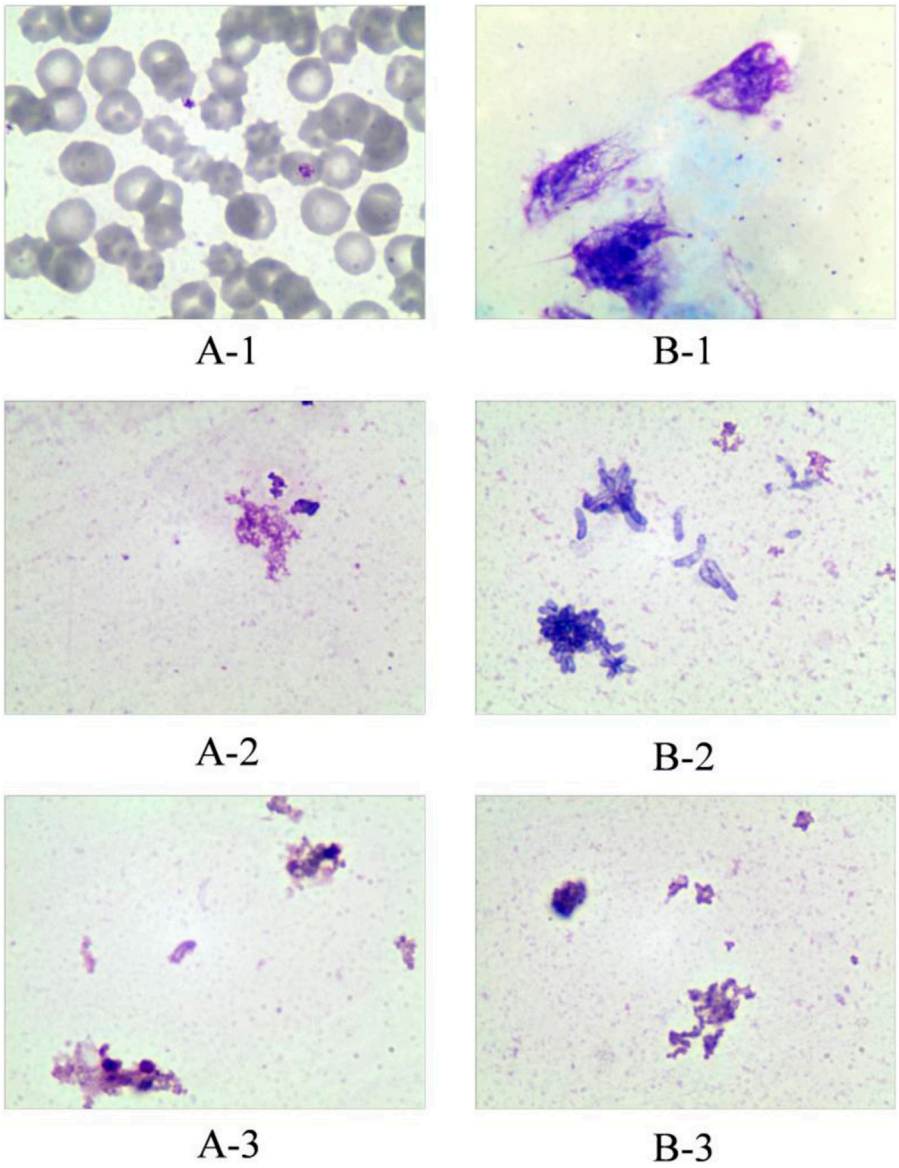

FIGURE 2
Effect of different treatments on red blood cell disruption. Group A represents fresh whole blood; group B represents cryopreserved whole blood. A-1: Fresh whole blood spiked only; A-2: fresh whole blood precipitated with methanol and mixed up-and-down; A-3: fresh whole blood precipitated with methanol and vortexed for 10 min. B-1: Cryopreserved whole blood spiked only; B-2: cryopreserved whole blood precipitated with methanol and mixed up-and-down; B-3: cryopreserved whole blood precipitated with methanol and vortexed for 10 min.

3.4 Enzyme multiplied immunoassay technique assay

A calibration curve with a range of 3.00–36.0 ng/ml was automatically obtained from the Viva-E automatic enzyme immunoassay analyzer, while the analyzer has a reportable concentration range of 3.50 ng/ml (based on detection limit and instrument sensitivity) to 30.0 ng/ml. Quantitative results above 30.0 ng/ml can be evaluated by diluting and re-assaying the sample at a higher concentration and multiplying the result by the dilution factor. The concentration was calculated by the formula as shown in Table 6.

TABLE 3 Intra-batch and inter-batch precision and accuracy for SRL in cryopreserved and fresh human whole blood.

Matrix	Intra-batch (n = 6)								Inter-batch (n = 6 × 3)							
	LLOQ QC		LQC		MQC		HQC		LLOQ QC		LQC		MQC		HQC	
	A	P	A	P	A	P	A	P	A	P	A	P	A	P	A	P
Cryopreserved human whole blood	−2.4	8.0	−0.7	12.8	−2.7	6.8	4.3	7.7	−4.0	8.8	−11.3	10.5	1.3	7.9	5.7	8.5
Fresh human whole blood	11.8	2.9	4.0	6.4	0.0	6.7	3.0	9.0	5.0	13.0	2.0	10.5	0.0	7.3	6.8	7.3

Note: A, accuracy and data are expressed as relative error (RE, %); P, precision, and data are expressed as the relative standard deviation (RSD, %); n, number of replicates; LLQC, 0.500 ng/ml; LQC, 1.50 ng/ml; MQC, 15.0 ng/ml; HQC, 40.0 ng/ml.

TABLE 4 Recovery and matrix effect of SRL in cryopreserved and fresh human whole blood.

Nominal conc. (ng/ml)	Recovery (n = 6)						IS-normalized matrix factor (n = 3 × 6)					
	Cryopreserved human whole blood			Fresh human whole blood			Cryopreserved human whole blood			Fresh human whole blood		
	Mean (%)	RSD (%)	Total RSD (%)	Mean (%)	RSD (%)	Total RSD (%)	Mean ± SD (%)	RSD (%)	Total RSD (%)	Mean ± SD (%)	RSD (%)	Total RSD (%)
1.50	88.6	5.6	4.7	96.7	12.6	9.4	112.2 ± 7.6	6.8	4.2	109.0 ± 3.1	2.8	3.1
15.0	81.0	4.8		80.7	6.4		103.8 ± 4.1	3.9		102.6 ± 3.3	3.2	
40.0	87.2	6.1		93.7	12.1		111.1 ± 8.0	7.2		104.8 ± 3.5	3.3	

Note: RSD, relative standard deviation; total RSD, the RSD for three concentration levels; n, number of replicates.

TABLE 5 Stability of SRL in cryopreserved and fresh human whole blood (n = 3).

Matrix	Storage conditions		RE (%)	RSD (%)
Cryopreserved human whole blood	Room temperature stability	LQC	−2.0	7.5
	(25°C, 24 h)	HQC	0.5	11.2
	Freeze–thaw stability	LQC	0.0	6.7
	(−80°C, five cycles)	HQC	7.8	3.0
	Autosampler stability	LQC	10.7	12.0
	(4°C, 2 d 17 h)	HQC	7.0	3.3
	Long-term stability	LQC	13.3	6.5
	(−80°C, 31 d)	HQC	0.5	3.0
Fresh human whole blood	Room temperature stability	LQC	13.3	5.3
	(25°C, 24 h)	HQC	9.5	8.7
	Freeze–thaw stability	LQC	−10.0	13.3
	(−80°C, five cycles)	HQC	1.5	9.6
	Autosampler stability	LQC	8.7	12.9
	(4°C, 2 d 17 h)	HQC	3.2	8.0
	Long-term stability	LQC	9.3	0.6
	(−80°C, 31 d)	HQC	3.2	10.4

Note: RE, relative error; RSD, relative standard deviation; LQC, 1.50 ng/ml; HQC, 40.0 ng/ml.

TABLE 6 EMIT Formula for SRL concentration calculation.

A = a (I) + b (I) * (C − C (I)) *c (I) * (C − C (I))^2 + B (I) * (C − C (I))^3

a (0) = −4.80830E-005	b (0) = 0.00000E+000	c (0) = 1.77636E+001	d (0) = −2.08016E-001
a (1) = −6.54051E-005	b (1) = −2.46666E-006	c (1) = 1.77636E+001	d (1) = 9.57422E-002
a (2) = −2.06495E-005	b (2) = −4.74276E-006	c (2) = 1.77636E+001	d (2) = 3.01801E-001
a (3) = 5.99687E-005	b (3) = −5.91977E-006	c (3) = 1.77636E+001	d (3) = 6.39310E-001
a (4) = 6.59947E-006	b (4) = −3.24694E-007	c (4) = 1.77636E+001	d (4) = 1.19176E+000

Inaccuracy = 1.32798E+000.

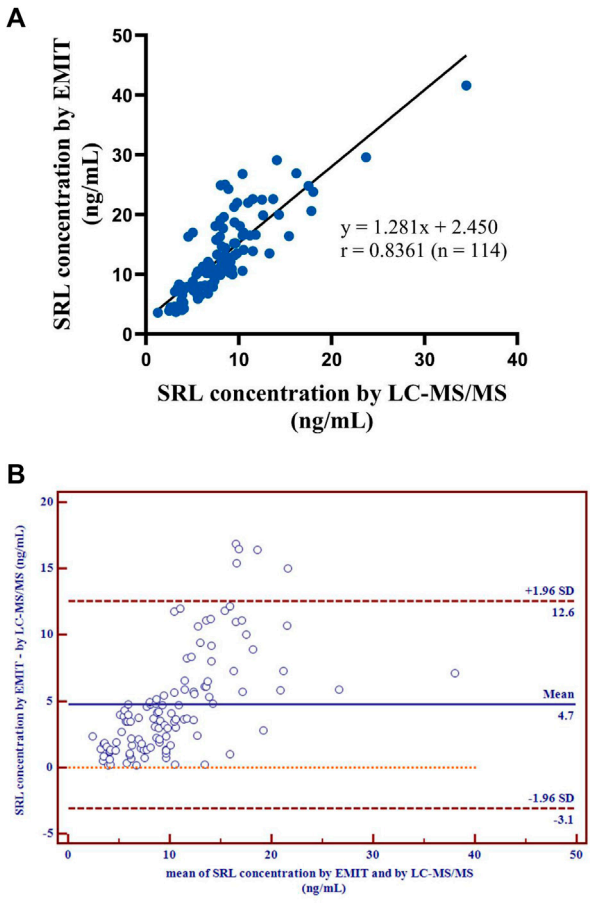

FIGURE 3
Correlation of the regression curve for LC-MS/MS and EMIT assay (*n* = 114) **(A)**. Differences between mean whole blood SRL concentrations (ng/ml) generated by LC-MS/MS and by EMIT assay expressed as absolute bias (*n* = 114) **(B)**.

Our laboratory conducted three concentration levels of QC samples to control inter-day variation. The deviations of QC samples over the period of clinical sample collection and detection were from −13.6% to 14.6%.

3.5 Comparison of sirolimus concentrations generated by liquid chromatography–tandem mass spectrometry and by enzyme multiplied immunoassay technique

To the best of our knowledge, this is the first study focusing on the consistency evaluation of SRL concentrations generated by the EMIT and LC-MS/MS. Briefly, 114 blood samples were measured by two methods. SRL concentrations measured by the EMIT and by LC-MS/MS were 11.0 ng/ml (median, range 3.60–41.6 ng/ml) and 7.61 ng/ml (median, range 1.27–34.5 ng/ml), respectively. The median concentration of whole blood SRL determined by the EMIT was higher by 1.45 fold than that by LC-MS/MS.

Kolmogorov–Smirnov analysis and D'Agostino–Pearson test both revealed that the distribution style of the concentration data obtained from the LC-MS/MS or EMIT method was non-normal distribution. Spearman's correlation analysis indicated that the data from two assays were significantly correlated ($p < 0.0001$). A regression equation was obtained as follows:

[***EMIT***] = 1.281 × [***LC–MS/MS***] + 2.450

with r = 0.8361 (Figure 3A), which revealed a good correlation between the two methods.

There were disparities between the SRL concentrations generated by the EMIT and by LC-MS/MS plotted against the mean level determined by two methods (Figure 3B). The levels of the whole blood SRL measured by the EMIT were higher than those determined by LC-MS/MS [positive bias: 4.7 ng/ml; 95% CI: (−3.1, 12.6)]. The Bland–Altman difference plot in Figure 4 shows the relative difference calculated by [(EMIT)–(LC-MS/MS)/(LC-MS/MS)], plotted against the LC-MS/MS results. There was a mean positive bias of 63.1% [95% CI: (−36.1, 162.3)] compared with the LC-MS/MS assay. Overall, the Bland–Altman difference plots suggested that the EMIT systematically overestimated SRL levels in whole blood compared to LC-MS/MS data. In addition, the data comparison was also performed by Weighted Deming regression. The Deming plot also revealed a mean positive bias for the EMIT (Figure 5).

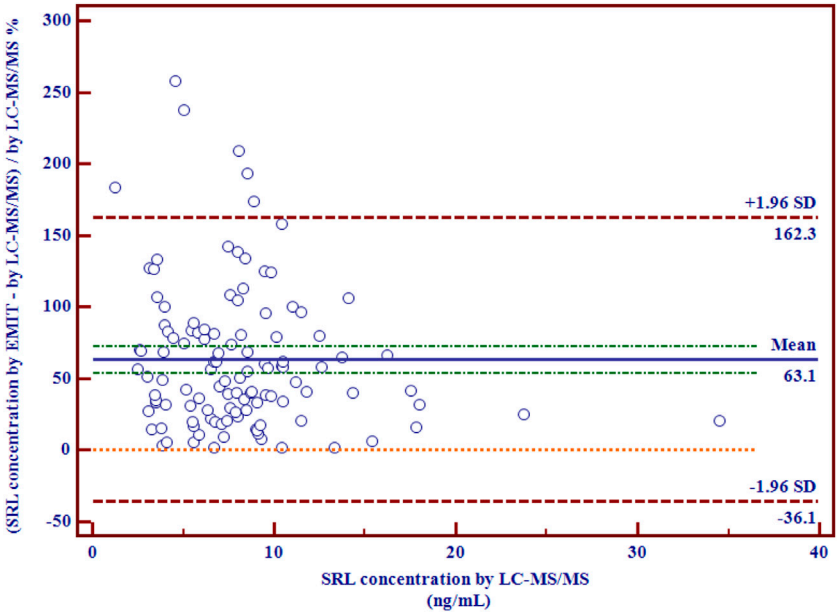

FIGURE 4
Relative differences between mean whole blood SRL concentrations (ng/ml) generated by LC-MS/MS and by the EMIT assay expressed in percentage (n = 114).

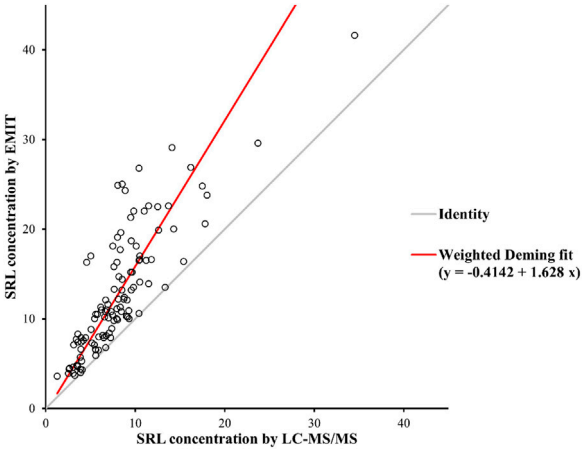

FIGURE 5
Weighted Deming Plot between SRL concentrations generated by the EMIT and LC-MS/MS methods.

The EMIT is easily operated but has a number of shortcomings such as high cost per sample, low specificity, and falsely elevated concentrations (Mika and Stepnowski, 2016). LC-MS/MS is currently used as a gold standard assay for measuring the concentration of SRL because it is known for negligible interference (Lee, Kim et al., 2019). In the current study, the whole blood concentration of SRL from the EMIT was higher than that generated by the LC-MS/MS method. A mean overestimation of about 63.1% was observed. Similar results were reported in other comparison studies performed to investigate the difference between the immunoassay and LC-MS/MS. Fillee, Mourad et al. (2005) found a global overestimation of about 15% by microparticle enzyme immunoassay (MEIA) compared with LC-MS/MS. The mean MEIA bias was found to be 11.5% compared with LC-MS/MS in a correlation study by Vicente, Smith et al. (2006), and Salm, Taylor et al. (2000) revealed a mean overestimation of 42.5% by MEIA compared with LC-MS/MS. The difference between these MEIA studies and the present study may be due to the different determination principles of MEIA and the EMIT.

In general, immunoassay results were overestimated compared to LC-MS/MS (Lee, Kim et al., 2019). LC-MS/MS has excellent reproducibility and low interference, suggesting that it is an unlikely source of overestimation. The most likely explanation for the bias would be non-specific binding to antibodies, known as cross-reactivity. Immunoassay cross-reactivity has been demonstrated between SRL and its 41-O-desmethyl (86–127%) and hydroxy (44–50%) metabolites (Jones, Saadat-Lajevard et al., 2000). In addition, SRL and its major metabolites have significant cross-reactivity with

everolimus (Baldelli, Crippa et al., 2006; Bouzas and Tutor, 2007; Khoschsorur, Fruehwirth et al., 2007), although they are unlikely to be administered simultaneously to patients. Moreover, the matrix effect can also significantly compromise the performance of immunoassays (Sallustio, Noll et al., 2011). Additionally, deviations may also be caused by inaccurate calibration before measurement and hematocrit (Sallustio, Noll et al., 2011; Sturgeon and Viljoen, 2011). Therefore, all of these potential causes likely act in a synergic way, and the final effect observed is hardly due to the cross-reactivity.

One more question needs to be further considered. Early studies suggested a whole blood SRL therapeutic window of 5–15 ng/ml or 6–12 ng/ml (in combination with tacrolimus) using MEIA as the detection method (MacDonald, Scarola et al., 2000; McAlister, Gao et al., 2000). Another report in the same year showed that a trough concentration window of 5–15 ng/ml measured by an HPLC instrument combined with an ultraviolet detector (HPLC-UV) could be regarded as the putative target for dose tailoring (Kahan, Napoli et al., 2000). Furthermore, the therapeutic window recommended for trough SRL concentration in patients on triple therapy with cyclosporine, corticosteroids, and SRL was 4–12 ng/ml, determined by HPLC-UV or LC-MS/MS (Oellerich, Armstrong et al., 2004). These reports revealed that the detection methods had no influence on the target range definition for blood SRL monitoring. Our study found a good correlation between the EMIT and LC-MS/MS, indicating that switching between the two methods was feasible. However, when switching from the EMIT to an alternative LC-MS/MS method, clinical TDM laboratories need to explain the results to clinicians and patients that the decrease in concentration results was due to an overestimation of the previous EMIT. More emphasis should be simultaneously placed on efficacy and safety rather than just concentration data.

4 Conclusion

This study compared the whole blood SRL concentrations generated by a routine EMIT and by a newly validated LC-MS/MS assay using a number of whole blood samples from children with vascular anomalies. In summary, there was a close correlation between the two methods, but EMIT assay significantly overestimated SRL concentrations by 63.1% compared with the LC-MS/MS method. Switching from the EMIT to the LC-MS/MS technique for routine TDM of SRL deserves great concern. Moreover, the results generated by LC-MS/MS are closer to the true values; therefore, necessary re-evaluation for the target therapeutic reference range may be required when methods are switched within the same clinical laboratory or results are compared between different laboratories.

Data availability statement

The original contributions presented in the study are included in the article/Supplementary Material; further inquiries can be directed to the corresponding authors.

Ethics statement

The studies involving human participants were reviewed and approved by the Children's Hospital of Nanjing Medical University ethics committee. Written informed consent from the participants' legal guardian/next of kin was not required to participate in this study in accordance with the national legislation and the institutional requirements.

Author contributions

Y-TZ, Y-HH, and FC: principal investigators for the study, data analysis, and primary authors of the manuscript. H-RD, YL, Y-YZ, and H-LG: performed the data collection and analysis. X-SD: assisted in the design and performance of the study and the writing of the manuscript. Y-TZ: writing—original draft. Y-HH and FC: supervision, writing—review and editing. Y-HH and FC: provided financial support. All the authors reviewed and agreed on the final manuscript.

Funding

This study was supported by the Specially Appointed Medical Expert Project of the Jiangsu Commission of Health (2019). This study was also supported by the Scientific Research Support Foundation for Top Young Scholars at the Children's Hospital of Nanjing Medical University (2020).

Conflict of interest

The authors declare that the research was conducted in the absence of any commercial or financial relationships that could be construed as a potential conflict of interest.

Publisher's note

References

Baldelli, S., Crippa, A., Gabrieli, R., Fiocchi, R., Perico, N., Merlini, S., et al. (2006). Comparison of the Innofluor Certican Assay with HPLC-UV for the Determination of Everolimus Concentrations in Heart Transplantation. *Clin. Biochem.* 39 (12), 1152–1159. doi:10.1016/j.clinbiochem.2006.08.013

Bogusz, M. J., Enazi, E. A., Hassan, H., Abdel-Jawaad, J., Ruwaily, J. A., and Tufail, M. A. (2007). Simultaneous LC-MS-MS Determination of Cyclosporine A, Tacrolimus, and Sirolimus in Whole Blood as Well as Mycophenolic Acid in Plasma Using Common Pretreatment Procedure. *J. Chromatogr. B Anal. Technol. Biomed. Life Sci.* 850 (1-2), 471–480. doi:10.1016/j.jchromb.2006.12.048

Borgman, M. P., Hiemer, M. F., Molinelli, A. R., Ritchie, J. C., and Jortani, S. A. (2012). Improved Sensitivity for Methotrexate Analysis Using Enzyme Multiplied Immunoassay Technique on the Siemens Viva-E Instrument. *Ther. Drug Monit.* 34 (2), 193–197. doi:10.1097/FTD.0b013e31824b93a5

Bouzas, L., and Tutor, J. C. (2007). Determination of Everolimus in Whole Blood Using the Abbott IMx Sirolimus Microparticle Enzyme Immunoassay. *Clin. Biochem.* 40 (1-2), 132–136. doi:10.1016/j.clinbiochem.2006.08.005

Chen, F., Li, H. L., Tan, Y. F., Lai, W. Y., Qin, Z. M., Cai, H. D., et al. (2014). A Sensitive and Cost-Effective LC-ESI-MS/MS Method for Quantitation of Euscaphic Acid in Rat Plasma Using Optimized Formic Acid Concentration in the Mobile Phase. *Anal. Methods* 6 (21), 8713–8721. doi:10.1039/c4ay01894j

Cui, J. J., Wang, L. Y., Tan, Z. R., Zhou, H. H., Zhan, X., and Yin, J. Y. (2020). Mass Spectrometry-Based Personalized Drug Therapy. *Mass Spectrom. Rev.* 39 (5-6), 523–552. doi:10.1002/mas.21620

Fillee, C., MouradM.Squifflet, J. P., Malaise, J., Lerut, J., Reding, R., et al. (2005). Evaluation of a New Immunoassay to Measure Sirolimus Blood Concentrations Compared to a Tandem Mass-Spectrometric Chromatographic Analysis. *Transpl. Proc.* 37 (6), 2890–2891. doi:10.1016/j.transproceed.2005.05.034

Fu, Y., Barkley, D., Li, W., Picard, F., and Flarakos, J. (2020). Evaluation, Identification and Impact Assessment of Abnormal Internal Standard Response Variability in Regulated LC-MS Bioanalysis. *Bioanalysis* 12 (8), 545–559. doi:10.4155/bio-2020-0058

Ivanova, M., Artusi, C., Polo, G., Zaninotto, M., and Plebani, M. (2011). High-throughput LC-MS/MS Method for Monitoring Sirolimus and Everolimus in the Routine Clinical Laboratory. *Clin. Chem. Lab. Med.* 49 (7), 1151–1158. doi:10.1515/CCLM.2011.192

Jandera, P. (2006). Can the Theory of Gradient Liquid Chromatography Be Useful in Solving Practical Problems? *J. Chromatogr. A* 1126 (1-2), 195–218. doi:10.1016/j.chroma.2006.04.094

Jones, K., Saadat-Lajevard, S., Lee, T., HoRwatt, R., Hicks, D., Johnston, A., et al. (2000). An Immunoassay for the Measurement of Sirolimus. *Clin. Ther.* 22, B49–B61. doi:10.1016/s0149-2918(00)89022-0

Kahan, B. D., Napoli, K. L., Kelly, P. A., Podbielski, J., HusseIn, I., Urbauer, D. L., et al. (2000). Therapeutic Drug Monitoring of Sirolimus: Correlations with Efficacy and Toxicity. *Clin. Transpl.* 14 (2), 97–109. doi:10.1034/j.1399-0012.2000.140201.x

Khoschsorur, G., Fruehwirth, F., Zelzer, S., Stettin, M., and Halwachs-Baumann, G. (2007). Comparison of Fluorescent Polarization Immunoassay (FPIA) versus HPLC to Measure Everolimus Blood Concentrations in Clinical Transplantation. *Clin. Chim. Acta.* 380 (1-2), 217–221. doi:10.1016/j.cca.2007.01.017

Koster, R. A., Alffenaar, J. W. C., Greijdanus, B., and Uges, D. R. A. (2013). Fast LC-MS/MS Analysis of Tacrolimus, Sirolimus, Everolimus and Cyclosporin A in Dried Blood Spots and the Influence of the Hematocrit and Immunosuppressant Concentration on Recovery. *Talanta* 115, 47–54. doi:10.1016/j.talanta.2013.04.027

Koster, R. A., Dijkers, E. C. F., and Uges, D. R. A. (2009). Robust, High-Throughput LC-MS/MS Method for Therapeutic Drug Monitoring of Cyclosporine, Tacrolimus, Everolimus, and Sirolimus in Whole Blood. *Ther. Drug Monit.* 31 (1), 116–125. doi:10.1097/FTD.0b013e318192304c

Laplante, M., and Sabatini, D. M. (2012). mTOR Signaling in Growth Control and Disease. *Cell.* 149 (2), 274–293. doi:10.1016/j.cell.2012.03.017

Lee, E. J., Kim, H. K., Ahn, S., Lee, W., Kim, H. S., Chun, S., et al. (2019). Accuracy Evaluation of Automated Electrochemiluminescence Immunoassay for Everolimus and Sirolimus Compared to Liquid Chromatography-Tandem Mass Spectrometry. *J. Clin. Lab. Anal.* 33 (7), e22941. doi:10.1002/jcla.22941

Li, L., Tian, D., Chen, F., Yang, J., Yu, K., and Sun, Y. (2012). Strategies for Improving the Quantitative Bioanalytical Performance of LC-MS in Pharmacokinetic Studies. *Curr. Drug Metab.* 13 (9), 1206–1212. doi:10.2174/138920012803341320

Lowes, S., Jersey, J., Shoup, R., Garofolo, F., Savoie, N., Mortz, E., et al. (2011). Recommendations on: Internal Standard Criteria, Stability, Incurred Sample Reanalysis and Recent 483s by the Global CRO Council for Bioanalysis. *Bioanalysis* 3 (12), 1323–1332. doi:10.4155/bio.11.135

MacDonald, A., Burke, J. T., and Zimmerman, J. J. (2000). Clinical Pharmacokinetics and Therapeutic Drug Monitoring of Sirolimus. *Clin. Ther.* 22, 101–121. doi:10.1016/s0149-2918(00)89027-x

Mano, N., Sato, M., Nozawa, M., Matsumoto, Y., Mori, M., Yamaguchi, H., et al. (2011). An Accurate Quantitative LC/ESI-MS/MS Method for Sirolimus in Human Whole Blood. *J. Chromatogr. B Anal. Technol. Biomed. Life Sci.* 879 (13-14), 987–992. doi:10.1016/j.jchromb.2011.03.013

McAlister, V. C., Gao, Z., PelteKian, K., Domingues, J., Mahalati, K., and MacDonald, A. S. (2000). Sirolimus-tacrolimus Combination Immunosuppression. *Lancet* 355 (9201), 376–377. doi:10.1016/S0140-6736(99)03882-9

Mika, A., and Stepnowski, P. (2016). Current Methods of the Analysis of Immunosuppressive Agents in Clinical Materials: A Review. *J. Pharm. Biomed. Anal.* 127, 207–231. doi:10.1016/j.jpba.2016.01.059

Morgan, P. E., Brown, N. W., and Tredger, J. M. (2014). A Direct Method for the Measurement of Everolimus and Sirolimus in Whole Blood by LC-MS/MS Using an Isotopic Everolimus Internal Standard. *Ther. Drug Monit.* 36 (3), 358–365. doi:10.1097/FTD.0000000000000006

Morgan, P., Nwafor, M., and Tredger, M. (2016). Use of a Small Particle Solid-Core Packing for Improved Efficiency and Rapid Measurement of Sirolimus and Everolimus by LC-MS/MS. *Biomed. Chromatogr.* 30 (6), 983–985. doi:10.1002/bmc.3628

Nguyen, D. T., Guillarme, D., Rudaz, S., and Veuthey, J. L. (2006). Fast Analysis in Liquid Chromatography Using Small Particle Size and High Pressure. *J. Sep. Sci.* 29 (12), 1836–1848. doi:10.1002/jssc.200600189

Nguyen, T. T., Duong, V. A., Vo, D. K., Jo, J., and Maeng, H. J. (2021). Development and Validation of a Bioanalytical LC-MS/MS Method for Simultaneous Determination of Sirolimus in Porcine Whole Blood and Lung Tissue and Pharmacokinetic Application with Coronary Stents. *Molecules* 26 (2), E425. doi:10.3390/molecules26020425

O'Halloran, S., and Ilett, K. F. (2008). Evaluation of a Deuterium-Labeled Internal Standard for the Measurement of Sirolimus by High-Throughput HPLC Electrospray Ionization Tandem Mass Spectrometry. *Clin. Chem.* 54 (8), 1386–1389. doi:10.1373/clinchem.2008.103952

Oellerich, M., Armstrong, V. W., Streit, F., Weber, L., and Tonshoff, B. (2004). Immunosuppressive Drug Monitoring of Sirolimus and Cyclosporine in Pediatric Patients. *Clin. Biochem.* 37 (6), 424–428. doi:10.1016/j.clinbiochem.2004.04.001

Sallustio, B. C., Noll, B. D., and Morris, R. G. (2011). Comparison of Blood Sirolimus, Tacrolimus and Everolimus Concentrations Measured by LC-MS/MS, HPLC-UV and Immunoassay Methods. *Clin. Biochem.* 44 (2-3), 231–236. doi:10.1016/j.clinbiochem.2010.10.005

Salm, P., Taylor, P. J., and Pillans, P. I. (2000). The Quantification of Sirolimus by High-Performance Liquid Chromatography-Tandem Mass Spectrometry and Microparticle Enzyme Immunoassay in Renal Transplant Recipients. *Clin. Ther.* 22, B71–B85. doi:10.1016/s0149-2918(00)89024-4

Scott, J. R., Courter, J. D., Saldana, S. N., Widemann, B. C., Fisher, M., Weiss, B., et al. (2013). Population Pharmacokinetics of Sirolimus in Pediatric Patients with Neurofibromatosis Type 1. *Ther. Drug Monit.* 35 (3), 332–337. doi:10.1097/FTD.0b013e318286dd3f

Sehgal, S. N., Baker, H., and Vezina, C. (1975). Rapamycin (AY-22, 989), a New Antifungal Antibiotic. II. Fermentation, Isolation and Characterization. *J. Antibiot.* 28 (10), 727–732. doi:10.7164/antibiotics.28.727

Sehgal, S. N. (1995). Rapamune (Sirolimus, Rapamycin): an Overview and Mechanism of Action. *Ther. Drug Monit.* 17 (6), 660–665. doi:10.1097/00007691-199512000-00019

Shi, R. Z., El Gierari, E. T. M., Faix, J. D., and Manicke, N. E. (2016). Rapid Measurement of Cyclosporine and Sirolimus in Whole Blood by Paper Spray-Tandem Mass Spectrometry. *Clin. Chem.* 62 (1), 295–297. doi:10.1373/clinchem.2015.245191

Shipkova, M., and Svinarov, D. (2016). LC-MS/MS as a Tool for TDM Services: Where Are We? *Clin. Biochem.* 49 (13-14), 1009–1023. doi:10.1016/j.clinbiochem.2016.05.001

Stenton, S. B., Partovi, N., and Ensom, M. H. H. (2005). Sirolimus: the Evidence for Clinical Pharmacokinetic Monitoring. *Clin. Pharmacokinet.* 44 (8), 769–786. doi:10.2165/00003088-200544080-00001

Sturgeon, C. M., and Viljoen, A. (2011). Analytical Error and Interference in Immunoassay: Minimizing Risk. *Ann. Clin. Biochem.* 48, 418–432. doi:10.1258/acb.2011.011073

Taylor, P. J. (2004). Therapeutic Drug Monitoring of Immunosuppressant Drugs by High-Performance Liquid Chromatography-Mass Spectrometry. *Ther. Drug Monit.* 26 (2), 215–219. doi:10.1097/00007691-200404000-00023

U.S. Food and Drug Administration (2018). Bioanalytical Method Validation Guidance for Industry. Retrieved from https://www.fda.gov/media/70858/download.

Valbuena, H., Shipkova, M., Kliesch, S. M., Muller, S., and Wieland, E. (2016). Comparing the Effect of Isotopically Labeled or Structural Analog Internal Standards on the Performance of a LC-MS/MS Method to Determine Ciclosporin A, Everolimus, Sirolimus and Tacrolimus in Whole Blood. *Clin. Chem. Lab. Med.* 54 (3), 437–446. doi:10.1515/cclm-2015-0519

van den Ouweland, J. M., and Kema, I. P. (2012). The Role of Liquid Chromatography-Tandem Mass Spectrometry in the Clinical Laboratory. *J. Chromatogr. B Anal. Technol. Biomed. Life Sci.* 883-884, 18–32. doi:10.1016/j.jchromb.2011.11.044

Vezina, C., Kudelski, A., and Sehgal, S. N. (1975). A New Antifungal Antibiotic. I. Taxonomy of the Producing Streptomycete and Isolation of the Active Principle. *J. Antibiot.* 28 (10), 721–726. doi:10.7164/antibiotics.28.721

Vicente, F. B., Smith, F. A., Peng, Y., and Wang, S. (2006). Evaluation of an Immunoassay of Whole Blood Sirolimus in Pediatric Transplant Patients in Comparison with High-Performance Liquid Chromatography/tandem Mass Spectrometry. *Clin. Chem. Lab. Med.* 44 (4), 497–499. doi:10.1515/CCLM.2006.080

Vogeser, M., Fleischer, C., Meiser, B., Groetzner, J., Spohrer, U., and Seidel, D. (2002). Quantification of Sirolimus by Liquid Chromatography-Tandem Mass Spectrometry Using On-Line Solid-phase Extraction. *Clin. Chem. Lab. Med.* 40 (1), 40–45. doi:10.1515/CCLM.2002.008

Yatscoff, R., LeGatt, D., Keenan, R., and Chackowsky, P. (1993). Blood Distribution of Rapamycin. *Transplantation* 56 (5), 1202–1206. doi:10.1097/00007890-199311000-00029

Yuan, C., Payto, D., Gabler, J., and Wang, S. (2014). A Simple and Robust LC-MS/MS Method for Measuring Sirolimus and Everolimus in Whole Blood. *Bioanalysis* 6 (12), 1597–1604. doi:10.4155/bio.14.43

Zochowska, D., BartlomIejczyk, I., KAminskA, A., Senatorski, G., and Paczek, L. (2006). High-performance Liquid Chromatography versus Immunoassay for the Measurement of Sirolimus: Comparison of Two Methods. *Transpl. Proc.* 38 (1), 78–80. doi:10.1016/j.transproceed.2005.12.008

frontiers | Frontiers in Pediatrics

TYPE Original Research
PUBLISHED 07 September 2022
DOI 10.3389/fped.2022.949783

OPEN ACCESS

EDITED BY
Xiaoling Wang,
Beijing Children's Hospital, Capital Medical University, China

REVIEWED BY
Elisabetta Tozzi,
University of L'Aquila, Italy
Ashwin Karanam,
Pfizer, United States

*CORRESPONDENCE
Xiao-Peng Lu
lxp20071113@sina.com
Feng Chen
cy.chen508@gmail.com

†These authors have contributed equally to this work

SPECIALTY SECTION
This article was submitted to Obstetric and Pediatric Pharmacology, a section of the journal Frontiers in Pediatrics

RECEIVED 21 May 2022
ACCEPTED 19 August 2022
PUBLISHED 07 September 2022

CITATION
Li Y, Guo H-L, Zhang Y-Y, Dong N, Hu Y-H, chen J, Lu X-P and Chen F (2022) Plasma lacosamide monitoring in children with epilepsy: Focus on reference therapeutic range and influencing factors.
Front. Pediatr. 10:949783.
doi: 10.3389/fped.2022.949783

Plasma lacosamide monitoring in children with epilepsy: Focus on reference therapeutic range and influencing factors

Yue Li[1†], Hong-Li Guo[1†], Yuan-Yuan Zhang[1], Na Dong[2], Ya-Hui Hu[1], Jing chen[3], Xiao-Peng Lu[3*] and Feng Chen[1*]

[1]Department of Pharmacy, Pharmaceutical Sciences Research Center, Children's Hospital of Nanjing Medical University, Nanjing, China, [2]Institute of Pharmaceutical Sciences, China Pharmaceutical University, Nanjing, China, [3]Department of Neurology, Children's Hospital of Nanjing Medical University, Nanjing, China

Background: Lacosamide (LCM) is a newer anti-seizure medication (ASM) that was approved in China in 2018, but its real-world clinical data and plasma concentrations in Chinese children with epilepsy are very limited. Of note, the reference range for routine LCM therapeutic drug monitoring is still unknown. The purpose of this study was to investigate the efficacy and safety of LCM as a monotherapy or an adjunctive treatment with other ASMs and to evaluate the potential factors affecting its efficacy and variable LCM plasma concentrations in Chinese children with epilepsy.

Methods: Children with epilepsy (<18 years) with routine plasma LCM monitoring from March 2019 to December 2021 at the Department of Pharmacy, Children's Hospital of Nanjing Medical University were retrospectively collected. Clinical data were obtained from the hospital information system.

Results: 76 pediatric patients (52 males) were finally enrolled. Mean age was 7.9 years (1.3–17.3 years) with a mean dose of LCM 6.3 mg/kg/day (2.0–11.3 mg/kg/day). The TDM data as a whole showed that the median plasma trough concentration (C_0) was 3.42 μg/mL (1.25–8.31 μg/mL). A 6-month LCM add-on therapy produced 70% of patients achieving ≥50% seizure frequency reductions, and the number was 81% for the one-year follow-up findings. Interestingly, more patients who took LCM monotherapy achieved seizure freedom over the same periods of follow-up observations. Under maintenance dosages, approximately 92.1% of the C_0 values were 2.0–7.0 μg/mL. The plasma-C_0-to-daily dose (C_0/Dose) ratio was significantly associated with age and body weight (BW). The C_0/Dose ratio in patients aged 1–≤6 and 6–≤12 years was significantly higher by 81% and 29% than those aged 12–≤18 years, respectively. The C_0/Dose ratio in patients with a BW of ≥40 kg was 1.7-fold lower than in patients with a BW of ≤20 kg. In addition, complex LCM-ASMs interactions were observed. Oxcarbazepine significantly decreased the C_0/Dose ratio of LCM by 28%.

Conclusion: This retrospective study confirmed the effectiveness and tolerability of the LCM treatment used alone or with other ASMs in children with focal epilepsy. Children with higher BW and older age have lower C_0/Dose

ratio. Complex drug interactions between LCM and other concomitant ASMs were revealed. Notably, based on the data in our hands, the reference range, *i.e.*, 2.0–7.0 μg/mL, for routine LCM monitoring may be feasible. The real-world evidence of this study supports LCM as a promising option in children with focal epilepsy.

KEYWORDS

focal epilepsy, lacosamide, children, therapeutic drug monitoring, C_0/Dose ratio

Introduction

China has ∼10 million people with epilepsy (1), and around two-thirds of people are under 18 years of age (2). Childhood epilepsies present broad management challenges that are unique to this age group. These challenges mainly include the precision diagnoses; the therapy options; the developmental, cognitive, and behavioral comorbidities of epilepsy; and the likelihood that those different factors interact with developmental processes in the young brain (3). Nearly 20 different anti-seizure medications (ASMs) and non-pharmacological options are now available in China, but there are still unmet needs for epilepsy management (1), with therapeutic aims not only to achieve overt freedom from seizures, but also to actively abolish abnormal electrical activity in the developing brain.

With new-generation ASMs, such as lacosamide (LCM), seizure control with less side effects and food- and/or drug-drug interactions is expected, in an attempt to target the causes and mechanisms of epilepsy rather than its symptoms (4). LCM, the R-enantiomer of 2-acetamido-N-benzyl-3-methoxypropionamide, is a functionalized amino acid analog of D-serine. LCM exerts distinct mechanisms of action over other ASMs by selectively changing voltage-gated sodium channel into a slow and inactivated state, resulting in stabilization of hyperexcitable neuronal membranes; and by binding to the collapsin response mediator protein 2, which plays critical roles in the process of neuronal differentiation, growth, polarization, control of axonal outgrowth and probably also epileptogenesis (5, 6). These unique properties lead to its powerful anti-seizure effects while retaining normal brain functions.

The US FDA approved LCM as an adjunctive therapy for partial-onset (focal) seizures in October 2008 (5). Nowadays, as a prescription medicine, LCM is used to treat focal-onset seizures in people 1 month of age and older or used with other medicines to treat primary generalized tonic-clonic seizures in people 4 years of age and older, according to the revised version of package insert in 2021. Nevertheless, it is unclear if LCM is safe and effective for partial-onset seizures in children under 1 month of age or for primary generalized tonic-clonic seizures in children under 4 years of age. Recent study revealed that LCM might also be useful as the first-line monotherapy for adults with newly diagnosed epilepsy (7). In China, LCM was approved in 2018 as an adjunctive therapy to treat focal-onset seizures in people 4 years of age and older. However, the safety and effectiveness profiles of LCM stay understudied in Chinese pediatric patients. The approval was granted mainly based on the extrapolation of efficacy and safety data from those western pediatric subjects (8). Therefore, the efficacy, tolerability, and pharmacokinetics of LCM are worthy of further validation by enrolling both RCTs and real-world observational studies with different time-period treatments (9).

A long-term, open-label extension of a randomized, controlled trial revealed that LCM was well-tolerated as long-term adjunctive therapy in Chinese adults with epilepsy and uncontrolled focal seizures, with improvements in seizure reduction maintained over 36 months of treatment (10, 11). Notably, a retrospective study of 72 pediatric patients with epilepsy in Uygur, China, showed that LCM therapy is safe and effective for epilepsy in children, resulting in a reduction in the seizure frequency (8). However, there is limited data on the effectiveness and safety of LCM in Han Chinese children with epilepsy.

On the other hand, it is evident that the systemic exposure to LCM depends partly on age and sex, thereby requiring pharmacokinetic monitoring to define the optimal dosage that guarantees therapeutic efficacy with tolerable side effects (4). Interestingly, Zhao et al. (12) found that *ABCB1* polymorphisms might affect LCM serum concentrations and treatment efficacy in Uygur pediatric patients with epilepsy, leading to drug resistance. In addition, evidence of drug-drug interactions also justifies monitoring epileptic patients taking LCM (13). In a sense, LCM monitoring demands sensitive and robust bioanalytical techniques that guarantee an accurate LCM measurement in plasma or serum. Moreover, it is also meaningful to define a specific reference range of LCM for Chinese people, especially for pediatric patients. Although several ranges have been recommended, the optimal therapeutic range is still inconclusive for those western populations (14).

This retrospective study aimed to (1) review the efficacy and safety of LCM as a monotherapy or an adjunctive treatment with other ASMs in Chinese children with epilepsy; (2) identify the potential factors affecting its plasma concentrations; and (3) suggest a specific plasma reference range for LCM.

Patients and methods

Patients

This study retrospectively reviewed children (<18 years) who were diagnosed with epilepsy and did the LCM treatment at the Children's Hospital of Nanjing Medical University from March 2019 to December 2021 (Figure 1). Diagnosis of epileptic seizures and syndromes was based on the Classification of Epileptic Seizures (15), after reviewing the semiology of seizures, electroencephalography (EEG), and magnetic resonance imaging (MRI) findings. Patients were excluded from the study if: (1) they received LCM treatment but did not have routine LCM concentration monitoring data; (2) if they had an underlying metabolic and systemic disorder; (3) if their detailed information was absent in the hospital information system (HIS). The Ethics Committee of the Children's Hospital of Nanjing Medical University granted the ethical approval for the study (Protocol number 202204021-1). Written consents were waivered due to the retrospective nature of the study.

Treatment protocol

All patients included in this study received oral LCM as monotherapy or add-on therapy.

For children aged 4 to 17 years, the starting dose was 2 mg/kg/day, which was raised to an initial therapeutic dose of 4 mg/kg/day after 1 week. Based on clinical response and tolerability, the maintenance dose might be increased weekly by 2 mg/kg/day. Gradually titrate the dose until the best response was achieved. Of note, for children weighing ≥11 but <30 kg, due to the increased total clearance compared with adults, the maximum dose did not exceed 12 mg/kg/day, and the maintenance dose was 6 to 12 mg/kg/day. For children weighing ≥30, but <50 kg, the maximum dose was 8 mg/kg/day, and the maintenance dose was 4 to 8 mg/kg/day. The daily dose was taken in two divided doses. For children weighing ≥50 kg, the starting dose is 50 mg twice a day, then the dose was increased to an initial therapeutic dose of 100 mg twice a day, in the morning and evening, after 1 week.

For pediatric patients below the age of 4 years with focal epilepsy, the informed consent was obtained from a parent of each patient due to the off-label use nature. According to the package insert, the dose tailoring was performed based on the body weight (BW), *i.e.*, the recommended dosages for weighing 6 kg to 11 kg and weighing <6 kg.

Collectively, the mean initial dose of LCM was 2.13 mg/kg/day, and the mean maintenance dose was 6.29 mg/kg/day. After three consecutive days of the administration, the trough concentration (C_0) of LCM was measured by LC-MS/MS method before the morning dose, and then each patient was followed up periodically for monitoring efficacy, safety, LCM levels, and laboratory tests.

Definitions of clinical response

Diagnosis of epileptic seizures and syndromes was based on the Classification of Epileptic Seizures (15), after reviewing the semiology of seizures, EEG, and MRI findings. The seizure frequency of 1 month before starting LCM therapy was set as a baseline value. To measure the curative effect of LCM therapy, the seizure frequency at 1, 3, 6, 12, and 24 months after starting LCM therapy were recorded.

The definitions for clinical response to the treatment as following were based on the seizure frequency compared with the baseline values: (1) seizure-freedom (SF), *i.e.*, absence of seizures on unchanged medication; (2) seizure frequency reduction (SFR), *i.e.*, patients with 50% or more reduction of baseline seizure frequency on unchanged medication; (3) ineffectiveness (IE), *i.e.*, patients with <50% reduction in seizure frequency on unchanged medication. Accordingly, children with seizure freedom, ≥50% seizure reduction, and <50% seizure frequency induction for a period of at least 6 months were considered as complete responders, responders, and non-responders, respectively.

Data collection

We collected various data on age, sex, BW, types of seizures, EEG findings, neuroimaging, duration of epilepsy before starting LCM therapy, duration of LCM treatment, number and type of previous ASMs treatment, concomitant ASMs used, treatment response, reported side effects. Specific data on LCM including its initial and maximal dose, and routine therapeutic drug monitoring if possible were also reviewed. The efficacy measures were analyzed based on the change in seizure frequency.

Routine therapeutic monitoring of LCM

Whole blood samples are routinely transported to our lab for monitoring steady-state plasma LCM levels in pediatric patients with LCM monotherapy or adjunctive therapy. The bioanalysis was performed on an LC-MS/MS system. In brief, the LC-MS/MS system consisted of a Triple Quad^{TM} 4500MD mass spectrometer (AB Sciex Pte. Ltd, Singapore) interfaced *via* a Turbo V^{TM} ion source with a Jasper^{TM} liquid chromatography system (AB Sciex Pte. Ltd, Singapore), which comprises a binary pump (Sciex Dx^{TM}), an online degasser (Sciex Dx^{TM}), an autosampler (Sciex Dx^{TM}), and a column oven (Sciex Dx^{TM}). The AB-SCIEX Analyst software packages (version 1.6.3) were used to control the LC-MS/MS system, as well as for data acquisition and processing. The chromatographic separation was achieved on a Kinetex C18 column (2.1 x 50 mm, 5 μm, Phenomenex) with a security Guard-C18 column (4 x 2.0 mm, Phenomenex), pumped at a flow rate of 0.35 mL/min. Gradient

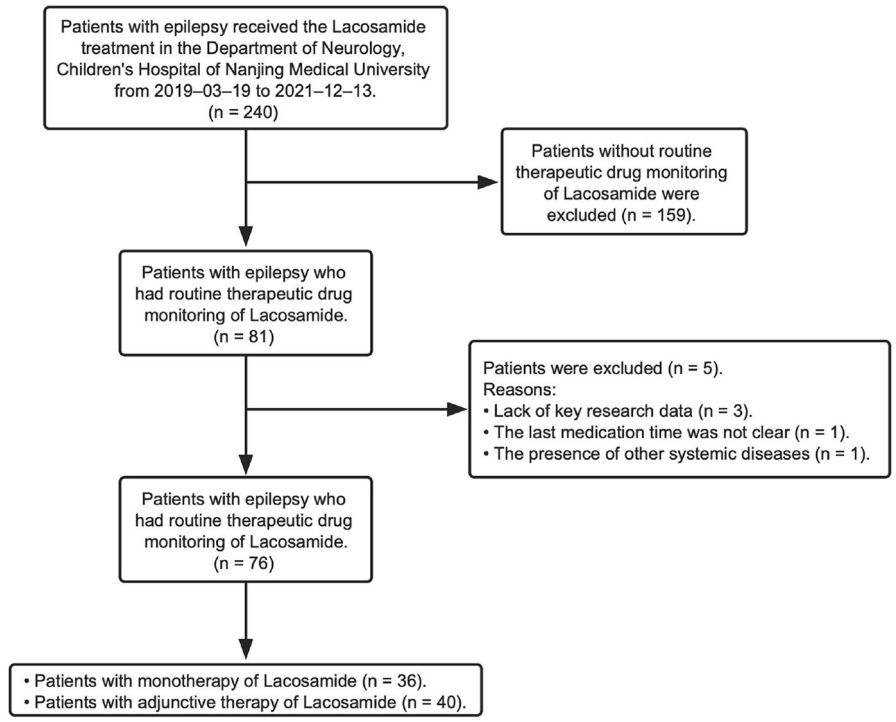

FIGURE 1
Numbers of patients who were eligible for this study.

elution was carried out with mobile phase A consisting of 0.008 mM FA in water and mobile phase B of MeOH containing the same FA level. The gradient elution program was as follows: 0–0.3 min, 1% B; 0.3–0.4 min, 1–20% B; 0.4–2.7 min, 20–50% B; 2.7–6.5 min, 50% B; 6.6–8.8 min, 100% B; 8.8–8.9 min, 100–1% B;8.9–10.0 min, 1% B. The column and auto-sampler were maintained at 30 and 4°C, respectively. MeOH precipitation was used for sample clean-up and the 5 μL supernatant was injected into LC-MS/MS for analysis. Ionization mode was ESI positive and two mass transitions (m/z 251.3→ 108.1 and 257.1→ 108.1) were monitored for LCM and its internal standard. LCM quantification was normalized by using stable-isotope-labeled LCM-d6. Collectively, no matrix effect or carryover was observed. The intra- and inter-day accuracy and precision of the assay were all acceptable according to US FDA guidance. The method development and validation data for simultaneous determination of 15 ASMs including LCM has been published elsewhere (16).

Statistical analysis

All data were statistically analyzed using GraphPad Prism 9 (GraphPad Software, La Jolla, CA, United States) and SPSS version 26.0 software (IBM, Armonk, USA). Shapiro-Wilk tests were used to assess normality. Demographic data and clinical characteristics were described as the frequency for categorical variables, means and standard deviations for normally distributed continuous variables, and median with an interquartile range for non-normally distributed continuous variables, respectively. Continuous variables were compared using the Mann–Whitney U test. Differences between independent groups were assessed using the Kruskal–Wallis test and Dunn's test. Correlations were tested by Spearman's correlation coefficient analysis. A P-value of < 0.05 was considered statistically significant.

Results

Characteristics of pediatric patients

A total of 76 children (52 males) met the inclusion criteria (Table 1). 98.7% of patients were diagnosed with focal seizures. The median epilepsy duration from the time of first seizure was 18 months (IQR 31.5). The median number of ASMs used before starting LCM treatment was one (IQR 2), and the median number of concomitant ASMs after LCM therapy initiation was two (IQR 2) (Table 1).

LCM therapy was initiated when the patient was at a median age of 6.6 (IQR 5) years. Ten children were 4 years of age or younger, but none of them aged 1 month to 12 months. The median treatment duration was 5.5 months (IQR 9.4).

TABLE 1 Clinical characteristics of patients.

Characteristics	Value
Age (year)	
Mean ± SD	7.9 ± 3.5
Range	1.3–17.3
Sex	
M	52
F	24
Weight (kg)	
Range	10–75
Type of seizures, *n* (%)	
Focal seizures	75 (98.7%)
Unknown	1 (1.3%)
Dose (mg/kg)	
Mean ± SD	6.3 ± 1.9
Range	2.0–11.3
Number of previous ASMs	
Median	1
IQR	2
Number of ASMs when LCM initiated, *n* (%)	
0	36 (47.4%)
1	21 (27.6%)
2	15 (19.7%)
3	3 (3.9%)
4	1 (1.3%)
Concomitant ASMs, *n* (%)	
VPA	24 (31.6%)
LEV	15 (19.7%)
OXC	11 (14.5%)
PER	6 (7.9%)
LMT	5 (6.5%)
CZP	3 (3.9%)
TPM	1 (1.3%)

M, male; F, female; ASM, antiseizure medicine; LCM, lacosamide; VPA, valproic acid; LEV, levetiracetam; OXC, oxcarbazepine; PER, perampanel; LMT, lamotrigine; CZP, clonazepam; TPM, topiramate.

Mean maintenance LCM dose was 6.3 mg/kg daily (range 2.0–11.3 mg/kg/day).

Clinical outcomes

The seizure frequency at 1, 3, 6, 12, and 24 months after starting LCM therapy were recorded and compared with the baseline values (Tables 2, 3). Before starting LCM therapy, 92% ($n = 70$) of patients had experienced unsuccessful epilepsy control. Notably, over a follow-up period of 6 months, 15 and 10 patients became seizure free while receiving LCM as monotherapy and add-on therapy, respectively. Moreover,

TABLE 2 The seizure frequencies at 1, 3, 6, 12, and 24 months after starting LCM adjunctive therapy.

Time (month)	IE	SFR	SF
Baseline	34 (85%)	6 (15%)	0
1	12 (30.8%)	6 (15.4%)	21 (53.8%)
3	13 (37.1%)	4 (11.4%)	18 (51.4%)
6	9 (30%)	6 (20%)	15 (50%)
12	4 (19%)	4 (19%)	13 (62%)
24	3 (33.3%)	4 (44.4%)	2 (22.2%)

IE, ineffectiveness, *i.e.*, patients with <50% reduction in seizure frequency on unchanged medication; SFR, seizure frequency reduction, *i.e.*, patients with 50% or more reduction of baseline seizure frequency on unchanged medication; SF, seizure-freedom, *i.e.*, absence of seizures on unchanged medication.

TABLE 3 The seizure frequencies at 1, 3, 6, 12, and 24 months after starting LCM monotherapy.

Time (month)	IE	SFR	SF
Baseline	36 (100%)	0	0
1	6 (16.7%)	2 (5.6%)	28 (77.7%)
3	1 (3.8%)	1 (3.8%)	24 (92.3%)
6	NA	NA	10 (100%)
12	NA	NA	4 (100%)
24	NA	NA	NA

IE, ineffectiveness, *i.e.*, patients with <50% reduction in seizure frequency on unchanged medication; SFR, seizure frequency reduction, *i.e.*, patients with 50% or more reduction of baseline seizure frequency on unchanged medication; SF, seizure-freedom, *i.e.*, absence of seizures on unchanged medication; NA, not available.

6 more patients achieved on seizure reduction and only 9 patients (30%) were poorly responsive to the LCM adjunctive therapy. Collectively, a 6-month LCM add-on therapy produced complete or partial remission of 70% ($n = 21$) of patients, and the number was 81% ($n = 17$) for the 1-year follow-up findings. However, no any clinical improvement was noted in 3 of nine children (33.3%) after a 2-year follow-up with LCM add-on therapy (Table 2). Interestingly, more patients who took LCM monotherapy achieved on seizure freedom (*i.e.*, higher remission rate) over a similar period of follow-up observation (Table 3).

In addition, all patients could tolerate the LCM medications. During the 2-year treatment period, 3 (3.9%) patients had dizziness; 1 (1.3%) had hypersomnia; 1 (1.3%) had diplopia and hypersomnia.

Plasma C_0 of LCM

The blood C_0 was monitored throughout the entire treatment period. To avoid introducing bias from multiple samples from each individual patients, the first measure was

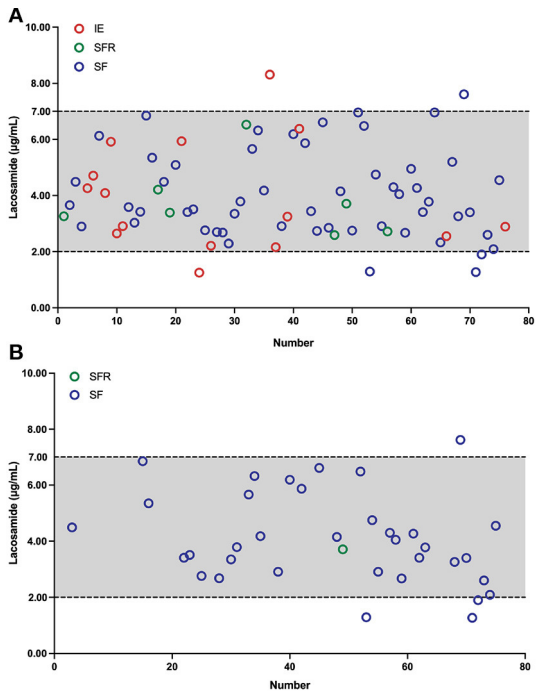

FIGURE 2
Plasma LCM concentrations C_0 (μg/mL) in children with epilepsy, the x-axis shows the number of patients. Two dotted lines depict the measured C_0 values in our findings. Different colored circles denote C_0 measurements after the maintenance dosage. Red circles indicate C_0 measurements of the ineffectiveness (IE) group, green circles represent C_0 measurements of the seizure frequency reduction (SFR) group, and blue circles denote C_0 measurements of the seizure-freedom (SF) group, respectively. **(A)** As an adjunctive therapy, LCM C_0 (μg/mL) values in 76 children with epilepsy. **(B)** As a monotherapy, LCM C_0 (μg/mL) measurements in 36 children with epilepsy.

used when more than one result was available. In total, 76 measurements were recorded for all the 76 patients, with C_0 values found to be between 1.25 and 8.31 μg/mL (Figure 2A). Notably, approximately 92.1% of the monitored C_0 values ranged from 2.0 to 7.0 μg/mL. Intriguingly, in the range of 2.0–7.0 μg/mL, 71.4% (n = 50) of patients were in the SF group, which demonstrated that most patients became seizure free after LCM treatment. When we fixed our eyes on the LCM monotherapy, 36 measurements were recorded. Moreover, approximately 88.8% of the C_0 values scattered at 2.0–7.0 μg/mL and 96.9% (n = 31) of patients became seizure free (Figure 2B).

Age, BW, sex and the C_0/Dose ratio of LCM

We observed a weak positive correlation between monitored C_0 values and LCM doses (r = 0.265, P = 0.02; Figure 3A) if we did not distinguish between monotherapy and combination therapy. In those patients, we found a significant negative correlation between age and C_0/Dose ratio (r = − 0.605, P < 0.0001; Figure 3B). Specifically, the dose-corrected C_0 values were significantly higher in children with 1–≤6 (n = 23) and 6–≤12 years of age (n = 43) than those patients with 12–≤18 year of age (n = 10, P < 0.001) by 81 and 29%, respectively. Similarly, we also revealed a negative correlation between BW and C_0/Dose ratio (r = - 0.532, P < 0.0001; Figure 3C), and the values in children with a BW of ≥40 kg were 1.7-fold and 1.2-fold lower than those in patients with a BW of ≤20 kg and between 20 to 40 kg, respectively (P < 0.001). In addition, no significant differences were found in C_0/Dose ratio between individuals of both sexes (P = 0.973; Figure 3D). Nevertheless, males exposed to higher LCM levels.

We next tested whether the above-mentioned findings were still retained when the adjunctive therapy data were removed. No correlation was found between C_0 values and doses of LCM (r = 0.143, P = 0.407; Figure 4A). Notably, the significant negative correlation between age and C_0/Dose ratio (r = - 0.644, P < 0.0001; Figure 4B) could still be observed. The same was true for BW and C_0/Dose ratio (r = - 0.516, P = 0.0013; Figure 4C).

Concomitant drugs and the C_0/dose ratio of LCM

To test whether coadministration contributes to the C_0/Dose ratio, we evaluated the influences of various concomitant therapies on plasma LCM levels. Notably, oxcarbazepine (OXC), but not valproic acid (VPA) or levetiracetam (LEV), significantly decreased the C_0/Dose ratio of LCM by 28% (P = 0.031; Figure 5). Interestingly, the coadministration with other ASMs did not put any impact on the C_0/Dose ratio of LCM (*i.e.*, LCM + ASMs *vs.* LCM).

We next evaluated the potential influences of concomitant ASMs with different mechanisms of action, including sodium channel blocking (SCB) agents [*i.e.*, OXC, lamotrigine (LMT), and topiramate (TPM); LCM + SCBs, n = 7], and non-SCB medications [*i.e.*, levetiracetam (LEV), perampanel (PER), or clonazepam (CZP); LCM + non-SCB, n = 9]. Of note, the add-on SCB medications (P = 0.047), predominantly OXC, significantly decreased the C_0/Dose ratio of LCM (Figure 5).

Other factors affecting the C_0/dose ratio of LCM

Since epilepsy is a chronic disease, we wondered if some other factors play potential roles. To test this, we evaluated the duration of LCM treatment, disease duration, MRI and EEG readings in these pediatric patients. Only negligible effects were

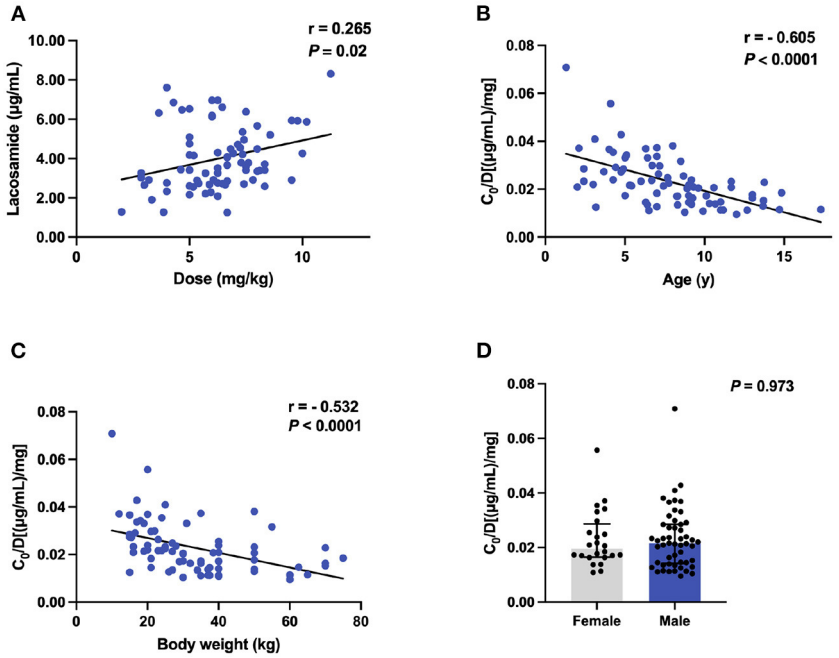

FIGURE 3
The C_0 and C_0/Dose ratio [(μg/mL)/mg] of LCM in polytherapy (n = 76). **(A)** Correlation between C_0 and dose (mg/kg); **(B)** Correlation between C_0/Dose ratio and ages; **(C)** Correlation between C_0/Dose ratio and BW; **(D)** A comparison of C_0/Dose ratio in both sexes.

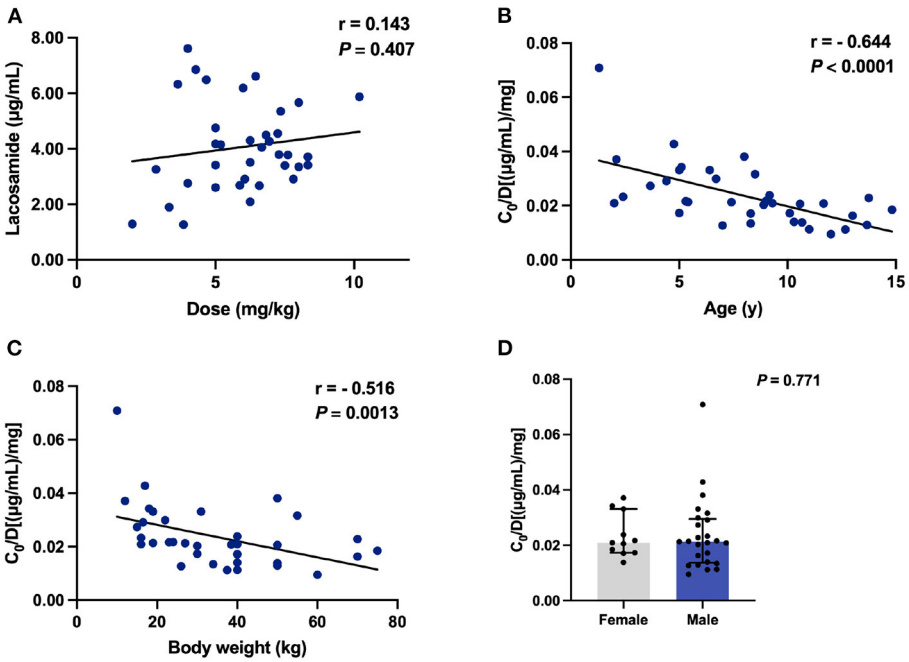

FIGURE 4
The C_0 and C_0/Dose ratio [(μg/mL)/mg] of LCM in monotherapy (n = 36). **(A)** Correlation between C_0 and dose (mg/kg); **(B)** Correlation between C_0/Dose ratio and ages; **(C)** Correlation between C_0/Dose ratio and BW; **(D)** A comparison of C_0/Dose ratio in both sexes.

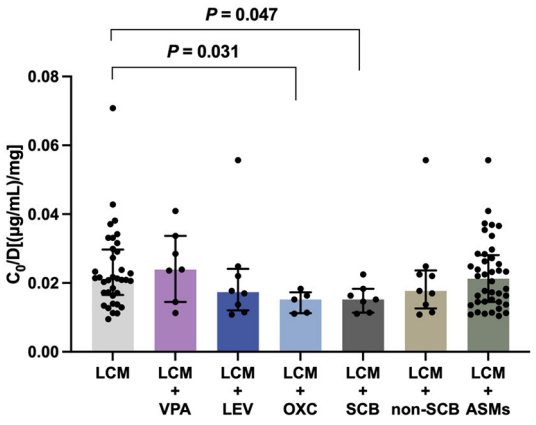

FIGURE 5
The C_0/Dose ratio [(μg/mL)/mg] of LCM in polytherapy. A comparison of C_0/Dose ratio between monotherapy and coadministration with valproic acid (VPA), levetiracetam (LEV), oxcarbazepine (OXC), sodium channel blocking (SCB) agents and non-SCB medications.

observed. Interestingly, there were no any statistically significant differences between complete responders, responders, and non-responders groups regarding C_0 and C_0/Dose ratio.

Discussion

Seizures pose risks, especially for pediatric patients, and the main goal of pharmacological treatment for epilepsy is to eliminate seizures completely while minimizing the adverse effects of ASMs, or no adverse events. To achieve this, drug dosages need to be individualized. In fact, the clinical use of a new ASM follows a stepwise vigorous approach to better understand its mechanism of action, efficacy, pharmacokinetics, and tolerability. LCM gained its approval from China government in 2018, but reports on its clinical experience with LCM as an add-on or first-line monotherapy in Chinese children, even in adults, with epilepsy are still rare (8–11, 17). No or only sparse data on LCM concentration monitoring at this young age group are available. Therefore, real-world data collected during routine clinical care for young pediatric patients have received increasing attention as a source of valuable information to support dosage optimization. This retrospective study assessed the efficacy of LCM as mono- and add-on therapy in a Chinese pediatric population. Specifically, in the current study, we explored for the first time the effect of demographic and clinical variables on the LCM plasma concentration in children with focal epilepsy in our clinical practice.

In this study, adjunctive therapy of LCM was shown to be effective and safe with as many as approximately 81 and 67% of children experiencing ≥50% seizure frequency reduction by the end of a 1- and 2-year follow-up period, respectively (Table 2). For LCM monotherapy, 10 and 4 patients completed a 6- and 12-months follow-up observation, respectively, and all of them became seizure free (Table 3). One very recent retrospective study of pediatric patients with epilepsy in the Uygur area of China has revealed that the addition of LCM to antiseizure therapy resulted in a positive response in approximately 69% of children over a minimum 1-year follow-up period (8). Some retrospective studies in pediatric patients of other nations so fat have shown that the proportion of responders varies between ∼30 and 70% (18–24). Collectively, our efficacy findings are overall comparable to those previously reported from Western and Asian countries.

A major finding of this study was that a reference therapeutic C_0 range of LCM (*i.e.*, 2.0–7.0 μg/mL) (Figure 2) was established to match the efficacy and tolerability seen in our pediatric patients. Therapeutic drug monitoring (TDM) of ASMs assists in guiding and tailoring ASM therapy, while also avoiding potential associated toxicity in routine clinical practice, because the clinical response has been shown to correlate better with the drug concentration than the dose (25). In fact, TDM requirement whether or not and the reference range for LCM monitoring in children and adults are still controversial (14). Previously, 2.5–10 μg/mL has been suggested as a target range, but those values were partly derived from non-drug-fasting blood samples (26). Burns et al. (27) revealed that 94% of patients had serum concentrations in the reference range of 3–10 μg/mL in Norway, and a similar reference range of 2.25–8.75 μg/mL is used in Denmark. However, Perrenoud et al. (28) concluded that the reference range of 10–20 μg/mL was more effective in reducing seizures. But to emphasize again, the reference range for LCM monitoring in Chinese children is not available. In our study, under maintenance dosages, approximately 92.1% of the C_0 values varied from 2.0 to 7.0 μg/mL and the matched mean daily dose was 6.38 mg/kg (range 2.86–10.19 mg/kg/day). More than 81.4% of C_0 values in children achieved on >50% seizure frequency reduction (Figure 2A). Similar findings (*i.e.*, 2.0–7.0 μg/mL) were obtained for children who received LCM monotherapy, and a very impressive proportion of 70.6% was seen in those 17 patients who became seizure free over a minimum 3-month follow-up therapy (Figure 2B; Table 3). Therefore, our data in hands suggest that aiming at a C_0 (2.0–7.0 μg/mL) may be feasible when LCM is used as monotherapy or adjunctive therapy for Chinese children with focal epilepsy.

One of the major strengths of the current study was our ability to monitor the LCM plasma levels and thus we could evaluate the effects of various variables on the dose-adjusted plasma levels (*i.e.*, C_0/Dose) of LCM in our study subjects. The demographic characteristics (sex, age and ethnicity) have been identified as the right factors that affect LCM pharmacokinetics (4). Moreover, previous evidence supports the opinion that LCM exposure depends on age and sex, requiring PK monitoring

to define the optimal posology that guarantees therapeutic efficacy with tolerable adverse effects (4). In the present study, a combined data from LCM monotherapy and adjunctive therapy in C_0/Dose ratio revealed no significant difference between patients of both sexes (Figures 3D, 4D). Sex had no relevant effects on the LCM C_0/Dose ratio in healthy adults and adults with focal epilepsy (29), but no similar study is available in children up to now.

In our study, of note, the increasing age decreased the C_0/Dose ratio of LCM used either alone or in combination with other ASMs (Figures 3B, 4B), which could be partly explained by an inverse relationship between plasma concentration and systemic clearance. Specifically, the C_0/Dose ratio in patients aged 1–≤6 and 6–≤12 years was significantly higher than those aged 12–≤18 years, by 81 and 29%, respectively, which is in line with a previous report (27). Interestingly, a decrease in C_0/Dose was seen with age indicating an increase in total clearance with age which is in line with the ontogeny of CYP3A4, CYP2C9, and CYP2C19 involved in LCM metabolism.

Also, we have found a lower C_0/Dose ratio in children who have a higher BW. The C_0/Dose ratio in patients with a BW of ≥40 kg was 1.7-fold lower than in patients with a BW of ≤20 kg. Similar findings had been reported in our previous study on tacrolimus concentration-to-dose ratio in children with refractory nephrotic syndrome (30). Why older children with higher BW presented lower C_0/Dose ratio of LCM than those younger counterparts could be partly explained by PK characteristics. The preferential distribution of LCM in extracellular fluids implies that total body water determines plasma concentration (4, 31).

Another important finding in the present study was the assessment of potential drug-drug interactions between LCM and other ASMs. Notably, LCM coadministration with OXC, but not LEV or VPA, significantly decreased the C_0/Dose ratio by comparison with LCM monotherapy ($P = 0.031$; Figure 5). This result suggested a potential PK interaction from the perspective of drug action mechanisms. Pratima Gulati et al. (32) previously suggested that the concomitant use of SCBs did not significantly influence response to LCM. In the present study, there was a clear trend that SCB agents may decreased LCM plasma levels (Figure 5). Particularly, OXC substantially lowered LCM plasma levels, which might result in a reduced efficacy of LCM. Thus, a higher LCM dose might be needed for patients taking concomitant OXC, albeit on an individual patient basis. Collectively, our study provided evidence of complex drug-drug interactions between LCM and concomitant ASMs. More research is required for a complete and clear description of the potential drug interactions, reinforcing the importance of LCM concentration monitoring.

However, our study has several limitations due to its retrospective design nature. Firstly, this was a single-center study with a small sample size because of the new approval in China for pediatric patients. Thus, our findings as a reference should be interpreted with caution. Secondly, 76 children were included but they had variable therapy periods and we had to rely on the real-world clinical reporting rather than prospective patient seizure diaries. This prompted us to summarize the effectiveness data of LCM, alone or adjunctive, over different periods with variable numbers of patients. Thirdly, adverse reactions may be underreported due to the data collected sporadically rather than by a structured questionnaire at clinical visits. Nevertheless, the real-world clinical findings in this study for efficacy and safety, especially for LCM plasma monitoring in children, may be very useful for pediatric clinicians and TDM pharmacists when they try to tailor LCM dosages for precision therapy.

Conclusions

In conclusion, this retrospective study found that LCM treatment used alone or with other ASMs in children with focal epilepsy can reduce the seizure frequency with adverse reactions reported in a minority. We also identified several contributing factors to variable C_0/Dose ratio of LCM in children with epilepsy. Children with higher BW and older age have a lower C_0/Dose ratio. Complex drug interactions between LCM and other concomitant ASMs were revealed. Based on the data in our hands, the reference range, *i.e.*, 2.0–7.0 μg/mL, for routine LCM monitoring may be feasible when LCM is taken as a monotherapy or combined with other ASMs in Chinese children with epilepsy.

Data availability statement

The raw data supporting the conclusions of this article will be made available by the authors, without undue reservation.

Ethics statement

The studies involving human participants were reviewed and approved by the Ethics Committee of the Children's Hospital of Nanjing Medical University granted the ethical approval for the study (Protocol number 202204021-1). Written informed consent to participate in this study was provided by the participants' legal guardian/next of kin. Written informed consent was obtained from the individual(s), and minor(s)' legal guardian/next of kin, for the publication of any potentially identifiable images or data included in this article.

Author contributions

YL and H-LG had full access to all the data in the study and take responsibility for the integrity of the data and the accuracy of the data analysis. Concept and design:

JC and X-PL. Drafting of the manuscript: YL and FC. Critical revision of the manuscript: FC. Administrative, technical, or material support, and supervision: FC and X-PL. Acquisition, analysis, or interpretation of data, contributed to the article, and approved the submitted version: all authors.

Funding

This research was supported by the Specially Appointed Medical Expert Project of the Jiangsu Commission of Health (2019), Jiangsu Research Hospital Association for Precision Medication (JY202108), and by the CAAE Epilepsy Research Fund of China Association against Epilepsy (CU-2022-024).

Conflict of interest

The authors declare that the research was conducted in the absence of any commercial or financial relationships that could be construed as a potential conflict of interest.

Publisher's note

References

1. Ding D, Zhou D, Sander JW, Wang W, Li S, Hong Z. Epilepsy in China: major progress in the past two decades. *Lancet Neurol.* (2021) 20:316–26. doi: 10.1016/S1474-4422(21)00023-5

2. Yang C, Yu D, Li J, Zhang L. Prevalence of medication adherence and factors influencing adherence to antiepileptic drugs in children with epilepsy from western China: a cross-sectional survey. *Epilepsy Behav.* (2020) 104:106662. doi: 10.1016/j.yebeh.2019.106662

3. Wilmshurst JM, Berg AT, Lagae L, Newton CR, Cross JH. The challenges and innovations for therapy in children with epilepsy. *Nat Rev Neurol.* (2014) 10:249–60. doi: 10.1038/nrneurol.2014.58

4. Carona A, Bicker J, Silva R, Fonseca C, Falcao A, Fortuna A. Pharmacology of lacosamide: from its molecular mechanisms and pharmacokinetics to future therapeutic applications. *Life Sci.* (2021) 275:119342. doi: 10.1016/j.lfs.2021.119342

5. Perucca E, Yasothan U, Clincke G, Kirkpatrick P. Lacosamide. *Nat Rev Drug Discov.* (2008) 7:973–4. doi: 10.1038/nrd2764

6. Chen D, Lin Y, Chen T, Zhang Q, Lin Y, Si Y, et al. Dose effects of lacosamide as add-on therapy for partial-onset seizure in adult. *Neurol Sci.* (2016) 37:907–20. doi: 10.1007/s10072-016-2512-2

7. Baulac M, Rosenow F, Toledo M, Terada K, Li T, De Backer M, et al. Efficacy, safety, and tolerability of lacosamide monotherapy versus controlled-release carbamazepine in patients with newly diagnosed epilepsy: a phase 3, randomised, double-blind, non-inferiority trial. *Lancet Neurol.* (2017) 16:43–54. doi: 10.1016/S1474-4422(16)30292-7

8. Zhao T, Li HJ, Ma L, Feng J, Wang TT, Yu J, et al. Safety, efficacy, and tolerability of lacosamide for the treatment of epilepsy in pediatric patients in Uygur, China. *Epilepsy Behav.* (2021) 117:107814. doi: 10.1016/j.yebeh.2021.107814

9. Hou L, Peng B, Zhang D, Yang J, Wang Y, Tong L, et al. Clinical efficacy and safety of lacosamide as an adjunctive treatment in adults with refractory epilepsy. *Front Neurol.* (2021) 12:712717. doi: 10.3389/fneur.2021.712717

10. Hong Z, Inoue Y, Liao W, Meng H, Wang X, Wang W, et al. Efficacy and safety of adjunctive lacosamide for the treatment of partial-onset seizures in Chinese and Japanese adults: a randomized, double-blind, placebo-controlled study. *Epilepsy Res.* (2016) 127:267–75. doi: 10.1016/j.eplepsyres.2016.08.032

11. Inoue Y, Liao W, Wang X, Du X, Tennigkeit F, Sasamoto H, et al. Safety and efficacy of adjunctive lacosamide in Chinese and Japanese adults with epilepsy and focal seizures: a long-term, open-label extension of a randomized, controlled trial. *Epilepsy Res.* (2021) 176:106705. doi: 10.1016/j.eplepsyres.2021.106705

12. Zhao T, Li HJ, Feng J, Zhang HL, Ma L, Yu J, et al. Impact of ABCB1 polymorphisms on lacosamide serum concentrations in uygur pediatric patients with epilepsy in China. *Ther Drug Monit.* (2021) 44:455–64. doi: 10.1097/FTD.0000000000000927

13. Cawello W. Clinical pharmacokinetic and pharmacodynamic profile of lacosamide. *Clin Pharmacokinet.* (2015) 54:901–14. doi: 10.1007/s40262-015-0276-0

14. Schultz L, Mahmoud SH. Is therapeutic drug monitoring of lacosamide needed in patients with seizures and epilepsy? *Eur J Drug Metab Pharmacokinet.* (2020) 45:315–49. doi: 10.1007/s13318-019-00601-8

15. Scheffer IE, Berkovic S, Capovilla G, Connolly MB, French J, Guilhoto L, et al. ILAE classification of the epilepsies: position paper of the ILAE commission for classification and terminology. *Epilepsia.* (2017) 58:512–21. doi: 10.1111/epi.13709

16. Zhang YY, Xia Y, Guo HL, Hu YH, Wen XY, Chen J, et al. An LC-ESI-MS/MS assay for the therapeutic drug monitoring of 15 anti-seizure medications in plasma of children with epilepsy. *Biomed Chromatogr.* (2022) 23:e5484. doi: 10.1002/bmc.5484

17. Wu T, Chuang YC, Huang HC, Lim SN, Hsieh PF, Lee WT, et al. A prospective, multicenter, noninterventional study in Taiwan to evaluate the safety and tolerability of lacosamide as adjunctive therapy for epilepsy in clinical practice. *Epilepsy Behav.* (2020) 113:107464. doi: 10.1016/j.yebeh.2020.107464

18. Toupin JF, Lortie A, Major P, Diadori P, Vanasse M, Rossignol E, et al. Efficacy and safety of lacosamide as an adjunctive therapy for refractory focal epilepsy in paediatric patients: a retrospective single-centre study. *Epileptic Disord.* (2015) 17:436–43. doi: 10.1684/epd.2015.0782

19. McGinnis E, Kessler SK. Lacosamide use in children with epilepsy: retention rate and effect of concomitant sodium channel blockers in a large cohort. *Epilepsia.* (2016) 57:1416–25. doi: 10.1111/epi.13466

20. Rosati A, Ilvento L, Rizzi R, Doccini V, Leo MC, Pugi A, et al. Long-term efficacy of add-on lacosamide treatment in children and adolescents with refractory epilepsies: a single-center observational study. *Epilepsia.* (2018) 59:1004–10. doi: 10.1111/epi.14071

21. Sanmarti-Vilaplana F, Diaz-Gomez A. The effectiveness and safety of lacosamide in children with epilepsy in a clinical practice setting. *Epilepsy Behav.* (2018) 79:130–7. doi: 10.1016/j.yebeh.2017.11.024

22. Farkas V, Steinborn B, Flamini JR, Zhang Y, Yuen N, Borghs S, et al. Efficacy and tolerability of adjunctive lacosamide in pediatric patients with focal seizures. *Neurology.* (2019) 93:e1212–26. doi: 10.1212/WNL.0000000000008126

23. Hmaimess G, Sabbagh S, Dirani M, Hotait M, Beydoun AA, Nasreddine W. Efficacy and tolerability of treatment with lacosamide in children: postmarketing experience from the middle east. *Seizure.* (2020) 79:75–9. doi: 10.1016/j.seizure.2020.04.016

24. Ishikawa N, Eguchi Y, Izumo H, Tateishi Y, Tani H, Kobayashi Y, et al. Clinical impact of the dose and blood concentration of lacosamide in Japanese pediatric patients with epilepsy: a cohort study. *Epilepsy Behav.* (2022) 129:108614. doi: 10.1016/j.yebeh.2022.108614

25. Aicua-Rapun I, Andre P, Rossetti AO, Ryvlin P, Hottinger AF, Decosterd LA, et al. Therapeutic drug monitoring of newer antiepileptic drugs: a randomized trial for dosage adjustment. *Ann Neurol.* (2020) 87:22–9. doi: 10.1002/ana.25641

26. Svendsen T, Brodtkorb E, Baftiu A, Burns ML, Johannessen SI, Johannessen Landmark C. Therapeutic drug monitoring of lacosamide in norway: focus on pharmacokinetic variability, efficacy and tolerability. *Neurochem Res.* (2017) 42:2077–83. doi: 10.1007/s11064-017-2234-8

27. Larsen Burns M, Nikanorova M, Baftiu A, Borg Rasmussen J, Johannessen SI, Johannessen Landmark C. Pharmacokinetic variability and clinical use of lacosamide in children and adolescents in Denmark and Norway. *Ther Drug Monit.* (2019) 41:340–7. doi: 10.1097/FTD.0000000000000599

28. Perrenoud M, Andre P, Alvarez V, Stahli C, Decosterd LA, Rossetti AO, et al. Intravenous lacosamide in status epilepticus: correlation between loading dose, serum levels, and clinical response. *Epilepsy Res.* (2017) 135:38–42. doi: 10.1016/j.eplepsyres.2017.05.007

29. Schaefer C, Cawello W, Waitzinger J, Elshoff JP. Effect of age and sex on lacosamide pharmacokinetics in healthy adult subjects and adults with focal epilepsy. *Clin Drug Investig.* (2015) 35:255–65. doi: 10.1007/s40261-015-0277-7

30. Guo HL, Xu J, Sun JY, Li L, Guo HL, Jing X, et al. Tacrolimus treatment in childhood refractory nephrotic syndrome: a retrospective study on efficacy, therapeutic drug monitoring, and contributing factors to variable blood tacrolimus levels. *Int Immunopharmacol.* (2020) 81:106290. doi: 10.1016/j.intimp.2020.106290

31. May TW, Brandt C, Helmer R, Bien CG, Cawello W. Comparison of lacosamide concentrations in cerebrospinal fluid and serum in patients with epilepsy. *Epilepsia.* (2015) 56:1134–40. doi: 10.1111/epi.13022

32. Gulati P, Cannell P, Ghia T, Bint L, Walsh P, Ghosh S, et al. Lacosamide as adjunctive therapy in treatment-resistant epilepsy in childhood. *J Paediatr Child Health.* (2015) 51:794–7. doi: 10.1111/jpc.12850

frontiers | Frontiers in Pharmacology

TYPE Brief Research Report
PUBLISHED 07 September 2022
DOI 10.3389/fphar.2022.916253

OPEN ACCESS

EDITED BY
Xiaoling Wang,
Capital Medical University, China

REVIEWED BY
Prajwal Paudel,
Department of Neonatology, Paropakar, Nepal
Mamta Jajoo,
University of Delhi, India
Surulivelrajan Mallayasamy,
Manipal Academy of Higher Education, India

*CORRESPONDENCE
Yan Xu,
xuyanxy2006@163.com
Wei Zhao,
zhao4wei2@hotmail.com

†These authors have contributed equally to this work and share first authorship

‡These authors have contributed equally to this work

SPECIALTY SECTION
This article was submitted to Obstetric and Pediatric Pharmacology, a section of the journal Frontiers in Pharmacology

RECEIVED 09 April 2022
ACCEPTED 15 August 2022
PUBLISHED 07 September 2022

CITATION
Shang Z-H, Wu Y-E, Lv D-M, Zhang W, Liu W-Q, van den Anker J, Xu Y and Zhao W (2022), Optimal dose of cefotaxime in neonates with early-onset sepsis: A developmental pharmacokinetic model-based evaluation.
Front. Pharmacol. 13:916253.
doi: 10.3389/fphar.2022.916253

Optimal dose of cefotaxime in neonates with early-onset sepsis: A developmental pharmacokinetic model-based evaluation

Zhen-Hai Shang[1†], Yue-E Wu[2†], Dong-Mei Lv[1], Wei Zhang[2], Wen-Qiang Liu[3], John van den Anker[4,5,6], Yan Xu[3*‡] and Wei Zhao[2,7*‡]

[1]Department of Pharmacy, The Affiliated Hospital of Xuzhou Medical University, Xuzhou, China, [2]Department of Clinical Pharmacy, Key Laboratory of Chemical Biology (Ministry of Education), School of Pharmaceutical Sciences, Cheeloo College of Medicine, Shandong University, Jinan, China, [3]Department of Neonatology, The Affiliated Hospital of Xuzhou Medical University, Xuzhou, China, [4]Division of Clinical Pharmacology, Children's National Hospital, Washington, DC, United States, [5]Departments of Pediatrics, Pharmacology & Physiology, Genomics and Precision Medicine, School of Medicine and Health Sciences, George Washington University, Washington, DC, United States, [6]Department of Paediatric Pharmacology and Pharmacometrics, University Children's Hospital Basel, University of Basel, Basel, Switzerland, [7]NMPA Key Laboratory for Clinical Research and Evaluation of Innovative Drug, Qilu Hospital of Shandong University, Shandong University, Jinan, China

Objective: The perspective of real-world study is especially relevant to newborns, enabling dosage regimen optimization and regulatory approval of medications for use in newborns. The aim of the present study was to conduct a pharmacokinetic analysis of cefotaxime and evaluate the dosage used in newborns with early-onset sepsis (EOS) using real-world data in order to support the rational use in the clinical practice.

Methods: This prospective, open-label study was performed in newborns with EOS. A developmental pharmacokinetic-pharmacodynamic model of cefotaxime in EOS patients was established based on an opportunistic sampling method. Then, clinical evaluation of cefotaxime was conducted in newborns with EOS using real-world data.

Results: A one-compartment model with first-order elimination was developed, using 101 cefotaxime concentrations derived from 51 neonates (30.1–41.3°C weeks postmenstrual age), combining current weight and postnatal age. The pharmacokinetic-pharmacodynamic target was defined as the free cefotaxime concentration above MIC during 70% of the dosing interval (70% fT > MIC), and 100% of neonates receiving the dose of 50 mg/kg, BID attained the target evaluated using the model. Additionally, only two newborns had adverse reactions possibly related to cefotaxime treatment, including diarrhea and feeding intolerance.

Conclusion: This prospective real-world study demonstrated that cefotaxime (50 mg/kg, BID) had a favorable efficacy and an accepted safety profile for neonates with EOS.

KEYWORDS
cefotaxime, early-onset sepsis, pharmacokinetics analysis, effectiveness, safety

Introduction

Early-onset neonatal sepsis (EOS) is a life-threatening systemic infection in newborns with an onset during the first 72 h of life (Hornik et al., 2012; Simonsen et al., 2014). With the improvement of perinatal management and evidence-based application of intrapartum antibiotics, the incidence of EOS has decreased (Polin, 2012). However, EOS is still one of the main causes of morbidity and mortality in neonates, and it presents with a huge challenge because the variable clinical presentation in these infants resulting in a delayed treatment (Scheel and Perkins, 2018).

The selection of empirical antibiotics for treatment of EOS is based on the local epidemiology of the responsible pathogens. In high-income countries, Group B *streptococcus* (GBS) and *Escherichia coli* are the most common pathogens involved in EOS accounting for approximately 70% of infections (Stoll et al., 2011; Schrag et al., 2016; Mukhopadhyay and Puopolo, 2017; Brown and Denison, 2018). Therefore, the initial treatment for EOS is generally ampicillin combined with an aminoglycoside (usually gentamicin) (Polin, 2012). However, a distinctive pathogen distribution exists among neonates with EOS in different countries, for example *Escherichia coli* is the most common pathogens associated with EOS in China (Guo et al., 2019; Jiang et al., 2019). Thus, third-generation cephalosporins, such as cefotaxime, are usually applied to treat EOS in clinical practice, owing to its broad-spectrum antimicrobial activity covering more of the pathogens implicated in neonatal sepsis (Odio, 1995). Cefotaxime undergoes hydrolysis by esterases contained in plasma and the liver to form the active metabolite desacetylcefotaxime, and approximately 50%–60% of a dose is excreted unchanged in the urine, whereas 15%–20% appears as desacetylcefotaxime (Kearns and Young, 1995). The amount of desacetyl cefotaxime formed reduced with increasing liver damage, and cefotaxime clearance markedly declined when the creatinine clearance fell below 10 ml/min (Wise and Wright, 1985; Paap et al., 1991). The dosage adjustment may be necessary for cefotaxime in patients with hepatic and renal dysfunction.

The rational use of cefotaxime in EOS is still hampered by uncertainty about the optimal dose. The dosage regimens of cefotaxime used in different neonatal units vary (75–180 mg/kg/day) due to the absence of a powerful developmental pharmacokinetic-pharmacodynamic study in EOS patients (Leroux et al., 2015b). Pacifici et al. reported that the pharmacokinetics of cefotaxime in newborn babies were primarily studied in the 1980s with a limited number of patients (Pacifici, 2011). The study design and methods limited the power to recommend a precise dosage regimen of cefotaxime in the neonate population using pharmacokinetic data, as the influences of covariates (i.e., hepatic or renal function) on dosage were not fully evaluated. A model-based dosing recommendation was available in children (between the ages of 1 month and 19 years) with Sickle Cell disease. It clearly indicates that the use of a standard dose of cefotaxime is not appropriate for these patients and the dose should be increased in order to optimize efficacy, depending on the children's clinical presentation and characteristics (Maksoud et al., 2018). The pharmacokinetic profile of most drugs relies on the patient's covariates and may be influenced by the specific disease. The lack of pharmacokinetic data of the specific population and specific disease may increase the risk of unreasonable use of antibiotics, which could lead to the occurrence of adverse drug reaction or the spread of antibiotic resistance. Thus we aimed to conduct a pharmacokinetic analysis of cefotaxime in EOS patients and evaluate the dosage used in a real-world setting to provide data in terms of pharmacokinetic-pharmacodynamic target achievement, effectiveness and safety to support rational use of cefotaxime in neonates with EOS.

Methods

Study design

This prospective, open-label clinical study was conducted in the neonatal intensive care unit (NICU) of the Affiliated Hospital of Xuzhou Medical University, Jiangsu, China. Newborn infants ≤72 h of life who met the standard of starting antibiotic treatment in accordance with NICE guidelines (National Collaborating Centre for and Children's, 2012) were enrolled in this study, receiving intravenous cefotaxime as part of standard therapy. The standard of initiating antibiotic therapy was as follows: one high risk factor or more than one low risk factor is present (Wu et al., 2021). The exclusion criteria were severe congenital malformation, expected survival time less than the duration of the treatment, undergoing surgery in the first week after birth, participating in another clinical trial, or other circumstances that the investigator deemed unsuitable for enrollment. This study was approved by the Ethics Committee of the Affiliated Hospital of Xuzhou Medical University and abode by the Helsinki Declaration II. Written informed consent was obtained from guardian(s) of each newborn.

Clinical procedures

Cefotaxime (Huamin Pharmaceutical Co., Ltd., Hebei, China) was administered intravenously within 30 min using a dose of 50 mg/kg/dose BID. The therapeutic effect evaluation was

performed by the neonatologist, and the decision to discontinue cefotaxime treatment was made based on clinical manifestations of neonates, the levels of C-reactive protein (CRP) and blood culture results. The first evaluation for discontinuation was made at 36 h after initiating cefotaxime treatment. Cefotaxime would be discontinued if the baby's clinical presentation associated with sepsis and the levels of CRP remained normal, and blood culture was negative. CRP abnormality was defined as >10 mg/L. If the blood culture was positive, the duration of cefotaxime treatment would last at least 7 days, after which the blood culture required to be reexamined in order to make next decision. After 36 h of cefotaxime treatment, despite negative blood cultures, the baby's current clinical conditions and the levels of CRP should be reviewed at least once every 24 h, to consider whether it was appropriate to discontinue cefotaxime therapy. Effectiveness and safety profile of cefotaxime were well recorded by clinical research pharmacist during the whole treatment period.

Sampling and determination of cefotaxime

An opportunistic sampling method was adopted for collecting blood samples (Leroux et al., 2015a). The total number of study-specific blood samples was restricted to two per patient. After routine biochemical examinations, the remaining blood was collected for pharmacokinetic assay. The plasma volume of samples for analyses was 0.1 ml per sample. The time of infusion and sampling was accurately recorded according to standard operating procedure. Each sample was centrifuged for 10 min at 4,000 rpm and 4°C, and plasma samples were stored at −80°C until determination of cefotaxime concentration. High-performance liquid chromatography method with UV detection at 254 nm was adopted to determine cefotaxime plasma concentrations, with tinidazole as internal standard. The chromatographic seperation was performed on a Insustain C18 column (250*4.6 mm, 5 μm, Shimadzu, Japan), with acetonitrile and 0.01 mol/L potassium dihydrogen phosphate solution at a flow rate of 1.0 ml/min. The calibration curve ranged from 0.5 to 200 μg/ml, with 0.5 μg/ml as the lower limit of quantification (LOQ), using 50 μl of plasma samples. The intraday and interday coefficients of variation for the controls were 2.4% and 4.1%, respectively.

Pharmacokinetic analysis

The non-linear mixed effects modeling program NONMEM V7.4 (Icon Development Solutions, United States) was adopted for pharmacokinetic analysis. The one- and two-compartment model were tested and the results were compared before choosing the structural model. The first-order conditional estimation (FOCE) method with interaction was employed to estimate the pharmacokinetic parameters and their variations. The exponential model was used to estimate the inter-individual differences in pharmacokinetic parameters and expressed as follows:

$$\theta i = \theta \,\mathrm{mean}^{*} e\eta i$$

where θ i indicates the value of the ith patient, θmean the typical value of the parameter in the population and ηi the differences in subjects which is supposed to follow a normal distribution with a mean of zero and a variance of ω2.

The forward and backward selection process was employed for covariate analysis. The covariates of birth weight, gestational age, current weight, postnatal age and postmenstrual age were explored as potential variables affecting pharmacokinetic parameters. The impact of each covariate on model parameters was evaluated by the likelihood ratio test.

A covariate was incorporated if the objective function value (OFV) reduction was >3.84 ($p < 0.05$) compared with value of the basic model. All the covariates that had a significant effect were included simultaneously to the model. Then, each covariate was removed in sequence from the model. The covariate was regarded as significant and therefore retained in the final model if the increase in the OFV was more than 6.635 ($p < 0.01$).

Graphical and statistical criteria were adopted to verify the power of the model. Plots of observed concentrations (DV) versus population prediction (PRED), DV versus individual prediction (IPRED), conditional weighted residuals (CWRES) versus time and CWRES versus PRED were applied to verify the performance of the model.

The reliability and stability of the final model was confirmed by a non-parametric bootstrap with resampling and replacement. The non-parametric bootstrap procedure was replicated 1000 times. The values of estimated parameters from the non-parametric bootstrap procedure were compared with those derived from the original data set. PsN (v2.30) was employed to complete the whole procedure in an automated fashion. Eventually, 1000 datasets were simulated with the final population model parameters. R package (v1.2) was used to display QQ-plot and histogram of the NPDE, which was expected to abide by the N (0, 1) distribution. Additionally, pcVPC was used to evaluate the simulation performance.

Pharmacokinetic-pharmacodynamic target attainment

The pharmacokinetic-pharmacodynamic target was defined as the free cefotaxime concentration above MIC during 70% of the dosing interval (70% fT > MIC). The protein binding rate of cefotaxime was reported to between 27% and 50% (Harding et al., 1981; LeFrock et al., 1982; Patel et al., 1995), and in the cefotaxime label, the protein binding rate is 30%–50%, thus

40% was selected for the calculation of pharmacokinetic-pharmacodynamic target attainment. The MIC of 2 mg/L was assigned as the pharmacokinetic-pharmacodynamic breakpoint for its coverage of most common pathogens (*E. coli* and CoNS) for EOS. The pharmacokinetic-pharmacodynamic target attainment analysis was conducted using the individual empirical Bayesian estimates method by NONMEM software. For each neonate, the simulated drug-free concentration at 70% dosing interval was compared with the MIC value to determine whether the target was reached. The percentage of patients who met the target was calculated. In addition, the $AUC_{0\text{-}24}$ at steady-state was calculated by dividing the dose by clearance.

Effectiveness and safety evaluation

The main indicator for effectiveness assessment of cefotaxime treatment was treatment failure rate. Treatment failure was defined as a recurrence of infection that required extra course of antibiotic therapy within 72 h after ceasing cefotaxime treatment, and/or changing antibiotics owing to exacerbation or no improvement of patient's conditions, and/or culture-proven pathogens reported resistant to the antibiotic.

The adverse events monitoring covers adverse drug reaction documented in the package insert of cefotaxime and the laboratory testing outliers. The adverse drug reactions recorded in cefotaxime instructions included rash, nausea, vomiting, diarrhea, phlebitis, leukopenia, thrombocytopenia, elevated serum amino transferase level and urea nitrogen and creatinine level. Clinical features and laboratory examination including blood cell analysis, blood gas assay, and biochemical tests were monitored during cefotaxime treatment. Laboratory tests were conducted based on the patient's condition, not intentionally for study purposes. The causal relation between adverse events and cefotaxime treatment was evaluated by a pediatrician and a clinical pharmacist, and classified as follows: definitely related, probably related, possibly related, not related, or unable to determine.

Results

Study population

A total of 54 newborns were enrolled in our study according to the inclusion and exclusion criteria. Three neonates discontinued the trial because of being transferred to another medical center (n = 1), change to another antibiotic due to the worsening of patient's condition before the planned assessment (n = 2). Eventually, fifty-one newborns (31 male patients and 20 female patients) accomplished cefotaxime treatment and were included in the following effectiveness and safety evaluation. The clinical baseline characteristics of all neonates were summarized in Table 1. The median (range) values of GA and PNA in the 51 neonates were 35.7 (30.0–41.1) weeks and 1.0 (1.0–3.0) days, respectively. The median (range) values of BW and CW were 2310 (1220–3970) and 2310 (1220–3970) grams respectively.

Eight (15.7%) of the 51 newborns started cefotaxime treatment with one "high risk factor" and ≥0 "low risk factor", while 43 (84.3%) newborns with 0 "high risk factor" and ≥2 "low risk factor" (Supplementary Material). The major maternal factor for initiating cefotaxime therapy was "suspected or confirmed rupture of membranes for more than 18 h in a preterm birth" in 18 (56.3%) neonates, followed by "preterm birth following spontaneous labor (before 37 weeks' gestation)" in 6 (11.8%) babies. By contrast, the most common clinical indicator in neonates with EOS was "altered behavior or responsiveness" in 34 (23.0%) newborns, followed by "signs of respiratory distress" in 29 (19.6%) neonates.

Pharmacokinetic analysis and target attainment

A total of 101 cefotaxime concentrations were available for modeling of population pharmacokinetics. The cefotaxime concentrations ranged from 7.18 to 347.61 μg/ml. Supplementary Figure S1 described the cefotaxime concentration versus time profile. In the current work, the OFV values of the one-compartment model and the two-compartment model were similar, but the one-compartment model with first-order elimination best described the data. The model was parameterized in terms of volume of distribution (V) and clearance (CL) of cefotaxime. An exponential model was adopted to describe inter-individual variability, and residual variability was expressed as a proportional model.

The current weight was included into the basic model using the allometric estimated size approach, which resulted in a significant drop in the OFV of 70.3 points (allometric fixed size approach ΔOFV: 66.3). Postnatal age was confirmed as the most important covariate on CL, with a drop in the OFV of 36.2 units (GA-ΔOFV: 3.62; PMA-ΔOFV: 6.89). No other covariates have a significant effect. The parameter estimates of the final pharmacokinetic model was shown in Table 2. The estimated weight-normalized CL and volume of distribution median (range) values were 0.04 (0.02–0.09) L/h/kg and 0.36 (0.21–0.63) L/kg, respectively. The $AUC_{0\text{-}24}$ at steady-state ranged from 974 to 5755 mg*h/L. Clearance of cefotaxime increased allometrically according to current weight.

Favorable goodness-of-fit results for the final model of cefotaxime were validated by means of model diagnostics. As exhibited in Figures 1A,B, the predictions are unbiased. There is no tendency in the diagnostic plots of CWRES versus time and PRED (Figures 1C,D). Additionally, the median parameter estimates deriving from the bootstrap

TABLE 1 Baseline characteristics of 51 neonates in effectiveness and safety analysis.

	Median (range)	Number
Patients		51
Male/female		31/20
GA (weeks)	35.7 (30.0–41.1)	
PNA (days)	1.0 (1.0–3.0)	
PMA (weeks)	35.9 (30.1–41.3)	
BW (g)	2310 (1220–3970)	
CW (g)	2310 (1220–3970)	
Commencing antibiotics treatment evaluation		
Patients with one 'high risk factor' and ≥0 'low risk factor'		8
Patients with 0 'high risk factor' and ≥2 'low risk factor'		43
Maternal factors		
Prelabour rupture of membranes		4
Preterm birth following spontaneous labour (before 37 weeks' gestation)		6
Suspected or confirmed rupture of membranes for more than 18 h in a preterm birth		18
Intrapartum fever higher than 38°C, or confirmed or suspected chorioamnionitis		3
Parenteral antibiotic treatment given to the woman for confirmed or suspected invasive bacterial infection (such as septicaemia) at any time during labour, or in the 24-h periods before and after the birth [This does not refer to intrapartum antibiotic prophylaxis]		1
Clinical indicators		
Altered behaviour or responsiveness		34
Altered muscle tone (for example, floppiness)		2
Feeding difficulties (for example, feed refusal)		3
Feed intolerance, including vomiting, excessive gastric aspirates and abdominal distension		1
Signs of respiratory distress		29
Hypoxia (for example, central cyanosis or reduced oxygen saturation level)		25
Jaundice within 24 h of birth		3
Seizures		1
Need for mechanical ventilation in a preterm baby		15
Need for mechanical ventilation in a term baby		16
Unexplained excessive bleeding, thrombocytopenia, or abnormal coagulation (International Normalised Ratio greater than 2.0)		5
Altered glucose homeostasis (hypoglycaemia or hyperglycaemia)		4
Local signs of infection (for example, affecting the skin or eye)		10

GA, gestational age; PNA, postnatal age; BW, birth weight; CW, current weight.

procedure are closely consistent with the values from the final population model, suggesting that the final model is stable and reliable (Table 2). The distribution and histogram of NPDE were in accordance with the theoretical N (0, 1) distribution and density, reflecting a good fit of the model to the individual data (Figures 1E,F). The mean and variance of NPDE were 0.039 and 1, respectively. The pcVPC result is shown in Figure 2. The simulated concentrations are in agreement with the prediction-corrected observed concentrations, validating the predictive performance of the model.

Using this pharmacokinetic model, the dosage regimen of cefotaxime prescribed in the study (50 mg/kg, BID) resulted 100% of neonates achieving the target (70% fT > MIC) at steady state.

Effectiveness evaluation

As described in Supplementary Table S1, 98.0% (n = 50) neonates were successfully cured, and only 2.0% (n = 1) newborns experienced treatment failure. The one newborn babies altered antibiotic treatment due to the progression of clinical conditions (switched to meropenem on Day 5). In our study, the median time to start cefotaxime treatment after birth was 3.07 (range 1.0–55.6) hours, while the median duration of cefotaxime therapy in 51 newborns was 6.6 (range 1.5–15.5) days. The median length of hospitalization was 13.0 (range 3.0–36.0) days in all the subjects. Cefotaxime discontinuance criteria were reached in 46 (92%) patients. Approximately half of neonates (23%, 46%) ceased cefotaxime treatment in the third round of discontinuation evaluation (96–144 h), and almost all subjects discontinued

TABLE 2 Population pharmacokinetic parameters of cefotaxime and bootstrap results.

Parameters	Full dataset		Bootstrap	
	Final estimate	RSE (%)	Median	5th–95th
V (L)				
$V = \theta 1$				
θ1	0.873	5.00	0.872	0.792–0.952
CL (L/h)				
$CL = \theta 2 \times (CW/2310)^{\theta 3} \times F_{age}$				
θ2	0.0803	6.00	0.0802	0.0713–0.0900
θ3	1.68	9.00	1.70	1.42–2.00
$F_{age}=(PNA/1)^{\theta 4}$				
θ4	0.444	15.3	0.452	0.312–0.583
Inter-individual variability (%)				
V	21.1	14.3	20.9	12.8–28.1
CL	20.0	18.9	19.2	13.3–25.3
Residual variability (%)	14.2	15.7	13.7	7.86–17.5

V, volume of distribution; CL, clearance; CW, current weight in gram; PNA, postnatal age in days.

cefotaxime therapy in the fourth stage of discontinuation assessment (144–216 h).

Safety evaluation

In our current study, no subjects ceased cefotaxime treatment or changed the dosage regimen due to AEs. Two AEs occurred in 2 (3.9%) neonates which were regarded as possibly related to cefotaxime therapy, while there were 4 AEs in 4 (7.8%) cases which were recognized as not related to cefotaxime. No patients had AEs which were definitely or probably related to cefotaxime. AEs possibly related to cefotaxime included diarrhea (n = 1) and moderate feeding intolerance (n = 1). AEs not related to cefotaxime treatment included seizures (n = 1) and feeding difficulties (n = 3). No infection-related death involved in cefotaxime treatment occurred in the first month after birth.

Discussion

Our present work using real-world data was the first population pharmacokinetics, effectiveness and safety evaluation of cefotaxime in neonates with EOS in China. The findings of the work revealed that a one-compartment model with first-order elimination best fitted the pharmacokinetics data of cefotaxime. Additionally, this prospective real-world study demonstrated that according to the model results, all of studied neonates treated with cefotaxime (50 mg/kg BID) attained the pharmacokinetic-pharmacodynamic target, which had a favorable efficacy and an accepted safety profile for newborns with EOS.

Since cefotaxime is mainly eliminated *via* a renal route, renal anatomical and function maturation is considered to have an essential influence on cefotaxime CL and dosing in newborn babies. Our results showed that current weight and postnatal age had a crucial impact on cefotaxime clearance, indicating that postnatal renal maturation had an important effect on cefotaxime CL, consistent with principally renally eliminated antibiotics (Rodieux et al., 2015).

Low birth weight is a major risk factor for EOS. In the United States, the overall incidence of EOS was 10.96‰ (10.96 per 1000 live newborns) in very low birth weight (VLBW) babies with a BW of <1500 g, 1.38‰ among low birth weight (LBW) babies with a BW of 1500–2500 g, 0.57‰ among normal birth weight (NBW) babies with a BW > 2500 g (Stoll et al., 2011). In the present study, 28 LBW infants and two VLBW infants were subjected to EOS, accounting for 58.8% of 51 cases. Therefore, for LBW or VLBW infants, once suspected or confirmed EOS, prompt and effective treatment should be adopted. Additionally, another important risk factor for neonatal sepsis is maternal membrane rupture. An obstetric risk factor—membrane rupture >18 hours—was found in 13.5% of group B streptococcal (GBS) cases and 26.7% of other sepsis (Schuchat et al., 2000). Compared to neonatal clinical indicators, maternal risk factors are more important for the diagnosis of EOS and the starting of antibiotic treatment. In our study, the top three reasons to initiate antibiotic therapy were maternal risk factors, including "suspected or confirmed rupture of membranes for more than 18 h in a preterm birth", "preterm birth following spontaneous

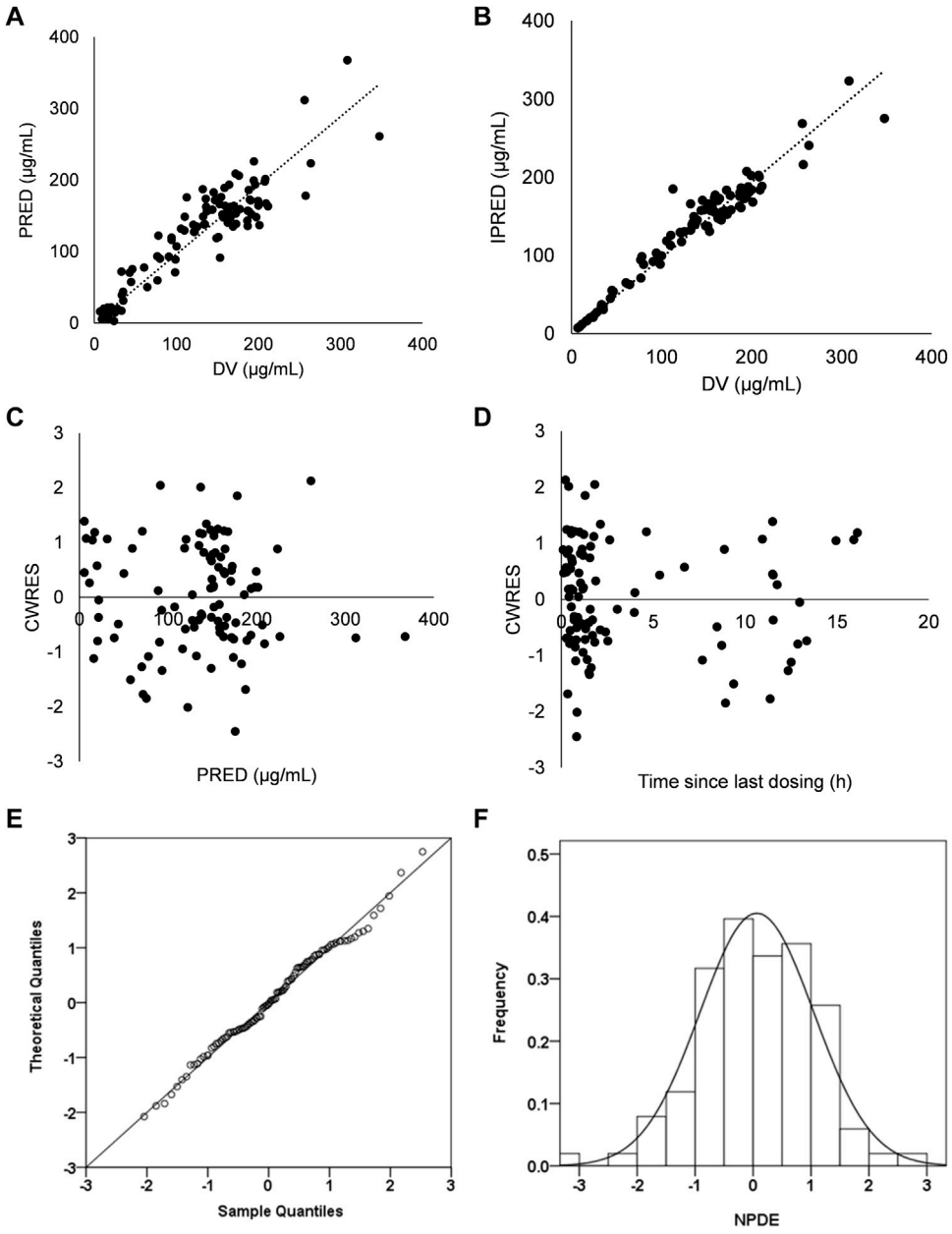

FIGURE 1
Model evaluation for cefotaxime **(A)** Population predicted concentrations (PRED) versus observed concentrations (DV). **(B)** Individual predicted concentrations (IPRED) versus DV **(C)** Conditional weighted residuals (CWRES) versus PRED. **(D)** CWRES versus time. **(E)** QQ-plot of the distribution of the Normalized Prediction Distribution Errors (NPDE) versus the theoretical N (0,1) distribution. **(F)** Histogram of the distribution of the NPDE.

labour (before 37 weeks' gestation)", and "prelabour rupture of membranes".

Antibiotics are frequently prescribed in the treatment of neonatal sepsis due to the high rates of incidence and mortality (Hornik et al., 2012; Oliver et al., 2017; Stocker et al., 2017). However, many medications used in neonatal clinical practice are unlicensed, owing to the absence of evidence-based dosing regimen (Schrier et al., 2020). Undoubtedly, empirical antibiotic treatment in newborns brings the risk of either drug-resistant bacteria due to underdose or side effects owing to overdose. The adoption of real-world evidence (RWE) is becoming increasingly essential for the evaluation of effectiveness and safety and the rational use of drugs in children (Lamberti et al., 2018; Lasky et al., 2020). A

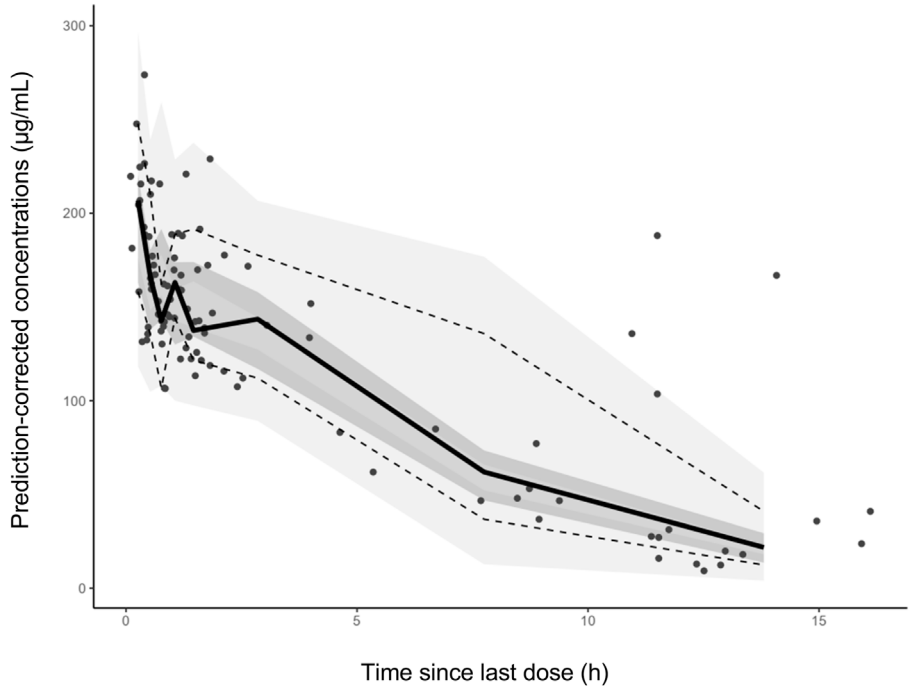

FIGURE 2
The prediction corrected visual predictive checks. The circles represent the prediction-corrected observed concentrations. The solid line represent the median prediction-corrected observed concentrations and semitransparent gray field represents simulation-based 95% confidence intervals for the median. The observed 5th and 95th percentiles are indicated by dashed lines, and the 95% intervals for the model-predicted percentiles are in a lighter translucent gray.

combination of ampicillin and an aminoglycoside was recognized as a standard regimen of EOS. However, aminoglycosides are not allowed to treat EOS in China because of a higher risk of ototoxicity. Instead, local neonatologists are more likely to prescribe third-generation cephalosporins, such as cefotaxime, based on its antibacterial spectrum and the distribution of pathogens. Obviously, it is crucial to generate real world evidence derived from real world data of alternative medication for neonatal EOS.

In the effectiveness and safety evaluation, in view of ambiguous signs and symptoms, low detection rate of blood culture and requirement for timely diagnosis and treatment, we designed the clinical trial according to NICE guidelines including maternal factors or clinical indicators, to assess the effectiveness and safety of cefotaxime in newborn babies with EOS. In the present study, the average time to initiate cefotaxime therapy after birth was 3.07 h, longer than 2.0 h in previous research (Stocker et al., 2017), which may be explained by the discrepancy of clinical practice in different medical centers. In addition, the average duration of cefotaxime treatment was 6.6 days, longer than 5 days in Cordero's study (Cordero and Ayers, 2003). This may be partially explained by the fact that delayed start of antibiotics treatment resulted in prolonged administration of antimicrobial agents (>5 days). Extended treatment duration of empirical antibiotics, especially third-generation cephalosporins, is associated with subsequent adverse outcomes, including late onset sepsis (LOS), necrotizing enterocolitis (NEC), invasive candidiasis and death (Cotten et al., 2009; Alexander et al., 2011; Kuppala et al., 2011; Cantey et al., 2018; Raba et al., 2019). Therefore, considering severe harmful outcomes implicated in prolonged use of antibiotics, the need to develop a precise strategy which can determine the duration of antibiotics treatment is essential for lower incidence of severe adverse outcomes.

As for effectiveness evaluation, cefotaxime demonstrated favorable therapeutic effect in the treatment of EOS. In the current work, 98.0% (n = 50) neonates with EOS were effectively cured, and only 2.0% (n = 1) newborns were evaluated as treatment failure. There is no definite value (27%–50%) for the protein binding rate of cefotaxime in human according to the reported data (Harding et al., 1981; LeFrock et al., 1982; Patel et al., 1995). In the cefotaxime label, the protein binding rate is 30%–50%, thus a median value of 40% was selected for PD target evaluation. The pharmacokinetic-pharmacodynamic target attainment was reached in 51 (100%) neonates, which enabled a consistent conclusion, reflecting a satisfying dosing regimen for this population. From the perspective of safety, there were limited adverse events implicated in cefotaxime treatment in newborns (Kearns and Young, 1995).

The side effects are mainly presented as hypersensitivity and gastrointestinal reactions, and cefotaxime rarely leads to nephrotoxicity and seizures (Roberts et al., 2014; Fanos and Dall'Agnola, 1999). The acceptable safety profile found in our study is consistent with these findings. Despite some studies have noted a rise in the incidence of invasive candidiasis, necrotizing enterocolitis and late onset sepsis because of the initial use of cefotaxime (Bryan et al., 1985; Manzoni et al., 2006; Polin, 2012), these serious adverse outcomes did not occur in our present study. However, out of prudence and safety, cefotaxime would be ceased promptly if the baby's clinical presentation associated with sepsis and the levels of CRP turned normal after evaluation, and meanwhile these cases should be paid more attention and given careful nursing during cefotaxime treatment, in order to avoid the severe adverse outcomes involved in cefotaxime.

Several limitations existed in our study. Extremely low birth weight (<1000 g) neonates are missing in the present study. Thus, our results can simply not be extrapolated to this population. Additionally, cefotaxime performed well in the effectiveness and safety evaluation over a one-month follow-up period. The long-term safety of cefotaxime in larger samples needs to further investigation.

Conclusion

We evaluated the effectiveness and safety of cefotaxime using real-world data, and the drug exhibited a favorable clinical benefits and safety in neonates. Innovative approach should be promoted to assess off-label drugs in newborns for rational use.

Data availability statement

The original contributions presented in the study are included in the article/Supplementary Material, further inquiries can be directed to the corresponding authors.

Ethics statement

The studies involving human participants were reviewed and approved by the Affiliated Hospital of Xuzhou Medical University. Written informed consent to participate in this study was provided by the participants' legal guardian/next of kin.

Author contributions

YX and WZ coordinated and supervised data collection and critically reviewed and revised the manuscript. Z-HS collected the clinical data and wrote the first version of the manuscript. Y-EW performed data analysis and revised the manuscript. D-ML and W-QL managed the patient and collected blood samples. WZ performed data analysis. JA provided advice, critically reviewed and revised the manuscript. All the authors contributed to write the manuscript and approved the final manuscript as submitted.

Funding

This work was supported by Clinical Technical Backbone Research Program of Xuzhou (grant number 2018GG032); the National Natural Science Foundation of China (grant number 82173897); Young Taishan Scholars Program of Shandong Province; and Distinguished Young and Middle-aged Scholar of Shandong University. The funders had no role in the study design, data collection and analysis, decision to publish, or preparation of the manuscript.

Conflict of interest

The authors declare that the research was conducted in the absence of any commercial or financial relationships that could be construed as a potential conflict of interest.

Publisher's note

Supplementary material

The Supplementary Material for this article can be found online at: https://www.frontiersin.org/articles/10.3389/fphar.2022.916253/full#supplementary-material

References

Alexander, V. N., Northrup, V., and Bizzarro, M. J. (2011). Antibiotic exposure in the newborn intensive care unit and the risk of necrotizing enterocolitis. *J. Pediatr.* 159, 392–397. doi:10.1016/j.jpeds.2011.02.035

Brown, A. P., and Denison, F. C. (2018). Selective or universal screening for gbs in pregnancy (review). *Early Hum. Dev.* 126, 18–22. doi:10.1016/j.earlhumdev.2018.09.002

Bryan, C. S., John, J. F., Jr., Pai, M. S., and Austin, T. L. (1985). Gentamicin vs cefotaxime for therapy of neonatal sepsis. Relationship to drug resistance. *Am. J. Dis. Child.* 139, 1086–1089. doi:10.1001/archpedi.1985.02140130024022

Cantey, J. B., Pyle, A. K., Wozniak, P. S., Hynan, L. S., and Sánchez, P. J. (2018). Early antibiotic exposure and adverse outcomes in preterm, very low birth weight infants. *J. Pediatr.* 203, 62–67. doi:10.1016/j.jpeds.2018.07.036

Cordero, L., and Ayers, L. W. (2003). Duration of empiric antibiotics for suspected early-onset sepsis in extremely low birth weight infants. *Infect. Control Hosp. Epidemiol.* 24, 662–666. doi:10.1086/502270

Cotten, C. M., Taylor, S., Stoll, B., Goldberg, R. N., Hansen, N. I., Sánchez, P. J., et al. (2009). Prolonged duration of initial empirical antibiotic treatment is associated with increased rates of necrotizing enterocolitis and death for extremely low birth weight infants. *Pediatrics* 123, 58–66. doi:10.1542/peds.2007-3423

Fanos, V., and Dall'agnola, A. (1999). Antibiotics in neonatal infections: A review. *Drugs* 58, 405–427. doi:10.2165/00003495-199958030-00003

Guo, J., Luo, Y., Wu, Y., Lai, W., and Mu, X. (2019). Clinical characteristic and pathogen spectrum of neonatal sepsis in guangzhou city from june 2011 to june 2017. *Med. Sci. Monit.* 25, 2296–2304. doi:10.12659/msm.912375

Harding, S. M., Monro, A. J., Thornton, J. E., Ayrton, J., and Hogg, M. I. (1981). The comparative pharmacokinetics of ceftazidime and cefotaxime in healthy volunteers. *J. Antimicrob. Chemother.* 8, 263–272. doi:10.1093/jac/8.suppl_b.263

Hornik, C. P., Fort, P., Clark, R. H., Watt, K., Benjamin, D. K., Jr., Smith, P. B., et al. (2012). Early and late onset sepsis in very-low-birth-weight infants from a large group of neonatal intensive care units. *Early Hum. Dev.* 88, S69–S74. doi:10.1016/s0378-3782(12)70019-1

Jiang, S., Hong, L., Gai, J., Shi, J., Yang, Y., Lee, S. K., et al. (2019). Early-onset sepsis among preterm neonates in China, 2015 to 2018. *Pediatr. Infect. Dis. J.* 38, 1236–1241. doi:10.1097/inf.0000000000002492

Kearns, G. L., and Young, R. A. (1995). Pharmacokinetics of cefotaxime and desacetylcefotaxime in the Young. *Diagn. Microbiol. Infect. Dis.* 22, 97–104. doi:10.1016/0732-8893(95)00052-c

Kuppala, V. S., Meinzen-Derr, J., Morrow, A. L., and Schibler, K. R. (2011). Prolonged initial empirical antibiotic treatment is associated with adverse outcomes in premature infants. *J. Pediatr.* 159, 720–725. doi:10.1016/j.jpeds.2011.05.033

Lamberti, M. J., Kubick, W., Awatin, J., Mccormick, J., Carroll, J., and Getz, K. (2018). The use of real-world evidence and data in clinical research and postapproval safety studies. *Ther. Innov. Regul. Sci.* 52, 778–783. doi:10.1177/2168479018764662

Lasky, T., Carleton, B., Horton, D. B., Kelly, L. E., Bennett, D., Czaja, A. S., et al. (2020). Real-world evidence to assess medication safety or effectiveness in children: Systematic review. *Drugs Real World Outcomes* 7, 97–107. doi:10.1007/s40801-020-00182-y

LeFrock, J. L., Prince, R. A., and Leff, R. D. (1982). Mechanism of action, antimicrobial activity, pharmacology, adverse effects, and clinical efficacy of cefotaxime. *Pharmacotherapy* 2, 174–184. doi:10.1002/j.1875-9114.1982.tb03185.x

Leroux, S., Turner, M. A., Guellec, C. B., Hill, H., Van Den Anker, J. N., Kearns, G. L., et al. (2015a). Pharmacokinetic studies in neonates: The utility of an opportunistic sampling design. *Clin. Pharmacokinet.* 54, 1273–1285. doi:10.1007/s40262-015-0291-1

Leroux, S., Zhao, W., Bétrémieux, P., Pladys, P., Saliba, E., Jacqz-Aigrain, E., et al. (2015b). Therapeutic guidelines for prescribing antibiotics in neonates should Be evidence-based: A French national survey. *Arch. Dis. Child.* 100, 394–398. doi:10.1136/archdischild-2014-306873

Maksoud, E., Koehl, B., Facchin, A., Ha, P., Zhao, W., Kaguelidou, F., et al. (2018). Population pharmacokinetics of cefotaxime and dosage recommendations in children with Sickle cell disease. *Antimicrob. Agents Chemother.* 62, e00637-17. doi:10.1128/aac.00637-17

Manzoni, P., Farina, D., Leonessa, M., D'oulx, E. A., Galletto, P., Mostert, M., et al. (2006). Risk factors for progression to invasive fungal infection in preterm neonates with fungal colonization. *Pediatrics* 118, 2359–2364. doi:10.1542/peds.2006-1311

Mukhopadhyay, S., and Puopolo, K. M. (2017). Clinical and microbiologic characteristics of early-onset sepsis among very low birth weight infants: Opportunities for antibiotic stewardship. *Pediatr. Infect. Dis. J.* 36, 477–481. doi:10.1097/inf.0000000000001473

National Collaborating Centre For, W. S and Children's, H. (2012). *Antibiotics for early-onset neonatal infection: Antibiotics for the Prevention and treatment of early-onset neonatal infection*. London: RCOG Press Copyright © 2012, National Collaborating Centre for Women's and Children's Health.National institute for health and clinical excellence: Guidance

Odio, C. M. (1995). Cefotaxime for treatment of neonatal sepsis and meningitis. *Diagn. Microbiol. Infect. Dis.* 22, 111–117. doi:10.1016/0732-8893(95)00093-p

Oliver, E. A., Reagan, P. B., Slaughter, J. L., Buhimschi, C. S., and Buhimschi, I. A. (2017). Patterns of empiric antibiotic administration for presumed early-onset neonatal sepsis in neonatal intensive care units in the United States. *Am. J. Perinatol.* 34, 640–647. doi:10.1055/s-0036-1596055

Paap, C. M., Nahata, M. C., Mentser, M. A., Mahan, J. D., Puri, S. K., and Hubbard, J. W. (1991). Pharmacokinetics of cefotaxime and its active metabolite in children with renal dysfunction. *Antimicrob. Agents Chemother.* 35, 1879–1883. doi:10.1128/aac.35.9.1879

Pacifici, G. M. (2011). Pharmacokinetics of cephalosporins in the neonate: A review. *Clinics* 66, 1267–1274. doi:10.1590/s1807-59322011000700024

Patel, K. B., Nicolau, D. P., Nightingale, C. H., and Quintiliani, R. (1995). Pharmacokinetics of cefotaxime in healthy volunteers and patients. *Diagn. Microbiol. Infect. Dis.* 22, 49–55. doi:10.1016/0732-8893(95)00072-i

Polin, R. A. (2012). Management of neonates with suspected or proven early-onset bacterial sepsis. *Pediatrics* 129, 1006–1015. doi:10.1542/peds.2012-0541

Raba, A. A., O'sullivan, A., Semberova, J., Martin, A., and Miletin, J. (2019). Are antibiotics a risk factor for the development of necrotizing enterocolitis-case-control retrospective study. *Eur. J. Pediatr.* 178, 923–928. doi:10.1007/s00431-019-03373-0

Roberts, J. K., Stockmann, C., Constance, J. E., Stiers, J., Spigarelli, M. G., Ward, R. M., et al. (2014). Pharmacokinetics and pharmacodynamics of antibacterials, antifungals, and antivirals used most frequently in neonates and infants. *Clin. Pharmacokinet.* 53, 581–610. doi:10.1007/s40262-014-0147-0

Rodieux, F., Wilbaux, M., Van Den Anker, J. N., and Pfister, M. (2015). Effect of kidney function on drug kinetics and dosing in neonates, infants, and children. *Clin. Pharmacokinet.* 54, 1183–1204. doi:10.1007/s40262-015-0298-7

Scheel, M., and Perkins, S. (2018). Hit or miss? A review of early-onset sepsis in the neonate. *Crit. Care Nurs. Clin. North Am.* 30, 353–362. doi:10.1016/j.cnc.2018.05.003

Schrag, S. J., Farley, M. M., Petit, S., Reingold, A., Weston, E. J., Pondo, T., et al. (2016). *Epidemiology of Invasive Early-Onset Neonatal Sepsis*, 138. doi:10.1542/peds.2016-2013*Pediatrics*

Schrier, L., Hadjipanayis, A., Stiris, T., Ross-Russell, R. I., Valiulis, A., Turner, M. A., et al. (2020). Off-label use of medicines in neonates, infants, children, and adolescents: A joint policy statement by the European Academy of paediatrics and the European society for developmental perinatal and pediatric pharmacology. *Eur. J. Pediatr.* 179, 839–847. doi:10.1007/s00431-019-03556-9

Schuchat, A., Zywicki, S. S., Dinsmoor, M. J., Mercer, B., Romaguera, J., O'sullivan, M. J., et al. (2000). Risk factors and opportunities for prevention of early-onset neonatal sepsis: A multicenter case-control study. *Pediatrics* 105, 21–26. doi:10.1542/peds.105.1.21

Simonsen, K. A., Anderson-Berry, A. L., Delair, S. F., and Davies, H. D. (2014). Early-onset neonatal sepsis. *Clin. Microbiol. Rev.* 27, 21–47. doi:10.1128/cmr.00031-13

Stocker, M., Van Herk, W., El Helou, S., Dutta, S., Fontana, M. S., Schuerman, F., et al. (2017). Procalcitonin-guided decision making for duration of antibiotic therapy in neonates with suspected early-onset sepsis: A multicentre, randomised controlled trial (neopins). *Lancet* 390, 871–881. doi:10.1016/s0140-6736(17)31444-7

Stoll, B. J., Hansen, N. I., Sánchez, P. J., Faix, R. G., Poindexter, B. B., Van Meurs, K. P., et al. (2011). Early onset neonatal sepsis: The burden of group B streptococcal and E. Coli disease continues. *Pediatrics* 127, 817–826. doi:10.1542/peds.2010-2217

Wise, R., and Wright, N. (1985). The pharmacokinetics of cefotaxime and ceftriaxone in renal and hepatic dysfunction. *Infection* 13, S145–S150. doi:10.1007/bf01644237

Wu, Y. E., Wang, T., Yang, H. L., Tang, B. H., Kong, L., Li, X., et al. (2021). Population pharmacokinetics and dosing optimization of azlocillin in neonates with early-onset sepsis: A real-world study. *J. Antimicrob. Chemother.* 76, 699–709. doi:10.1093/jac/dkaa468

frontiers | Frontiers in Pharmacology

TYPE Review
PUBLISHED 07 September 2022
DOI 10.3389/fphar.2022.957376

OPEN ACCESS

EDITED BY
Jian Gao,
Shanghai Children's Medical Center, China

REVIEWED BY
Meixing Yan,
Qingdao Women and Children's Hospital, China
Jing Tang,
Fudan University, China

*CORRESPONDENCE
Yulian Zhu,
1054507078@qq.com
Yong Yang,
yyxpower@163.com

SPECIALTY SECTION
This article was submitted to Obstetric and Pediatric Pharmacology, a section of the journal Frontiers in Pharmacology

RECEIVED 31 May 2022
ACCEPTED 05 July 2022
PUBLISHED 07 September 2022

CITATION
Zhang Z, Li Q, Shen X, Liao L, Wang X, Song M, Zheng X, Zhu Y and Yang Y (2022), The medication for pneumocystis pneumonia with glucose-6-phosphate dehydrogenase deficiency patients.
Front. Pharmacol. 13:957376.
doi: 10.3389/fphar.2022.957376

The medication for pneumocystis pneumonia with glucose-6-phosphate dehydrogenase deficiency patients

Ziyu Zhang[1,2], Qinhui Li[3], Xiaoyan Shen[4], Lankai Liao[5], Xia Wang[1], Min Song[1], Xi Zheng[2], Yulian Zhu[6]* and Yong Yang[2,7]*

[1]Department of Pharmacy, The First People's Hospital of Ziyang, Ziyang, China, [2]Department of Pharmacy, Sichuan Academy of Medical Sciences & Sichuan Provincial People's Hospital, School of Medicine, University of Electronic Science and Technology of China, Chengdu, China, [3]Department of Medical, Sichuan Academy of Medical Sciences & Sichuan Provincial People's Hospital, School of Medicine, University of Electronic Science and Technology of China, Chengdu, China, [4]Department of Pharmacy, Chengdu Qingbaijiang District People's Hospital, Chengdu, China, [5]Intensive Care Unit, The Third Hospital of Mianyang, Mianyang, China, [6]Department of Pharmacy, Ziyang People's Hospital, Ziyang, China, [7]Personalized Drug Therapy Key Laboratory of Sichuan Province, School of Medicine, University of Electronic Science and Technology of China, Chengdu, China

Pneumocystis pneumonia (PCP) is an opportunity acquired infection, which is usually easy to occur in patients with AIDS, organ transplantation, and immunosuppressive drugs. The prevention and treatment must be necessary for PCP patients with immunocompromise. And the oxidants are currently a typical regimen, including sulfanilamide, dapsone, primaquine, etc. Glucose-6-phosphate dehydrogenase (G6PD) deficiency is an X-linked gene-disease that affects about 400 million people worldwide. The lack of G6PD in this population results in a decrease in intracellular glutathione synthesis and a weakening of the detoxification ability of the oxidants. As a result, oxidants can directly damage haemoglobin in red blood cells, inducing methemoglobin and hemolysis. When patients with G6PD deficiency have low immunity, they are prone to PCP infection, so choosing drugs that do not induce hemolysis is essential. There are no clear guidelines to recommend the drug choice of this kind of population at home and abroad. This paper aims to demonstrate the drug choice for PCP patients with G6PD deficiency through theoretical research combined with clinical cases.

KEYWORDS

PCP, G6PD, immunocompromise, oxidant, hemolysis

1 Introduction

G6PD deficiency is an X-chromosome-linked genotypic disease and was first found by investigating hemolytic development in patients receiving primaquine (Beutler, 1959; Mbanefo et al., 2017). The incidence of G6PD deficiency in southern Chinese cities such as Guangdong, Guangxi, Sichuan, and Hainan province was as high as 4–11% (Jiang et al., 2006; Liu et al., 2012). Except for red blood cells, G6PD may exist in other tissues, but these issues do not seem to be damaged by the lack of the enzyme. The primary purpose of this enzyme in red blood cells is to protect haemoglobin from oxidation. The critical factor in safeguarding haemoglobin from oxidation in red blood cells is glutathione (Prankerd, 1964). As the substrate of glutathione proenzyme, Glutathione protects cells from the toxicity of hydrogen peroxide produced by oxidizing drugs (Cohen and Hochstein, 1963). Due to the lack of G6PD, the cells cannot provide enough nicotine adenine dinucleotides phosphate (NADP) to maintain Glutathione. Glutathione will overused after taking some antioxidants or eating fava beans. The remaining oxygen-free radicals will directly damage red blood cells, leading to cell rupture and hemolytic anaemia. Such oxidant drugs usually include sulfonamides, sulfones, nitrofurantoin, p-aminosalicylic acid, chloramphenicol, and isoniazid (Allen and Wilkerson, 1972). After the onset of the disease, medicine is unuseful for these people but only with relief of symptoms, so avoiding the excessive consumption of glutathione caused by low G6PD activity is the primary measure. The World Health Organization (WHO) recommended that people in areas where the prevalence of G6PD deficiency is more than 5% should be routinely tested for enzymes at birth. However, the coverage rate of this detection is low. There are still many G6PD deficiency positive patients with hemolytic anaemia after using oxidant drugs. There is sufficient evidence that patients with G6PD deficiency are prohibited from using the following seven drugs: dapsone, methylthioninium chloride (methylene blue), nitrofurantoin, phenazopyridine, primaquine, rasburicase, and tolonium chloride (Youngster et al., 2010).

Pneumocystis pneumonia is an opportunistic infection, its prevention and treatment are essential. The dangerous factors for PCP infection are severe immune deficiency for instance HIV, long-term use of glucocorticoids, tumour, transplantation and severe malnutrition. In that case, the mortality rate exceeds 90% (Hughes et al., 1975; Dei-Cas, 2000; Herrag et al., 2010; Gilroy and Bennett, 2011; Weyant et al., 2021). Sulfonamides and sulfoxides commonly used for PCP patients, and may cause serious adverse reactions in patients with G6PD deficiency. Therefore, it is difficult to choose drugs when patients with such enzyme deficiency are complicated with PCP infection. This article will focus on the prevention and treatment of PCP drugs and analyze the impact of these drugs on patients with G6PD deficiency. To reduce the harm of drugs to such patients, providing the best choice for the prevention and treatment of PCP in patients with G6PD deficiency.

2 G6PD deficiency

G6PD is not specific to red blood cells. It is a housekeeping enzyme that exists in almost all human cells. The monomer of G6PD is composed of 515 amino acids with a molecular weight of about 59 kDa (Cappellini and Fiorelli, 2008). G6PD can catalyze the oxidation of glucose-6 - phosphate (G6P), convert NADP into NADPH, and provide the reduction capacity for body cells in the form of NADPH (Cappellini and Fiorelli, 2008). NADPH can promote the production of reduced glutathione (GSH), thereby reducing the oxidative stress response of oxidants to body cells (Tsai et al., 1998). In most human cells, NADPH is a crucial component in many biosynthesis processes, including the synthesis of fatty acids, cholesterol, and steroid hormones, and the generation of deoxyribose. G6PD plays an important role in reducing hydrogen peroxide and oxygen free radicals and maintaining hemoglobin and other erythrocyte proteins. In most cells, in addition to G6PD, there are many enzymes catalyzed dehydrogenase reactions to produce NADPH, so even G6PD deficiency cells do not lead to short of NADPH. However, NADPH production in red blood cells is entirely different. The difference is that, with red blood cell differentiation and other enzyme inactivation, NADPH has no other source than the pentose phosphate pathway (Luzzatto et al., 2016). Therefore, red blood cells defend against oxidative stress depending on G6PD and are more vulnerable to G6PD deficiency than other cells. The defects of G6PD are primarily incomplete, and the NADPH produced by the remaining G6PD activity is sufficient to maintain RBC operation but usually short-lived. At this time, if there is exogenous oxidant stimulation, G6PD-deficient red blood cells will not produce enough NADPH and GSH for consumption, which will cause damage to haemoglobin or other proteins, and eventually, lead to red blood cell rupture and hemolysis.

2.1 Genetic characteristics of G6PD deficiency

The G6PD gene is composed of 13 exons of 515 amino acid protein subunits. Except for the binding site between NADP substrate and G6P substrate, each subunit has a closely bound NADP molecule (Au et al., 2000). G6PD deficiency is caused by G6PD gene mutation, resulting in varying degrees of enzyme deficiency and protein variation, which is related to various clinical subtypes. The most usual clinical diseases are neonatal hyperbilirubinemia and acute hemolytic anemia, and exogenous drug use is the main cause.

In the case of G6PD deficiency, the genetic defect is located in the subtelomere region of the long arm of the X chromosome and is also affected by X chromosome inactivation. (Beutler et al., 1962). X linkage has an essential effect on the genetic characteristics of G6PD deficiency. There are only two genotypes in males: hemizygote normal and half zygote G6PD deficiency, while females, have three genotypes: homozygote normal, homozygous deficient, and heterozygote (Cappellini and Fiorelli, 2008). It is generally considered incorrect that the incidence of G6PD deficiency is higher in males than in females since homozygote female are less likely than hemizygote men. Still, there are many more heterozygous females, from the basic principles of population genetics (Hardy-Weinberg equilibrium). These heterozygotic females usually show that half of the red blood cells are G6PD deficient, and half of the red blood cells are G6PD normal. Some heterozygous female patients offer a normal state, and some show a disease state similar to homozygous, which has apparent clinical significance (Rinaldi et al., 1976).

2.2 Epidemiological characteristics of G6PD deficiency

The geographical distribution of G6PD deficiency is extensive, with the frequency peak of infections found in Africa, the Middle East the Mediterranean region, and Asia; however, due to recent migration, this disease occurs in the United States and Northern Europe. The prevalence of the disease is highest in Africa, Asia, the Middle East, Latin America and the Mediterranean. Among them: Kurdish Jews 60–70%, Sardinia 4–35%, Nigeria22%, Thailand17%, Greece6%, South China6%, India3%. The lack of G6PD affects black Americans, of which up to 24% are carriers, and about 10% are affected by black males (Harcke et al., 2019). It is found that the distribution of G6PD deficiency is similar to that of malaria endemic areas. This indirect evidence suggests that G6PD deficiency is resistant to malaria (Ruwende and Hill, 1998), but it does not prove that malaria selects for the gene that causes G6PD deficiency. Natural selection seems responsible for the higher mortality rates of children from malaria in endemic areas. By comparing the incidence of malaria, parasiteia levels, or the severity of malaria in children with G6PD normal and deficiency, studies conducted in Africa and other regions showed that the lack of G6PD appeared to have a protective effect on severe malaria (Rockett et al., 2014; Luzzatto et al., 2016), but the results need more data to support.

According to the law of natural selection, the genetic characteristics associated with the X-linked G6PD gene tend to be stable if both males and females with protective genes increase adaptability (Luzzatto, 2012). However, there is no evidence that population genes have evolved into G6PD deficiency in malaria-prone areas. Although so much current research shows that G6PD deficiency protects against malaria, especially falciparum malaria, the evidence is still insufficient. Therefore, the idea that G6PD deficiency is a protective factor for malaria requires more research data.

2.3 Clinical manifestations of G6PD deficiency

Patients with G6PD deficiency usually have no obvious clinical manifestations but can lead to disease only under exogenous stimulation. In infants with G6PD deficiency, neonatal jaundice (NNJ) risk is higher. There is not enough evidence for this phenomenon, but this may be the most common cause of NNJ in countries where G6PD deficiency is widespread. Serious complications may occur in semi-zygotic boys and girls with G6PD deficiency (Doxiadis et al., 1964). Another clinical manifestation of acute hemolysis is often caused by exogenous substances, including fava beans or some drugs, such as chloroquine, sulfanilamide, naphthalic acid, etc.

Red blood cells (RBC) may rupture after eating fava beans in G6PD deficiency patients. Ruptured RBC can lead to a sharp drop in haemoglobin, acute hemolysis, and hemoglobinuria. A particular glycoside in fava beans causes this phenomenon and can occur at any age, but it is more usual and dangerous in childhood (Luzzatto et al., 2016). Studies have shown that patients with G6PD are more likely to develop sepsis, so treatment for patients with G6PD deficiency needs to be more cautious (Spolarics et al., 2001). Infectious diseases are also one of the risk factors for hemolysis. So, it is challenging to distinguish whether the cause of hemolysis is disease or drugs. When a patient with G6PD deficiency is co-infected, the choice of medicine will be critical (Youngster et al., 2010).

3 Pneumocystis pneumonia

3.1 Definition

PCP can lead to aggravation of diseases and even death in patients with immunocompromised, especially with HIV infection (Huang et al., 2006; Herrag et al., 2010; Huang, 2011). Initially, Plasmodium Cysticercosis was initially classified as protozoans because of their morphological characteristics similar to those of protozoans and their sensitivity to antiprotozoal drugs. Because its cytoderm composition and nucleotides are identical to fungi, they have recently been classified as fungi. The earliest molecular biological evidence also suggests that Plasmodium cysticercosis is a fungus (Santamauro et al., 2002; Lu and Lee, 2008).

3.2 Clinical manifestations

The symptoms and signs of pneumocystis pneumonia are atypical and are often mistaken for infections caused by other bacteria or viruses (Weyant et al., 2021). The common symptoms of PCP include dyspnea, fever, and hacking cough, and there are other atypical symptoms, such as chest pain, hemoptysis, hypoxia, and diffuse dry rale during an examination (Singhal et al., 2005; Fujii et al., 2007; Thomas and Limper, 2007). The clinical manifestations of HIV complicated with PCP infection are different from those of other causes of immune dysfunction. The course of the PCP in patients with HIV is often longer, usually manifested as a hidden course with symptoms; some studies showed the duration could be as long as 28 days (Catherinot et al., 2010). Patients with immunodeficiency without HIV tend to have more severe symptoms and a higher risk of respiratory failure and death (Krajicek et al., 2008; Weyant et al., 2021).

3.3 Characteristics of the disease

It may not be abnormal or accompanied by strange respiratory sounds in the initial chest examination. Still, later, the disseminated rale and pulmonary shadow will be severe if not treated. The typical manifestations are diffuse interstitial syndrome on x-ray chest film and diffuse bilateral ground-glass shadow on CT, mainly in the perihilar inferior areas. Other features include focal patchy parenchymal consolidation, cysts, solid nodules, pneumothorax, and some cavity and honeycomb lesions (Santamauro et al., 2002; Fujii et al., 2007; Thomas and Limper, 2007). Zaman et al. proposed that elevated serum lactate dehydrogenase (LDH) levels are closely associated with PCP infection. In AIDS patients, the absolute level greater than 450 IU may suggest the infection of pneumocystis pneumonia, while normal levels indicate a lower likelihood of PCP infection (Zaman and White, 1988). However, LDH is not a specific indicator, especially in some potential malignant tumors or patients with liver dysfunction. Whether or not the people affected by HIV or the level of LDH is within the normal range, these patients may develop pneumocystis pneumonia (Santamauro et al., 2002). Sputum induction is a susceptible method for diagnosing pneumocystis pneumonia in laboratory tests, with a sensitivity between 55 and 95% for PCP in HIV-infected persons (Santamauro et al., 2002). Bronchoalveolar lavage fluid is another practical test for PCP in immunosuppressed patients, and the test has almost 100% sensitivity and peculiarity. In addition, the current methods used to detect PCP-positive microorganisms are immunofluorescence (IFL), cytology, polymerase chain reaction (PCR), or silver staining, in which PCR is more sensitive but cannot distinguish colonization from infection (Santamauro et al., 2002; Azoulay et al., 2009; Catherinot et al., 2010; Wilson et al., 2011).

3.4 Susceptible population

Generally, Pneumocystis mainly causes infection in immunocompromised patients but can colonize in individuals with standard immune systems and spread to patients with immune impairment (Ponce et al., 2010). Among them, the causes of immune deficiency are HIV, glucocorticoids, and cellular immune deficiency. *Cancer* (especially haematological malignancies), hematopoietic stem cell transplantation (HSCT), or solid organ transplantation acceptor are the leading causes. Following, connective tissue diseases, systemic diseases, rheumatism, severe immunodeficiency, and severe malnutrition also play a role (Dei-Cas, 2000; Herrag et al., 2010; Sadanand, 2011; Weyant et al., 2021). In patients without HIV infection, the most critical risk factor for PCP was glucocorticoids and cell-mediated immunity deficiencies (Sepkowitz et al., 1992; Sepkowitz et al., 1995).

3.5 Treatment programmes

According to the symptoms, signs, and chest radiography of PCP patients, the disease status is divided into three grades: mild, moderate, and severe. Despite other medications for pneumocystis pneumonia, trimethoprim-sulfamethoxazole (TMP-SMX) remains the recommended first-line treatment for mild to middle infections, which has good oral bioavailability (Singhal et al., 2005; Carmona and Limper, 2011). Intravenous or oral administration can achieve appropriate serum levels in patients without impaired gastrointestinal function. TMP-SMX (15 mg/kg every 6–8 h) was routinely administered according to renal function. As for non-critical patients who can take oral medication, two double dosage tablets every 8 h are recommended (Goto and Oka, 2011). Sulfoxide combined with trimethoprim, primaquine combined with clindamycin, and atovaquone is the second-line treatment options for mild to moderate PCP patients. The first-line drug for patients with severe infection is still TMP-SMX. And primaquine combined with clindamycin, caspofungin combined with TMP-SMX, and intravenous injection of Pentamidine is the second-line drugs. Besides, In some cases, methotrexate plus calcium folinate can be used as a rescue treatment for PCP (Huang et al., 2006; Calderón et al., 2010; Rouyer et al., 2015). Glucocorticoids can reduce pulmonary inflammation caused by pulmonary cysticercosis for patients with severe PCP. It significantly prevents oxidative deterioration, mortality, and intubation in the first 7 days of HIV treatment (50 percent reduction) (Briel et al., 2005). For non-HIV patients with severe PCP, daily doses

of prednisone greater than or equal to 60 mg were more effective than lower doses (Pareja et al., 1998).

3.6 Preventive measures

In patients with HIV, the count of CD4 T cells is a helpful marker and classifies the risk of PCP. TPCP patients need Primary prevention when the count of CD4 cells is lower than 200/mm^3. However, in patients without AIDS, there were no valuable markers for monitoring immune status (Santamauro et al., 2002). TMP-SMX is the first selection to prevent PCP; sulfoxide is the second-line drug to prevent PCP, which is banned in G6PD enzyme deficiency patients (Bellamy, 2008). Atovaquone is a suspension that only fatty foods can promote its absorption. It has been widely studied in the human immunodeficiency virus population and small-scale trials of solid organ transplantation recipients. It can be used as a second-track drug to prevent PCP. Compared with TMP-SMX, sulfoxide, or Atovaquone, inhaled injection of Pentamidine is less effective and should be regarded as a third-line drug to prevent PCP. In the study of HIV patients, clindamycin combined with pyrimidine was neither less effective than TMP-SMX nor sulfoxide or pentamidine (Davey and Masur, 1990; Goto and Oka, 2011; Rouyer et al., 2015; Brakemeier et al., 2018).

4 The effect of drugs in pneumocystis pneumonia with G6PD deficiency

The most severe consequence of patients with G6PD deficiency is that the red blood cells of some patients will cause oxidative damage and acute hemolysis under drugs, acute diseases, and certain foods (such as broad beans). If patients can avoid using some medications to reduce oxidative stress exposure, the incidence of hemolysis may be significantly reduced. Some oxidant medicines for the prevention and treatment of PCP can lead to acute hemolysis in patients with G6PD deficiency. In the following, we will analyze the drugs used for PCP prevention and treatment one by one to evaluate the hemolysis risk of these drugs in patients with G6PD deficiency.

4.1 The influence of oxidants

At present, sulfonamides are the main recommended drugs in the first line for PCP, among which TMP-SMX is the optimal choice for these patients. The main alternatives include sulfoxide, trimethoprim, primaquine, clindamycin, etc. However, sulfoxide-trimethoprim and clindamycin-primaquine regimens are prohibited in Use in G6PD deficiency (Warren et al., 1997; Castro, 1998; Sadanand, 2011). These common oxidant drugs may cause a risk for acute hemolysis in G6PD deficiency. Hemolytic anaemia caused by G6PD deficiency is a self-constraint process; sometimes, anemia may not be apparent. The WHO classifies G6PD deficiency into five grades based on the wide range of enzyme activity in genotypes and heterozygotes: grade 1 showed severe deficiency, accompanied by chronic non-spherical hemolytic anaemia, grade 2 severe deficiency (enzyme activity was 1–10%), grade 3 moderate deficiency (the range of enzyme activity is 10–60%), grade 4 regular (enzyme activity 60–150%) The activity of grade 5 was enhanced (>150%) (WHO Working Group, 1989). Although the enzyme activity is different, oxidant drugs can cause hemolytic anaemia in various stages of enzyme deficiency. Several drugs are associated with acute hemolysis in G6PD deficient population, such as Primaquine, Sulfanilamide, Sulfapyridine, TMP-SMX, dapsone, Nitrofurantoin, Co-trimoxazole (Beutler, 1964; Beutler, 1996).

4.1.1 Sulfonamides

TMP-SMX, as the most optimized selection for PCP, can reduce mortality and intubation rates. Compared with controls, A Cochrane meta-analysis reports a 91% reduction in the incidence of PCP and an 83% reduction in mortality (Hughes et al., 1975; Maschmeyer et al., 2016). At the same time, metabolic disorders, drugs, and hepatitis are also factors of hemolysis in G6PD deficiency. Patients with PCP infection who use sulfonamides may increase the danger of hemolysis due to the influence of ailment and drugs. TMP-SMX has been associated with severe side effects of medicine source hemolytic anemia due to lack of G6PD activity (Frank, 2005). In an early study, 75% of patients with G6PD deficiency developed hemolysis after treatment with sulfonamides. However, sulfonamides are not contraindications for all patients with G6PD. In black women, there was a low risk of severe hemolysis after therapy with sulfonamides in G6PD deficiency (Norden et al., 1968). In the Chan et al. Study, ten infants with G6PD deficiency were treated with TMP-SMX at a dose of 5–10 mg/kg, and the daily dose is about 30–50 mg. Before and 5 days after treatment, we reviewed the haemoglobin, hematocrit, reticulocyte count, and blood smear and found no signs of hemolysis in the infant. We found an experiment result; even if the G6PD deficiency showed the same activity as the G6PD enzyme, it could lead to differences in drug metabolism due to liver and kidney function changes or some uncertain metabolic characteristics, or other coexisting diseases (Chan et al., 1976). Whether or not these sulfonamides cause severe hemolytic anaemia, the World Health Organization and many studies have banned their use in the G6PD deficiency population. Above all, it is best to prevent G6PD deficiency patients from choosing such drugs and selecting other medicines.

4.1.2 Primaquine

Primaquine, combined with clindamycin as an alternative treatment for PCP, is an antiparasitic agent used primarily to prevent and treat malaria. A controlled study of primaquine for safety and tolerance showed that the average hematocrit of G6PD deficiency patients taking primaquine decreased significantly on the 7th, 8th, and 9th day (p = 0.015, 0.027, 0.048) (Krudsood et al., 2006). Some early tests demonstrated that primaquine at a daily dose caused intravascular hemolysis in glutathione-deficient red blood cells, with severity associated with glutathione, and suggested that ascorbic acid might alleviate such hemolysis (Greenberg and Wong, 1961). So, we must be careful about using primaquine in patients with a G6PD deficiency.

Several studies have shown that primaquine has dose-dependent hemolysis: a higher dosage of primaquine may lead to significant clinical hemolysis in G6PD heterozygotic women. A prospective study of 801 malaria patients showed that in Thailand, where the epidemic variation of G6PD deficiency was relatively mild, many sufferers with G6PD deficiency could not tolerate large doses of primaquine. In a subject with G6PD deficiency, high doses of primaquine may be contraindicated, but standard doses of primaquine with careful monitoring of hematocrit may also be a treatment option (Silachamroon et al., 2003). It has been found that giving primaquine twice a week provides more hemolytic effect than once a week. In contrast, the control group without G6PD deficiency does not cause anaemia (Zipursky et al., 1965; Tine et al., 2017).

Low doses of primaquine are safer than high doses of primaquine: the WHO recommended combined therapy of a single dose of 0.25 mg/kg. Standard artemisinin is safe in treating acute uncomplicated Plasmodium falciparum malaria, whether or not patients have G6PD deficiency. Other tests also showed a lower risk of hemolysis after daily administration of primaquine with a single dosage of 0.25 mg/kg (Eziefula et al., 2014; Bancone et al., 2016; Mwaiswelo et al., 2016; Bastiaens et al., 2018; Dysoley et al., 2019). In a systematic evaluation of primaquine in the therapy of malaria, the higher dose of the remedy, the higher the rish of anaemia in G6PD deficiency compared with placebo. However, there was no significant difference in haemoglobin decrease on the 7th day compared with placebo at low doses such as 0.25 mg/kg (Uthman et al., 2017).

The hemolysis caused by primaquine and chloroquine in Caucasians or Asians with g6pd deficiency has not been thoroughly studied. Still, enzyme deficiency is more severe in these groups than in blacks, and even given low doses of drugs can cause more severe hemolysis (Brewer and Zarafonetis, 1967). The severity of hemolysis in G6PD deficiency flocks relies on enzyme deficiency, the accumulated dose, drug exposure time, and other agents such as infection, age, and haemoglobin (Hb) concentration (Cappellini and Fiorelli, 2008).

4.1.3 Dapsone

Dapsone is a sulfone antibiotic that can prevent pneumocystis pneumonia in patients with sulfonamide allergy. The primary adverse reaction was hemolytic anaemia caused by sulfone drugs. The hdroxylamine is a toxic metabolite, the leading cause of hemolysis. It is mainly produced by the metabolism of cytochrome P450 enzymes after the absorption of dapsone in the gastrointestinal tract into the blood system through the portal vein to the liver. It generates free radicals, which cause haemoglobin damage and hemolytic anaemia forasmuch as glutathione consumption. In patients with G6PD deficiency, these hydroxylamine metabolites consume large amounts of glutathione, rapidly deplete its stores and increase the chance of hemolytic anaemia (Grossman and Jollow, 1988; Jollow et al., 1995; Zhu and Stiller, 2001). In addition, the antioxidants vitamin C or other vitamins cannot neutralize the metabolites produced by dapsone, and such antioxidants do not reduce the incidence of hemolytic anaemia.

There are some adverse reactions associated with dapsone in transplant patients. In individuals with G6PD deficiency, children who received sulfoxide treatment for malaria developed hemolytic anaemia more frequently than those who received the treatment of artemisinin (29%) (Van Malderen et al., 2012). Animal experiments showed that individuals lacking G6PD showed a tripling sensitivity to hemolytic anaemia induced by sulfoxide (Grossman et al., 1995). The Enzyme activity detection is a routine test for G6PD deficiency, but molecular analysis of female heterozygotes may be required. We found a Greek woman whose G6PD enzyme activity was detected to decrease and developed severe acute hemolysis following initiation of dapsone therapy (Lee and Geetha, 2015). A multicenter randomized controlled study of thousands of people showed signs of hemolysis in almost all G6PD deficient children receiving sulfoxide, with normal erythrocyte morphology before treatment and a significant decrease in haemoglobin after treatment (Pamba et al., 2012). A study in North America reported that in a population with stem cell transplantation (SCT), dapsone had a higher risk of hemolysis than dapsone and TMP-SMX in preventing PCP. Although most of the patients who received sulfoxide prophylaxis were negative for G6PD activity fluorescence screening tests, there is still existed hemolysis induced by dapsone (Zhu and Stiller, 2001). Another trial also showed that dapsone had a higher risk of hemolysis than TMP-SMX (87 vs. 0%, p = 0.001) (Olteanu et al., 2012). Four patients switched from TMP-SMX to dapsone in renal transplants due to allergy to sulfonamides and subsequently developed methemoglobinemia. So, early identification and discontinuation of sulfoxide were essential (Salim et al., 2017). Another study showed that 46% of 26 renal transplants using sulfoxide also developed methemoglobin

(Mitsides et al., 2014). A randomized controlled clinical trial of complicated falciparum malaria in Africa also suggested that the risk of haemoglobin decline in patients with G6PD deficiency was even higher in the Chlorproguanidine - dapsone group than in the sulfadoxine-pyrimethamine group (Alloueche et al., 2004). Several studies have found that the incidence of methemohemoglobin induced by dapsone is higher than that of TMP-SMX. This may be due to the differentiation in the formation, disposal, virulence and detoxification of TMP-SMX and dapsone hydroxylamine metabolites (Reilly et al., 1999). The above studies showed that sulfoxide is more likely to consume reduced glutathione in red blood cells as an oxidant, so we do not advise patients with G6PD deficiency to choose sulfoxide to prevent or treat PCP.

4.2 The effect of non-oxidants

As for the prevention and treatment of PCP, gene screening and enzyme activity examination are the first step in patients with G6PD deficiency. Then, we recommended different drugs according to the degree of enzyme deficiency. We should conduct Long-term follow-ups in patients with a serious degree of G6PD deficiency, and tell the one and their families about the food and drugs which is prohibited and cautious to use. Regardless of the degree of enzyme deficiency in patients, we should also give the appropriate medication guidance to patients to prevent hemolytic diseases. In this paper, we summarize several PCP prophylaxes and therapeutic drugs for the patients with G6PD deficiency.

4.2.1 Atovaquone

Atovaquone is traditionally known as a broad-spectrum antiparasitic drug. It is similar to the coenzyme Q, which inhibits the electron transport chain by preventing ubiquinone from binding to cytochrome B (Baggish and Hill, 2002). HIV-infected patients with TMP-SMX or sulfoxide tolerance, especially patients with G6PD deficiency (also known as favism), can be treated with Atovaquone. Although Atovaquone is not as effect availability as TMP-SMX in the PCP, its main advantage is oral administration, tolerable side effects, and fewer adverse reactions, so it is the replacement therapy for mild to moderate PCP (Weyant et al., 2021). Among solid organ transplant recipients with regular G6PD activity, dapsone had more significant haemoglobin reduction and drug discontinuation rates compared with Atovaquone (Hedvat et al., 2021). Douzinas et al. reported A clinical case in a G6PD deficiency patient with severe PCP infection have completely cured with Atovaquone (Douzinas et al., 2010). However, Atovaquone cannot be used in combination with rifampin, azanavir and weilun, because these drugs can reduce its blood concentration.

4.2.2 Pentamidine

Pentamidine is an aromatic diamidine with a wider scope of antimicrobial effects. And it has an optimal investigation in antigenic animals such as trypanosomiasis and leishmaniasis. It is given that it has a broad antibacterial mechanism. It can reduce polyamine synthesis by inhibiting the ornithine carboxylase and binding the Trypanosoma motor DNA and RNA to reduce polyamine synthesis. It can also inhibit polymerase impairment of ribosome function and the synthesis of nucleic acid and protein. The mechanism of action remains unclear. There is currently sufficient evidence for the use of pentamidine in the treatment of PCP, and we recommend intravenous injection as a major alternative to TMP-SMX for moderate to severe PCP (Calderón et al., 2010). The effective rate of atomizing Pentamidine in preventing the first attack of PCP in HIV- infected patients was 60–70%. There were no apparent side effects except cough (Hirschel et al., 1991). A systematic review of the second-line treatment of PCP suggests that Pentamidine may be more commonly used in patients with severe PCP but may lead to more deaths than TMP-SMX due to the adverse risk of spraying amidine (Benfield et al., 2008). In addition, a retrospective research of adverse reactions caused by pentamidine treatment of PCP showed that nephrotoxicity, abnormal blood glucose, hepatotoxicity, hyperkalemia, and hyperamylasemia accounted for 80%, and hemolytic anaemia was not reported (O'Brien et al., 1997). So, Pentamidine is a relatively safe option in patients with G6PD deficiency.

4.2.3 Clindamycin

Clindamycin is one of the Lincomycin derivatives and has good antimicrobial activity against Gram's positive bacterium and Gram-negative anaerobes. The primary mechanism is to inhibit the ribosome of 50s and prevent the synthesis of proteins. In protozoa, the target of clindamycin is a parasite-specific organelle (a plastid organelle), which reduces toxin production in bacterial staphylococci and streptococci. However, the mechanism of its use in the treatment of PCP is not precise (Fichera and Roos, 1997). Clindamycin combined with primaquine as a second-line treatment is more effective than Pentamidine in patients with TMP-SMX intolerance, according to a study (Kim et al., 2009). In a meta-analysis by Smego et al., the success rate of clindamycin combined with primaquine in the treatment of PCP was 92% higher than that of Atovaquone and Pentamidine (Smego et al., 2001). There are no reports of hemolytic anaemia caused by clindamycin in patients with G6PD deficiency. However, clindamycin and primaquine are often combined to prevent and treat PCP. As an oxidant, primaquine has a particular effect on G6PD deficiency

patients. However, studies in recent years have reported that low-dose primaquine has less risk of hemolytic anaemia in G6PD deficiency (Eziefula et al., 2014; Bancone et al., 2016; Mwaiswelo et al., 2016; Uthman et al., 2017; Bastiaens et al., 2018; Dysoley et al., 2019). Clindamycin combined with low dose primaquine may be a potential solution for PCP patients with G6PD deficiency, but more clinical trials are needed to validate this regimen.

4.2.4 Echinocandins

Echinocandins (such as caspofungin, micafungin, etc.) are a new class of antifungal drugs targeting β (1, 3)-D-glucan. Because there is β (1, 3)-D-glucan in the cell wall of cysticercosis, Echinocandins can kill pneumocystis by inhibiting the synthesis of β (1, 3)-D-glucan. Some animal experiments showed that the drug was influential in the animal model of PCP (Furuta et al., 1997; Kamboj et al., 2006). There is no wide prospective analysis on the management of PCP with Echinocandins, and many case reports or cohort studies reported the clinical data as a remedial measure for the failure of TMP-SMX (Annaloro et al., 2006; Hof and Schnülle, 2008; Armstrong-James et al., 2011). Herbert Hof reported a 60-year-old patient with PCP complicated with Wegener granulomatosis. After failing to respond to TMP-SMX treatment, the patient switched to intravenous caspofungin at a load dosage of 70 mg and a maintenance dose of 50 mg/day. Symptoms improved 3 weeks later (Hof and Schnülle, 2008). The success of this case suggests that echinocandin may be a reliable candidate for the treatment of PCP, which deserves more research and attention.

Similarly, ten patients who could not tolerate first-line therapy used caspofungin in a European retrospective clinical study of HIV with PCP. Eight patients were successfully treated (one patient died of pneumothorax, and one died of lymphoma). Who suggested that caspofungin was effective as a salvage treatment (Armstrong-James et al., 2011). There is less data on Echinocandins in G6PD deficiency and PCP. Still, some clinical cases presented that an HIV-infected patient diagnosed with PCP and G6PD deficiency achieved successful results after 3 weeks of treatment with Anidulafungin when TMP-SMX was disabled (Chang et al., 2018).

4.3 Assisting effect

4.3.1 Glucocorticoids

Glucocorticoids as immunosuppressants may increase the chance of Pneumocystis pneumonia infection. Higher doses of glucocorticoids have been reported in some studies related to higher mortality in patients with PCP (Ando et al., 2019). So, is glucocorticoid appropriate as a treatment for PCP patients with G6PD deficiency? We found the answer through some clinical reports. For patients with severe HIV-associated PCP, adjunctive corticosteroids are an advocate in PCP patients whose arterial oxygen partial pressure is lower than 70 mmHg. Early use of glucocorticoids can reduce pulmonary inflammation and edema, improve respiratory status, reduce the risk of respiratory failure, and improve the severe adverse reactions caused by sulfonamides (Bozzette et al., 1990; Gagnon et al., 1990; Wazir and Ansari, 2004). A meta-analysis showed that adjuvant corticosteroid therapy could reduce the hazard of death in the HIV-associated PCP population with hypoxia. Still, there is no evidence that adjuvant glucocorticoid therapy was effective for mild PCP (Briel et al., 2005). Moreover there are limited data to support the action of adjuvant corticosteroids in the therapy of non-HIV-associated PCP, and further research is needed to explain the role of corticosteroids in PCP (Injean et al., 2017). So, for patients with severe PCP, early glucocorticoid use seems beneficial. However, there is little evidence that auxiliary glucocorticoid is effective for mild PCP.

5 Summary

There are several different degrees according to enzyme activity in G6PD deficiency. Patients with a mild enzyme activity deficiency may not have any adverse reactions. Still, patients with a moderate and severe lack of enzymes may have hemolytic anaemia and other severe consequences after using oxidants, such as sulfanilamide, dapsone and primaquine. Therefore, it is challenging to select medicines for PCP when the activity of G6PD is unknown. If medical conditions permit, we recommend measuring the G6PD enzyme activity before using oxidant drugs. The patient's hematocrit and the clinical manifestation of hemolysis should be monitored regularly during oxidant drugs (Todd et al., 1994; Belfield and Tichy, 2018). For patients with G6PD deficiency, according to the enzyme activity, the most effective measure is to avoid exposure to oxidant drugs. Choose atovaquone and pentamidine, which have more evidence in the alternative plan. Other drugs, such as clindamycin, Echinocandins, and glucocorticoid, can be used as a single or combined remedy.

6 Discussion

The screening of G6PD deficiency in China is still not routine surveillance, and its pathogenesis belongs to X chromosome linkage incomplete dominant inheritance. Male patients usually show a significant decrease in enzyme activity, while female patients are mainly heterozygotes. The range of G6PD enzyme activity varies widely, and the diagnosis is difficult, which challenges the choice of drugs. If such patients use oxidant drugs, they may have serious consequences: such as sulfonamides, which can lead to dangerous or fatal hemolytic anaemia

(Bernstein and Lorincz, 1981; Norby et al., 1981). For G6PD deficiency, primaquine should be avoided or carefully used under the supervision of experts (Kovacs and Masur, 2009; Lalloo et al., 2016). In addition, even after taking the standard dose of primaquine, the specific volume of blood cells began to decrease at 2–4 days, reached the lowest level at 8–12 days, and developed reticulocytosis 4–6 days later, accompanied by elevated serum bilirubin, as well as a series of symptoms of fatigue, grief, fever, and jaundice (Reinke et al., 1995). Therefore, we generally do not recommend oxidant-type drugs for patients with G6PD deficiency who need to prevent or treat PCP.

Pneumocystis pneumonia is the most common life-threatening infection in immunocompromised populations. A study reported that in the absence of prevention, the incidence of PCP in solid organ transplant recipients was 6.8–22%, so it is recommended to receive PCP prevention at least 6 months after organ transplantation (Al-Raisi et al., 2009). People living with HIV, recipients of hematopoietic stem cell transplantation (HCT) or solid organ transplantation, cancer patients (especially patients with hematological malignancies), and people with low immunity receiving glucocorticoids, chemotherapy drugs and other immunosuppressive drugs are all at high risk for PCP infection. The National Comprehensive *Cancer* Network (NCCN) Clinical Practice Guidelines in Oncology recommend that in acute lymphoblastic leukemia, the prevention of PCP should run through the entire anti-leukemia treatment process. We successfully implemented PCP prevention for a 4 - year-old child with G6PD deficiency and acute T-lymphocyte leukemia. The patient was screened in Sichuan Provincial People's Hospital at birth and found to have decreased G6PD enzyme activity and diagnosed with G6PD deficiency. The boy was diagnosed with acute T-cell lymphoblastic leukemia in September 2021. He had been treated with vincristine, daunorubicin, thiopurine, and dexamethasone, and intrathecal injection of methotrexate, cytarabine, and dexamethasone to prevent central leukemia. According to the NCCN guidelines, patients with acute lymphoblastic leukemia who were treated with chemotherapy drugs were at high risk of PCP infection. We implemented measures to prevent PCP in the boy. Due to the lack of G6PD, clindamycin 5 mg/kg was selected as the second-line regimen to prevent PCP thrice a day. During the treatment of leukemia for half a year, the infection of PCP was successfully avoided in children, indicating that clindamycin can be used as a preventive drug for such patients, with good safety and no adverse reactions such as hemolytic anemia.

Combined with clinical cases and previous experience, we suggest that for patients with G6PD deficiency, it is recommended that red blood cells, haemoglobin, reticulocytes, etc., should be monitored regularly before or after the use of sulfonamides or sulfoxide and other oxidant drugs, because some adverse reactions such as hemolytic anaemia may subside when sulfonamides stop taking drugs (Bernstein and Lorincz, 1981). Not clear about the inspection indicators will affect our diagnosis of G6PD deficiency and may have adverse effects on the future when using oxidant drugs. For patients with G6PD deficiency, regardless of their enzyme activity, our recommendation is to avoid the application of control for PCP and to choose other drugs as alternative treatments; we recommend six options as follows:

1) Atovaquone is rarely used in China, making it difficult to obtain these drugs, especially in many primary hospitals in China. However, it is still an adequate substitute for the PCP's prophylactic and therapeutic. For patients with G6PD deficiency, we recommend that Atovaquone 750 mg be taken twice a day for oral treatment or 1500 mg once daily for prevention (Dennis and Kasper, 2019).
2) Pentamidine is a recommended alternative drug for PCP in the current guidelines, including 3~4 mg/kg, given intravenously once a day, or 300 mg monthly atomization therapy to prevent PCP (Dennis and Kasper, 2019). The efficacy is worse than that of Atovaquone, TMP-SMX, or dapsone, but its occurrence of hemolytic anaemia in patients with G6PD deficiency is minor. So, it is also our recommended drug.
3) In recent years, there have been reports and studies on the adverse reactions to haemoglobin reduction of primaquine. Whether or not patients suffer from G6PD deficiency, many studies have confirmed that there is no a significant difference in the adverse reactions of hemolytic anaemia between patients with G6PD deficiency and ordinary patients when primaquine is used with a low dose of 0.25 mg/kg/d. Therefore, we suggest that without other better options, patients with G6PD deficiency can be given low dose primaquine 0.25 mg/kg/d under the supervision of a doctor. Not more than 7 days of use, and need to monitor haemoglobin, red blood cells, reticulocytes, and so on.
4) In our case, Clindamycin is also a good choice about it successfully prevented PCP infection in a 4-year-old child. Regarding clindamycin treatment, we generally do not recommend a single drug treatment because its single drug use effect is poor. As the PCP alternatives treatment, we recommend clindamycin 300–450 mg Every 6 h, or 600 mg, Every 6–8 h (Dennis and Kasper, 2019)combined with primaquine 0.25 mg/kg/d. Pay close attention to the use of related blood indicators.
5) Caspofungin is an alternative therapy for PCP. However, there are few reports, and several literature reports on the treatment of PCP of sulfonamides are not suitable for successful examples. In addition, Carpofungin is metabolized slowly by hydrolysis and n-acetylation and spontaneous chemical degradation without the inhibition of the CYP system. According to the treatment experience, our recommended dose is 70 mg/d for the first time, followed by 50 mg/d, and the course of treatment depends on the patient's remission (Annaloro et al., 2006; Hof and Schnülle, 2008; Armstrong-James et al., 2011). It may be a wonderful

choice for PCP patients with G6PD deficiency who cannot tolerate sulfonamides, dapsone, primaquine and other drugs.

6) Although the evidence is limited, prednisone or methylprednisolone 40 mg once or twice a day for 5 days in patients with moderate to severe PCP is recommended (Bozzette et al., 1990; Gagnon et al., 1990). A reasonable method is to treat patients by taking at least 20 mg of prednisone a day for more than 1 month (Kovacs and Masur, 2009).

There were differences in the risk of drug use in patients with G6PD deficiency due to genetic polymorphism. Although a few case reports suggest that some patients have a low risk of hemolysis after medication, we still should monitor during treatment. Our suggestions come from clinical studies and case reports. We have not found randomized controlled trials or meta-analyses to demonstrate our views, so our opinions have some limitations. We expect that there will be more clinical studies on the prevention and treatment of PCP infection in G6PD patients in the future to provide the basis and guarantee for the safety of drug use in these patients.

Author contributions

In this paper, ZZ, QL, XS, LL, XW, and MS have sorted out the literature and wrote the paper. XZ provides medication guidance in cases and article revisions. YZ and YY modifies and guides the manuscript. All the authors read the manuscript and approved the submission.

Funding

This research is supported by the key R&D project of Science and Technology Department of Sichuan Province (No. 2022YFS0059).

Acknowledgments

We acknowledge the support from Sichuan Academy of Medical Sciences and Sichuan Provincial People's Hospital, University of Electronic Science and Technology of China, The First People's Hospital of Ziyang, Ziyang People's Hospital, and the Qingbaijiang District people's Hospital.

Conflict of interest

The authors declare that the research was conducted in the absence of any commercial or financial relationships that could be construed as a potential conflict of interest.

Publisher's note

All claims expressed in this article are solely those of the authors and do not necessarily represent those of their affiliated organizations, or those of the publisher, the editors and the reviewers. Any product that may be evaluated in this article, or claim that may be made by its manufacturer, is not guaranteed or endorsed by the publisher.

References

Allen, S. D., and Wilkerson, J. L. (1972). The importance of glucose-6-phosphate dehydrogenase screening in a urologic practice. *J. Urol.* 107 (2), 304–305. doi:10.1016/s0022-5347(17)61010-3

Alloueche, A., Bailey, W., Barton, S., Bwika, J., Chimpeni, P., Falade, C. O., et al. (2004). Comparison of chlorproguanil-dapsone with sulfadoxine-pyrimethamine for the treatment of uncomplicated falciparum malaria in young african children: double-blind randomised controlled trial. *Lancet* 363 (9424), 1843–1848. doi:10.1016/s0140-6736(04)16350-2

Al-Raisi, F., Al-Mawali, G., Al-Naamani, H., and Al-Barwani, U. (2009). Prophylaxis for opportunistic infections for kidney transplantation recipients at the royal hospital in Oman. *Oman Med. J.* 24 (1), 37–40. doi:10.5001/omj.2009.10

Ando, T., Abe, Y., Endo, Y., Tada, K., Yamaji, K., Tamura, N., et al. (2019). Rapid glucocorticoid tapering therapy to reduce mortality from pneumocystis pneumonia in patients with rheumatic disease. *Mod. Rheumatol.* 29 (4), 656–661. doi:10.1080/14397595.2018.1496873

Annaloro, C., Della Volpe, A., Usardi, P., Lambertenghi Deliliers, G., and DellA Volpe, A. (2006). Caspofungin treatment of Pneumocystis pneumonia during conditioning for bone marrow transplantation. *Eur. J. Clin. Microbiol. Infect. Dis.* 25 (1), 52–54. doi:10.1007/s10096-005-0065-z

Armstrong-James, D., Stebbing, J., John, L., Murungi, A., Bower, M., Gazzard, B., et al. (2011). A trial of caspofungin salvage treatment in PCP pneumonia. *Thorax* 66 (6), 537–538. doi:10.1136/thx.2010.135350

Au, S. W., Gover, S., Lam, V. M., and Adams, M. J. (2000). Human glucose-6-phosphate dehydrogenase: the crystal structure reveals a structural NADP(+) molecule and provides insights into enzyme deficiency. *Structure* 8 (3), 293–303. doi:10.1016/s0969-2126(00)00104-0

Azoulay, É., Bergeron, A., Chevret, S., Bele, N., Schlemmer, B., Menotti, J., et al. (2009). Polymerase chain reaction for diagnosing pneumocystis pneumonia in non-HIV immunocompromised patients with pulmonary infiltrates. *Chest* 135 (3), 655–661. doi:10.1378/chest.08-1309

Baggish, A. L., and Hill, D. R. (2002). Antiparasitic agent atovaquone. *Antimicrob. Agents Chemother.* 46 (5), 1163–1173. doi:10.1128/aac.46.5.1163-1173.2002

Bancone, G., Chowwiwat, N., Somsakchaicharoen, R., Poodpanya, L., Moo, P. K., Gornsawun, G., et al. (2016). Single low dose primaquine (0.25 mg/kg) does not cause clinically significant haemolysis in G6PD deficient subjects. *PLoS One* 11 (3), e0151898. doi:10.1371/journal.pone.0151898

Bastiaens, G. J. H., Tiono, A. B., Okebe, J., Pett, H. E., Coulibaly, S. A., Gonçalves, B. P., et al. (2018). Safety of single low-dose primaquine in glucose-6-phosphate dehydrogenase deficient falciparum-infected African males: two open-label, randomized, safety trials. *PLoS One* 13 (1), e0190272. doi:10.1371/journal.pone.0190272

Belfield, K. D., and Tichy, E. M. (2018). Review and drug therapy implications of glucose-6-phosphate dehydrogenase deficiency. *Am. J. Health. Syst. Pharm.* 75 (3), 97–104. doi:10.2146/ajhp160961

Bellamy, R. J. (2008). HIV: treating pneumocystis pneumonia (PCP). *BMJ Clin. Evid.* 2008, 2501.

Benfield, T., Atzori, C., Miller, R. F., and Helweg-Larsen, J. (2008). Second-line salvage treatment of AIDS-associated pneumocystis jirovecii pneumonia: a case

series and systematic review. *J. Acquir. Immune Defic. Syndr.* 48 (1), 63–67. doi:10.1097/QAI.0b013e31816de84d

Bernstein, J. E., and Lorincz, A. L. (1981). Sulfonamides and sulfones in dermatologic therapy. *Int. J. Dermatol.* 20 (2), 81–88. doi:10.1111/j.1365-4362.1981.tb00406.x

Beutler, E., Yeh, M., and Fairbanks, V. F. (1962). The normal human female as a mosaic of X-chromosome activity: studies using the gene for C-6-PD-deficiency as a marker. *Proc. Natl. Acad. Sci. U. S. A.* 48 (1), 9–16. doi:10.1073/pnas.48.1.9

Beutler, E. (1959). The hemolytic effect of primaquine and related compounds: a review. *Blood* 14 (2), 103–139. doi:10.1182/blood.v14.2.103.103

Beutler, E. (1964). Drug-induced blood dyscrasias.III.hemolytic anemia. *JAMA* 189, 143–144. doi:10.1001/jama.1964.03070020071015

Beutler, E. (1996). G6PD: Population genetics and clinical manifestations. *Blood Rev.* 10 (1), 45–52. doi:10.1016/s0268-960x(96)90019-3

Bozzette, S. A., Sattler, F. R., Chiu, J., Wu, A. W., Gluckstein, D., Kemper, C., et al. (1990). A controlled trial of early adjunctive treatment with corticosteroids for Pneumocystis carinii pneumonia in the acquired immunodeficiency syndrome. California Collaborative Treatment Group. *N. Engl. J. Med.* 323 (21), 1451–1457. doi:10.1056/nejm199011223232104

Brakemeier, S., Pfau, A., Zukunft, B., Budde, K., and Nickel, P. (2018). Prophylaxis and treatment of Pneumocystis Jirovecii pneumonia after solid organ transplantation. *Pharmacol. Res.* 134, 61–67. doi:10.1016/j.phrs.2018.06.010

Brewer, G. J., and Zarafonetis, C. J. (1967). The haemolytic effect of various regimens of primaquine with chloroquine in American Negroes with G6PD deficiency and the lack of an effect of various antimalarial suppressive agents on erythrocyte metabolism. *Bull. World Health Organ.* 36 (2), 303–308.

Briel, M., Boscacci, R., Furrer, H., and Bucher, H. C. (2005). Adjunctive corticosteroids for pneumocystis jiroveci pneumonia in patients with HIV infection: a meta-analysis of randomised controlled trials. *BMC Infect. Dis.* 5, 101. doi:10.1186/1471-2334-5-101

Calderón, E. J., Gutiérrez-Rivero, S., Durand-Joly, I., and Dei-Cas, E. (2010). Pneumocystis infection in humans: diagnosis and treatment. *Expert Rev. Anti. Infect. Ther.* 8 (6), 683–701. doi:10.1586/eri.10.42

Cappellini, M. D., and Fiorelli, G. (2008). Glucose-6-phosphate dehydrogenase deficiency. *Lancet* 371 (9606), 64–74. doi:10.1016/s0140-6736(08)60073-2

Carmona, E. M., and Limper, A. H. (2011). Update on the diagnosis and treatment of Pneumocystis pneumonia. *Ther. Adv. Respir. Dis.* 5 (1), 41–59. doi:10.1177/1753465810380102

Castro, M. (1998). Treatment and prophylaxis of Pneumocystis carinii pneumonia. *Semin. Respir. Infect.* 13 (4), 296–303.

Catherinot, E., Lanternier, F., Bougnoux, M. E., Lecuit, M., Couderc, L. J., Lortholary, O., et al. (2010). Pneumocystis jirovecii pneumonia. *Infect. Dis. Clin. North Am.* 24 (1), 107–138. doi:10.1016/j.idc.2009.10.010

Chan, T. K., Todd, D., and Tso, S. C. (1976). Drug-induced haemolysis in glucose-6-phosphate dehydrogenase deficiency. *Br. Med. J.* 2 (6046), 1227–1229. doi:10.1136/bmj.2.6046.1227

Chang, H. C., Yang, W. T., and Chen, T. C. (2018). Pneumocystis jirovecii pneumonia in a human immunodeficiency virus-infected patient with G6PD deficiency-successful treatment with anidulafungin. *Eur. Rev. Med. Pharmacol. Sci.* 22 (24), 8961–8964. doi:10.26355/eurrev_201812_16666

Cohen, G., and Hochstein, P. (1963). Glutathione peroxidase: the primary agent for the elimination of hydrogen peroxide in erythrocytes. *Biochemistry* 2, 1420–1428. doi:10.1021/bi00906a038

Davey, R. T., and Masur, H. (1990). Recent advances in the diagnosis, treatment, and prevention of Pneumocystis carinii pneumonia. *Antimicrob. Agents Chemother.* 34 (4), 499–504. doi:10.1128/aac.34.4.499

Dei-Cas, E. (2000). Pneumocystis infections: the iceberg? *Med. Mycol.* 38 (1), 23–32. doi:10.1080/mmy.38.s1.23.32

Dennis, L., and Kasper, A. S. F. (2019). *Harrison's™ infectious diseases*. Shanghai: McGraw-Hill Education and Shanghai Scientific and Techical publishers.

Douzinas, E. E., Flevari, K., Andrianakis, I., and Betrosian, A. P. (2010). Oral atovaquone for the treatment of severe Pneumocystis jirovecii pneumonia in a patient with glucose-6-phosphate dehydrogenase deficiency. *Scand. J. Infect. Dis.* 42 (1), 76–78. doi:10.3109/00365540903321606

Doxiadis, S. A., Karaklis, A., Valaes, T., and Stavrakakis, D. (1964). Risk of severe jaundice in glucose-6-phosphate-dehydrogenase deficiency of the newborn. Differences in population groups. *Lancet (London, England)* 2 (7371), 1210–1212. doi:10.1016/s0140-6736(64)91044-x

Dysoley, L., Kim, S., Lopes, S., Khim, N., Bjorges, S., Top, S., et al. (2019). The tolerability of single low dose primaquine in glucose-6-phosphate deficient and normal falciparum-infected Cambodians. *BMC Infect. Dis.* 19 (1), 250. doi:10.1186/s12879-019-3862-1

Eziefula, A. C., Pett, H., Grignard, L., Opus, S., Kiggundu, M., Kamya, M. R., et al. (2014). Glucose-6-phosphate dehydrogenase status and risk of hemolysis in Plasmodium falciparum-infected African children receiving single-dose primaquine. *Antimicrob. Agents Chemother.* 58 (8), 4971–4973. doi:10.1128/aac.02889-14

Fichera, M. E., and Roos, D. S. (1997). A plastid organelle as a drug target in apicomplexan parasites. *Nature* 390 (6658), 407–409. doi:10.1038/37132

Frank, J. E. (2005). Diagnosis and management of G6PD deficiency. *Am. Fam. Physician* 72 (7), 1277–1282.

Fujii, T., Nakamura, T., and Iwamoto, A. (2007). Pneumocystis pneumonia in patients with HIV infection: clinical manifestations, laboratory findings, and radiological features. *J. Infect. Chemother.* 13 (1), 1–7. doi:10.1007/s10156-006-0484-5

Furuta, T., Muramatsu, H., Fujie, A., and Fujihira, S. (1997). Therapeutic effect of a water soluble echinocandin compound on Pneumocystis pneumonia in animals. *J. Eukaryot. Microbiol.* 44 (6), 53s. doi:10.1111/j.1550-7408.1997.tb05774.x

Gagnon, S., Boota, A. M., Fischl, M. A., Baier, H., Kirksey, O. W., La Voie, L., et al. (1990). Corticosteroids as adjunctive therapy for severe Pneumocystis carinii pneumonia in the acquired immunodeficiency syndrome. A double-blind, placebo-controlled trial. *N. Engl. J. Med.* 323 (21), 1444–1450. doi:10.1056/nejm199011223232103

Gilroy, S. A., and Bennett, N. J. (2011). Pneumocystis pneumonia. *Semin. Respir. Crit. Care Med.* 32 (6), 775–782. doi:10.1055/s-0031-1295725

Goto, N., and Oka, S. (2011). Pneumocystis jirovecii pneumonia in kidney transplantation. *Transpl. Infect. Dis.* 13 (6), 551–558. doi:10.1111/j.1399-3062.2011.00691.x

Greenberg, M. S., and Wong, H. (1961). Studies on the destruction of glutathione-unstable red blood cells. The influence of fava beans and primaquine upon such cells *in vivo*. *J. Lab. Clin. Med.* 57, 733–746.

Grossman, S. J., and Jollow, D. J. (1988). Role of dapsone hydroxylamine in dapsone-induced hemolytic anemia. *J. Pharmacol. Exp. Ther.* 244 (1), 118–125.

Grossman, S., Budinsky, R., and Jollow, D. (1995). Dapsone-induced hemolytic anemia: role of glucose-6-phosphate dehydrogenase in the hemolytic response of rat erythrocytes to N-hydroxydapsone. *J. Pharmacol. Exp. Ther.* 273 (2), 870–877.

Harcke, S. J., Rizzolo, D., and Harcke, H. T. (2019). G6PD deficiency: an update. *JAAPA* 32 (11), 21–26. doi:10.1097/01.JAA.0000586304.65429.a7

Hedvat, J., Poladi, N., Salerno, D. M., Dube, G. K., and Lange, N. W. (2021). An evaluation of PJP prophylaxis and anemia among renal transplant recipients. *Transpl. Infect. Dis.* 23 (3), e13543. doi:10.1111/tid.13543

Herrag, M., Elfassy Fihry, M. T., and Alaoui Yazidi, A. (2010). Pneumocystis jirovecii: what does this mean? *Rev. Pneumol. Clin.* 66 (6), 342–346. doi:10.1016/j.pneumo.2009.09.007

Hirschel, B., Lazzarin, A., Chopard, P., Opravil, M., Furrer, H. J., Rüttimann, S., et al. (1991). A controlled study of inhaled pentamidine for primary prevention of Pneumocystis carinii pneumonia. *N. Engl. J. Med.* 324 (16), 1079–1083. doi:10.1056/nejm199104183241602

Hof, H., and Schnülle, P. (2008). Pneumocystis jiroveci pneumonia in a patient with Wegener's granulomatosis treated efficiently with caspofungin. *Mycoses* 51 (1), 65–67. doi:10.1111/j.1439-0507.2008.01530.x

Huang, L., Morris, A., Limper, A. H., and Beck, J. M. (2006). An Official ATS workshop summary: recent advances and future directions in pneumocystis pneumonia (PCP). *Proc. Am. Thorac. Soc.* 3 (8), 655–664. doi:10.1513/pats.200602-015MS

Huang, L. (2011). Clinical and translational research in pneumocystis and pneumocystis pneumonia. *Parasite* 18 (1), 3–11. doi:10.1051/parasite/2011181003

Hughes, W. T., Feldman, S., Aur, R. J., Verzosa, M. S., Hustu, H. O., Simone, J. V., et al. (1975). Intensity of immunosuppressive therapy and the incidence of Pneumocystis carinii pneumonitis. *Cancer* 36 (6), 2004–2009. doi:10.1002/cncr.2820360912

Injean, P., Eells, S. J., Wu, H., McElroy, I., Gregson, A. L., McKinnell, J. A., et al. (2017). A systematic review and meta-analysis of the data behind current recommendations for corticosteroids in non-HIV-related PCP: knowing when you are on shaky foundations. *Transpl. Direct* 3 (3), e137. doi:10.1097/txd.0000000000000642

Jiang, W., Yu, G., Liu, P., Geng, Q., Chen, L., Lin, Q., et al. (2006). Structure and function of glucose-6-phosphate dehydrogenase-deficient variants in Chinese population. *Hum. Genet.* 119 (5), 463–478. doi:10.1007/s00439-005-0126-5

Jollow, D. J., Bradshaw, T. P., and McMillan, D. C. (1995). Dapsone-induced hemolytic anemia. *Drug Metab. Rev.* 27 (1-2), 107–124. doi:10.3109/03602539509029818

Kamboj, M., Weinstock, D., and Sepkowitz, K. A. (2006). Progression of Pneumocystis jiroveci pneumonia in patients receiving echinocandin therapy. *Clin. Infect. Dis.* 43 (9), e92–94. doi:10.1086/508282

Kim, T., Kim, S. H., Park, K. H., Cho, O. H., Sung, H., Kim, M. N., et al. (2009). Clindamycin-primaquine versus pentamidine for the second-line treatment of pneumocystis pneumonia. *J. Infect. Chemother.* 15 (5), 343–346. doi:10.1007/s10156-009-0710-z

Kovacs, J. A., and Masur, H. (2009). Evolving health effects of pneumocystis: One hundred years of progress in diagnosis and treatment. *JAMA* 301 (24), 2578–2585. doi:10.1001/jama.2009.880

Krajicek, B. J., Limper, A. H., and Thomas, C. F. (2008). Advances in the biology, pathogenesis and identification of Pneumocystis pneumonia. *Curr. Opin. Pulm. Med.* 14 (3), 228–234. doi:10.1097/MCP.0b013e3282f94abc

Krudsood, S., Wilairatana, P., Tangpukdee, N., Chalermrut, K., Srivilairit, S., Thanachartwet, V., et al. (2006). Safety and tolerability of elubaquine (bulaquine, CDRI 80/53) for treatment of Plasmidium vivax malaria in Thailand. *Korean J. Parasitol.* 44 (3), 221–228. doi:10.3347/kjp.2006.44.3.221

Lalloo, D. G., Shingadia, D., Bell, D. J., Beeching, N. J., Whitty, C. J. M., and Chiodini, P. L. (2016). UK malaria treatment guidelines 2016. *J. Infect.* 72 (6), 635–649. doi:10.1016/j.jinf.2016.02.001

Lee, S. M., and Geetha, D. (2015). Dapsone induced hemolysis in a patient with ANCA associated glomerulonephritis and normal G6PD level and implications for clinical practice: case report and review of the literature. *Springerplus* 4, 29. doi:10.1186/s40064-015-0816-y

Liu, W. L., Li, F., He, Z. X., Jiang, H. Y., and Ai, R. (2012). Glucose-6-phosphate dehydrogenase qingzhen: identification of a novel splice mutation (IVS5-1 G>A). *Pediatr. Blood Cancer* 58 (5), 825–826. doi:10.1002/pbc.23345

Lu, J. J., and Lee, C. H. (2008). Pneumocystis pneumonia. *J. Formos. Med. Assoc.* 107 (11), 830–842. doi:10.1016/s0929-6646(08)60199-0

Luzzatto, L., Nannelli, C., and Notaro, R. (2016). Glucose-6-Phosphate dehydrogenase deficiency. *Hematol. Oncol. Clin. North Am.* 30 (2), 373–393. doi:10.1016/j.hoc.2015.11.006

Luzzatto, L. (2012). G6PD deficiency and malaria selection. *Hered. (Edinb)* 108 (4), 456. doi:10.1038/hdy.2011.90

Maschmeyer, G., Helweg-Larsen, J., Pagano, L., Robin, C., Cordonnier, C., and Schellongowski, P. (2016). ECIL guidelines for treatment of Pneumocystis jirovecii pneumonia in non-HIV-infected haematology patients. *J. Antimicrob. Chemother.* 71 (9), 2405–2413. doi:10.1093/jac/dkw158

Mbanefo, E. C., Ahmed, A. M., Titouna, A., Elmaraezy, A., Trang, N. T., Phuoc Long, N., et al. (2017). Association of glucose-6-phosphate dehydrogenase deficiency and malaria: a systematic review and meta-analysis. *Sci. Rep.* 7, 45963. doi:10.1038/srep45963

Mitsides, N., Green, D., Middleton, R., New, D., Lamerton, E., Allen, J., et al. (2014). Dapsone-induced methemoglobinemia in renal transplant recipients: more prevalent than previously thought. *Transpl. Infect. Dis.* 16 (1), 37–43. doi:10.1111/tid.12161

Mwaiswelo, R., Ngasala, B. E., Jovel, I., Gosling, R., Premji, Z., Poirot, E., et al. (2016). Safety of a single low-dose of primaquine in addition to standard artemether-lumefantrine regimen for treatment of acute uncomplicated Plasmodium falciparum malaria in Tanzania. *Malar. J.* 15, 316. doi:10.1186/s12936-016-1341-3

Norby, L. H., Bethencourt, D., and Schwartz, J. H. (1981). Dual effect of carbonic anhydrase inhibitors on H+ transport by the turtle bladder. *Am. J. Physiol.* 240 (5), F400–F405. doi:10.1152/ajprenal.1981.240.5.F400

Norden, C. W., Desforges, J. F., and Kass, E. H. (1968). Hemolytic effect of sulfonamides in patients with erythrocytes deficient in glucose-6-phosphate dehydrogenase. *N. Engl. J. Med.* 279 (1), 30–31. doi:10.1056/nejm196807042790107

O'Brien, J. G., Dong, B. J., Coleman, R. L., Gee, L., and Balano, K. B. (1997). A 5-year retrospective review of adverse drug reactions and their risk factors in human immunodeficiency virus-infected patients who were receiving intravenous pentamidine therapy for Pneumocystis carinii pneumonia. *Clin. Infect. Dis.* 24 (5), 854–859. doi:10.1093/clinids/24.5.854

Olteanu, H., Harrington, A. M., George, B., Hari, P. N., Bredeson, C., Kroft, S. H., et al. (2012). High prevalence of Dapsone-induced oxidant hemolysis in North American SCT recipients without glucose-6-phosphate-dehydrogenase deficiency. *Bone Marrow Transpl.* 47 (3), 399–403. doi:10.1038/bmt.2011.83

Pamba, A., Richardson, N. D., Carter, N., Duparc, S., Premji, Z., Tiono, A. B., et al. (2012). Clinical spectrum and severity of hemolytic anemia in glucose 6-phosphate dehydrogenase-deficient children receiving dapsone. *Blood* 120 (20), 4123–4133. doi:10.1182/blood-2012-03-416032

Pareja, J. G., Garland, R., and Koziel, H. (1998). Use of adjunctive corticosteroids in severe adult non-HIV Pneumocystis carinii pneumonia. *Chest* 113 (5), 1215–1224. doi:10.1378/chest.113.5.1215

Ponce, C. A., Gallo, M., Bustamante, R., and Vargas, S. L. (2010). Pneumocystis colonization is highly prevalent in the autopsied lungs of the general population. *Clin. Infect. Dis.* 50 (3), 347–353. doi:10.1086/649868

Prankerd, T. A. (1964). Enzymes and drug sensitivity. Glucose 6-phosphate dehydrogenase deficiency. *Proc. R. Soc. Med.* 57, 506–508. doi:10.1177/003591576405700626

Reilly, T. P., Woster, P. M., and Svensson, C. K. (1999). Methemoglobin formation by hydroxylamine metabolites of sulfamethoxazole and dapsone: implications for differences in adverse drug reactions. *J. Pharmacol. Exp. Ther.* 288 (3), 951–959.

Reinke, C. M., Thomas, J. K., and Graves, A. H. (1995). Apparent hemolysis in an AIDS patient receiving trimethoprim/sulfamethoxazole: case report and literature review. *J. Pharm. Technol.* 11 (6), 256–262. doi:10.1177/875512259501100607

Rinaldi, A., Filippi, G., and Siniscalco, M. (1976). Variability of red cell phenotypes between and within individuals in an unbiased sample of 77 heterozygotes for G6PD deficiency in Sardinia. *Am. J. Hum. Genet.* 28 (5), 496–505.

Rockett, K. A., Clarke, G. M., Fitzpatrick, K., Hubbart, C., Jeffreys, A. E., Rowlands, K., et al. (2014). Reappraisal of known malaria resistance loci in a large multicenter study. *Nat. Genet.* 46 (11), 1197–1204. doi:10.1038/ng.3107

Rouyer, M., Stoclin, A., and Blanc, F. X. (2015). Pneumocystis pneumonia in HIV-negative adults. *Rev. Mal. Respir.* 32 (10), 985–990. doi:10.1016/j.rmr.2015.06.007

Ruwende, C., and Hill, A. (1998). Glucose-6-phosphate dehydrogenase deficiency and malaria. *J. Mol. Med.* 76 (8), 581–588. doi:10.1007/s001090050253

Sadanand, S. (2011). Harrison's infectious diseases. *Yale J. Biol. Med.* 84, 327.

Salim, S. A., Ramachandran Nair, L., Palabindala, V., and Craici, I. (2017). Upward trend of dapsone-induced methemoglobinemia in renal transplant community. *Clin. Nephrol.* 88 (9), 156–161. doi:10.5414/cn109181

Santamauro, J. T., Aurora, R. N., and Stover, D. E. (2002). Pneumocystis carinii pneumonia in patients with and without HIV infection. *Compr. Ther.* 28 (2), 96–108. doi:10.1007/s12019-002-0047-3

Sepkowitz, K. A., Brown, A. E., Telzak, E. E., Gottlieb, S., and Armstrong, D. (1992). Pneumocystis carinii pneumonia among patients without AIDS at a cancer hospital. *J. Am. Med. Assoc.* 267 (6), 832–837. doi:10.1001/jama.267.6.832

Sepkowitz, K. A., Brown, A. E., and Armstrong, D. (1995). Pneumocystis carinii pneumonia without acquired immunodeficiency syndrome. More patients, same risk. *Arch. Intern. Med.* 155 (11), 1125–1128. doi:10.1001/archinte.155.11.1125

Silachamroon, U., Krudsood, S., Treeprasertsuk, S., Wilairatana, P., Chalearmrult, K., Mint, H. Y., et al. (2003). Clinical trial of oral artesunate with or without high-dose primaquine for the treatment of vivax malaria in Thailand. *Am. J. Trop. Med. Hyg.* 69 (1), 14–18. doi:10.4269/ajtmh.2003.69.14

Singhal, R., Mirdha, B. R., and Guleria, R. (2005). Human pneumocystosis. *Indian J. Chest Dis. Allied Sci.* 47 (4), 273–283.

Smego, R. A., Nagar, S., Maloba, B., and Popara, M. (2001). A meta-analysis of salvage therapy for Pneumocystis carinii pneumonia. *Arch. Intern. Med.* 161 (12), 1529–1533. doi:10.1001/archinte.161.12.1529

Spolarics, Z., Siddiqi, M., Siegel, J. H., Garcia, Z. C., Stein, D. S., Ong, H., et al. (2001). Increased incidence of sepsis and altered monocyte functions in severely injured type A- glucose-6-phosphate dehydrogenase-deficient African American trauma patients. *Crit. Care Med.* 29 (4), 728–736. doi:10.1097/00003246-200104000-00005

Thomas, C. F., and Limper, A. H. (2007). Current insights into the biology and pathogenesis of Pneumocystis pneumonia. *Nat. Rev. Microbiol.* 5 (4), 298–308. doi:10.1038/nrmicro1621

Tine, R. C., Sylla, K., Faye, B. T., Poirot, E., Fall, F. B., Sow, D., et al. (2017). Safety and efficacy of adding a single low dose of primaquine to the treatment of adult patients with Plasmodium falciparum malaria in Senegal, to reduce gametocyte carriage: a randomized controlled trial. *Clin. Infect. Dis.* 65 (4), 535–543. doi:10.1093/cid/cix355

Todd, P., Samaratunga, I. R., and Pembroke, A. (1994). Screening for glucose-6-phosphate dehydrogenase deficiency prior to dapsone therapy. *Clin. Exp. Dermatol.* 19 (3), 217–218. doi:10.1111/j.1365-2230.1994.tb01168.x

Tsai, K. J., Hung, I. J., Chow, C. K., Stern, A., Chao, S. S., and Chiu, D. T. (1998). Impaired production of nitric oxide, superoxide, and hydrogen peroxide in glucose

6-phosphate-dehydrogenase-deficient granulocytes. *FEBS Lett.* 436 (3), 411–414. doi:10.1016/s0014-5793(98)01174-0

Uthman, O. A., Graves, P. M., Saunders, R., Gelband, H., Richardson, M., Garner, P., et al. (2017). Safety of primaquine given to people with G6PD deficiency: systematic review of prospective studies. *Malar. J.* 16 (1), 346. doi:10.1186/s12936-017-1989-3

Van Malderen, C., Van Geertruyden, J. P., Machevo, S., González, R., Bassat, Q., Talisuna, A., et al. (2012). Glucose-6-phosphate dehydrogenase deficiency, chlorproguanil-dapsone with artesunate and post-treatment haemolysis in African children treated for uncomplicated malaria. *Malar. J.* 11, 139. doi:10.1186/1475-2875-11-139

Warren, E., George, S., You, J., and Kazanjian, P. (1997). Advances in the treatment and prophylaxis of Pneumocystis carinii pneumonia. *Pharmacotherapy* 17 (5), 900–916.

Wazir, J. F., and Ansari, N. A. (2004). Pneumocystis carinii infection. Update and review. *Arch. Pathol. Lab. Med.* 128 (9), 1023–1027. doi:10.1043/1543-2165(2004)128<1023:PCI>2.0.CO;2

Weyant, R. B., Kabbani, D., Doucette, K., Lau, C., and Cervera, C. (2021). Pneumocystis jirovecii: a review with a focus on prevention and treatment. *Expert Opin. Pharmacother.* 22 (12), 1579–1592. doi:10.1080/14656566.2021.1915989

WHO Working Group (1989). Glucose-6-phosphate dehydrogenase deficiency. *Bull. World Health Organ.* 67 (6), 601–611.

Wilson, J. W., Limper, A. H., Grys, T. E., Karre, T., Wengenack, N. L., Binnicker, M. J., et al. (2011). Pneumocystis jirovecii testing by real-time polymerase chain reaction and direct examination among immunocompetent and immunosuppressed patient groups and correlation to disease specificity. *Diagn. Microbiol. Infect. Dis.* 69 (2), 145–152. doi:10.1016/j.diagmicrobio.2010.10.021

Youngster, I., Arcavi, L., Schechmaster, R., Akayzen, Y., Popliski, H., Shimonov, J., et al. (2010). Medications and glucose-6-phosphate dehydrogenase deficiency: an evidence-based review. *Drug Saf.* 33 (9), 713–726. doi:10.2165/11536520-000000000-00000

Zaman, M. K., and White, D. A. (1988). Serum lactate dehydrogenase levels and pneumocystis carinii pneumonia. Diagnostic and prognostic significance. *Am. Rev. Respir. Dis.* 137 (4), 796–800. doi:10.1164/ajrccm/137.4.796

Zhu, Y. I., and Stiller, M. J. (2001). Dapsone and sulfones in dermatology: Overview and update. *J. Am. Acad. Dermatol.* 45 (3), 420–434. doi:10.1067/mjd.2001.114733

Zipursky, A., Rowland, M., Peters, J. C., and Israels, L. G. (1965). Congenital non-spherocytic hemolytic anemia. *Can. Med. Assoc. J.* 93 (22), 1141–1146.

frontiers | Frontiers in Pharmacology

TYPE Original Research
PUBLISHED 23 September 2022
DOI 10.3389/fphar.2022.957980

OPEN ACCESS

EDITED BY
Catherine M. T. Sherwin,
Wright State University, United States

REVIEWED BY
Dmitriy Sychev,
Ministry of Health, Russia
Tara McMorrow,
University College Dublin, Ireland
Jonathan Constance,
The University of Utah, United States

*CORRESPONDENCE
Xiaoling Wang,
wangxiaoling@bch.com.cn
Xiaoxia Peng,
pengxiaoxia@bch.com.cn

†These authors have contributed equally to this work and share senior authorship

SPECIALTY SECTION
This article was submitted to Obstetric and Pediatric Pharmacology, a section of the journal Frontiers in Pharmacology

RECEIVED 31 May 2022
ACCEPTED 15 August 2022
PUBLISHED 23 September 2022

CITATION
Yu Y, Nie X, Zhao Y, Cao W, Xie Y, Peng X and Wang X (2022), Detection of pediatric drug-induced kidney injury signals using a hospital electronic medical record database. *Front. Pharmacol.* 13:957980. doi: 10.3389/fphar.2022.957980

Detection of pediatric drug-induced kidney injury signals using a hospital electronic medical record database

Yuncui Yu[1,2], Xiaolu Nie[3], Yiming Zhao[1], Wang Cao[1,2], Yuefeng Xie[4], Xiaoxia Peng[3*†] and Xiaoling Wang[1,2*†]

[1]Department of Pharmacy, National Center for Children's Health, Beijing Children's Hospital, Capital Medical University, Beijing, China, [2]Clinical Research Center, National Center for Children's Health, Beijing Children's Hospital, Capital Medical University, Beijing, China, [3]Center for Clinical Epidemiology and Evidence-Based Medicine, National Center for Children's Health, Beijing Children's Hospital, Capital Medical University, Beijing, China, [4]Information Center, National Center for Children's Health, Beijing Children's Hospital, Capital Medical University, Beijing, China

Background: Drug-induced kidney injury (DIKI) is one of the most common complications in clinical practice. Detection signals through post-marketing approaches are of great value in preventing DIKI in pediatric patients. This study aimed to propose a quantitative algorithm to detect DIKI signals in children using an electronic health record (EHR) database.

Methods: In this study, 12 years of medical data collected from a constructed data warehouse were analyzed, which contained 575,965 records of inpatients from 1 January 2009 to 31 December 2020. Eligible participants included inpatients aged 28 days to 18 years old. A two-stage procedure was adopted to detect DIKI signals: 1) stage 1: the suspected drugs potentially associated with DIKI were screened by calculating the crude incidence of DIKI events; and 2) stage 2: the associations between suspected drugs and DIKI were identified in the propensity score-matched retrospective cohorts. Unconditional logistic regression was used to analyze the difference in the incidence of DIKI events and to estimate the odds ratio (OR) and 95% confidence interval (CI). Potentially new signals were distinguished from already known associations concerning DIKI by manually reviewing the published literature and drug instructions.

Results: Nine suspected drugs were initially screened from a total of 652 drugs. Six drugs, including diazepam (OR = 1.61, 95%CI: 1.43–1.80), omeprazole (OR = 1.35, 95%CI: 1.17–1.54), ondansetron (OR = 1.49, 95%CI: 1.36–1.63), methotrexate (OR = 1.36, 95%CI: 1.25–1.47), creatine phosphate sodium (OR = 1.13, 95%CI: 1.05–1.22), and cytarabine (OR = 1.17, 95%CI: 1.06–1.28), were demonstrated to be associated with DIKI as positive signals. The remaining three drugs, including vitamin K1 (OR = 1.06, 95%CI: 0.89–1.27), cefamandole (OR = 1.07, 95%CI: 0.94–1.21), and ibuprofen (OR = 1.01, 95%CI: 0.94–1.09), were found not to be associated with DIKI. Of these, creatine phosphate sodium was considered to be a possible new DIKI signal as it had not been reported in both adults and children previously. Moreover, three other drugs, namely, diazepam, omeprazole, and ondansetron, were shown to be new potential signals in pediatrics.

Conclusion: A two-step quantitative procedure to actively explore DIKI signals using real-world data (RWD) was developed. Our findings highlight the potential of EHRs to complement traditional spontaneous reporting systems (SRS) for drug safety signal detection in a pediatric setting.

KEYWORDS

drug-induced kidney injury, children, active monitoring, electronic health records, signal detection

1 Introduction

Drug-induced kidney injury (DIKI), as one of the most common adverse drug reactions (ADRs), is a significantly increased clinical problem worldwide. It may lead to clinical symptoms such as oliguria, anuria, and acute renal failure (Radi, 2019). Studies have shown that the incidence of DIKI in hospitalized patients is about 2%–5%, accounting for 19%–40% of acute kidney injury (AKI) (Hosohata, 2016). Children are at higher risk of developing DIKI compared with adults; several factors contribute to the pediatric renal damage onset, including the immaturity of renal functions and specific pathological conditions (Faught et al., 2015a). Data from critically ill children who have DIKI suggest that survivors develop a risk for the development of chronic kidney disease (Hanna et al., 2016). In addition to that, DIKI is more likely to occur in the post-marketing of drugs than in the pre-marketing setting as its incidence is low (Faught et al., 2015b). This is particularly true for children since they are not frequently included in clinical trials. It is of great value to prevent and reduce DIKI in pediatrics through a post-marketing approach.

In most countries all over the world, national pharmacovigilance relies heavily on spontaneous reporting systems (SRS), in which suspected ADRs are reported to a national coordinating center by health professionals, manufacturers, or directly by patients. However, as a passive monitoring method, SRS has its inherent limitations, such as poor-quality reports, underreporting, and the inability to estimate rates and frequencies of ADRs (Pitts and Le Louet, 2018). Previous studies have demonstrated that 50%–90% of DIKI were unreported using SRS (Yang et al., 2015). Additional resources and methods are, therefore, needed to actively monitor the quantitative aspects of drug safety and to characterize ADRs associated with specific drugs and in specific populations. Recently, real-world data (RWD), especially data collected during routine clinical care in the form of electronic health records (EHRs), have been adopted by healthcare professionals, regulators, and providers to inform decision-making about drug safety. Several emerging pharmacovigilance programs extend the pharmacovigilance capabilities by monitoring drug safety signals actively using EHRs, such as the "Sentinel Initiative" in the United States (Toh et al., 2016), the "Exploring and Understanding Adverse Drug Reaction Project (EU-ADR)" in Europe (de Bie et al., 2015), and the "Adverse Drug Events Active Surveillance and Assessment System (ADE-ASAS)" in China (Chen et al., 2020). More attempts have also been made to develop data-mining methods based on EHRs, such as the "Global Trigger Tool (GTT)" (Garrett et al., 2013) and the "Comparison of the Laboratory Extreme Abnormality Ratio (CLEAR) algorithm" (Yoon et al., 2012). However, these methods are not applicable for the detection of DIKI signals because the confounding factors affecting DIKI are not fully considered. Moreover, most of these studies are conducted on adults, and so far, little is known about pediatric patients in relation to this issue.

Hence, the present study aims at developing a novel quantitative algorithm for DIKI signal detection using a hospital electronic medical record database and analyzing the correlation and characteristics of DIKI signals with the specific drugs in the pediatric population.

2 Methods

2.1 Data sources

This study was conducted using the retrospective inpatient data warehouse of Beijing Children's Hospital (BCH) from 1 January 2009 to 31 December 2020 (Yu et al., 2020). Approximately, 575,965 records of inpatients under 18 years old were included along with their detailed diagnoses, medications, and laboratory tests. Considering the immature kidney function in the neonates, only inpatients aged 28 days to 18 years old were included. All eligible patient data were exported and de-identified to protect their privacy.

The protocol of the study was approved by the Institutional Review Board (IRB) of BCH, Capital Medical University (approval number: 2018-129), with a waiver of informed consent. This work was reported critically according to the RECORD statement for pharmacoepidemiology (RECORD-PE) statement (Supplementary Table S1).

2.2 Laboratory criterion of DIKI

According to the published Kidney Disease: Improving Global Outcomes (KDIGO) (Ostermann et al., 2020), the serum creatinine (SCr) and the glomerular filtration rate (GFR) were the most important renal function parameters for

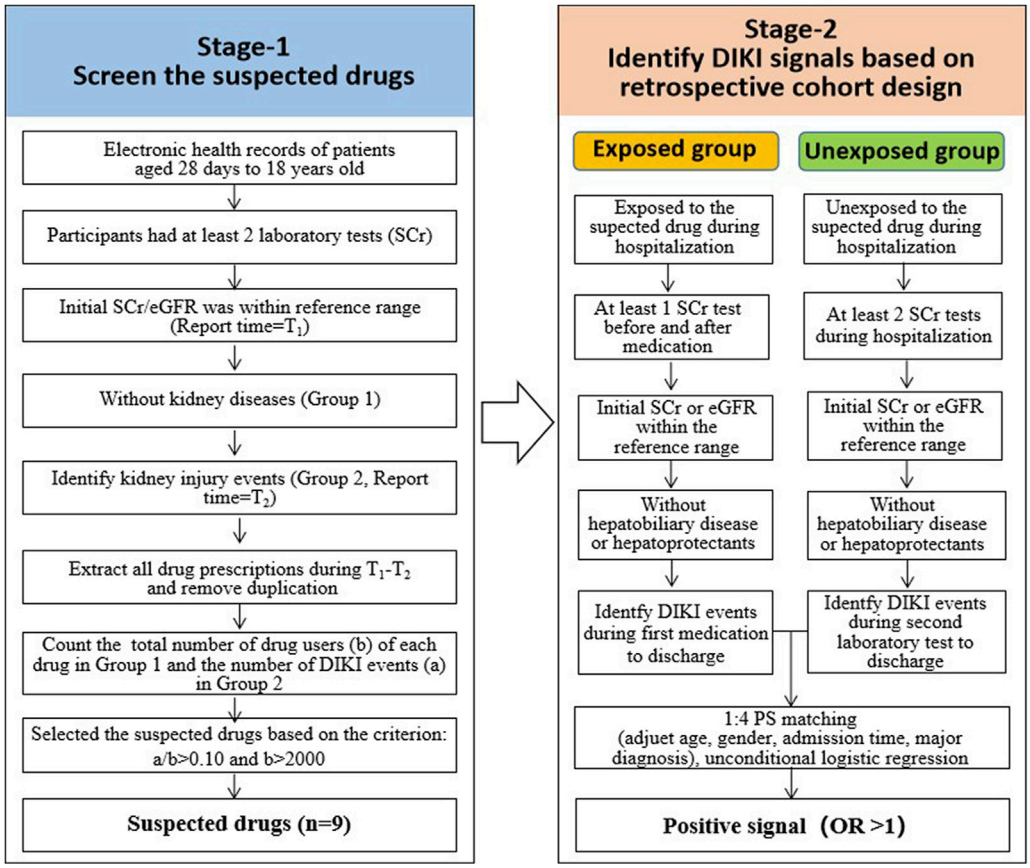

FIGURE 1
Workflow for identifying potential DIKI signals based on the retrospective cohort design. Abbreviations: DIKI: drug-induced kidney injury; EHRs: electronic health records. SCr: serum creatinine; eGFR: estimate glomerular filtration rate; OR: odds ratio.

determining DIKI. Because of the difficulty in measuring directly in clinical settings, the estimated GFR (eGFR) was usually used instead of the GFR and was calculated using the following formula, based on Scr and the normalization constant (Q) (Hoste et al., 2014):

$$eGFR = 107.3 \times (1 - e^{-Age/0.5}) / (SCr/Q).$$

(For children, Q is the median or the average Scr concentration for healthy children and depends linearly on age)

The fourth-degree polynomials for Q are as follows:

$$Q = 17.8 + 6.68 \times Age - 0.907 \times Age^2 + 0.0687 \times Age^3 - 0.00152 \times Age^4 \, (boys)$$

$$Q = 18.2 + 5.54 \times Age - 0.602 \times Age^2 + 0.0421 \times Age^3 - 0.00993 \times Age^4 \, (girls)$$

After completing the calculation, the normal pediatric reference interval of the eGFR was as follows: 33–84(3–6 months), 57–122(6–12 months), 78–132(12–15 months), 84–150(15–24 months), and 83–143 (24 months–18 years old).

Thus, according to the KDIGO guidelines and the reference interval of pediatric kidney parameters (Zhu, 2015), the trigger for pediatric DIKI was defined as the following events that occurred after medication within the appropriate therapeutic dose range: (1):SCr>130 mmol/L; or (2) out of the reference interval of the eGFR for pediatrics.

2.3 Establishment of the two-stage signal detection model for DIKI

2.3.1 Stage 1: Screening suspected drugs

The main purpose of this step was to identify the suspected drugs that may cause DIKI to provide candidate drugs for the subsequent correlation analysis. The main steps were as follows (Figure 1):

1) The records with at least two SCr tests in the eligible participants were selected.

2) The records with the initial SCr or eGFR value within the reference range were further included. The report time of SCr tests was recorded as T1. This step aimed to ensure that kidney function was normal before medication.
3) The records with the diagnosis of kidney-related diseases were excluded (Supplementary Table S2). This step aimed to exclude the records where changes in laboratory parameters were primarily due to the progression of the kidney-related disease itself, rather than DIKI. The remaining records were marked as group 1.
4) The records with abnormal SCr or eGFR test findings, which were considered as DIKI events, were marked as group 2. The time of the first abnormal result was recorded as T2.
5) All drugs during T1-T2 were extracted, and duplicates were removed from groups 1 and 2. Thus, the number of DIKI events (a) and the total number of drug users (b) of each drug were obtained.
6) We calculated the ratio of a/b for each drug. The threshold of the a/b ratio was set according to the range of a/b values of solvents for intravenous infusions, such as normal saline and glucose injections, which can be regarded as the reference value since it is well known that they do not affect DIKI. The a/b values of solvents for intravenous infusions ranged from 0.081 to 0.095. In addition to that, for drugs with less than 2000 users, the number of DIKI events in the exposed group was too low. There may be a greater risk of bias in the subsequent statistical analysis due to insufficient samples. Thus, the criteria for suspected drugs were as follows: (1): ratio (a/b) > 0.10 and (2) b > 2000.

2.3.2 Stage 2: Identifying potential DIKI signals based on the retrospective cohort design

This step aimed to compare the incidence of DIKI events between the exposed group (i.e., taking the suspected drugs) and the unexposed group (i.e., not taking the suspected drugs) whilst also adjusting for confounding factors through retrospective analysis. This was performed to explore the association between drugs and kidney damage. The following analysis was performed on all suspected drugs found in stage 1 (Figure 1):

2.3.2.1 Exposure group

1) All records containing suspected drugs were identified.
2) The records with at least one SCr test before and after medication were screened.
3) The records with an initial SCr or eGFR result that was within the normal range before the first medication were included.
4) The records with competing kidney diseases were excluded (Supplementary Table S2).
5) In cases where records showing abnormal SCr or eGFR findings during hospitalization, the records with kidney-protecting drugs before the first report time of the abnormal test were excluded (Supplementary Table S3); for records without SCr or eGFR abnormalities, those who have used kidney-protecting drugs during the entire hospitalization were excluded.

2.3.2.2 Unexposed group

1) All records without the suspected drug were identified.
2) The records with at least two SCr tests during hospitalization remained.
3) The records with an initial SCr or eGFR that was within the normal range after admission were included.
4) The records with competing kidney diseases were excluded (Supplementary Table S2).
5) In cases where records showing abnormal SCr or eGFR findings during hospitalization, the records with kidney-protecting drugs before the first report time of the abnormal test were excluded (Supplementary Table S3); for records without SCr or eGFR abnormalities, those who have used kidney-protecting drugs during the entire hospitalization were excluded.

2.3.3 Signal detection

1) Each exposed record was paired with four unexposed records randomly after adjusting age, gender, admission time, and major diagnosis.
2) The association between suspected drugs and kidney injury was analyzed by unconditional logistic regression. The odds ratio (OR) and 95% confidence interval (CI) were calculated.
3) An OR>1.0 (with the 95%CI lower band >1) indicated a positive signal; otherwise, a negative signal was considered.

2.4 Evaluation of the DIKI signals

A literature search and the summary of product characteristics (SPCs) were used as available knowledge to evaluate the novelty of the positive DIKI signals. Type I signals were defined as those signals that have not been previously documented in research in both children and adults. Type II signals were defined as those drug–DIKI associations that have not been reported in children, although they have been reported in adults. The SPCs were checked from the FDA website (https://www.fda.gov), Micromedex (https://www.ibm.com/watson-health/learn/micromedex), and the drug instructions (https://www.yaozh.com/). Literature research was conducted using PubMed (https://pubmed.ncbi.nlm.nih.gov), Embase (https://www.embase.com), Wanfang (http://www.wanfang.data.com.cn/index.html), and CNKI (http://www. cnki.net/).

2.5 Statistical analysis

MySQL software version 14.14 (Oracle, California, United States) was used as a database management system. The pandas v1.2.2 package in Python 3.7 was performed to summarize data. R 4.2.0 software was used for statistical

TABLE 1 Suspected drugs related to DIKI in pediatrics in stage 1.

Drug name	Pharmacological classification	ATC code	Number of DIKI events (a)	Total number of drug usages (b)	Ratio (a/b)
Diazepam	Sedative–hypnotic drugs	N05BA01	889	4,016	0.22
Vitamin K1	Vitamins	B02BA01	538	2,661	0.20
Cefamandole	Cephalosporins	J01DC03	1,028	5,212	0.20
Omeprazole	Mucosal protective agents	A02BC01	792	4,817	0.16
Ondansetron	Antiemetics	A04AA01	836	6,501	0.13
Ibuprofen	Antipyretics	M01AE01	2,313	18,990	0.12
Methotrexate	Antineoplastic agents	L04AX03	1,066	9,377	0.11
Creatine phosphate sodium	Cardioprotective drugs	NA	2,875	25,485	0.11
Cytarabine	Antineoplastic agents	L01BC01	881	8,343	0.11

Abbreviations: DIKI: drug-induced kidney injury; ATC: anatomical therapeutic chemical classification.

analysis. The forest plot was visualized by GraphPad Prism 9.3 software.

The propensity score matching (PSM) was used to match the exposed group and unexposed group for the ratio of 1:4. As demographic variables, the distribution of age and gender needs to be comparable in exposed and unexposed groups. Laboratory testing equipment, methods, and capability may change over time in the hospital, which can affect the results of laboratory parameters such as Scr. The patients admitted at similar times in the two groups were, therefore, more comparable. In addition, as the patient's underlying medical condition may affect the effectiveness of the drugs on renal function, cases with similar diagnoses in two groups need to be matched. Thus, four variables, namely, age, gender, admission time, and main diagnosis, were considered as confounding factors. The logistic regression model was used to calculate propensity scores, with drug exposure or not as dependent variables and four confounding factors as covariates. The nearest neighbor matching principle was used with a caliper of 0.1.

An unconditional logistic regression was used to analyze the association between suspected drugs and kidney injury. All p-values were reported as two-sided, and $p < 0.05$ represented statistical significance.

3 Results

3.1 Nine suspected drugs were screened in stage 1

A total of 652 drugs were initially screened in stage 1. After combining drugs with the same ingredients and anatomical therapeutic chemical (ATC) classification, 346 drugs remained. After excluding external drugs and solvents for intravenous infusions (such as normal saline and glucose injection), 48 drugs were left (Supplementary Table S4). According to the inclusion criteria (a/b > 0.10 and b > 2000), a total of nine suspected drugs (diazepam, vitamin K1, cefamandole, omeprazole, ondansetron, ibuprofen, methotrexate, creatine phosphate sodium, and cytarabine) were finally identified. More information is shown in Table 1.

3.2 Six positive DIKI signals were identified in stage 2

The data extraction workflow of the nine suspected drugs is shown in Supplementary Table S5. The clinical information between the exposed group and the unexposed group is described in Supplementary Table S6. Retrospective cohort analysis showed that nine drugs met the inclusion criteria. Six drugs, namely, diazepam ($p = 3.47 \times 10^{-15}$, OR = 1.61, and 95% CI: 1.43–1.80), omeprazole ($p = 4.46 \times 10^{-5}$, OR = 1.35, and 95% CI: 1.17–1.54), ondansetron ($p = 1.95 \times 10^{-16}$, OR = 1.49, and 95% CI: 1.36–1.63), methotrexate ($p = 1.17 \times 10^{-13}$, OR = 1.36, and 95% CI: 1.25–1.47), creatine phosphate sodium ($p = 2.94 \times 10^{-3}$, OR = 1.13, and 95% CI: 1.05–1.22), and cytarabine ($p = 1.76 \times 10^{-3}$, OR = 1.17, and 95% CI: 1.06–1.28), were found to be associated with DIKI as positive signals. Although the three remaining drugs, namely, vitamin K1 ($p = 0.54$, OR = 1.06, and 95% CI: 0.89–1.27), cefamandole ($p = 0.40$, OR = 1.07, and 95% CI: 0.94–1.21), and ibuprofen ($p = 0.77$, OR = 1.01, and 95% CI: 0.94–1.09), tended toward a positive association with kidney injury, it did not reach statistical significance. The results of nine drugs and their associations with DIKI are shown in Table 2 and Figure 2.

3.3 Four new signals for DIKI in pediatrics were evaluated

According to the current available knowledge, the novelty of the six positive DIKI signals observed in stage 2 was further

TABLE 2 Signal detection of drug-induced kidney injury using PS matching in stage 2.

Suspect drug	Exposed group		Unexposed group		Adjusted *p*-value[a]	Or (95% CI)
	Number of cases with DIKI events	Number of cases without DIKI events	Number of cases with DIKI events	Number of cases without DIKI events		
Diazepam	571	2,363	1,558	10,178	3.47×10^{-15}	1.61 (1.43, 1.80)
Vitamin K1	214	1,111	808	4,492	0.54	1.06 (0.89, 1.27)
Cefamandole	436	1873	1,627	7,609	0.40	1.07 (0.94, 1.21)
Omeprazole	391	2,203	1,402	8,974	4.46×10^{-05}	1.35 (1.17, 1.54)
Ondansetron	779	5,530	2,875	22,361	1.95×10^{-16}	1.49 (1.36, 1.63)
Ibuprofen	1,168	9,796	3,367	30,106	0.77	1.01 (0.94, 1.09)
Methotrexate	1,027	7,646	3,640	31,052	1.17×10^{-13}	1.36 (1.25, 1.47)
Creatine phosphate sodium	1,271	11,248	2,931	24,636	2.94×10^{-3}	1.13 (1.05, 1.22)
Cytarabine	773	7,001	2,981	28,115	1.76×10^{-3}	1.17 (1.06, 1.28)

[a]: The *p*-value was adjusted by the Benjamini–Hochberg method.

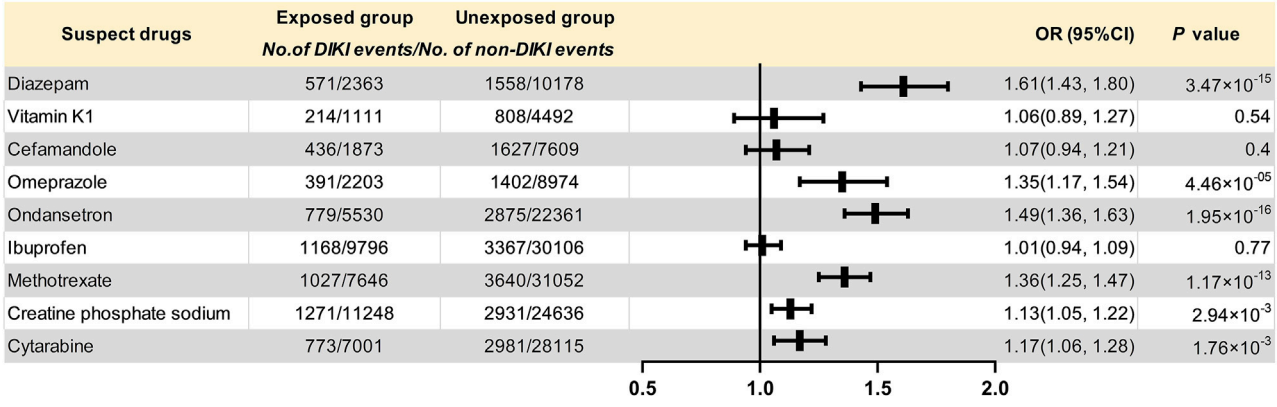

FIGURE 2
Forest plot for the association of suspected drugs with DIKI. Abbreviations: DIKI: drug-induced kidney injury; OR: odds ratio; CI: confidence interval.

evaluated (Table 3). Of these, creatine phosphate sodium was found to be a type I signal as it had not previously been reported in either adults or children. Three other drugs, namely, diazepam, omeprazole, and ondansetron, were demonstrated to be type II signals in pediatrics. The other drug–DIKI associations have been confirmed in previous studies.

4 Discussion

Medications are the relatively common cause of AKI, especially in pediatrics. DIKI is related to a drugs' inherent toxicity and how the kidneys are able to handle it. It poses several challenges for clinicians mainly because of the difficulties

TABLE 3 Evaluation of drug-induced kidney injury signals.

Suspect drug	Literature (PubMed/ Embase)		Literature (CNKI/ Wangfang)[a]		SPC[b]	Signal type*
	Adults	Children	Adults	Children		
Diazepam	√	×	×	×	×	II
Omeprazole	√	×	√	×	√	II
Ondansetron	√	×	×	×	×	II
Methotrexate	√	√	√	√	√	Known
Creatine phosphate sodium	×	×	×	×	√	I
Cytarabine	√	×	√	√	√	Known

AbbreviationsDIKI: drug-induced kidney injury; SPCs: summary of product characteristics.
[a]: Literature reviewed: 1) PubMed: https://pubmed.ncbi.nlm.nih.gov; 2) Embase: https://www.embase.com; 3) Wanfang: http://www.wanfangdata.com.cn/index.html); and 4) CNKI: https://www.cnki.net.
[b]: SPCs reviewed: 1) Micromedex: https://www.ibm.com/watson-health/learn/micromedex); 2) FDA website: https://www.fda.gov/; and 3) drug instructions: https://www.yaozh.com/.
*Signal type **I**: the specific drug-DIKI signal had never been reported in the literature; **II**: the specific drug-DIKI signal had been reported in the literature about adults, but no reports about children could be found in the literature; known: the specific drug-DIKI association had been reported in both adults and children.

in timely identification of drugs with potential nephrotoxicity (Starr et al., 2021). In this context, research on RWD is growing for its implication in the surveillance of drug safety. The EHR, as one of the routine RWDs, is a good data source for pharmacovigilance because of its detailed information on clinical events related to medications (Patadia et al., 2015). This study established and applied a two-stage method for detecting DIKI signals in children using an EHR database: first to identify potential suspected drugs and then to conduct a retrospective cohort to analyze the correlation between the specific suspected drugs and renal impairment. We initially discovered nine candidate drugs related to DIKI, and six positive signals for DIKI were identified in further analyses. To the best of our knowledge, one of the drug-DIKI associations (creatine phosphate sodium) has not been previously described in current literature evidence, either in adults or in children. Three other drug-DIKI associations (diazepam, omeprazole, and ondansetron) were not previously reported in children but have already been reported in adults. These drugs may become the critical target drugs for active surveillance and causality assessment in further research.

4.1 Potential new signals

The association of creatine phosphate sodium with DIKI was found to be a possible new signal in this study. Creatine phosphate sodium is one of the cardioprotective drugs and is widely used in the protection of abnormal myocardial metabolism during myocardial ischemia. A previous study showed that 14.40% cases (28/200) of children were treated with sodium creatine phosphate as prophylactic treatment without a diagnosis, suggesting that there was an overdosage of sodium creatine phosphate in pediatrics (Jin et al., 2022). Another study showed that high doses of creatine phosphate sodium injection may cause large amounts of phosphate intake, which may affect renal function through calcium and purine metabolism disorders, as well as unstable hormone secretion (Yan et al., 2011). Recently, the National Medical Products Administration (NMPA) in China has recommended that serum calcium, serum phosphorus, and renal function should be monitored during the use of creatine phosphate sodium in neonates and premature infants, which also provides a reference for children of other ages. Although creatine phosphate sodium has been on the market for many years, the mechanisms underlying the association between its use and the deterioration of kidney function are still unclear. In light of these findings, further studies should assess the mechanism of kidney injury induced by creatine phosphate sodium in children. For patients with DIKI, suspected drugs were discontinued immediately, followed by symptomatic treatment to preserve the kidney. At the same time, clinicians should also pay attention to regular renal function in children who need long-term and high-dose use of creatine phosphate sodium to better promote the rational use of this drug.

Three other drug-DIKI associations (diazepam, omeprazole, and ondansetron) were identified as potentially new signals in the pediatric population. Diazepam is a common sedative–hypnotic drug in clinical settings, and the ADRs described in SPC include drowsiness, fatigue, muscle weakness, urinary retention, or incontinence. A nationwide population-based retrospective cohort study showed that diazepam had a significant correlation with increased chronic kidney disease risk in the population aged >18 years old (adjusted hazard ratio (HR) = 1.627, 95 CI%:1.527–1.736) (Liao et al., 2020). One of the possible mechanisms is that propylene glycol is contained in parenteral formulations of diazepam, which may cause AKI and proximal tubule injury (Cawley, 2001). In addition, omeprazole is a proton

pump inhibitor (PPI) that selectively inhibits the H + -K + -ATPase in the gastric parietal cell membrane. It is widely used in the treatment of peptic ulcers, reflux esophagitis, and Zollinger–Ehrlich syndrome in pediatrics (Kato et al., 2021). Serious ADRs such as acute interstitial nephritis (AIN) and renal failure have also been reported in adults (Nadri and Althaf, 2014). Simpson et al. (2006) reported that the incidence of AIN caused by omeprazole was 8/100,000 (95% Cl: 2.6/100,000 to 18.7/100,000) (Simpson et al., 2006). Other studies have shown that omeprazole can cause a high incidence of renal damage in the elderly (Klatte et al., 2017). The underlying mechanism was drug-induced immune damage, including acute and chronic interstitial nephritis and tubulointerstitial nephritis (Torlot and Whitehead, 2016). Furthermore, ondansetron is a preferred anti-emetic in critical care to treat nausea and vomiting. A recent pharmacoepidemiology study reported that ondansetron may be associated with an increased risk of AKI (Gray et al., 2022). Another work showed that ondansetron can enhance cisplatin-induced nephrotoxicity *via* inhibition of multiple toxins and extrusion proteins (Li et al., 2013). However, the associations between the aforementioned three drugs and renal impairment were mainly reported in adults. We should also remember that most of the drugs currently used in pediatric clinical practices were originally developed for adults, and for the majority of them, the mechanism of renal toxicity in children is still to be clarified. Our results may provide more clues and need to be validated in a larger pediatric population.

This study also found that both methotrexate (MTX) and cytarabine were associated with a degree of kidney injury, which was consistent with previous reports in the literature. They are both common antineoplastic agents and are widely used in acute lymphoblastic leukemia (ALL) and non-Hodgkin's lymphoma in pediatrics. A retrospective analysis found that the first high-dose methotrexate (HDMTX) course (OR = 1.767) and methotrexate dose per body surface area (OR = 1.944) significantly correlated with AKI in 336 ALL children (Cheng et al., 2018). HDMTX-associated AKI with delayed MTX clearance has been linked to an excess in MTX-induced toxicities (Heuschkel et al., 2022). AKI develops due to the precipitation of MTX and its metabolites within the tubular lumens of the kidney (Perazella and Izzedine, 2015). Furthermore, MTX has been shown to induce the formation of oxygen radicals with subsequent cellular injury, associated with decreased adenosine deaminase activity (Pinheiro et al., 2010). In addition, a case report showed that low-dose cytarabine could induce hepatic and renal dysfunction in a patient with myelodysplastic syndrome, indicating that careful observation should be carried out in clinical practice (Tanaka et al., 1999). As an anti-tumor drug with weak cell specificity, cytarabine affects all actively growing cells by inhibiting the synthesis of DNA, including renal tubular epithelial cells, thereby causing nephrotoxicity (Pannu and Nadim, 2008). The aforementioned results support the reliability of our two-stage method in DIKI signal detection.

4.2 Strengths and limitations

The main strength of this study is its capability to retrospectively observe a large number of children and adolescents in a "real-world" setting by combining data from longitudinal EHRs. This two-stage designed approach has certain advantages in comparison with other methods based on abnormal values of laboratory tests (Yoon et al., 2012) or GTT. In the first stage, we roughly assessed the potential to select the suspected drugs, increasing the efficiency of subsequent analysis. Furthermore, more confounders, such as kidney disease and medications that may affect the level of laboratory indicators, were considered. In addition, the algorithm execution does not require manual review and can be developed into an automated program in the future, which is more suitable for the detection of ADEs based on large-scale databases. The final results suggest that our method can be used as a useful tool to detect DIKI signals for use by clinicians and regulatory agencies.

Despite the strengths of EHRs, they have inherent limitations, including incomplete case capture, selection bias, unmeasured confounding, and the inability to infer causality. Thus, some limitations to this study should be considered. First, only the records that met the criteria were included in the study. The associations between suspected drugs and DIKI remain unknown in those excluded records. Second, while our method has controlled four important variables, it does not adjust drug–drug interactions, drug–dose response, or disease severity covariates in the model. Third, the EHR data from a single-site system was used in this study. More efforts are needed to validate the feasibility of the approach and the DIKI signals in other EHR databases in the future. Lastly, it is important to realize that this method is a tool to assist with signal detection but does not ensure causality assessment of ADRs. All potentially new signals require further evaluation in hypothesis-testing studies to better account for bias and confounding.

In summary, this study shows that the RWDs, especially the EHRs, are potentially valuable resources for post-marketing drug safety surveillance. Our findings provide six candidate drug-DIKI associations using medical record databases. Future research is warranted to assess the causality of DIKI signals and formulate strategies for drug risk management in pediatrics. Nowadays, China has initiated the project "China ADR Sentinel Surveillance Alliance" (CASSA) with at least 300 medical facilities. Also of note, BCH was the first pediatric hospital in CASSA. More attention will be paid to integrating the method based on the CASSA platform to explore multi-center pharmacovigilance research.

5 Conclusion

DIKI is one of the most common problems in clinical practice, especially in hospitalized patients. In this work, we

proposed a quantitative two-stage procedure to explore potential DIKI signals using RWD. Six positive signals of DIKI, including four new signals in children, were detected. Our findings highlight the potential of EHRs to complement traditional SRS for drug safety signal detection and strengthening in a pediatric setting. It is hoped that current efforts to identify DIKI signals will allow us to modify practice and reduce unnecessary harm in the future.

Data availability statement

The raw data supporting the conclusion of this article will be made available by the authors, without undue reservation.

Ethics statement

The protocol of the study was approved by the Institutional Review Board (IRB) of Beijing Children's Hospital, Capital Medical University (approval number: 2018-129), with a waiver of informed consent.

Author contributions

XW and XP undertook work of framework design and overall guidance of the whole research. YY and XN took responsibility for the data collection. YY, YZ, and YX performed data processing and statistical analysis. YY and WC were responsible for the manuscript writing and data interpretation. XP provided important methodological advice.

Funding

This work was supported by the Clinical Toxicology Program of the Chinese Society of Toxicology (CST2020CT108), the Children's Medication Project of Beijing Children's Hospital (2020) (YZYB202006), the National Natural Science Foundation of China (Nos. 72174128, 82102688 and 82204149), the Hainan Free Trade Port Boao Hope City Real World Study Project (HNLC2022RWS015), and the Clinical Technology Training Program for Comprehensive Evaluation of Pediatric Medication (CNHDRC-KJ-W-2021-58).

Conflict of interest

The authors declare that the research was conducted in the absence of any commercial or financial relationships that could be construed as a potential conflict of interest.

Publisher's note

All claims expressed in this article are solely those of the authors and do not necessarily represent those of their affiliated organizations, or those of the publisher, the editors, and the reviewers. Any product that may be evaluated in this article, or claim that may be made by its manufacturer, is not guaranteed or endorsed by the publisher.

Supplementary material

The Supplementary Material for this article can be found online at: https://www.frontiersin.org/articles/10.3389/fphar.2022.957980/full#supplementary-material.

References

Cawley, M. J. (2001). Short-term lorazepam infusion and concern for propylene glycol toxicity: Case report and review. *Pharmacotherapy* 21 (9), 1140–1144. doi:10.1592/phco.21.13.1140.34611

Chen, C., Jia, W., Guo, D., Zhu, M., Xu, Y., Wang, X., et al. (2020). Development of a computer-assisted adverse drug events alarm and assessment system for hospital inpatients in China. *Ther. Innov. Regul. Sci.* 54 (1), 32–41. doi:10.1007/s43441-019-00027-z

Cheng, D-H., Lu, H., Liu, T-T., Zou, X-Q., and Pang, H-M. (2018). Identification of risk factors in high-dose methotrexate-induced acute kidney injury in childhood acute lymphoblastic leukemia. *Chemotherapy* 63 (2), 101–107. doi:10.1159/000486823

de Bie, S., Coloma, P. M., Ferrajolo, C., Verhamme, K. M., Trifiro, G., Schuemie, M. J., et al. (2015). The role of electronic healthcare record databases in paediatric drug safety surveillance: A retrospective cohort study. *Br. J. Clin. Pharmacol.* 80 (2), 304–314. doi:10.1111/bcp.12610

Faught, L. N., Greff, M. J., Rieder, M. J., and Koren, G. (2015). Drug-induced acute kidney injury in children. *Br. J. Clin. Pharmacol.* 80 (4), 901–909. doi:10.1111/bcp.12554

Faught, L. N., Greff, M. J. E., Rieder, M. J., and Koren, G. (2015). Drug-induced acute kidney injury in children. *Br. J. Clin. Pharmacol.* 80 (4), 901–909. doi:10.1111/bcp.12554

Garrett, P. R., Jr., Sammer, C., Nelson, A., Paisley, K. A., Jones, C., Shapiro, E., et al. (2013). Developing and implementing a standardized process for global trigger tool application across a large health system. *Jt. Comm. J. Qual. Patient Saf.* 39 (7), 292–297. doi:10.1016/s1553-7250(13)39041-2

Gray, M., Priyanka, P., Kane-Gill, S., Wang, L., and Kellum, J. A. (2022). Kidney and mortality Outcomes associated with ondansetron in critically ill patients. *J. Intensive Care Med.*, 088506662110735. doi:10.1177/08850666211073582

Hanna, M. H., Askenazi, D. J., and Selewski, D. T. (2016). Drug-induced acute kidney injury in neonates. *Curr. Opin. Pediatr.* 28 (2), 180–187. doi:10.1097/MOP.0000000000000311

Heuschkel, S., Kretschmann, T., Teipel, R., Bonin, S., Richter, S., Quick, S., et al. (2022). Half-dose glucarpidase as efficient rescue for toxic methotrexate levels in patients with acute kidney injury. *Cancer Chemother. Pharmacol.* 89 (1), 41–48. doi:10.1007/s00280-021-04361-8

Hosohata, K. (2016). Role of oxidative stress in drug-induced kidney injury. *Int. J. Mol. Sci.* 17 (11), E1826. doi:10.3390/ijms17111826

Hoste, L., Dubourg, L., Selistre, L., De Souza, V. C., Ranchin, B., Hadj-Aissa, A., et al. (2014). A new equation to estimate the glomerular filtration rate in children, adolescents and young adults. *Nephrol. Dial. Transpl.* 29 (5), 1082–1091. doi:10.1093/ndt/gft277

Jin, X., Xinghui, Z., Jiong, L., and Qingtao, W. (2022). Establishment and application of DUE criteria for creatine phosphate sodium in a Children's hospital. *China Pharm.* 23 (5), 923–925.

Kato, K., Mizuno, T., Koseki, T., Ito, Y., Hatano, M., Takahashi, K., et al. (2021). Concomitant proton pump inhibitors and immune checkpoint inhibitors increase nephritis frequency. *Vivo* 35 (5), 2831–2840. doi:10.21873/invivo.12570

Klatte, D. C. F., Gasparini, A., Xu, H., Deco, P., Trevisan, M., Johansson, A. L. V., et al. (2017). Association between proton pump inhibitor use and risk of progression of chronic kidney disease. *Gastroenterology* 153 (3), 702–710. doi:10.1053/j.gastro.2017.05.046

Li, Q., Guo, D., Dong, Z., Zhang, W., Zhang, L., Huang, S-M., et al. (20132013). Ondansetron can enhance cisplatin-induced nephrotoxicity via inhibition of multiple toxin and extrusion proteins (MATEs). *Toxicol. Appl. Pharmacol.* 273 (1), 100–109. doi:10.1016/j.taap.2013.08.024

Liao, C. Y., Chung, C. H., Lu, K. C., Cheng, C. Y., Yang, S. S., Chien, W. C., et al. (2020). Taking sleeping pills and the risk of chronic kidney disease: A nationwide population-based retrospective cohort study. *Front. Pharmacol.* 11, 524113. doi:10.3389/fphar.2020.524113

Nadri, Q., and Althaf, M. M. (2014). Granulomatous tubulointerstitial nephritis secondary to omeprazole. *BMJ Case Rep.*, bcr2014203842. doi:10.1136/bcr-2014-203842

Ostermann, M., Bellomo, R., Burdmann, E. A., Doi, K., Endre, Z. H., Goldstein, S. L., et al. (2020). Controversies in acute kidney injury: Conclusions from a kidney disease: Improving global Outcomes (KDIGO) conference. *Kidney Int.* 98 (2), 294–309. doi:10.1016/j.kint.2020.04.020

Pannu, N., and Nadim, M. K. (2008). An overview of drug-induced acute kidney injury. *Crit. Care Med.* 36, S216–S223. doi:10.1097/CCM.0b013e318168e375

Patadia, V. K., Schuemie, M. J., Coloma, P., Herings, R., van der Lei, J., Straus, S., et al. (2015). Evaluating performance of electronic healthcare records and spontaneous reporting data in drug safety signal detection. *Int. J. Clin. Pharm.* 37 (1), 94–104. doi:10.1007/s11096-014-0044-5

Perazella, M. A., and Izzedine, H. (2015). New drug toxicities in the onco-nephrology world. *Kidney Int.* 87 (5), 909–917. doi:10.1038/ki.2015.30

Pinheiro, F. V., Pimentel, V. C., Bona, K. S. D., Scola, G., Salvador, M., Funchal, C., et al. (2010). Decrease of adenosine deaminase activity and increase of the lipid peroxidation after acute methotrexate treatment in young rats: Protective effects of grape seed extract. *Cell. biochem. Funct.* 28 (1), 89–94. doi:10.1002/cbf.1627

Pitts, P. J., and Le Louet, H. (2018). Advancing drug safety through prospective pharmacovigilance. *Ther. Innov. Regul. Sci.* 52 (4), 400–402. doi:10.1177/2168479018766887

Radi, Z. A. (2019). Kidney pathophysiology, Toxicology, and drug-induced injury in drug development. *Int. J. Toxicol.* 38 (3), 215–227. doi:10.1177/1091581819831701

Simpson, I. J., Marshall, M. R., Pilmore, H., Manley, P., Williams, L., Thein, H., et al. (2006). Proton pump inhibitors and acute interstitial nephritis: Report and analysis of 15 cases. *Nephrology* 11 (5), 381–385. doi:10.1111/j.1440-1797.2006.00651.x

Starr, M. C., Charlton, J. R., Guillet, R., Reidy, K., Tipple, T. E., Jetton, J. G., et al. (2021). Advances in neonatal acute kidney injury. *Pediatrics* 148 (5), e2021051220. doi:10.1542/peds.2021-051220

Tanaka, M., Kanamori, H., Yamaji, S., Mishima, A., Fujita, H., Fujisawa, S., et al. (1999). Low-dose cytarabine-induced hepatic and renal dysfunction in a patient with myelodysplastic syndrome. *Anticancer. Drugs* 10 (3), 289–291. doi:10.1097/00001813-199903000-00006

Toh, S., Hampp, C., Reichman, M. E., Graham, D. J., Balakrishnan, S., Pucino, F., et al. (2016). Risk for hospitalized heart failure among new users of saxagliptin, sitagliptin, and other antihyperglycemic drugs: A retrospective cohort study. *Ann. Intern. Med.* 164 (11), 705–714. doi:10.7326/M15-2568

Torlot, F. J., and Whitehead, D. J. (2016). Acute interstitial nephritis caused by two different proton pump inhibitors. *Br. J. Hosp. Med.* 77 (1), 50–51. doi:10.12968/hmed.2016.77.1.50

Yan, H., Jichun, Z., and Xiaoyue, X. (2011). Evaluation on the safety of creatine phosphate sodium for injection. *Chin. J. Hosp. Pharm.* 31 (22), 1871–1874.

Yang, L., Xing, G., Wang, L., Wu, Y., Li, S., Xu, G., et al. (2015). Acute kidney injury in China: A cross-sectional survey. *Lancet* 386 (10002), 1465–1471. doi:10.1016/S0140-6736(15)00344-X

Yoon, D., Park, M. Y., Choi, N. K., Park, B. J., Kim, J. H., and Park, R. W. (2012). Detection of adverse drug reaction signals using an electronic health records database: Comparison of the Laboratory Extreme Abnormality Ratio (CLEAR) algorithm. *Clin. Pharmacol. Ther.* 91 (3), 467–474. doi:10.1038/clpt.2011.248

Yu, Y., Nie, X., Song, Z., Xie, Y., Zhang, X., Du, Z., et al. (2020). Signal detection of potentially drug-induced liver injury in children using electronic health records. *Front. Pediatr.* 8, 171. doi:10.3389/fped.2020.00171

Zhu, K. S. (2015). *Practice of pediatrics*. Beijing: People's Medical Publishing House.

frontiers | Frontiers in Pharmacology

TYPE Original Research
PUBLISHED 26 September 2022
DOI 10.3389/fphar.2022.993923

OPEN ACCESS

EDITED BY
Jian Gao,
Shanghai Children's Medical Center, China

REVIEWED BY
Maria Elizete Almeida Araujo,
Federal University of Amazonas, Brazil
Jiangwei Tian,
China Pharmaceutical University, China

*CORRESPONDENCE
Chengxian Guo,
gchxyy@163.com
Zhiling Li,
lizhiling22@163.com

SPECIALTY SECTION
This article was submitted to Obstetric and Pediatric Pharmacology, a section of the journal Frontiers in Pharmacology

RECEIVED 14 July 2022
ACCEPTED 05 September 2022
PUBLISHED 26 September 2022

CITATION
Hu B, Ye L, Li T, Feng Z, Huang L, Guo C, He L, Tan W, Yang G, Li Z and Guo C (2022), Drug-induced kidney injury in Chinese critically ill pediatric patients. *Front. Pharmacol.* 13:993923. doi: 10.3389/fphar.2022.993923

Drug-induced kidney injury in Chinese critically ill pediatric patients

Biwen Hu[1], Ling Ye[1], Tong Li[1], Zeying Feng[1], Longjian Huang[2], Chengjun Guo[3], Li He[4], Wei Tan[5], Guoping Yang[1], Zhiling Li[6]* and Chengxian Guo[1]*

[1]Center of Clinical Pharmacology, The Third Xiangya Hospital, Central South University, Changsha, Hunan, China, [2]West Guangxi Key Laboratory for Prevention and Treatment of High-Incidence Diseases, Youjiang Medical University for Nationalities, Baise, China, [3]School of Applied Mathematics, Guangdong University of Technology, Guangzhou, China, [4]Department of Pediatrics, The Third Xiangya Hospital, Central South University, Changsha, Hunan, China, [5]Department of Neonatology, Maternal and Child Health Hospital of Guangxi Zhuang Autonomous Region, Nanning, Guangxi Zhuang Region, China, [6]Department of Pharmacy, Shanghai Children's Hospital, School of Medicine, Shanghai Jiao Tong University, Shanghai, China

Background: Drug-induced acute kidney injury (DIKI) is a common adverse drug reaction event but is less known in pediatric patients. The study explored the DIKI in Chinese pediatric patients using the Pediatric Intensive Care database (PIC).

Method: We screened pediatric patients with acute kidney injury (AKI) using the KDIGO criteria from the PIC and then assessed the relationship between their drugs and DIKI using the Naranjo scale. For the fifteen frequently used DIKI-suspected drugs, we divided patients into drug-exposed and non-exposed groups, using the outcome of whether DIKI was presented or not. Propensity score matching (PSM) was used to control for the effects of four confounders, age, gender, length of hospital stay, and major diagnosis. Unconditional logistic regression was used to identify statistically significant differences between the two groups.

Results: A total of 238 drugs were used 1,863 times by the 81 patients with DIKI during their hospital stay. After screening the Naranjo scale to identify the top 15 suspected DIKI drugs with a high frequency of use, we found that furosemide injection (p = 0.001), midazolam injection (p = 0.001), 20% albumin prepared from human plasma injection (p = 0.004), fentanyl citrate injection (p = 0.001), compound glycyrrhizin injection (p = 0.026), vancomycin hydrochloride for intravenous (p = 0.010), and milrinone lactate injection (p = 0.009) were associated with DIKI.

Conclusion: In critically ill pediatric patients, DIKI is more likely to occur after using furosemide injection, midazolam injection, 20% albumin prepared from human plasma injection, fentanyl citrate injection, compound glycyrrhizin injection, vancomycin hydrochloride for intravenous, milrinone lactate injection.

KEYWORDS

drug-induced kidney injury, acute kidney injury, rational drug use, rational medication, pediatrics

Introduction

AKI is a common problem in hospitalized children, and its overall incidence can be as high as 33.7% (Xu et al., 2018; Feiten et al., 2019). It is also associated with higher mortality and sequelae and may lead to chronic kidney disease in adulthood (Kaddourah et al., 2017; Levey and James, 2017). As the use of drugs is unavoidable in pediatric patients in intensive care, the identification and attention to nephrotoxic drugs play a key role in reducing morbidity as well as mortality in this population (Slater et al., 2017; Joyce et al., 2019). There has been a great deal of research into drug-induced kidney injury in adult inpatients. It is shown that the use of drugs such as NSAIDs and diuretics is an independent risk factor for AKI in adult hospitalized patients (Yu C. et al., 2020). The use of iodine-based contrast media can also lead to acute kidney injury during hospitalization and eventually to persistent renal insufficiency or end-stage renal disease (Cheng et al., 2020; Weisbord et al., 2020). In addition, prolonged antibiotic therapy with vancomycin also greatly increases the risk of acute kidney injury (O'Callaghan et al., 2020). Immune-related adverse events caused by immune checkpoint inhibitors when used in cancer treatment can affect the kidneys, leading to acute kidney injury associated with immune checkpoint inhibitor therapy (Meraz-Muñoz et al., 2020). There is also a series of studies on drug-induced kidney injury in pediatric inpatients. It was found that increased exposure to nephrotoxic drugs was associated with the development of AKI in pediatric inpatients (Searns et al., 2020). The use of drugs such as NSAIDs and proton pump inhibitors, which are more common in hospitalized children, also increases the risk of acute kidney injury during hospitalization (Xu et al., 2018; Su et al., 2021). Antibacterial drugs such as vancomycin and aminoglycoside antibiotics can affect renal function through different mechanisms of action, leading to acute kidney injury in children (Downes et al., 2017; Downes et al., 2020). Medication needs to be used with even greater caution in the complex conditions of the intensive care unit. However, there is still a lack of systematic research on the relationship between medications in this setting and the development of acute kidney injury.

Here, we used the PIC database to study 13,449 patients at the Children's Hospital of Zhejiang University School of Medicine from 2010 to 2019 (Zeng et al., 2020), mainly collecting information on serum creatinine values and medication use of patients. The purpose of this study was to analyze the type and distribution of drugs for DIKI in pediatric patients and explain the occurrence of AKI by the mechanism of medications, to provide medical advice for children.

Methods

Study population

We conducted a retrospective case-control study, using the PIC database. The pediatric in-patients aged between 1 month and 18 years were included in the study (Ingelfinger et al., 2016; Xu et al., 2018). Patients with one of the following conditions were excluded: 1) age less than 1 month; 2) lacking records of prescriptions; 3) less than two serum creatinine tests; 4) baseline creatinine beyond the normal range; 5) an admitting diagnosis of acute renal failure (community-acquired AKI), chronic kidney disease, end-stage renal disease, renal transplantation, urinary tract infection, or pyelonephritis; 6) unexplained high serum creatinine values or low serum creatinine values (may be data entry errors). Physician-diagnosed AKI on admission or at discharge was determined according to the International Coding Definitions Version 10 (ICD-10).

Data collection

Demographic data were abstracted from the database, including age and sex from ADMISSION, the name, and dose of drugs from PRESCRIPTION, and serum creatinine values from LABEVENT. When the difference between the two serum creatinine values met one of the Kidney Disease Improving Global Outcomes (KDIGO, 2012), patients were judged to have AKI. We considered that the AKI occurred when the earliest test of serum creatinine defining AKI happened. As the frequency of serum creatinine testing varied between pediatric patients, we also calculated and recorded the time difference between their serum creatinine test at the time of AKI and the previous one. Drug usage was defined as all the drugs the patient used before AKI.

Identification of AKI

We used the KDIGO criteria to screen the patients with AKI in the PIC database, where AKI is defined as an increase in serum creatinine by 0.3 mg/dl within 48 h or a 50% increase in serum creatinine from the baseline within 7 days. Because no urine output was recorded in the database, we only used serum creatinine values to define AKI. The database only records patients' data after admission, so we used the lowest serum creatinine level on the hospitalized days as the baseline serum creatinine level. Meanwhile, the baseline value was required to be within the normal range (Siew and Matheny, 2015).

Relevance evaluation between drugs and AKI

Combined with patients' drug usage during hospitalization, the Naranjo scale was used to further judge DIKI patients and DIKI suspected drugs on the AKI patients screened from the PIC database (Naranjo et al., 1981). The relevance evaluation of the criteria was: affirmative: ≥9 points; very likely: 5-8 points; possible: 1–4 points; impossible: ≤0 points. All cases with a score greater than 1 were considered DIKI, and the drugs which had a score greater than 1were considered DIKI-suspected signals.

Validation of suspected drugs

After scoring the drugs using the Naranjo scale, we screened for suspected drugs associated with the occurrence of DIKI. Among these DIKI-suspected signals, the 15 most frequently used drugs were further analyzed. We divide patients from the PIC database into drug-exposed and non-exposed groups, with DIKI as an outcome. The inclusion and exclusion criteria for patients in both groups were consistent with the Identification of AKI section above. PSM was using for 15 drugs to adjust four confounders, including age, sex, length of stay, and major diagnosis, with two groups matched with a ratio of 1:1 by setting the caliper value (Yu Y. et al., 2020). After matching, unconditional logistic regression was performed on both groups to investigate the relationship between the suspected signals and DIKI. Chi-square test was used to compare mortality between the two groups.

Statistical analysis

Descriptive analysis was used to present the medication information of the patients. Categorical variables are expressed using frequency. PSM was performed using R4.1.1 software, the "MatchIt" package version 4.4.0. The unconditional logistic regression and chi-square test were performed for the exposed and unexposed groups using SPSS version 18.0 statistical software. $p < 0.05$ indicates that the difference is statistically significant.

Results

Clinical characteristics of pediatric patients with DIKI

We screened 13,449 patients from the PIC database. A total of 178 patients met the age requirement and were rated as having developed AKI according to the KDIGO criteria. However, 79 patients with AKI were excluded from the study due to the absence of prescriptions. According to the Naranjo scale, 1 patient had a case score of 5 and was considered likely to have DIKI, and 80 patients had a case score of 1–4 and were considered likely to have DIKI, leaving 4 patients with a case score ≤0. After a careful review of the prescriptions for 85 patients with AKI, 81 patients considered to be potentially associated with DIKI were included in the study.

The clinical features of patients with DIKI are shown below (Table 1). 66.7% of the 81 patients included in the study with DIKI were male and 33.3% were female, giving a male to female ratio of 2:1. Overall, 45.7% of pediatric patients were aged 1 month to 1 year, 43.2% were aged 2–10 years, and 11.1% were aged 11–18 years. The top two major diseases were tumors (24.7%) and respiratory diseases (18.5%). Because of different status of the pediatric patients or incomplete database records, the frequency of serum creatinine testing was 42% (n = 34) of DIKI patients tested twice within 24h, 24.7% (n = 20) of patients tested once within 24h and 33.3% (n = 27) of patients tested once more than 48 h. There were 43.2% of DIKI patients in Stage 1, 24.7% in Stage 2, and 32.1% in Stage 3 according to the KDIGO criteria. Their median length of stay was 13 days (6, 22.5), and 48.1% of patients died during their stay. Before discharge or death, renal function was fully recovered in 17.3% of patients, partially recovered in 21.0% of patients, and not recovered in 61.7% of patients.

For pediatric patients with different AKI Stage, their use of suspected DIKI drugs is largely similar (Supplementary Table S1). This is also shown in pediatric patients with different renal recovery (Supplementary Table S2).

Screening for suspected DIKI signals

A total of 238 drugs were used 1,863 times by 81 patients with DIKI during their hospital stay. We evaluated all drugs used before AKI using the Naranjo scale. Overall, The Naranjo score for 102 kinds of drugs was ≤0, for 134 kinds of was 1–4, for 2 kinds of drugs was 5. We considered that 136 kinds of drugs with Naranjo score greater than 1 were likely to be associated with the occurrence of AKI. About the 136 suspected DIKI drugs, 5.29% were systemic hormone preparations, 14.21% were anti-infectives, 5.15% were NSAIDs, 6.13% were respiratory system drugs, 1.11% were anti-tumor agents and immunomodulators, 16.57% were nervous system drugs, 8.77% were digestive and metabolism drugs, 11.14% were diuretics, 9.19% were cardiovascular system drugs, 18.38% were drugs related with the blood and blood-forming organs, and 4.04% belonged to other categories (Figure 1). After excluding drugs with Naranjo scores <0, the frequency of medication use in the 81 patients with DIKI was compiled (Supplementary Table S3).

TABLE 1 Demographic information and clinical characteristics of patients with drug-induced kidney injury.

	N (%)
Gender	
Male	54 (66.7%)
Female	27 (33.3%)
Age	
Infancy,1 mo to 1 yr	37 (45.7%)
Childhood, 2–10 years	35 (43.2%)
Adolescence, 11–18 years	9 (11.1%)
Major Diagnosis	
Neoplasms	20 (24.7%)
Respiratory system	15 (18.5%)
Blood and blood-forming organs	8 (9.9%)
Congenital malformations, deformations and chromosomal abnormalities	8 (9.9%)
Circulatory system	7 (8.6%)
Nervous system	6 (7.4%)
Digestive system	5 (6.2%)
Injury, poisoning and certain other consequences of external causes	4 (4.9%)
Endocrine, nutritional and metabolic diseases	2 (2.5%)
musculoskeletal system and connective tissue	2 (2.5%)
Symptoms, signs and abnormal clinical and laboratory findings, not elsewhere classified	2 (2.5%)
Genitourinary system	1 (1.2%)
External causes of morbidity and mortality	1 (1.2%)
AKI stage	
Stage 1	35 (43.2%)
Stage 2	20 (24.7%)
Stage 3	26 (32.1%)
Length of stay, d	13 (6, 22.5)
In-hospital death	
Yes	39 (48.1%)
No	42 (51.9%)
Renal Recovery	
Full Recovery	14 (17.3%)
Partial Recovery	17 (21.0%)
Failure to Recovery	50 (61.7%)

Abbreviation: AKI, acute kidney injury.

Validation of DIKI signals

These drugs were used in the top 15 of all drugs used in the 81 patients with DIKI, with furosemide injection being the most frequently used (Figure 2). There were 1,417 cases in which furosemide injection was used, along with 1,096 cases with midazolam injection, 1,273 cases with 20% albumin prepared from human plasma injection, 792 cases with fentanyl citrate injection, 1,134 cases with ibuprofen suspension, 1,704 cases with diazepam injection, 1,162 cases with methylprednisolone sodium succinate for injection, 738 cases with compound glycyrrhizin injection, 468 cases with vancomycin hydrochloride for intravenous, 1,222 cases with adrenaline hydrochloride injection, 506 cases with milrinone lactate injection, 803 cases with meropenem for injection, 688 cases with human immumoglobulin for intravenous injection, 804 cases with aminomethylbenzoic acid injection, and 1,015 cases with etamsylate injection (Supplementary Table S4). After conducting statistics on them separately using logistic regression, we found that 7 drugs were found to be associated with the development of DIKI. Vancomycin hydrochloride for intravenous (p = 0.010, OR = 14.40, $95\%CI$ = 1.89–109.96) as a highly effective diuretic and nephrotoxin furosemide injection (p = 0.001, OR = 12.71, $95\%CI$ = 3.00–53.75) were strongly associated with DIKI. The pediatric patients in ICU using them independently increased the odds of DIKI. In our result, it appeared the anaesthetics midazolam injection (p = 0.001, OR = 8.16, $95\%CI$ = 2.45–27.17), fentanyl citrate injection (p = 0.001, OR = 7.87, $95\%CI$ = 2.35–26.31) could also increase the risk of DIKI. In additions, milrinone lactate injection (p = 0.009, OR = 7.17, $95\%CI$ = 1.62–31.72), 20% albumin prepared from human plasma injection (p = 0.004, OR = 4.25, $95\%CI$ = 1.60–11.32), and compound glycyrrhizin injection (p = 0.026, OR = 3.55, $95\%CI$ = 1.16–10.83) (Table 2). To explore the impact of drug use on patient mortality, we also compared the mortality rates of the two groups. We found that mortality rates were higher in the exposed group than in the unexposed group, except for milrinone lactate injection (Supplementary Table S5).

Discussion

In the current study, we evaluated patients in the PIC database for AKI according to the KDIGO criteria. Then, using the Naranjo scale, we determined the correlation between patients' AKI and the medications used during hospitalization, and further validated the above judgments using statistical analysis. Most of the drugs that led to DIKI in patients belonged to drugs related to the blood and blood-forming organs, nervous system drugs, and diuretics (Figure 1). Meanwhile, among the suspected drugs associated with AKI, furosemide injection, midazolam injection, and 20% human albumin injections were considered to be highly associated with the occurrence of DIKI. This result deepens our understanding of nephrotoxic drugs and provides inspiration to search for new signals of DIKI.

After further validation of 15 drugs, we found that 7 drugs were considered to be correlated with the occurrence of AKI. They were furosemide injection, midazolam injection, 20% albumin prepared from human plasma injection, fentanyl citrate injection, compound glycyrrhizin injection, vancomycin hydrochloride for intravenous, and milrinone lactate injection. As two drugs closely associated with

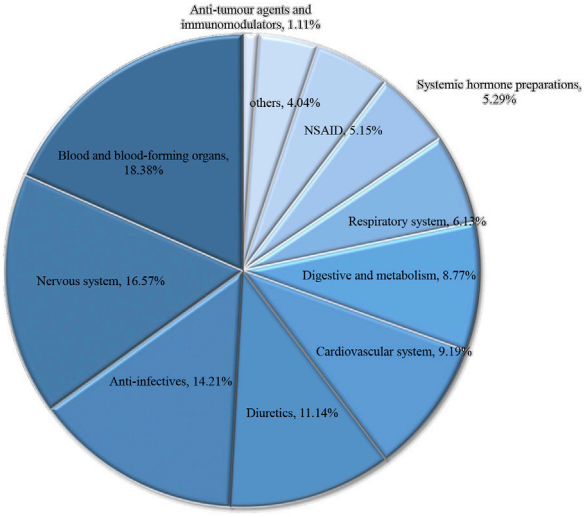

FIGURE 1
Drug categories and high frequency of drug for Pediatric patients with DIKI. Abbreviation: DIKI, drug-induced kidney injury.

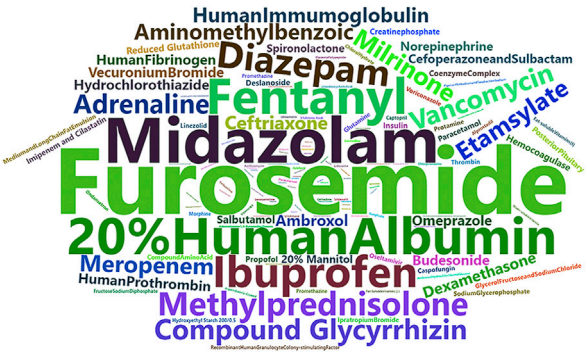

FIGURE 2
The suspected DIKI drugs. Abbreviation: DIKI, drug-induced kidney injury.

AKI, vancomycin hydrochloride for intravenous and furosemide injection have been the subject of many relevant studies so far. Numerous studies have shown that critically ill patients who have used vancomycin are more likely to develop AKI and that vancomycin-associated nephrotoxicity is often associated with higher serum vancomycin levels (Hanrahan et al., 2015; Feiten et al., 2019). The mechanism by which vancomycin causes the onset of AKI remains poorly understood, but it is currently believed that the oxidative effects of vancomycin lead to renal tubular ischemia (Elyasi et al., 2012). Pathology reports showing acute tubular necrosis have also been reported in pediatric patients with vancomycin-induced AKI who underwent renal biopsy (Wu et al., 2007). Unlike vancomycin, furosemide injection is not a nephrotoxic drug. It can be used to treat oedema caused by diseases such as congestive heart failure and cirrhosis (Joannidis et al., 2019; Zhao et al., 2020). When renal perfusion is inadequate, furosemide can reduce the potential risk of tubular injury due to ischaemia by inhibiting the Nn-2Cr co-transporter (NKCC2), reducing ion channel activity and decreasing cellular oxygen consumption. However, prior fluid replacement is required to correct hypovolemia, otherwise the use of furosemide in hypovolemic patients is likely to promote the development of AKI (Shah et al., 2017; Joannidis et al., 2019). It has also been demonstrated that the use of furosemide in pediatric patients in intensive care units increases the risk of AKI in patients (Slater et al., 2017). In our results, the proportion of patients who used furosemide injection and developed a DIKI with a preliminary diagnosis of heart disease was particularly low. Thus, we ruled out this possibility of AKI occurring as a result of cardio-renal syndrome. From our results, it appears that the use of furosemide can increase the risk of AKI in pediatric patients. Before using furosemide in critically ill patients, it is important to note the status of patients. The 20% albumin prepared from human plasma injection can be used to treat shock due to blood loss or burns, elevated cranial pressure due to cerebral edema and injury, or edema or ascites due to cirrhosis and renal disease. We can draw inspiration from the hypothesis of renal failure described by Moran and Kapsner (Moran and Kapsner, 1987): Glomerular Filtration Rate (GFR) is related to the imbalance of renal perfusion pressure and oncotic forces at the membrane of the glomeruli; when the colloid osmotic pressure increases, glomerular filtration decreases or stops. It can be used to correct blood volume deficiencies and maintain plasma colloid osmotic pressure. A studies found that the use of hypertonic albumin injections may increase the risk of AKI in patients needing fluid resuscitation for shock (Schortgen et al., 2008). In addition, a study had also found that albumin administration is associated with an increased risk of AKI after cardiac surgery in a dose-dependent manner (Frenette et al., 2014). However, as can be seen from the distribution of our patients' major diagnosis (Table 1), the proportion of DIKI patients with heart disease was not high (8.6%). We also used PSM in the exposed and non-exposed groups to avoid the effect of the primary diagnosis on the outcome. When using 20% Human Albumin Injection, excessive blood volume may result once the infusion dose and infusion rate are not adjusted to the patient's circulatory status. Continued supplementation of human albumin in the presence of excess blood volume can exacerbate the patient's risk of AKI. Therefore, when using this drug, it is important to focus on the patient's circulatory status first to prevent the development of DIKI. Midazolam is a sedative drug, which is commonly used for endoscopic procedures, general anesthesia, and sedation of patients with tracheal intubation and mechanical ventilation. Fentanyl citrate injection, a drug commonly used in compound general anesthesia today, is frequently used for sedation and analgesia before, during, and after anesthesia. Midazolam and fentanyl are commonly used in pediatric intensive care units

TABLE 2 Exposure and non-exposure of suspected drugs and the risk of DIKI.

Drug ID	Drugs name	Exposed group		Unexposed group		Beta	P	OR (95%CI)
		+	−	+	−			
1	Furosemide Injection	25	1,392	2	1,415	2.54	0.001	12.71 (3.00–53.75)
2	Midazolam Injection	24	1,072	3	1,093	2.10	0.001	8.16 (2.45–27.17)
3	20% Albumin Prepared From Human Plasma Injection	21	1,252	5	1,268	1.45	0.004	4.25 (1.60–11.32)
4	Fentanyl citrate Injection	23	769	3	789	2.06	0.001	7.87 (2.35–26.31)
5	Ibuprofen Suspension	14	1,120	7	1,127	0.70	0.132	2.01 (0.81–5.00)
6	Diazepam Injection	15	1,689	14	1,690	0.07	0.852	1.07 (0.52–2.23)
7	Methylprednisolone sodium succinate for Injection	13	1,149	9	1,153	0.37	0.394	1.45 (0.62–3.40)
8	Compound Glycyrrhizin Injection	14	724	4	734	1.27	0.026	3.55 (1.16–10.83)
9	Vancomycin Hydrochloride for Intra Venous	14	454	1	467	2.67	0.010	14.40 (1.89–109.96)
10	Adrenaline Hydrochlaride Injection	9	1,213	9	1,213	0.00	1.000	1.000 (0.40–2.53)
11	Milrinone Lactate Injection	14	492	2	504	1.97	0.009	7.17 (1.62–31.72)
12	Meropenem for Injection	10	793	9	794	0.11	0.818	1.11 (0.45–2.75)
13	Human Immumoglobulin for Intravenous Injection	11	677	7	681	0.46	0.347	1.52 (0.61–4.10)
14	Aminomethylbenzoic Acid Injection	10	794	9	795	0.11	0.818	1.11 (0.45–2.75)
15	Etamsylate Injection	9	1,006	11	1,004	−0.203	0.654	0.82 (0.34–1.98)

Abbreviation: DIKI, drug-induced kidney injury; OR, odds ratio.

(PICUs). The UK Pediatric Intensive Care Society's consensus have recommended the combination of midazolam and fentanyl in continuous infusion as the first choice for sedation/ analgesia in PICUs patients (Playfor et al., 2006). Fentanyl belongs to the synthetic class of opioid receptor agonists. Opioids can cause kidney damage by causing excessive sedation, hypoxia and decreased renal blood flow in pediatric patients (Schenk et al., 1995; Feng et al., 2015; Mallappallil et al., 2017). Midazolam Injection belongs to the benzodiazepine group of drugs and is also often used in combination with fentanyl injection in our results, which can make it more dangerous and more likely to lead to excessive sedation and cause AKI. Therefore, pediatric patients should be alert to the development of AKI when using midazolam injection and fentanyl citrate injection, especially when they are used in combination. Compound glycyrrhizin injection can be used to treat chronic liver disease, improve abnormal liver function, and treat eczema, dermatitis, and urticaria. Its main component is glycyrrhizin, which is extracted from *Glycyrrhiza* glabra (Deutch et al., 2019). There are no studies on the association of Compound glycyrrhizin injection with the development of AKI and it is not clear what causes it to occur. However, its structure is similar to that of aldosterone, which enables it to mimic the sodium-retaining and potassium-removing effects of aldosterone. It can also inhibit the activity of 11β-hydroxysteroid dehydrogenase, leading to the increased release of other aldosterone-like components and resulting in the development of hypokalemia. Once hypokalaemia occurs, it may lead to dysfunction of the sodium-potassium pump, extracellular calcium entry of extracellular calcium into cells, increased intracellular free calcium ion concentration, activation of intracellular proteases by calcium overload, causing necrosis of myocytes and muscle fibres, release of harmful components into the extracellular fluid and blood, and ultimately renal impairment. Meanwhile, milrinone lactate injection is primarily used for the short-term treatment of patients with acute decompensated heart failure. In pediatric patients, it can be used to prevent cardiac output syndrome after cardiac surgery. These patients are likely to be treated with Cardiopulmonary bypass (CPB) at the same time. It has been reported that there is a significant association between the perioperative use of milrinone and acute kidney risk or injury in pediatric patients who have received CPB (Chiravuri et al., 2011). However, CPB has also been shown to be a risk factor for the development of AKI in pediatric patients (Aydin et al., 2012; Pedersen, 2012). Thus, we cannot clarify the effect of milrinone lactate injection on the development of AKI in pediatric patients other than the effect of CPB, but the use of milrinone injection in pediatric patients receiving CPB may also increase the risk of AKI.

In our study, there are several shortcomings. First of all, due to the small sample of patients, it is hard to explore the factors influencing adverse drug reactions. It is an urgent need for larger population-based studies to validate and further investigate the drugs that we found to be associated with the occurrence of AKI. Secondly, as it was a retrospective study using a secondary database, the information recorded in the database on the patients will not exactly match the purpose of our study, and for these patients we need to exclude. Half of patients were

excluded due to missing records of medication information or apparently incorrect records of data. Third, there are many factors that can contribute to the development of AKI in the PICU and medication is only one part of them. We learned that some factors such as hemodynamic status and cardiac surgery were risk factors for the development of AKI, but we were unable to include these important factors in our analysis because no such information was available in the database for the duration of the patient's hospitalization.

Our study found that furosemide injection, midazolam injection, 20% albumin prepared from human plasma injection, fentanyl citrate injection, compound glycyrrhizin injection, vancomycin hydrochloride for intravenous and milrinone lactate injection were risk factors for the development of AKI in critically ill pediatric patients. These results suggest that, because of the many complex factors that may be encountered in critical care units, the administration of medications for these patients needs to be more rigorous and rational, according to their own conditions, to avoid adverse effects caused by these drugs, as much as possible.

Conclusion

In order to search for drugs associated with critically ill pediatric patients with DIKI, we assessed and validated the relationship between patients and suspected drugs, screening patients in the PIC database, finally we found some drugs related to DIKI. We hope to provide some reference for physicians and pharmacists when administering drugs to critically ill pediatric patients to reduce adverse reactions of drugs.

Data availability statement

The raw data supporting the conclusions of this article will be made available by the authors, without undue reservation.

Ethics statement

The studies involving human participants were reviewed and approved by the study protocol was approved by the Institutional Review Board (AAHRPP-accredited) of the Third Xiangya Hospital of Central South University. The data used in this study were de-identified so the statement of informed consent from the Institutional Review Board was waived for this study.

Author contributions

CXG and ZL designed the study. BH, LY, TL, and ZF extracted and analyzed the data. BH, LJH, and CJG drafted the first draft of the manuscript. LH, WT, GY, and CXG interpreted the results and revised the first draft of the manuscript. CXG and ZL organized the study as an overall supervisor. All the authors approved the final version of the manuscript and agreed on submitting it to Annals of Intensive Care. All authors read and approved the final manuscript.

Funding

This work was supported by National Natural Science Foundation of China under Grant number 81974511; Natural Science Foundation of Hunan Province under Grant number 2020JJ4832, Natural Science Foundation of Guangdong Province under Grant number 2018A030313871, the Scientific and Technological Project of Changsha under Grant number kq2004147, and the Wisdom Accumulation and Talent Cultivation Project of the Third Xiangya Hospital of Central South University under Grant number YX202110.

Conflict of interest

The authors declare that the research was conducted in the absence of any commercial or financial relationships that could be construed as a potential conflict of interest.

Publisher's note

Supplementary material

The Supplementary Material for this article can be found online at: https://www.frontiersin.org/articles/10.3389/fphar.2022.993923/full#supplementary-material

References

Aydin, S. I., Seiden, H. S., Blaufox, A. D., Parnell, V. A., Choudhury, T., Punnoose, A., et al. (2012). Acute kidney injury after surgery for congenital heart disease. *Ann. Thorac. Surg.* 94 (5), 1589–1595. doi:10.1016/j.athoracsur.2012.06.050

Cheng, W., Wu, X., Liu, Q., Wang, H. S., Zhang, N. Y., Xiao, Y. Q., et al. (2020). Post-contrast acute kidney injury in a hospitalized population: Short-mid-and long-term outcome and risk factors for adverse events. *Eur. Radiol.* 30 (6), 3516–3527. doi:10.1007/s00330-020-06690-3

Chiravuri, S. D., Riegger, L. Q., Christensen, R., Butler, R. R., Malviya, S., Tait, A. R., et al. (2011). Factors associated with acute kidney injury or failure in children undergoing cardiopulmonary bypass: A case-controlled study. *Paediatr. Anaesth.* 21 (8), 880–886. doi:10.1111/j.1460-9592.2011.03532.x

Deutch, M. R., Grimm, D., Wehland, M., Infanger, M., and Krüger, M. (2019). Bioactive candy: Effects of licorice on the cardiovascular system. *Foods* 8 (10), E495. doi:10.3390/foods8100495

Downes, K. J., Cowden, C., Laskin, B. L., Huang, Y. S., Gong, W., Bryan, M., et al. (2017). Association of acute kidney injury with concomitant vancomycin and piperacillin/tazobactam treatment among hospitalized children. *JAMA Pediatr.* 171 (12), e173219. doi:10.1001/jamapediatrics.2017.3219

Downes, K. J., Hayes, M., Fitzgerald, J. C., Pais, G. M., Liu, J., Zane, N. R., et al. (2020). Mechanisms of antimicrobial-induced nephrotoxicity in children. *J. Antimicrob. Chemother.* 75 (1), 1–13. doi:10.1093/jac/dkz325

Elyasi, S., Khalili, H., Dashti-Khavidaki, S., and Mohammadpour, A. (2012). Vancomycin-induced nephrotoxicity: Mechanism, incidence, risk factors and special populations. A literature review. *Eur. J. Clin. Pharmacol.* 68 (9), 1243–1255. doi:10.1007/s00228-012-1259-9

Feiten, H. D. S., Okumura, L. M., Martinbiancho, J. K., Andreolio, C., Da Rocha, T. S., Antonacci Carvalho, P. R., et al. (2019). Vancomycin-associated nephrotoxicity and risk factors in critically ill children without preexisting renal injury. *Pediatr. Infect. Dis. J.* 38 (9), 934–938. doi:10.1097/inf.0000000000002391

Feng, G., Luo, Q., Guo, E., Yao, Y., Yang, F., Zhang, B., et al. (2015). Multiple organ dysfunction syndrome, an unusual complication of heroin intoxication: A case report and review of literature. *Int. J. Clin. Exp. Pathol.* 8 (9), 11826–11830.

Frenette, A. J., Bouchard, J., Bernier, P., Charbonneau, A., Nguyen, L. T., Rioux, J. P., et al. (2014). Albumin administration is associated with acute kidney injury in cardiac surgery: A propensity score analysis. *Crit. Care* 18 (6), 602. doi:10.1186/s13054-014-0602-1

Hanrahan, T. P., Kotapati, C., Roberts, M. J., Rowland, J., Lipman, J., Roberts, J. A., et al. (2015). Factors associated with vancomycin nephrotoxicity in the critically ill. *Anaesth. Intensive Care* 43 (5), 594–599. doi:10.1177/0310057x1504300507

Ingelfinger, J. R., Kalantar-Zadeh, K., and Schaefer, F. (2016). Ingelfinger JR, kalantar-zadeh K, schaefer F; for the world kidney day steering committee. Averting the legacy of kidney disease-focus on childhood. Kidney int. 2016;89:512-518. *Kidney Int.* 89 (6), 1405. doi:10.1016/j.kint.2016.04.001

Joannidis, M., Klein, S. J., and Ostermann, M. (2019). 10 myths about frusemide. *Intensive Care Med.* 45 (4), 545–548. doi:10.1007/s00134-018-5502-4

Joyce, E. L., Kane-Gill, S. L., Priyanka, P., Fuhrman, D. Y., and Kellum, J. A. (2019). Piperacillin/Tazobactam and antibiotic-associated acute kidney injury in critically ill children. *J. Am. Soc. Nephrol.* 30 (11), 2243–2251. doi:10.1681/asn.2018121223

Kaddourah, A., Basu, R. K., Bagshaw, S. M., and Goldstein, S. L. (2017). Epidemiology of acute kidney injury in critically ill children and young adults. *N. Engl. J. Med.* 376 (1), 11–20. doi:10.1056/NEJMoa1611391

KDIGO (2012). Kidney disease: Improving global outcomes (KDIGO) acute kidney injury work group. KDIGO clinical practice guideline for acute kidney injury. *Kidney Int. Suppl.* 2 (1), 1–138. doi:10.1038/kisup.2012.1

Levey, A. S., and James, M. T. (2017). Acute kidney injury. *Ann. Intern. Med.* 167 (9), ITC66-ITC80–itc80. doi:10.7326/aitc201711070

Mallappallil, M., Sabu, J., Friedman, E. A., and Salifu, M. (2017). What do we know about opioids and the kidney? *Int. J. Mol. Sci.* 18 (1), E223. doi:10.3390/ijms18010223

Meraz-Muñoz, A., Amir, E., Ng, P., Avila-Casado, C., Ragobar, C., Chan, C., et al. (2020). Acute kidney injury associated with immune checkpoint inhibitor therapy: Incidence, risk factors and outcomes. *J. Immunother. Cancer* 8 (1), e000467. doi:10.1136/jitc-2019-000467

Moran, M., and Kapsner, C. (1987). Acute renal failure associated with elevated plasma oncotic pressure. *N. Engl. J. Med.* 317 (3), 150–153. doi:10.1056/nejm198707163170306

Naranjo, C. A., Busto, U., Sellers, E. M., Sandor, P., Ruiz, I., Roberts, E. A., et al. (1981). A method for estimating the probability of adverse drug reactions. *Clin. Pharmacol. Ther.* 30 (2), 239–245. doi:10.1038/clpt.1981.154

O'callaghan, K., Hay, K., Lavana, J., and Mcnamara, J. F. (2020). Acute kidney injury with combination vancomycin and piperacillin-tazobactam therapy in the ICU: A retrospective cohort study. *Int. J. Antimicrob. Agents* 56 (1), 106010. doi:10.1016/j.ijantimicag.2020.106010

Pedersen, K. (2012). Acute kidney injury in children undergoing surgery for congenital heart disease. *Eur. J. Pediatr. Surg.* 22 (6), 426–433. doi:10.1055/s-0032-1322540

Playfor, S., Jenkins, I., Boyles, C., Choonara, I., Davies, G., Haywood, T., et al. (2006). Consensus guidelines on sedation and analgesia in critically ill children. *Intensive Care Med.* 32 (8), 1125–1136. doi:10.1007/s00134-006-0190-x

Schenk, H. D., Radke, J., Ensink, F. B., Drobnik, L., Kettler, D., Sonntag, H., et al. (1995). Interactions between renal and general hemodynamics in fentanyl, droperidol, ketamine, thiopental and in peridural anesthesia--animal studies. *Anaesthesiol. Reanim.* 20 (3), 60–70.

Schortgen, F., Girou, E., Deye, N., and Brochard, L. (2008). The risk associated with hyperoncotic colloids in patients with shock. *Intensive Care Med.* 34 (12), 2157–2168. doi:10.1007/s00134-008-1225-2

Searns, J. B., Gist, K. M., Brinton, J. T., Pickett, K., Todd, J., Birkholz, M., et al. (2020). Impact of acute kidney injury and nephrotoxic exposure on hospital length of stay. *Pediatr. Nephrol.* 35 (5), 799–806. doi:10.1007/s00467-019-04431-3

Shah, R., Wood, S. J., Khan, S. A., Chaudhry, A., Rehan Khan, M., and Morsy, M. S. (2017). High-volume forced diuresis with matched hydration using the RenalGuard system to prevent contrast-induced nephropathy: A meta-analysis of randomized trials. *Clin. Cardiol.* 40 (12), 1242–1246. doi:10.1002/clc.22817

Siew, E. D., and Matheny, M. E. (2015). Choice of reference serum creatinine in defining acute kidney injury. *Nephron* 131 (2), 107–112. doi:10.1159/000439144

Slater, M. B., Gruneir, A., Rochon, P. A., Howard, A. W., Koren, G., and Parshuram, C. S. (2017). Identifying high-risk medications associated with acute kidney injury in critically ill patients: A pharmacoepidemiologic evaluation. *Paediatr. Drugs* 19 (1), 59–67. doi:10.1007/s40272-016-0205-1

Su, L., Li, Y., Xu, R., Luo, F., Gao, Q., Chen, R., et al. (2021). Association of ibuprofen prescription with acute kidney injury among hospitalized children in China. *JAMA Netw. Open* 4 (3), e210775. doi:10.1001/jamanetworkopen.2021.0775

Weisbord, S. D., Palevsky, P. M., Kaufman, J. S., Wu, H., Androsenko, M., Ferguson, R. E., et al. (2020). Contrast-associated acute kidney injury and serious adverse outcomes following angiography. *J. Am. Coll. Cardiol.* 75 (11), 1311–1320. doi:10.1016/j.jacc.2020.01.023

Wu, C. Y., Wang, J. S., Chiou, Y. H., Chen, C. Y., and Su, Y. T. (2007). Biopsy proven acute tubular necrosis associated with vancomycin in a child: Case report and literature review. *Ren. Fail.* 29 (8), 1059–1061. doi:10.1080/08860220701643773

Xu, X., Nie, S., Zhang, A., Mao, J., Liu, H. P., Xia, H., et al. (2018). Acute kidney injury among hospitalized children in China. *Clin. J. Am. Soc. Nephrol.* 13 (12), 1791–1800. doi:10.2215/cjn.00800118

Yu, C., Guo, D., Yao, C., Yang, H., Liu, S., Zhu, Y., et al. (2020a). Clinical characteristics of hospitalized patients with drug-induced acute kidney injury and associated risk factors: A case-control study. *Biomed. Res. Int.* 2020, 9742754. doi:10.1155/2020/9742754

Yu, Y., Nie, X., Song, Z., Xie, Y., Zhang, X., Du, Z., et al. (2020b). Signal detection of potentially drug-induced liver injury in children using electronic health records. *Front. Pediatr.* 8, 171. doi:10.3389/fped.2020.00171

Zeng, X., Yu, G., Lu, Y., Tan, L., Wu, X., Shi, S., et al. (2020). PIC, a paediatric-specific intensive care database. *Sci. Data* 7 (1), 14. doi:10.1038/s41597-020-0355-4

Zhao, G. J., Xu, C., Ying, J. C., Lü, W. B., Hong, G. L., Li, M. F., et al. (2020). Association between furosemide administration and outcomes in critically ill patients with acute kidney injury. *Crit. Care* 24 (1), 75. doi:10.1186/s13054-020-2798-6

frontiers | Frontiers in Pharmacology

TYPE Review
PUBLISHED 27 September 2022
DOI 10.3389/fphar.2022.941182

OPEN ACCESS

EDITED BY
Xiaoling Wang,
Capital Medical University, China

REVIEWED BY
Nikola Kotur,
University of Belgrade, Serbia
Sarah McGarrity,
Harvard Medical School, Boston,
United States

*CORRESPONDENCE
Feng Chen,
cy.chen508@gmail.com
Li Zhou,
zhoulinjey@163.com
Tao Li,
ltcrlcq@yeah.net

SPECIALTY SECTION
This article was submitted to Obstetric and Pediatric Pharmacology, a section of the journal Frontiers in Pharmacology

RECEIVED 11 May 2022
ACCEPTED 02 August 2022
PUBLISHED 27 September 2022

CITATION
Guo H-L, Zhao Y-T, Wang W-J, Dong N, Hu Y-H, Zhang Y-Y, Chen F, Zhou L and Li T (2022), Optimizing thiopurine therapy in children with acute lymphoblastic leukemia: A promising "MINT" sequencing strategy and therapeutic "DNA-TG" monitoring. *Front. Pharmacol.* 13:941182. doi: 10.3389/fphar.2022.941182

Optimizing thiopurine therapy in children with acute lymphoblastic leukemia: A promising "MINT" sequencing strategy and therapeutic "DNA-TG" monitoring

Hong-Li Guo[1], Yue-Tao Zhao[2,3], Wei-Jun Wang[2,3], Na Dong[4,5], Ya-Hui Hu[1], Yuan-Yuan Zhang[1], Feng Chen[1]*, Li Zhou[6]* and Tao Li[7]*

[1]Pharmaceutical Sciences Research Center, Department of Pharmacy, Children's Hospital of Nanjing Medical University, Nanjing, China, [2]School of Basic Medicine and Clinical Pharmacy, China Pharmaceutical University, Nanjing, China, [3]Visiting Graduate Student from School of Basic Medicine and Clinical Pharmacy, Pharmaceutical University, Nanjing, China, [4]Institute of Pharmaceutical Science, China Pharmaceutical University, Nanjing, China, [5]School of Institute of Pharmaceutical Science, Pharmaceutical University, Nanjing, China, [6]Hematology and Oncology Department, Children's Hospital of Nanjing Medical University, Nanjing, China, [7]Department of Solid Oncology, Children's Hospital of Nanjing Medical University, Nanjing, China

Thiopurines, including thioguanine (TG), 6-mercaptopurine (6-MP), and azathioprine (AZA), are extensively used in clinical practice in children with acute lymphoblastic leukemia (ALL) and inflammatory bowel diseases. However, the common adverse effects caused by myelosuppression and hepatotoxicity limit their application. Metabolizing enzymes such as thiopurine S-methyltransferase (TPMT), nudix hydrolase 15 (NUDT15), inosine triphosphate pyrophosphohydrolase (ITPA), and drug transporters like multidrug resistance-associated protein 4 (MRP4) have been reported to mediate the metabolism and transportation of thiopurine drugs. Hence, the single nucleotide polymorphisms (SNPs) in those genes could theoretically affect the pharmacokinetics and pharmacological effects of these drugs, and might also become one of the determinants of clinical efficacy and adverse effects. Moreover, long-term clinical practices have confirmed that thiopurine-related adverse reactions are associated with the systemic concentrations of their active metabolites. In this review, we mainly summarized the pharmacogenetic studies of thiopurine drugs. We also evaluated the therapeutic drug monitoring (TDM) research studies and focused on those active metabolites, hoping to continuously improve monitoring strategies for thiopurine therapy to maximize therapeutic efficacy and minimize the adverse effects or toxicity. We proposed that tailoring thiopurine dosing based on *MRP4*, *ITPA*, *NUDT15*, and *TMPT* genotypes, defined as "MINT" panel sequencing strategy, might contribute toward improving the efficacy and safety of thiopurines. Moreover, the DNA-incorporated thioguanine nucleotide (DNA-TG) metabolite level was more suitable for red cell 6-thioguanine nucleotide (6-

TGNs) monitoring, which can better predict the efficacy and safety of thiopurines. Integrating the panel "MINT" sequencing strategy with therapeutic "DNA-TG" monitoring would offer a new insight into the precision thiopurine therapy for pediatric acute lymphoblastic leukemia patients.

KEYWORDS

thiopurines, myelosuppression, pharmacogenetics, "MINT" sequencing strategy, therapeutic "DNA-TG" monitoring

Introduction

Thioguanine (TG), 6-mercaptopurine (6-MP), and azathioprine (AZA), collectively known as thiopurines, are broadly applied as anti-cancer and immunosuppressive agents. 6-MP is one of the backbone drugs for the maintenance therapy of acute lymphoblastic leukemia (ALL) in children and adults (Schmiegelow et al., 2014). 6-MP and AZA are also commonly prescribed in maintaining the clinical remission of patients with steroid-dependent inflammatory bowel diseases (IBD) (Andoh et al., 2021). Thiopurines are pro-drugs devoid of any intrinsic activity and need metabolic transformation to their pharmacologically active metabolites, 6-thio-guanine nucleotides (6-TGNs), which are structurally similar to the endogenous purine-base guanine, are fraudulent bases being integrated into the DNA of leucocytes, leading to the inhibition of purine *de novo* synthesis and cell death (Karran and Attard, 2008). It is worth noting that, while thioguanine enters the DNA to play a therapeutic role, it also creates conditions for the occurrence of common and serious adverse reactions. Hepatotoxicity, pancreatitis, gastric intolerance, and leukopenia are common adverse drug reactions associated with thiopurines (Koren et al., 1990; Lee et al., 2022). In particular, life-threatening leukopenia, caused by thiopurines, might interrupt or even discontinue the effective treatment, resulting in a high risk of subsequent disease recurrence in ALL (Fotoohi et al., 2010). Hence, the narrow therapeutic index of thiopurines indicates an urgent demand for us to utilize precision medicine strategies to make better use of these drugs.

Polymorphisms of genes encoding various drug-metabolizing enzymes and transporters could exert an effect on the efficacy and toxicity of thiopurines. In fact, the first pharmacogenetic marker by means of a pharmacology-guided approach was recognized as single nucleotide polymorphisms (SNPs) in thiopurine S-methyltransferase (TPMT) (Weinshilboum and Sladek, 1980), and its predictive role in 6-MP-related adverse effects is regarded as an important development in this field. In recent years, other related enzymes including Nudix hydrolase 15 (NUDT15) (Yang et al., 2014), inosine triphosphate pyrophosphohydrolase (ITPA) (Barba et al., 2022), and multidrug resistance-associated protein (e.g., MRP4) (Wielinga et al., 2002) have been reported to dramatically affect the pharmacokinetics and pharmacological properties of thiopurines, thereby becoming critical determinants of their therapeutic efficacy and toxicity. However, the significant differences in the distribution and frequency of these SNPs among different ethnic groups pose certain challenges for a practical clinical application of genotype-based precision therapy.

Previously, monitoring the drug concentration of thioguanine nucleotides (TGNs) in red blood cells (RBCs) has played an important role in maximizing the clinical efficacy and reducing adverse effects of these drugs, and has also been helpful for individualized dose adjustment (Nygaard et al., 2004; Hedeland et al., 2010; Nielsen et al., 2016). Unfortunately, there is a broad agreement that too high or too low TGN concentrations should be avoided, but the exact definition of both upper and lower limits, even if such rigid threshold values should be generally used at all, is still debated in different studies. Furthermore, as RBCs are not the active target of thiopurines, some researchers proposed that the cytotoxicity of thiopurines was caused by the incorporation of thioguanine nucleotides into the DNA, called DNA-TG, the true culprit in the nucleus. The concentration of DNA-TG has been quantified by using liquid chromatography–mass spectrometry (Moriyama et al., 2017; Larsen et al., 2021a). Therefore, DNA-TG monitoring is much more helpful in evaluating an inadequate dose or non-adherence, or distinguishing patients with abnormal metabolic spectrums (Nielsen et al., 2017).

In this review, we summarize the pharmacogenetic studies related to those enzymes and transporters taking responsibility for the disposition of thiopurines, focusing on the association between SNPs and the clinical efficacy and side effects of thiopurines. We also review the current status of the TDM of thiopurines in children with ALL. Combining "MINT" panel sequencing with DNA-TG monitoring is a more feasible strategy when implementing thiopurine precision medicine for those pediatric patients.

Metabolism and material action basis of thiopurines

As prodrugs that lack intrinsic activity or with low activity, thiopurines need to be transformed to 6-TGNs inside the cells through multi-enzymatic reactions and then exert

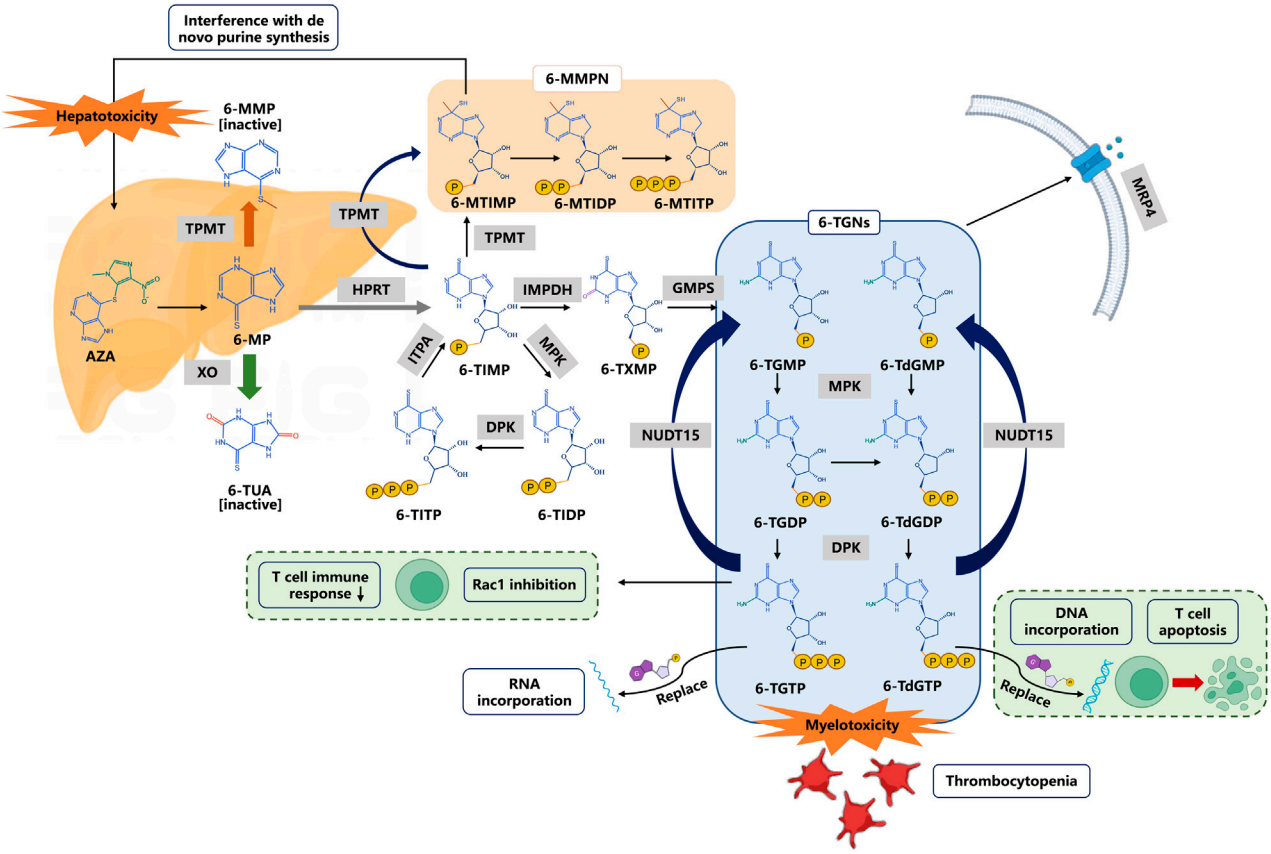

FIGURE 1
Thiopurine metabolism and transportation. 6-Thioguanine nucleotides (6-TGNs) are pharmacologic active products. 6-TGMP 6-thioguanine monophosphate, 6-TGDP 6-thioguanine diphosphate, 6-TGTP 6-thioguanine triphosphate, 6-TdGMP 6-thio-deoxyguanine monophosphate, 6-TdGDP 6-thio-deoxyguanine diphosphate, 6-TdGTP 6-thio-deoxyguanine triphosphate. Abbreviations: AZA azathioprine, 6-MP 6-mercaptopurine, 6-MMP 6-methylmercaptopurine, 6-TUA 6-thiouric acid, 6-TIMP 6-thioinosine monophosphate, 6-MMPN 6-methylmercaptopurine nucleotides, 6-MTIMP 6-methylthioinosine 5′-monophosphate, 6-MTIDP 6-methylthioinosine 5′ -diphosphate, 6-MTITP 6-methylthioinosine 5′-triphosphate, 6-TIDP 6-thioinosine diphosphate, 6-TITP 6-thioinosine triphosphate, 6-TXMP 6-thioxanthosine monophosphate. Enzymes or transporters are shown in gray boxes: TPMT thiopurine S-methyl transferase, XO xanthine oxidase, HPRT hypoxanthine phosphoribosyl transferase, MPK monophosphate kinase, DPK diphosphate kinase, ITPA inosine triphosphate pyrophosphohydrolase, IMPDH inosine monophosphate dehydrogenase, GMPS guanosine monophosphate synthetase, and MRP4 multidrug resistance-associated protein 4.

pharmacological effects. The three major metabolic pathways of 6-MP are well described (Figure 1). Xanthine oxidase (XO) and thiopurine-S-methyltransferase (TPMT) are the two dominant enzymes in the metabolism of 6-MP, and produce inactive metabolites 6-thiouric acid and 6-methylmercaptopurine (6-MMP), respectively. However, the formation of 6-TGNs is a “long journey” involving multiple enzymes. 6-MP is first converted into thioIMP (6-TIMP) by hypoxanthine-guanine phosphoribosyltransferase (HGPRT), and finally, 6-TIMP metabolized to 6-TGNs, the active forms, which are successively mediated by hypoxanthine monophosphate dehydrogenase (IMPDH) and guanylate synthase (GMPS), respectively. Meanwhile, the multidrug resistance protein 4 (MRP4) can pump these active metabolites out of the cells. In this journey, TPMT can also metabolize intermediate 6-TIMP into methyl-thioIMP (6-MTIMP), an active metabolite that can suppress *de novo* purine synthesis, and has been reported to have an association with hepatotoxicity (Adam de Beaumais et al., 2011). 6-TIMP also can be catalyzed into 6-thioinosine diphosphate (6-TIDP) by monophosphate kinase (MPK), and into 6-thioinosine triphosphate (6-TITP) by diphosphate kinase (DPK), and finally back to 6-TIMP by ITPA forming a complete cycle.

6-TGNs are active metabolites, consisting of 6-thioguanine monophosphate (6-TGMP), 6-thio-deoxyguanine monophosphate (6-TdGMP), 6-thioguanine diphosphate (6-TGDP), 6-thio-deoxyguanine diphosphate (6-TdGDP), 6-thioguanine triphosphate (6-TGTP), and 6-thio-deoxyguanine

TABLE 1 Frequencies of the TPMT and NUDT15 alleles/phenotypes in major race/ethnic groups.

—	Allele	African	Central/South Asian	East Asian	European	Phenotype	African	Central/South Asian	East Asian	European
TPMT	*1	92.34%	98.14%	97.96%	95.31%	NM	85.27%	96.31%	95.97%	90.84%
	*2	0.53%	0.02%	0.01%	0.21%	IM	6.89%	3.41%	3.34%	8.42%
	*3A	0.80%	0.42%	0.03%	3.43%	PIM	0.29%	0.00%	0.01%	0.02%
	*3B	0.00%	0.17%	0.00%	0.27%	PM	0.14%	0.03%	0.03%	0.20%
	*3C	2.40%	1.12%	1.64%	0.47%	Indeterminate	7.41%	0.24%	0.65%	0.53%
NUDT15	*1	99.69%	93.00%	87.90%	99.31%	NM	99.38%	86.49%	77.26%	0.53%
	*2	0.00%	14.3%	3.50%	0.00%	IM	0.27%	12.55%	16.79%	8.42%
	*3	0.10%	6.70%	6.05%	0.20%	PIM	0.00%	0.03%	0.49%	90.84%
	*4	0.03%	0.00%	0.09%	0.00%	PM	0.00%	0.46%	0.91%	0.20%
	*5	0.00%	0.04%	1.11%	0.00%	Indeterminate	0.35%	0.46%	4.55%	0.02%
	*6	0.15%	0.20%	1.30%	0.30%					

NM: Normal metabolizer; IM: Intermediate metabolizer; PIM: Possible intermediate metabolizer; PM: Poor metabolizer.
Data from PharmGKB (https://www.pharmgkb.org) and study of Banerjee R and colleagues (Banerjee et al., 2020).

triphosphate (6-TdGTP). The aforementioned 6 metabolites are catalyzed by MPK, DPK, and NUDT15, respectively, to form another metabolic cycle. On one hand, 6-TdGTPs are integrated into DNA (6-TdGTP) and RNA (6-TGTP), leading to nucleotide suppression and protein synthesis and cause cell apoptosis (Paugh et al., 2010). On the other hand, 6-TGTPs have been reported to block the activity of Vav on RAC proteins and thus to prevent the development of an effective immune response in T cells (Poppe et al., 2006). It is generally accepted that the adverse reactions of thiopurines are closely associated with those active metabolites, especially high levels of 6-TGNs resulting in dose-dependent side effects typified by leukopenia (Relling et al., 1999). Therefore, the genetic variation of key enzymes in metabolic transformations (such as TPMT, ITPA, and NUDT15) would have an important impact on the pharmacokinetics, pharmacodynamics, and side effects of thiopurines.

Pharmacogenetics of thiopurines

Thiopurine S-methyltransferase

As one of the most critical enzymes in the biotransformation of thiopurines, TPMT is the earliest and most comprehensive pharmacogenetic predictor used in clinical practice. Loss of the TPMT function leads to excessive levels of 6-TGNs, which greatly increase the risk of leukopenia. In 1980, Weinshiboum and Sladek first reported the significant individual variations of erythrocyte TPMT activity in Caucasians, with 88.6% of high, 11.1% of intermediate, and 0.3% of undetectable activities, respectively (Weinshilboum and Sladek, 1980). Since then, this classification method has been widely used. Moreover, SNPs resulting in loss of function of the TPMT have also been identified (Ansari et al., 2002). More than 40 allelic variants (**2–*44*) in the *TPMT* gene have been discovered (Iu et al., 2017; Zimdahl Kahlin et al., 2019), but the loss-of-function variants mainly include *TPMT*2*, *TPMT*3A*, *TPMT*3B*, and *TPMT*3C* (Azimi et al., 2014). Therefore, the TPMT phenotype is usually determined by the aforementioned mutant variants. Especially, *TPMT* genotypes **3A* and **3C* had the strongest associations with toxicity (Rudin et al., 2017). In 2011, the Clinical Pharmacogenetics Implementation Consortium (CPIC) guidelines for *TPMT* genotype and thiopurine dosing (Relling et al., 2011) recommend pre-emptive genotyping for *TPMT* before the initiation of thiopurine treatment, and that patients with heterozygous **1* allele and with **2/*3A/*3C/*4* alleles (intermediate metabolizers) should start at 30–70% of the full dose (6-MP 50 mg/m^2/day or 0.75 mg/kg/day). However, for poor metabolizers, the thiopurine dose should be purposefully started with 10% of the full dose, and administered weekly thrice instead of daily. This approach has been proven to decrease the incidence of acute toxicity while having no negative effect on the relapse rates in ALL (Relling et al., 2006).

Despite the success of *TPMT* pharmacogenetic testing, the most important issue is that the prevalence of loss-of-function *TPMT* alleles varies across ethnic groups (Table 1, https://www.pharmgkb.org). In Europeans and African Americans, the common alleles that cause TPMT deficiency are *TPMT*2*, **3A*, **3B*, and **3C*, while in Asians, **3C* is the most common mutant allele. A recent extensive whole-genome re-sequencing study in 3,554 Japanese showed that alleles **3A* and **3B* were absent (not observed), and only allele **3C* was

TABLE 2 Frequencies of the ITPA and MRP4 variants in major race/ethnic groups.

—	Allele	African	Latino	East Asian	European	South Asian
ITPA	rs1127354 (C > A/G)	4.46%	4.18%	16.87%	7.06%	12.17%
	rs7270101 (A > C)	7.11%	8.21%		12.92%	1.53%
MRP4	rs3765534 (C > T)	0.08%	2.74%	7.64%	0.89%	5.11%
	rs2274407 (C > A/G/T)	20.95%	6.20%	18.45%	8.05%	17.08%

Data from PharmGKB (https://www.pharmgkb.org).

confirmed to be present (0.96%) (Nagasaki et al., 2015; Yamaguchi-Kabata et al., 2015). Furthermore, in a study including 253 Chinese patients, none of the three alleles **2*, **3A*, and **3B* were observed, and the allelic frequency of **3C* was 1.6% (Zhu et al., 2016). In this study, leukopenia occurred in 25.7% of patients, and no strong association was observed between the disease and **3C* genotypes. Clearly, the low-mutation frequency (<2%) of variants in the *TPMT* gene did not explain the high frequency of adverse reactions (>20%) occurring in East Asian populations, suggesting that pre-emptive *TPMT* genotyping in Asians might not be the same as that in Caucasians. On the other hand, there are a plethora of genetic variants (**1~*44*) of *TPMT* as mentioned previously, and it is hard to determine a patient's exact genotype solely based on one commercial kit which usually cannot provide all target variations. Moreover, other genetic variants may contribute to inter-patient variability. Hopefully, those problems would be readily solved as testing costs are reduced and pharmacogenetic implementations become very popular.

Another concern is that results from a pharmacogenetic test are incapable of covering the other co-factors contributing to the TPMT phenotype such as age, renal insufficiency, or drug–drug interactions (Wu et al., 2019). From this perspective, measuring TPMT activity is a more accurate strategy for predicting the appropriate dose of thiopurines than genotyping test. Actually, TPMT phenotype testing is fairly common in some countries (Fargher et al., 2007; Weitzel et al., 2018). However, it is worth noting that TPMT enzyme activity is usually measured in fresh red blood cells directly (Mokhtari et al., 2020), or consumes a longer turnaround test time (Weitzel et al., 2018). Moreover, in patients who have received blood transfusions recently or in leukemia patients, because of atypical hematopoiesis, the result could not reflect the true enzymatic activity (Mokhtari et al., 2020).

Interestingly, genotype–phenotype discordance was reported at a rate of 5% in patients who underwent both tests (Weitzel et al., 2018). In patients with a discordant situation, the use of genotypes to guide thiopurine dosing is consistent with a previous study that states that optimum accuracy of the *TPMT* genotype test was achieved as compared with the enzyme activity assay (Donnan et al., 2011).

Nucleoside diphosphate-linked moiety X-type motif 15

In 2014, Yang and others first reported that *NUDT15* (rs116855232, referred to as c.415C > T or p.R139C variant hereafter) was highly associated with thiopurine-induced leukopenia among Korean patients who suffered from IBD (Yang et al., 2014). Subsequently, loss-of-function *NUDT15* diplotypes were found to be consistently related to the intolerance of thiopurine during ALL therapy (Yang et al., 2015; Moriyama et al., 2016). Based on these studies, CPIC in 2018 updated its guidelines for the dosage adjustment of 6-MP, suggesting that ALL patients should be guided by *TPMT* and *NUDT15* genotyping for the initial dose selection of 6-MP (Relling et al., 2019).

NUDT15 is a purine-specific nudix hydrolase that controls the hydrolysis of nucleosides–diphosphates (Gad et al., 2014). This enzyme catalyzes the conversion of TGTP and deoxy-TGTP (TdGTP) metabolites to the low-toxic TGMP and deoxy-TGMP (TdGMP), respectively (Valerie et al., 2016). Defective NUDT15-mediated degradation of TdGTP results in more available TdGTP which can be used for the integration into the DNA (namely DNA-TG, the primary anti-leukemic metabolite). Simultaneously, NUDT15 deficiency also results in more TGTP, which promotes the binding of TGTP to Rac1 and also promotes the transportation of TGTP into the RNA. Therefore, it is hypothesized that NUDT15 negatively regulates thiopurine activation and its cytotoxicity (Moriyama et al., 2016). Although 6-MP-induced leukopenia is known to be related to increased 6-TGNs levels, no significant difference was found between the 6-TGN levels and *NUDT15* variants (Asada et al., 2016). Interestingly, results obtained from a series of model systems in a Moriyama laboratory and ALL patients jointly indicated that NUDT15 deficiency directly led to the excessive DNA-TG levels and increased adverse effects (Moriyama et al., 2016). Therefore, the DNA-TG metabolite levels are preferred over 6-TGNs in forming *NUDT15* genotype-guided dose adjustments (Moriyama et al., 2017).

As the first *NUDT15* SNP linked to thiopurine toxicity, p.R139C was the most studied in patients receiving thiopurine therapy, and the results showed that *NUDT15* p.R139C mutation had no influence on the enzymatic activity. Instead, it negatively

affected the protein stability (Valerie et al., 2016). In children diagnosed with ALL, the tolerability of homozygotes for the p.R139C variant allele was only 8% of the standard dose of 6-MP, while the tolerable dosages were 63 and 83.5% of the standard doses of 6-MP, respectively, in those patients with heterozygous and wild-type genotypes (Yang et al., 2015). To date, a total of 20 haplotypes with star allele names of *NUDT15* (**1-*20*) have been identified (Moriyama et al., 2016; Moriyama et al., 2017; Schaeffeler et al., 2019) (https://www.pharmvar.org/gene/NUDT15). It was found that in Chinese IBD patients, the predictive sensitivity of *NUDT15* p.R139C was 49.2 %. But, the combined analysis of Val18Ile and p.Val18_Val19insGlyVal, designed to identify diplotypes by detecting haplotypes **5* and **6*, successfully increased the sensitivity to 55.4 % (Chao et al., 2017). However, compared with p.R139C, other variants are rare, and their correlations with thiopurine-induced toxicity in clinical practice remain unclear. As shown in Table 1, the frequency of the decreased function NUDT15 variants is higher in Asians and Hispanics, but lower in Europeans and Africans. Interestingly, the frequency is just reverse for *TPMT* variants. Therefore, as the CPIC guideline recommended, if genetic tests are available for only one gene (*TPMT* or *NUDT15*, but not both), the matched decision-making will be implemented by clinical labs. More importantly, the potential association of rare mutations with efficacy and adverse reactions of thiopurines remains to be confirmed by large cohort studies.

Inosine triphosphate pyrophosphohydrolase

ITPA can catalyze the phosphorylation of inosine triphosphate (ITP) and convert the latter to inosine monophosphate (IMP), which is a key substance in the purine metabolism. In the metabolism of 6-MP, ITPA is the catalyst that helps to complete the hydrolysis process from 6-TITP to 6-TIMP, and the ITPA deficiency leads to an abnormal accumulation of 6-TITP, which results in toxicity (Marinaki et al., 2004). There are 11 *ITPA* variants that have been reported (Sakamoto et al., 2020), and the two most common SNPs are 94C > A as well as IVS2 + 21A > C. Several studies have examined the role of these two variants in the *ITPA* gene with 6-MP metabolism, as well as adverse drug reactions including hepatotoxicity, flu-like symptoms, arthralgia, and pancreatitis (Arenas et al., 2007; Zabala-Fernandez et al., 2011; Wroblova et al., 2012) with promising results. However, consistent with *TPMT* polymorphism, the frequency of the *ITPA* (94C > A) A allele differed significantly by ethnicity and was higher in Asians (11–19%) than in Caucasian, Hispanics, and Africans (1–7%) (Okada et al., 2009). Interestingly, the reverse situation would appear for the frequency of the *ITPA* 94C > A allele and *TPMT* polymorphisms in the same populations (Marsh and Van Booven, 2009).

Naturally, research studies on the relationship between the *ITPA* gene polymorphism and the adverse reactions of thiopurines are inconsistent partly due to the ethnic differences in allele frequencies (Table 2). For instance, Uchiyama found that the *ITPA* 94C > A mutation occurred more frequently than *TPMT* variants in Japanese patients diagnosed with thiopurine-induced leukopenia (Uchiyama et al., 2009). Also, ALL patients with allele *ITPA* 94A were more likely to suffer from fever and hepatotoxicity from 6-MP, while the prevalence of *TPMT* variants was too low to be well applied in Malays, Chinese, and Indian populations (Wan Rosalina et al., 2012). Therefore, Asians may be more sensitive to the toxicity of AZA/6-MP based on the *ITPA* mutation than *TPMT*. However, a lack of association between the *ITPA* 94C > A polymorphism and AZA-related adverse effects was found in a New Zealander (Gearry et al., 2004). In addition, *ITPA* genotyping has no predictive significance for the clarity and development of the AZA side effects (van Dieren et al., 2005). In the Netherlands, the mean doses of 6-MP did not differ in ALL patients with or without *ITPA* variants (Kouwenberg et al., 2020). Another study came to a similar conclusion (Wahlund et al., 2020). The aforementioned results suggested that, before the beginning of maintenance treatment for ALL in these populations, the *ITPA* genotype should not to be regarded as a part of the accepted assessment.

Stocco and others analyzed a group of St. Jude patients with ALL whose 6-MP doses were not adjusted based on their *TPMT* genotype or TGN concentrations. Notably, the probability of grade 3–4 infections was not significantly related to the *ITPA* genotype in the aforementioned conditions. But if the doses were tailored for *TPMT* and *ITPA*, then they had a great effect on the likelihood of febrile neutropenia (Stocco et al., 2010). According to the authors, most studies suggested that the dose of 6-MP taken by patients was not fully adjusted for the *TPMT* genotype. Their results revealed that it might be the cause of why the influence of the *ITPA* genotype had been inconsistent in previous studies. Some researchers tend to suggest that physicians should first ponder over the genotyping for *ITPA* variants, together with *TPMT* and *NUDT15*, before deciding to treat a patient with 6-MP (Moradveisi et al., 2019). Of note, the association between *ITPA* 94 C > A and neutropenia in children with ALL was verified in recent systematic reviews and meta-analysis (Barba et al., 2022; Lee et al., 2022). A total of 1,072 and 974 ALL pediatric patients were included in the meta-analysis, respectively. Specifically, pediatric ALL patients with an *ITPA* 94 C > A variant had an approximately 2.5 times higher risk of suffering from neutropenia (Barba et al., 2022; Lee et al., 2022). Moreover, due to the existing ethnic differences in the *ITPA* 94 C > A mutation frequency, both the studies had stratified their data analysis based on the races. For neutropenia, the results did not show any different outcome between Asians and Caucasians (Barba et al., 2022), while for hepatotoxicity, the 94C > A variant was significantly associated with an increased risk in Asians and

Middle Easterners (Lee et al., 2022).Moreover, IBD patients with *ITPA* variant alleles exhibited higher 6-TGN levels than those with the wild-type allele (Luo et al., 2022). These findings support that *ITPA* polymorphisms could be used as predictive biomarkers for thiopurine-related adverse effects. Nevertheless, considering the variable frequency across different ethnicities, the clinical implementation of *ITPA* gene tests for precision thiopurine treatment also warrants further studies.

Multi-drug resistance protein 4

MRP4 is a member of the ATP-binding cassette transporter family, encoded by the *ABCC4* gene, responsible for transporting monophosphorylated nucleosides (Wielinga et al., 2002). Murine models with MRP4 deficiency confirmed that MRP4 protects against thiopurine-induced hematopoietic toxicity by reducing the accumulation of intracellular TGNs (Takenaka et al., 2007; Krishnamurthy et al., 2008). In clinics, Hiromistu Ban and others were the first to demonstrate an association of *MRP4* G2269A (rs3765534) polymorphisms with thiopurine sensitivity (Ban et al., 2010). The authors found that patients with the *MRP4* variant had higher 6-TGN levels in erythrocytes and a higher risk of leukopenia, compared with patients with the wild-type alleles. In addition, another study highlighted the significance of *MRP4* polymorphisms related to 6-MP dose tolerance in ALL maintenance therapy (Tanaka et al., 2015). Moreover, ALL patients with intermediate active *NUDT15* and *ABCC4* variants experienced higher 6-MP intolerability, compared with the group with either of the variants (Tanaka et al., 2018). In a very recent study, the co-occurrence of the *ABCC4* (c.912G > T, rs2274407) and *ITPA* (c.94C > A) variants in 145 Chinese children with ALL witnessed a significant positive association with 6-MP intolerance (Fan et al., 2022). Meanwhile, *ABCC4* c.2128G > A (rs3765534) carriers experienced a significant increase in the DNA-TG to 6-MP dose ratio, which was associated with a high risk of leukopenia (Fan et al., 2022). Similarly, *ABCC4* SNP rs2274407 was found to be related to the increased 6-TGN to 6-MP dose ratio (Choi et al., 2019). In addition, a study in Thai ALL pediatric patients found that the average absolute neutrophil count (ANC) at the 6th month of the maintenance phase was significantly lower in *ABCC4* SNP rs3765534 carriers, compared to patients carrying wild-type alleles, and the risk of grade 4 neutropenia was higher in *ABCC4* GA carriers than wild-type patients, but was not statistically significant (Khaeso et al., 2022). Of note, the allele frequency of variants in *ABCC4* showed ethnic difference (Table 2), and more evidence needs to be accumulated to establish the potential association between *ABCC4* variants and 6-MP-induced adverse effects in the future.

Other genetic polymorphisms

In 2012, Stocco's team first reported that *PACSIN2* (protein kinase C and casein kinase II interacting protein-2 or Syndapin 2) was the most fundamental trans-acting gene. *PACSIN2* has also been shown to be a genetic variant which could affect TPMT activity (Stocco et al., 2012). Moreover, a SNP of *PACSIN2* (rs2413739) was closely associated with severe gastrointestinal toxicity in children with ALL treated with 6-MP. Recently, another study confirmed these results (Franca et al., 2020). Furthermore, *PACSIN2* polymorphism was shown to be linked with thiopurine-induced hematological toxicity in children receiving maintenance therapy aimed at treating ALL (Smid et al., 2016). As an earlier study had identified, PACSIN2 was a Rac1 interactor that regulated the diffusion of Rac1-mediated cells (de Kreuk et al., 2011). Therefore, the interaction of PACSIN2 with Rac1 might increase the likelihood of hematotoxicity, resulting in increased sensitivity of cells to 6-MP, thereby exposing patients to a higher risk of hematotoxicity.

Cytosolic 5′-nucleotidase II (NT5C2) is an allosteric catabolic enzyme that hydrolyzes IMP, GMP, and AMP. The thiopurine nucleotides thio-GMP, thio-IMP, and methylthioIMP are all converted by NT5C2 (Brouwer et al., 2005). Increased *in vitro* nucleotidase activity has been identified in NT5C2 mutant proteins. Also, when expressed in ALL lymphoblasts, these proteins were resistant to the chemotherapy with 6-MP/6-TG (Tzoneva et al., 2013). Tulstrup and others found that the thiopurine metabolism can be altered by *NT5C2*-germline variants associated with acquired recurrent *NT5C2* mutations in childhood acute lymphoblastic leukemia (Tulstrup et al., 2018). Moreover, sub-clonal *NT5C2* mutations determine relapses related to the high risks in treatment failure in patients, while emphasizing their complicated role in the outcome over mutant *NT5C2*, which acts as a targetable driver during relapse progression. Therefore, a thorough, rigorous, and retrospective study is warranted so that we could identify *NT5C2* mutations, further deepening our understanding and better treating the relapse subtype of aggressive ALL (Barz et al., 2020).

Recently, folate metabolic variants including thymidylate synthetase (*TYMS*) and dihydrofolate reductase (*DHFR*) were shown to be potential biomarkers of 6-MP-induced myelotoxicity, which could be employed for the individualization of 6-MP therapy when childhood ALL treatment reaches its maintenance phase (Milosevic et al., 2019). In Chinese pediatric patients, the *MTHFR* rs1801133 variant was found to have a 4.46-fold higher risk of hepatotoxicity than the wild-type genotype (Zhou et al., 2020). In this study, the authors also found that *IMPDH1* (rs2278293) was associated with a high risk of leukopenia (Zhou et al., 2020), which is consistent with Rihwa Choi's earlier study in Korean ALL patients (Choi et al., 2019). Moreover, Rihwa Choi and

TABLE 3 Main efficacy, safety results, and TDM of thiopurines in ALL pediatric patients.

NO.	First author year	Study design and population	Treatment regimen and duration	Concomitant medication	Gene	Measured metabolites	Matrix	Metabolites range	Principal findings	Reference
1	Lennard 1983	Prospective, 22 patients, pediatric, European	6-MP 75 mg/m2/d > 2 weeks	Methotrexate Steroids Vincristine	—	6-TGN	RBC	0–802 (210 ± 149) (pmol/8 × 108 RBC)	As for the group not influenced by co-trimoxazole, as long as RBC 6-TG nucleotide at day 0 reaches >210 pmol/8 × 108 RBC, folate deficiency or neutropenia can be foreseen to happen by day 14	Lennard et al., (1983)
2	Lilleyman 1984	Prospective, 22 patients, pediatric, European	6-MP 75 mg/m2/d 11 months	Methotrexate Steroids Vincristine	—	6-TGN	RBC	girls: 0–720 boys: 42–958 (pmol/8 × 108 RBC)	For the girls involved in the study, statistically significant relevance between the doses of 6-MP and 6-TGN was shown, whereas this was not found in the boys	Lilleyman et al., (1984)
3	Lennard 1990	Retrospective, 95 patients, pediatric, European	6-MP 75 mg/m2/d > 2 months	Methotrexate Steroids Vincristine	TPMT	6-TGN	RBC	132–832 (pmol/8 × 108 RBC)	Among the 16 patients, 15 of them suffered a relapse, and this might be due to their lower 6-TGN concentrations, which did not attain the group median level. And this was a statistically significant excess, as it proved to be	Lennard et al., (1990)
4	Schmiegelow 1990	Prospective, 31 patients, pediatric, European	6-MP 50–75 mg/m2/d at least 3 months	Methotrexate	—	6-TGN	RBC	85–286 (nmol/mmol Hb)	Mean white cell count was used as an indicator to measure the degree of myelosuppression in this research and it was found that the degree of myelosuppression was correlated with 6-TGN.	Schmiegelow and Bruunshuus, (1990)
5	Berkovitch 1996	Retrospective, 25 patients, pediatric, North American	6-MP GI symptoms: 73 ± 23 mg/m2/d	Methotrexate Steroids Vincristine	—	6-MMPN 6-TGN	RBC	3000–27900 (pmol/8 × 108 RBC) 171–463 (pmol/8 × 108 RBC)	6-TGN as well as 6-MMPN levels in RBC, did not differ significantly in patients who had hepatotoxicity, when compared to those without hepatotoxicity	Berkovitch et al., (1996)
6	Lancaster 1998	Retrospective 23 patients, pediatric, European	6-MP 75 mg/m2/d > 12 weeks	Methotrexate Steroids Vincristine	—	6-TGN	RBC	205–1310 (pmol/8 × 108 RBC)	For participants who took TG on average, their 6-TGN levels were found to be 5-fold higher. At the same time, in the group of children on MP, 6-TGN levels had no obvious relevance to myelotoxicity, the results demonstrated	(Lancaster et al., (1998)

(Continued on following page)

10.3389/fphar.2022.941182

TABLE 3 (*Continued*) Main efficacy, safety results, and TDM of thiopurines in ALL pediatric patients.

NO.	First author year	Study design and population	Treatment regimen and duration	Concomitant medication	Gene	Measured metabolites	Matrix	Metabolites range	Principal findings	Reference
7	Chrzanowska 1999	Retrospective 19 patients, pediatric, European	6-MP 50 mg/m2/d > 1 month	Methotrexate	—	6-MMPN 6-TGN	RBC	<150–19000 (pmol/8 × 108 RBC) <60–833 (pmol/8 × 108 RBC)	There was a significant relevance observed between WBC count and RBC 6-TGN. Also, the same thing applies to neutrophil count and RBC 6-TGN.	Chrzanowska et al., (1999)
8	Innocenti 2000	Retrospective 19 patients, pediatric, European	6-MP 50 mg/m2/d 3–18 months	Methotrexate Cytosine Steroids Vincristine	—	6-TGN	RBC	74–628 (pmol/8 × 108 RBC)	It was demonstrated to be significantly correlated that as RBC 6-TGN levels increased, the decrease of WBC, ANC, erythrocyte, and platelet counts was observed	Innocenti et al., (2000)
9	Dervieux 2001	Retrospective 78 patients, pediatric, European	6-MP 50 mg/m2/d > 5 months	Methotrexate	TPMT	6-TGN	RBC	173–1334 (pmol/8 × 108 RBC)	As steady-state 6-TGN concentrations became higher, leukocyte counts turned lower, the former and latter were significantly related	Dervieux et al., (2001) (Dervieux et al., 2001)
10	Stoneham 2003	Retrospective 99 patients, pediatric, European	6-MP (37%) or 6-TG (63%) >1 year	—	—	6-TGN	RBC	without VOD: 1231–1979 with VOD: 1240–1965 (pmol/8 × 108 RBC)	Risk factors responsible for VOD included male sex and 6-TG.	Stoneham et al., (2003)
11	Nygaard 2004	Retrospective 43 patients, pediatric, European	6-MP 75 mg/m2/d > 4 weeks	Methotrexate	TPMT	6-MMPN 6-TGN	RBC	1843–12422 (nmol/mmol Hb) 162–488 (nmol/mmol Hb)	Weighted means of aminotransferase levels were significantly related to the average doses of 6-MP, erythrocyte levels of 6-MMPN, and TPMT activity. Weighted means of aminotransferase levels were negatively correlated with the erythrocyte levels of 6-TGN and were not related to the average doses of methotrexate or erythrocyte levels of methotrexate and its polyglutamates	Nygaard et al., (2004)
12	Halonen 2006	Prospective 16 patients, pediatric, European	6-MP 75 mg/m2/d 2.3 years (SR) 1.7 years (IR)	Methotrexate Steroids Vincristine	—	6-TGN	RBC	86–301 (nmol/mmol Hb)	Throughout the therapy period, serum median ALT levels related significantly in a positive manner to the cumulative doses of 6-MP, but this correlation was not found when it came to the cumulative doses of 6-TGN.	Halonen et al., (2006)

(Continued on following page)

10.3389/fphar.2022.941182

TABLE 3 (*Continued*) Main efficacy, safety results, and TDM of thiopurines in ALL pediatric patients.

NO.	First author year	Study design and population	Treatment regimen and duration	Concomitant medication	Gene	Measured metabolites	Matrix	Metabolites range	Principal findings	Reference
13	Lennard 2006	Prospective 744 patients, pediatric, European	6-MP 75 mg/m2/d > 7 days	—	TPMT	6-TGN	RBC	682–4,072 (pmol/8 × 108 RBC)	The range of 6-TGNs in either the persistent splenomegaly group or the splenomegaly and VOD cohort did not differ from the range recorded in control children taking 6-MP.	Lennard et al., (2006)
14	Ganping 2008	Prospective 10 patients, pediatric, Asian	6-MP 75 mg/m2/d > 2 months	Methotrexate	—	6-TGN	RBC	day 7: 264–866 days 14: 290–450 (pmol/8 × 108 RBC)	275–750 pmol/8 × 108/sup RBC was the established and recognized target level range of 6-TGN. Just by determining the level of 6-TGN in blood sample as well as modifying the 6-MP dosage in accordance with 6-TGN concentrations. It's workable to achieve the individualization and personalization of 6-MP.	Ganping Zhou et al., (2008)
15	Adam de Beaumais 2011	Prospective 66 patients, pediatric, European	6-MP 50 mg/m2/d 15 months	Methotrexate Aracytine Steroids	TPMT	6-MMPN	RBC	TPMT WT: 11290 TPMT HT: 5,010 (pmol/8 × 108 RBC)	In terms of 6-TGN concentrations and hepatotoxicity, no strong relationship was determined between the two	[Adam de Beaumais et al., (2011)]
						6-TGN		TPMT WT: 336 TPMT HT: 757 (pmol/8 × 108 RBC)		
16	Wojtuszkiewicz 2014	Prospective 236 patients, pediatric, European	6-MP week 6–161	—	—	6-TGN	RBC	week 25: 38–934 weeks 53: 68–881 weeks 109: 84–1048 (pmol/8 × 108 RBC)	Greater *in vitro* antileukemic activity was demonstrated to tend to be associated with high levels of 6-TGN. And elevated 6-TGN concentrations were proved to be strongly related to grade III/IV leucopenia	Wojtuszkiewicz et al., (2014)
17	Moriyama 2017	Prospective 55 patients, pediatric, Asian	6-MP 50 mg/m2/d > 13 weeks	—	NUDT15	DNA-TG	WBC	78.1–1054.0 (fmol TG/μg DNA)	For NUDT15-deficient patients, the ratio of DNA-TG to TGN was dramatically raised; To judge the adjustments of NUDT15 genotype-guided dose, compared to TGN, DNA-TG is a more pertinent MP metabolite	Moriyama et al., (2017)
						6-TGN	RBC	0.46–315.5 (pmol/4 × 108 RBC)		

(Continued on following page)

10.3389/fphar.2022.941182

TABLE 3 (*Continued*) Main efficacy, safety results, and TDM of thiopurines in ALL pediatric patients.

NO.	First author year	Study design and population	Treatment regimen and duration	Concomitant medication	Gene	Measured metabolites	Matrix	Metabolites range	Principal findings	Reference
18	Nielsen 2017	Prospective 1266 patients, pediatric, European	6-MP 75 mg/m2/d TPMT heterozygous: 50 mg/m2/d TPMT-deficient: 10 mg/m2/d > 37 weeks	Methotrexate Steroids Vincristine	—	DNA-TG	WBC	phase 1: 23–1591 phase 2: 44–1559 (fmol TG/μg DNA)	DNA-TGN concentration was found to have significant correlation with relapse-free survival; elevated concentrations of DNA-TGN indicated raised relapse-free survival	Nielsen et al., (2017)
19	Gerbek 2018	Prospective 132 patients, pediatric, European	6-MP TPMTWT: 75 mg/m2/24 h	Methotrexate Steroids Vincristine	TPMT ITPA	6-TGN	RBC	178–305 (nmol/mmol Hb)	When wild-type patients were used as the baseline, in low-activity patients it was found their median DNA-TG levels were higher in TPMT and ITPA.	Gerbek et al., (2018)
						6-MMPN		9787–22233 (nmol/mmol Hb)		
						DNA-TG	WBC	272–458 (fmol TG/μg DNA)		
20	Choi 2019	Retrospective 139 patients, Pediatric, Asian	6-MP 50 mg/m2/d > 1 month	Methotrexate Steroids Vincristine Cytarabine Hydrocortisone	TPMT NUDT15 ITPA MRP4	6-TGN	RBC	301.1–555.2 (pmol/4 × 108 RBC)	The levels of thiopurine metabolites (6-TGN and 6-MMPN) were significantly associated with 6-MP dosage	Choi et al., (2019)
21	Ju 2021	Prospective 71 patients, pediatric, Asian	6-MP 50 mg/m2/d > 2 weeks	—	NUDT15 TPMT	DNA-TG	WBC	1.0–903.1 (fmol TG/μg DNA)	During the time when patients suffered from the leukopenia episodes, the DNA-TGN concentrations varied between 27.8 and 54.8 fmol TG/μg DNA.	Ju et al., (2021)
22	Larsen 2021	Prospective 52 patients, pediatric, European	6-MP	Methotrexate Steroids Vincristine	—	DNA-TG	WBC	31–2888 (fmol TG/μg DNA)	A dependable profile of DNA-TG levels could be offered by measuring DNA-TG at 2–4 week intervals	Larsen et al., (2021a)
23	Larsen 2021	Prospective 34 patients, pediatric and adult European	6-MP+6-TG >10 weeks	Methotrexate	—	DNA-TG	WBC	764 (mean) (fmol TG/μg DNA)	It is a novel and practicable method to add incremental doses of 6-thioguanine to methotrexate/6-mercaptopurine, maintenance therapy, which can enhance the therapy, and consequently boost greater DNA-TG with no extra toxicity induced	Larsen et al., (2021b)

(Continued on following page)

10.3389/fphar.2022.941182

TABLE 3 (*Continued*) Main efficacy, safety results, and TDM of thiopurines in ALL pediatric patients.

NO.	First author year	Study design and population	Treatment regimen and duration	Concomitant medication	Gene	Measured metabolites	Matrix	Metabolites range	Principal findings	Reference
24	Nielsen 2021	Retrospective 918 patients, pediatric, European	6-MP TPMT heterozygous: 50 mg/m2/d	Methotrexate Steroids Vincristine Asparaginase	TPMT	DNA-TG	WBC	wildtype: 492.7 heterozygous: 760.9 (fmol TG/μg DNA)	TPMT heterozygous patients had higher DNA-TG levels	Nielsen et al., (2021)
25	Rosdiana 2021	Cross-sectional 106 patients, pediatric, Asian	6-MP 50 mg/m2/d > 1 month	Methotrexate Steroids Vincristine	TPMT	6-MMPN	RBC	3.5–3167.01 (pmol/8 × 108 RBC)	6-MMPN plasma concentrations and 6-MMPN/6-TGN ratio were found to be linked with the occurrence of hematotoxicity	Rosdiana et al., (2021)
						6-TGN		6–234.04 (pmol/8 × 108 RBC)		
26	Toksvang 2021	Prospective 1234 patients, pediatric and adult, European	6-MP 75 mg/m2/d TMPT heterozygous: 50 mg/m2/d	Methotrexate PegASP Steroids	TPMT	6-MMPN	RBC	0–103323 (nmol/mmol Hb)	By determining and judging 6 MP and MTX metabolites, the intensity of maintenance therapy could be ascertained, and it had no relationship with the danger of getting osteonecrosis	Toksvang et al., (2021)
						6-TGN		0–5,966 (nmol/mmol Hb)		
						DNA-TG	WBC	30–5,610 (fmol TG/μg DNA)		
27	Fan, P. 2022	Retrospective 145 patients, pediatric, Asian	6-MP 50 mg/m2/d > 6 months	Methotrexate	TPMT NUDT15 ITPA MRP4	DNA-TG	WBC	246.5 ± 267.8 (fmol TG/μg DNA)	A significantly higher DNA-TG to dose ratio was indicated in the patients who experienced one or more leukopenia episodes	Fan et al., (2022)

ADR, adverse drug reaction; PegASP, Pegylated-asparaginase; GI, symptoms: gastrointestinal symptoms; VOD, vena-occlusive disease; SR, standard risk; IR, intermediate risk; WT, wild-type; HT, carrier of one variant allele; 6-MP, 6-mercaptopurine; TPMT, thiopurine S-methyl transferase; NUDT15, Nudix hydrolase 15; 6-TGN, 6-thioguanine nucleotides; 6-MMPN, methyl-thioIMP; DNA-TG, DNA-incorporated thioguanine; ITPA, inosine triphosphate pyrophosphatase; RBC, red blood cells; WBC, white blood cells.

10.3389/fphar.2022.941182

others analyzed 103 SNPs and found that, in addition to the *TPMT* genotype, thiopurine metabolism and any adverse effects were linked with a total of 32 SNPs in 24 genes (Choi et al., 2019). A series of genetic polymorphisms such as *ADK*, *ATIC*, *GART*, *GMPS*, *GSTP1*, *SLC29A1*, *KCNMA1*, *SLC19A1*, *MOCOS*, *MTRR*, *SLC28A3*, *SLCO1B1*, and *XDH* have been linked with thiopurine-related adverse effects that have not been previously assessed.

Generally, the association between genotype and phenotype in pharmacogenetic studies is complex. As shown in Supplementary Table S1, we summarize the effects of *TMPT*, *NUDT15*, *ITPA*, and *MRP4* polymorphisms on the clinical outcomes of thiopurines in ALL pediatric patients. We propose that the ongoing research will surely manifest the value of pharmacogenetics in predicting the optimal dose and reducing adverse events, thereby contributing to better treatment for ALL patients.

Therapeutic drug monitoring of thiopurines

The pharmacodynamics and pharmacogenetics of thiopurines have evolved considerably over the past 30 years. In addition to genotype–phenotype related research studies, long-term clinical practice has confirmed that thiopurine-associated adverse events and ALL relapses are related to metabolite levels, including 6-TGNs, 6-methylmercaptopurine nucleotides (6-MMPN), or the ratio of 6-MMPN/6-TGNs, and DNA-TG levels (Table 3). Therefore, integrating TDM of these active metabolites with pharmacogenetics may facilitate the development of a more personalized dosing method than the traditional weight-based one.

Concentrations of 6-TGNs in RBCs is related to neutropenia and relapsed risk

In ALL patients, the 6-TGN concentrations in RBCs have been recognized to correlate with neutropenia and tolerable 6-MP doses in the 1980s (Lennard et al., 1983; Lilleyman et al., 1984; Lennard and Lilleyman, 1989), whereas the well-established reference range of 6-TGN therapeutic levels has not yet been agreed (Schmiegelow and Bruunshuus, 1990; Lancaster et al., 1998; Innocenti et al., 2000; Stoneham et al., 2003; Halonen et al., 2006; Lennard et al., 2006). A study by Chrzanowska et al. showed the 6-TGN concentrations that ranged from <60 to 833 pmol/8 × 10^8 RBC in patients receiving 6-MP dosed at 50 mg/m^2/day (Chrzanowska et al., 1999). In the study by Bhatia et al., patients received a higher dose of 6-MP, 75 mg/m^2/day and the 6-TGN levels remained 0.3–714.1 pmol/8 × 10^8 RBC (Bhatia et al., 2015). Nevertheless, the levels obtained in the study by Rosdiana et al. were 6–234.04 pmol/8 × 10^8 RBC with a 6-MP dose of 50 mg/m^2/day (Rosdiana et al., 2021). Interestingly, Zhou Y and others proposed the existence of a target threshold of 197.50 pmol/8 × 10^8 RBCs to predict the risk of leukopenia in Chinese pediatric patients tormented by ALL (Zhou et al., 2020). Notably, not all studies found a correlation between metabolite concentrations and adverse effects (Halonen et al., 2006), which may due to the different therapy regimens (Lancaster et al., 1998; Lennard et al., 2006). More importantly, 6-TGN concentrations were associated with relapsed risk (Lennard et al., 1990; Wojtuszkiewicz et al., 2014). Therefore, there is an urgent to conduct a multicenter study involving more patients to find a suitable target range of therapeutic targets.

Ratio of 6-MMPN/6-TGN is associated with the efficacy and tolerance of thiopurines

As previously described, a clear correlation between 6-MMPN concentrations and the development of hepatotoxicity was found in ALL patients treated with 6-MP (Nygaard et al., 2004; Adam de Beaumais et al., 2011). The findings of Nygaard et al. (Nygaard et al., 2004) indicated that the 6-MMPN contents were the most important pharmacological determinants of elevated aminotransferase levels during the 6-MP maintenance therapy in childhood ALL. A later study of Beaumais et al. showed that the threshold concentration of 6-MMPN, 4,884 pmol/8 × 10^8 RBC could predict the risk of hepatotoxicity with a positive predictive value of 95.7% (Adam de Beaumais et al., 2011). As well known, patients carrying *TPMT* mutations had higher TGN levels than their wild-type counterparts, but this genetic variation only interprets the intolerance in 30–60% patients who received full doses of 6-MP or AZA (Relling et al., 2011). Some heterozygotes might be sufficiently thiopurine-tolerant because they have lower 6-MMPN concentrations than those with homozygous wild-type carriers (and thus fewer toxic effects), and therefore tolerated higher 6-TGNs. For example, in Dervieux's study, wild-type patients experienced higher 6-MMPN concentrations (median: 6,137 pmol/8 × 10^8 cells) than those carrying *TPMT* mutations (median: 307 pmol/8 × 10^8 cells) (Dervieux et al., 2001). In this study, the 6-MMPN concentrations in RBCs were determined in the last patients enrolled in the trail, with a median concentration of 5,749 pmol/8 × 10^8 cells (range 20–19682). The authors confirmed that higher 6-MP dosage and infectious events were associated with higher 6-MMPN concentrations. More recently, studies have shown a link between the ratio of 6-MMPN/6-TGN and the incidence of grade 3–4 neutropenia (Rosdiana et al., 2021). The researchers therefore proposed that the balance between RBC 6-MMPN and 6-TGN levels was important for predicting efficacy and improving the tolerance of thiopurines. Unfortunately, the therapeutic ratio of 6-MMPN/6-TGN is also unclear up to now.

DNA-incorporated thioguanine nucleotides and relapse-free survival during ALL maintenance therapy

Pharmacologically, leukocyte DNA-TG, a cytotoxic agent and the end-point metabolite of 6-MP (Karran and Attard, 2008), appears to be more appropriately and accurately reflecting therapy intensity in the nucleated target cells in ALL, and it has recently been associated with 6-TGNs and 6-MMPN in RBCs (Hedeland et al., 2010; Ebbesen et al., 2013; Vang et al., 2015). Moreover, using an on-therapy blood count model, Nielsen and others attempted to estimate the degree of myelosuppression using the DNA-TG levels, a parameter available on-therapy that could be indicative of the treatment intensity. However, the results were contradictory. On-therapy ANC decreased with increasing DNA-TGN level ($p < 0.001$, model adjusted for off-therapy ANC), whereas on-therapy absolute lymphocyte counts (ALC) could not be modeled reliably (Nielsen et al., 2016). The authors claimed that measurements of the DNA-TG levels could provide blood counts when evaluating therapy intensity, but required prospective validation. Subsequently, a prospective sub-study of a phase 3 trial (NOPHO ALL 2008) has confirmed that the DNA-TG concentration (adjusted hazard ratio 0·81 per 100 fmol/μg DNA increase, 95%CI 0.67–0.98; $p = 0.029$) was closely related to relapse-free survival (Nielsen et al., 2017). Although higher DNA-TG was associated with a decreased relapse rate, it was worth noting that the cytotoxicity of maintenance therapy in ALL was also dependent on DNA-TG formation. Larsen and others added a low-dose 6-TG to MTX/6 MP maintenance therapy, termed as "TEAM" strategy, which proved to be a novel and practicable method to enhance the maintenance therapy, resulting in higher DNA-TGs without causing additional toxicity (Larsen et al., 2021b). They recommended that a reliable profile of DNA-TG levels could be provided by measuring DNA-TGs in leucocytes every 2–4 weeks (Larsen et al., 2021a). On the other hand, as pharmacogenomics significantly influence the metabolism of 6-MP, numerous studies have investigated the influence of genotypes on the DNA-TG levels. In Gerbek's study, Gerbek found that *TPMT* heterozygous patients held notably higher DNA-TG levels than *TPMT* wild-type carriers (Gerbek et al., 2018). Another study of Nielsen was consistent with those results (Nielsen et al., 2021). Gerbek and others also found that the DNA-TG levels were significantly elevated in ITPA heterozygotes compared with *ITPA* wild-type carriers (Gerbek et al., 2018). In addition, DNA-TG accumulated with higher efficiency *in vivo* as the amount of risk alleles increased in the *NUDT15* gene (Moriyama et al., 2017).

We speculate that those large inter-individual variations in previous studies might be caused by variations in 6-MP absorption and disposition, drug–drug interactions, different TPMT enzyme activities, ethnic differences, and by patients' compliance. In addition, the stratification according to those risk factors could be performed, but many chemotherapies are still used in the same way when treating all types of ALL. Hence, as optimal metabolite levels may vary by indications, it is important for physicians to adapt posology so that toxicity can be reduced while efficacy is not affected.

Conclusion and outlook

Thiopurines have been broadly used for over 5 decades in the treatment of a wide range of diseases. However, side effects for thiopurines ranging from mild rashes, flu-like symptoms to severe life-threatening myelosuppression, and hepatotoxicity have hindered their clinical application. Although pharmacogenetics and TDM for thiopurines may contribute to and influence clinical practice, there are still several problems that need to be addressed urgently.

Although the pharmacogenetics of thiopurines is one of the most successful clinical applications, the large intra- and inter-individual variations of thiopurines, especially the high incidence of side effects in Asian populations, remain difficult to explain well. One possible explanation is that, thiopurine-related toxicity phenotype could not be determined only by one or two genotyping analyses (e.g. *TPMT* and *NUDT15*). Conversely, while high-throughput techniques allow researchers to map thousands of genetic polymorphisms in a single test, it still remains an enormous challenge to identify and figure out which one exerts the most considerable impact on both efficacy and toxicity. We now propose in this review, that a comprehensive consideration of the "MINT" sequencing strategy including *MRP4*, *ITPA*, *NUDT15*, and *TPMT* genes, combined with patients' clinical characteristics, will provide more accurate information for the precise medication of thiopurines. Furthermore, if rare SNPs could dramatically alter the properties of transporter proteins or enzymes in victims with thiopurine-related side effects, it would be beneficial to continue further research. Unfortunately, we still have a long way to go before incorporating pharmacogenetic tests into routine clinical practice, which can help predict the outcomes and effects of thiopurine therapy.

For TDM of active metabolites, the therapeutic levels of 6-TGNs, 6-MMPN, or their cut-offs remain inconsistent. Therefore, in clinical practice, physicians should be cautious about the calculated optimal threshold for adverse events. On the other hand, most studies measure the level of metabolites in RBCs to evaluate the effect of drug treatment, which are not representative of the drugs in lymphocytes. This may be the reason why various studies have come to different conclusions. Recent studies have found that the levels of DNA-TG may be more related to the clinical efficacy and adverse reactions of thiopurines, which is the development direction of TDM

monitoring in the future. The standardization of procedures for the evaluation of metabolites should be attached great importance in the near future.

In conclusion, we propose that integrating the "MINT" sequencing strategy with routine DNA-TG- and 6-MMPN-monitoring might be more feasible toward improving the efficacy and tolerability of thiopurines. Nevertheless, multicenter studies with large samples in different ethnic populations need to be performed in the future.

Author contributions

H-LG, FC, LZ and TL: Concept and design. H-LG: Principal investigators for the review, literature summary, and primary author of the manuscript. Y-TZ, W-JW, ND, Y-HH, and Y-YZ: Performed the original articles' collection and analysis, made the figures. H-LG and FC: Drafted of the manuscript. LZ, and TL: Assisted in the design and performance of the study and the writing of the manuscript. FC: Critical revision of the manuscript.

Funding

This research was supported by the Specially Appointed Medical Expert Project of the Jiangsu Commission of Health (2019), Jiangsu Research Hospital Association for Precision Medication (JY202108). This study was also sponsored by the Scientific Research Support Foundation for Top Young Scholars at the Children's Hospital of Nanjing Medical University (2020).

Conflict of interest

The authors declare that the research was conducted in the absence of any commercial or financial relationships that could be construed as a potential conflict of interest.

Publisher's note

All claims expressed in this article are solely those of the authors and do not necessarily represent those of their affiliated organizations, or those of the publisher, the editors, and the reviewers. Any product that may be evaluated in this article, or claim that may be made by its manufacturer, is not guaranteed or endorsed by the publisher.

Supplementary material

The Supplementary Material for this article can be found online at: https://www.frontiersin.org/articles/10.3389/fphar.2022.941182/full#supplementary-material

References

Adam de Beaumais, T., Fakhoury, M., Medard, Y., Azougagh, S., Zhang, D., Yakouben, K., et al. (2011). Determinants of mercaptopurine toxicity in paediatric acute lymphoblastic leukemia maintenance therapy. *Br. J. Clin. Pharmacol.* 71, 575–584. doi:10.1111/j.1365-2125.2010.03867.x

Andoh, A., Kawahara, M., Imai, T., Tatsumi, G., Inatomi, O., and Kakuta, Y. (2021). Thiopurine pharmacogenomics and pregnancy in inflammatory bowel disease. *J. Gastroenterol.* 56, 881–890. doi:10.1007/s00535-021-01805-z

Ansari, A., Hassan, C., Duley, J., Marinaki, A., Shobowale-Bakre, E. M., Seed, P., et al. (2002). Thiopurine methyltransferase activity and the use of azathioprine in inflammatory bowel disease. *Aliment. Pharmacol. Ther.* 16, 1743–1750. doi:10.1046/j.1365-2036.2002.01353.x

Arenas, M., Duley, J., Sumi, S., Sanderson, J., and Marinaki, A. (2007). The ITPA c.94C>A and g.IVS2+21A>C sequence variants contribute to missplicing of the ITPA gene. *Biochim. Biophys. Acta* 1772, 96–102. doi:10.1016/j.bbadis.2006.10.006

Asada, A., Nishida, A., Shioya, M., Imaeda, H., Inatomi, O., Bamba, S., et al. (2016). NUDT15 R139C-related thiopurine leukocytopenia is mediated by 6-thioguanine nucleotide-independent mechanism in Japanese patients with inflammatory bowel disease. *J. Gastroenterol.* 51, 22–29. doi:10.1007/s00535-015-1142-4

Azimi, F., Jafariyan, M., Khatami, S., Mortazavi, Y., and Azad, M. (2014). Assessment of thiopurine-based drugs according to thiopurine S-methyltransferase genotype in patients with acute lymphoblastic leukemia. *Iran. J. Ped. Hematol. Oncol.* 4, 32–38.

Ban, H., Andoh, A., Imaeda, H., Kobori, A., Bamba, S., Tsujikawa, T., et al. (2010). The multidrug-resistance protein 4 polymorphism is a new factor accounting for thiopurine sensitivity in Japanese patients with inflammatory bowel disease. *J. Gastroenterol.* 45, 1014–1021. doi:10.1007/s00535-010-0248-y

Banerjee, R., Ravikanth, V. V., Pal, P., Bale, G., Avanthi, U. S., Goren, I., et al. (2020). NUDT15 C415T variant compared with TPMT genotyping in predicting azathioprine-induced leucopenia: Prospective analysis of 1014 inflammatory bowel disease patients in India. *Aliment. Pharmacol. Ther.* 52, 1683–1694. doi:10.1111/apt.16137

Barba, E., Kontou, P. I., Michalopoulos, I., Bagos, P. G., and Braliou, G. G. (2022). Association of ITPA gene polymorphisms with adverse effects of AZA/6-MP administration: A systematic review and meta-analysis. *Pharmacogenomics J.* 22, 39–54. doi:10.1038/s41397-021-00255-3

Barz, M. J., Hof, J., Groeneveld-Krentz, S., Loh, J. W., Szymansky, A., Astrahantseff, K., et al. (2020). Subclonal NT5C2 mutations are associated with poor outcomes after relapse of pediatric acute lymphoblastic leukemia. *Blood* 135, 921–933. doi:10.1182/blood.2019002499

Berkovitch, M., Matsui, D., Zipursky, A., Blanchette, V. S., Verjee, Z., Giesbrecht, E., et al. (1996). Hepatotoxicity of 6-mercaptopurine in childhood acute lymphocytic leukemia: Pharmacokinetic characteristics. *Med. Pediatr. Oncol.* 26, 85–89. doi:10.1002/(SICI)1096-911X(199602)26:2<85::AID-MPO3>3.0.CO;2-Q

Bhatia, S., Landier, W., Hageman, L., Chen, Y., Kim, H., Sun, C. L., et al. (2015). Systemic exposure to thiopurines and risk of relapse in children with acute lymphoblastic leukemia: A Children's oncology group study. *JAMA Oncol.* 1, 287–295. doi:10.1001/jamaoncol.2015.0245

Brouwer, C., Vogels-Mentink, T. M., Keizer-Garritsen, J. J., Trijbels, F. J., Bokkerink, J. P., Hoogerbrugge, P. M., et al. (2005). Role of 5'-nucleotidase in thiopurine metabolism: Enzyme kinetic profile and association with thio-GMP levels in patients with acute lymphoblastic leukemia during 6-mercaptopurine treatment. *Clin. Chim. Acta.* 361, 95–103. doi:10.1016/j.cccn.2005.05.006

Chao, K., Wang, X., Cao, Q., Qian, J., Wu, K., Zhu, X., et al. (2017). Combined detection of NUDT15 variants could highly predict thiopurine-induced leukopenia

in Chinese patients with inflammatory bowel disease: A multicenter analysis. *Inflamm. Bowel Dis.* 23, 1592–1599. doi:10.1097/MIB.0000000000001148

Choi, R., Sohn, I., Kim, M. J., Woo, H. I., Lee, J. W., Ma, Y., et al. (2019). Pathway genes and metabolites in thiopurine therapy in Korean children with acute lymphoblastic leukaemia. *Br. J. Clin. Pharmacol.* 85, 1585–1597. doi:10.1111/bcp.13943

Chrzanowska, M., Kolecki, P., Duczmal-Cichocka, B., and Fiet, J. (1999). Metabolites of mercaptopurine in red blood cells: A relationship between 6-thioguanine nucleotides and 6-methylmercaptopurine metabolite concentrations in children with lymphoblastic leukemia. *Eur. J. Pharm. Sci.* 8, 329–334. doi:10.1016/s0928-0987(99)00027-5

de Kreuk, B. J., Nethe, M., Fernandez-Borja, M., Anthony, E. C., Hensbergen, P. J., Deelder, A. M., et al. (2011). The F-BAR domain protein PACSIN2 associates with Rac1 and regulates cell spreading and migration. *J. Cell Sci.* 124, 2375–2388. doi:10.1242/jcs.080630

Dervieux, T., Medard, Y., Verpillat, P., Guigonis, V., Duval, M., Lescoeur, B., et al. (2001). Possible implication of thiopurine S-methyltransferase in occurrence of infectious episodes during maintenance therapy for childhood lymphoblastic leukemia with mercaptopurine. *Leukemia* 15, 1706–1712. doi:10.1038/sj.leu.2402259

Donnan, J. R., Ungar, W. J., Mathews, M., and Rahman, P. (2011). Systematic review of thiopurine methyltransferase genotype and enzymatic testing strategies. *Ther. Drug Monit.* 33, 192–199. doi:10.1097/FTD.0b013e31820810cd

Ebbesen, M. S., Nersting, J., Jacobsen, J. H., Frandsen, T. L., Vettenranta, K., Abramsson, J., et al. (2013). Incorporation of 6-thioguanine nucleotides into DNA during maintenance therapy of childhood acute lymphoblastic leukemia-the influence of thiopurine methyltransferase genotypes. *J. Clin. Pharmacol.* 53, 670–674. doi:10.1002/jcph.81

Fan, P. O. L., Leung, K. T., Chan, K. Y. Y., Leung, A. W. K., Lam, G. K. S., Chow, T. T. W., et al. (2022). ABCC4, ITPA, NUDT15, TPMT and their interaction as genetic predictors of 6-mercaptopurine intolerance in Chinese patients with acute lymphoblastic leukemia. *Pediatr. Hematol. Oncol.* 39, 254–266. doi:10.1080/08880018.2021.1973628

Fargher, E. A., Tricker, K., Newman, W., Elliott, R., Roberts, S. A., Shaffer, J. L., et al. (2007). Current use of pharmacogenetic testing: A national survey of thiopurine methyltransferase testing prior to azathioprine prescription. *J. Clin. Pharm. Ther.* 32, 187–195. doi:10.1111/j.1365-2710.2007.00805.x

Fotoohi, A. K., Coulthard, S. A., and Albertioni, F. (2010). Thiopurines: Factors influencing toxicity and response. *Biochem. Pharmacol.* 79, 1211–1220. doi:10.1016/j.bcp.2010.01.006

Franca, R., Stocco, G., Favretto, D., Giurici, N., Del Rizzo, I., Locatelli, F., et al. (2020). PACSIN2 rs2413739 influence on thiopurine pharmacokinetics: Validation studies in pediatric patients. *Pharmacogenomics J.* 20, 415–425. doi:10.1038/s41397-019-0130-0

Gad, H., Koolmeister, T., Jemth, A. S., Eshtad, S., Jacques, S. A., Strom, C. E., et al. (2014). MTH1 inhibition eradicates cancer by preventing sanitation of the dNTP pool. *Nature* 508, 215–221. doi:10.1038/nature13181

Ganping Zhou, Z. C., Zhou, S., Feng, Z., Xu, F., and Xu, F. (2008). A simplistic individualization method for 6-mercaptopurine in acute lymphoblastic leukemia children. *Int. J. Pharmacol.* 4, 64–66. doi:10.3923/ijp.2008.64.66

Gearry, R. B., Roberts, R. L., Barclay, M. L., and Kennedy, M. A. (2004). Lack of association between the ITPA 94C>A polymorphism and adverse effects from azathioprine. *Pharmacogenetics* 14, 779–781. doi:10.1097/00008571-200411000-00010

Gerbek, T., Ebbesen, M., Nersting, J., Frandsen, T. L., Appell, M. L., and Schmiegelow, K. (2018). Role of TPMT and ITPA variants in mercaptopurine disposition. *Cancer Chemother. Pharmacol.* 81, 579–586. doi:10.1007/s00280-018-3525-8

Halonen, P., Mattila, J., Mäkipernaa, A., Ruuska, T., and Schmiegelow, K. (2006). Erythrocyte concentrations of metabolites or cumulative doses of 6-mercaptopurine and methotrexate do not predict liver changes in children treated for acute lymphoblastic leukemia. *Pediatr. Blood Cancer* 46, 762–766. doi:10.1002/pbc.20442

Hedeland, R. L., Hvidt, K., Nersting, J., Rosthoj, S., Dalhoff, K., Lausen, B., et al. (2010). DNA incorporation of 6-thioguanine nucleotides during maintenance therapy of childhood acute lymphoblastic leukaemia and non-Hodgkin lymphoma. *Cancer Chemother. Pharmacol.* 66, 485–491. doi:10.1007/s00280-009-1184-5

Innocenti, F., Danesi, R., Favre, C., Nardi, M., Menconi, M. C., Di Paolo, A., et al. (2000). Variable correlation between 6-mercaptopurine metabolites in erythrocytes and hematologic toxicity: Implications for drug monitoring in children with acute lymphoblastic leukemia. *Ther. Drug Monit.* 22, 375–382. doi:10.1097/00007691-200008000-00002

Iu, Y. P. H., Helander, S., Kahlin, A. Z., Cheng, C. W., Shek, C. C., Leung, M. H., et al. (2017). One amino acid makes a difference-Characterization of a new TPMT allele and the influence of SAM on TPMT stability. *Sci. Rep.* 7, 46428. doi:10.1038/srep46428

Ju, H. Y., Lee, J. W., Cho, H. W., Hyun, J. K., Ma, Y., Yi, E. S., et al. (2021). DNA-thioguanine nucleotide as a treatment marker in acute lymphoblastic leukemia patients with NUDT15 variant genotypes. *PLoS One* 16, e0245667. doi:10.1371/journal.pone.0245667

Karran, P., and Attard, N. (2008). Thiopurines in current medical practice: Molecular mechanisms and contributions to therapy-related cancer. *Nat. Rev. Cancer* 8, 24–36. doi:10.1038/nrc2292

Khaeso, K., Komvilaisak, P., Chainansamit, S. O., Nakkam, N., Suwannaying, K., Kuwatjanakul, P., et al. (2022). NUDT15 is a key genetic factor for prediction of hematotoxicity in pediatric patients who received a standard low dosage regimen of 6-mercaptopurine. *Drug Metab. Pharmacokinet.* 43, 100436. doi:10.1016/j.dmpk.2021.100436

Koren, G., Ferrazini, G., Sulh, H., Langevin, A. M., Kapelushnik, J., Klein, J., et al. (1990). Systemic exposure to mercaptopurine as a prognostic factor in acute lymphocytic leukemia in children. *N. Engl. J. Med.* 323, 17–21. doi:10.1056/NEJM199007053230104

Kouwenberg, T. W., van den Bosch, B. J. C., Bierau, J., Te Loo, D., Coenen, M. J. H., and Hagleitner, M. M. (2020). Dosage of 6-mercaptopurine in relation to genetic TPMT and ITPA variants: Toward individualized pediatric acute lymphoblastic leukemia maintenance treatment. *J. Pediatr. Hematol. Oncol.* 42, e94–e97. doi:10.1097/MPH.0000000000001707

Krishnamurthy, P., Schwab, M., Takenaka, K., Nachagari, D., Morgan, J., Leslie, M., et al. (2008). Transporter-mediated protection against thiopurine-induced hematopoietic toxicity. *Cancer Res.* 68, 4983–4989. doi:10.1158/0008-5472.CAN-07-6790

Lancaster, D. L., Lennard, L., Rowland, K., Vora, A. J., and Lilleyman, J. S. (1998). Thioguanine versus mercaptopurine for therapy of childhood lymphoblastic leukaemia: A comparison of haematological toxicity and drug metabolite concentrations. *Br. J. Haematol.* 102, 439–443. doi:10.1046/j.1365-2141.1998.00812.x

Larsen, R. H., Hjalgrim, L. L., Degn, M., Nersting, J., Als-Nielsen, B., Grell, K., et al. (2021). Dynamics of leucocyte DNA thioguanine nucleotide levels during maintenance therapy of childhood acute lymphoblastic leukemia. *Cancer Chemother. Pharmacol.* 88, 53–60. doi:10.1007/s00280-020-04219-5

Larsen, R. H., Utke Rank, C., Grell, K., Norgaard Moller, L., Malthe Overgaard, U., Kampmann, P., et al. (2021). Increments in DNA-thioguanine level during thiopurine enhanced maintenance therapy of acute lymphoblastic leukemia. *Haematologica* 106 (11), 2824–2833. doi:10.3324/haematol.2020.278166

Lee, Y., Jang, E. J., Yoon, H. Y., Yee, J., and Gwak, H. S. (2022). Effect of ITPA polymorphism on adverse drug reactions of 6-mercaptopurine in pediatric patients with acute lymphoblastic leukemia: A systematic review and meta-analysis. *Pharm. (Basel)* 15, 416. doi:10.3390/ph15040416

Lennard, L., Lilleyman, J. S., Van Loon, J., and Weinshilboum, R. M. (1990). Genetic variation in response to 6-mercaptopurine for childhood acute lymphoblastic leukaemia. *Lancet* 336, 225–229. doi:10.1016/0140-6736(90)91745-v

Lennard, L., and Lilleyman, J. S. (1989). Variable mercaptopurine metabolism and treatment outcome in childhood lymphoblastic leukemia. *J. Clin. Oncol.* 7, 1816–1823. doi:10.1200/JCO.1989.7.12.1816

Lennard, L., Rees, C. A., Lilleyman, J. S., and Maddocks, J. L. (1983). Childhood leukaemia: A relationship between intracellular 6-mercaptopurine metabolites and neutropenia. *Br. J. Clin. Pharmacol.* 16, 359–363. doi:10.1111/j.1365-2125.1983.tb02178.x

Lennard, L., Richards, S., Cartwright, C. S., Mitchell, C., Lilleyman, J. S., Vora, A., et al. (2006). The thiopurine methyltransferase genetic polymorphism is associated with thioguanine-related veno-occlusive disease of the liver in children with acute lymphoblastic leukemia. *Clin. Pharmacol. Ther.* 80, 375–383. doi:10.1016/j.clpt.2006.07.002

Lilleyman, J. S., Lennard, L., Rees, C. A., Morgan, G., and Maddocks, J. L. (1984). Childhood lymphoblastic leukaemia: Sex difference in 6-mercaptopurine utilization. *Br. J. Cancer* 49, 703–707. doi:10.1038/bjc.1984.111

Luo, X., Yan, S., Jin, L., Zhu, H., Zhang, X., and Ge, W. (2022). Inosine triphosphate pyrophosphatase and NUDT15 are good predictors of clinical outcomes in thiopurine-treated Chinese patients with inflammatory bowel disease. *Ther. Drug Monit.* 44, 391–395. doi:10.1097/FTD.0000000000000965

Marinaki, A. M., Ansari, A., Duley, J. A., Arenas, M., Sumi, S., Lewis, C. M., et al. (2004). Adverse drug reactions to azathioprine therapy are associated with polymorphism in the gene encoding inosine triphosphate pyrophosphatase (ITPase). *Pharmacogenetics* 14, 181–187. doi:10.1097/00008571-200403000-00006

Marsh, S., and Van Booven, D. J. (2009). The increasing complexity of mercaptopurine pharmacogenomics. *Clin. Pharmacol. Ther.* 85, 139–141. doi:10.1038/clpt.2008.219

Milosevic, G., Kotur, N., Lazic, J., Krstovski, N., Stankovic, B., Zukic, B., et al. (2019). Influence of variants in folate metabolism genes on 6-mercaptopurine induced toxicity during treatment for childhood acute lymphocytic leukemia. *J. BUON* 24, 2075–2083.

Mokhtari, M., Mostanbet, F., Nekooee Fard, S., Shekarkhar, G., Sepaskhah, M., and Sadati, M. S. (2020). Thiopurine S-methyltransferase and pemphigus vulgaris: A phenotype-genotype study. *Iran. J. Pathol.* 15, 299–305. doi:10.30699/ijp.2020.121365.2320

Moradveisi, B., Muwakkit, S., Zamani, F., Ghaderi, E., Mohammadi, E., and Zgheib, N. K. (2019). ITPA, TPMT, and NUDT15 genetic polymorphisms predict 6-mercaptopurine toxicity in Middle eastern children with acute lymphoblastic leukemia. *Front. Pharmacol.* 10, 916. doi:10.3389/fphar.2019.00916

Moriyama, T., Nishii, R., Lin, T. N., Kihira, K., Toyoda, H., Jacob, N., et al. (2017). The effects of inherited NUDT15 polymorphisms on thiopurine active metabolites in Japanese children with acute lymphoblastic leukemia. *Pharmacogenet. Genomics* 27, 236–239. doi:10.1097/FPC.0000000000000282

Moriyama, T., Nishii, R., Perez-Andreu, V., Yang, W., Klussmann, F. A., Zhao, X., et al. (2016). NUDT15 polymorphisms alter thiopurine metabolism and hematopoietic toxicity. *Nat. Genet.* 48, 367–373. doi:10.1038/ng.3508

Nagasaki, M., Yasuda, J., Katsuoka, F., Nariai, N., Kojima, K., Kawai, Y., et al. (2015). Rare variant discovery by deep whole-genome sequencing of 1, 070 Japanese individuals. *Nat. Commun.* 6, 8018. doi:10.1038/ncomms9018

Nielsen, S. N., Grell, K., Nersting, J., Abrahamsson, J., Lund, B., Kanerva, J., et al. (2017). DNA-Thioguanine nucleotide concentration and relapse-free survival during maintenance therapy of childhood acute lymphoblastic leukaemia (NOPHO ALL2008): A prospective substudy of a phase 3 trial. *Lancet. Oncol.* 18, 515–524. doi:10.1016/S1470-2045(17)30154-7

Nielsen, S. N., Grell, K., Nersting, J., Frandsen, T. L., Hjalgrim, L. L., and Schmiegelow, K. (2016). Measures of 6-mercaptopurine and methotrexate maintenance therapy intensity in childhood acute lymphoblastic leukemia. *Cancer Chemother. Pharmacol.* 78, 983–994. doi:10.1007/s00280-016-3151-2

Nielsen, S. N., Toksvang, L. N., Grell, K., Nersting, J., Abrahamsson, J., Lund, B., et al. (2021). No association between relapse hazard and thiopurine methyltransferase geno- or phenotypes in non-high risk acute lymphoblastic leukemia: A NOPHO ALL2008 sub-study. *Cancer Chemother. Pharmacol.* 88, 271–279. doi:10.1007/s00280-021-04281-7

Nygaard, U., Toft, N., and Schmiegelow, K. (2004). Methylated metabolites of 6-mercaptopurine are associated with hepatotoxicity. *Clin. Pharmacol. Ther.* 75, 274–281. doi:10.1016/j.clpt.2003.12.001

Okada, Y., Nakamura, K., Hiromura, K., Nojima, Y., Horiuchi, R., and Yamamoto, K. (2009). Pro32Thr polymorphism of inosine triphosphate pyrophosphatase gene predicts efficacy of low-dose azathioprine for patients with systemic lupus erythematosus. *Clin. Pharmacol. Ther.* 85, 527–530. doi:10.1038/clpt.2008.261

Paugh, S. W., Stocco, G., and Evans, W. E. (2010). Pharmacogenomics in pediatric leukemia. *Curr. Opin. Pediatr.* 22, 703–710. doi:10.1097/MOP.0b013e32833fde85

Poppe, D., Tiede, I., Fritz, G., Becker, C., Bartsch, B., Wirtz, S., et al. (2006). Azathioprine suppresses ezrin-radixin-moesin-dependent T cell-APC conjugation through inhibition of Vav guanosine exchange activity on Rac proteins. *J. Immunol.* 176, 640–651. doi:10.4049/jimmunol.176.1.640

Relling, M. V., Gardner, E. E., Sandborn, W. J., Schmiegelow, K., Pui, C. H., Yee, S. W., et al. (2011). Clinical Pharmacogenetics Implementation Consortium guidelines for thiopurine methyltransferase genotype and thiopurine dosing. *Clin. Pharmacol. Ther.* 89, 387–391. doi:10.1038/clpt.2010.320

Relling, M. V., Hancock, M. L., Rivera, G. K., Sandlund, J. T., Ribeiro, R. C., Krynetski, E. Y., et al. (1999). Mercaptopurine therapy intolerance and heterozygosity at the thiopurine S-methyltransferase gene locus. *J. Natl. Cancer Inst.* 91, 2001–2008. doi:10.1093/jnci/91.23.2001

Relling, M. V., Pui, C. H., Cheng, C., and Evans, W. E. (2006). Thiopurine methyltransferase in acute lymphoblastic leukemia. *Blood* 107, 843–844. doi:10.1182/blood-2005-08-3379

Relling, M. V., Schwab, M., Whirl-Carrillo, M., Suarez-Kurtz, G., Pui, C. H., Stein, C. M., et al. (2019). Clinical pharmacogenetics implementation Consortium guideline for thiopurine dosing based on TPMT and NUDT15 genotypes: 2018 update. *Clin. Pharmacol. Ther.* 105, 1095–1105. doi:10.1002/cpt.1304

Rosdiana, D. S., Setiabudy, R., Andalusia, R., Gatot, D., Louisa, M., Bardosono, S., et al. (2021). TPMT genetic variability and its association with hematotoxicity in Indonesian children with acute lymphoblastic leukemia in maintenance therapy. *Pharmgenomics. Pers. Med.* 14, 199–210. doi:10.2147/PGPM.S288988

Rudin, S., Marable, M., and Huang, R. S. (2017). The promise of pharmacogenomics in reducing toxicity during acute lymphoblastic leukemia maintenance treatment. *Genomics Proteomics Bioinforma.* 15, 82–93. doi:10.1016/j.gpb.2016.11.003

Sakamoto, M., Kouhei, D., Haniffa, M., Silva, S., Troncoso, M., Santander, P., et al. (2020). A novel ITPA variant causes epileptic encephalopathy with multiple-organ dysfunction. *J. Hum. Genet.* 65, 751–757. doi:10.1038/s10038-020-0765-3

Schaeffeler, E., Jaeger, S. U., Klumpp, V., Yang, J. J., Igel, S., Hinze, L., et al. (2019). Impact of NUDT15 genetics on severe thiopurine-related hematotoxicity in patients with European ancestry. *Genet. Med.* 21, 2145–2150. doi:10.1038/s41436-019-0448-7

Schmiegelow, K., and Bruunshuus, I. (1990). 6-Thioguanine nucleotide accumulation in red blood cells during maintenance chemotherapy for childhood acute lymphoblastic leukemia, and its relation to leukopenia. *Cancer Chemother. Pharmacol.* 26, 288–292. doi:10.1007/BF02897232

Schmiegelow, K., Nielsen, S. N., Frandsen, T. L., and Nersting, J. (2014). Mercaptopurine/methotrexate maintenance therapy of childhood acute lymphoblastic leukemia: Clinical facts and fiction. *J. Pediatr. Hematol. Oncol.* 36, 503–517. doi:10.1097/MPH.0000000000000206

Smid, A., Karas-Kuzelicki, N., Jazbec, J., and Mlinaric-Rascan, I. (2016). PACSIN2 polymorphism is associated with thiopurine-induced hematological toxicity in children with acute lymphoblastic leukaemia undergoing maintenance therapy. *Sci. Rep.* 6, 30244. doi:10.1038/srep30244

Stocco, G., Crews, K. R., and Evans, W. E. (2010). Genetic polymorphism of inosine-triphosphate-pyrophosphatase influences mercaptopurine metabolism and toxicity during treatment of acute lymphoblastic leukemia individualized for thiopurine-S-methyl-transferase status. *Expert Opin. Drug Saf.* 9, 23–37. doi:10.1517/14740330903426151

Stocco, G., Yang, W., Crews, K. R., Thierfelder, W. E., Decorti, G., Londero, M., et al. (2012). PACSIN2 polymorphism influences TPMT activity and mercaptopurine-related gastrointestinal toxicity. *Hum. Mol. Genet.* 21, 4793–4804. doi:10.1093/hmg/dds302

Stoneham, S., Lennard, L., Coen, P., Lilleyman, J., and Saha, V. (2003). Veno-occlusive disease in patients receiving thiopurines during maintenance therapy for childhood acute lymphoblastic leukaemia. *Br. J. Haematol.* 123, 100–102. doi:10.1046/j.1365-2141.2003.04578.x

Takenaka, K., Morgan, J. A., Scheffer, G. L., Adachi, M., Stewart, C. F., Sun, D., et al. (2007). Substrate overlap between Mrp4 and Abcg2/Bcrp affects purine analogue drug cytotoxicity and tissue distribution. *Cancer Res.* 67, 6965–6972. doi:10.1158/0008-5472.CAN-06-4720

Tanaka, Y., Manabe, A., Fukushima, H., Suzuki, R., Nakadate, H., Kondoh, K., et al. (2015). Multidrug resistance protein 4 (MRP4) polymorphisms impact the 6-mercaptopurine dose tolerance during maintenance therapy in Japanese childhood acute lymphoblastic leukemia. *Pharmacogenomics J.* 15, 380–384. doi:10.1038/tpj.2014.74

Tanaka, Y., Nakadate, H., Kondoh, K., Nakamura, K., Koh, K., and Manabe, A. (2018). Interaction between NUDT15 and ABCC4 variants enhances intolerability of 6-mercaptopurine in Japanese patients with childhood acute lymphoblastic leukemia. *Pharmacogenomics J.* 18, 275–280. doi:10.1038/tpj.2017.12

Toksvang, L. N., Andrés-Jensen, L., Rank, C. U., Niinimäki, R., Nersting, J., Nielsen, S. N., et al. (2021). Maintenance therapy and risk of osteonecrosis in children and young adults with acute lymphoblastic leukemia: A NOPHO ALL2008 sub-study. *Cancer Chemother. Pharmacol.* 88, 911–917. doi:10.1007/s00280-021-04316-z

Tulstrup, M., Grosjean, M., Nielsen, S. N., Grell, K., Wolthers, B. O., Wegener, P. S., et al. (2018). NT5C2 germline variants alter thiopurine metabolism and are associated with acquired NT5C2 relapse mutations in childhood acute lymphoblastic leukaemia. *Leukemia* 32, 2527–2535. doi:10.1038/s41375-018-0245-3

Tzoneva, G., Perez-Garcia, A., Carpenter, Z., Khiabanian, H., Tosello, V., Allegretta, M., et al. (2013). Activating mutations in the NT5C2 nucleotidase gene drive chemotherapy resistance in relapsed ALL. *Nat. Med.* 19, 368–371. doi:10.1038/nm.3078

Uchiyama, K., Nakamura, M., Kubota, T., Yamane, T., Fujise, K., and Tajiri, H. (2009). Thiopurine S-methyltransferase and inosine triphosphate pyrophosphohydrolase genes in Japanese patients with inflammatory bowel disease in whom adverse drug reactions were induced by azathioprine/6-mercaptopurine treatment. *J. Gastroenterol.* 44, 197–203. doi:10.1007/s00535-008-2307-1

Valerie, N. C., Hagenkort, A., Page, B. D., Masuyer, G., Rehling, D., Carter, M., et al. (2016). NUDT15 hydrolyzes 6-thio-DeoxyGTP to mediate the anticancer efficacy of 6-thioguanine. *Cancer Res.* 76, 5501–5511. doi:10.1158/0008-5472.CAN-16-0584

van Dieren, J. M., van Vuuren, A. J., Kusters, J. G., Nieuwenhuis, E. E., Kuipers, E. J., and van der Woude, C. J. (2005). ITPA genotyping is not predictive for the development of side effects in AZA treated inflammatory bowel disease patients. *Gut* 54, 1664.

Vang, S. I., Schmiegelow, K., Frandsen, T., Rosthoj, S., and Nersting, J. (2015). Mercaptopurine metabolite levels are predictors of bone marrow toxicity following high-dose methotrexate therapy of childhood acute lymphoblastic leukaemia. *Cancer Chemother. Pharmacol.* 75, 1089–1093. doi:10.1007/s00280-015-2717-8

Wahlund, M., Nilsson, A., Kahlin, A. Z., Broliden, K., Myrberg, I. H., Appell, M. L., et al. (2020). The role of TPMT, ITPA, and NUDT15 variants during mercaptopurine treatment of Swedish pediatric patients with acute lymphoblastic leukemia. *J. Pediatr.* 216, 150–157. doi:10.1016/j.jpeds.2019.09.024

Wan Rosalina, W. R., Teh, L. K., Mohamad, N., Nasir, A., Yusoff, R., Baba, A. A., et al. (2012). Polymorphism of ITPA 94C>A and risk of adverse effects among patients with acute lymphoblastic leukaemia treated with 6-mercaptopurine. *J. Clin. Pharm. Ther.* 37, 237–241. doi:10.1111/j.1365-2710.2011.01272.x

Weinshilboum, R. M., and Sladek, S. L. (1980). Mercaptopurine pharmacogenetics: Monogenic inheritance of erythrocyte thiopurine methyltransferase activity. *Am. J. Hum. Genet.* 32, 651–662.

Weitzel, K. W., Smith, D. M., Elsey, A. R., Duong, B. Q., Burkley, B., Clare-Salzler, M., et al. (2018). Implementation of standardized clinical processes for TPMT testing in a diverse multidisciplinary population: Challenges and lessons learned. *Clin. Transl. Sci.* 11, 175–181. doi:10.1111/cts.12533

Wielinga, P. R., Reid, G., Challa, E. E., van der Heijden, I., van Deemter, L., de Haas, M., et al. (2002). Thiopurine metabolism and identification of the thiopurine metabolites transported by MRP4 and MRP5 overexpressed in human embryonic kidney cells. *Mol. Pharmacol.* 62, 1321–1331. doi:10.1124/mol.62.6.1321

Wojtuszkiewicz, A., Barcelos, A., Dubbelman, B., De Abreu, R., Brouwer, C., Bökkerink, J. P., et al. (2014). Assessment of mercaptopurine (6MP) metabolites and 6MP metabolic key-enzymes in childhood acute lymphoblastic leukemia. *Nucleosides Nucleotides Nucleic Acids* 33, 422–433. doi:10.1080/15257770.2014.904519

Wroblova, K., Kolorz, M., Batovsky, M., Zboril, V., Suchankova, J., Bartos, M., et al. (2012). Gene polymorphisms involved in manifestation of leucopenia, digestive intolerance, and pancreatitis in azathioprine-treated patients. *Dig. Dis. Sci.* 57, 2394–2401. doi:10.1007/s10620-012-2163-y

Wu, F., Melis, R., McMillin, G. A., and Johnson-Davis, K. L. (2019). Retrospective data analysis of the influence of age and sex on TPMT activity and its phenotype-genotype correlation. *J. Appl. Lab. Med.* 3, 827–838. doi:10.1373/jalm.2018.027276

Yamaguchi-Kabata, Y., Nariai, N., Kawai, Y., Sato, Y., Kojima, K., Tateno, M., et al. (2015). iJGVD: an integrative Japanese genome variation database based on whole-genome sequencing. *Hum. Genome Var.* 2, 15050. doi:10.1038/hgv.2015.50

Yang, J. J., Landier, W., Yang, W., Liu, C., Hageman, L., Cheng, C., et al. (2015). Inherited NUDT15 variant is a genetic determinant of mercaptopurine intolerance in children with acute lymphoblastic leukemia. *J. Clin. Oncol.* 33, 1235–1242. doi:10.1200/JCO.2014.59.4671

Yang, S. K., Hong, M., Baek, J., Choi, H., Zhao, W., Jung, Y., et al. (2014). A common missense variant in NUDT15 confers susceptibility to thiopurine-induced leukopenia. *Nat. Genet.* 46, 1017–1020. doi:10.1038/ng.3060

Zabala-Fernandez, W., Barreiro-de Acosta, M., Echarri, A., Carpio, D., Lorenzo, A., Castro, J., et al. (2011). A pharmacogenetics study of TPMT and ITPA genes detects a relationship with side effects and clinical response in patients with inflammatory bowel disease receiving Azathioprine. *J. Gastrointestin. Liver Dis.* 20, 247–253.

Zhou, Y., Wang, L., Zhai, X. Y., Wen, L., Tang, F., Yang, F., et al. (2020). Precision therapy of 6-mercaptopurine in Chinese children with acute lymphoblastic leukaemia. *Br. J. Clin. Pharmacol.* 86, 1519–1527. doi:10.1111/bcp.14258

Zhu, X., Wang, X. D., Chao, K., Zhi, M., Zheng, H., Ruan, H. L., et al. (2016). NUDT15 polymorphisms are better than thiopurine S-methyltransferase as predictor of risk for thiopurine-induced leukopenia in Chinese patients with Crohn's disease. *Aliment. Pharmacol. Ther.* 44, 967–975. doi:10.1111/apt.13796

Zimdahl Kahlin, A., Helander, S., Skoglund, K., Soderkvist, P., Martensson, L. G., and Appell, M. L. (2019). Comprehensive study of thiopurine methyltransferase genotype, phenotype, and genotype-phenotype discrepancies in Sweden. *Biochem. Pharmacol.* 164, 263–272. doi:10.1016/j.bcp.2019.04.020

frontiers | Frontiers in Pharmacology

TYPE Clinical Trial
PUBLISHED 05 October 2022
DOI 10.3389/fphar.2022.961863

OPEN ACCESS

EDITED BY
Jian Gao,
Shanghai Children's Medical Center, China

REVIEWED BY
Hairong Huang,
Beijing Chest Hospital, Capital Medical University, China
Leping Ye,
First Hospital, Peking University, China

*CORRESPONDENCE
Wei Zhao,
zhao4wei2@hotmail.com
Adong Shen,
shenadong@bch.com.cn

†These authors have contributed equally to this work

SPECIALTY SECTION
This article was submitted to Obstetric and Pediatric Pharmacology, a section of the journal Frontiers in Pharmacology

RECEIVED 05 June 2022
ACCEPTED 09 September 2022
PUBLISHED 05 October 2022

CITATION
Wang Z, Bi J, You D, Tang Y, Liu G, Yu J, Jin Z, Jiang T, Tian X, Qi H, Dong L, Dong L, Zhang Q, Zhao W and Shen A (2022), Improving the efficacy for meropenem therapy requires a high probability of target attainment in critically ill infants and children. *Front. Pharmacol.* 13:961863. doi: 10.3389/fphar.2022.961863

Improving the efficacy for meropenem therapy requires a high probability of target attainment in critically ill infants and children

Zeming Wang[1,2†], Jing Bi[3†], Dianping You[4†], Yu Tang[5], Gang Liu[6], Jinqian Yu[7], Zhipeng Jin[5], Tingting Jiang[3], Xue Tian[1], Hui Qi[1], Lei Dong[4], Lili Dong[5], Qunqun Zhang[5], Wei Zhao[8,9*†] and Adong Shen[1,5*†]

[1]Beijing Key Laboratory of Pediatric Respiratory Infection Diseases, Key Laboratory of Major Diseases in Children, Ministry of Education, National Clinical Research Center for Respiratory Diseases, National Key Discipline of Pediatrics (Capital Medical University), Beijing Pediatric Research Institute, Beijing Children's Hospital, Capital Medical University, National Center for Children's Health, Beijing, China, [2]Department of Pediatrics, Beijing Friendship Hospital, Capital Medical University, Beijing, China, [3]Baoding Children's Hospital, Baoding, China, [4]Children's Hospital of Hebei Province, Shijiazhuang, China, [5]Children's Hospital Affiliated to Zhengzhou University, Henan Children's Hospital, Zhengzhou Children's Hospital, Zhengzhou, China, [6]Department of Infection Diseases, Beijing Children's Hospital, Capital Medical University, National Center for Children's Health, Beijing, China, [7]Department of Neonatology, Sunyi Women's and Children's Hospital of Beijing Children's Hospital, Beijing, China, [8]Department of Clinical Pharmacy, School of Pharmaceutical Sciences, Cheeloo College of Medicine, Shandong University, Jinan, China, [9]NMPA Key Laboratory for Clinical Research and Evaluation of Innovative Drug, Qilu Hospital of Shandong University, Shandong University, Jinan, China

Probability of target attainment is the key factor influencing the outcome of meropenem therapy. The objective of the present study was to evaluate the relationship between the time in which the plasma free concentration of meropenem exceeds the minimum inhibitory concentration of pathogens ($fT_{>MIC}$) during therapy and the clinical outcome of treatment to optimize meropenem therapy. Critically ill children with infections who had received intravenous meropenem monotherapy were included. The relationship between $fT_{>MIC}$ of meropenem and effectiveness and safety were explored. Data from 53 children (mean age ± standard deviation, 26 months ± 38) were available for final analysis. Children with $fT_{>MIC} \geq 5.6$ h ($n = 14$) had a more significant improvement in antibacterial efficacy in terms of decrease in fever ($p = 0.02$), white blood cell count ($p = 0.014$), and C-reactive protein ($p = 0.02$) compared with children with $fT_{>MIC} < 5.6$ h ($n = 39$) after meropenem therapy completed. No drug-related adverse events were shown to have a causal association with meropenem therapy. Our study shows the clinical benefits of sufficient target attainment of meropenem therapy. Meeting a suitable pharmacodynamic target attainment of meropenem is required to ensure better antibacterial efficacy in critically ill infants and children.

Clinical Trial Registration: clinicaltrials.gov, Identifier NCT03643497.

KEYWORDS

$fT_{>MIC}$, meropenem, children, critically ill, pharmacodynamic target attainment

Introduction

Meropenem is the most widely used carbapenem in children for the treatment of severe infections owing to its broad antimicrobial spectrum (including multidrug-resistant bacteria) and favorable safety profile (Thalhammer and Horl, 2000; Cies et al., 2014). Meropenem shows time-dependent antibacterial activity related to the time that the plasma free concentration of meropenem exceeds the minimum inhibitory concentration (MIC) of the pathogen ($fT_{>MIC}$) (Mathew et al., 2016). Despite its wide use, the standard dosing regimen, administered as 10–40 mg/kg/dose (q8h) infused for 0.5 h, for critically ill infants, children (Kongthavonsakul et al., 2016; Cies et al., 2017; Hassan et al., 2019; Wang et al., 2020) and adults(Alsultan et al., 2021) may fail to meet pharmacodynamic (PD) targets.

Probability of target attainment (PTA) is the key factor influencing the outcome of meropenem therapy. A higher target $fT_{>MIC}$ value ≥70% of the dosage interval has been suggested for patients with severe bacterial infections to ensure bactericidal effectiveness, however, limited data are available in children to support this target (Wang et al., 2020, Cies et al., 2017). Additionally, for some critically ill children without renal impairment, clearance (CL) of therapeutics is augmented thereby decreasing plasma levels, and the volume of distribution (V_d) is increased due to a hyper dynamic state in response to inflammation (Wang et al., 2020; Cies et al., 2017; Rapp et al., 2019). As a result, the probability of target attainment (PTA) of 70% $fT_{>MIC}$ with a standard meropenem dosing regimen is low in critically ill children (Wang et al., 2020). Failure to combat the causative pathogen adequately as a result of a low PTA clearly reduces the probability of successful treatment.

We hypothesized that PTA is the key factor for meropenem treatment success in critically ill children. To optimize meropenem therapy, the relationship between 70% $fT_{>MIC}$ of meropenem [70% × 8 h (the dosage interval) = 5.6 h] and clinical outcome was evaluated in this study.

Methods

Study design

A multicenter prospective, open-label PD study of meropenem was conducted in Beijing Children's Hospital, Baoding Children's Hospital, Henan Children's Hospital, Hebei Children's Hospital from 2019 to 2021. Children hospitalized in pediatric intensive care units with bacterial meningitis [National Institute for Health and Care Excellence (NICE), 2018], sepsis (Dellinger et al., 2013) or severe pneumonia (Subspecialty Group of Respiratory Diseases, 2013) who had received meropenem monotherapy (Dainippon Sumitomo Pharma, Osaka, Japan) for a clinically suspected or proven bacterial infection as an intravenous infusion for 0.5–1 h at 20–40 mg/kg/dose (q8h) were included. Exclusion criteria included a history or evidence of chronic pathology of any organ system, receiving meropenem for ≤48 h, non-bacterial infections, and incomplete clinical information. Demographic data, clinical "characteristics," and response to/adverse events (AE) associated with meropenem therapy were recorded in H6WORLD system (https://www.h6world.cn/home) for the management of clinical data independently.

Calculation of $fT_{>MIC}$ for meropenem

Opportunistic PK samples were collected and plasma concentrations of meropenem were quantified using high-performance liquid chromatography (HPLC) as described in our previous study (Wang et al., 2020). On the basis of the population pharmacokinetic (PK)-PD parameters of meropenem in critically ill infants and children with infections reported (Wang et al., 2020), the $fT_{>MIC}$ for each patient was calculated using the following equation (Dudley and Ambrose, 2000; Bradley et al., 2008; Yun et al., 2010):

$$\frac{In\frac{Dose}{Vd} - In\,MIC}{\frac{0.693}{T_{1/2}}} \quad (1)$$

where V_d is the volume of distribution, $T_{1/2}$ is the serum elimination half-life, and Dose is the single dose administered. The information associated with V_d and $T_{1/2}$ value is detailed in our article (Wang et al., 2020). Meropenem has excellent activity against Gram-positive bacteria, including *Streptococcus pneumoniae*, and Gram-negative organisms such as *Escherichia coli*, *Haemophilus influenzae*, *Klebsiella pneumonia*, and *Neisseria meningitidis*; these were the most common bacterial pathogens observed in our study. The MICs for almost all pathogens were ≤1 mg/L (CLSI supplement M100. Wayne, 2019) and the PTA was 18.7% (MIC = 1 mg/L) and 5.8% (MIC = 2 mg/L) at the standard dosing regimen for meropenem under 70% $fT_{>MIC}$ based on our microbiological data (Wang et al., 2020). In order to ensure enough children in the PD target attainment group for efficacy analysis, MIC = 1 mg/L with higher PTA was selected. It should be highlighted that the choice of the 5.6-h cut-off value for meropenem was based on a high PTA at 70% $fT_{>MIC}$ (8-h dose interval). The 70% $fT_{>MIC}$ (defined as the time that the plasma free concentration of meropenem exceeds the MIC) value of meropenem was calculated as 70% × 8 h (the dosage interval) = 5.6 h. Patients with $fT_{>MIC}$ values ≥ 5.6 h were identified as achieving $fT_{>MIC}$ of at least 70% and meeting the target attainment. The relationship between meropenem $fT_{>MIC}$ and effectiveness and safety were explored.

Effectiveness assessment

The assessment of response to meropenem therapy was based on clinical characteristics (signs and symptoms of infection and inflammatory markers) and/or radiological (X-ray or computed tomography scans) findings at first 48–72 h after meropenem treatment and the point when meropenem therapy was completed. Clinical response was defined as improvements in signs and symptoms, laboratory testing values, and infection resolution without worsening of severe pneumonia by chest X-ray examination. Failure was defined as the demonstration of no improvement or deterioration of signs and symptoms, laboratory testing values, or the requirement of additional antibiotics (Schuler, 1995). The effective rates (ER) were calculated using the following equation:

$$ER = \frac{\mathrm{Ni}}{\mathrm{N}} \times 100\% \quad (2)$$

where Ni is the numbers of patients with clinical improvement in children with $fT_{>\mathrm{MIC}} \geq 5.6$ h or children with $fT_{>\mathrm{MIC}} < 5.6$ h, N is the total numbers of children in the corresponding group above.

Safety assessment

AEs that occurred during meropenem use were recorded and classified by severity (mild, moderate, severe, or life-threatening) and relationship (possibly, probably, certainly, probably not, or certainly not related) to treatment by the investigator independently before and after therapy (Cohen-Wolkowiez et al., 2012; Liu et al., 2018).

Statistical analysis

Data are expressed as the means ± standard deviation (SD). Proportions were compared by the χ^2 or Fisher's exact tests, as appropriate. Continuous variables were compared by the *t*-test or Wilcoxon test, as appropriate. Statistical significance was defined by a two-sided p value of 0.05. All statistical analyses were performed using IBM SPSS software version 25.0.

Results

Patients

From July 2019 to November 2021, 98 critically ill children with infections who had received intravenous meropenem were screened. There were 53 patients (18 bacterial meningitis, 24 sepsis, and 11 severe pneumonia patients) available for PD analysis after exclusion of 35 patients on two antibiotics (including meropenem), one patient with Kawasaki disease, three patients out of study, three patients with trauma, two patients who had been infected with virus combined and one patient with meropenem treatment for 1 day. The mean age and weight of the 53 children at the time of study were 26 ± 38 months and 12.67 ± 11.07 kg, respectively. There were no significant differences in diseases distribution between the two groups (Table 1).

Calculation of meropenem $fT_{>\mathrm{MIC}}$ levels

Meropenem was administrate in the enrolled patients with sepsis, severe pneumonia (20 mg/kg/dose) and bacterial meningitis (40 mg/kg/dose) respectively. The median duration of therapy was 13 days. 111 meropenem concentrations were obtainable. The median number of samples per patients was 2 (range, 1–4). The median meropenem concentration of PK samples was 1.16 (range, 0.2–147.24) μg/ml. The median $fT_{>\mathrm{MIC}}$ was 4.38 h (range, 3.48–8.0 h).

Effectiveness assessment

$fT_{>\mathrm{MIC}}$ of meropenem was <5.6 h in 39 cases (73.58%) and ≥5.6 h in 14 cases (26.42%). Significant improvement in antibacterial efficacy at first 48–72 h after meropenem treatment (ER: 78.57% v 35.90%, $p = 0.006$) and the point when meropenem therapy was completed (ER: 92.86% v 64.10%, $p = 0.04$) was found in children with $fT_{>\mathrm{MIC}} \geq 5.6$ h compared with children with $fT_{>\mathrm{MIC}} < 5.6$ h. Significantly decreases in fever were present between the two groups at first 48–72 h ($p = 0.002$) and the point meropenem therapy completed ($p = 0.02$). Additionally, Clear decreases in white blood cell (WBC) counts ($p = 0.014$) and C-reactive protein (CRP) ($p = 0.02$) were also observed between the two groups after meropenem treatment. No significant differences were observed for other effectiveness parameters (Table 2).

$fT_{>\mathrm{MIC}}$ of meropenem was <5.6 h in 14 cases (77.78%) and ≥5.6 h in 4 cases (22.22%) in children with bacterial meningitis. More decreases in fever, WBC and CRP were found between the two groups at first 48–72 h and the point meropenem therapy completed. However, only improvement in fever was significant at the early treatment stage($p = 0.023$) (Table 3).

Safety assessment

All 53 patients were assessed for treatment safety. Fourteen mild AEs were reported in ten (18.87%) patients, including granulocytopenia (6), aspartate aminotransferase (5), alanine aminotransferase increase (2), and rash (1). There was no statistically significant difference in meropenem $fT_{>\mathrm{MIC}}$

TABLE 1 Demographic parameters.

Variable	Meropenem $T_{>MIC}$ (hour)		*p*
	≥5.6 h (*n* = 14)	<5.6 h (*n* = 39)	
Demographic data			
Age (months), mean (SD)	14 (24)	30 (41)	0.194
Boys, n (%)	10 (71.43)	21 (53.85)	0.252
Weight (kg), mean (SD)	8.97 (5.15)	14.00 (12.26)	0.151
Creatinine clearance (ml/min/1.73 m^2), mean (SD)	129.56 (75.66)	177.26 (66.09)	***0.03***
Severe infectious diseases *n* (%)			
Sepsis	8 (57.14)	16 (41.03)	0.299
Bacterial meningitis	4 (28.57)	14 (35.90)	0.620
Severe pneumonia	2 (14.29)	9 (23.08)	0.487
Pathogens, *n* (%)			
Klebsiella pneumoniae	0 (0.00)	3 (7.69)	
Staphylococcus aureus	1 (7.14)	2 (5.13)	
Listeria monocytogenes	0 (0.00)	1 (2.56)	
Pseudomonas aeruginosa	2 (14.29)	0 (0.00)	
Streptococcus pneumoniae	1 (7.14)	1 (2.56)	
Escherichia coli	1 (7.14)	0 (0.00)	
Haemophilus influenzae	0 (0.00)	1 (2.56)	
Acinetobacter baumannii	1(7.14)	0 (0.00)	
Viridans streptococci	1(7.14)	0 (0.00)	
Streptococcus constellatus	0 (0.00)	1 (2.56)	
No pathogens found	8 (57.14)	30 (76.92)	
Duration of antibiotic treatment (days), mean (SD)	11.79 (7.24)	13.18 (7.82)	0.57
Duration of hospitalization (days), mean (SD)	15.64 (10.35)	19.74 (16.01)	0.378

The bold and Italics indicated that the *p* value was less than 0.05. The difference was statistically between children with fT>MIC ≥ 5.6 h and children with fT>MIC < 5.6 h.

between children with or without AEs ($p = 0.715$). No patients discontinued meropenem treatment in response to AEs and no drug-related AEs were causally associated with meropenem treatment.

Discussion

Optimizing PK exposure of antibiotics to meet suitable target attainment in critically ill patients could improve infection-related outcomes and reduce bacterial antibiotic resistance. A previous study reported that adjusting doses to achieve a $fT_{>MIC}$ of at least 70% of the dosage interval was more likely to eradicate the causative pathogen (Scaglione et al., 2009). To the best of our knowledge, our study shows the clinical benefits of a high PTA for meropenem therapy in critically ill children.

To ensure better clinical outcome, 70% $fT_{>MIC}$ was selected as the PD target in critically ill infants and children associated with immunodeficient states (Ariano et al., 2005; Scaglione et al., 2009; Franciscus van der Meer et al., 2011). Our study did find that there was significantly clinical improvement in children with $fT_{>MIC} \geq 5.6$ h than children with $fT_{>MIC} < 5.6$ h. We further simulated the clinical efficacy of meropenem with lower $fT_{>MIC}$ (60% of the dosage interval = 4.8 h) as the PD target in these children. However, it was no significant difference between the children with $fT_{>MIC} \geq 4.8$ h and children with $fT_{>MIC} < 4.8$ h ($p > 0.05$, range 0.141–0.905).

According to the instructions, meropenem was administered at 40 or 20 mg/kg in children with bacterial meningitis or other infections, respectively. There was no difference in disease distribution between two groups ($p = 0.299$–0.620). Therefore minor effect under different doses for meropenem was related with our conclusion. In addition, our study showed the better clinical benefits (fever, WBC and CRP) of a high PTA of meropenem therapy in children with bacterial meningitis ($n = 18$). Unfortunately, most of the differences were not significant which associated with the limited patients enrolled. Similar results were also found in children ($n = 35$) with severe pneumonia ($n = 11$) and sepsis ($n = 24$) (Table 3). When the analysis was performed target the whole patients, the differences between the two groups were dramatical as the total population increased (Table 2).

TABLE 2 Clinical response to meropenem therapy in children.

Response	Meropenem $T_{>MIC}$ (hour)		*p*
	≥5.6 h (*n* = 14)	<5.6 h (*n* = 39)	
Total patients, *n* (%)			
Improvement			
Meropenem treatment after first 48–72 h	11 (78.57)	14 (35.90)	***0.006***
Meropenem treatment completed	13 (92.86)	25 (64.10)	***0.04***
Failure			
Meropenem treatment after first 48–72 h	3 (21.43)	25 (64.10)	***0.006***
Meropenem treatment completed	1 (7.14)	14 (35.90)	***0.04***
Fever, patients *n* (%)			
Improvement			
Meropenem treatment after first 48–72 h	13 (92.86)	18 (46.15)	***0.002***
Meropenem treatment completed	13 (92.86)	23 (58.97)	***0.02***
Failure			
Meropenem treatment after first 48–72 h	1 (7.14)	21 (53.85)	***0.002***
Meropenem treatment completed	1 (7.14)	16 (41.03)	***0.02***
WBC, patients *n* (%)			
Meropenem treatment after first 48–72 h	10 (71.43)	27 (69.23)	0.878
Meropenem treatment completed	13 (92.86)#	22 (56.41)#	***0.014***
CRP, patients *n* (%)			
Meropenem treatment after first 48–72 h	13 (92.86)	26 (66.67)	0.057
Meropenem treatment completed	13 (92.86)*	23 (58.97)*	***0.02***

White blood cell (WBC) count decreased under 10×10^9/L; * C-reactive protein (CRP) decreased under 10 mg/L; *p* represents statistical significance between children with $fT_{>MIC} \geq 5.6$ h and children with $fT_{>MIC} < 5.6$ h.
The bold and Italics indicated that the *p* value was less than 0.05. The difference was statistically between children with fT>MIC ≥ 5.6 h and children with fT>MIC < 5.6 h.

TABLE 3 Clinical response to meropenem therapy in children with bacterial meningitis or spesis and severe pneumonia.

Response	Meropenem $T_{>MIC}$ (hour)		*p*	Meropenem $T_{>MIC}$ (hour)		*p*
	≥5.6 h (*n* = 4)	<5.6 h (*n* = 14)		≥5.6 h (*n* = 10)	<5.6 h (*n* = 25)	
Total patients, *n* (%)	**Bacterial meningitis**			**Spesis and severe pneumonia**		
Improvement						
Meropenem treatment after first 48–72 h	3 (75.00)	5 (35.71)	0.163	8 (80.00)	9 (36.00)	***0.019***
Meropenem treatment completed	4 (100.00)	7 (50.00)	0.07	9 (90.00)	18 (72.00)	0.252
Fever, patients *n* (%)						
Improvement						
Meropenem treatment after first 48–72 h	4 (100.00)	5 (35.71)	***0.023***	9 (90.00)	13 (52.00)	***0.036***
Meropenem treatment completed	4 (100.00)	7 (50.00)	0.07	9 (90.00)	16 (64.00)	0.124
WBC, patients *n* (%)						
Meropenem treatment after first 48–72 h	3 (75.00)	9 (64.29)	0.688	7 (70.00)	18 (72.00)	0.906
Meropenem treatment completed	4 (100.00)#	8 (57.14)#	0.109	9 (90.00)#	14 (56.00)#	0.056
CRP, patients *n* (%)						
Meropenem treatment after first 48–72 h	4 (100.00)	8 (57.14)	0.109	9 (90.00)	18 (72.00)	0.252
Meropenem treatment completed	4 (100.00)*	8 (57.14)*	0.109	9 (90.00)*	15 (60.00)*	0.084

White blood cell (WBC) count decreased under 10×10^9/L; * C-reactive protein (CRP) decreased under 10 mg/L; *p* represents statistical significance between children with $fT_{>MIC} \geq 5.6$ h and children with $fT_{>MIC} < 5.6$ h.
The bold and Italics indicated that the *p* value was less than 0.05. The difference was statistically between children with fT>MIC ≥ 5.6 h and children with fT>MIC < 5.6 h.

In our study, clinical signs improved in 71.70% cases, which is similar to what Punpanich et al. (2012) reported (68.1%) with a standard dosing regimen for meropenem. However, their regimen could not reach the PD target for susceptible and multi-resistant organisms in critically ill children (Wang et al., 2020). As shown here, optimization of the dose regimen for meropenem is a viable means of improving its efficacy. Children with a high PTA had a significant improvement in antibacterial efficacy compared with children with low target attainment at both the early and final stages of meropenem treatment. Length of hospitalization also decreased in children with a high PTA, although the difference between the two groups was not statistically significant, which is possibly attributed to the limited number of patients. Furthermore, the proportion of patients with decreased inflammatory markers in the group with $fT_{>MIC} \geq 5.6$ h was lower than that in the group with $fT_{>MIC} < 5.6$ h, but this was also not significant. However, for the patients with inflammatory markers reduced to normal levels, there were significant differences between the two groups. Taken together, a high PTA observably increases the probability of recovery.

We further found that the children with $fT_{>MIC} < 5.6$ h had higher creatinine clearance than children with $fT_{>MIC} \geq 5.6$ h (177.26 v129.56 ml/min/1.73 m^2), which resulted in rapid excretion of meropenem and lower $fT_{>MIC}$. To determine the optimal dosage regimens, we evaluated treatment frequency and infusion time, showing that 40 mg/kg/dose (q8h) with 4-h infusion and 110 mg/kg/day with continuous infusion can achieve PTA for bacteria with a low MIC (≤2 mg/L) and high MIC (2–8 mg/L), respectively (Wang et al., 2020). Multicenter random clinical trials associated with the efficacy and safety of these recommended regimens are under way.

There are several limitations in our study. Firstly, this study was limited by the small number of children enrolled. Secondly, the selection of the cut-off value (70% $fT_{>MIC} = 5.6$ h, MIC = 1 mg/L) for PTA of meropenem was mainly based on our microbiological and PK-PD data. Different values and MICs might be targeted with bacterial pathogens with higher MICs. Finally, only patients on meropenem monotherapy were included in this study. Because combined antimicrobial therapy might introduce additional complicating factors in the interpretation of the relationship between PTA of meropenem and clinical outcome.

Conclusion

Our study demonstrates the clinical benefits of a high PTA with meropenem therapy in critically ill children with infections. Children with meropenem $fT_{>MIC} \geq 5.6$ h showed better antibacterial efficacy. Prospective trials to confirm this discovery in a larger pediatric population will be conducted in future studies.

Data availability statement

The original contributions presented in the study are included in the article, further inquiries can be directed to the corresponding authors.

Ethics statement

The studies involving human participants were reviewed and approved by the Ethics Committee of each participating hospital (2019-k-185, 2020-6-1) and registered on clinicaltrials.gov (ID: NCT03643497). Written informed consent to participate in this study was provided by the participants' legal guardian/next of kin.

Author contributions

ZW, JB, and DY contributed equally to this paper. ZW, WZ, and AS conceived and designed the study. ZW, JB, DY, GL, YT, JY, ZJ, TJ, XT, HQ, LeD, LiD, and QZ contributed to patient recruitment, data collection, data analysis and data interpretation. ZW wrote the first draft of the manuscript. JB, DY, WZ, and AS provided administrative, technical, or material support. WZ and AS supervised the study. ZW, WZ, and AS contributed to the critical revision of the manuscript for important intellectual content. WZ and AS contributed equally to this work. All authors reviewed and approved the final version of the manuscript.

Funding

The study was funded by the Special Research Project of Capital Health Development (2020-1-1991) and Beijing Natural Science Foundation (J200005). The funders had no role in the study design, data collection and analysis, decision to publish, or preparation of the manuscript.

Acknowledgments

We would like to acknowledge the support of Beijing Children's Hospital, Capital Medical University, National Center for Children's Health, Baoding Children's Hospital, Hebei Children's Hospital, Henan Children's Hospital and Beijing Friendship Hospital, Capital Medical University.

Conflict of interest

The reviewer HH declared a shared parent affiliation with the authors ZW, GL, XT, HQ, and AS to the handling editor at the time of review.

The authors declare that the research was conducted in the absence of any commercial or financial relationships that could be construed as a potential conflict of interest.

Publisher's note

References

Alsultan, Abdullah, Dasuqi, Shereen A., Aljamaan, Fadi, Omran, Rasha A., Ali Syed, Saeed, AlJaloud, Turki, et al. (2021). Pharmacokinetics of meropenem in critically ill patients in Saudi Arabia. *Saudi Pharm. J.* 29, 1272–1277. doi:10.1016/j.jsps.2021.09.017

Ariano, Robert E., Anna, Nyhlén, Donnelly, J. Peter, Sitar, Daniel S., Harding, Godfrey K. M., and Zelenitsky, Sheryl A. (2005). Pharmacokinetics and pharmacodynamics of meropenem in febrile neutropenic patients with bacteremia. *Ann. Pharmacother.* 39, 32–38. doi:10.1345/aph.1E271

Author Anonymous (2018). *2018 surveillance of meningitis (bacterial) and meningococcal septicaemia in under 16s: Recognition, diagnosis and management*. London: NICE guideline CG102.

Bradley, John S., Sauberan, Jason B., Ambrose, Paul G., Bhavnani, Sujata M., Rasmussen, Maynard R., and Capparelli, Edmund V. (2008). Meropenem pharmacokinetics, pharmacodynamics, and Monte Carlo simulation in the neonate. *Pediatr. Infect. Dis. J.* 27, 794–799. doi:10.1097/INF.0b013e318170f8d2

Cies, J. J., Moore, W. S., Enache, A., and Chopra, A. (2017). Population pharmacokinetics and pharmacodynamic target attainment of meropenem in critically ill young children. *J. Pediatr. Pharmacol. Ther.* 22, 276–285. doi:10.5863/1551-6776-22.4.276

Cies, Jeffrey J., Moore, Wayne S., J Dickerman, Mindy, Small, Christine, Carella, Dominick, Chopra, Arun, et al. (2014). Pharmacokinetics of continuous-infusion meropenem in a pediatric patient receiving extracorporeal life support. *Pharmacotherapy* 34, e175–e179. doi:10.1002/phar.1476

Cohen-Wolkowiez, Michael, Poindexter, Brenda, Bidegain, Margarita, Schelonka, Robert L., Randolph, David A., Ward, Robert M., et al. (2012). Safety and effectiveness of meropenem in infants with suspected or complicated intra-abdominal infections. *Clin. Infect. Dis.* 55, 1495–1502. doi:10.1093/cid/cis758

Dellinger, R. Phillip, Levy, Mitchell M., Rhodes, Andrew, Annane, Djillali, Gerlach, Herwig, Opal, Steven M., et al. (2013). Surviving sepsis campaign: International guidelines for management of severe sepsis and septic shock: 2012. *Crit. Care Med.* 41, 580–637. doi:10.1097/CCM.0b013e31827e83af

Dudley, M. N., and Ambrose, P. G. (2000). Pharmacodynamics in the study of drug resistance and establishing *in vitro* susceptibility breakpoints: Ready for prime time. *Curr. Opin. Microbiol.* 3, 515–521. doi:10.1016/s1369-5274(00)00132-6

Franciscus van der Meer, A., Marcus, Marco A. E., DaniëlTouw, J., JohannesProost, H., and Neef, Cees (2011). Optimal sampling strategy development methodology using maximum a posteriori Bayesian estimation. *Ther. Drug Monit.* 33, 133–146. doi:10.1097/FTD.0b013e31820f40f8

Hassan, Hazem E., Ivaturi, Vijay, Gobburu, Jogarao, and Green, Thomas P. (2019). Dosage regimens for meropenem in children with Pseudomonas infections do not meet serum concentration targets. *Clin. Transl. Sci.* 13, 301–308. doi:10.1111/cts.12710

Kongthavonsakul, Kritsana, Lucksiri, Aroonrut, Eakanunkul, Suntara, Roongjang, Somjing, and Oberdorfer, Peninnah (2016). Pharmacokinetics and pharmacodynamics of meropenem in children with severe infection. *Int. J. Antimicrob. Agents* 48, 151–157. doi:10.1016/j.ijantimicag.2016.04.025

Liu, Shuping, Zheng, Yi, Wu, Xirong, Xu, Baoping, Liu, Xiuyun, Feng, Guoshuang, et al. (2018). Early target attainment of azithromycin therapy in children with lower respiratory tract infections. *J. Antimicrob. Chemother.* 73, 2846–2850. doi:10.1093/jac/dky273

Mathew, S. K., Mathew, B. S., Neely, M. N., Naik, G. S., Prabha, Ratna, Jacob, G. G., et al. (2016). A nonparametric pharmacokinetic approach to determine the optimal dosing regimen for 30-minute and 3-hour meropenem infusions in critically ill patients. *Ther. Drug Monit.* 38, 593–599. doi:10.1097/FTD.0000000000000323

Punpanich, Warunee, Srisarang, Suchada, and Prachantasen, Uraiwan (2012). Therapeutic effectiveness of the generic preparation of meropenem (Mapenem) in the treatment of moderate to severe infection in children. *J. Med. Assoc. Thai* 95, 895–902.

Rapp, Mélanie, Urien, Saïk, Foissac, Frantz, Béranger, Agathe, Bouazza, Naïm, Benaboud, Sihem, et al. (2019). Population pharmacokinetics of meropenem in critically ill children with different renal functions. *Eur. J. Clin. Pharmacol.* 76, 61–71. doi:10.1007/s00228-019-02761-7

Scaglione, F., Esposito, S., Leone, S., Lucini, V., Pannacci, M., Ma, L., et al. (2009). Feedback dose alteration significantly affects probability of pathogen eradication in nosocomial pneumonia. *Eur. Respir. J.* 34, 394–400. doi:10.1183/09031936.00149508

Schuler, D. (1995). Safety and efficacy of meropenem in hospitalised children: Randomised comparison with cefotaxime, alone and combined with metronidazole or amikacin. Meropenem paediatric study group. *J. Antimicrob. Chemother.* 36, 99–108. doi:10.1093/jac/36.suppl_a.99

Subspecialty Group of Respiratory Diseases (2013). The society of pediatrics, Chinese medical association, editorial board, Chinese journal of pediatrics [guidelines for management of community acquired pneumonia in children (the revised edition of 2013) (I)]. *Zhonghua Er Ke Za Zhi* 51, 745–752.

Thalhammer, F., and Hörl, W. H. (2000). Pharmacokinetics of meropenem in patients with renal failure and patients receiving renal replacement therapy. *Clin. Pharmacokinet.* 39, 271–279. doi:10.2165/00003088-200039040-00003

Wang, Ze-Ming, Chen, Xiao-Yu, Jing, Bi, Wang, Mei-Ying, Xu, Bao-Ping, Tang, Bo-Hao, et al. (2020). Reappraisal of the optimal dose of meropenem in critically ill infants and children: A developmental pharmacokinetic-pharmacodynamic analysis. *Antimicrob. Agents Chemother.* 64, e00760. doi:10.1128/AAC.00760-20

Wayne, P. A. (2019). *Performance standards for antimicrobial susceptibility testing*. 29th ed. Wayne, PA: Clinical and Laboratory Standards InstituteCLSI supplement M100.

Yun, Zhuo, Nian, Hua, Shang, Hong, GuoSun, Quan, Shang, H., and Sun, G. Q. (2010). Pharmacokinetic-pharmacodynamic profiling of four antimicrobials against gram-negative bacteria collected from Shenyang, China. *BMC Infect. Dis.* 10, 171. doi:10.1186/1471-2334-10-171

frontiers | Frontiers in Pediatrics

TYPE Original Research
PUBLISHED 18 January 2023
DOI 10.3389/fped.2022.958622

OPEN ACCESS

EDITED BY
Yang Zhou,
Brown University, United States

REVIEWED BY
Matej Stuhec,
University of Maribor, Slovenia
Li Sun,
Peking University Sixth Hospital, China

*CORRESPONDENCE
Jacob T. Brown
jtbrown@d.umn.edu

SPECIALTY SECTION
This article was submitted to Obstetric and Pediatric Pharmacology, a section of the journal Frontiers in Pediatrics

RECEIVED 31 May 2022
ACCEPTED 21 November 2022
PUBLISHED 18 January 2023

CITATION
Brown JT, Beery N, Taran A, Stevens T, Henzler C, Badalamenti J, Regal R and McCarty CA (2023) Associations between *CES1* variants and dosing and adverse effects in children taking methylphenidate.
Front. Pediatr. 10:958622.
doi: 10.3389/fped.2022.958622

Associations between *CES1* variants and dosing and adverse effects in children taking methylphenidate

Jacob T. Brown[1]*, Nancy Beery[2], Allise Taran[3], Tyler Stevens[4], Christine Henzler[5], Jonathan Badalamenti[6], Ron Regal[3] and Catherine A. McCarty[7]

[1]University of Minnesota College of Pharmacy, Department of Pharmacy Practice and Pharmaceutical Sciences, Duluth,/c MN, United States, [2]Essentia Health Department of Pediatrics, Duluth, MN, United States, [3]Essentia Institute of Rural Health, Duluth, MN, United States, [4]Essentia Health Department of Pharmacy, Duluth, MN, United States, [5]University of Minnesota Supercomputing Institute, Minneapolis, MN, United States, [6]University of Minnesota Genomics Center, Minneapolis, MN, United States, [7]Department of Family Medicine and BioBehavioral Health, University of Minnesota Medical School, Duluth Campus, Duluth, MN, United States

Background: Methylphenidate is the most prescribed stimulant to treat attention deficit-hyperactivity disorder (ADHD). Despite its widespread usage, a fair proportion of children are classified as non-responders to the medication. Variability in response and occurrence of adverse events with methylphenidate use may be due to several factors, including drug-drug interactions as well as pharmacogenetic differences resulting in pharmacokinetic and/or pharmacodynamic variances within the general population. The objective of this study was to analyze the effect of carboxylesterase 1 (*CES1*) variants on the frequency of adverse effects and dosing requirements of methylphenidate in children with ADHD.

Methods: This was a retrospective cohort study of children and adolescents who met the inclusion criteria and had a routine visit during the enrollment period were invited to participate. Inclusion criteria included: ADHD diagnosis by a healthcare provider, between 6 and 16 years of age at the time of permission/assent, had not previously been prescribed methylphenidate, and treatment with any methylphenidate formulation for at least three consecutive months. Three months of records were reviewed in order to assess changes in dose and frequency of discontinuing methylphenidate. Participants' ADHD symptoms, medication response, adverse effects, select vitals, and dose were extracted from the electronic health record. Saliva samples were collected by trained study coordinators. Haplotypes were assigned based on copy number in different portions of the CES1 gene. Due to limited numbers, diplotypes (combinations of two haplotypes) were grouped for analysis as CES1A1/CES1A1, CES1A1/CES1A1c and CES1A1c/CES1A1c.

Results: A total of 99 participants (n = 30 female; n = 69 male) had both clinical data and *CES1* sequencing data, with an average age of 7.7 years old (range 3–15 years). The final weight-based dose in all individuals was 0.79 mg/kg/day. The most common adverse effects reported were decreased appetite (n = 47), weight loss (n = 24), and sleep problems (n = 19). The mean final weight-based dose by haplotype was 0.92 mg/kg for CES1A2/CES1A2, 0.81 mg/kg for CES1A2/CES1P1, and 0.78 mg/kg for CES1P1/CES1P1. After

correction for multiple hypothesis testing, only one SNV, rs114119971, was significantly associated with weight-based dosing in two individuals. The individuals with the rs114119971 SNV had a significantly lower weight-based dose (0.42 mg/kg) as compared to those without (0.88 mg/kg; $p < 0.001$).

Discussion: Variation in CES1 activity may impact dose requirements in children who are prescribed methylphenidate, as well as other CES1 substrates. Although intriguing, this study is limited by the retrospective nature and relatively small sample size.

KEYWORDS

pediatrics, ADHD, methylphenidate, CES1, pharmacogenetics

Introduction

Attention deficit hyperactivity disorder (ADHD) prevalence worldwide varies considerably, and is estimated to be around 5%, ranging from 2%–7% (1). Among children 6–17 years of age in the United States, ADHD is the most prevalent neurodevelopmental disorder, with 9.5% of all U.S. children between 6 and 17 years of age having received a diagnosis of ADHD at any point in their lifetime (2). The overall prevalence in children 3–17 years of age has increased by 33% from 1997–1999 to 2006–2008 (3). Additionally, a previously estimated cost of illness of ADHD estimated the annual individual costs of ADHD to be between $12,005 and $17,458, and the total annual societal cost between $36 and $52.4 billion (4). ADHD currently has a prevalence estimated to be around 5% (5).

Methylphenidate is first-line treatment in children and adults, is available in several formulations, and is the most prescribed stimulant to treat attention deficit-hyperactivity disorder (ADHD), as well as the most dispensed medication to adolescents 12–17 years with approximately 10 million prescriptions per year from 2002 to 2010 in children 0–17 years of age (6, 7). Despite its widespread usage, a fair proportion of children are classified as non-responders to the medication, while roughly half remain on the medication after one year (8). This variation in response may be due in part to individual pharmacokinetic differences in metabolism and/or pharmacodynamic differences in receptors and transporters. Methylphenidate is a stimulant that works by inhibiting the reuptake of norepinephrine and dopamine into presynaptic neurons, thus increasing these neurotransmitters in the brain. Due to methylphenidate's mechanism of action, research has focused on several genes looking at individual response to treatment, including the dopamine transporter, dopamine receptor, and norepinephrine transporter. Studies comparing genetic variation within these genes have led to mixed results thus far and have resulted in minimal clinical impact (9–11).

Methylphenidate is metabolized to the inactive metabolite ritalinic acid by the enzyme carboxylesterase 1 (CES1) (12). Numerous single nucleotide variants (SNVs) and copy number variants (CNVs) have been identified within the *CES1* gene, with some resulting in altered enzyme activity, and either increased or decreased levels of methylphenidate plasma concentrations at standard doses (13, 14). These differences in overall exposure may lead to differences in both clinical response and adverse effects.

Few clinical studies have been completed describing the relationship between CES1 and methylphenidate with adverse event and clinical response rates. Zhu et al. demonstrated marked pharmacokinetic differences of methylphenidate in an individual with two variants in the *CES1* gene. One variant described a nonconservative amino acid substitution of glycine to glutamic acid (G143E; rs71647871), while the second was a frameshift mutation of *CES1*. This individual experienced a markedly increased area under the curve (AUC), maximum concentration, and half-life as compared to 19 other participants, as well as greater hemodynamic increase. While the frameshift mutation is considered rare (<1%), the glycine to glutamic acid was found in 3.7%, 4.3%, and 2.0% of white, black, and Hispanic populations (13). Furthermore, the G143E variant has also been shown to impair the bioactivation of oseltamivir, which is also a substrate for CES1 (15).

Variability in response and occurrence of adverse events with methylphenidate use may be due to pharmacogenetic differences resulting in pharmacokinetic and/or pharmacodynamic variances within the general population. These differences may be the result of varying levels of drug exposure among individuals at comparable doses, which may directly impact the occurrence of adverse effects and clinical response rates. Improving treatment by selecting the most appropriate dose for an individual may lead to better utilization of ADHD medications, resulting in less treatment failure and better symptomatic control. The objective of this study was to analyze the effect of *CES1* variants on the frequency and severity of adverse effects and dosing requirements of methylphenidate in children with ADHD.

Materials and methods

Study design

This was a retrospective cohort study examining variation in the *CES1* gene and clinical characteristics in children and

adolescents with ADHD prescribed any formulation of methylphenidate. Children and adolescents who met the inclusion criteria and had a routine visit during the enrollment period were invited to participate through mailed invitation letters and a follow-up phone call from study staff. Inclusion criteria included: ADHD diagnosis by a healthcare provider included in their medical record, between 6 and 16 years of age at the time of permission/assent, no previous trial of methylphenidate, and treatment with methylphenidate for at least three consecutive months without concomitant use of another drug to treat ADHD or MAOIs. Exclusion criteria included those with hypersensitivity to methylphenidate, marked agitation, anxiety, or tension, motor tics, diagnosis of Tourette syndrome, or any cardiac abnormality. Informed parental permission, child assent, and saliva collection were obtained at the participant's regularly scheduled appointment by trained study coordinators in cooperation with their health care provider and nursing staff. This study was reviewed and approved by the Essentia Health Institutional Review Board.

Clinical assessment

The primary outcomes of interest included known methylphenidate adverse effects and daily dose. Participants' ADHD symptoms, medication response, adverse effects, and select vitals (height, weight, blood pressure, and heart rate) were assessed using data extracted from the electronic health record through analytics and manual abstraction conducted by research staff.

Study data were collected and managed using REDCap electronic data capture tools hosted at Essentia Health. REDCap (Research Electronic Data Capture) is a secure, web-based application designed to support data capture for research studies, providing: (1) an intuitive interface for validated data entry; (2) audit trails for tracking data manipulation and export procedures; (3) automated export procedures for seamless data downloads to common statistical packages; and (4) procedures for importing data from external sources (16, 17).

Participants and their accompanying parent or guardian were asked at the time of saliva collection to self-report race and ethnicity based on standardized data collection tools (phenxtoolkit.org) as well as the names and dates of birth of the participant's biological parents and grandparents (if available) to determine and account for relatedness of study participants at the time of analysis.

Sample collection and CES1 sequencing

Saliva samples were collected by trained study coordinators using Oragene® DISCOVER (OGR-500 and OGR-575) saliva collection kits, and were stored in a laboratory setting until DNA extraction and gene sequencing were conducted. Each sample was extracted following the automated QIAamp DNA Mini Kit (QIAGEN, Hilden, Germany) protocol for the QIAcube (QIAGEN, Hilden, Germany). Purified DNA extracts were set to elute in 2 increments of 100 µl of AE buffer (200 µl total elution volume). DNA quantification was performed in triplicate using the Qubit™ dsDNA HS Assay Kit (Thermo-Fisher, Waltham, MA) for the 2.0 Qubit™ fluorometric quantification system according to manufacturer's instructions.

Amplicon design and approximate primer placement were performed using Geneious Primer v. 2019.2.3 against the repeat-masked CES1 locus that included 20 kbp up- and downstream (build hg38 in UCSC Genome Browser). Concurrent GC% and conserved SNP tracks were plotted in Geneious alongside the reference to facilitate visual inspection of candidate regions for primer placement such that (1) resulting amplicons had a final size of ∼6 kbp +/− 15%, and (2) amplicons overlapped by at least 200 bp. Genomic coordinates for these candidate ranges were used to iteratively design primers for each amplicon using NCBI PrimerBLAST to have a final length of 20–26 nt and calculated Tm between 58 and 62 °C. Where possible 3′ GC clamps were included and homopolymers limited to 5 nt. Oligonucleotide primers were synthesized by Integrated DNA Technologies (Coralville, IA) with standard desalting and included a single phosphorothioate linkage before the terminal 3′ base to reduce off-target amplification from primer editing (18).

Amplicons were generated using Q5 HiFi HotStart mastermix (New England Biolabs, Ipswich, MA) in a 20-µl PCR containing 10 µl 2× mastermix, 1 µl of forward primer (10 µM), 1 µl of reverse primer (10 µM), 7 µl nuclease-free water, and 1 µl (10 ng/µl) of extracted gDNA. Amplification was performed according to the following cycling conditions (all except region (4): 98 °C for 30 s, followed by 30 cycles of 98 °C for 10 s, 64 °C for 15 s, and 72 °C for 3 min, and a final extension at 72 °C for 5 min. Region 4 used an extension time of 3 min 30 s. PCR products were purified using 0.5× (v/v) Ampure XP beads (Beckman-Coulter), quantified using Picogreen, and normalized to 10 ng/µl. Normalized amplicons from the same individual were pooled at equal volume (2 µl each) and concentrated to ∼5 µl by evaporation before undergoing PacBio library creation (SMRT Bell Express Template Kit 2.0, Pacific Biosciences, Menlo Park, CA) with sample barcodes added *via* ligation. Once barcoded, all libraries were pooled together and sequenced on 1 PacBio 8M SMRT cell (3 pM loading concentration) with 2-h pre-extension.

Circular consensus reads (CCS) were generated for all samples using PacBio's ccs v.6.0.0, the default minimum of 3 full passes (three full reads through the amplicon), a minimum target length of 4,000 and a maximum target

length of 8,000. Reads were aligned to the human genome (GrCh38) using pbmm2 v.1.4.0, PacBio's wrapper for minimap2 (19). Bedtools v2.29.2 (20) was used to measure coverage for both CES1 and CES1P1 (to check for off-target, non-specific amplification.) For each amplicon, 30× coverage was required for a sample to be included in the final analysis. For most amplicons, only four or fewer samples had insufficient depth to be retained in the final analysis, however amplicon 4 failed to amplify for 26 samples. There was virtually no amplification of CES1P1 (as designed). The highest coverage in any sample at any point in CES1P1 was 14× (while the same sample had an average coverage of CES1P1 of only 0.08× and a minimum of 2,654× coverage for CES1).

Variants were called from the aligned bams using freebayes v.1.3.4 (21) using the following parameters: (1) Requiring a minimum of 5 reads and 10% of reads supporting an alternate call (-C 5, -F 0.10), (2) Restricting calls to just the amplified regions, (3) "Output all alleles which pass input filters regardless of genotyping outcome or model." (–pooled-continuous) (–haplotype-length 0), (4) Haplotype length set to 0 to emit simple SNP and indel calls (rather than complex haplotype calls) (–haplotype-length 0). Variant calls were filtered with bcftools v.1.6 (22) to remove calls with a quality score < 20. SNPs were phased using whatshap v.1.0 (23).

In a parallel analysis to the alignment and variant calling, PacBio's (long amplicon analysis tool v.2.4.2 (LAA) [https://github.com/PacificBiosciences/pblaa]) was used to collapse reads into phased haplotypes, representing distinct allele sequences for each amplicon within each sample. The relative number of reads supporting each haplotype from this analysis was used as additional confirmation of the copy number calling. Haplotypes were assigned based on copy number in different portions of the *CES1* gene, using custom R code. Due to limited numbers diplotypes (i.e., combinations of two haplotypes) were grouped for analysis as CES1A1/CES1A1, CES1A1/CES1A1c and CES1A1c/CES1A1c.

The relationship between individual SNVs and clinical correlates were assessed for a list of SNVs determined from the literature. Linkage disequilibrium was calculated for all SNVs, and to account for the most closely linked SNVs, for every pair of SNVs with an $R^2 > 0.95$ the SNV present in the highest number of samples was chosen for further analysis. (If two SNVs were in the same number of samples, the first one was chosen.) This dropped the number of key SNVs analyzed against clinical correlates to 19. (**Supplementary File**) SNVs were treated as simply present or absent, and were tested against binary clinical traits (e.g., side effects) with Fisher's exact test, and against continuous traits {e.g., log2[dose by weight (mg/kg)]} with a *t*-test. The Benjamini-Hochberg correction was used to correct for multiple hypothesis tests across all tests (all SNVs and all clinical correlates) (**Figure 1**).

Results

A total of 99 participants ($n = 30$ female; $n = 69$ male) had both clinical data and *CES1* sequencing data (**Figure 2**), with an average age of 7.7 years old (range 3–15 years) at their initial visit. Of note, methylphenidate is approved for children 6 years and older, but is sometimes used in younger children, and our data included children as young as three years of age.

Age was significantly associated with both the final absolute dose ($p = 0.018$) and weight-based dose (mg/kg; $p = 0.005$), though the r^2 values for both were relatively low at 0.056 (**Figure 3**) and 0.078, respectively. The final average absolute dose in all participants was 24.2 mg/day (22.4 mg/day in females vs. 25.0 mg/day in males), while the final weight-based dose in all individuals was 0.79 mg/kg/day (0.74 mg/kg/day in females vs. 0.81 mg/kg/day in males). In total, 65 participants had any change in dose, 61 had a dose increase, and 15 had a dose decrease. Adverse effects were reported for 69 (female = 20, male = 49) of the individuals. The most common adverse effects reported were decreased appetite ($n = 47$; 14 females, 33 males), other ($n = 27$), weight loss ($n = 24$; 10 females, 14 males), and sleep problems ($n = 19$; 4 females, 15 males). The mean final weight-based dose by haplotype is described in **Table 1**.

The CES1 locus and 12 kb upstream were sequenced with overlapping ~6 kb amplicons and PacBio Sequel sequencing. Nine tiled, overlapping primer sets were designed to cover all CES1 and 12 kb upstream, but primer sets 8 and 9, targeting the 3′ end of the gene, were not successful and not included in the final project. Additionally, amplicon 4 performed poorly and a subset of samples are either missing amplicon 4 or have low coverage. Amplicon 4 covers exon 2 and 3. As a result, the final sequencing data cover 12 kb upstream of CES1 to partway through intron 11 of the 14-exon CES1 gene for 99 individuals, and 19 individuals are missing data for exons 2 and 3 (amplicon 4). Most samples (77 of the 99 final samples) had no amplicons with less than the threshold 30× coverage required for further analysis, and most amplicons had vastly more than 30× coverage (median coverage for all exons was >2000×). Of the 22 samples where an amplicon was below 30× coverage, in 20 samples only one amplicon was <30×, and in the other two samples, it was two amplicons. Given the good coverage across amplicons, haplotypes could reasonably be inferred for 99 samples that also had clinical correlates (**Supplementary File**).

Before correction for multiple hypothesis testing, nine SNVs showed significant associations, three with weight-based doses, five with weight loss, and one with both weight loss and dose increase. The three SNVs associated with weight-based doses [determined by t-test of log2(last dose in mg/kg) for children with and without the SNV] were rs114119971 ($p = 4.3e{-}13$), (**Figure 4**) rs4122238 (0.77 with the SNV mg/kg vs. 1.1 mg/kg

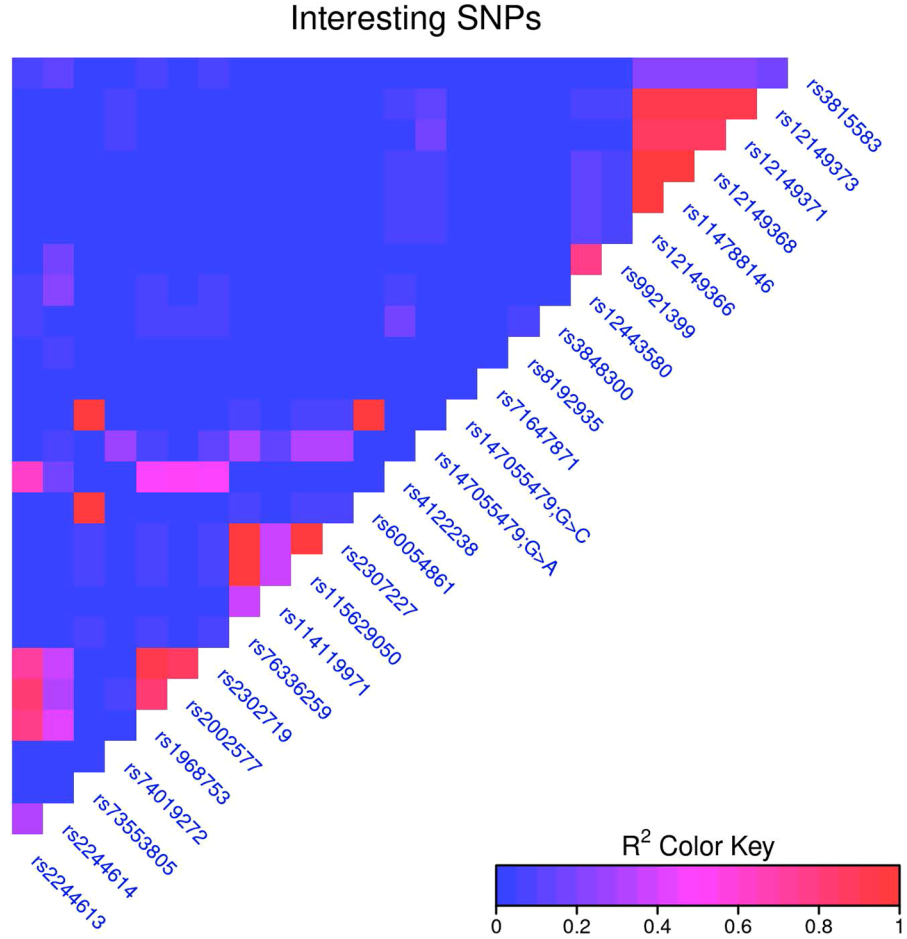

FIGURE 1
Notable CES1 SNPs.

without the SNV; $p = 0.0095$), (**Figure 5**) and rs74019272 (0.28 mg/kg with the SNV vs. 0.81 mg/kg; $p = 0.023$). (**Figure 6**) The six SNVs associated with weight loss were rs32171764 ($p = 0.003$), rs2244614 ($p = 0.0039$), rs1968753 ($p = 0.0065$), rs2302719 ($p = 0.014$), rs2244613 ($p = 0.032$), and rs2002577 ($p = 0.039$). SNV rs3217164 was also associated with dose increase ($p = 0.032$). Correction for multiple hypothesis testing assumes independence of tests. While the SNVs with the highest linkage disequilibrium were filtered from the dataset so only one of each pair of highly-linked SNVs was analyzed further, there was still considerable linkage disequilibrium among the remaining SNVs. As such, the remaining SNVs tested may not be truly independent, and the Benjamini-Hochberg correction for multiple hypothesis testing may be too stringent. It is worth considering the tests that were still significant after multiple hypothesis correction as the strongest result, but those that were only significant prior to the correction may also be worth consideration for further research.

After correction for multiple hypothesis testing, only one SNV, the previously mentioned rs114119971, was significantly associated with weight-based dosing, and included only two individuals with the SNV. The two individuals with the rs114119971 SNV had a significantly lower weight-based dose [as determined by a t-test of log2(final dose in mg/kg) in children with and without the SNV, final dose with rs114119971 = 0.42 mg/kg] as compared to those without the SNV (final dose = 0.88 mg/kg; $p = 4.3e{-}13$, adjusted $p = 1.3e{-}10$). One individual was identified as having the rs71647871 SNV, with a final absolute dose of 27 mg and weight-based of 0.37 mg/kg.

Discussion

Due to the many variables involved, clinical implementation of pharmacogenetic testing in children with ADHD has proven challenging. Although this study was unable to discern any associations between clinical response to methylphenidate and

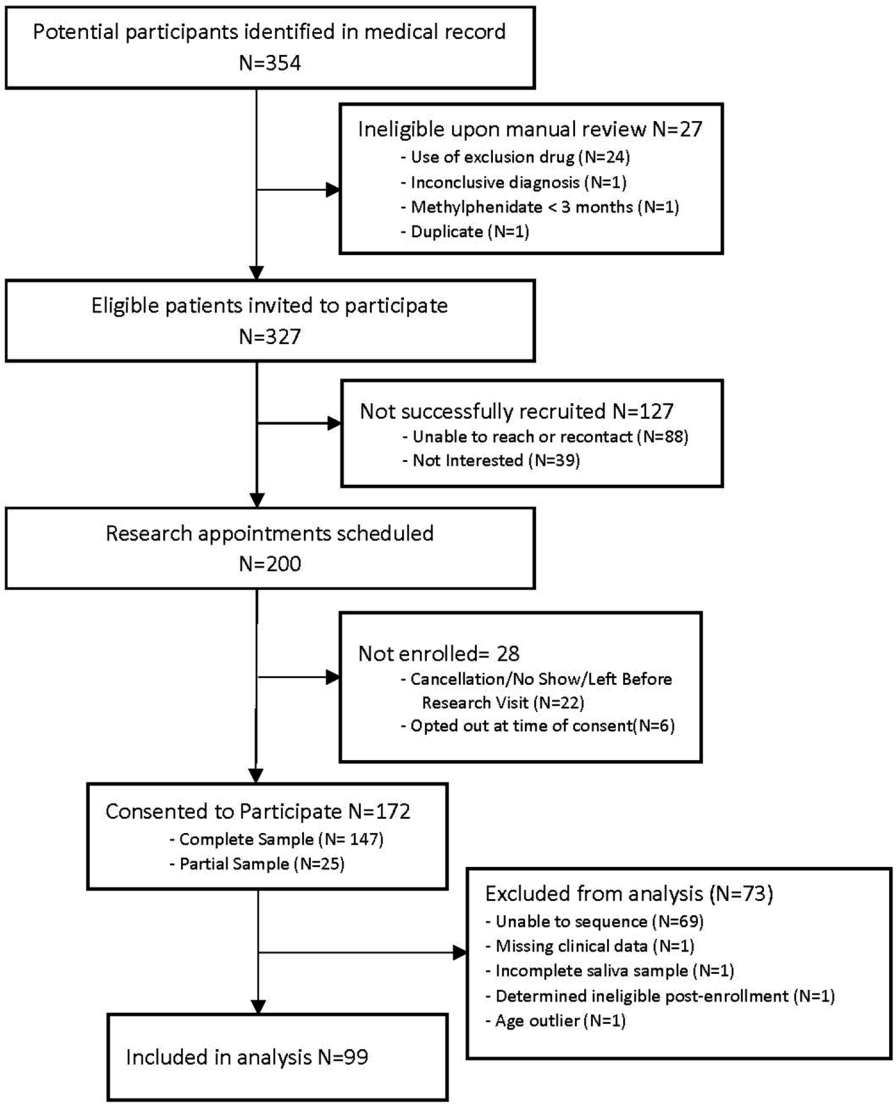

FIGURE 2
Study flowchart.

CES1 genetic variation, we did identify several *CES1* SNVs associated with weight-based dosing and weight loss; however, after correction for multiple hypothesis testing only a single SNV remained statistically significant. While sparsely studied, associations between *CES1* and methylphenidate dose, response, and adverse effects have been previously reported.

Previously, pharmacokinetic studies have described a handful of variants significantly associated with methylphenidate exposure. The previously noted Zhu et al. article described two functional *CES1* variants in a single adult resulting in decreased enzyme activity as shown by increased exposure to methylphenidate (13). Additionally, Stage et al. showed a similar increased exposure to methylphenidate of the rs71647871 SNV in a group of Danish adults (14). Similar effects for the rs71647871 variant were shown when examined as the metabolic ratio of ritalinic acid to methylphenidate (24). While the pharmacokinetic impact of this variant is well defined, only a single individual with this variant was included in this study.

Nemoda et al. described children classified as responders to methylphenidate with the glycine to glutamic variant allele require significantly smaller dosing requirements as compared to responders without the variant allele (0.41 vs. 0.57 mg/kg) (25). However, these results are limited as they were based upon five individuals with the variant allele. We were unable to compare our own results to these, as only one individual completing all study procedures also had this variant. Of the variants with significant associations with weight-based

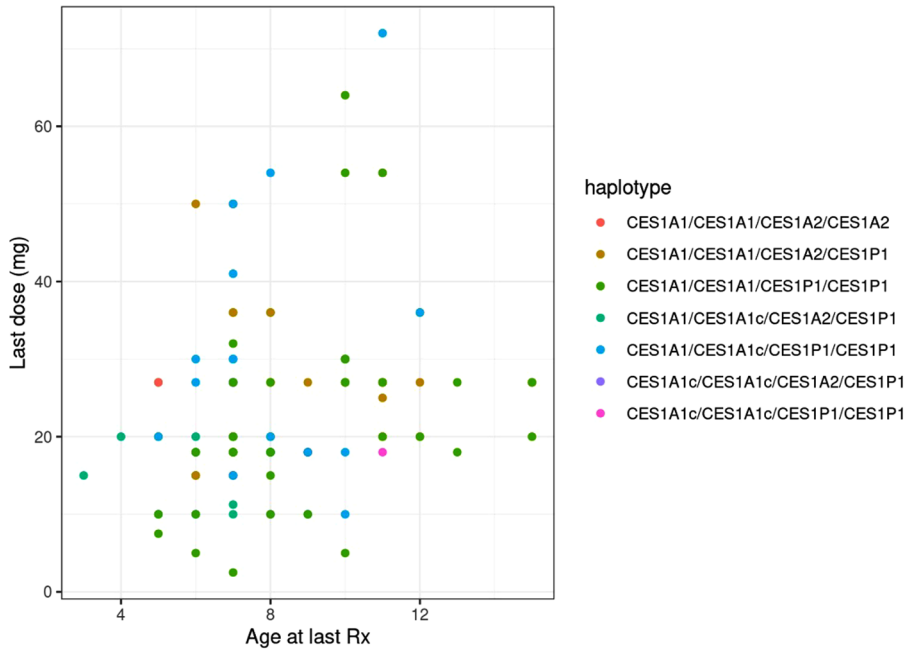

FIGURE 3
Comparing age and final methylphenidate dose across CES1 haplotypes.

dosing, the rs114119971 SNP is a missense variant, while the rs4122238 and rs74019272 are both intron variants.

The rs114119971 SNP identified as being significantly associated with weight-based dosing after multiple hypothesis correction is a missense variant with a low allele frequency (0.2%–0.9%). No other studies were identified describing this variant with methylphenidate (or any other CES1 substrate) dosing or clinical response, and this SNP was found in only two participants in the study described herein. Of note, these two individuals required significantly lower doses as compared to those without the rs114119971 variant. Further study examining the pharmacokinetic effect of this variant on methylphenidate and other CES1 substrates may be warranted.

Recent clinical studies have compared side effect profile with genetic variation in the *CES1* gene in children taking methylphenidate for ADHD. Specifically, Johnson et al. identified two *CES1* SNV markers (rs2244613 and rs2002577)

TABLE 1 Methylphenidate dose by CES1 haplotype (mg/kg).

Haplotype	All	Males	Females
CES1A1/CES1A1/CES1A2/CES1A2 ($n = 3$)	0.92	0.92	–
CES1A1/CES1A1/CES1A2/CES1P1 ($n = 16$)	0.88	0.99	0.70
CES1A1/CES1A1/CES1P1/CES1P1 ($n = 45$)	0.75	0.77	0.69
CES1A1/CES1A1c/CES1A2/CES1P1 ($n = 8$)	0.66	0.79	0.44
CES1A1/CES1A1c/CES1P1/CES1P1 ($n = 22$)	0.90	0.88	0.94
CES1A1c/CES1A1c/CES1A2/CES1P1 ($n = 2$)	0.81	0.81	–
CES1A1c/CES1A1c/CES1P1/CES1P1 ($n = 3$)	0.38	0.38	–

in linkage disequilibrium with two SNVs in the norepinephrine transporter gene associated with sadness as a side effect (26). While our study did not find an association between these SNPs and sadness, they were found to be associated with weight loss prior to multiple hypothesis correction. The rs2244613 variant has also been associated with low trough concentrations of dabigatran, which is also a CES1 substrate requiring bioactivation, with an allele frequency of approximately 13.2%–40.3% (27). Additionally, Bruxel et al. described a different *CES1* variant (rs3815583) where carriers had a significant odds ratio of 3.5 for appetite reduction worsening as compared to those who lacked the variant (28), although we did not find a similar association.

Of the five SNPs associated with weight loss, all were intron variants with high allele frequencies. The rs2244614 variant has an allele frequency of 18%–50% and was not shown to impact the pharmacokinetics or toxicity of capecitabine in colorectal cancer patients (29). An additional study examining the pharmacodynamic effects of CES1 variation, including rs2244614, in patients treated with angiotensin converting enzyme (ACE) inhibitors with congestive heart failure did not show significant associations (30). The rs1968753 variant has an allele frequency of 19%–45% and was previously shown to possibly be a candidate for risk prediction of antituberculosis drug-induced hepatotoxicity (31). The rs2244613 variant is relatively well described in CES1 substrates other than methylphenidate and has an allele frequency of 15%–40%. The rs2244613 variant has been associated with lower

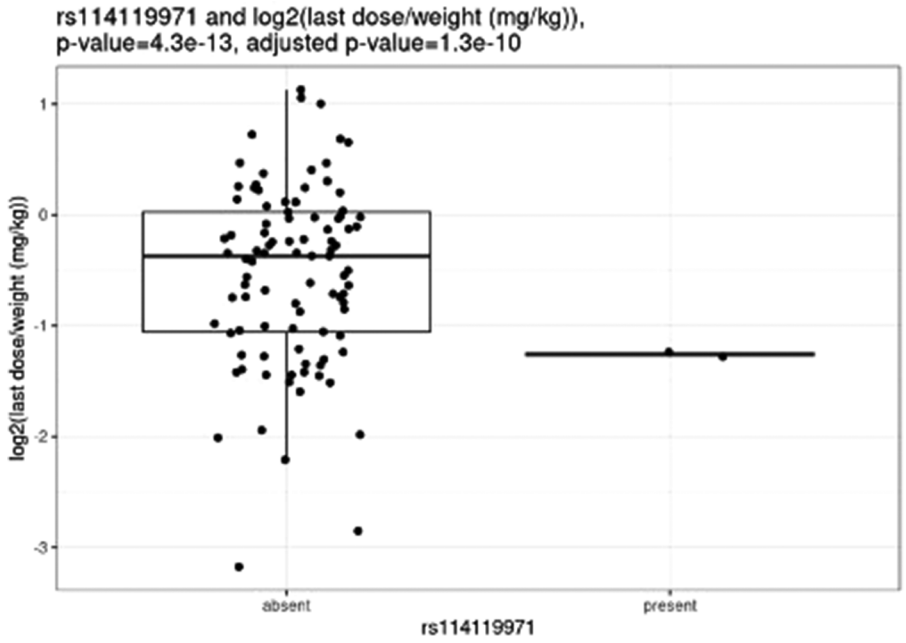

FIGURE 4
Comparing dose (mg/kg) with rs114119971.

dabigatran trough concentrations (27), reduced risk of diarrhea with irinotecan treatment (32), and lower peak and trough enalaprilat concentrations (33). The rs2302719 and rs2002577 SNVs are both intron variants with relatively high allele frequencies, though no studies were identified describing these.

While this study focused on the impact of variation in CES1 on methylphenidate dosing and adverse effects, other

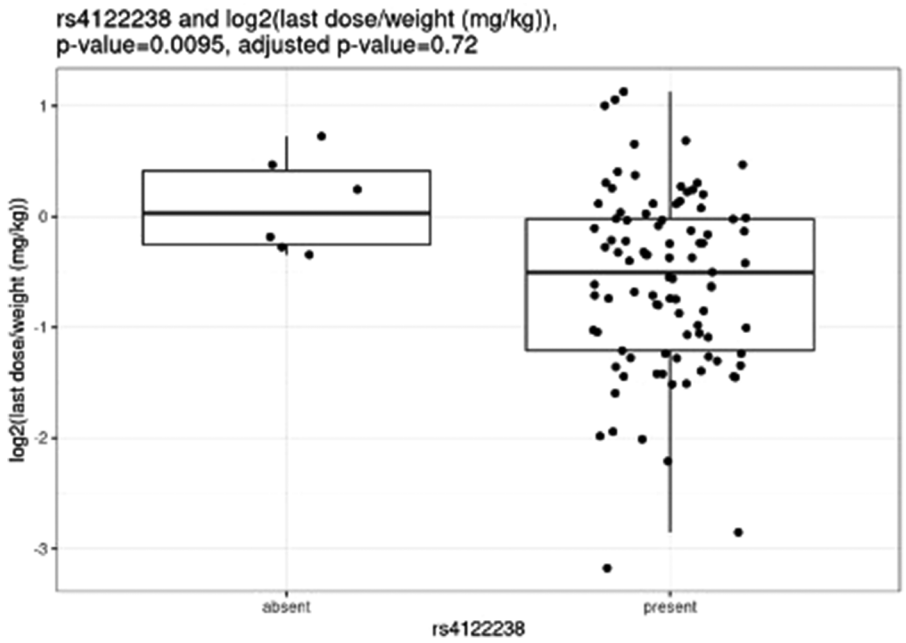

FIGURE 5
Comparing dose (mg/kg) with rs4122238.

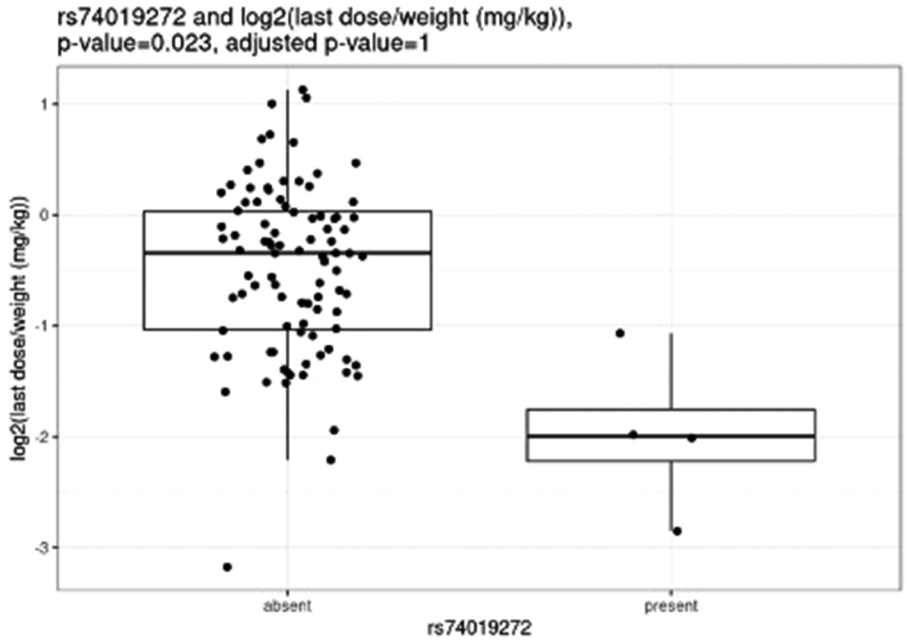

FIGURE 6
Comparing dose (mg/kg) with rs74019272.

non-genetic factors also contribute to CES1 activity. These include natural products capable of inhibiting CES1 activity (34), alcohol (35), and therapeutic agents which may result in drug-drug interactions (36). Additionally, variation in several other genes have been described as it relates to methylphenidate adverse events and clinical response (37, 38).

Although studies describing the pharmacokinetic and pharmacodynamic effects of CES1 on medications such as methylphenidate, ACE-inhibitors, and dabigatran are increasing, CES1 is rarely included in commercially available pharmacogenetic testing panels. Based on registered laboratories through the National Library of Medicine Genetic Testing Registry, only six laboratories include *CES1* genetic testing, five of which are located within the United States. Variants such as rs71647871 that have been shown to increase exposure to CES1 substrates could be clinically useful in identifying individuals who may respond better to a lower dose or an alternative medication.

This study is limited by the retrospective nature of the clinical and adverse effect data, and is dependent on medical records. It is also limited by the inclusion of all methylphenidate formulations considered as the total daily dose of methylphenidate. Additionally, given the considerable variation of *CES1* the sample size is relatively small to show clinically significant differences in dosing or adverse effects.

Contributions of this study include improving researchers' and clinicians' understanding of how genetic variation in the *CES1* gene primarily responsible for the metabolism of methylphenidate impacts adverse events and dose requirements in children with ADHD.

Data availability statement

The original contributions presented in the study are publicly available. This data can be found here: https://www.ncbi.nlm.nih.gov/bioproject/PRJNA919062.

Ethics statement

Written informed consent to participate in this study was provided by the participants and their legal guardian.

Author contributions

JTB, NB, AT, RR, and CAM designed the study. AT and TS performed the data abstraction. CH and JB performed the gene sequencing and data analysis. All authors contributed to the article and approved the submitted version.

Funding

This work was supported in part by a grant from the Essentia Health Foundation (A1512).

Acknowledgments

The study team would like to acknowledge Austin Land who programmed data pulls from the electronic health record, Nathan Tesch who performed data collection, and Hillary Henzler-Buckingham who also performed data collection.

Conflict of interest

The authors declare that the research was conducted in the absence of any commercial or financial relationships that could be construed as a potential conflict of interest.

Publisher's note

All claims expressed in this article are solely those of the authors and do not necessarily represent those of their affiliated organizations, or those of the publisher, the editors and the reviewers. Any product that may be evaluated in this article, or claim that may be made by its manufacturer, is not guaranteed or endorsed by the publisher.

Supplementary material

The Supplementary Material for this article can be found online at: https://www.frontiersin.org/articles/10.3389/fped.2022.958622/full#supplementary-material.

References

1. Sayal K, Prasad V, Daley D, Ford T, Coghill D. ADHD In children and young people: prevalence, care pathways, and service provision. *Lancet Psychiatry*. (2018) 5(2):175–86. doi: 10.1016/S2215-0366(17)30167-0

2. Pastor PN, Reuben CA. Diagnosed attention deficit hyperactivity disorder and learning disability: united States, 2004–2006. *Vital Health Stat*. (2008) 10 (237):1–14.

3. Boyle CA, Boulet S, Schieve LA, Cohen RA, Blumberg SJ, Yeargin-Allsopp M, et al. Trends in the prevalence of developmental disabilities in US children, 1997–2008. *Pediatrics*. (2011) 127(6):1034–42. doi: 10.1542/peds.2010-2989

4. Pelham WE, Foster EM, Robb JA. The economic impact of attention-deficit/hyperactivity disorder in children and adolescents. *Ambul Pediatr Off J Ambul Pediatr Assoc*. (2007) 7(1 Suppl):121–31. doi: 10.1016/j.ambp.2006.08.002

5. Polanczyk G, Rohde LA. Epidemiology of attention-deficit/hyperactivity disorder across the lifespan. *Curr Opin Psychiatry*. (2007) 20(4):386–92. doi: 10.1097/YCO.0b013e3281568d7a

6. Chai G, Governale L, McMahon AW, Trinidad JP, Staffa J, Murphy D. Trends of outpatient prescription drug utilization in US children, 2002-2010. *Pediatrics*. (2012) 130(1):23–31. doi: 10.1542/peds.2011-2879

7. Bolea-Alamañac B, Nutt DJ, Adamou M, Asherson P, Bazire S, Coghill D, et al. Evidence-based guidelines for the pharmacological management of attention deficit hyperactivity disorder: update on recommendations from the British association for psychopharmacology. *J Psychopharmacol Oxf Engl*. (2014) 28(3):179–203. doi: 10.1177/0269881113519509

8. McGough JJ. Attention-deficit/hyperactivity disorder pharmacogenomics. *Biol Psychiatry*. (2005) 57(11):1367–73. doi: 10.1016/j.biopsych.2004.10.021

9. McGough JJ, McCracken JT, Loo SK, Manganiello M, Leung MC, Tietjens JR, et al. A candidate gene analysis of methylphenidate response in attention-deficit/hyperactivity disorder. *J Am Acad Child Adolesc Psychiatry*. (2009) 48 (12):1155–64. doi: 10.1097/CHI.0b013e3181bc72e3

10. Kambeitz J, Romanos M, Ettinger U. Meta-analysis of the association between dopamine transporter genotype and response to methylphenidate treatment in ADHD. *Pharmacogenomics J*. (2014) 14(1):77–84. doi: 10.1038/tpj.2013.9

11. Stevens T, Sangkuhl K, Brown JT, Altman RB, Klein TE. PharmGKB summary: methylphenidate pathway, pharmacokinetics/pharmacodynamics. *Pharmacogenet Genomics*. (2019) 29(6):136–54. doi: 10.1097/FPC.0000000000000376

12. Sun Z, Murry DJ, Sanghani SP, Davis WI, Kedishvili NY, Zou Q, et al. Methylphenidate is stereoselectively hydrolyzed by human carboxylesterase CES1A1. *J Pharmacol Exp Ther*. (2004) 310(2):469–76. doi: 10.1124/jpet.104.067116

13. Zhu HJ, Patrick KS, Yuan HJ, Wang JS, Donovan JL, DeVane CL, et al. Two CES1 gene mutations lead to dysfunctional carboxylesterase 1 activity in man: clinical significance and molecular basis. *Am J Hum Genet*. (2008) 82 (6):1241–8. doi: 10.1016/j.ajhg.2008.04.015

14. Stage C, Jürgens G, Guski LS, Thomsen R, Bjerre D, Ferrero-Miliani L, et al. The impact of CES1 genotypes on the pharmacokinetics of methylphenidate in healthy danish subjects. *Br J Clin Pharmacol*. (2017) 83(7):1506–14. doi: 10.1111/bcp.13237

15. Tarkiainen EK, Backman JT, Neuvonen M, Neuvonen PJ, Schwab M, Niemi M. Carboxylesterase 1 polymorphism impairs oseltamivir bioactivation in humans. *Clin Pharmacol Ther*. (2012) 92(1):68–71. doi: 10.1038/clpt.2012.13

16. Harris PA, Taylor R, Thielke R, Payne J, Gonzalez N, Conde JG. Research electronic data capture (REDCap)–a metadata-driven methodology and workflow process for providing translational research informatics support. *J Biomed Inform*. (2009) 42(2):377–81. doi: 10.1016/j.jbi.2008.08.010

17. Harris PA, Taylor R, Minor BL, Elliott V, Fernandez M, O'Neal L, et al. The REDCap consortium: building an international community of software platform partners. *J Biomed Inform*. (2019) 95:103208. doi: 10.1016/j.jbi.2019.103208

18. Gohl D, Vangay P, Garbe J, MacLean A, Hauge A, Becker A, et al. Systematic improvement of amplicon marker gene methods for increased accuracy in microbiome studies. *Nat Biotechnol*. (2016) 34:942–9. doi: 10.1038/nbt.3601

19. Li H. Minimap2: pairwise alignment for nucleotide sequences. *Bioinforma Oxf Engl*. (2018) 34(18):3094–100. doi: 10.1093/bioinformatics/bty191

20. Quinlan AR, Hall IM. BEDTools: a flexible suite of utilities for comparing genomic features. *Bioinforma Oxf Engl*. (2010) 26(6):841–2. doi: 10.1093/bioinformatics/btq033

21. Garrison E, Marth G. Haplotype-based variant detection from short-read sequencing. arXiv; 2012 [cited 2022 May 31]. Available at: http://arxiv.org/abs/1207.3907. doi: 10.48550/arXiv.1207.3907

22. Danecek P, Bonfield JK, Liddle J, Marshall J, Ohan V, Pollard MO, et al. Twelve years of SAMtools and BCFtools. *GigaScience*. (2021) 10(2):giab008. doi: 10.1093/gigascience/giab008

23. Martin M, Patterson M, Garg S, Fischer S O, Pisanti N, Klau GW, et al. Whatshap: fast and accurate read-based phasing. *Bioinformatics*. (2016). [cited 2022 May 31]. Available at: http://biorxiv.org/lookup/doi/10.1101/085050

24. Stage C, Dalhoff K, Rasmussen HB, Schow Guski L, Thomsen R, Bjerre D, et al. The impact of human CES1 genetic variation on enzyme activity assessed by ritalinic acid/methylphenidate ratios. *Basic Clin Pharmacol Toxicol*. (2019) 125(1):54–61. doi: 10.1111/bcpt.13212

25. Nemoda Z, Angyal N, Tarnok Z, Gadoros J, Sasvari-Szekely M. Carboxylesterase 1 gene polymorphism and methylphenidate response in ADHD. *Neuropharmacology*. (2009) 57(7–8):731–3. doi: 10.1016/j.neuropharm.2009.08.014

26. Johnson KA, Barry E, Lambert D, Fitzgerald M, McNicholas F, Kirley A, et al. Methylphenidate side effect profile is influenced by genetic variation in the attention-deficit/hyperactivity disorder-associated CES1 gene. *J Child Adolesc Psychopharmacol*. (2013) 23(10):655–64. doi: 10.1089/cap.2013.0032

27. Paré G, Eriksson N, Lehr T, Connolly S, Eikelboom J, Ezekowitz MD, et al. Genetic determinants of dabigatran plasma levels and their relation to bleeding. *Circulation*. (2013) 127(13):1404–12. doi: 10.1161/CIRCULATIONAHA.112.001233

28. Bruxel EM, Salatino-Oliveira A, Genro JP, Zeni CP, Polanczyk GV, Chazan R, et al. Association of a carboxylesterase 1 polymorphism with appetite reduction in children and adolescents with attention-deficit/hyperactivity disorder treated with methylphenidate. *Pharmacogenomics J*. (2013) 13(5):476–80. doi: 10.1038/tpj.2012.25

29. Matsumoto N, Kubota Y, Ishida H, Sekido M, Ohkuma R, Ishiguro T, et al. Variants of carboxylesterase 1 have no impact on capecitabine pharmacokinetics and toxicity in capecitabine plus oxaliplatin treated-colorectal cancer patients. *Cancer Chemother Pharmacol*. (2020) 85(6):1119–28. doi: 10.1007/s00280-020-04087-z

30. Nelveg-Kristensen KE, Bie P, Ferrero L, Bjerre D, Bruun NE, Egfjord M, et al. Pharmacodynamic impact of carboxylesterase 1 gene variants in patients with congestive heart failure treated with angiotensin-converting enzyme inhibitors. *PloS One*. (2016) 11(9):e0163341. doi: 10.1371/journal.pone.0163341

31. Xue-qiong W, Dong-lin Z, Jun-xian Z, Zhong Y, Xi Y, Hui-ru A, et al. The relationship between carboxylesterase 1 gene polymorphisms and susceptibility to antituberculosis drug-induced hepatotoxicity. *Zhonghua Nei Ke Za Zhi*. (2012) 51 (7):524–30.

32. Teft WA, Welch S, Lenehan J, Parfitt J, Choi YH, Winquist E, et al. OATP1B1 And tumour OATP1B3 modulate exposure, toxicity, and survival after irinotecan-based chemotherapy. *Br J Cancer*. (2015) 112(5):857–65. doi: 10.1038/bjc.2015.5

33. Ikonnikova A, Rodina T, Dmitriev A, Melnikov E, Kazakov R, Nasedkina T. The influence of the CES1 genotype on the pharmacokinetics of enalapril in patients with arterial hypertension. *J Pers Med*. (2022) 12(4):580. doi: 10.3390/jpm12040580

34. Qian Y, Markowitz JS. Natural products as modulators of CES1 activity. *Drug Metab Dispos Biol Fate Chem*. (2020) 48(10):993–1007. doi: 10.1124/dmd.120.000065

35. Her L, Zhu HJ. Carboxylesterase 1 and precision pharmacotherapy: pharmacogenetics and nongenetic regulators. *Drug Metab Dispos Biol Fate Chem*. (2020) 48(3):230–44. doi: 10.1124/dmd.119.089680

36. Zhu HJ, Appel DI, Peterson YK, Wang Z, Markowitz JS. Identification of selected therapeutic agents as inhibitors of carboxylesterase 1: potential sources of metabolic drug interactions. *Toxicology*. (2010) 270(2–3):59–65. doi: 10.1016/j.tox.2010.01.009

37. Elsayed NA, Yamamoto KM, Froehlich TE. Genetic influence on efficacy of pharmacotherapy for pediatric attention-deficit/hyperactivity disorder: overview and current Status of research. *CNS Drugs*. (2020) 34(4):389–414. doi: 10.1007/s40263-020-00702-y

38. Joensen B, Meyer M, Aagaard L. Specific genes associated with adverse events of methylphenidate use in the pediatric population: a systematic literature review. *J Res Pharm Pract*. (2017) 6(2):65–72. doi: 10.4103/jrpp.JRPP_16_161

Frontiers in Pharmacology

Explores the interactions between chemicals and living beings

The most cited journal in its field, which advances access to pharmacological discoveries to prevent and treat human disease.

Discover the latest Research Topics

See more →

Frontiers

Avenue du Tribunal-Fédéral 34
1005 Lausanne, Switzerland
frontiersin.org

Contact us

+41 (0)21 510 17 00
frontiersin.org/about/contact